

IFIP AICT 450



Luis M. Camarinha-Matos
Thais A. Baldissera
Giovanni Di Orio
Francisco Marques
(Eds.)

Technological Innovation for Cloud-Based Engineering Systems

6th IFIP WG 5.5/SOCOLNET Doctoral Conference
on Computing, Electrical and Industrial Systems,
DoCEIS 2015
Costa de Caparica, Portugal, April 13–15, 2015
Proceedings

 Springer

Editor-in-Chief

Kai Rannenber, Goethe University Frankfurt, Germany

Editorial Board

Foundation of Computer Science

Jacques Sakarovitch, Télécom ParisTech, France

Software: Theory and Practice

Michael Goedicke, University of Duisburg-Essen, Germany

Education

Arthur Tatnall, Victoria University, Melbourne, Australia

Information Technology Applications

Erich J. Neuhold, University of Vienna, Austria

Communication Systems

Aiko Pras, University of Twente, Enschede, The Netherlands

System Modeling and Optimization

Fredi Tröltzsch, TU Berlin, Germany

Information Systems

Jan Pries-Heje, Roskilde University, Denmark

ICT and Society

Diane Whitehouse, The Castlegate Consultancy, Malton, UK

Computer Systems Technology

Ricardo Reis, Federal University of Rio Grande do Sul, Porto Alegre, Brazil

Security and Privacy Protection in Information Processing Systems

Yuko Murayama, Iwate Prefectural University, Japan

Artificial Intelligence

Tharam Dillon, Curtin University, Bentley, Australia

Human-Computer Interaction

Jan Gulliksen, KTH Royal Institute of Technology, Stockholm, Sweden

Entertainment Computing

Matthias Rauterberg, Eindhoven University of Technology, The Netherlands

IFIP – The International Federation for Information Processing

IFIP was founded in 1960 under the auspices of UNESCO, following the First World Computer Congress held in Paris the previous year. An umbrella organization for societies working in information processing, IFIP's aim is two-fold: to support information processing within its member countries and to encourage technology transfer to developing nations. As its mission statement clearly states,

IFIP's mission is to be the leading, truly international, apolitical organization which encourages and assists in the development, exploitation and application of information technology for the benefit of all people.

IFIP is a non-profitmaking organization, run almost solely by 2500 volunteers. It operates through a number of technical committees, which organize events and publications. IFIP's events range from an international congress to local seminars, but the most important are:

- The IFIP World Computer Congress, held every second year;
- Open conferences;
- Working conferences.

The flagship event is the IFIP World Computer Congress, at which both invited and contributed papers are presented. Contributed papers are rigorously refereed and the rejection rate is high.

As with the Congress, participation in the open conferences is open to all and papers may be invited or submitted. Again, submitted papers are stringently refereed.

The working conferences are structured differently. They are usually run by a working group and attendance is small and by invitation only. Their purpose is to create an atmosphere conducive to innovation and development. Refereeing is also rigorous and papers are subjected to extensive group discussion.

Publications arising from IFIP events vary. The papers presented at the IFIP World Computer Congress and at open conferences are published as conference proceedings, while the results of the working conferences are often published as collections of selected and edited papers.

Any national society whose primary activity is about information processing may apply to become a full member of IFIP, although full membership is restricted to one society per country. Full members are entitled to vote at the annual General Assembly. National societies preferring a less committed involvement may apply for associate or corresponding membership. Associate members enjoy the same benefits as full members, but without voting rights. Corresponding members are not represented in IFIP bodies. Affiliated membership is open to non-national societies, and individual and honorary membership schemes are also offered.

More information about this series at <http://www.springer.com/series/6102>

Luis M. Camarinha-Matos · Thais A. Baldissera
Giovanni Di Orio · Francisco Marques (Eds.)

Technological Innovation for Cloud-Based Engineering Systems

6th IFIP WG 5.5/SOCOLNET Doctoral Conference
on Computing, Electrical and Industrial Systems,
DoCEIS 2015

Costa de Caparica, Portugal, April 13–15, 2015
Proceedings

Editors

Luis M. Camarinha-Matos
NOVA University of Lisbon
Monte da Caparica
Portugal

Giovanni Di Orio
NOVA University of Lisbon
Monte da Caparica
Portugal

Thais A. Baldissera
NOVA University of Lisbon
Monte da Caparica
Portugal

Francisco Marques
NOVA University of Lisbon
Monte da Caparica
Portugal

ISSN 1868-4238

ISSN 1868-422X (electronic)

IFIP Advances in Information and Communication Technology

ISBN 978-3-319-16765-7

ISBN 978-3-319-16766-4 (eBook)

DOI 10.1007/978-3-319-16766-4

Library of Congress Control Number: 2015935201

Springer Cham Heidelberg New York Dordrecht London

© IFIP International Federation for Information Processing

This work is subject to copyright. All rights are reserved by the Publisher, whether the whole or part of the material is concerned, specifically the rights of translation, reprinting, reuse of illustrations, recitation, broadcasting, reproduction on microfilms or in any other physical way, and transmission or information storage and retrieval, electronic adaptation, computer software, or by similar or dissimilar methodology now known or hereafter developed.

The use of general descriptive names, registered names, trademarks, service marks, etc. in this publication does not imply, even in the absence of a specific statement, that such names are exempt from the relevant protective laws and regulations and therefore free for general use.

The publisher, the authors and the editors are safe to assume that the advice and information in this book are believed to be true and accurate at the date of publication. Neither the publisher nor the authors or the editors give a warranty, express or implied, with respect to the material contained herein or for any errors or omissions that may have been made.

Printed on acid-free paper

Springer International Publishing AG Switzerland is part of Springer Science+Business Media
(www.springer.com)

Preface

This proceedings book, which collects selected results produced in engineering doctoral programs, focuses on development and application of Cloud-based Engineering Systems. These systems leverage the emerging “network effect” and rely on the access to large pools of computational resources that are available in the “cloud” to overcome the limitations of environments with scarce processing and information storage capability. Potential benefits can be found in all engineering fields and at all levels, e.g., supporting management, operation, and services provision in small and medium enterprises, facilitating high-level sensorial perception based on sensor networks with limited local intelligence, supporting monitoring, and diagnosis of a machine with limited computer power, etc.

This approach is changing the way engineering systems are designed, giving rise to new subareas such as the so-called cloud manufacturing, while leading to exciting challenges for researchers and industrial practitioners. Instead of trying to increase local computational resources at the level of each component/ subsystem, which in some cases might be technically difficult, the efforts can be channeled to give connectivity and communication capabilities to such components, connecting them to “the cloud”. As a result, not only elasticity and more robust security mechanisms may be acquired, but also wider access to larger pools of resources available on the Internet, opening the opportunity for the development of higher value-added services. Furthermore, it also challenges systems engineers to pay attention to the underlying business models, security concerns, and user acceptability aspects.

The DoCEIS series of advanced doctoral conferences on Computing, Electrical and Industrial Systems aims at creating a space for sharing and discussing ideas and results from doctoral research in these interrelated areas of engineering, while promoting a strong multidisciplinary dialog. As such, participants were challenged to look beyond their specific research question and relate their work to the selected theme of the conference, namely to identify in which ways their research topics can benefit from, or contribute to cloud-based solutions. Current trends in strategic research programs are confirming the fundamental role of multidisciplinary and interdisciplinary approaches in innovation. As a matter of fact, more and more funding agencies are including this element as a key requirement in their calls for proposals. In such a way, the “exercise” requested by DoCEIS can be seen as a contribution to the process of acquiring such skills, which are mandatory in the profession of a PhD.

The sixth edition of DoCEIS, which is sponsored by SOCOLNET, IFIP, and IEEE IES, attracted a considerable number of paper submissions from a large number of PhD students and their supervisors from 23 countries. This book comprises the works selected by the International Program Committee for inclusion in the main program and covers a wide spectrum of application domains. As such, research results and ongoing work are presented, illustrated, and discussed in areas such as:

- Collaborative networks
- Cloud-based manufacturing
- Reconfigurable manufacturing
- Distributed computing and embedded systems
- Perception and signal processing
- Healthcare
- Smart monitoring systems
- Renewable energy and energy-related management, decision support, simulation, and power conversion

As anticipated, and confirmed by the submissions, it is shown that virtually any research topic in this broad engineering area can either benefit from a cloud-based engineering systems perspective, or be a direct contributor with models, approaches, and technologies for further development of such systems.

We expect that this book will provide readers with an inspiring set of promising ideas and new challenges, presented in a multidisciplinary context, and that by their diversity these results can trigger and motivate richer research and development directions.

We would like to thank all the authors for their contributions. We also appreciate the efforts and dedication of the DoCEIS Program Committee members who both helped with the selection of articles and contributed with valuable comments to improve their quality.

February 2015

Luis M. Camarinha-Matos
Thais A. Baldissera
Giovanni Di Orio
Francisco Marques

Organization



6th IFIP/SOCOLNET Advanced Doctoral Conference
on COMPUTING, ELECTRICAL AND
INDUSTRIAL SYSTEMS
Costa de Caparica, Portugal, April 13–15, 2015

Conference and Program Chair

Luis M. Camarinha-Matos New University of Lisbon, Portugal

Organizing Committee Co-chairs

Luis Gomes New University of Lisbon, Portugal

João Goes New University of Lisbon, Portugal

João Martins New University of Lisbon, Portugal

International Program Committee

Andy Adamatzky, UK

Hamideh Afsarmanesh, The Netherlands

Rui Aguiar, Portugal

José Júlio Alferes, Portugal

Juan Rodríguez Andina, Spain

Helder Araujo, Portugal

Américo Azevedo, Portugal

José Barata, Portugal

Olga Battaia, France

Marko Beko, Portugal

Luis Bernardo, Portugal

Nik Bessis, UK

Vedran Bilas, Croatia

Xavier Boucher, France

Erik Bruun, Denmark

Giuseppe Buja, Serbia

Luis M. Camarinha-Matos, Portugal

Roberto Canonico, Italy

João Catalão, Portugal

Wojciech Cellary, Poland

Alok Choudhary, UK

Fernando J. Coito, Portugal

Luis Correia, Portugal

Luís Cruz, Portugal

Ed Curry, Ireland

Jose de la Rosa, Spain

Joaquim António Dente, Portugal

Jorge Dias, Portugal

Rolf Drechsler, Germany

Pedro Encarnação, Portugal

Ip-Shing Fan, UK

Florin G. Filip, Romania

Maria Helena Fino, Portugal

José M. Fonseca, Portugal

João Goes, Portugal

Fausto P. Garcia, Spain

Paulo Gil, Portugal

Luis Gomes, Portugal

Antoni Grau, Spain
Nuno Horta, Portugal
Michael Huebner, Germany
David Hutchison, UK
Giulio Iannello, Italy
Tomasz Janowski, Macau
Ricardo Jardim-Gonçalves, Portugal
Hans-Jörg Kreowski, German
J. Tenreiro Machado, Portugal
Ratko Magjarevic, Croatia
João Martins, Portugal
Paulo Miyagi, Brazil
Lars Moench, Germany
Dimitris Mourtzis, Greece
Horacio Neto, Portugal
Paulo Novais, Portugal
Henrique O’Neill, Portugal
Luis Oliveira, Portugal
Manuel D. Ortigueira, Portugal
Angel Ortiz, Spain
Gordana Ostojic, The Netherlands
Peter Palensky, Austria
Luis Palma, Portugal
Nuno Paulino, Portugal

Antonio Pescapè, Italy
Willy Picard, Poland
Luigi Piegari, Italy
Simon Pietro, Italy
Paulo Pinto, Portugal
Armando Pires, Portugal
Ricardo Rabelo, Brazil
Sven-Volker Rehm, Germany
Rita Ribeiro, Portugal
Enrique Romero, Spain
Imre Rudas, Hungary
Thilo Sauter, Austria
Gheorghe Scutaru, Romania
Pierluigi Siano, Italy
Fernando Silva, Portugal
Adolfo Steiger-Garção, Portugal
Thomas Strasser, Austria
João Manuel Tavares, Portugal
Klaus-Dieter Thoben, Germany
Stanimir Valtchev, Portugal
Manuela Vieira, Portugal
Pavel Vrba, Czech Republic
Ahmed F. Zobaa, UK

Organizing Committee (PhD Students)

André Rocha
Elsa Marcelino-Jesus
Fernando Pereira
Francisco Marques
Giovanni Di Orio
Kevin Nagorny

Leonardo Martins
Mário Marques
Nuno Pereira
Oliver Kotte
Sérgio Correia
Thais A. Baldissera

Technical Sponsors



Society of Collaborative Networks



IFIP WG 5.5 COVE
Co-operation Infrastructure for Virtual Enterprises
and Electronic Business



IEEE–Industrial Electronics Society

Organizational Sponsors



Organized by: PhD Program on Electrical and Computer Engineering FCT-UNL.

Contents

Introduction

Towards Cloud-Based Engineering Systems	3
<i>João Martins, Luis M. Camarinha-Matos, João Goes, and Luis Gomes</i>	

Collaborative Networks

Dealing with the Alignment of Strategies Within the Collaborative Networked Partners	13
<i>Beatriz Andres and Raul Poler</i>	

The Need of Performance Indicators for Collaborative Business Ecosystems	22
<i>Paula Graça and Luis M. Camarinha-Matos</i>	

Negotiation Environment and Protocols for Collaborative Service Design . . .	31
<i>Ana Inês Oliveira and Luis M. Camarinha-Matos</i>	

An Emotional Support System for Collaborative Networks	42
<i>Filipa Ferrada and Luis M. Camarinha-Matos</i>	

Trust-Based Access Control in Storage Middleware Grids: A Reference Framework Proposal to Deploy in the Financial Sector	54
<i>Francisco Nunes and Henrique O'Neill</i>	

Cloud-Based Manufacturing

Service Composition in the Cloud-Based Manufacturing Focused on the Industry 4.0	65
<i>Marcos A. Pisching, Fabricio Junqueira, Diolino J. Santos Filho, and Paulo E. Miyagi</i>	

Cloud-Based Framework for Practical Model-Checking of Industrial Automation Applications	73
<i>Sandeep Patil, Dmitrii Drozdov, Victor Dubinin, and Valeriy Vyatkin</i>	

A Cloud-Based Infrastructure to Support Manufacturing Resources Composition	82
<i>Giovanni Di Orio, Diogo Barata, André Rocha, and José Barata</i>	

Reconfigurable Manufacturing

Modeling of Mechanisms for Reconfigurable and Distributed Manufacturing Control System. 93
Robson Marinho da Silva, Edson H. Watanabe, Maurício F. Blos, Fabrício Junqueira, Diolino J. Santos Filho, and Paulo E. Miyagi

PRIME as a Generic Agent Based Framework to Support Pluggability and Reconfigurability Using Different Technologies 101
Andre Dionisio Rocha, Diogo Barata, Giovanni Di Orio, Tiago Santos, and José Barata

The Migration from Conventional Manufacturing Systems for Multi-Agent Paradigm: the First Step 111
João Alvarez Peixoto, José Antonio Barata Oliveira, André Dionísio Rocha, and Carlos Eduardo Pereira

Distributed Computing

Experimental Assessment of Cloud Software Dependability Using Fault Injection. 121
Lena Herscheid, Daniel Richter, and Andreas Polze

Usability of Scientific Workflow in Dynamically Changing Environment . . . 129
Anna Bánáti, Eszter Kail, Péter Kacsuk, and Miklós Kozlovsky

Graph-Transformational Swarms with Stationary Members 137
Larbi Abdenebaoui, Hans-Jörg Kreowski, and Sabine Kuske

Embedded Systems

Analysis and Generation of Logical Signals for Discrete Events Behavioral Modeling. 147
Rogério Campos-Rebelo, Anikó Costa, and Luís Gomes

EmbedCloud – Design and Implementation Method of Distributed Embedded Systems 157
Kazimierz Krzywicki, Marian Adamski, and Grzegorz Andrzejewski

Cloud based IOPT Petri Net Simulator to Test and Debug Embedded System Controllers 165
Fernando Pereira and Luís Gomes

Perception and Signal Processing

Improved Denoising with Robust Fitting in the Wavelet Transform Domain 179
Adrienn Dineva, Annamária R. Várkonyi-Kóczy, and József K. Tar

Selection of Large-Scale 3D Point Cloud Data using Gesture Recognition. . . 188
Robin Burgess, António J. Falcão, Tiago Fernandes, Rita A. Ribeiro, Miguel Gomes, Alberto Krone-Martins, and André Moitinho de Almeida

Context Classifier for Service Robots 196
Tiago Ferreira, Fábio Miranda, Pedro Sousa, José Barata, and João Pimentão

Distributed RSS-Based Localization in Wireless Sensor Networks with Node Selection Mechanism. 204
Slavisa Tomic, Marko Beko, Rui Dinis, Goran Dimic, and Milan Tuba

Signal Processing in Medicine

Continuous Speech Classification Systems for Voice Pathologies Identification 217
Hugo Cordeiro, Carlos Meneses, and José Fonseca

3D Human Scanning Solution for Medical Measurements 225
Balázs Süttő, Zsolt Könnnyű, Zsolt Tölgyesi, Tibor Skala, Imre Rudas, and Miklos Kozlovszky

Semi-Automated Quantitative Validation Tool for Medical Image Processing Algorithm Development 231
Viktor Zoltan Jonas, Miklos Kozlovszky, and Bela Molnar

High Resolution Digital Tissue Image Processing using Texture Image Databases. 239
Gábor Kiss, Orsolya Eszter Cseri, Ádám Altsach, István Imre Bándi, Levente Kovács, and Miklos Kozlovszky

Smart Monitoring Systems

Georeferenced Dynamic Event Handling 251
Sérgio Onofre, João Paulo Pimentão, and Pedro Sousa

Implementation of User-Oriented Smart Services into an Innovative DC Low Voltage Net 259
Manja Görner, Thomas Göschel, Stephan Kassel, Thomas Klein, and Sabrina Sander

Light Memory Operation Based on a Double Pin SiC Device 265
V. Silva, M. Barata, M.A. Vieira, P. Louro, and M. Vieira

Brain Inspired Health Monitoring Supported by the Cloud. 273
Fernando Luis-Ferreira, Sudeep Ghimire, and Ricardo Jardim-Goncalves

Renewable Energy

Optimal Generation Scheduling of Wind-CSP Systems in Day-Ahead Electricity Markets 285
H.M.I. Pousinho, P. Freire, J. Esteves, V.M.F. Mendes, C. Pereira Cabrita, and M. Collares-Pereira

Influence of Large Renewable Energy Integration on Insular Grid Code Compliance 296
Eduardo M.G. Rodrigues, Radu Godina, Tiago D.P. Mendes, João C.O. Matias, and João P.S. Catalão

Optimal Behavior of Demand Response Aggregators in Providing Balancing and Ancillary Services in Renewable-Based Power Systems 309
E. Heydariyan-Forushani, M.E.H. Golshan, M. Shafie-khah, and João P.S. Catalão

A Heuristic Approach for Economic Dispatch Problem in Insular Power Systems 317
G. João Osório, J.M. Lujano-Rojas, J.C.O. Matias, and João P.S. Catalão

Energy: Management

Experimental Wireless Wattmeter for Home Energy Management Systems . . . 327
Eduardo M.G. Rodrigues, T. Caramelo, Tiago D.P. Mendes, Radu Godina, and João P.S. Catalão

Use of Web Based Meters to Improve Energy Efficiency and Power Quality in Buildings 337
Licínio Moreira, Sérgio Leitão, Zita Vale, and João Galvão

A Model-Based Approach for Resource Constrained Devices Energy Test and Simulation 345
Edgar M Silva, Luís Gomes, João Rodrigues, and Pedro Maló

Energy: Improvement

- Analysis of Causes and Effects of Harmonic Distortion in Electric Power Systems and Solutions to Comply with International Standards Regarding Power Quality 357
Mercedes Ruiz-Cortés, María Isabel Milanés-Montero, Fermín Barrero-González, and Enrique Romero-Cadaval
- Risk Analysis and Behavior of Electricity Portfolio Aggregator 365
Eduardo Eusébio, Jorge de Sousa, and Mário Ventim Neves
- Combined Operation of an Unified Power Quality Conditioner and a Superconducting Magnetic Energy Storage System for Power Quality Improvement 374
Nuno Amaro, Luís Casimiro, João Murta Pina, João Martins, and José Maria Ceballos

Energy: Decision Support

- Offering Strategies of Wind Power Producers in a Day-Ahead Electricity Market 385
R. Laia, H.M.I. Pousinho, R. Melício, V.M.F. Mendes, and M. Collares-Pereira
- New Multi-objective Decision Support Methodology to Solve Problems of Reconfiguration in the Electric Distribution Systems. 395
Sérgio F. Santos, Nikolaos G. Paterakis, and João P.S. Catalão
- Cloud-Based Decision Support Ecosystem for Renewable Energy Providers. . . . 405
Ioana Andreea Stănescu, Antoniu Stefan, and Florin Gheorghe Filip

Energy: Simulation

- Development of a Simulink Model of a Saturated Cores Superconducting Fault Current Limiter 415
Nuno Vilhena, Pedro Arsénio, João Murta-Pina, Anabela Gonçalves Pronto, and Alfredo Álvarez
- Simulation of a-Si PV System Linked to the Grid by DC Boost and Three-Level Inverter Under Cloud Scope 423
L. Fialho, R. Melício, V.M.F. Mendes, and M. Collares-Pereira
- Modeling Reserve Ancillary Service as Virtual Energy Carrier in Multi-Energy Systems 431
M.Y. Damavandi, Mohsen Parsa Moghaddam, M.-R. Haghifam, M. Shafie-khah, and João P.S. Catalão

Simulation of Offshore Wind System with Three-Level Converters:
 HVDC Power Transmission in Cloud Scope 440
*M. Seixas, R. Melício, V.M.F. Mendes, M. Collares-Pereira,
 and M.P. dos Santos*

Energy: Power Conversion I

Disc Motor with Rotor Made of Aluminium or Polycrystalline High
 Temperature Superconductor 451
David Inácio, João Murta Pina, Mário Ventim Neves, and Alfredo Álvarez

Investigation of the Tesla Transformer as a Device for One-Wire Power
 and Signaling and as a Device for Power and Signaling
 Through the Ground 459
*Kaloyan Mihaylov, Rui Neves-Medeiros, Rumen Arnaudov,
 and Stanimir Valtchev*

Experimental Magnetic Field Mapping of a Polycrystalline Superconducting
 YBCO Disc for an Axial Flux Motor 467
*David Inácio, João Murta Pina, José Maria Ceballos,
 Mário Ventim Neves, and Alfredo Álvarez*

Energy: Power Conversion II

Analysis of a Multi-Ratio Switched Capacitor DC-DC Converter
 for a Supercapacitor Power Supply 477
Hugo Serra, Ricardo Madeira, and Nuno Paulino

A Piezoelectric Device for Measurement and Power Harvesting
 Applications 486
M. Alves, J.M. Dias Pereira, and J.M. Fonseca

Design of High Voltage Full-Bridge Inverter Using Marx
 Derived Switches 494
*Nelson Santos, J. Fernando Silva, Vasco Soares, Sónia F. Pinto,
 and Duarte Sousa*

Stable Integration of Power Electronics-Based DG Links to the Utility Grid
 with Interfacing Impedance Uncertainties 502
S. Kazem Hoseini, Edris Pouresmaeil, Jafar Adabi, and João P.S. Catalão

Erratum to: Selection of Large-Scale 3D Point Cloud Data
 Using Gesture Recognition E1
*Robin Burgess, António J. Falcão, Tiago Fernandes, Rita A. Ribeiro,
 Miguel Gomes, Alberto Krone-Martins, and André Moitinho de Almeida*

Author Index 513

Introduction

Towards Cloud-Based Engineering Systems

João Martins, Luis M. Camarinha-Matos^(✉), João Goes, and Luis Gomes

Department of Electrical Engineering, Faculty of Sciences and Technology,
Universidade Nova de Lisboa, 2829-516 Caparica, Portugal
{jf.martins,lugo}@fct.unl.pt, {cam,jg}@uninova.pt

Abstract. Cloud-based Engineering Systems offer new possibilities to leverage the emerging “network effect”, by relying on the access to large pools of computational resources that are available in the “cloud” to overcome the limitations of environments with scarce processing and information storage capability. The impact of this approach is already observed in most engineering domains. Motivating engineering doctoral students to look into the potential of this novel research area is essential for their education. With this aim, the doctoral conference DoCEIS’15 focused on technological innovation for Cloud-based Engineering Systems, challenging the contributors to analyze in which ways their technical and scientific work could contribute to or benefit from this paradigm. The results of this initiative are briefly analyzed in this chapter.

Keywords: Cloud-based systems · Cloud computing · Internet of things

1 Introduction

With the increasing demand on engineering systems applications and the rapid development of Internet technologies, cloud-based engineering systems appear as a multi-paradigm for sharing information, software and hardware, within the Internet-based environment.

Cloud-based Engineering Systems provide a truly multi-dimensional approach for modern engineering. The application scope is not only restricted to *regular* cloud computing, where information and services sharing are considered on both Internet and Intranet (giving clients the power to decide what information or services to use), but it goes beyond the infrastructures, towards areas such as design, manufacturing, and supervision, where users are able to configure, select and use customized information, resources and services for product / systems achievement and operation. The location of physical resources and devices being accessed are typically not known to the end user. It also provides facilities for users to develop, deploy and manage their applications ‘on the cloud’, which entails virtualization of resources that maintain and manage themselves. This is achieved through the synergetic multidisciplinary integration of several service components: Infrastructure-as-a-Service, Storage-as-a-Service, Database-as-a-Service, Information-as-a-Service, Process-as-a-Service, Platform-as-a-Service, Hardware-as-a-Service, and Software-as-a-Service and Integration-as-a-Service.

As a result, a large variety of multidisciplinary research challenges appear, where the Electrical and Computer Engineering related disciplines play a relevant role. Ranging from basic hardware to advanced software solutions, through state-of-the-art manufacturing and operation systems, the impact of Cloud-based Engineering Systems is expected to be enormous in the upcoming years.

Considering that a substantial amount of technological innovation results from the research works of doctoral students, it is important to call their attention for the potential of the Cloud-based Engineering Systems and the role they can play in the innovation process. The DoCEIS'15 (6th Advanced Doctoral Conference on Computing, Electrical and Industrial Systems) was thus organized with this mission and some of the results are summarized in this introductory chapter.

2 Related Concepts and Trends

The origins of the term *cloud computing*, or *cloud* to make it shorter, are difficult to identify. These terms reached some popularity after Google and Amazon began to use them around 2006 to refer to the way people can have access to computer resources over the Web, either software, computer power, or data files, in opposition to having them on their own desktops. However, as pointed out in [1], a first reference to cloud computing appeared as early as 1996, in a Compaq Computer Corporation internal document, where internet cloud would accommodate moving all business software to the Web.

As a matter of fact, cloud computing has become a common jargon used to describe different kinds of solutions, or even misused to describe already available (old) products. As typically happens with other jargons, cloud computing can mean different things to different people. For some, cloud computing is only an additional marketing term. Nevertheless, the attention the area has got also motivated further developments on a number of technological facets such as security mechanisms, resource sharing, virtualization of processing capabilities, distributed storage, etc., in order to make it a reliable approach to business applications.

According to NIST (National Institute of Standards and Technology) [2], cloud computing model is composed of five essential characteristics, three service models, and four deployment models. The five essential characteristics include on-demand self-service, broad network access, resource pooling, rapid elasticity, and measured service, while the three service models are Software as a Service (SaaS), Platform as a Service (PaaS), and Infrastructure as a Service (IaaS). Three main deployment models are considered: private cloud, community cloud, and public cloud. A fourth deployment model, hybrid cloud, is characterized as a combination of two or more distinct deployment models. The essential characteristics of cloud computing typically mentioned in the literature include:

- ***On-demand self-service:*** A consumer can access to computing capabilities, such as server time and network storage, as needed automatically without requiring human interaction with the service providers.

- **Ubiquitous network access:** Capabilities are available over the network and accessed through standard mechanisms that promote use by heterogeneous thin or thick client platforms (e.g. mobile phones, tablets, laptops).
- **Location-independent resource pooling:** The customer generally has no control or knowledge over the exact location of the provided resources. The service provider assigns different physical and virtual resources dynamically according to consumer demand.
- **Rapid elasticity:** Capabilities can be rapidly and elastically provisioned to quickly scale up and released to quickly scale down.
- **Measured servicing:** Cloud systems automatically control and optimize resource use by leveraging a metering capability at some level of abstraction appropriate to the type of service. This measurement is the basis for billing of the used resources.

Within the engineering areas, the cloud symbol has been used for ages to represent networks. More recently, the term has been used to describe innovative application relying on Web usage. Remarkably, as an example of how widely the concept has been adopted, two major players in the EDA (electronic design automation) community, as Cadence and Synopsis, already started migration of their EDA tools in the cloud. Synopsis claimed that their VCS tool (Functional Verification for SoC Design) is the first EDA product to become available on a public cloud, as a Software as a Service (SaaS) offering. Other than having a potential strong impact on getting access to a vast network of computational resources, adoption of cloud computing has a direct impact in terms of version update and maintenance of the application, because they are not needed to be installed on each user's computer.

In terms of research, many projects have been launched to explore the opportunities offered by cloud computing to the development of novel engineering systems. While several of them have been addressing the development of new platforms and base components for cloud computing (e.g. ASCETIC, BETaaS, Broker@Cloud, Cactus, CELAR, Cloud4SOA, CoherentPaaS, CloudScale, CloudSpaces, CumuloNimbo, HARNESS, HEADS, MIDAS, MODAClouds, MONDO, PaaSage, Panacea, REMICS, RISCOSS, SeaClouds, SUCRE, VISION Cloud), various others are addressing the development of cloud-based engineering systems (examples in Table 1).

As an example, Fig. 1 illustrates the GloNet project [3] concept which relies on cloud-computing to deliver integrated multi-stakeholder business services enhancing complex products such as solar energy plants and intelligent buildings. Through sharing resources over a cloud-based platform and using collaboration spaces on top of this platform, networks of small and medium size enterprises can collaborate to provide services in interaction with the customer and local suppliers close to the customer, possibly located in different geographical regions.

Also in engineering education, cloud computing has been contributing to change the picture, as more and more students rely for their learning activities on resources available from the cloud, as in [4], which also support collaborative work, even carried on from different locations.

Table 1. A few examples of cloud-based engineering projects

Project	Focus	URL
ARTIST	Software modernization approach based on Model Driven Engineering techniques to automate the reverse and forward engineering of legacy applications to and from platform independent models, based Cloud Computing and related business models.	www.artist-project.eu/
BigFoot	Platform-as-a-Service solution for processing and interacting with large volumes of data coming from ICT Security, Smart Grid and other application areas	www.bigfootproject.eu/
ClodFlow	Enabling the remote use of computational services distributed on the cloud, seamlessly integrating these within established engineering design workflows and standards.	www.eu-cloudflow.eu/
CloudSME	Scalable platform for small or larger scale simulations, and enable the wider take-up of simulation technologies in manufacturing and engineering SMEs.	www.cloudsme.org/
ClouT	Leveraging cloud computing as an enabler that bridges the Internet of Things with the Internet of People via the Internet of Services, in support of smart cities	http://clout-project.eu/
GloNet	Design, develop, and deploy an agile virtual enterprise environment for collaborative networks of SMEs involved in highly customized and service-enhanced products through a cloud-based platform	www.glonet-fines.eu/
MSEE	Establishing foundations for service-oriented virtual factories and enterprises, including service Clouds.	www.msee-ip.eu

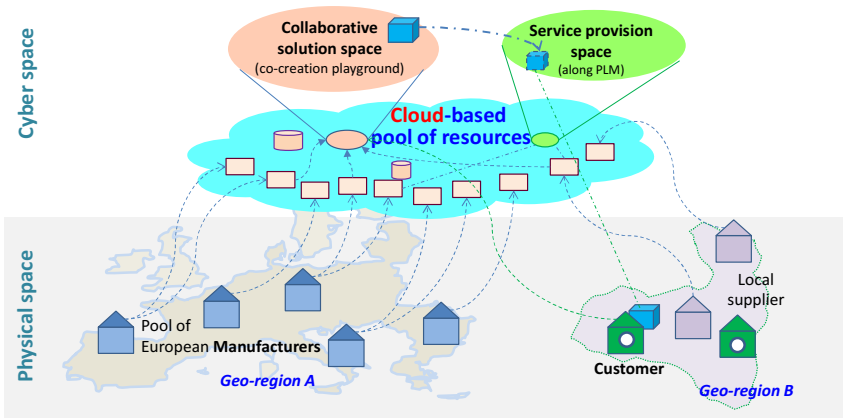


Fig. 1. GloNet cloud-based engineering approach to service-enhance products

Also a number of other related terms have emerged to represent partially overlapping perspectives or focused application contexts. Some examples are:

Cloud-Based Industrial Cyber-Physical Systems - it is expected that cyber-physical systems (CPS) will benefit from emerging cloud computing technologies, including resource-flexibility and scalability [5]. This has the potential to improve the functionality of cyber-physical systems, as well as enabling a much wider usage of CPS's data and services.

Service-oriented Architecture (SOA) - Cloud computing adopts concepts from Service-oriented Architecture, where the user may decompose a problem into services that can be integrated to provide a solution.

Grid computing - Cloud computing can be considered as a kind of grid computing, where a cluster of networked, loosely coupled computers can cooperate in order to perform large computational intensive tasks.

Internet of Things (IoT): Understood as “a dynamic global network infrastructure with self-configuring capabilities based on standard and interoperable communication protocols where physical and virtual “things” have identities, physical attributes, and virtual personalities and use intelligent interfaces, and are seamlessly integrated into the information network” [6]. In this context, a “thing” can be understood as a real/physical or digital/virtual entity that exists and moves in space and time and is capable of being identified [7].

Big data / data science: The expansion of sensing capabilities, sensor networks, smart devices, and other sources, generating huge amounts of data, requires large and elastic storage capabilities, thus a clear candidate for cloud computing.

3 Example Contributions

Cloud-based Engineering Systems (CES) involve a set of challenges that are particularly relevant for Electrical and Computer Engineering (ECE) researchers and professionals. Most professionals (and students) focus on a specialization sub-field, rarely mastering a comprehensive view of the whole field. However, addressing each individual problem normally requires the capability to address problems from a multi-disciplinary perspective. Since CES require a "strong dialogue" among the various sub-fields of electrical and computer engineering (and other areas), it represents a particularly interesting subject to bring them together.

Under this assumption, a challenge was presented to DoCEIS'15 conference participants, which are doctoral students from various countries and different sub-fields, as summarized in the following alternative questions:

– *In which aspects your research is directly related with **Cloud-based Engineering Solutions**?*

Or, in alternative,

– *In which aspects your area of work could benefit from **Cloud-based Engineering Systems**?*

As a result, all contributors made an effort to analyze the relationship between their specific research work and the CES. Among the accepted papers there is a quite balanced distribution between those that can benefit from CES adoption and those that contribute to the development of support technologies and models for CES. A summary is given in Fig. 2, which also includes the percentage of contributions in each specific sub-field.

Smart grids, Energy Management (42%)	<ul style="list-style-type: none"> ▪ Home and building energy management systems, including power consumption monitoring ▪ Efficient supply systems for sustainable cloud data centers ▪ Trading strategies in the electricity market and cloud-based decision support ecosystems ▪ User oriented smart services for low voltage networks ▪ Renewables energy smart and optimized management ▪ Super-capacitors and superconducting current limiters ▪ Magnetic energy storage systems
Cloud Computing for Advanced Services, robotics and manufacturing (30%)	<ul style="list-style-type: none"> ▪ Event behavioral modeling applied in the creation of cloud-based services ▪ Geo-referenced dynamic event handling ▪ Data interoperability ▪ Service robots ▪ Collaboration platforms on the cloud ▪ Collaborative business ecosystems applied to cloud platforms ▪ Multi-agent, re-configurability approaches applied to manufacturing ▪ Context classifier in robotics domain ▪ Reconfigurable service-oriented event-driven systems ▪ Cloud-based manufacturing ▪ Fault injection to access cloud software dependability ▪ Supply chain risk management
Sensors, Actuators, Electronics, Telecommunications Embedded Systems and Advanced signal processing techniques (17%)	<ul style="list-style-type: none"> ▪ Design of distributed embedded systems (e.g. controllers) using cloud services and Petri nets cloud based simulators ▪ Energy harvesting, DC-DC converter and power monitoring for extended autonomy in wireless sensor devices that connect to cloud platforms ▪ Piezoelectric devices for energy harvesting to be used in systems located in remote places ▪ Light memory devices ▪ Distributed RSS based localization in cloud based wireless sensor networks ▪ Distributed embedded systems ▪ Wireless sensor networks (WSN) ▪ Advanced signal-processing techniques (wavelets, graph-transformational swarms, etc.)
Healthcare, Elderly care and Human Interaction (11%)	<ul style="list-style-type: none"> ▪ 3D visualization point cloud data using hand gesture recognition ▪ Pathological speech and voice identification using cloud reference databases ▪ 3D Human scanning solutions for medical measurements ▪ Brain-inspired health monitoring systems ▪ Health monitoring supported on real-time cloud services ▪ Medical high resolution image processing

Fig. 2. DoCEIS'15: Relationship to (and Benefits from) Cloud-based Engineering Systems

Amongst the areas that can either benefit from a CES or with a direct relationship with CES, energy management is the most represented in terms of submissions to the conference. This is certainly a result of the current challenges faced by society regarding the development of sustainable energy solutions. The materialization of smart grids strongly relies on ICT and sensing / measuring capabilities in order to shift the emphasis from the traditional “predict and supply” model to a more flexible and responsive “demand-based” model [8]. The integration of grid and cloud will be one of the key trends in CES development, in order to optimize cloud-based services, grid services and e-infrastructures. The full realization of this idea requires highly distributed cyber-physical functionalities, but also the involvement of the customers in close (collaborative) interaction with providers, a process that should go far beyond the traditional client-supplier relationship. The concept of cloud-based engineering systems can help reaching a shared vision of long-term sustainability and facilitate more effective use of resources.

Manufacturing is another area indicated as major potential beneficiary. “Cloud Manufacturing (CM) is a customer-centric manufacturing model that exploits on-demand access to a shared collection of diversified and distributed manufacturing resources to form temporary, reconfigurable production lines which enhance efficiency, reduce product lifecycle costs, and allow for optimal resource loading in response to variable-demand customer generated tasking” [9]. In reality, cloud manufacturing is a misleading or meaningless term; it should better be referred to as cloud-based manufacturing. Achieving truly agile manufacturing systems, able to dynamically adjust to market dynamics, requires novel approaches that take the shop-floor as a collaborative ecosystem of (progressively more) intelligent and autonomous machines / resources. On the other hand, there is a need for stronger synergies among the various engineering areas involved in product design, manufacturing system design, manufacturing system deployment, manufacturing system operation, etc., which can also benefit from the conceptual insights of cloud-based systems.

In terms of conceptual and technological contributions to the development of CES, DoCEIS'15 includes a vast number of elements, ranging from the hardware level (electronic devices, sensors, telecommunication devices and systems), to software (interfacing and computing methods and models, advanced signal processing techniques, etc.), including specific approaches for embedded systems design.

Last but not less important, other important areas indicated as major potential beneficiaries are healthcare and elderly care, and human interaction. Application examples such as, 3D hand gesture recognition, 3D human scanning solutions, health monitoring systems, high-resolution medical imaging processing and pathological speech and voice identification benefit naturally from CES since huge amounts of data have to be acquired, stored and processed in real time.

Given the scope of DoCEIS, the mentioned contributions are naturally biased by an engineering perspective. The development of advanced cloud-based engineering systems would, however, require the involvement of other disciplines.

4 Concluding Remarks

The increasing development of Cloud-based Engineering Systems will surely have a strong impact in many sectors of society, where some impacts are already visible.

This development will be enlarged by flexible architectures, advanced compatibility mechanisms and new engineering methods. The increased Internet resources will stimulate market-oriented applications, while the integration of grids and cloud surely provide new services and e-infrastructures, opening excellent opportunities for the area of Electrical and Computer Engineering. Several current topics, ranging from the impact of emerging technologies on Cloud-based Engineering Systems to which services/enterprises/business are suitable to move to the cloud, are clearly reflected in the contributions to the DoCEIS'15 doctoral conference.

Acknowledgments. This work was supported in part by the GloNet project (FP7 program) funded by the European Commission, as well as partially financed by Portuguese Agency "FCT - Fundação para a Ciência e a Tecnologia" in the framework of project PEst-OE/EEI/UI0066/2011.

References

1. Regalado, A.: Who Coined 'Cloud Computing'?. *Technology Review (MIT)* (2011). <http://www.technologyreview.com/news/425970/who-coined-cloud-computing/>
2. Mell, P., Grance, T.: The NIST Definition of Cloud Computing. NIST Special Publication 800-145 (2011). <http://csrc.nist.gov/publications/nistpubs/800-145/SP800-145.pdf>
3. Camarinha-Matos, L.M., Ferrada, F., Oliveira, A.I.: Interplay of Collaborative Networks in Product Servicing. In: Camarinha-Matos, L.M., Scherer, R.J. (eds.) *PRO-VE 2013. IFIP AICT*, vol. 408, pp. 51–60. Springer, Heidelberg (2013)
4. Gomes, L., Costa, A.: Cloud based development framework using IOPT Petri nets for embedded systems teaching; In: *ISIE 2014 – 2014 IEEE International Symposium on Industrial Electronics*, Istanbul, Turkey, June 1-4, 2014, pp. 2202–2206 (2014). doi:10.1109/ISIE.2014.6864959
5. Colombo, A., Bangemann, T., Karnouskos, S., Delsing, J., Stluka, P., Harrison, R., Jammes, F., Lastra, J.L. (eds.) *Industrial Cloud-Based Cyber-Physical Systems - The IMC-AESOP Approach*. Springer, 245 p. (2014)
6. Sundmaeker, H., Guillemin, P., Friess, P., Woelfflé, S. (eds.) *Vision and Challenges for Realising the Internet of Things*. CERP-IoT, European Commission (2010)
7. Camarinha-Matos, L.M., Goes, J., Gomes, L., Martins, J.: Contributing to the internet of things. In: Camarinha-Matos, L.M., Tomic, S., Graça, P. (eds.) *DoCEIS 2013. IFIP AICT*, vol. 394, pp. 3–12. Springer, Heidelberg (2013)
8. Fang, X., Misra, S., Xue, G., Yang, D.: Managing smart grid information in the cloud: opportunities, model, and applications. *IEEE Network* **26**(4), 32–38 (2012)
9. Wu, D., Greer, M.J., Rosen, D.W., Schaefer, D.: Cloud manufacturing: Strategic vision and state-of-the-art. *Journal of Manufacturing Systems* **32**(4), 564–579 (2013)

Collaborative Networks

Dealing with the Alignment of Strategies Within the Collaborative Networked Partners

Beatriz Andres^(✉) and Raul Poler

Centro de Investigación en Gestión e Ingeniería de la Producción, Escuela
Politécnica Superior de Alcoy, Universitat Politècnica de València, Centre
d'Innovació i Investigació, Calle Alarcón, 03801 Alcoy, Alicante, Spain
{beaanna, rpoler}@cigip.upv.es

Abstract. Over the last years, enterprises awareness towards establishing collaborative processes has significantly grown due to the benefits obtained when participating in a collaborative network (CN). This paper is a continuation of the work developed by Andres and Poler [1] in which a set of collaborative processes are identified. This paper particularly focuses on the *strategies alignment (SA) process*, highlighting its influence on the success of a CN. A preliminary framework is outlined to address the collaborative process of SA, consisting of a model, a method and a methodology. Highlighting the importance of the use of cloud-based systems to support small and medium enterprises (SMEs) to deal with the SA process. The implementation of the proposed framework allows identifying what are the strategies that are aligned and how its activation increases the network performance, resulting in more stable and sustainable collaborative relationships, and assuring the proper operation of the CNs.

Keywords: Strategies alignment (SA) · Collaborative networks (CN) · Collaborative processes · Sustainability · SMEs · Cloud-based engineering systems.

1 Introduction

Along the last fifteen years, a wide research activity has been carried out in the CN context; this research especially focuses in small and medium enterprises (SMEs) due to their higher lack of resources and capabilities to conduct collaborative processes. A wide range of models, guidelines and tools have been developed along the literature to assist enterprises to comply the requirements demanded by the CNs, and cope with the appearance of possible obstacles derived from the collaborative processes participation [2]. Despite the challenges enterprises have to face up when establishing collaborative processes, taking part in a CN leads them to obtain higher competitive advantages and greater degrees of agility, facilitating their survival in the current competitive and globalised environments.

According to the definition provided by [3] a CN consist of a set of heterogeneous and autonomous entities, which collaborate to better achieve common or compatible goals. Each autonomous entity defines its own objectives and formulates its own strategies apart from defining a common goal. The raised strategies encompass a set of

actions described to achieve the objectives defined, whose accomplishment is measured through key performance indicators (KPIs). Once the strategies are formulated the enterprises have to decide which ones activate in order to achieve the objectives defined and obtain the desired performance [4]. When deciding what strategies activate, an enterprise may opt for making this decision from an isolate perspective, that is, by only taking into account the extent to which the activation of its strategies will benefit the achievement of its own objectives. An enterprise that makes this decision, by only taking into account its own objectives, may trigger a contradictory situation in which the strategies activated by one enterprise positively influence the objectives defined in the same enterprise but could negatively influence the achievement of the objectives defined by the other network enterprises, leading to a partnership failure. On the other hand, an enterprise can opt for deciding what are the strategies to activate by considering not only its own objectives, but also taking into account the achievement of the objectives defined by the other network partners.

1.1 Research Question

CNs are characterised by the heterogeneity of the enterprises and the objectives they define, consequently, a high diversity of strategies are formulated, to achieve these objectives, which at times might contradict one each other. In order to support the network partners on deciding about what strategies to activate, so that they positively influence all the objectives defined by network partners, a set of collaborative mechanisms are needed with the main aim of identifying the strategies that are aligned. In the light of this, a research question emerges:

What would be an adequate model, method and methodology to identify amongst all the strategies, formulated by the network partners, those that must be activated so that there are aligned and positively influence the objectives of all the partners?

The opportunities derived from the proper selection of strategies opens new ways to decide what strategies to activate, considering all the objectives defined by the enterprises. In this context, the research challenge emerges evolving from the null consideration of the objectives defined by all the network partners towards deciding what strategies to activate by considering how they affect to the objectives achievement of the rest of enterprises. The measurement of the increase of KPIs when certain strategies are activated will allow SMEs to identify what is the combination of strategies that results on higher increases on the KPIs. As will be justified then, the information gathering required to implement the framework proposed to deal with the SA process will be supported by cloud-based systems. Accordingly, the paper is organised as follows: Section 2 identifies how the SA process can benefit from the application of cloud-based systems; in Section 3 the SA concept is defined and a brief overview of how this concept has been treated in the literature is given; Section 4 provides a summarised description of the proposed framework, consisting of a model, a method and a guideline to address the SA process; conclusions and future research lines are presented in Section 5.

2 Benefits from Cloud-Based Engineering Systems

According to [5] the cloud-service term is understood as an Internet-based technology used as a repository of information and IT services provided to the enterprises (seen as customers) that updates the data, computes the required issues (computation) and maintains the IT (software). The SA process, established in a CN context, involves a large diversity of SMEs having their own information. To address the proposed SA model interoperable information systems are required to exchange the data demanded. Cloud-based systems allow achieving data interoperability between different applications belonging to different SMEs; exchanging, connecting and integrating the data required to feed the model developed to deal with the SA process [6]. Considering the characteristics affecting the widely distributed SMEs, for which the proposed SA framework is designed, cloud-computing resources contribute to overcome some limitations of the SMEs in terms of (i) increasing their capability to process and storage the information, (ii) reducing the lack of interoperability in their applications, and (iii) shortening their limited computed power, with appropriate computational resources, technologies and software. One useful application of cloud-based systems in the context of SA is the integration of the simulation software used to solve the proposed SA model: *AnyLogic@* [7]. This system dynamics simulation software will be included in the cloud in order to support all the enterprises, belonging to the collaborative network, on the decision making of which strategies to activate in order to be aligned one with each other.

3 Definition and State of Art

In this section a definition of what in this paper is meant by the SA concept, is offered. Besides this, a brief overview on how the alignment concept has been treated in the literature is given.

Strategies Alignment (SA) Concept. Considering that the strategies are the set of actions to be performed in order to fulfil the objectives defined, there are characterised by being aligned when: each activated strategy not only promotes the achievement of the objectives defined by the enterprise that raises such strategy, but also positively influences the accomplishment of the objectives defined by the rest of the network partners. The SA concept is linked with the strategies *complementarity*, in which two or more strategies, apart from being able to exist together harmoniously if simultaneously activated (compatibility), enhance the benefits obtained in the associated objectives, receiving positive influences from the set of activated strategies

The literature has used different terms to refer to the alignment concept in the CNs context, such CN participants' alignment [8], strategic alliance [9], collaborative strategy [10] or values alignment [11]. As regards the alignment in the specific context of strategies, different works have been developed, by considering in most of the cases the alignment of two particular strategies (table 1).

The analysis of the selected works has allowed identifying a common feature about how the alignment concept is treated. Concluding that, the approaches developed so far to deal with the alignment of strategies deals with the strategies *compatibility*. What is to say that, the alignment term is used to promote the simultaneous activation of pairs of specific strategies, which make a good combination, but does not involves, necessarily, that the enterprises performance increase when compatible strategies are activated. Accordingly, none of the works, provided so far, give a global view of the whole range of strategies defined by all the enterprises of the CN. In the light of this, the SA framework proposed in this paper goes further and develops a holistic approach identifying *complementary* strategies, in which the collaborative network system is analysed as a whole, considering all the strategies formulated by the enterprises that comprise it. The holistic nature of the proposed approach allows determining how the objectives of each company behave (increasing or decreasing its performance levels) as a result of the synergies arising from the activated strategies.

Table 1. Alignment of specific strategies and authors

Alignment of specific strategies	Authors
Business Strategy & IT Strategy	Cuenca et al. [12]
Business Strategy & Information Assurance Efforts	Jean-Noël et al. [13]
Business Strategy & e-Business	Raymond and Bergeron [14]
Supply Strategies	Cousins [15]
Global Sourcing Strategies	Selen and Ashayeri [16]
Marketing Strategy & Sourcing Strategy	Green et al. [17]
Supply Chain Configuration & Distribution Channels	Wu et al. [18]
Product Design Strategies	Dell'Era and Verganti [19]
Product & SC characteristics	Lyons and Ma'aram [20]
Product & SC Processes	Stavroulaki and Davis [21]
Green SCM & Business Strategy	Whitelock [22]

4 Research Contribution in Strategies Alignment

The strategies alignment process is considered a key factor that, if carried out, leads the CN to have higher levels of performance, and therefore, success. The problem identified in this paper is the strategies misalignment, which may lead to partnership failure. In order to deal with this relevant problem, the paper bases its research on a theoretical body of knowledge regarding Collaborative Networks, Industrial Management, and System Dynamics. The research scientific methodology used has its ground on the *Constructive Research* method [23]. A framework consisting of (i) a *model*, to represent the links between the objectives and the strategies formulated by all the networked partners, (ii) a *method*, selected to solve the particular modelled process, the SA, and (iii) a *methodology*, to guide the CN enterprises on how to apply the model, to solve the specific problem of SA, is proposed. This framework identifies the set of strategies to activate in order to be aligned.

4.1 Strategies Alignment Modelling

The SA model addresses the decision making of what strategies to activate though an approach that allows to identify the set of strategies that if activated positively influence (or its negative influence is minimum) all the objectives defined by all the network partners. The model computes the increase (or decrease) of the KPIs, used to measure the objectives, depending on what strategies are activated. Accordingly, the model is based on deciding which strategies to activate so that the increase of the KPIs is maximised. The set of parameters characterising the SA model are depicted in (table 2). These parameters allow defining the function that models the influence the strategies exert over the KPIs (fig 1).

Table 2. Parameters and its classification in systems dynamic

Index		
net	set of networks ($net = 1, \dots, N$)	k set of KPIs ($k = 1, \dots, K$)
i	set of enterprises ($i = 1, \dots, I$)	s set of strategies ($s = 1, \dots, S$)
x	set of objectives ($o = 1, \dots, O$)	
Parameters		Type of variable
kpi_{ixk}	KPI k defined by enterprise i to measure the objective x	Auxiliary
kpi_i	KPI at enterprise level (the sum of the kpi_{ixk})	Variables (kpi_{ixk})
kpi_{net}	KPI at network level (the sum of the kpi_i)	
str_{is}	Strategy s defined by the enterprise i	
$u_{str_{is}}$	Units of strategies to activate of str_{is}	
$c_{str_{is}}$	Cost of one unit of strategy str_{is}	
$val_{str_{is}-kpi_{ixk}}$	Value estimated by the enterprise defining the increase or decrease of the kpi_{ixk} when one unit of str_{is} is activated	
$ti_{str_{is}}$	Time of initialisation of str_{is}	
$tf_{str_{is}}$	Time of finalisation of str_{is}	Auxiliary
$d1_{str_{is}}$	Delay time, period of time in which, once the str_{is} is initiated, the str_{is} does not exerts influence over the kpi_{ixk}	Variables (str_{is})
$d2_{str_{is}}$	The influence that str_{is} exerts on the kpi_{ixk} is not immediate, unlike it takes a time to reach the maximum level of influence ($val_{str_{is}-kpi_{ixk}}$)	
$slope_{str_{is}-kpi_{ixk}}$	The progressive influence during $d2_{str_{is}}$	
$d4_{str_{is}}$	Duration of strategy str_{is}	
$inf_{str_{is}-kpi_{ixk}}$	Maximum level of influence of str_{is} in kpi_{ixk}	
bi	Budget owned by enterprise i to activate the strategies	Stock Variables
$\forall kpi_{ixk}$	Increase of the KPI when the strategies are activated	
$F_{inf_{str_{is}-kpi_{ixk}}$	Function of influence that the kpi_{ixk} experiences when the strategy str_{is} is activated (fig 1)	Flow Variable

The objective function is defined by maximising the parameter kpi_{net} through modifying the decision variables defined by $ti_{str_{is}}$ and $u_{str_{is}}$.

$$\max. kpi_{net} \tag{1}$$

$$kpi_{net} = \sum_i i kpi_i \tag{2}$$

$$kpi_i = \sum_k \nabla kpi_{ixk} \tag{3}$$

$$\nabla kpi_{ixk} = \int F_{str_{is} kpi_{ixk}}^{inf} (t) \cdot dt \tag{4}$$

$$F_{inf_str_{is} kpi_{ixk}} = \begin{cases} 0; & t < t_{i_str_{is}} + d_{1_str_{is}} \wedge t < t_{f_str_{is}} \\ slope_str_{is} kpi_{ixk}; & t_{i_str_{is}} + d_{1_str_{is}} \leq t \leq t_{i_str_{is}} + d_{1_str_{is}} + d_{2_str_{is}} \\ inf_str_{is} kpi_{ixk}; & t_{i_str_{is}} + d_{1_str_{is}} + d_{2_str_{is}} < t \leq t_{f_str_{is}} \end{cases} \tag{5}$$

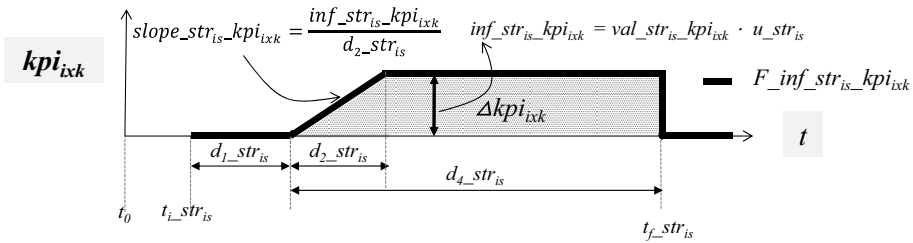


Fig. 1. Function modelling the KPIs behaviour when a strategy is activated $F_{str_{is} kpi_{ik}}$.

4.2 Method: Systems Dynamic (SD)

The systems dynamic [24] is the method selected to solve the SA model, due to allows characterising the causal relationships between the strategies and the objectives, and models the influences that the objectives experience when certain set of strategies are activated. The parameters that characterise the model are arranged according to the classification given by SD method: stock variables, flow variables and auxiliary variables (table 2, *Type of Variables* column) [25]. The tool used to solve the SA model is *AnyLogic*® [7], allowing simulating in SD. This software includes an optimiser package that allows obtaining the best set of parameters ($t_{i_str_{is}}$, $u_{str_{is}}$) that maximise the network performance (kpi_n).

4.3 Methodology

The collection of steps that allows enterprises to identify the set of aligned strategies that optimise the network performance is described. The methodology consist of: (i) selecting the enterprises that participate in the SA process; (ii) identifying for each enterprise the objectives defined: the kpi_{ixk} used to measure these objectives and the strategies formulated (str_{is}) to be potentially activated; (iii) gathering the data: each

enterprise estimates the value, $val_str_{is_kpi_{ixk}}$, that determines the strategies (str_{is}) influence on the kpi_{ixk} when the first ones are activated, besides this, all the data regarding the strategies characterisation is also collected (costs and durations). The use of cloud-based systems support enterprises on gathering the data; (iv) feeding the model with the gathered data; (v) the SA model is simulated in *AnyLogic*® software. The number of units to activate of each strategy, u_str_{is} , and the time unit in which each strategy is initiated, t_str_{is} , are determined, maximising the kpi_{ix} . The use of cloud-based systems is used to provide to all the collaborative SMEs with software. We refer readers to Andres and Poler [25] for a detailed numerical example applying the above-developed model.

5 Conclusions and Future Work

This paper focuses on the SA process, addressing it through modelling the influences that the strategies exert on the KPIs, defined to measure the objectives achievement. The System Dynamics is the method used to solve the model. *AnyLogic*® software is selected to implement the modelled process of SA. The provided approach supports the decision making process of which strategies activate at enterprise level from an holistic perspective considering all the strategies defined by the enterprises of a CN, allowing obtaining optimal network performance levels. Cloud-based systems are useful tools to support enterprises on gathering the information required by the SMEs in order to feed and implement the model. Despite the advantages obtained from the application of the SA framework, there is a limitation related with the information gathering, as regards the estimation of the value $val_str_{is_kpi'_{ixk}}$, specially if the strategy str_{is} has never been activated or there is a lack of information flow between the CN enterprises. The drawbacks as regards the information exchange and uncertainty inherent to CN must be considered in the formulation of the model and definition of the methodology. In the light of this, future work is lead to (i) extend the work developed so far defining a complete model and methodology in order to deal with the identified limitations, (ii) validate the developed approach in a real supply network, and (iii) demonstrate the usefulness of the developed contribution through simulations comparing collaborative and non-collaborative scenarios, of the decision making regarding the strategies activation.

Acknowledgments. This work was funded by the *Programa Val i+d para investigadores en formación* (ACIF).

References

1. Andrés, B., Poler, R.: Research on collaborative processes in non hierarchical manufacturing networks. In: Camarinha-Matos, L.M., Barrento, N.S., Mendonça, R. (eds.) DoCEIS 2014. IFIP AICT, vol. 423, pp. 21–28. Springer, Heidelberg (2014)
2. Andres, B., Poler, R.: Relevant problems in collaborative processes of non-hierarchical manufacturing networks. *J. Ind. Eng. Manag.* **6**(3), 723–773 (2013)

3. Camarinha-Matos, L.M., Afsarmanesh, H.: Collaborative Networks: A new scientific discipline. *Journal of Intelligent Manufacturing* **16**(4), 439–452 (2005)
4. Andres, B., Poler, R.: Computing the strategies alignment in collaborative networks In: Mertins, K., et al. (eds.) *Enterprise Interoperability VI*. Springer International Publishing Switzerland
5. Bal, J., Issa, A., Ma, X.: Orchestrating new markets using cloud services. In: Camarinha-Matos, L.M., Afsarmanesh, H. (eds.) *PRO-VE 2014*. IFIP AICT, vol. 434, pp. 161–168. Springer, Heidelberg (2014)
6. Mell, P., Grance, T.: The NIST definition of cloud computing. *National Institute of Standards and Technology* **53**(6), 20 (2009)
7. Anylogic, AnyLogic® Software 7.0.3 University (2014). <http://www.anylogic.com/>
8. da Piedade Francisco, R., Azevedo, A., Bastos, J.: Managing performance to align the participants of collaborative networks: case studies results. In: Camarinha-Matos, L.M., Boucher, X., Afsarmanesh, H. (eds.) *PRO-VE 2010*. IFIP AICT, vol. 336, pp. 545–552. Springer, Heidelberg (2010)
9. Cante, C.J., Calluzzo, V.J., Schwartz, D.P., Schwartz, T.M.: Strategic alliances in food and beverage and executive recruiting industries. *Supply Chain Management: An Int. Journal* **9**(3), 230–240 (2004)
10. Campos, P., Brazdil, P., Mota, I.: Comparing Strategies of Collaborative Networks for R&D: an agent-based study. *Comput. Econ.* **42**(1), 1–22 (2013)
11. Macedo, P., Camarinha-Matos, L.M.: A qualitative approach to assess the alignment of Value Systems in collaborative enterprises networks. *Comput. Ind. Eng.* **64**(1), 412–424 (2013)
12. Cuenca, L., Boza, A., Ortiz, A.: An enterprise engineering approach for the alignment of business and information technology strategy. *Int. J. Comput. Integr. Manuf.* **24**(11), 974–992 (2011)
13. Ezingeard, J.-N., McFadzean, E., Birchall, D.: Mastering the art of corroboration. *Journal of Enterprise Information Management* **20**(1), 96–118 (2007)
14. Raymond, L., Bergeron, F.: Enabling the business strategy of SMEs through e#business capabilities. *Industrial Management & Data Systems* **108**(5), 577–595 (2008)
15. Cousins, P.D.: The alignment of appropriate firm and supply strategies for competitive advantage. *International Journal of Operations & Production Management* **25**(5), 403–428 (2005)
16. Selen, W., Ashayeri, J.: Global sourcing strategy alignment using business intelligence: a conceptual framework. *International Journal of Procurement Management* **1**(3), 342–358 (2008)
17. Green Jr., K.W., Whitten, D., Inman, R.A.: Aligning marketing strategies throughout the supply chain to enhance performance. *Ind. Mark. Manage.* **41**(6), 1008–1018 (2012)
18. Wu, T., Wang, W., Tang, C.S., Liu, D., Gao, F., Fang, C.: How do foreign cosmetics companies align their supply chains and distribution channels in China? *International Journal of Logistics: Research and Applications* **11**(3), 201–228 (2008)
19. Dell’Era, C., Verganti, R.: Collaborative strategies in design-intensive industries: knowledge diversity and innovation. *Long Range Plan.* **43**(1), 123–141 (2010)
20. Lyons, A.C., Ma’aram, A.: An examination of multi-tier supply chain strategy alignment in the food industry. *Int. J. Prod. Res.* **52**(7), 1911–1925 (2014)
21. Stavrulaki, E., Davis, M.: Aligning products with supply chain processes and strategy. *The International Journal of Logistics Management* **21**(1), 127–151 (2010)

22. Whitelock, V.G.: Alignment between green supply chain management strategy and business strategy. *International Journal of Procurement Management* **5**(4), 430–451 (2012)
23. Kasanen, E., Lukka, K., Siitonen, A.: The Constructive Approach in Management Accounting Research. *Journal of Management Accounting Research* **5**, 21 (1993)
24. Forrester, J.W.: *Industrial Dynamics*. MIT Press and Wiley, New York (1961)
25. Andres, B., Poler, R.: Identifying the strategies to be activated for optimising the performance in collaborative networks. In: *8th International Conference on Industrial Engineering and Industrial Management* (2014)

The Need of Performance Indicators for Collaborative Business Ecosystems

Paula Graça^{1(✉)} and Luis M. Camarinha-Matos^{1,2}

¹Centre for Technologies and Systems (CTS), UNINOVA,
Campus de Caparica, 2829-516 Caparica, Portugal

²Faculty of Sciences and Technology, Universidade Nova de Lisboa,
Campus de Caparica, 2829-516 Caparica, Portugal
mgraca@deetc.isel.ipl.pt, cam@uninova.pt

Abstract. During last decades there has been a trend to build collaboration platforms as enablers for groups of enterprises to jointly provide integrated services and products. As a result, the notion of business ecosystem is getting wider acceptance. However, a critical issue that is still open, despite some efforts in this area, is the identification of adequate performance indicators to measure and motivate sustainable collaboration. This work-in-progress addresses this concern, briefly presenting the state of the art of relevant contributing areas such as, collaborative networks, business ecosystems, enterprise performance indicators, social networks analysis, and supply chains. Complementarily, through an assessment of current gaps, the research challenges are identified and an approach for further development is proposed.

Keywords: Collaborative network · Digital ecosystem · Business ecosystem · Digital business ecosystem · Performance indicators

1 Introduction

The concept of Business Ecosystem was introduced by Moore in the 1990s [1], using natural ecosystems as a biological metaphor to explain a business environment. The author considers a business ecosystem “*an economic community supported by a foundation of interacting organizations and individuals - the organisms of the business world. This economic community produces goods and services of value to customers, who themselves are members of the ecosystem*”. Furthermore, he highlights the interdependence between all the actors of the ecosystem, who “*coevolve their capabilities and roles*” [2].

This concept has been refined in the last two decades, namely as a result of the enabling role of ICT. One example is the emergence of the term Digital Business Ecosystem (DBE) [3], which puts a stronger emphasis on the technological support perspective. The DBE concept was primarily introduced as a policy strategy to address the challenge of achieving for every industry, sector and region, an effective adoption of ICT, namely enabling SMEs to become more innovative and competitive in global markets [4]. As such, it can be considered as a natural evolution of the

business environment, from the e-mail and web-sites, to e-commerce and collaborative e-business. The DBE notion follows Moore's inspiration in natural ecosystems, but expressed it in terms of a "digital environment" populated by "digital species" which could be software components, applications, services, knowledge, business models, training modules, contractual frameworks, laws, etc. These "digital species", like the living species, interact, express an independent behavior, end evolve – or becomes extinct – following the laws of market selection [3].

On the other hand, the emergence of the discipline of Collaborative Networks [5] which has a wider scope, allowed to classify business ecosystems as a sub-class of a virtual organization breeding environment (VBE), which acts as a source network of organizations, providing an adequate collaborative environment (common business processes, interoperable infrastructures, mutual trust, among others) [6]. To answer to nowadays demanding market challenges, organizations must collaborate to overcome their weaknesses and strengthen their expertise, to offer better integrated services and gain competitive advantage. In order to emphasize this perspective, the term **Collaborative Business Ecosystem** can be adopted.

However, in spite of the potential benefits of collaboration, many networks face difficulties as it is not always obvious to each of its members what they can benefit. Unlike the case of individual enterprises management, for which there are well-known indicators and balanced scorecards [7], for enterprise networks in general, and even for business ecosystems in particular, there is still a lack of well identified and widely accepted performance indicators to measure collaborative benefits, motivating sustainability, and ensuring ecosystem's resiliency. This work is motivated by this need, and is led by the following research question:

What can be a suitable approach to assess collaboration performance and promote collaboration sustainability in collaborative business ecosystems?

For a better understanding of the proposed research contributing, this main research question is further divided into two sub-questions: What is a reasonable set of key performance indicators to measure and assess collaboration benefits in a collaborative business ecosystem? How to promote collaboration sustainability and resilience within a business ecosystem?

In order to find an answer for these questions, our research is guided by the following corresponding hypotheses: **(H1)** Collaboration benefits can be evaluated and made explicit if a set of indicators is established through a holistic combination of concepts on value and benefit derived from a number of research areas such as value systems, social networks analysis, supply chain performance, and theories of complexity. **(H2)** Sustainability and resilience of collaboration in business ecosystems can be promoted if a system of incentives, combined with transparent assessment methods, is implemented at the ecosystem level. In this context, this work corresponds to only the first stage, where the state of the art of the most relevant contributing research areas is analyzed, main gaps are identified, and promising directions to overcome these gaps are proposed.

2 Relationship to Cloud-Based Engineering Systems

Nowadays cloud computing is changing the way the organizations manage their ICT resources and expertise. Cloud servers, cloud storage, and more generically cloud platforms offer to enterprises, more economic, scalable, and secure infrastructures for them to manage their business. This trend is contributing to boost emergent collaborative platforms operating in the cloud and offering network infrastructures and tools to logically connect individual organizations, under a common collaboration context. Such context is defined as a set of services under a coordinated choreography on contributing for some valuable objective, allowing interoperability between people or systems that can work together for some business goals [8]. These generic collaboration spaces support virtual organizations and virtual organizations breeding environments, being particularly promising for SME networks [9]. Complementarily, the developments on Internet of Things, facilitating access to a large number of information sources, enable the materialization of the concept of *sensing enterprise* and the effective implementation of better performance measurement mechanisms.

3 Brief Survey of the State of the Art

Our attempt to establish performance indicators for collaborative business ecosystems considers input knowledge from a number of research areas such as collaborative networks, business ecosystems, enterprise performance indicators, social networks analysis, and supply chain. An overview of these areas is presented below, briefly characterizing them and highlighting important aspects for the proposed work:

Collaborative Networks (CNs), one of the main contributing scientific disciplines on which this research work is based. A CN is defined as “*a network consisting of a variety of entities (e. g. organizations and people) that are largely autonomous, geographically distributed, and heterogeneous in terms of their operating environment, culture, social capital and goals, but that collaborate to better achieve common or compatible goals, and whose interactions are supported by computer networks*” [5], [6]. Important foundations for this area were earlier established by projects such as THINKcreative, Vomap, VOSTER, ECOLEAD, and many others. A large diversity of collaborative networks can nowadays be identified on a variety of sectors in industry and services. In order to better understand this diversity, some efforts focused on the establishment of reference models, such as ARCON [6]. According to ARCON, collaborative networks are divided into two main groups, the organized collaboration and the ad-hoc collaboration. The organized collaborative networks are in turn divided into long-term strategic networks and goal-oriented networks, where participants are linked together to drive a continuous specific activity, or to grab a business opportunity. Under this classification, a Business Ecosystem is seen as a subclass of long-term strategic networks. Supply chains are considered as a particular case of goal-oriented networks. In fact, traditional supply chains tend to evolve to more collaborative structures, leading to the concept of Supply Chain Collaboration (SCC). A SCC can be defined “*as a long-term partnership process where supply*

chain partners with common goals work closely together to achieve mutual advantages that are greater than the firms would achieve individually” [10].

While most works on collaborative networks have mainly addressed issues of collaboration support infrastructures and tools, organizational and governance models, very few references can be found on performance measurement in enterprise networks. The exception is perhaps the case of supply chains for which some works can be found. For instance, [11] identifies different levels or intensity in the collaboration, which are categorized into two types of collaborative practices. The first one considers the exchange of information as the most basic form of collaboration, distinguishing two broad groups depending on the closeness, information exchange or process integration, also called structural collaboration [12]. The second one considers three gradual organizational and decision-making levels (operational, tactical and strategic), i.e. the higher the degree of partners' relationships towards process integration, the stronger the interaction, sophisticated information technology, and organizational commitment among them.

Business Ecosystems. Since the introduction of the Business Ecosystem concept by Moore [1], [2], several other researchers have focused on the ICT support to this organizational structure, as illustrated by the notion of Digital Business Ecosystem [3][4]. Various authors have explored analogies between natural ecosystems and mechanisms provided by computational models such as service-orientation, multi-agent systems, and swarm intelligence. Two examples can be found in [13], [14]. These authors worked towards the establishment of the basis of a digital ecosystem, considering it as a collaborative environment, where the key elements are the “species” and the environment comprising support technologies and services. The species are “*biological - humans*”, “*economic – organizations*”, and “*digital - computers, software, applications,...*” linked by networks and interacting with each other to achieve benefits and objectives. Another example is given by the work of Briscoe [15], [16], which uses modeling techniques from complex adaptive systems and multi-agent systems to create a generic definition inspired by biological ecosystems, which abstractly defines the key properties, behavior, and structure of an ecosystem. The emphasis in this line of research has been, so far, more oriented to the structure, organization, behavior, and technological support of the ecosystem. Therefore, and to the best of our knowledge, the aspects of performance of such systems remain an open issue.

Performance Indicators (PI) are financial and non-financial metrics used to quantify objectives and reflect strategic performance of an organization. This kind of metrics has been largely developed for individual enterprises management but not so much to assess collaborative strategy and benefits. Nevertheless, some research lines have generated a number of elements that can be taken as a basis for the development of performance indicators tailored to collaborative networks. One of these lines has pursued the identification and characterization of collaboration benefits and value systems. Another relevant line is the social networks analysis, which has established several metrics related to graph structures. In summary:

Collaboration Benefits. A number of works have tried to model (business) benefits resulting from collaboration. One example is an estimation model for business benefits in horizontal collaborative networks for product development [17], which considers four phases: 1) Estimation of the opportunities that should be generated by the network; 2) Construction of the product realization graph giving a weight to each opportunity, 3) Identification of the best consortium to develop the product, and 4) Summation of the earnings. Another work [18] suggests a set of collaboration benefits through the identification of cooperation variables and respective target goals. In this work it is argued that the perception of collaboration benefits are related to the two strategic goals perspectives - performance increase and survival capacity. Our research question is somehow in line with this perception. Although these early works have contributed to a better understanding of collaboration benefits, the proposed indicators have not been specifically tailored to collaborative business ecosystems. Furthermore, validation of these indicators in terms of their contribution to promote collaboration sustainability and resilience has not been extensively done yet.

Value Systems. Progress has been made in terms of conceptualization of value systems for collaborative networks, namely through combining views coming from the social sciences and the economy. One example is a conceptual model for value systems for collaborative networks [19], based on the identification of objects that can be evaluated, and the elements that represent the mechanisms of evaluation. More recent developments of this work [20] suggest methods to assess the alignment of value systems of different members of a network. The proposed system remains, however, quite limited when it comes to the evaluation mechanisms. Another proposal for a conceptual model, formalizes a value system for a VBE [21], and a corresponding performance measurement system. This system intends to evaluate the value co-creation process through a set of indicators that quantify the VBE results, making easier to monitor its progress. The authors also propose the balanced scorecards (BSC) to monitor the performance measurement. A BSC is a classical method [7] composed of a set of performance indicators strongly aligned with the vision and strategy of the enterprise, and which represents an innovation compared to other types of metrics existing at the time focused only on financial indicators, by the combination of lagging and leading indicators, resulting not only in historical indicators, but also in predictable results. These proposals, e.g. [21], remain, however, at a general conceptual level, without providing concrete indicators.

Social Network Analysis. The large adherence of people to social networks has motivated a substantial amount of research, often under the umbrella of Social Network Analysis (SNA). A number of research works have also attempted to borrow methods and indicators from SNA to apply in collaborative networks. But there are also a number of arguments pointing to the limitations of SNA when adopted for the analysis of business networks, namely: i) the empirical link between organizational-level structure and firm-level performance is not adequately demonstrated; ii) links in a social network allow a structural analysis, such as degrees of separation between nodes, “betweenness”, “closeness”, among others, but do not address economic or social value creation; iii) all links in a social network are of the same nature and only

one link is represented between actors, not allowing, for instance, to distinguish social or economic exchanges; and iv) to analyze and interpret the network patterns requires high level of expertise. An attempt to overcome these limitations is the work of Allee [22], which introduces the concept of Value Network Analysis (VNA). A VNA is defined as “any purposeful group of people or organizations creating social and economic good through complex dynamic exchanges of tangible and intangible value” [22]. According to the author, a value network is a “human-centric, role-based, network view of any business activity”. A set of metrics for managing collaborative work have been proposed in this context, representing a promising direction.

4 Research Approach

The analysis of the literature, as briefly shown above, shows that an adequate approach to measure and manage performance in collaborative business ecosystems is not available yet. However, several partial and, to some extent, complementary contributions can be found in a number of research fields. Bringing together all these contributions, can provide a promising direction towards identifying suitable performance indicators that not only help in performance measurement, but also contribute to the promotion of collaboration sustainability and resilience. As a result, our research approach is driven by 3 main pillars as illustrated in Fig. 1: (1) An organizational and collaborative framework, to provide an understanding of the structure, organization and behavioral aspects of the collaborative business ecosystem; (2) Performance indicators and mechanisms, to allow quantitative assessment of performance and potential benefits for the ecosystem members and the ecosystem as a whole; (3) A set of enablers, mainly provided by ICT infrastructures and new computational models that inspire and support various alternatives of organizational structures and simulation models.

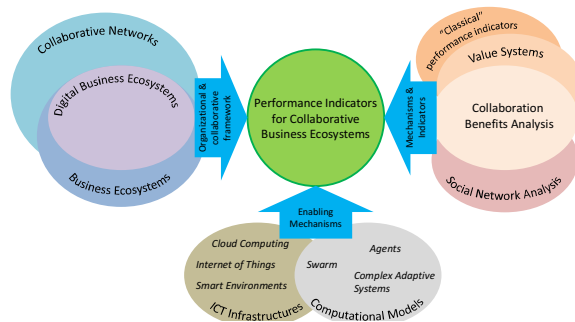


Fig. 1. Research strategy

The initial phase of the work allowed identifying the potential contributions from each of the mentioned areas and putting them into a context. One difficulty with establishing performance indicators is that their actual value depends, to a large extent, on their acceptance by the involved community. Therefore, it is not strictly and issue

of “proving” their validity in classical research terms. If a set of indicators are reasonably coherent, and based on a logical foundation, their value depends on their acceptance. As such, our approach tries to (1) guarantee the first requirements, and (2) create conditions for their acceptance.

Regarding the first aspect, at the current stage, a consolidation and formalization of concepts is being developed, together with the design of measurement mechanisms. In addition to inputs from the contributing areas mentioned above, grounded theory methods are also considered as they are likely to facilitate the capture of knowledge about the reality, behavior and interactions of the participants in a shared social context, the business ecosystem. All collected data from different formal and informal sources, allow an identification of key concepts and its categorization, leading to the establishment of collaborative performance indicators. Grounded theory emerged from the discipline of sociology, focused on society and the individual. However it has been broadening to incorporate issues with significant behavioral implications, such as ethical marketing, social marketing, green issues and experiential consumption [23], thus appearing to be also suitable for business ecosystems. A business ecosystem can be characterized by a set of key properties taken from a generic ecosystem inspired by biological ecosystems, combining attributes of digital, business, and social ecosystems: i) the environment is the economy of society, where agents are the businesses which influence and are influenced by the environment; ii) the population and evolution match the business domain, in which the evolutionary theory of capabilities and behavior of business firms is applicable; iii) the community matches the social domain, referring to a social unit that shares common values regardless of physical location, since, instead of being located in the same geographical region, participants are connected by a digital common infrastructure supported by ICT technologies [16].

Regarding the second aspect, we pursue the second research sub-question related to the use of the performance indicators to promote collaboration resilience and sustainability. The vision is that achieving resilience and sustainability will give a strong argument to promote wide acceptance of the proposed indicators.

At the same time, suitable validation scenarios are being analyzed. The main obstacle to the implementation of this approach is the lack of historic data or benchmarks to support effective validation. Furthermore, the main goals of using such performance indicators to promote collaboration sustainability and resilience can only be verified in the long term, a typical difficulty in most research on Collaborative Networks. Therefore, the designed validation strategy combines a mix of methods including: (partial) case studies, simulation, ethnographic methods (mainly involving business ecosystem managers), and grounded theory. Furthermore, the simulation seems to be a promising strategy, because existing specific models consistent with evolutionary theory, can be applied to business ecosystems.

5 Conclusions and Further Work

The analysis of the state of the art in relevant areas shows that although various relevant contributions can be found, there is still an important gap: the inexistence of adequate and effective methods for evaluation of collaboration benefits in business

ecosystems. This gap points to the need of identifying suitable performance indicators and associated measurement mechanisms that can promote collaboration and cohesion of the ecosystem's members. Thus, a research strategy was designed towards developing a contribution to the survival of organizations in an aggressive and turbulent market environment. After the first stage of our work, the research framework and a preliminary solution design are achieved. The development and validation steps correspond to ongoing work.

References

1. Moore, J.F.: Predators and prey: a new ecology of competition. *Harvard Business Review* **71**(3), 75–86 (1993)
2. Moore, J.F.: *The death of competition: leadership and strategy in the age of business ecosystems*. Harper Business, New York (1996)
3. Nachira, F.: *Towards a network of digital business ecosystems fostering the local development*. Technical report, DG Information Society and Media, EC (2002)
4. Nachira, F., Dini, P., Nicolai, A.: *A network of digital business ecosystems for Europe: roots, processes and perspectives*. European Commission, Introductory Paper (2007)
5. Camarinha-Matos, L.M., Afsarmanesh, H.: Collaborative networks: A new scientific discipline. *J. Intelligent Manufacturing* **16**(4–5), 439–452 (2005)
6. Camarinha-Matos, L. M., Afsarmanesh, H.: *Collaborative Networks: Reference Modeling: Reference Modeling*. Springer (2008)
7. Kaplan, R. S., Norton, D. P.: *The balanced scorecard: translating strategy into action*. Harvard Business Press (1996)
8. Osório, A., Camarinha-Matos, L.M., Afsarmanesh, H.: Cooperation enabled systems for collaborative networks. In: Camarinha-Matos, L.M., Pereira-Klen, A., Afsarmanesh, H. (eds.) *PRO-VE 2011. IFIP AICT*, vol. 362, pp. 400–409. Springer, Heidelberg (2011)
9. Osório, A., Camarinha-Matos, L.M., Afsarmanesh, H.: Enterprise collaboration network for transport and logistics services. In: Camarinha-Matos, L.M., Scherer, R.J. (eds.) *PRO-VE 2013. IFIP AICT*, vol. 408, pp. 267–278. Springer, Heidelberg (2013)
10. Cao, M., Vonderembse, M.A., Zhang, Q., Ragu-Nathan, T.S.: Supply chain collaboration: conceptualisation and instrument development. *International Journal of Production Research* **48**(22), 6613–6635 (2010)
11. Botta-Genoulaz, V., Campagne, J.-P., Llerena, D., Pellegrin, C. (eds.): *Supply Chain Performance: Collaboration, Alignment, and Coordination*. John Wiley & Sons (2013)
12. Vereecke, A., Muyllé, S.: Performance improvement through supply chain collaboration in Europe. *IJ Operations & Production Manag.* **26**(11), 1176–1198 (2006)
13. Chang, E., West, M.: Digital Ecosystems A Next Generation of the Collaborative Environment. In: *iiWAS*, pp. 3–24 (2006)
14. Boley, H., Chang, E.: Digital Ecosystems: Principles and Semantics. In: *Inaugural IEEE-IIES Digital EcoSystems and Technologies Conference, DEST 2007*, pp. 398–403 (2007)
15. Briscoe, G.: Digital ecosystems. arXiv preprint arXiv:0909.3423 (2009)
16. Briscoe, G.: Complex adaptive digital ecosystems. In: *Proceedings of the Int. Conference on Management of Emergent Digital EcoSystems*, pp. 39–46. ACM (2010)
17. Piot, G., Pouly, M., Cheikhrouhou, N., Glardon, R.: An estimation model for business benefits in horizontal collaborative networks. In: *Establishing the Foundation of Collaborative Networks*, pp. 345–352. Springer, US (2007)

18. Abreu, A., Camarinha-Matos, L. M.: A benefit analysis model for collaborative networks. In: Collaborative networks: Reference modeling, pp. 253–276. Springer (2008)
19. Camarinha-Matos, L.M., Macedo, P.: A conceptual model of value systems in collaborative networks. *Journal of Intelligent Manufacturing* **21**(3), 287–299 (2010)
20. Macedo, P., Camarinha-Matos, L.M.: A Qualitative Approach to Assess the Alignment of Value Systems in Collaborative Enterprises Networks. *Journal Computers & Industrial Engineering* **64**, 412–424 (2013)
21. Romero, D., Galeano, N., Molina, A.: A conceptual model for virtual breeding environments value systems. In: Establishing the foundation of collaborative networks, pp. 43–52. Springer (2007)
22. Allee, V.: Value Networks and the true nature of collaboration. Digital edition edn. ValueNet Works and Verna Allee Associates (2011)
23. Goulding, C.: Grounded theory, ethnography and phenomenology: A comparative analysis of three qualitative strategies for marketing research. *European Journal of Marketing* **39**(3/4), 294–308 (2005)

Negotiation Environment and Protocols for Collaborative Service Design

Ana Inês Oliveira^{1,2(✉)} and Luis M. Camarinha-Matos^{1,2}

¹CTS, Uninova, 2829-516 Caparica, Portugal

²Faculdade de Ciências e Tecnologia, Universidade Nova de Lisboa, Campus da Caparica,
Quinta da Torre, 2829-516 Monte Caparica, Portugal
{aio, cam}@uninova.pt

Abstract. During the last decade, in manufacturing and service industries, collaboration among small and medium enterprises (SMEs) has focused on competencies and resources sharing as an approach to both create new competitive environments, as well as to achieve agility to rapidly respond to new market demands. Also, with the increasing level of customization of products and services required by customers, the notion of co-creation of products and business services leads to an increase of collaboration with customers and local suppliers. In this context, this paper presents an approach based on a negotiation support environment that structures the design of new business services under a collaborative perspective. The adopted protocol to facilitate interaction among the multi-users in the negotiation dialog is described.

Keywords: Collaborative networks · Negotiation support environment · Business services · Co-design · Co-creation · Negotiation protocol

1 Introduction

Due to market unpredictability and new requirements, companies and organizations need to adapt themselves to maintain competitiveness. One option is to move from the “traditional enterprise” concept to a new business paradigm where enterprises can strategically access to each other’s markets by joining competences and sharing skills and costs, resulting in a new collaboration structure of enterprises. The collaborative network concept is increasingly adopted to support organizations and companies in this change of paradigm, as it can provide agility and survival mechanisms that facilitate companies to survive to market turbulences [1]. Nevertheless, there are some obstacles, for example: how to find or choose the right partners; lack of common or standard formats for basic profile of organizations; how to define and reach agreements for roles and responsibilities of each partner and of course how to predict associated collaboration risks.

Another important aspect that requires attention is the increasing demand from customers for highly customized products. Therefore, one tendency for manufacturers is to associate business services to the products they offer [1]. From a collaborative perspective, these services are designed and created by multiple stakeholders to meet

the individual customer's needs and/or requirements. This also brings the need to follow some service design methodology, which typically is a non-structured approach. In this context, the European research project GloNet was carried out with the aim to design, develop and deploy an environment to facilitate networks of SMEs to collaborate and achieve highly customized service-enhanced products [2]. The interaction with the customer and local suppliers is fundamental and leads to the notion of co-creation of products and business services. For the formation of such networks, one important requirement is the existence of an established negotiation process to improve the generation of agreements that facilitate collaboration and lead to the governing rules and principles of the consortium during its operation phase [3].

Considering this background context [4] that supports and fosters the creation of dynamic virtual organizations (VOs), the research question addressed by this work is:

How can an electronic negotiation support environment increase the agility in the process of successfully creating dynamic virtual organizations?

An important motivation for this work is that by contextualizing the design of a new business service in a collaborative environment, it can also use the same negotiation support environment mechanisms to reach agreements, as the ones that are used for the VO creation process [5, 6, 7].

2 Relationship to Cloud-Based Solutions

Cloud computing provides its users with different levels of solutions in the form of services: infrastructure, platform, and software as a service. Depending on the user requirements, it provides services based on a distributed and parallel processing, improving reliability, storage capacity, and service efficiency [8] when compared to traditional solutions. In the existing market volatility, it is crucial for companies to guarantee that their applications and services are always accessible. So, through a cloud-based solution companies can, in principle, reduce their costs [8, 9], as they don't have to keep complex private infrastructures.

While in the manufacturing and services industry the trend is to move towards a global networked economy, cloud-based solutions potentiate collaboration platforms to support the establishment and operation of the involved enterprise networks [10]. Considering the co-design of new business services where different and diverse stakeholders intervene in the process to achieve new business services design, the cloud-based solutions appear with relevance once they can facilitate the development of new collaborative processes [10]. This work is developed in such context and builds on top of a cloud-based collaboration platform [11].

3 Context and Related Areas

To contextualize the negotiation support for service co-design and related negotiation protocol, this section gives a brief overview of the literature.

Business Services and Composite Business Services. A business service refers to an organized set of added value activities from a business perspective [12], considering issues such as the delivery conditions, service level agreements, period, availability, etc. [1]. It corresponds to the service provided to the customer, and can be implemented by manual services and/or software services whose flow can be modeled through business processes. Also, business services provided to the customer can be composed of several atomic business services [10]. In such situation, service providers of each business services can together form a virtual organization to deliver the composite business through a new entity that is the service integrator (that acts as the service provider of the composite business service) [13].

GloNet co-Creation Network. One of the GloNet project assumptions is that if networks of SMEs are supported by an environment that facilitate collaboration, then they can achieve highly customized service-enhanced products [2]. Here the notion of co-creation networks appears as a concept that is based on collaboration between manufacturers, customers, and members of customers' community [1]. These networks aim to co-design and co-innovate value-added services for products when new promising business ideas emerge [14]. Also, an analysis of the IT implementation requirements of those business applications can be performed [15].

Service Design. This is an interdisciplinary area that emerged as a contribution to a changing context from the growing economy of the services sector and the traditional culture of design [16]. Service design integrates relevant stakeholders in the design of services through some methodological approach [17]. Service design aims at designing user-oriented services making them useful, effective and different from existing ones. It potentiates co-creation between the different users of a service, and the providers [18]. In the different service design activities, especially in co-creation, not all stakeholders need to be involved at the same time; they can be involved just in the specific moments or situation in which they take part [19], which applies to the co-creation and co-design case of GloNet. There are a number of methods and tools for service design that have been emerging [20], some of which can be found in <http://www.servicedesigntools.org/>.

Negotiation Protocols. In negotiation processes it is fundamental that a protocol is defined so that an agreement can be achieved. The negotiation process includes several interactions that are based on the exchanging of some arguments and opinions on the form of dialogues [21]. The dialogues that take place can include some form of argumentation in favor or against certain statements [22]. Depending on the context, the arguments used can be constructed from a knowledge base in an argumentative system [23], or from a rule-based system [22]. Typically protocols for negotiation based on argumentation can be found in agent systems where agents have a certain level of intelligence and at some point have to make their options and create some arguments [24,25]. In these cases, although there are already some agent communication languages such as ACL, KQML, etc., that try to cope with some of the requirements for negotiation [26], there are still open issues, namely the existence of some limitations in multilateral negotiation when compared to one-to-one bilateral negotiations [25].

4 Research Contribution and Innovation

According to the different natures of collaborative networks, namely virtual organizations (VOs), the formation process of new VOs for collaboration can be diverse. Nevertheless, as illustrated in Fig. 1, typically, involved processes include some common steps, that go from the new business or collaboration opportunity (BO/CO) discovery, to the formation of the new consortium to rapidly respond to it [5]. Although the selection of the adequate partners to form the consortium is of extreme relevance, the consensus that is reached among them is of no less importance once it can serve as the basis for the operating principles of the VO. Therefore, if the process of reaching and negotiating agreements among participants can be supported by an ICT environment, then the entire process of VO formation and negotiation can become smoother [5,6,7]. When designing a new business service (BS), a team of interested stakeholders already exist (acting like a VO) with the aim of reaching agreements on the design requirements of the new BS.

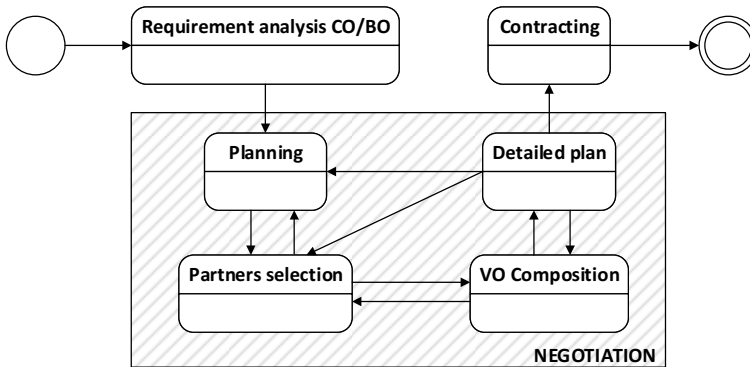


Fig. 1. VO formation process

In line with the previous assumptions and with the research question mentioned in section 1, the hypothesis that supports the current research work is:

The process of creating dynamic virtual organizations can become more agile if an appropriate electronic negotiation wizard environment is established with the necessary soft modeling characteristics to structure and conduct the entire negotiation process, making it traceable, reducing the collaboration risks, and managing the participants' expectations. Moreover, the negotiation environment should be customizable according to different collaboration levels, either in terms of commitment or in terms of duration.

Therefore, a negotiation support environment is also expected to facilitate and boost the participation in business service design allowing its participants to collaborate in a co-creation environment, reducing the potential collaboration risks, and supporting different levels of collaboration. Given so, the main mechanisms for the negotiation support environment are, on one hand, to support negotiation for the classical VO formation that includes: negotiation towards the selected partners; negotiation details with partners; and negotiation with the customer; and on the other hand, to support negotiation in co-design and co-innovation.

Service Design Methodology. To design new business services, a service design methodology has been adopted [7]. This methodology identifies and defines the needed services and their interactions with the customer, and their nature. The methodology is summarized in Table 1.

Table 1. Service Design Methodology in co-creation teams

<i>Service Design steps</i>	<i>Description</i>
Identify needed service	Brainstorming exercise involving an analysis of the needs and characteristics of the customer.
Design touchpoints diagram	To identify user interaction points with the service.
Design blueprint diagram	To describe the nature and the characteristics of the service interaction to verify, implement and maintain it. It includes: temporal order, timings, and line of visibility (denoting what the customer sees and <i>back-office</i>).
Storyboard / storytelling	Representation of use cases, through a series of drawings or textual description put together in a narrative sequence, which illustrates a sequence of events such as a customer journey.
Service prototyping	Involving the selection, assembly and integration of the various service components (atomic services).

For the current research work, the aim is to use this service design methodology and adapt it to a philosophy of co-design where new business services can be designed in a collaborative environment involving multiple stakeholders and the customer.

Although a number of methods and tools are available for some aspects of services design [20], most of them are based on simple manual methods. Therefore the proposed environment supports the collaborative process of the different stakeholders in some steps of the adopted methodology.

Service Co-design Negotiation Support System. Being the service co-design negotiation support system (CoDeN), intended to provide a collaborative environment for the design of new business services where the various involved participants can reach agreements on what needs to be decided, for the developed system it is assumed that the needed service is already identified and the relevant stakeholders (participants in the negotiation process) are previously defined. The negotiation process is guided by defined templates that follow the described service design methodology for the design of touchpoints and blueprint diagram, also addressing the identification of the business service related stakeholders mapping.

Besides the important roles of customer and involved participants (co-creation team), also, to conduct the entire negotiation process, the role of co-creation team mediator is introduced (acting like the classical VO Planner). Therefore, to properly model the core processes involved in co-design, the main actors with the correspondent roles are identified in Table 2 and the correspondent dependencies between them are illustrated in Fig. 2 using the *i** modelling framework.

Table 2. Actors and roles in co-creation teams

<i>Actor</i>	<i>Role</i>
Co-creation Team	The Co-creation Team represents all the involved actors within the collaborative space aimed for co-design of services. These actors are essentially the VO Partners and the Customer.
Co-creation team mediator	The Co-creation team mediator is the VO partner responsible to conduct the entire co-design process. He acts similarly to the VO Planner in generic VOs.
VO Partners	The VO Partner is part of the co-creation team, and, gives support for the service co-design and co-innovation according to its knowledge and skills.
Customer	The Customer is also part of the co-creation team, and together with the VO Partners plays an important role in the service co-design once his satisfaction must be attained. He maybe also responsible for providing the services requirements and for giving feedback during the collaboration processes.

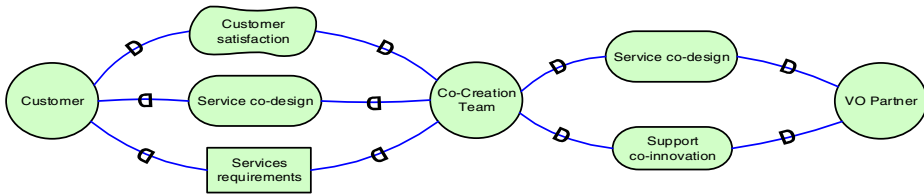


Fig. 2. Strategic dependency model for co-design

Negotiation Protocol. The process of reaching consensus among the various participants, besides being guided through the negotiation environment, has to follow a determined protocol in order to be effective. In this specific case, a logical language was followed [22] to define the negotiation protocol that is used to specify when a determined decision can be made by an intervention of the process. Therefore, the negotiation protocol is used to specify when a particular *move* can be made in the course of the negotiation dialogue [21], being *move* here understood as the statement and/or decision that a participant can make.

Although there are different protocols for negotiation, and different defined *moves* for different scenarios [25], the benefit from the used protocol is that it is generic and can be used when addressing different negotiation contexts. Therefore, the adopted protocol relies of the following *moves*:

$$M_{(N)} = \{request(N), refuse(N), accept(N), withdraw(N)\}$$

and

$$M_{(NT, K_{NT})} = \{propose(NT, K_{NT}), refuse(NT), accept(NT), counterpropose(NT, K_{NT}), withdraw(NT)\}$$

being:

- $M_{(N)}$ the set of moves allowed to participate in the negotiation of a new business service design (where N stands for the specific negotiation); and
- $M_{(NT,K_{NT})}$ the set of moves allowed to participate in the negotiation of a specific topic/template (where NT represents the negotiation topic, and K_{NT} represents the content of NT).

The defined moves consider that, in some occasions in VO formation negotiations, for each negotiation topic only a subset of participants are involved and can even be replaced by others [6, 7]. That is why the moves $refuse(NT)$, $accept(NT)$ are considered. In the co-creation case (in the main focus of this paper), all participants are requested to participate in the design of all templates (diagrams). So the participants' interaction with the system reduces the $M_{(NT,K_{NT})}$ to the following:

$$M_{(NT,K_{NT})} = \{propose(NT, K_{NT}), counterpropose(NT, K_{NT}), withdraw(NT)\}$$

being all other moves made internally by the system.

While participants can make several of the mentioned moves in the course of a negotiation dialogue, they have to do it in a pre-determined way. They may even have to wait for the other participants' moves so that actions can be made accordingly. For example, an evident restriction is that a participant cannot accept to participate on a negotiation process without the Team Mediator requesting his participation in advance. Table 3 summarizes some of the pre- and post-conditions to some moves.

Table 3. Pre- and post- conditions for the negotiation protocol

m1: $request(N)$	pre: no condition post: $accept(N)$, $refuse(N)$
m2: $accept(N)$	pre: $request(N)$ post: other moves are consequence of certain triggers
m3: $refuse(N)$	pre: $request(N)$ post: no moves may occur from the participant that $refuse(N)$
m4: $withdraw(N)$	pre: $request(N)$ followed by $refuse(N)$; or $refuse(NT)$ on the negotiation of a specific topic post: no further move
m5: $propose(NT)$	pre: $accept(N)$ post: $accept(NT)$, $refuse(NT)$, $counterpropose(NT, K_{NT})$
m6: $accept(NT)$	pre: $propose(NT)$ post: other moves are consequence of certain triggers
m7: $refuse(NT)$	pre: $propose(NT)$ post: no moves may occur from the participant that $refuse(NT)$
m8: $counterpropose(NT, K_{NT})$	pre: $propose(NT)$ post: maybe followed by $propose(NT)$
m9: $withdraw(NT)$	pre: $propose(NT)$ post: maybe followed by a $withdraw(N)$

Fig. 3 illustrates the relation of the described moves in reference to the Team Mediator's possible states.

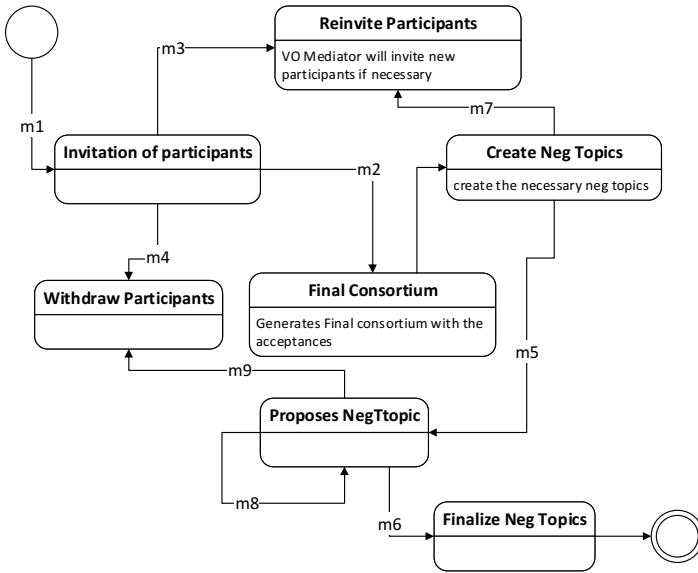


Fig. 3. Team Mediator states and related negotiation moves

Implementation and Validation. For the described work, a software prototype has been developed in order to check the feasibility of the proposed concepts. The prototype system was implemented in JAVA, with the VAADIN framework, and allows the generation of general information on the co-creation consortium, as well as to upload supporting documentation. For the negotiation of the templates of diagrams to guide the new service design, functionalities are also available and cope with the described negotiation protocol. The main output is a generated .pdf document that includes a summary of all the information that is generated in the course of negotiation. Fig. 4 illustrates the involved concepts and prototype usability for a general scenario.

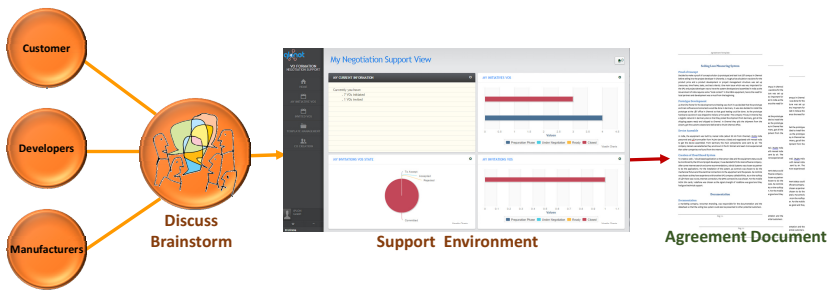


Fig. 4. CoDeN usability

Being the present work part of a PhD work, the validation process is mainly through peer validation but also through the participation on the mentioned European research project GloNet. Also, close interaction with end-users in the solar energy domain is being done to perform a more accurate analysis of the achieved results. Through these means, some of the concepts and preliminary results have already been positively validated.

5 Conclusions and Further Work

In the work presented in this paper, the aim is to have a negotiation environment to support networks of SMEs in the form of co-creation teams to achieve agreements on the design of new business services. For this purpose, a negotiation support environment has been developed and briefly summarized, highlighting the main requirements and approach. Also, the adopted negotiation protocol to specify the adequate rules was also detailed. In this case, what is intended is not to have an artificial agent system acting on behalf of organizations, but to have the human actors interacting with the system and following the adopted protocol. Therefore, one of the challenges in the definition of the protocol is to ensure that it can easily be followed and accepted by all involved stakeholders.

Acknowledgments. This work has been supported by the *Collaborative Networks and Distributed Industrial Systems* Research Group of Uninova and partly by the GloNet project (FP7 programme) funded by the European Commission.

References

1. Camarinha-Matos, L.M., Macedo, P., Ferrada, F., Oliveira, A.I.: Collaborative business scenarios in a service-enhanced products ecosystem. In: Camarinha-Matos, L.M., Xu, L., Afsarmanesh, H. (eds.) *Collaborative Networks in the Internet of Services*. IFIP AICT, vol. 380, pp. 13–25. Springer, Heidelberg (2012)
2. Camarinha-Matos, L.M., Afsarmanesh, H., Koelmel, B.: Collaborative networks in support of service-enhanced products. In: Camarinha-Matos, L.M., Pereira-Klen, A., Afsarmanesh, H. (eds.) *PRO-VE 2011*. IFIP AICT, vol. 362, pp. 95–104. Springer, Heidelberg (2011)
3. Rabelo, R.J., Costa, S.N., Romero, D.: A governance reference model for virtual enterprises. In: Camarinha-Matos, L.M., Afsarmanesh, H. (eds.) *Collaborative Systems for Smart Networked Environments*. IFIP AICT, vol. 434, pp. 60–70. Springer, Heidelberg (2014)
4. Di Maio, P. Ure, J.: An open conceptual framework for operationalising collective awareness and social sensing. In: *Proceedings of the 3rd International Conference on Web Intelligence, Mining and Semantics*. ACM (2013)
5. Oliveira, A.I., Camarinha-Matos, L.M., Pouly, M.: Agreement negotiation support in virtual organisation creation—an illustrative case. *Production Planning & Control* **21**(2), 160–180 (2010)

6. Oliveira, A.I., Camarinha-Matos, L.M.: Electronic Negotiation Support Environment in Collaborative Networks. In: Camarinha-Matos, L.M., Shahamatnia, E., Nunes, G. (eds.) DoCEIS 2012. IFIP AICT, vol. 372, pp. 21–32. Springer, Heidelberg (2012)
7. Oliveira, A.I., Camarinha-Matos, L.M.: Negotiation support for co-design of business services. In: Camarinha-Matos, L.M., Afsarmanesh, H. (eds.) Collaborative Systems for Smart Networked Environments. IFIP AICT, vol. 434, pp. 98–106. Springer, Heidelberg (2014)
8. Ma, N., Yuan, M., Cao, G.: Integration of digital campus resources based on cloud computing. In: Proceedings of the 2012 International Conference on Cybernetics and Informatics, pp. 1957–1963. Springer, New York (2014)
9. Ostermann, S., Iosup, A., Yigitbasi, N., Prodan, R., Fahringer, T., Epema, D.: A performance analysis of EC2 cloud computing services for scientific computing. In: Avresky, D.R., Diaz, M., Bode, A., Ciciani, B., Dekel, E. (eds.) CloudComp 2009. LNICST, vol. 34, pp. 115–131. Springer, Heidelberg (2010)
10. Camarinha-Matos, L.M., Afsarmanesh, H., Oliveira, A.I., Ferrada, F.: Cloud-Based collaborative business services provision. In: Hammoudi, S., Cordeiro, J., Maciaszek, L.A., Filipe, J. (eds.) ICEIS 2013. LNBIP, vol. 190, pp. 366–384. Springer, Heidelberg (2014)
11. Surajbali, B., Bauer, M., Bär, H., Alexakis, S.: A cloud-based approach for collaborative networks supporting serviced-enhanced products. In: Camarinha-Matos, L.M., Scherer, R.J. (eds.) PRO-VE 2013. IFIP AICT, vol. 408, pp. 61–70. Springer, Heidelberg (2013)
12. Brentani, U.: Innovative versus incremental new business services: different keys for achieving success. *Journal of Product Innovation Management* **18**(3), 169–187 (2001)
13. Camarinha-Matos, L. M., Afsarmanesh, H., Oliveira, A. I., Ferrada, F.: Collaborative Business Services Provision. In: ICEIS, vol. 2, pp. 380–390 (2013)
14. Camarinha-Matos, L. M., Ferrada, F., Oliveira, A. I., Afsarmanesh, H.: Supporting product-servicing networks. In: Proceedings of 2013 International Conference on Industrial Engineering and Systems Management (IESM), pp. 1–7. IEEE (2013)
15. Yang, S., Zhang, S., Kong, L.: Research on the cooperative decision of business application needs in IT governance. In: 2012 IEEE 16th International Conference on 2012 Computer Supported Cooperative Work in Design (CSCWD). IEEE (2012)
16. Sangiorgi, D.: Building up a framework for service design research. In: 8th European Academy of Design conference , pp. 415–420 (April 2009)
17. Mager, B., Sung, T.: Special issue editorial: Designing for services. *International Journal of Design* **5**(2), 1–3 (2011)
18. Sandberg, F.: Co-creating collaborative food service opportunities through work context maps. In: Proceedings of 3rd Service Design and Service Innovation Conference, ServDes. 2012: Linköping Electronic Conference Proceedings, vol. 67. Linköping University Electronic Press, Sweden (2012)
19. Sanders, E.B.-N., Stappers, P.J.: Co-creation and the new landscapes of design. *Co-design* **4**(1), 5–18 (2008)
20. Wild, P.J.: Review of Service Design Methods. In: IPAS project deliverable I15.6. University of Cambridge, Cambridge (2009)
21. Moschoyiannis, S., Krause, P., Bryant, D., McBurney, P.: Verifiable protocol design for agent argumentation dialogues. In: 3rd IEEE International Conference on Digital Ecosystems and Technologies, DEST 2009, pp. 630–635. IEEE (June 2009)
22. Caminada, M., Amgoud, L.: On the evaluation of argumentation formalisms. *Artificial Intelligence* **171**(5), 286–310 (2007)

23. Prakken, H.: An abstract framework for argumentation with structured arguments. *Argument and Computation* **1**(2), 93–124 (2010)
24. Aknine, S., Pinson, S., Shakun, M.F.: An extended multi-agent negotiation protocol. *Autonomous Agents and Multi-Agent Systems* **8**(1), 5–45 (2004)
25. Wang, G., Wong, T.N., Wang, X.: A hybrid multi-agent negotiation protocol supporting agent mobility in virtual enterprises. *Information Sciences* **282**, 1–14 (2014)
26. Beer, M., D’inverno, M., Luck, M., Jennings, N., Preist, C., Schroeder, M.: Negotiation in multi-agent systems. *The Knowledge Engineering Review* **14**(03), 285–289 (1999)

An Emotional Support System for Collaborative Networks

Filipa Ferrada¹(✉) and Luis M. Camarinha-Matos^{1,2}

¹ CTS, Uninova, Departamento de Engenharia Electrotécnica,
Faculdade de Ciências e Tecnologia, FCT, Universidade Nova de Lisboa,
2829-518 Caparica, Portugal
{faf, cam}@uninova.pt

² Departamento de Engenharia Electrotécnica,
Faculdade de Ciências e Tecnologia, FCT, Universidade Nova de Lisboa,
2829-518 Caparica, Portugal

Abstract. A particular challenge in the management of collaborative networks is the effective handling of the interactions among participants, especially in what concerns the management of “soft” issues that are not currently available in the execution processes of such networks. These issues can include inter- and intra-organizational abilities, problems in keeping team cohesion, leadership, among others. Moreover, one cannot forget that organizations are composed of people, and people have intrinsically associated emotions which are present in all interactions. In this sense, when not properly handled, some participant’s emotions might put in jeopardy the quality of the collaboration. On the other hand the collective emotional state of the collaborative network can also affect each participant’s emotions. As a contribution to keep the emotional equilibrium of the network, this paper presents the design of an emotional support system, including the identification and categorization of the most influencing positive and negative collective emotions and also the specification and prototyping of the sub-system services.

Keywords: Emotions · Collective emotions · Collaborative networks · Collaboration health

1 Introduction

Over the past decades there has been a great interest in the nature and role of emotions in community and work contexts, and a growing recognition of their centrality in facilitating or not connections between people [1]. In this line, the understanding of the role of emotions within networks of organizations is becoming a challenge due to its organizational, dynamic and “soft” nature. Furthermore, emotions might have a central role in the quality of communications and interaction among participants, in keeping network cohesion, in decision-making, in conflicts resolution, in leadership, among others. Having these considerations into account, it becomes interesting to

understand to what extent having an emotional equilibrium in the network contributes to the health of the collaboration.

In this context the main research question for this work is: *What could be a suitable set of models, methods and tools to promote emotional health in collaborative networks, namely allowing the diagnosis of the networks' emotional state and assisting in conflicts resolution?*

The development of effective supervision functionalities to monitor and manage the emotional climate/state – or the “collective virtual emotions” – of collaborative networks with the intention of maintaining the emotional equilibrium of the community, forecasting and attempting to *heal* potential conflicts among participants and external communities are important elements for the success of the network [2]. In fact, several studies reveal that emotions are very often the cause for misunderstandings and conflicts which, in some cases might lead to the failure of collaborative networks [3]. However, very little progress has been made in this direction. A particularly challenging issue is the acquisition, via non-intrusive methods, of multi-modal emotional input for achieving awareness of the participants' as well as the collective emotional state.

As a contribution to help keeping the emotional equilibrium of the network, this paper presents an emotional support system for collaborative networks developed on top of the GloNet platform. It includes the identification and categorization of the most influencing positive and negative collective emotions and also the specification and prototyping of the sub-system services. The remainder of this paper is organized as follows: Section 2 identifies the relationship of this work to cloud-based engineering systems; Section 3 gives a brief description of the related literature, namely in what concerns emotions in organizations and group-based emotions; Section 4 presents the emotions support system, its framework and prototype; and finally Section 5 concludes.

2 Benefits from Cloud-Based Engineering Systems

Several research projects and business initiatives show trend to develop collaboration platforms on the cloud. The consolidation of this approach is likely to facilitate an increase of collaboration among small and medium enterprises (SMEs) as, in this case, they do not need to acquire and maintain complex computational infrastructures. The work presented in this paper is developed in such context in the scope of the GloNet project: networks of SMEs involved in complex service-enhanced products [4] are supported by a cloud-based platform. This platform not only facilitates the collaboration processes among participants but also allows the emotional support system to more easily access the information that is needed to assess and manage the emotional equilibrium within the collaborative networks.

Besides the benefits of freeing enterprises from the burden of keeping their own infrastructures, the scalability property of cloud-computing allows for greater agility, which is quite relevant in our use case on supporting the full life cycle of solar plants. Each solar plant (a complex product) and the associated business services to be pro-

vided along its life cycle are highly customized (one of a kind) and might involve the need to store increasing amount of data. On the other hand, security concerns, namely in terms of access to data and even direct access to the physical plant, are vital here. The solutions offered by cloud providers are more reliable than what could be guaranteed by proprietary development of a network of heterogeneous SMEs. On the other hand, even within a network of collaborating partners there are several levels of access to information that need to be properly defined according to the role played by each participant. The GloNet platform provides the base mechanisms for specification of those access rights [5] and these need to be taken into account by the emotional support system in delivering different access to members and administrator.

3 Related Literature

3.1 Emotions in Organizations

Organizations have been studied by several scientific areas as rationally designed and operated structures. Nevertheless, issues like bringing fruitful collective action, quality of interaction and relations between parties and incentives to motivate organization's participants to follow common goals were, for a while, treated as irrelevant or insignificant. Aspects of group dynamics [6] and factors of sociality were often disregarded such as the impact of complex social processes on organization's participants. However, they surely contribute for the ability that an organization has to integrate, create and reconfigure internal and external resources according to the changing environment. These "additional factors", to a large extent, form the "social glue" that keeps together the participants of the collective action [7]. Emotions started to be recognized as an important element of cognitive processes [8], a necessary component of individual activity motivation and have high importance in interpersonal communications. In other words, the influence of emotional factors provides significant impact for positive organizational dynamics. On the other hand, emotional factors might as well input some negative impacts in an organization [9, 10]. Namely, they can disrupt normal procedural flows, break working relationships, and disrupt reasoned judgment and decision-making.

3.2 Collective and Group-Based Emotions

Emotional Contagion. Emotional contagion is "a process in which a person or group influences the emotions or behavior of another person or group through the conscious or unconscious induction of emotion states and behavioral attitudes" [11]. Emotions are "caught" by group members when they are exposed to the emotional expressions of other group members. Hatfield et al. [12] advanced that the degree to which emotional contagion occurs is mediated by attentional processes, with greater emotional contagion occurring when more attention is allocated. Zurcher [13] argues that displays of positive emotion in group situations constitute an essential ingredient necessary for the establishment of group cohesion. Furthermore, Lawler [14] claims that emotion is the essential social process in group formation and maintenance. This is

because positive emotions strengthen feelings of control. As such, positive emotion is a necessary precursor of group cohesiveness. In the context of organizational work groups, George [15] has also shown that positive affection is a key ingredient for group effectiveness and satisfaction. Barsade [16] found that positive emotional contagion amongst group members affects individual-level attitudes and group processes. Group members who experienced positive emotional contagion demonstrated improved cooperation, decreased conflict, and increased perceived task.

Collective Emotions. Collective emotions have been defined in a relatively general way as emotions that are shared by large numbers of individuals in a certain society [17], while group-based emotions are defined as emotions that are felt by individuals as a result of their membership in a certain group or society [18]. According to Bar-Tal [19], both concepts suggest that individuals may experience emotions, not necessarily in response to their personal life events, but also in reaction to collective or societal experiences in which only a part of the group members have taken part. But while the former concept suggests that group members may share the same emotions for a number of different reasons, the latter refers only to emotions that individuals experience as a result of identifying themselves with their fellow group members. A number of scholars have also pointed to the important behavioral implications of collective or group-based emotions when there are conflicts between groups and societies. Moreover, Bar-Tal [19] argues that the emotional element of context has great potential to influence emotional reactions and subsequent behavior. Furthermore, he proposed that, in contrast to individual emotions which are sometimes related to a dispositional system or physiological mechanism, collective or group-based emotions are solely formed as a consequence of experiences in a particular societal context. Society members experience collective emotions not only as a result of directly experiencing events that evoke particular emotion but also by identifications with the society as a collective.

Emotional Atmosphere, Emotional Culture and Emotional Climate. In the initial work of de Rivera [20], he suggested that it is important to differentiate emotional atmosphere from emotional culture and emotional climate: *emotional atmosphere* or *collective mood* refers to the collective behavior that a group or society may manifest when it is focused on a common event, rather than to the emotional relationships between members of the society. Such an atmosphere appears when those who identify with a group celebrate a collective success, lament a tragedy, or suffer a common threat. *Emotional culture* refers to the emotional relations that are socialized in a particular culture, while *emotional climate* is “an objective group phenomenon that can be palpably sensed - as when one enters a party or a city and feels an atmosphere of gaiety or depression, openness or fear”. This basically refers to the collective emotions experienced as a result of a society’s response to its sociopolitical conditions. Thus, in times of political repression, people are afraid of expressing their ideas in public; in times of ethnic tension, there is hate and/or fear toward other groups, and so on. De Rivera gives the example of Chile’s Pinochet regime that was under a climate of fear and now it has changed to a climate of hope. Emotional climate is more stable

than emotional atmosphere and may be a useful construct for analyzing social dynamics in contexts of political violence [21].

4 Emotions Supporting Health in Collaboration

As mentioned above, it might be considered that the emotional equilibrium of a collaborative network contributes to supporting healthy collaboration. Individual participants experience emotions not only as a result of directly experiencing events (that involve/evoke their own particular emotions) but also through collaborative interactions and by identifying themselves with the network as a whole. As a consequence, the emotional health of the collaborative network might depend of the intricate interactions between the various participants developing, in this way, a collective emotion which is influenced by each participant's dominant emotions and the network's global performance evaluation. From an intuitive point of view, it seems plausible that the more positive the collective emotion is, the healthier the collaborative network becomes.

4.1 Which Emotions

Human emotions are known and although not universally categorized and defined, some authors invested considerable research efforts on establishing theories for categorizing basic and inferred emotions, e.g. [22, 23]. However, when it comes to the context of collaborative networks it becomes understandable that the emotions that are "felt" are not at the level of an individual but rather of a "collectivity". In this way, and under a simplified view of what should be the (collective) emotions that need to be further analyzed, the following examples can be considered:

Excitement Excitement is a positive emotion, "experienced" when the network as a whole feels excited, that might be triggered when the short- and/or long-term network objectives and partner's expectations and wishes are fully achieved. As a positive emotion, it maintains the network health calibrated ensuring, in this way, future successful interactions among network partners.

Contentment Contentment, like excitement, is a positive emotion, "experienced" when the network as a whole feels content, which might be triggered when the short- and/or long-term network objectives and partner's expectations and wishes were partially achieved. As a positive emotion, it indicates a successful achievement from the majority of the network participants and causes a slight alert to the network health to be regulated.

Frustration Frustration is a negative emotion, "experienced" when the network as a whole feels frustrated, that might be triggered when a partner's own actions, and/or others' actions in pursuit of the short- and/or long-term network objectives are mostly not achieved. As a negative emotion, it inhibits the achievement from the majority of network participants and down regulates the network health, increasing the chance of network "failure".

Depression Depression, like frustration, is a negative emotion, "experienced" when the network as a whole feels depressed, hopeless, uninterested and unable to focus on normal activities. Depression might be triggered when a partner's own actions and/or others' actions in pursuit of the short- and/or long-term network objec-

tives are a complete failure. As a negative emotion, it jeopardizes the network health, compromising the interactions among partners and potentially promoting conflicts.

4.2 Emotions Categorization

For both theoretical and practical reasons, some researchers define emotions according to one or more dimensions [24]. Dimensional descriptions capture essential properties of emotional states, such as arousal (active/passive) and valence (negative/positive). Emotion dimensions can be used to describe general emotional tendencies, including low-intensity emotions. In addition to these two, there are a number of other possible dimensions, such as power, control, or approach/avoidance, which add some refinement. Dimensional representations are attractive mainly because they provide a way of describing emotional states, which are more tractable than using words. A further attraction is the fact that dimensional descriptions can be translated into and out of verbal descriptions.

In the context of collaborative networks, we suggest that emotions can be defined according to three dimensions: Valence (positive/negative); Activation or arousal (active/passive); and Intensity (weak/moderate/strong).

4.3 Emotional Evidences/Information

In order to properly build an Emotional Support System, it is necessary to find (non-intrusive) mechanisms to measure/infer the emotion that the collaborative network is “feeling”. Therefore, emotional evidences (or emotional information) have to be defined and their sources identified. As collaborative networks are composed of organizations and people, each one of them can bring its own emotional tendencies to the network, helping in “producing” the network collective emotion. In this way two groups of emotional evidences/information are considered: the first concerning the information that will be useful for “measuring” each member’s emotional state and the second for “measuring” the collective emotion present in the collaborative network. The following tables illustrate the information envisaged, at this stage, for each group as well as were it can be collected. Due to the experimental nature of this work, this information might need to be revised later.

Table 1. Member’s Emotional Information

	<i>Emotional Information</i>	<i>Sources</i>
Individual Part	Needs & Expectations	Survey / Questionnaire
	Performance Data	Member Profile Performance Evaluation
	Past Emotional States	List of past <i>Estimated Emotional State</i>
Shared Part	Member Satisfaction	Survey / Questionnaire

# of belonging Groups	Member's Groups List
# of belonging VO's	Member's VO's List
# of Sharing Resources	Member's Shared Resources

Table 1. (Continued)

	Communication Data <ul style="list-style-type: none"> ▪ Member's Communication Flow (<i>direction of member interactions, as a sender or receiver</i>) ▪ Member's Communication Intensity (<i>frequency of interactions</i>) 	Social Network Analysis Tools
Inferred Part	Estimated Actual Emotional State <ul style="list-style-type: none"> ▪ Name of emotion [<i>EMOTION</i>] ▪ Valence [<i>POSITIVE, NEGATIVE</i>] ▪ Activation [<i>ACTIVE, PASSIVE</i>] ▪ Intensity of emotion [<i>WEAK, MODERATE, STRONG</i>] 	Algorithm using the above information

Table 2. Collaborative Network's Emotional Information

	<i>Emotional Information</i>	<i>Sources</i>
Network Part	Performance Data	Network Profile Performance Evaluation
	Past Collective Emotional States	List of past <i>Estimated Collective Emotional State</i>
	List of Members' Emotional Information	Members' emotional Information
	Total Number of VOs	Network VOs List
	Communication Data <ul style="list-style-type: none"> ▪ Communication Flows (<i>overall direction of interactions</i>) ▪ Communication Intensity (<i>overall frequency of interactions</i>) 	Social Network Analysis Tools
Inferred Part	Estimated Actual Collective Emotional State <ul style="list-style-type: none"> ▪ Name of emotion [<i>EMOTION</i>] ▪ Valence [<i>POSITIVE, NEGATIVE</i>] ▪ Activation [<i>ACTIVE, PASSIVE</i>] ▪ Intensity of emotion [<i>WEAK, MODERATE, STRONG</i>] 	Algorithm using all the above information

4.4 Emotional Support Sub-Systems

Having the above in mind, the Emotional Support System is divided into two sub-systems: the Member's Emotional State Support and the Collective Emotional State Support as illustrated in Fig. 1.

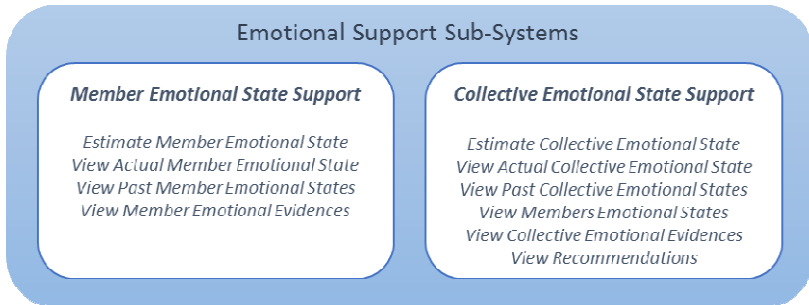


Fig. 1. – Global view of the Emotional Support System

Member's Emotional State Support Sub-System. The Member's Emotional State support sub-system aims to support gathering all the necessary information in order to estimate the current and past emotional state of a particular member.

Fig. 2 shows an adapted i* Rationale Strategic model where the involved actors as well as their dependency objectives are illustrated. Within the boundaries of the Member Emotional State Support sub-system the respective associated tasks/functionality are presented.

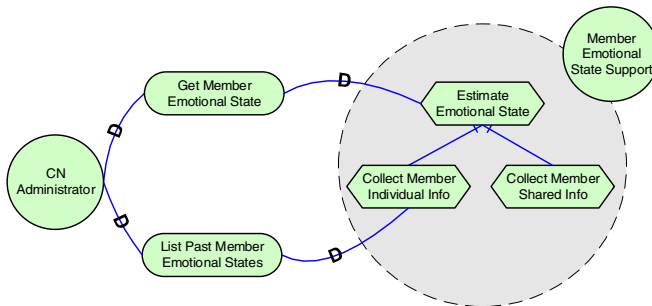


Fig. 2. Adapted i* Rationale Strategic Model for the Member Emotional State Support

The main functionalities of this sub-system are included in Table 3.

Collective Emotional State Support Sub-system. The Collective Emotional State support sub-system aims to support gathering all the necessary information in order to estimate the current and past emotional state of the network as a whole.

Table 3. Main Services of the Member's Emotional State support sub-system of Emotional Support

<i>Service Name</i>	<i>Service Description</i>
Estimate Member Emotional State	Functionality used to infer the emotional state of an identified member taking into account the current available emotional information.
View Actual Member Emotional States	This functionality serves to show the last estimated emotional state of an identified member.
View Past Member Emotional States	This functionality serves to show the list of the past emotional states of an identified member.
View Member Emotional Evidences	Functionality that permits the visualization of the identified member evidences that were used to estimate the emotional state.

Fig. 3 shows an adapted i* Rationale Strategic model where the involved actors as well as their dependency objectives are illustrated. Within the boundaries of the Collective Emotional State Support sub-system the respective associated tasks/functionality are presented.

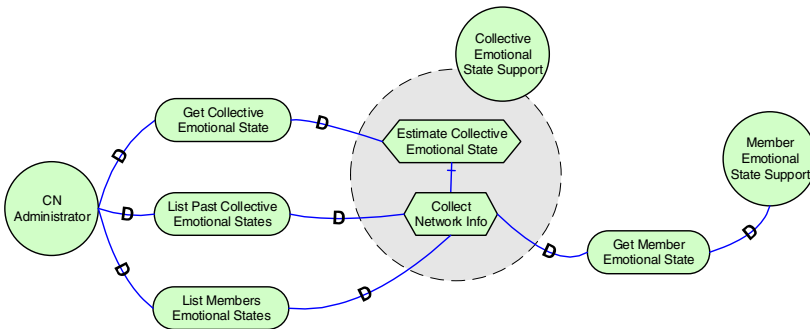


Fig. 3. Adapted i* Rationale Strategic Model for the Collective Emotional State Support

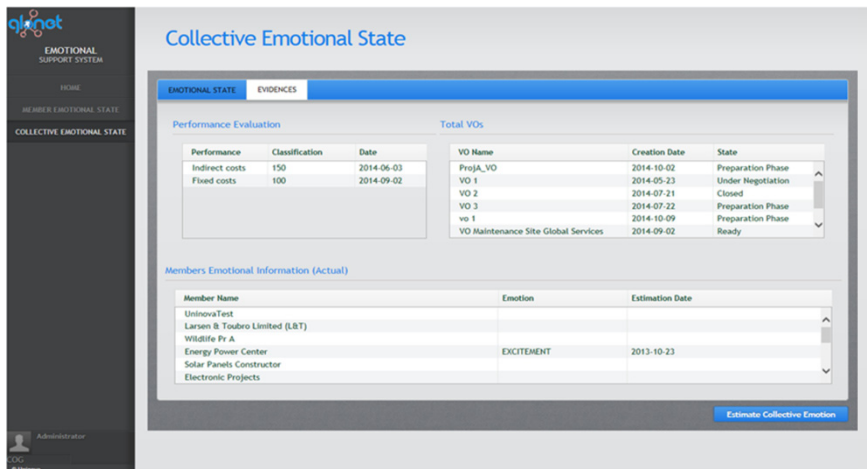
The main functionalities of this sub-system are included in Table 4.

Fig. 4 illustrates the interface of the implemented prototype on the Administrators' side.

This system is currently being evaluated and will be further validated in the context of the GloNet project, which addresses collaborative networks in support of complex service-enhanced products such as solar plants and intelligent buildings.

Table 4. Main Services of the Collective Emotional State support sub-system of Emotional Support

<i>Service Name</i>	<i>Service Description</i>
Estimate Collective Emotional State	Functionality used to infer the emotional state of the collaborative network taking into account the current available network emotional information.
View Actual Collective Emotional States	This functionality serves to show the last estimated emotional state of the network.
View Past Collective Emotional States	This functionality serves to show the list of the past collective emotional states of the collaborative network.
View Members Emotional States	This functionality serves to show the list of the current emotional states of the CN members.
View Collective Emotional Evidences	Functionality that permits the visualization of the evidences that were used to estimate the collective emotional state.
View Recommendations	Functionality that according to the collective emotion suggests recommendations to the network administrator.

**Fig. 4.** Developed prototype interface on the Administrators' side

5 Conclusions and Future Work

Collective emotions are becoming an important element in the management of organizations. In the collaborative networks context its effect is also of extreme significance due to the virtual, dynamic and “soft” nature of the interactions among organiza-

tion participants. Furthermore, it is also known that emotions might influence positively or negatively the network collaboration dynamics. Therefore, with the aim of maintaining the emotional equilibrium of the network, this paper presents the design of an emotional support system, including the identification and categorization of the most influencing positive and negative collective emotions and also the specification and prototyping of the sub-system services. Future work will rely on the progress of the emotional model that is used to estimate emotion according to the multi-modal non-intrusive evidences that were considered for the members and also for the network.

Acknowledgments. This work has been supported by the Collaborative Networks and Distributed Industrial Systems (CoDIS) Research Group of Uninova and partly by the GloNet project funded by the European Commission.

References

1. Stanley, R.O., Burrows, G.D.: Varieties and functions of human emotion. In: Payne, R.L., Cooper, C.L. (eds.) *Emotions at Work: Theory, Research and Applications in Management*, pp. 3–19. Wiley, Chichester (2001)
2. Ferrada, F., Camarinha-Matos, L.M.: Collective emotions supervision in the product-servicing networks. In: Camarinha-Matos, L.M., Tomic, S., Graça, P. (eds.) *DoCEIS 2013. IFIP AICT*, vol. 394, pp. 33–42. Springer, Heidelberg (2013)
3. Ferrada, F., Camarinha-Matos, L.M.: Emotions in collaborative networks: a monitoring system. In: Camarinha-Matos, L.M., Shahamatnia, E., Nunes, G. (eds.) *DoCEIS 2012. IFIP AICT*, vol. 372, pp. 9–20. Springer, Heidelberg (2012)
4. Camarinha-Matos, L.M., Afsarmanesh, H., Oliveira, A.I., Ferrada, F.: Cloud-based collaborative business services provision. In: Hammoudi, S., Cordeiro, J., Maciaszek, L.A., Filipe, J. (eds.) *ICEIS 2013. LNBIP*, vol. 190, pp. 366–384. Springer, Heidelberg (2014)
5. Surajbali, B., Bauer, M., Bär, H., Alexakis, S.: A cloud-based approach for collaborative networks supporting serviced-enhanced products. In: Camarinha-Matos, L.M., Scherer, R.J. (eds.) *PRO-VE 2013. IFIP AICT*, vol. 408, pp. 61–70. Springer, Heidelberg (2013)
6. Forsyth, D.R.: *Group dynamics*, 4th edn. Thomson Learning, Inc. (2006)
7. Luksha, P.O.: Emotions in organization: More than mere fluctuations. Paper presented at the XV World Congress of Sociology, Durban, South Africa (2006)
8. Lazarus, R.S.: Progress on a cognitive-motivational-relational theory of emotion. *American Psychologist* **46**, 819–834 (1991)
9. Ashkanasy, M.N., Härtel, E.J.C., Zerbe, J.W.: *Emotions in the workplace: research, theory, and practice*. Quorum Books, Westport (2000)
10. Brief, A.P., Weiss, H.M.: Organizational Behaviour: Affect in the Workplace. *Annual Review of Psychology* **53**(1), 279–307 (2002)
11. Schoenewolf, G.: *Turning points in analytic therapy: The Classic cases*. Jason Aronson Press, London (1990)
12. Hatfield, E., Cacioppo, J., Rapson, R.L.: *Emotional contagion*. Cambridge University Press, New York (1994)
13. Zucher, L.A.: The staging of emotion: A dramaturgical analysis. *Symbolic Interaction* **5**, 1–22 (1982)

14. Lawler, E.J.: Affective attachment to nested groups: A choice-process theory. *American Sociological Review* **57**, 327–339 (1992)
15. George, G.M.: Personality, affect, and behavior in groups. *Journal of Applied Psychology* **76**, 299–307 (1990)
16. Barsade, S.G.: The ripple effect: Emotional contagion and its influence on group behavior. *Administrative Science Quarterly* **47**, 644–675 (2002)
17. Stephan, W.G., Stephan, C.W.: An integrated threat theory of prejudice. In: Oskamp, S. (ed.) *Reducing Prejudice and Discrimination*, pp. 225–246. Erlbaum, Hillsdale (2000)
18. Smith, E.R.: Social identity and social emotions: Toward new conceptualization of prejudice. In: Mackie, D.M., Hamilton, D.L. (eds.) *Affect, Cognition and Stereotyping: Interactive Processes in Group Perception*, pp. 297–315. Academic Press, San Diego (1993)
19. Bar-Tal, D.: Sociopsychological Foundations of Intractable Conflicts. *American Behavioral Scientist* **50**(11), 1430–1453 (2007)
20. de Rivera, J.: Emotional climate: Social structure and emotional dynamics. In: Strongman, K.T. (ed.) *International Review of Studies on Emotion*, vol. 2, pp. 197–218. John Wiley & Sons Ltd., New York (1992)
21. Conejero, S., Etxebarria, I.: The Impact of the Madrid Bombing on Personal Emotions, Emotional Atmosphere and Emotional Climate. *Journal of Social Issues* **63**(2), 273–287 (2007)
22. Averill, J.R.: A constructivist view of emotion. In: Plutchik, R., Kellerman, H. (eds.) *Emotion: Theory, Research and Experience*, pp. 305–339. Academic Press, New York (1980)
23. Scherer, K.R.: What are emotions? And how can they be measured? *Social Science Information* **44**(4), 695–729 (2005). doi:10.1177/0539018405058216
24. Russell, J.A., Carroll, J.M.: On the bipolarity of positive and negative affect. *Psychological Bulletin* **125**, 3–30 (1999)

Trust-Based Access Control in Storage Middleware Grids: A Reference Framework Proposal to Deploy in the Financial Sector

Francisco Nunes^(✉) and Henrique O’Neill

ISCTE/IUL, Avenida das Forças Armadas, 1649-026 Lisboa, Portugal
fjfnunes@gmail.com, henrique.oneill@iscte.pt

Abstract. Fostered by the development of the Web, the financial sector has been able to develop a broad set of shared IT services. Despite the high levels of maturity that have been achieved there are still improvement opportunities concerning the sharing of services by financial institutions. This research addresses the sharing of data storage resources among different financial organizations to fulfil the needs for unplanned peaks of data storage, or to help shortening the time needed to start projects requiring allocation of storage space when this is not available in the organization. To answer to these requirements it was proposed a data grid infrastructure (SRM), centrally managed by a versatile storage resource manager middleware. Senior IT infrastructure managers of representative financial organizations have been questioned to assess the proposed solution. Security has been identified as a key concern that prevents the dissemination of this type of solutions. These solutions may be fostered by the adoption of a security mechanism that would consider the behaviour of the distinct organizations in the use of the shared resources. To meet this requirement the research proposes an algorithm for controlling the access to the storage resources based on trust, where the level of trust in the joint organizations will vary dynamically according to the fulfilment of the rules concerning the use of the shared storage by its users.

Keywords: Data storage systems · TBAC · Grid data storage · Virtual organizations

1 Introduction

This applied research project described in this paper has been sponsored by AdI under the “PhD in the Enterprise” initiative¹, a program that aims to contribute to the improvement of the Portuguese economy by addressing specific problems of the industry in topics that require further research. The project aims to improve the use of data storage resources by firms of the financial sector. It was developed in collaboration with two of the most important Portuguese banks. Like many other institutions in several sectors, banks have several ongoing IT projects of the most diverse nature.

¹AdI – Agência de Inovação – Doutoramento em Empresa

© IFIP International Federation for Information Processing 2015

L.M. Camarinha-Matos et al. (Eds.): DoCEIS 2015, IFIP AICT 450, pp. 54–61, 2015.

DOI: 10.1007/978-3-319-16766-4_6

Sometimes these organizations have some difficulty in initiating some of these projects that rely on computational power in general and in particular depend on the availability of space in data storage systems. These projects that need data space may begin immediately, if the disk space is available, or take up to three months or more if the disk space does not exist and involves an operation of procurement. To meet this need there are some institutions that aim to drastically reduce the average time of purchase and installation of new storage equipment by redesigning procurement processes.

After a thorough analysis of the problem [12] a framework was created to address the problem of availability of storage resources in order to deploy space in storage systems immediately or almost immediately, particularly for projects developed in the studied financial sector institutions. This framework will comprise the creation of a federated environment composed by different financial institutions with a centralized management. Each institution contributes with the storage resources that can provide at a given time, so it can help to fulfill immediate needs of any other institution belonging to this federated environment that does not have storage resources available at that time. The way to implement this framework implies that the shared storage resource management is done through the implementation of a common grid storage by using the same kind of middleware. The proposed middleware is based on the Storage Resource Manager (SRM) [1]. It meets the requirements of data operation of financial institutions and has been accepted by the architects and IT managers of these institutions. However the use of SRM for temporary data sharing lack security features (access control, access and operations log) [4]. This is an issue also identified by the experts of the institutions that participated in the investigation. So, an element of security to control data access based on dynamic trust management systems was created and added to the framework. It enables to manage not only the access and use of resources by users of various institutions with access to the pool of shared resources, but also assesses the reputation and trust of the entities that provide the resources.

This work relies on a series of research results on models on Trusted Based Access Control, collaboration and sharing to generate an integrated framework. It also addresses issues related with the technical feasibility of the infrastructure and its implementation.

2 Contribution to Cloud-Based Engineering Systems

Typically Cloud Computing refers to the hardware and software resources that are available via the Internet [2, 3]. The resources made available in this way are called IT services [4]. The features of these IT services are distinguished by being scalable, configurable, measurable and able to provide an easy access from the perspective of auto use.

The infrastructure that supports these services must be a structure with sufficient elasticity to satisfy the business services requirements. The infrastructure proposed in this research is based on a grid of data storage with clustering of resources dictated by the availability of each institution that belongs to the group that makes up the grid [4].

In the context of IT infrastructure and Cloud Computing the proposed grid data storage with centralized management, has precisely the main advantage of allowing of inclusion of resources in the grid space to meet peak needs or to remove these resources when there is less need for space data [5]. This requires the ability to monitor the needs of the users and to adjust the elasticity of the Cloud supply.

The application of this technology can support different types of offering Cloud Computing services [6]. An example is to use the platform as part of a shared services infrastructure, for example by deploying a Private Cloud serving various companies of the same economic group. An alternative approach will be to share resources between various financial enterprises despite the allocation of a resource to be assigned specifically to one of the group companies [9]. This sharing of resources will be partial and temporary in nature. It will be guaranteed not to harm the infrastructure, the resource will be temporarily allocated according to a set of rules and the recovery of the resource will be ensured. By using the Cloud with this collaborative network approach, those who provide resources for these effects will also benefit from them in times of unforeseen need. This versatility in the context of data storage can be materialized by a grid infrastructure for data storage with centralized management, able to integrate the storage devices capabilities of institutions that have joined this sharing group in the federate environment..

The uses of a data storage shared infrastructure can thus be a privileged resource in the context of Cloud systems, as the type of application described or other that will be implemented.

3 Related Work

For trust management, access policies and authorization different approaches have been explored in distributed environments with centralized management. However, no unified definition of trust exists in the current literature of computer science [8].

Most settings found in work related to the classification of trust tend to only use a number, a slight degree, a marker or a combination of all. In this context, there are several ways to define and establish a trustful relationship. The trust is paramount in a relationship and can be negotiated if the collaboration is established between actual organizations. In other scenarios, the trust agreement may be specified by one party (e.g. a service provider) and accepted by the other parties, without negotiation (e.g. a service consumer). Yet another example of establishing trust implies that the trust agreement may be declared by a supervisory authority and be applied by all parties involved (e.g., global policies declared by the supervisor of the federated environment).

In fact, one of the initial works that tried to provide a formal trust management, which could be used in computer science, was presented by Marsh (1994) [9]. Marsh's model is based on social trust properties and provides a motivation for the integration of some of the aspects of trust based on the concepts of sociology and psychology. But these sociological foundations proved that the model is quite complex and can hardly be implemented in electronic communities. Furthermore, the model places emphasis on the experiences of their own bodies, neglecting the views of others, a factor that prevents a network of trust to be built collectively. Later, 2009,

Boursas [8] developed a framework in order to manage federated environments that include a model of trust management that was accepted by the scientific community.

4 Shared Resources and Trusted Based Access Control

In this section we present the research developed around the middleware for grid storage control, its key features and capabilities. We will also present the Trusted Based Access Control algorithm inserted into the framework that allows varying levels of confidence of participants of the Sharing Group. Finally a prototype used to validate the developments carried out in the research model will be presented.

This work built a varying trust model that is the basis of a framework that allows trust based access control to shared resources by different institutions in the financial sector, in a federated environment of centralized management, which are themselves providers of resources storage (when resources are available) while customers of that environment.

4.1 Middleware Storage Resource Manager

The elected grid storage middleware management system was a modified version of the Storage Resource Manager (SRM) [10] implementation. The StoRM (Storage Resource Manager) works in a distributed fashion and with high availability across multiple systems ("Cluster", "GRID"). It allows to manage (share, transfer and access) data storage in an easy, fast and flexible way. The implementation can be distributed over several "datacenters" even when the geographical distance between them is very large. Its main characteristics are flexibility, scalability, high performance, able to run on various types of "filesystems" and independence of the storage manufacturer. It implements the mechanisms of SRM V2.2 interface standard (<https://sdm.lbl.gov/srm-wg/>). A StoRM application runs on Linux systems on "POSIX filesystems" (ext3, ext4, xfs, etc.), enabling the grid computing to simultaneously provide a direct of multiple systems to a common "filesystem" (e.g. GFS for Linux, HP-UX CFS and Veritas, IBM GPFS, etc.).

For sharing the storage resource data all suppliers and customers in the Sharing Group must have installed SRM in their infrastructure. SRM is used by various academic solutions from simple "grid map files" to Role Based Control Access (RBAC) systems, with Virtual Organizations Management Systems (VOMS) among other proposals [11], despite its breach in access control. This is not the case of the financial sector institutions which have tight security requirements. The implementation of TBAC in SRM and its application to financial sector was a major contribution of this research in order to solve the difficult problem of managing the storage resources in the day-to-day operation of the financial institutions. TBAC is one of the control access models that has large acceptance and works fine when we are dealing with IT communities. Because is a more interesting base to access control by level of trust in an entity than by the role the person has in his own organization (like RBAC did). It is believed that virtualization can help to significantly improve the application of more

stringent security policies and finer granularity with the SRM as a virtual machine that provides basic insulation through Virtual Organizations (VOs) to share resources and policies to monitor application properties. VO's are the way how an organization is created in the storage grid.

4.2 Algorithm for Trust Variation

The approach presented in this paper sought a quick and cost effective way to supplement the static nature of the federated environments, with a set of new mechanisms for dynamic reliability assessment, without affecting others or compromising the integrity of the federated environment [11]. A notable advantage of the presented solution is to reduce the effect of the arbitrariness of classical evaluation methods of confidence that are usually solely based on the classification of individuals. The proposed approach is based on the evaluation, updating and aggregation of trust by reputation and from past experiences. Three functions were used one to enhance, another to decrement and other neutral for the confidence levels and are used as follows:

$$f(x) = 1 - \frac{1}{2}e^{-\alpha^2(\Sigma \text{interaction}(x))}, x \in \{0, 0.5, 1\}, \alpha \in \mathbb{N}. \quad (1)$$

- The function (1) depends on the number of interactions, performs the incremental curve of confidence values that represent reliable behavior (above the axis of 0.5). The asymptotic values increases, but never touch the axis of one (indicating the absolute confidence) such that the confidence value is closer shaft requiring a large set of interactions. This function, on one hand, facilitates the rapid increase of the level of trust from the neutral level of trust for a higher level, but on the other hand, ensures that sufficient positive interactions must be made to achieve Absolute Trust Level.

$$g(x) = \frac{1}{2}e^{-\alpha^2(\Sigma \text{interaction}(x))}, x \in \{0, 0.5, 1\}, \alpha \in \mathbb{N}. \quad (2)$$

- The second function is the inverse function of the previous one. The same principle is defined for all values of trust representing an unreliability. Similarly, the curve rises rapidly to confidence values below 0.5, while rises more slowly when approaching the axis of 0 which represents the Absolute No Trust Level.

$$h(x) = 0, x \in \{0, 0.5, 1\}. \quad (3)$$

- The function (3) is a static function, zero, representing that no modifications are required by Neutral Trust Level, which of course can improve or degrade under the other two above functions
- (x) is a set of interactions with a rating level represented by discrete values: $x \in \{0, 0.5, 1\}$
- The parameter α represents the convergence factor of the curve of the exponential function.

4.3 Implementation of the Prototype

A prototype was implemented on virtual machines (Figure 1) where each machine implements a service and adopts the following authorization flow:

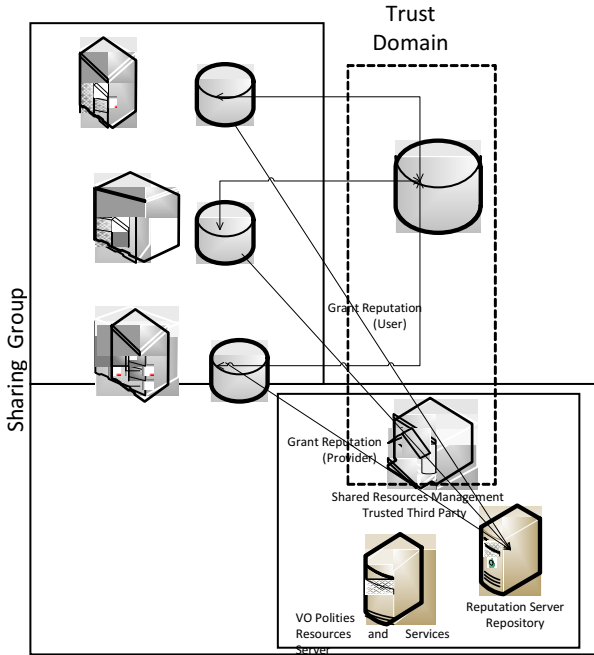


Fig. 1. Auth Flow

are stored on the server resource services (SSR).

3. The assets manager notifies the different participants, with user role, which has resources available.

4. The Bank C, needs resources and questions whether the SSR VOs are available in accordance with their technological needs and if the supplier complies with the desired level of trust. If so the SSR registers the request and analyzes the reputation of the Bank C, the requestor.

5. After the validations the SSR delivers the public key of B VO customer to Bank C. Thus the Bank C can enter the VO.

6. If the Bank C complies with the contractual agreement, the index will increment its trust in a reliable server, if some of the clauses violate the agreement its trust will be decremented. In the future, if there are many institutions competing for the same resource, it will be privileged the entity that holds the higher levels of trust.

5 Discussion of Results, their Validation, and Critical View

Given the nature of the research carried out, its assessment should be taken into account in its different dimensions. We considered two dimensions, one Formal and another

1. All the entities are made known to the system. Each one has to send an id and the role (user or provider) for the Services server that recognizes and keeps the records of the entities. If the entity that manages the shared resources confirms which entities are forwarded in accordance with the policies of the VO, and no reputation problems arises, then writes the data and the role of the user.

2. The Bank B, which aims to provide resources, creates and sends the VO, VO-id, the VO policy and public key pair for the server managers of the shared resources, which

Functional. Formal assessment was necessary to evaluate the coherence of the research where, in this case, comprised the validation by an expert panel of the acceptance in the sector and by other hand base the mathematical model that was proposed in other derivative models. Concerning the functional assessment we have to demonstrate that things really work and this was done by testing a prototype implementation and by validating that the grid storage solution may be applied to the financial sector, if the context meets certain requirements that enable the solution acceptance.

5.1 Formal Assessment

With respect to the adequacy of the Middleware Data Storage System Oriented for a Grid implementation to the financial sector, an expert panel was created and it was explained to the panel members the middleware that was developed to become a proof of concept. Unanimously the panel members agreed that the use of virtualization technology would be the way forward for the financial industry and even suggestions were given that provided good contributions to the prototype that was developed.

Regarding the adequacy of the dynamic variation of the trust model used, it was formally presented in the doctoral thesis of Marsh (1994) [9], which has profoundly demonstrated its validity as well as the mathematical representation of the belief model considered. Later, mentioned above, Boursas (2009) [8] with a variation introduced, applied this representation in the framework presented in her doctoral thesis. We proceeded to work in this setting, maintaining and ensuring semantic issues in the Body of Real Numbers, keeping unchanged its initial algorithmic essence.

5.2 Functional Assessment

In order to validate the acceptance by the financial industry an expert panel that studied the issue was created and agreed that the proposal made in this research was a good idea. The expert panel also contributed with suggestions that helped to improve the results of the research, namely in the security middleware component used in.

With respect to the prototype it has to be evaluated according to all the expected benefits that will be learned from its implementation. The performance has no significant impact in the operations. Conversely, the impact of their gaps must also be assessed to foster future improvements and extensions.

6 Conclusions and Further Work

The proposed trust model was developed just to solve an issue of lack of security found in the middleware that was adopted in the framework. The middleware was chosen as a solution to the needs of disk space available for start-up projects in the financial sector. The middleware was the option to provide central management of the Sharing Group. It was found to be suitable for the purpose since no prior knowledge of each element that needs to use the resources available in the group becomes necessary.

The adaptation of the framework applied to address the problem, assessing the suitability of the dynamic trust management model, as well as the formal evaluation of the developed mathematical model, are key components of the research developed. The suitability of the framework presented in this research was also sustained by

leveraging the knowledge base of frameworks previously investigated, developed and applied in doctoral thesis such as Boursas [8], which enabled to justify its application in this context the financial sector.

The mathematical model that was created followed the standards of mathematical inference of parametric models based on the Marsh's theory of belief (2004), thus justifying the application of the framework to the financial sector. The approach presented in this research complements the nature of more traditional systems with a new trust mechanism for evaluating trust dynamics. The proposal for a broader concept of trust, allowing dynamic trust values contributed to the body of knowledge of the specific area Trusted Based Access Control. This approach sought an efficient cooperation between members of the Sharing Group and any external organization without compromising the integrity inside the Sharing Group or affecting any third-party. Basically it allows a trade-off between flexibility, speed and degree of automation in the configuration of cooperation agreements and the level of security and privacy hit. As future work, certain points that can enable to evolve and enrich this research are:

- The research of inter-organizational trust and Service Level – there is a need to investigate this point since inter organizational trust agreements may conflict with organizational security policies, SLAs and restrictions
- Research of other dimensions of trust, aimed at identifying the behavior of other elements of trust. For instance the research of belief in case of an organization is absolute unknown of the group and the new contribution to the model once itself is very flexible.

References

1. Sim, A., Berkeley, L.: Grid, Storage and SRM (2008)
2. Armbrust, M., Fox, A., Griffith, R., Joseph, A.D., Katz, R., Konwinski, A., Lee, G., Patterson, D., Rabkin, A., Stoica, I., Zaharia, M.: A view of cloud computing. *Commun. ACM* **53**, 50–58 (2010)
3. Erdogmus, H.: Cloud Computing: Does Nirvana Hide behind the Nebula? *IEEE Software* **26**, 4–6 (2009)
4. Foster, I., Zhao, Y., Raicu, I., Lu, S.: Cloud Computing and Grid Computing 360-Degree Compared. In: 2008 Grid Computing Environments Workshop, pp. 1–10 (2008)
5. IBM Cloud Computing und Green IT - Ausbildung 2010. 49, 4887246-4887246 (2010)
6. Andreozzi, S., Forti, A., Magnoni, L., Zappi, R., Pichat, V.B.: Cloud Storage as a new Storage Class: QoS Characterization and Cost Analysis (S3) *, pp. 40127–40127 (2008)
7. Erlennmeyer, M.: Grid and Cloud Computing (2009)
8. Boursas, L.: Trust-Based Access Control in Federated Environments, vol. 10 (2009)
9. Marsh, S.: Formalising Trust as a Computational Concept (1994)
10. Alfieri, R., Cecchini, R., Ciaschini, V., dell'Agnello, L., Frohner, Á., Lörentey, K., Spataro, F.: From gridmap-file to VOMS: managing authorization in a Grid environment. *Future Generation Computer Systems* **21**, 549–558 (2005)
11. Boursas, L., Hegering, H.-G., Hommel, W.: Standards and New Technology for Systems and Virtualization Management: A Report on Svm 2008. *J. Netw. Syst. Manag.* **17**, 99–104 (2009)
12. Zissis, Dimitrios, Lekkas, Dimitrios: Addressing cloud computing security issues. *Future Generation Computer Systems* **28**(3), 583–592 (2012)

Cloud-Based Manufacturing

Service Composition in the Cloud-Based Manufacturing Focused on the Industry 4.0

Marcos A. Pisching^{1,2(✉)}, Fabrício Junqueira²,
Diolino J. Santos Filho² and Paulo E. Miyagi²

¹ Instituto Federal de Santa Catarina, Rua Heitor Villa Lobos, 222, Lages, SC, Brazil

² Escola Politécnica da Universidade de São Paulo, Cidade Universitária, Av.

Prof. Mello Moraes, 2231, São Paulo, SP, Brazil

{marcos.pisching, fabri, diolinos, pemiayagi}@usp.br

Abstract. The emerging Industry 4.0 concept, also called fourth industrial revolution and understood as smart factory, is based on integration of both Internet of Things and Cyber-Physical Systems. In smart factory, these two concepts are converging to the Internet of Services, which uses the cloud-based manufacturing for creating, publishing, and sharing the services that represent manufacturing processes, and could be offered by virtual enterprises. Therefore, any dispersed partner can meet the market demands according to their skills, capacities, and availability. This paper presents a survey about service composition in a cloud-based manufacturing over the Industry 4.0. To achieve it, the concepts and characteristics about the service composition based on cloud-manufacturing over the Industry 4.0 are presented, and then the advanced researches about it are summarized. After it, the main research challenges over these issues are shown. Finally, discussions on service composition are reported to contribute for the future researches.

Keywords: Cloud-based manufacturing · Cyber-physical systems · Industry 4.0 · Internet of things · Service composition · Virtual enterprises

1 Introduction

The Industry 4.0 is focused on creating smart products, procedures and processes. It was first presented in 2011 at Hannover Fair and launched in April, 2013 [1], [3]. This concept has meeting the smart manufacturing industry concerns that are dealing to spark design innovations and bring new products to market faster, and additionally, they are looking for satisfying the individual customer desires. In the Industry 4.0 this behavior changes the production concepts from mass to individualized production. Objects, sensors and actuators should communicate and exchange information among them all the time [2]. These tasks are realized by two concepts, the Cyber-Physical Systems (CPS) and Internet of Things (IoT) [1], [2], [3], [4].

In the Industry 4.0, also referred as smart factory, the CPS and IoT concepts are converging to the Internet of Services that widely uses the cloud-based approach for creating, publishing, and sharing the services [1], [2], [3], [20]. In this context, the

services represent manufacturing processes, which could be offered by virtual enterprises (VE). Thus, any dispersed partner around the world can meet the demands according to his ability, capacity, and availability. These issues have been gained force at worldwide industrial sector, and its complexity implies on the demand of collaborative and smart services, which should be available and shared on the Internet infrastructure [1], [4], [20].

Service composition is one of many concerns in the Industry 4.0. For example, the customer could require one virtual service, and then the virtual system must set a composition of services, in a way to comply with the customer specific demand. This research is centered on service composition and how can it be possible in a way to offer smart services and how it can integrate the real systems to the virtual systems, to contribute for Industry 4.0 expectations. This paper presents a survey about service composition in a cloud-based manufacturing over the Industry 4.0 context, for a future perspective of a collaborative and integrated environment, on which VE could be established to provide services and goods to the customers. It could help any enterprise regardless of size, but small and medium-size enterprises (SMEs) could be more competitive by joining business and knowledge.

2 Benefits from Cloud-Based Engineering Systems

In the Industry 4.0 the end-to-end engineering and the vertical and horizontal integration can have a significant increase by the extensive use of CPS and IoT. Consequently, it is expected that the number of projects, data and services over the Internet infrastructure should have an exponential growth. Therefore, the cloud-based engineering systems can benefit the emergent Industry 4.0 in a way to offer infrastructure, platforms, and software among the partners [1] and also contributing to the development of SMEs [1], [2], [3]. By these resources, the services and data could be available for any partner regardless of the platform and operational system. The cloud-based technology could be decentralized, and it is favorable for the deployment and sharing of services among the member of projects. In the worldwide context, where the service demands should rapidly increase, the stakeholders must be prepared to improve the ICT to answer the demands in a short time. The cloud-based infrastructure could be scalable and dynamic to attend the entrepreneur needs faster. In addition, these systems could support the service composition based on service-oriented architecture (SOA) for the establishment of VE, where SMEs could be favoured to the design of new products and, in the same time, to become faster in the answers to market fluctuations [9]. The Industry 4.0 and VE require more flexible environment and need autonomous system reconfiguration to support the market concerns. Then, according to [15], cloud-based manufacturing should comply task as service oriented, customer centric, and demand driven manufacturing, in a way to enable industrial control systems, service composition, and flexibility [8].

3 Fundamental Concepts

3.1 Industry 4.0

The Industry 4.0 concept, also referred as the fourth industrial revolution [5], integrated industry, or smart factory [4], is centered on network and Internet architecture [1], on which is possible to integrate the virtual world with the real world by using Information and Communication Technology (ICT). In the smart factory, all the relevant “things” involved in the manufacturing processes could be recognized, and then the hardware and software can automatically behave, with less human intervention, to perform all the tasks in a production line. It also depends on Cyber-Physical Systems (CPS) and Internet of Things (IoT) concepts. Its main purpose is to improve the efficiency and productivity of industrial processes by the smart automation environment and by the industry integration [1], [2]. According to [3] in the Industry 4.0 context the products can control their own manufacturing process, and additionally, the customer should be more involved in the creation processes of new products. This project has been leading by German government, German industries, and German Research and Development [2]. However this term is little known in the world, it has been spreading and being the issue in some technology conferences, and research and development [1], [3].

3.2 Cyber-Physical Systems and Internet of Things

The Cyber-Physical Systems (CPS) and Internet of Things (IoT) are the basis of Industry 4.0. The Fig. 1 shows the relation of CPS and IoT with the Industry 4.0. The CPS are related with the integration of computation technologies with physical processes [6]. The CPS are based on a structure composed by embedded systems (ES) and physical environment, on which are expected the ubiquitous computing that provide information anytime and anywhere [1]. Communication technology such as distributed application and service provision, and embedded system technologies such as robots, control systems, sensors and actuators are converging in a way to offer a distributed and embedded web-based system represented by services.

On the manufacturing, the CPS have been used at shop floor tools and equipment to integrate the manufacturing processes and to enable the machine-to-machine communication [7]. Additionally, the CPS infrastructure enables the communication between real and virtual systems, and vice-versa. By the virtual systems is possible to design, model and simulate products that should be exchanged to real world to be produced. On the other way, the physical processes for manufacturing products could be visualized by a virtual environment such as three-dimensional environment or augmented reality environment.

The IoT is a concept that is also based in the ICT, which uses the Internet infrastructure. It consists of sensory and smart object interconnection to offer connectivity of devices, systems and services. Its main purpose is to connect everything including resources, information, objects, people and machines to create the Internet of Things and Services [1]. In the IoT each object must be addressed with a unique identification that enable the interaction and cooperation with neighbours to reach common goals.

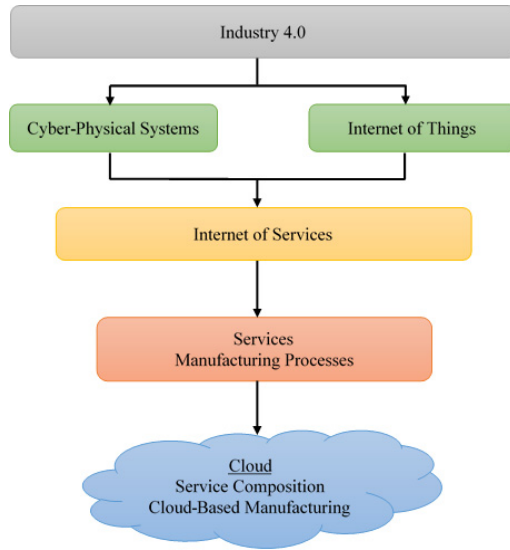


Fig. 1. The Industry 4.0 and its relation with CPS and IoT in a cloud-based manufacturing. Industry 4.0 depends on CPS and IoT technologies. These two concepts are converging to the Internet of Services that provide a set of services, which represent manufacturing processes. A cloud-based manufacturing is used to compose a set of services to offer solution for VE.

Both, CPS and IoT resources, could be virtualized as services, and then deployed over a cloud-based infrastructure, on which is possible to store, exchange, share, and process data. Furthermore, the stakeholders could deploy and share manufacturing processes as a service. All this resources can be used in a collaborative and integrated environment (CIE) to model and design goods and services by VE, and may be favorable for the SMEs and start-ups, in a way to facilitate design innovations and provide new products for an increasingly sophisticated, dynamic and demanding market.

3.3 Service Composition

In the context of manufacturing, all the objects, features and resources that represents their states, information, and mode operations are considered as services [10]. These services can be described, published, located, and invoked over a network, which purpose are to perform actions as answers from requests between service consumers and providers [11]. Services could be implemented on a single or on a large number of servers [11], and over the cloud-based technology. Such services, when working alone, could be more difficult to perform the actions according to demands. Therefore, the combination of exiting and available services from different enterprises, which is called service composition, can perform both simple or complex tasks [11], [12].

In the Industry 4.0, CPS components, hardware and software are represented as services. When it is published in a collaborative environment they could be used to

compose an integrated service, which aim to solve problems of common interest [12], [13]. The Fig. 2 depicts a single situation, where the stakeholders or partners, such as SMEs, can deploy and publish their virtual services on a cloud-based infrastructure in a way to establish virtual enterprises, which the main purpose is centered on a collaborative work to provide solutions according to the customers demand. Therefore, the customer could request a service by a virtual environment, and then a background system over the cloud should verify the availability of services and the best way to compose it to solve the customer need.

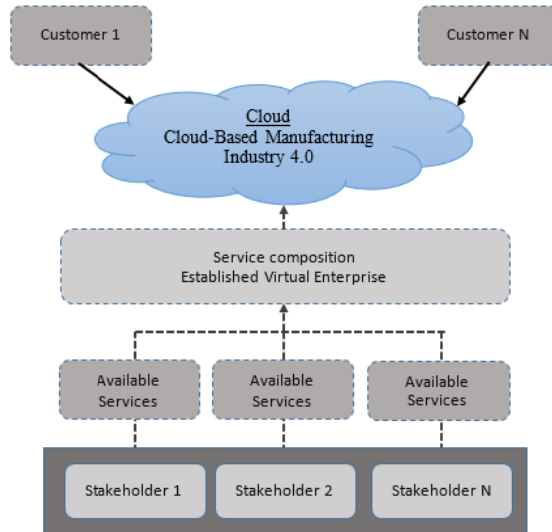


Fig. 2. Stakeholders publish their CPS components as services to provide a common solution in order to establish a VE to answer a specific market need

4 Research on Service Composition over the Industry 4.0 Concepts

The Industry 4.0 platform is in initial stage, hence the researches on this field must have many issues to explore and one of them is the service composition based on CPS and IoT concepts.

Based on CPS, [12] propose a dynamic manufacturing resource aggregation (MRA) architecture, on which they consider a virtualization model and describe in detail the implementation process of the manufacturing resources and a dynamic service composition.

In the [16] the CPS resources are related as components, for further modelling for complex and flexible process for smart environments. The authors present a process meta-model and use Unified Modelling Language (UML) to represent component composition using object-oriented approach, and then it is used to model process component and its composition.

For a cloud-manufacturing implementation focused on customer centric solutions, the [15] present an overview about cloud manufacturing, and show the current issues over the architectures, models and framework, for further exposure about the potential impact and future work. They also present the relation of service composition with the cloud-manufacturing systems, on which is presented a review about methods and implementation considering service composition in VE and virtual marketplace, for further presentation of model, framework, infrastructure, and architecture of cloud-manufacturing for flexible, cooperative and collaborative virtual enterprises.

Based on VE establishment, the work [14] adopt the everything-as-a-service concept to propose a service-oriented platform for on-demand virtual enterprise. The suggested platform supports flexible integration of networked resources and help the formation of VE considering trusted service composition, data service centric business collaboration, and business process utility. Considering collaborative and integrated environment, a modeling of service composition by interpreted Petri net for system integration is presented in [18], on which is proposed a coordinated and collaborative control of a dispersed productive system.

A widely approach about service composition based on ontology was realized in [17]. The authors present a method based on algorithms, on which automatic service composition is studied to decompose the requirements, the rules to determine the relation among the services, and the algorithms for composing services.

Associated to the new paradigms such as cloud computing and Web of Things, [19] report an overview about the lifecycle of web services composition (WSC) and present issues about standards, research prototypes, and platforms, which is assessed using a set of criteria. They show the state-of-the-art of WSC, and present a generic model for the lifecycle from it, which is used to compare with different prototypes using the defined criteria.

These studies show general issues and concerns around the service composition such as architecture, models, and methods that could be explored and applied on Industry 4.0.

5 Discussion on Service Composition for Industry 4.0

In the Industry 4.0 is expected a large growth of the objects and services available over the web due its worldwide trends involving the growing adoption of CPS, IoT and services.

Service composition, which is also applied in the smart manufacturing industry, is one of the essential problems of service-oriented computing [12]. In [15] the author points to the concerns over the automation and control, business model, information and resource sharing, distributed system simulation as services.

The research [11] points to the problem around the composability, adaptive, automatic composition, quality of services, and service governance, management, and administration.

The [16] suggests a decentralized and distributed workflow across several orchestration peers in a way to increase the availability of the workflow process. They also

work on a process component repository and a semantic domain-model for the classification of process components. Additionally, they will investigate the agent-based technology to find appropriate process composition.

The SMEs have been demonstrating significant importance around the economic growth of the European Union, on which several of them are consolidated and new companies have been created [9]. According to [9] these SMEs have been found difficulties to meet demands and react to the business changing due their manufacturing limitations, interoperability, and its lack of collaborative capabilities. It could be improved by SOA, which has been used to undertake inter-enterprise collaboration [13] by the orchestration and composition of services to join the SMEs in a interconnected network to form a virtual enterprise.

According to [17], subsequent research will extend the ontology approach for supporting the service composition in various domains. To [18], the integration and coordination of dispersed productive system is a problem that need investigation. In [19], web services composition has been an active sector for research and development, and activities including standardization, research, and system developments have been produced.

Considering the recommendation from [1], [3], [4], all these issues also need attention and could be exploited over the Industry 4.0. Additionally, issues like integration of CPS focused on collaborative, dynamic and smart services should be considered on smart industry researches.

6 Conclusions

The Industry 4.0 project promises to break-thru the boundaries of the conventional industries by the Information and Communication Technology (ICT). In addition, it is expected the increase of the number of members on the production chain in a collaborative environment, on which their location is indifferent and all the resource could be accessed by ubiquitous systems from any place of the world. In the same way it is expected that all the objects involved on the production processes can be available as services, and that they could communicate and exchange information among them.

The Industry 4.0 expectations and its complexity caused by the large number of interconnected machines, products, processes and people could increase the challenges and expand the opportunities for the research fields such as data security, standardization, and services interoperability. The SMEs may gain force on the Industry 4.0 by the virtual enterprise establishment. The shared skills, knowledge and resources as services over the cloud-manufacturing context, should leverage the business potential and improve the customer satisfaction. Although, strategies and methods should be adopted to improve the service composition among thousands of objects, services, and business.

Acknowledgments. The authors would like to thank the financial support of the Brazilian government agency MEC/CAPES, for funding the DINTER USP-IFSC.

References

1. Kagermann, H., Wahlster, W., Helbig, J.: Recommendations for Implementing the Strategic, Initiative Industrie 4.0. ACATECH, Frankfurt (2013)
2. Lasi, H., Kemper, H.-G., Fette, P., Feld, T., Hoffmann, M.: Industry 4.0. *Business & Information Systems Engineering* **4**, 239–242 (2014)
3. MacDougall, W.: Industrie 4.0 – Smart Manufacturing for the Future. Germany Trade & Invest, Berlin, Germany (2014). www.gtai.de
4. Heng, S.: Industry 4.0 – Upgrading of Germany’s Industrial Capabilities on the Horizon. Deutsche Bank Research, Frankfurt, Germany (2014). www.dbresearch.com
5. Schuh, G., Potente, T., Varandini, R., Schmitz, T.: Global Footprint Design on Genetic Algorithms – An “Industry 4.0” perspective. *CIRP Annals – MT* (2014)
6. Shi, J., Wan, J., Yan, H., Suo, H.: A Survey of Cyber-Physical Systems. *Wireless Communications and Signal Processing*, 1–6 (2011)
7. Jazdi, N.: Cyber Physical Systems in the Context of Industry 4.0. *AQTR - Automation, Quality and Testing, Robotics*, 1–4 (2014)
8. Xu, X.: From Cloud Computing to Cloud Manufacturing. *Robotics and Computer-Integrated Manufacturing* **28**, 75–86 (2012)
9. Gruner, F., Kassel, S.: Extending lifecycle of legacy systems – an approach for SME to enhance their supported business processes through a service-integration-system. In: Camarinha-Matos, L.M., Shahamatnia, E., Nunes, G. (eds.) *DoCEIS 2012. IFIP AICT*, vol. 372, pp. 43–50. Springer, Heidelberg (2012)
10. Wang, X., Xu, X.: An Interoperable Solution for Cloud Manufacturing. *Robotics and Computer-Integrated Manufacturing* **29**, 232–247 (2013)
11. Dustdar, S., Papazoglou, M.: Services and Service Composition. *IT - Information Technology* **50**, 86–92 (2008)
12. Liu, W., Su, J.: A solution of dynamic manufacturing resource aggregation in CPS. In: *IEEE: ITAIC*, vol. 2, Chongqing, pp. 65–71 (2011)
13. da Silva, R.M., Blos, M.F., Junqueira, F., Santos Filho, D.J., Miyagi, P.E.: A service-oriented and holonic control architecture to the reconfiguration of dispersed manufacturing systems. In: Camarinha-Matos, L.M., Barrento, N.S., Mendonça, R. (eds.) *DoCEIS 2014. IFIP AICT*, vol. 423, pp. 111–118. Springer, Heidelberg (2014)
14. Li, G., Wei, M.: Everything-as-a-service platform for on-demand virtual enterprises. *Information Systems Frontiers* **16**, 435–452 (2012)
15. Wu, D., Greer, M., Rosen, D., Schaefer, D.: Cloud Manufacturing: Strategic Vision and State-of-the-art. *Journal of Manufacturing Systems* **32**, 564–579 (2013)
16. Seiger, R., Keller, C., Niebling, F., Schlegel, T.: Modelling Complex and Flexible Processes for Smart Cyber-physical Environments. *Journal of Computational Science* **294** (2014)
17. Cai, G., Zhao, B.: An Approach for Composing Services based on Environment Ontology. *Journal Mathematical Problems in Engineering*, 1–11 (2013)
18. Fattori, C., Junqueira, F., Santos Filho, D., Miyagi, P.: Service composition modeling using interpreted petri net for system integration. In: *IEEE ICMA 2011*, pp. 696–701 (2011)
19. Sheng, Q., Qiao, X., Vasilakos, A., Szabo, C., Bourne, S., Xu, X.: Web Services Composition: A Decade’s Overview. *JIS* **280**, 218–238 (2014)
20. Ungurean, I., Gaitan, N.-C., Gaitan, V.G.: An IoT architecture for things from industrial environment. In: *10th COMM*, pp. 1–4. IEEE (2014)

Cloud-Based Framework for Practical Model-Checking of Industrial Automation Applications

Sandeep Patil^{1(✉)}, Dmitrii Drozdov^{1,2}, Victor Dubinin², and Valeriy Vyatkin^{1,3}

¹ Luleå University of Technology, Luleå, Sweden
{sandeep.patil, dmitrii.drozdov}@ltu.se

² Penza State University, Penza, Russia
victor_n_dubinin@yahoo.com

³ Aalto University, Helsinki, Finland
vyatkin@ieee.org

Abstract. In this paper we address practical aspects of applying the model-checking method for industrial automation systems verification. Several measures are proposed to cope with the high computational complexity of model-checking. To improve scalability of the method, cloud-based verification tools infrastructure is used. Besides, closed-loop plant controller modelling and synchronization of transitions in the SMV (input language for symbolic model checking) model aim at complexity reduction. The state explosion problem is additionally dealt with by using an abstraction of the model of the plant with net-condition event systems, which is then translated to SMV. In addition, bounded model-checking is applied, which helps to achieve results in cases when the state space is too high. The paper concludes with comparison of performance for different complexity reduction methods.

Keywords: Formal verification · Closed-loop modelling · Model-checking · SMV · NCES · Industrial automation · IEC 61499

1 Introduction

Formal verification is an act of proving or disproving an algorithm with respect to some specification or property and model-checking is one such formal verification approach introduced in early 1980s by Clarke and Emerson [1, 2]. A model-checker generates state space of the model that includes all or some states and transitions. Each path in the state space corresponds to one system's run or a single test case. Model-checking enables the unsupervised automatic verification process of a system by generating the state space and identifies system failure via counterexamples (a scenario (state trace) that breaks the safety property of the system). Properties to be verified are specified using many methods, including temporal logic, automata, etc. While model-checking is computationally resource hungry, it has been successfully used in other adjacent areas of computer systems engineering, such as hardware design, proving its ability to handle problems of reasonably large complexity [3, 4]. This suggests that it can be also applied in the industrial automation domain, and

there have been impressive number of research works towards this goal [5, 6]. For safety-critical applications, formal verification is one of the most efficient ways to prove system's correctness.

2 Cloud-Based Model-Checking Infrastructure

Verification tasks consume many resources and verification process can run for days and block all important personal computer resources. In this section, we present how we could run verification remotely on a service such as Amazon Elastic Compute Cloud that grows according to the need. A verification problem usually contains specifications that are to be evaluated to prove or disprove many properties and each property checking can run as a separate process. Hence the option to perform verification tasks in the cloud instead of running them on an own computer provides performance related improvements. The cloud-based solution takes advantage of highly scalable parallel computations and more cost-efficiency in comparison to supporting own computation infrastructure.

Fig. 1 shows possible decomposition of full verification with Bounded Model Checking (BMC). For each single bound, the NuSMV [7] verifier can generate a separate SAT-problem [7]. And all these SAT problems can be solved in parallel tasks (on many Amazon Cloud instances for example).

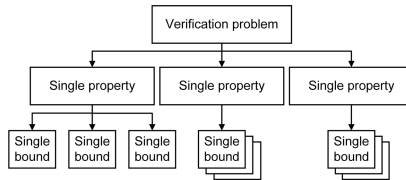


Fig. 1. Dividing the verification problem across multiple instances

In this work it is assumed that controllers are presented in terms of the function blocks of IEC 61499 standard that generalizes traditional programming paradigms of industrial automation for the case of component-based distributed systems.

For the function block models, memory consumption grows linearly for a single bound verification with NuSMV and this behaviour provides highly predictable resource needs. Reconfigurable clouds such as example Amazon EC2, enables us to tune cloud resources for specific model and reach high cost-efficiency.

3 Model Reduction with Plant Abstraction

In model-checking one of the most common problems is the state space explosion[8], which is tackled by various techniques [9]. In this section we present an abstraction technique in order to reduce the state space of the formal model that we use. This abstraction is built on top the closed-loop modelling previously proposed in model-checking of function block systems [10].

3.1 Plant Model Abstraction Using Net Condition-Event Systems (NCES)

In the closed-loop framework, both controller and plant are modelled with formalism, and then the combined model is exposed to model-checking. The controller model is automatically generated from the function block source code, using the function block (FB) operational semantics [11]. Therefore abstractions cannot be applied to the controller's model without loss of important execution aspects, hence we abstract on the model of the plant.

The control signals actuating the plant can be both value (level) and event (edge) signals. The formalism of NCES [12, 13] has sufficient expressiveness to represent them.

In works [10, 14] modelling and verification of closed-loop automation systems using NCES was described. In work [15] the methods to model Petri net in SMV [16] were proposed. Using first and second methods in combination with event signal transfer rules from FB operational semantics, hierarchical NCES models can be transformed into SMV.

The NCES model is wrapped into FB SMV module interface and contains input transition-place pairs (Fig. 2 (a)) which are designed such that all input transitions are fired synchronously. If an activation event occurs, transition rewrites place marking regard to 'data input' value, for simple plant models with Boolean inputs, considered in this paper, the place becomes marked if 'data input' value is TRUE, otherwise the place becomes unmarked.

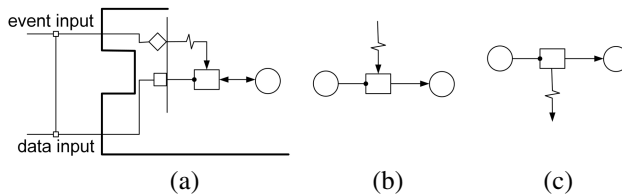


Fig. 2. (a) Synchronous transition-place pair and (b, c) typical NCES transitions

Fig. 2(b) shows a typical event activated transition (event consumer). The simple Petri net transition SMV module [15] can be transformed into NCES transition with event trigger by adding an event in 'enable' rule and simple unconditional event reset statement.

This approach mainly corresponds to events in FB operational semantics. The code snippet below shows the SMV module with the changes, line 2 shows the enable rule and the 'next()' statements show setting/resetting rules.

```

MODULE pnpVacuumOn(event_in, input, output)
DEFINE enabled := input & event_in;
ASSIGN
next(input) := case
    enabled : FALSE;
    TRUE   : input;

```

```

esac;
(*... Output goes here ... *)
next(event_in) := FALSE;

```

Fig. 2 (c) shows a typical event emitting transition. Event signal transmission is performed through signal buffers (SMV variables), which are set as ‘true’ when event emitting module fires and reset as ‘false’ every time an event consumer module runs. The code snippet below shows the SMV module exemplifies the setting and resetting of event emission.

```

MODULE pnpVacuumOn(input, output, event_out)
DEFINE enabled := input;
ASSIGN
next(input) := case
enabled : FALSE;
TRUE : input;
esac;
(*... Output goes here ... *)
next(event_out) := case
enabled : TRUE;
TRUE : event_out;
esac;

```

3.2 Example: A 3 Cylinder Pick-n-Place Manipulator

Fig. 3 (a) shows the 3-cylinder Pick-and-Place manipulator case study. It consists of 2 vertical and 1 horizontal cylinders and a suction unit (vacuum). Each cylinder has two sensors indicating two end positions of the piston. Full model verification with NCES was described in works [10, 14], in this paper we propose a way to verify full operational semantics-based controller model [11] with plant abstraction.

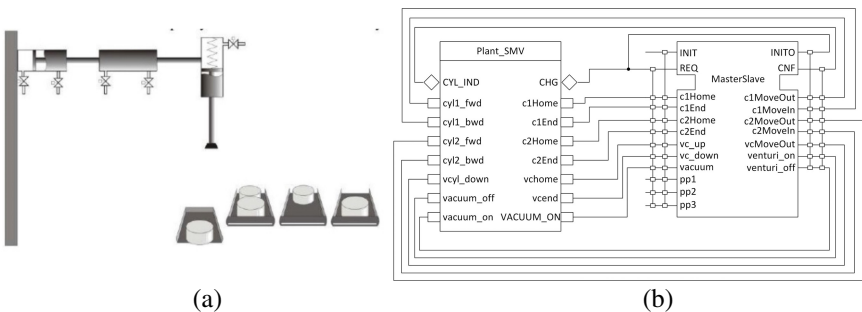


Fig. 3. 3-cylinder PnP manipulator and its closed-loop model (with NCES plant) schema

Fig. 3(b) shows the closed-loop model schema with MasterSlave controller[17] and the NCES plant model. At the initial state, the input ‘INIT’ has value ‘TRUE’, which

corresponds to the occurrence of event ‘INIT’ in the beginning of execution. Event output ‘INITO’ is connected to input ‘REQ’. This connection provides an entry point for system’s main execution path, which may be described as a cycle of the occurrence of events

$$REQ \rightarrow CNF \rightarrow CYL_IND \rightarrow CHG \rightarrow REQ \rightarrow \dots$$

Also, input pp1 is ‘true’ and pp2 and pp3 are ‘false’ (workpiece is present in place 1 and places 2 and 3 are empty) for model testing. But in real systems checking these variables can be left “free” to verify all possible system states, or they can be connected to environment emulation module.

The simplest abstract model of the cylinder consists of only two states: ‘home’ and ‘end’ and two transition between these states. Transition emits event ‘CHG’ when it fires. Vacuum model contains only two states as well.

Fig. 4(a) shows simple NCES models for vacuum and cylinder modules. The vacuum module has two inputs ‘vacuum_on’ and ‘vacuum_off’ and two outputs: ‘vacState’ and event ‘CHG’. Two places ‘On’ and ‘Off’ represent simple vacuum states and transitions between this states emit event ‘CHG’ when fire. Cylinder model has two inputs and two states as well, but transitions with inhibitor arcs provide operation regard to rules:

$$ToHome.enabled = fwd \& \overline{bwd};$$

$$ToEnd.enabled = \overline{fwd} \& bwd;$$

Fig. 4(b) shows the plant model with synchronous transitions inside the FB interface (wrapper). Inputs of NCES cylinders and vacuum are connected to synchronous transition-place pairs and outputs are merged with wrapper’s outputs (in this case, event signal buffers reset is managed by wrapper and “outer” SMV module regard to FB operational semantics).

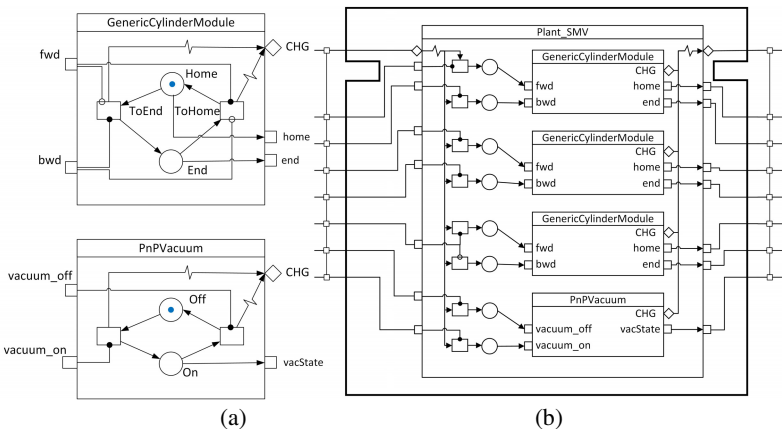


Fig. 4. (a) Vacuum and cylinder NCES-models and (b) Plant model with FB wrapper

4 Synchronous Function Block SMV Models

4.1 SMV Processes

Most of SMV language implementations support asynchronous module instances, implemented with keyword ‘process’ [16]. Usage of asynchronous processes provides simple representation of concurrent tasks but analysis of all possible execution orders together with increasing number of processes causes exponential state space growth (so-called state space combinatorial explosion). This problem affects resource consumption, for example memory and verification time.

FB application SMV model, based on FB operational semantics, proposed in work [11] uses FB instance mapping to asynchronous SMV processes. This approach provides intuitively clear FB types and instances mapping and allows avoiding the problem with access of multiple modules to one signal buffer. It is also the simplest way to model asynchronous execution discipline in SMV. Fig. 5 shows access of two modules to event signal buffer. Value ‘TRUE’ of the buffer SMV variable means the event occurred and has not been read yet. So one module “puts” an event to the buffer (set TRUE value to the buffer SMV variable) and another module receives event (reads the variable) and resets SMV variable value to FALSE.

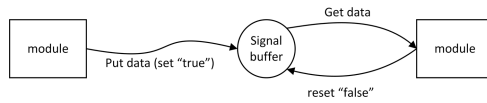


Fig. 5. Access to shared signal buffer

4.2 Synchronous Module Instances with External Buffer Controller

The approach to solve the multiple access problems with synchronous modules is based on external buffer controller, which contains all assignments of the shared buffer. (b)

Fig. 6(a) shows the controller that uses module selector variable to select one of many assignment rules, collected from accessing modules.

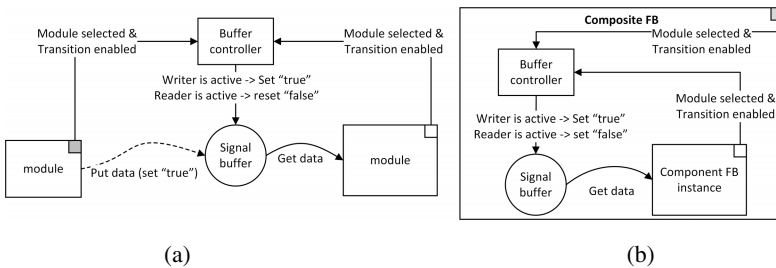


Fig. 6. (a) External buffer controller and (b) Buffer controller in composite FB

4.3 Synchronous FB Modules with Buffer Controller in SMV

In the function block SMV model, the execution order is fully determined by dispatchers. The problem of concurrent access to SMV variable occurs in event signal buffers, which are accessible from composite FB and its components. In this case, the schema shown in (b)

Fig. 6(a) can be modified and external buffer controller can be placed in a composite FB as it is shown in (b)

Fig. 6(b).

A composite FB model contains buffer SMV variables and it should contain buffer controllers. Composite FB SMV module and each asynchronous component instance contain own 'next' expressions to change shared event signal buffers (setting of output and resetting of input events). For synchronous modules this expressions from all component instances can be merged in composite FB and placed either in separated buffer controller modules, or in composite FB module definition.

signal_reset_rule and *signal_set_rule* in component FBs are declared with DEFINE statements. Alpha and beta rules should be defined in components and their 'next' statements should be merged into composite FB dispatcher.

For component event inputs.

```
next(event_signal) := case
  signal_set_rule : TRUE;
  component.signal_reset_rule
: FALSE;
  TRUE : event_signal;
esac;
```

For component event outputs.

```
next(event_signal) := case
  component.signal_set_rule :
TRUE;
  module_is_active : FALSE;
  -- unconditional reset
  TRUE : event_signal;
esac;
```

5 Results

Table 1 shows comparison of RAM usage and verification time for full PnP model and reduced with the first approach (described in section 3). Table 2 shows comparison of RAM usage and verification time for bounded model checking with single bounds for PnP model with asynchronous modules and synchronous ones.

Table 1. Model checking in Cadence SMV

Model	Time	RAM
Full PnP model	-	> 2GB*
Reduced PnP model	294 s	1082 MB

* On Win32 Cadence SMV running under Windows 7 x64, reaching of 2GB memory limit cause program failure, on Windows x32 versions, verification process stuck for hours without any results.

Table 2. Bounded model checking with the second approach

Single bound value	PnP model with async. instances		PnP model with sync. instances	
	Time	RAM	Time	RAM
20	42.93 s	2134 MB	20.37 s	1875 MB
50	> 12 hours	~7 GB	58.15 s	4721 MB
70	> 12 hours	~ 11 GB	73.18 s	5689 MB

6 Conclusion

Proposed modification of function blocks SMV models with synchronous modules allows for reduction of BMC verification time to reasonable limits. And the abstraction technique, using NCES to represent plant model, allows us to reduce model complexity when it necessary to keep within memory limits. Both, these techniques allow us to apply model-checking for verification of IEC 61499 closed-loop systems, and make this approach cost-efficient with cloud technologies.

Acknowledgments. This work was partially supported by the Federal Targeted Programme "Research and development in priority areas of elaboration of STC of Russia for 2014-2020" (agreement of 19.06.2014 № 14.574.21.0045), and by Luleå Tekniska Universitet, grants 381119, 381940 and 381121.

References

1. Clarke, E.M., Emerson, E.A.: Design and synthesis of synchronization skeletons using branching-time temporal logic. In: Logic of Programs Workshop (1982)
2. Emerson, E.A., Clarke, E.: Characterizing correctness properties of parallel programs using fixpoints. In: de Bakker, J., van Leeuwen, J. (eds.) Automata, Languages and Programming, vol. 85, pp. 169–181. Springer, Heidelberg (1980)
3. Fix, L.: Fifteen years of formal property verification in intel. In: Grumberg, O., Veith, H. (eds.) 25 Years of Model Checking. LNCS, vol. 5000, pp. 139–144. Springer, Heidelberg (2008)
4. Kern, C., Greenstreet, M.R.: Formal verification in hardware design: a survey. ACM Trans. Des. Autom. Electron. Syst. **4**, 123–193 (1999)
5. Hanisch, H.-M., Hirsch, M., Missal, D., Preuße, S., Gerber, C.: One decade of IEC 61499 modeling and verification-results and open issues. In: 13th IFAC Symposium on Information Control Problems in Manufacturing. V.A. Trapeznikov Institute of Control Sciences, Russia (2009)
6. Vyatkin, V., Hanisch, H.M.: Formal modeling and verification in the software engineering framework of IEC 61499: a way to self-verifying systems. In: Proceedings of the 8th IEEE International Conference on Emerging Technologies and Factory Automation, vol. 2, pp. 113–118 (2001)
7. Cimatti, A., Clarke, E., Giunchiglia, E., Giunchiglia, F., Pistore, M., Roveri, M., Sebastiani, R., Tacchella, A.: NuSMV 2: an opensource tool for symbolic model checking. In: Brinksma, E., Larsen, K.G. (eds.) CAV 2002. LNCS, vol. 2404, pp. 359–364. Springer, Heidelberg (2002)

8. Clarke, E., Grumberg, O., Jha, S., Lu, Y., Veith, H.: Progress on the state explosion problem in model checking. In: Wilhelm, R. (ed.) *Informatics: 10 Years Back, 10 Years Ahead*. LNCS, vol. 2000, pp. 176–194. Springer, Heidelberg (2001)
9. Clarke, E., Grumberg, O., Jha, S., Lu, Y., Veith, H.: Counterexample-guided abstraction refinement. In: Emerson, E.A., Sistla, A.P. (eds.) *CAV 2000*. LNCS, vol. 1855, pp. 154–169. Springer, Heidelberg (2000)
10. Patil, S., Bhadra, S., Vyatkin, V.: Closed-loop formal verification framework with non-determinism, configurable by meta-modelling. In: *IECON 2011 - 37th Annual Conference on IEEE Industrial Electronics Society*, pp. 3770–3775 (2011)
11. Patil, S., Dubinin, V., Pang, C., Vyatkin, V.: Neutralizing semantic ambiguities of function block architecture by modeling with ASM. In: *9th International Andrei Ershov Memorial Conference, PSI 2014, Peterhof, St. Petersburg, Russia* (2014)
12. Hanisch, H.-M., Lüder, A.: Modular modeling of closed-loop systems. In: *Proc of Colloquium on Petri Net Technologies for Modeling Communication Based Systems*, Berlin, Germany, pp. 103-126 (2000)
13. Pinzon, L., Jafari, M.A., Hanisch, H.M., Peng, Z.: Modeling admissible behavior using event signals. *IEEE Transactions on Systems, Man, and Cybernetics, Part B: Cybernetics* **34**, 1435–1448 (2004)
14. Patil, S., Vyatkin, V., Sorouri, M.: Formal verification of Intelligent Mechatronic Systems with decentralized control logic. In: *2012 IEEE 17th Conference on Emerging Technologies & Factory Automation (ETFA)*, pp. 1–7 (2012)
15. Wimmel, G.: *A BDD-based Model Checker for the PEP Tool*, Major Individual Project Report, Dept. (1997)
16. Cadence SMV Model Checker (March 4). <http://www.kenmcmil.com/smv.html>
17. Sorouri, M., Patil, S., Vyatkin, V.: Distributed control patterns for intelligent mechatronic systems. In: *2012 10th IEEE International Conference on Industrial Informatics (INDIN)*, pp. 259–264 (2012)

A Cloud-Based Infrastructure to Support Manufacturing Resources Composition

Giovanni Di Orio^(✉), Diogo Barata, André Rocha, and José Barata

CTS – UNINOVA Departamento de Engenharia Electrotécnica Faculdade de Ciências e Tecnologia, Universidade Nova de Lisboa, 2829-516 Caparica, Portugal {gido, andre.rocha, jab}@uninova.pt, Diogo.abarata@gmail.com

Abstract. Current development in emerging technologies, such as the Internet of Things (IoT), service-oriented and high-performance computing combined with the increasing advancement of manufacturing technologies and information systems, triggered a new manufacturing model. Modern industrial automation domain is characterized by heterogeneous equipment encompassing distinct functions, network interfaces and I/O specifications and controlled by distinct software/hardware platforms. To cope with such specificity, manufacturing enterprises are demanding for new service-oriented models that aim to abstract physical systems in terms of their functionalities/capabilities. In this scenario, Cloud Manufacturing (CMfg) arises as a new networked, service-oriented, customer centric and demand driven paradigm where manufacturing resources and capabilities are virtualized as services available in the cloud to users.

Keywords: Cloud manufacturing · Service-oriented architecture · Service composition · Device profile for web services

1 Introduction

Nowadays, manufacturing companies are more and more concerned with meeting the dynamic requirements imposed by the globalization [1]. Researchers and industry practitioners are striving for constant improvements and innovation in the business processes as a necessary condition for keeping the manufacturing companies competitive in market sharing [2]. In this scenario, the combination of new emerging technologies and paradigms such as IoT, Machine-to-machine (M2M), Cloud-computing/manufacturing, service-oriented architecture (SOA), service-oriented computing (SOC) together with the wider dissemination of information technology (IT) are driving powerful and, above all, new business opportunities for manufacturing enterprises. As deeply exposed in [3], for many years, business infrastructures has been mainly focused on connecting IT systems within the business environment. However, there are many businesses that are characterized by thousands of heterogeneous and geographically distributed devices deployed across the enterprise which are generating and consuming data and are isolated/separated from the enterprise IT backbone. This is particularly true in the manufacturing domain where the production processes are typically known for their plethora

© IFIP International Federation for Information Processing 2015

L.M. Camarinha-Matos et al. (Eds.): DoCEIS 2015, IFIP AICT 450, pp. 82–89, 2015.

DOI: 10.1007/978-3-319-16766-4_9

of heterogeneous equipment encompassing distinct functions, form factors, network interfaces and I/O specifications supported by different software and hardware platforms [4]. Today, mostly manufacturing enterprises have their operation technologies (OT) separated from the IT backbone infrastructure implying that the data generated by the field equipment is rarely used within business. As stated in [3], the business leaders of today are becoming more and more conscious about the possibilities and opportunities of gaining access to this data. In particular, data can be used for identifying important production events, predicting market fluctuations, savings costs and/or improving the overall quality of the products while optimizing their production processes. Furthermore, the rapid convergence of OT and IT – triggered by the proliferation of plant-floor Ethernet, smart devices, sensors networks, local computing solutions and network technologies – is rapidly changing the way the data can be used by enabling from one side the transformation of information into insight and from the other side extending the reach of the business [3][5]. In this context, cloud-based systems enable manufacturing enterprises to improve data management even further and move performance and profitability to a level once thought impossible while accommodating operational spikes more easily, procuring manufacturing resources when needed – and only when needed, on demand and as shared resource [6].

Finally, the introduction of cloud-based system in the world of manufacturing production systems can bring into the game the necessary degree of dynamicity and capability to change to enable enterprises to survive in current dynamic environment, i.e. to be able to respond to competitive challenges and to sustain their competitive advantage in order to reach the success [7].

2 Contribution to Cloud-Based Engineering Systems

The embedded technology progresses are promoting the transfer of more complex functionalities – currently hosted on powerful back end systems – in the world of manufacturing resources at shop floor level [2]. This technological revolution is radically changing the way production systems are designed and deployed, as well as, monitored and controlled. The dissemination of smart devices inside production processes confers new visibility on the production system while enabling for a more efficient and effective management of the operations. Taking advantage of the current technological trends, CMfg aims to integrate manufacturing resources into the cloud manufacturing services in order to expose them as a service to the users [8]. The binomial manufacturing resource/service will push the entire manufacturing enterprise visibility to another level while enabling the global optimization of the operation and processes of a production system and – at the same time – supporting its accommodation to the operational spike easily and with reduced impact on production. The present work implements a cloud-based infrastructure for achieving the resource/service value-added i.e. to facilitate the creation of services that are composition of currently available atomic services. In this context, manufacturing resource virtualization (i.e. formalization of resources capabilities into services accessible inside and outside the enterprise) and semantic representation/description are the pillars

for achieving resource service composition (RSC). In conclusion, the present work aims to act at the manufacturing resource layer where physical resources and shop floor capabilities are going to be provided to the user as SaaS (Software as a Service) and/or IaaS (Infrastructure as a Service).

3 Supporting Concepts

3.1 Cloud Manufacturing

CMfg is a new paradigm where manufacturing resources and capabilities are virtualized as services available in the cloud to users. This concept was firstly proposed by [9] with the intent to transform the manufacturing business into a new paradigm where manufacturing resources (i.e. physical devices, machines, products, processes, etc.) are transformed into cloud entities. This transformation is also called virtualization and enables for full sharing and circulation of virtualized resources that are capable of providing fundamental information about their own status. This information can potentially be used for local and global optimisation of the whole lifecycle of manufacturing. The current work addresses this theme by presenting a cloud-based infrastructure that enables manufacturing devices virtualization, deployment and selection by users for dynamically assembling them into a virtual manufacturing solution.

3.2 Service-Oriented Architecture (SOA)

SOA paradigm has emerged and rapidly grown as a standard solution for publishing and accessing information in an increasingly Internet-ubiquitous world. SOA defines an architectural model aiming to enhance efficiency, interoperability, agility and productivity of an enterprise by positioning services as the building blocks through which solution logic is represented in support of realization of strategic goals [10]. The existence of Web Services technology has enabled and stimulated the implementation and development of SOAs. The application of SOA and Web Services in the context of manufacturing layer is still scarce, since a set of persisting technical challenges exists as pointed in [11]. SOA and Web Service are considered promising techniques for integrating all the existing layers within a manufacturing enterprise spacing from business to the physical process. The capability of encapsulating functions and tools as services through standard interfaces and protocols, enables their access and usage by clients without the need to know and control their specific implementations. All these aspects promote the SOA paradigm and its most used implementing technology (Web Services) as the *de-facto* standards for fast, secure and, above all, easy integration of any new functionality within existing software solutions while electing them as one of the pillars for implementing the CMfg paradigm.

3.3 Service Composition

Services are the building block of a SOA, they provide simple interactions between client and server provider. However, sometimes atomic services need to be straightforwardly combined and/or assembled in order to generate more complex ones rising the service abstraction as referred by [12]. In this scenario as argued in [13], the term service composition is referred to the process of developing a composite service. Moreover, a composite service can be defined as the service that is obtained by the composition of the functionalities of several simplest services.

Currently in the domain of SOA-based systems, two main approaches can be used for the service composition, namely [14]: orchestration and choreography.

3.4 Devices Profile for Web Services

The Device Profile for Web Services (DPWS) is a standard by the OASIS Web Services Discovery¹ and Web Services Devices Profile Technical Committee². It defines two main elements: the device and the hosted services. The device element gathers all the meta-information about the attached physical device that is provided during the discovery activity. The hosted services gathers the main functionalities of the device. As explained in [15], the application of Web Services at device level implies significant improvements in both operational and development aspects while unifying the ICT protocols of a manufacturing enterprise by providing a single stack to communicate from device-level to MES or ERP level over Web Service technology.

4 Cloud-Based Infrastructure

The proposed infrastructure (see Fig. 1) is composed by three main components/resources, namely: the *deployer*, the *cloud server manager* and the *client UI*.

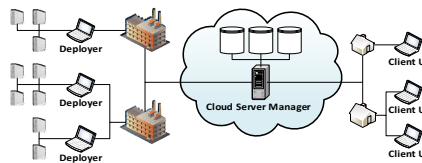


Fig. 1. Infrastructure Architecture

These three components/resources are together responsible for:

1. virtualizing the manufacturing resources available in the physical system in terms of capabilities and functionalities and deploying such virtualized resources in the cloud (cloud entities);

¹ <http://docs.oasis-open.org/ws-dd/ns/discovery/2009/01>

² <https://www.oasis-open.org/committees/ws-dd/>

2. Exposing the capabilities/functionalities of the cloud entities for enabling their invocation by external users that are accessing the cloud in order to execute certain tasks on the physical system.

In the next sections, a detailed description of the developed components/resources is given.

4.1 Deployer

The *deployer* is the component/resource responsible to scan the network (i.e. the local network in which it is connected) searching for *DPWS*-enabled devices. Whenever a new device is encountered then the following tasks are executed:

- **Virtualization:** an abstract description will be associated to each device in order to transform the physical device into a cloud entity.
- **Deployment:** make the virtualized devices available on the cloud for allowing the users to invoke the functionalities/services hosted by the device according to their needs.

Taking into account these tasks, the architecture of Fig. 2 has been designed and implemented for the *deployer*. The proposed architecture is constituted by the following core task-oriented components:

- **Device Explorer:** it allows to search the network for available *DPWS*-enabled device.
- **Device Virtualization:** once a device is discovered this component extracts all the information from the device with the objective of creating a virtual entity with all the capabilities of the physical device.
- **Device Repository:** it is responsible to store all the information about the devices in the network and push it into the cloud. This information will be internally used by the Device Handler (whenever a new request comes from the cloud) and externally by the *server* component/resource.
- **Device Handler:** it is responsible to handle requests asking for the execution of some functionality that come from the cloud.

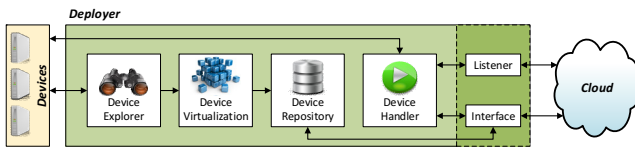


Fig. 2. Detail of the *deployer* architecture

4.2 Cloud Server Manager

The *cloud server manager* component/resource (see Fig. 3) is actually hosted into the Amazon Web Services³ (AWS) free tier. This cloud provide a virtualized resources

³ <http://aws.amazon.com/free/>

that enables the accessibility of the *cloud server manager* component/resource from everywhere while allowing the configuration of the storage and processing power according to the user needs. The *cloud server manager* component/resource provide two Web Service endpoint to permit from one side the communication with the *deployer* and from the other side the communication the *client*. Moreover, it includes a local database that is used to store all the information about the devices connected to the *deployer* and their related functionalities. Furthermore, the database also stores all the requests performed by the client using the *client UI* and all the responses to these requests performed by the *deployer*. Thereby, the *cloud server manager* is also responsible to guarantee the communication between *deployers* and *client UIs*.

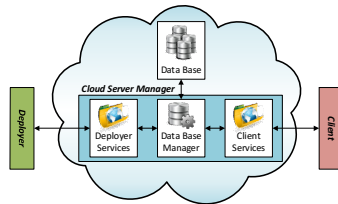


Fig. 3. Detail of the *cloud server manager* component/resource

4.3 Client UI

The *client UI* (User Interface) is a simple graphical form that allows the users connected to the cloud to both select the capabilities/functionalities that they need and to graphically compose them to create complex tasks to execute on the physical process. Therefore, the *client UI* is logically composed by two main components, namely: a graphical control that allows the creation of the composition of capabilities/functionalities and an internal engine that translates the graphical representation of the composite tasks into requests to be sent to the *cloud server manager*.

5 Experimental Setup

As proof of concept, the MOFA kit by Staudinger GmbH has been used. This educational kit simulates a flexible manufacturing system and is composed by four machines, a buffer area, a crane robot, local transporters (conveyors or tables) and sensors to detect product positions. The original control equipment was replaced by Inico⁴ S1000 components. The S1000 is a smart remote terminal unit (RTU) capable of real-time control, field data processing and web-based monitoring, programming and configuration tool. Moreover, it offers an embedded web server and implements a XML/SOAP interface based on DPWS standard. More details about the system used and its related monitoring and control solution can be found in [4].

⁴ <http://www.inicotech.com/index.html>

The developed cloud-based infrastructure has been instantiated on the presented kit. The system configuration is presented in Fig. 4. The *deployer* is a local entity that will gather all the information about the physical devices (Inico S1000) connected and the capabilities/functionalities hosted. This information is passed to the *cloud server manager* that will expose it in order to be accessed and eventually requested by cloud users. Moreover, the *cloud server manager* also keep the information about the *deployer* localization. Finally, the *cloud UI* will provide a user interface where the user can pick the capabilities/functionalities he required and compose them to create a process plan.

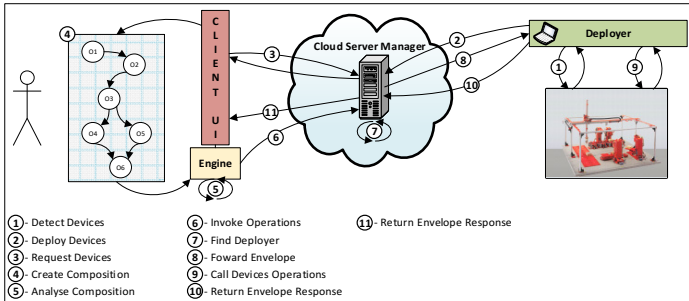


Fig. 4. Generic System configuration and workflow

For the time being, the focus of the present work was to provide an infrastructure capable from one side to transform manufacturing resources into virtualized cloud entities deployed into the cloud and, from the other side, to expose the resources capabilities in order to enable external users to create simple processes by combining the available capabilities (using the provided graphical tool).

6 Conclusions and Future Works

The present infrastructure provides a cloud-based manufacturing system where available manufacturing resources are virtualized as cloud entities and which capabilities/functionalities are exposed for enabling the creation of processes by composition of such capabilities/functionalities. During this work some fundamental pillars of the CMfg paradigm have been approached, namely: virtualization access, deployment into cloud and service encapsulation of physical manufacturing resources. The present work proves the feasibility of the CMfg paradigm if it is supported by smart/intelligent devices. Moreover, the implemented infrastructure provides a normalized layer where the typical heterogeneity of the automation domain is hidden into a generic semantic representation. Furthermore, since the solution is supported by open web standards it leaves the doors open for the integration of more internet-based solution such as Self-Learning solutions [16]. However, some improvements opportunities can also be found. First of all the integration of a more sophisticated graphical tool for service composition is required (BPMN, BPEL, etc.). Secondly, the semantic representation can be significantly improved by introducing ontologies (OWL, OWL-S, etc.).

Acknowledgments. This research was partially developed under the “ProSEco” project, Grant agreement no: 609143”, European Commission under the FP7 Programme.

References

1. Wu, D., Thames, J.L., Rosen, D.W., Schaefer, D.: Enhancing the Product Realization Process With Cloud-Based Design and Manufacturing Systems. *J. Comput. Inf. Sci. Eng.* **13**(4), 041004 (2013)
2. de Souza, L.M.S., Spiess, P., Guinard, D., Köhler, M., Karnouskos, S., Savio, D.: SOCRADES: a web service based shop floor integration infrastructure. In: Floerkemeier, C., Langheinrich, M., Fleisch, E., Mattern, F., Sarma, S.E. (eds.) *IOT 2008. LNCS*, vol. 4952, pp. 50–67. Springer, Heidelberg (2008)
3. Davidsen, L.: *IBM MQ: Integrated messaging to connect your enterprise*. IBM Corporation (2014)
4. Candido, G., Sousa, C., Di Orio, G., Barata, J., Colombo, A.W.: Enhancing device exchange agility in service-oriented industrial automation. In: 2013 IEEE International Symposium on Industrial Electronics (ISIE), pp. 1–6 (2013)
5. Rockwell Automation, The Connected Enterprise Maturity Model. CIE-WP002-EN-P (2014)
6. Katzel, J.: Power of the Cloud. *Control Engineering* **58**(12), 16–21 (2011)
7. Jassbi, J., Di Orio, G., Barata, D., Barata, J.: The impact of cloud manufacturing on supply chain agility. presented at the 12th IEEE International Conference on Industrial Informatics (INDIN 2014), Brazil (2014)
8. Zhang, L., Guo, H., Tao, F., Luo, Y.L., Si, N.: Flexible management of resource service composition in cloud manufacturing. In: 2010 IEEE International Conference on Industrial Engineering and Engineering Management (IEEM), pp. 2278–2282 (2010)
9. Li, B.-H., Zhang, L., Wang, S.-L., Tao, F., Cao, J., Jiang, X., Song, X., Chai, X.: Cloud manufacturing: a new service-oriented networked manufacturing model. *Comput. Integr. Manuf. Syst.* **16**(1), 1–7 (2010)
10. Erl, T.: *Service-Oriented Architecture: Concepts, Technology, and Design*. Prentice Hall PTR, Upper Saddle River (2005)
11. Ribeiro, L., Candido, G., Barata, J., Schuetz, S., Hofmann, A.: IT support of mechatronic networks: a brief survey. In: 2011 IEEE International Symposium on Industrial Electronics (ISIE), pp. 1791–1796 (2011)
12. Kavantzaz, N., Burdett, D., Ritzinger, G., Fletcher, T., Lafon, Y., Barreto, C.: *Web services choreography description language version 1.0, W3C Candidate Recomm.*, vol. 9 (2005)
13. Hazenberg, Meta Products. *Building the Internet of Things*. Uitgeverij Bis (2011)
14. Ashton, K.: That ‘internet of things’ thing. *RFiD J.* **22**, 97–114 (2009)
15. Candido, G., Jammes, F., de Oliveira, J.B., Colombo, A.W.: SOA at device level in the industrial domain: assessment of OPC UA and DPWS specifications. In: 2010 8th IEEE International Conference on Industrial Informatics (INDIN), pp. 598–603 (2010)
16. Di Orio, G.: *Adapter module for self-learning production systems*. FCT-UNL (2013)

Reconfigurable Manufacturing

Modeling of Mechanisms for Reconfigurable and Distributed Manufacturing Control System

Robson Marinho da Silva^{1,2}(✉), Edson H. Watanabe², Maurício F. Blos²
Fabrício Junqueira², Diolino J. Santos Filho², and Paulo E. Miyagi²

¹ Universidade Estadual de Santa Cruz, Ilhéus, BA, Brazil
rmsilva@uesc.br

² Escola Politécnica da Universidade de São Paulo, Butantã, SP, Brazil
{edsonh.watanabe,blosmauf,fabri,diolinos,pemiyagi}@usp.br

Abstract. This paper presents the modeling of fault diagnosis mechanisms extending a method to design reconfigurable and distributed manufacturing control system. The method combines different techniques: service-oriented architecture, holonic and multi-agent system, production flow schema and input-output place-transition Petri net. An application example demonstrates advantages of the proposal, such as at cloud-based engineering, reuse, implementation and reconfiguration flexibility.

Keywords: Reconfigurable control system · Service-oriented architecture · Holonic and multi-agent system · Petri net · Cloud manufacturing system

1 Introduction

Reconfigurable control systems have been proposed to implement manufacturing systems with different strategies because its business processes can modify due new demands and in case of fault occurrence [1]. Furthermore, geographically distributed manufacturing subsystems need communicating and collaborating with each other in a dynamic environment. To propose a feasible solution to design Reconfigurable and Distributed Manufacturing Control System (RDMCS), characteristics of different techniques should be combined. In [1,2], a method which associates top-down and bottom-up approaches through Petri Net (PN) [3, 4] combining Service-Oriented Architecture (SOA) [5] and Holonic and Multi-Agent System (HMAS) [6] concepts to model RDMCS was presented. The HMAS concept facilitates the development and integration of distributed and heterogeneous systems and SOA paradigm allows considering interoperability with other manufacturing systems. This paper extends that method to model RDMCS focusing on modeling of fault diagnosis mechanisms and describes an application example.

2 Relationship to Cloud-Based Solutions

In preview studies, the HMAS, SOA and PN concepts are combined to propose a method to design RDMCS [1, 2]. The basic assumption of this research is meeting the

needs of goal-directed behavior in a distributed, dynamic and unpredictable environment, using patterns to facilitate the development of new models and a suitable semantic. The SOA paradigm is applied to define interfaces for communication in models based on HMAS concepts. The semantic definition of business processes is combined in a top-down and bottom-up approach based on PN to organize specifications, reuse and integrate social structure. The dynamic models are edited using a web tool for Input Output Place Transition (IOPT) PN [7] which has modules for edition and simulation.

Therefore, according to cloud-based manufacturing statements [8], this method is related to this vision due characteristics as: (i) avoiding repetition and overlapping tasks through reuse; (ii) facilitating the analysis and communication between different design staffs through PN models and their available web tools; (iii) allowing reconfiguration flexibility for both rational use of resources and larger safety to fault detection through proposed control mechanisms; (iv) considering human interaction in dynamic environment of productive processes; and (v) allowing design a large complex system through modular models and collaboration between distributed subsystem.

3 State of the Art and Related Works

An overview of methodologies, architectures and applications as well as trends and challenges in HMAS are presented in [9]. Some architectures have a product-oriented vision and pay more attention to scalability and generic components of the system [10]. Others have a machine-oriented vision, paying more attention to an optimal utilization of the machine level than to the specific product performance [6]. However, in real applications much more complex and/or distributed subsystems may be combined into larger systems. On the other hand, SOA has revolutionized the distributed computing paradigm and made various kinds of inter-enterprise collaboration a reality [5]. Although SOA provides the framework for integrating cross-company services or technical interoperability, it does not address formal methods to ensure a systematic implementation of the design specifications [11]. According to [1, 3], the PFS associated to ordinary PN is a solution for transformation of abstraction into application level, a gap into design of discrete event systems and specifically in RDMCS. Furthermore, tools for edition of IOPT PN [4, 7] can be used to model a control system with the additional advantage that the models can quasi-automatically be converted to programs for industrial controllers.

4 Modeling of Diagnosis Mechanism for RDMCS

Modeling of the holons starts using a derivation of channel/ agent PN, called Production Flow Schema (PFS) [3]. The PFS models represent modifications on the flow¹ of items, activities and inter-activities. Then successive refinements are applied and the

¹ Terms associated to PN are in *Arial font*.

PFS model is more detailed at each level to generate the dynamic models in non-autonomous PN named IOPT [4]. This combined approach allows modeling system structures as well as system behaviors in a more simplified and transparent manner than ordinary Petri net representations.

The holons of this control architecture are: (i) *product holon (PrH)* which represents the *raw material*², *intermediate* or *final product*. The set of *PrHs* form the *production plan* holarchy which represents a recipe of how to join *raw material* and *intermediate products* to obtain the *final product*; (ii) *task holon (TH)* which represents the *business processes* strategies to attend the *product order*. The *TH* also is conceived to request the *reconfiguration* strategies; (iii) *supervisor holon (SuH)* which contains all the knowledge to coordinate the *operations*, registering components and the messages exchange and providing services combined with other entities; and (iv) *operational holon (OpH)* which represents the *resource* such as, the equipments, the staff manager and operators. Therefore, *PrH*, *TH* and *SuH* form the holarchies to represent the set of operations of the high level control (enterprise and factory control level); and each *OpH* represents an atomic service which can be combined with atomic services by other holons forming holarchies to represent the supervisory and shop floor control level.

Modeling of *PrHs* and *THs* is made by *activities* of PFS and the internal workflow is modeled using IOPT. To model the workflow, a *place* represents a state while a *transition* represents an event or operation that conducts the *flow* from one state to another. Modeling of *SuH* involves the workflow of resources abilities, messages exchange between holons, supervision and command to implement actions related to fault treatment. The register of messages are represented though PFS *distributors*. *OpHs* represent resources (control object) and are directly modeled in IOPT. To model them with the requirement of fault tolerance, each control object in IOPT includes normal and fault states (represented by *places*) and conditions (represented by *transitions*) for the change of states; these conditions are represented by logical represented by *guards*. Thus, the *OpHs* models consider real component behavior including influence of the environment and their faults. The synchronization of the holons can be made with *auxiliary places* or through *guard expression* which contains command signals represent by *input* or *output signal* which in turn can be fired by *input* or *output event*.

Concerning fault diagnostic, the method presents a mechanism called diagnoser. To model the diagnoser, it is necessary to define observable and non-observable events [12] that are related to fault specification. The steps for this modeling are: (i) diagnoser construction, initially considering normal operations only; (ii) linking the strategies implemented by means of *transitions* and *guard* to the possible observable and non-observable events that may occur from the initial state, and linking the states obtained according to *input* or *output signal* of actuators and sensors states; and (iii) linking the strategies implemented by means of *transitions* and *guard* to the events.

² Terms associated to ontology are in Courier font.

5 Modeling of Diagnosis Mechanism for RDMCS

The method is applied in a modular manufacturing system composed by WorkStations (WSs) described in Fig. 1. It is noteworthy that all the models are linked through of the PN elements representing real situations. Each WS controller is connected to internet allowing operators and clients interact with the system, that fits to the *engineering cloud* vision. The aim of this system is joining workpieces (*wps*). The devices, their control functions, commands and signals of actuation and detection of each WS are also identified. The identification is made according to specifications DIN/ISO 1219-2:1996-11 and IEC 61346-2:2000-12. For instance, in the nomenclature, 1S2: 1 = circuit number, S = device code, and 2 = device number.

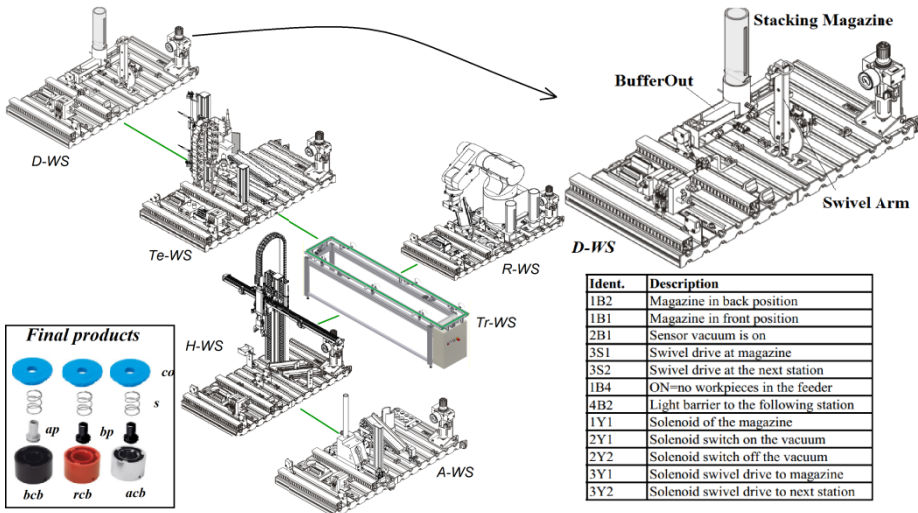


Fig. 1. Modular manufacturing system composed by workstations (WSs): distributing (*D-WS*), testing (*Te-WS*), transporting (*Tr-WS*), handling (*H-WS*), assembling (*A-WS*) and robot (*R-WS*). The aim is joining workpieces (*wps*): a cylinder body (black [*bcb*], red [*rcb*] or aluminum [*acb*]), a piston (black [*bp*] or aluminum [*ap*]), a spring [*s*] and a cover [*co*], to be obtained the final products: (i) [*bcb + ap + s + co*]; (ii) [*rcb + bp + s + co*]; and (iii) [*acb + bp + s + co*].

This paper describes some *D-WS* models, illustrated on the right of Fig. 1 with its related sensors and actuators. The *D-WS* function is providing [*bcb*], [*rcb*] or [*acb*] *wps* (on left at the bottom in Fig. 1) which are stored in the “stacking magazine” buffer. A double-acting piston pushes one *wp* out this buffer one at a time to the magazine. A swivel arm gets a *wp* in magazine via a suction gripper vacuum to move it to the transfer point of the *Te-WS*.

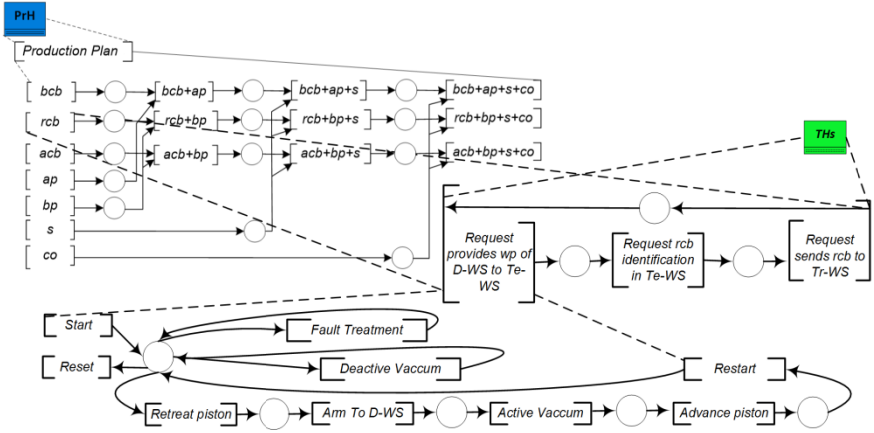


Fig. 2. PFS of workflow to obtain PrH-[rcb]. The services are represented by THs which are reuse in other products, such as [request to provide wp of D-WS to Te-WS] wich is used by all wps. The THs are: [request to provide wp of D-WS to Te-WS] in which D-WS through “swivel arm” takes a wp in its buffer out and put it in “buffer in” of Te-WS; [request rcb identification in Te-WS] in which Te-WSs checks color and height to identify wp; and [request sends rcb to Tr-WS] in which Te-WSs sends the identified wp to Tr-WS.

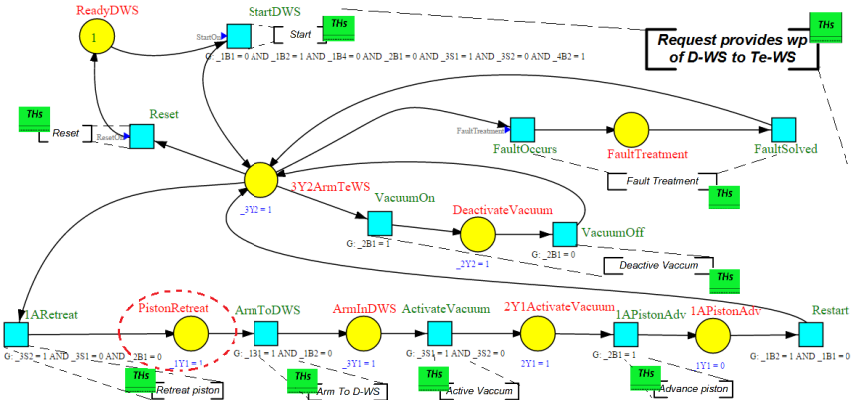


Fig. 3. IOPT for control of D-WS. Each transition has signals represented by “Guard (G)” which represent the equipments listed in Fig. 1. For instance, the “ArmToDWS” transition has associated the “G: 1B1=1 AND 1B2=0” that means “magazine is front position” and the “1B1 sensor” is sending signal “on”. Thus, a token is fired for “ArmInDWS” place sending an output signal “3Y1=1” that in turn modifies the state of this solenoid. This IOPT has also input events: (i) “StartOn” of “StartD-WS” transitions to initiate the D-WS, (ii) “ResetOn” to reset the D-WS, and (iii) “FaultTreatment” to solve fault occurrence.

Figure 2 illustrates the PFS of *production plan* of the modular manufacturing system, refinement of *intermediate product PrH-[rcb]* and sub-refinement of *TH-[request provides wp of D-WS to Te-WS]* which is detailed using IOPT model in Fig. 3. To clarify how communication/translation between different notations is assured, in this figure the related *activities* of the PFS in Fig. 2 are also illustrated inside the *transitions* and *places* of their IOPT model.

Figure 4 presents some control objects models of *D-WS* (represented according to codes listed in Fig. 1) which put the “magazine” in front or back position. As above stated, the *OpHs* are directly modeled in IOPT considering faults states.

Each *TH* has diagnoser and its sub-diagnosers model which are modeled at a similar manner of the models in Fig. 5 where an example for *D-WS* (represented by *TH-[Diagnostic for D-WS]* and *TH-[Diagnostic for 1ARetreating]*) are illustrated. The models evolve together and according to the executed control strategy, the possible states are diagnosed (see highlighted blue dashed line). The transformation of PFS into IOPT model is not presented but is similar to example in Fig. 3. Commands signals (represented in Fig. 3) and the *input* and *output signals* of all control objects of *D-WS* (such as represented in Fig. 4) are linked in these models.

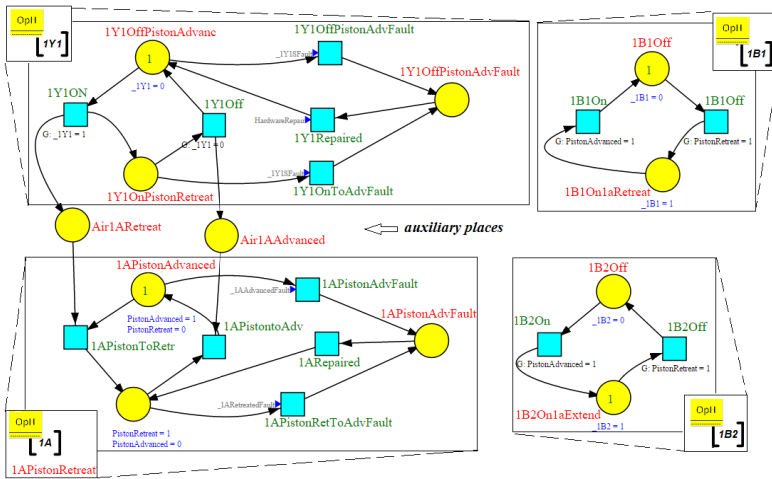


Fig. 4. OpHs of *D-WS* modeled with normal and fault states (see codes in Fig. 1). For instance, *OpH-[1Y1]* has normal states “1Y1Off” to advance piston and “1Y1On” to retreat piston; and fault state “1Y1OffPiston” which maintaining the piston only in advanced state. The models are linked, such as *OpH-[1Y1]* is linked to *OpH-[1A]* through “Air1ARetreat” and “Air1AAdvanced” *auxiliary places*; and *OpH-[1B1]* and *OpH-[1B2]* is linked to *OpH-[1Y1]* and *OpH-[1A]* through *input* and *output signals*. The *input events* represent external changes, which can be a fault, such as “1Y1SFault”.

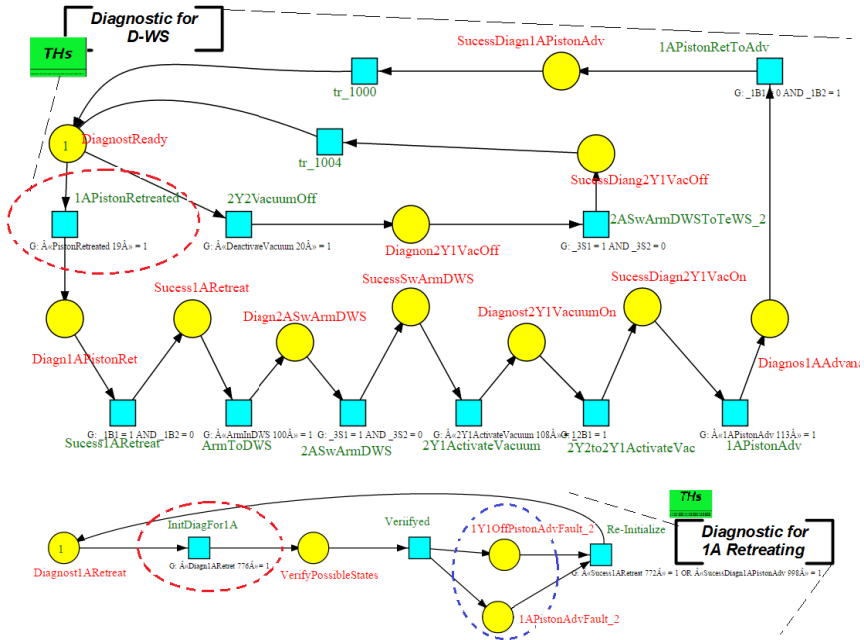


Fig. 5. Diagnoser for *D–WS* linked to control strategy and signals of control objects. For instance (see highlighted dashed red line in both figures), “Piston Retreated” control strategy (place in Fig. 3) is linked to “1APistonRetreated” transition of diagnoser through the guard “G:PistonRetreated”; while the “InitDiagFor1A” transition in *TH*[*Diagnostic for 1ARetreating*] has “G:Diagn1ARetreat” guard linking to *TH*[*Diagnostic for D-WS*].

6 Conclusions and Further Work

This paper proposes the modeling of fault diagnosis mechanisms for Reconfigurable and Distributed Manufacturing Control System (RDMCS). These mechanisms extend a method which uses holonic and multi-agent system and service-oriented architecture concepts through a combined top-down and bottom-up approach based on Petri nets extensions: production flow schema and input output place transition. This approach allows modeling the complex system structures of RDMCS as well as system behaviors in a more simplified and transparent manner than ordinary Petri net representations; avoiding repetition and overlapping tasks through reuse; utilization of web tools for automatic generation of controller languages; collaboration among distributed subsystems; and cloud engineering facilitating the analysis and communication between different design staffs. Furthermore, the fault-tolerant mechanisms allow reconfiguration flexibility for larger safety and new production demands. An application example presents the developing and composition of the models highlighting the advantages of the proposal. Plans for further work include modeling of decision-making mechanism as well as other case studies.

Acknowledgments. The authors thank the partial financial support of the agencies: CNPq, CAPES and FAPESP.

References

1. da Silva, R.M., Junqueira, F., dos Santos Filho, D.J., Miyagi, P.E.: A method to design a manufacturing control system considering flexible reconfiguration. In: 2014 12th IEEE International Conference on Industrial Informatics (INDIN), pp. 82–87 (July 2014)
2. da Silva, R.M., Blos, M.F., Junqueira, F., Santos Filho, D.J., Miyagi, P.E.: A service-oriented and holonic control architecture to the reconfiguration of dispersed manufacturing systems. In: Camarinha-Matos, L.M., Barrento, N.S., Mendonça, R. (eds.) DoCEIS 2014. IFIP AICT, vol. 423, pp. 111–118. Springer, Heidelberg (2014)
3. Hasegawa, K., Miyagi, P.E., Santos Filho, D.J., Takahashi, K., Ma, L., Sugisawa, M.: On resource arc for Petri net modelling of complex resource sharing system. *Journal of Intelligent and Robotic Systems* **26**(3-4), 423–437 (1999)
4. Gomes, L., Barros, J., Costa, A., Nunes, R.: The input-output place-transition petri net class and associated tools. In: 2007 5th IEEE International Conference on Industrial Informatics, INDIN 2007, pp. 27–32. IEEE (2007)
5. Candido, G., Barata, J., Jammes, F., Colombo, A.W.: Applications of Dynamic Deployment of Services in Industrial Automation. In: Camarinha-Matos, L.M., Pereira, P., Ribeiro, L. (eds.) DoCEIS 2010. IFIP AICT, vol. 314, pp. 151–158. Springer, Heidelberg (2010)
6. Barbosa, J., Leitão, P., Adam, E., Trentesaux, D.: Self-organized Holonic Manufacturing Systems Combining Adaptation and Performance Optimization. In: Camarinha-Matos, L.M., Shahamatnia, E., Nunes, G. (eds.) DoCEIS 2012. IFIP AICT, vol. 372, pp. 163–170. Springer, Heidelberg (2012)
7. Pereira, F., Moutinho, F., Ribeiro, J., Gomes, L.: Web based IOPT Petri net editor with an extensible plugin architecture to support generic net operations. In: IECON 2012-38th Annual Conference on IEEE Industrial Electronics Society, pp. 6151–6156. IEEE (2012)
8. Li, B.H., Zhang, L., Wang, S.L., Tao, F., Cao, J., Jiang, X., Song, X., Chai, X.: Cloud manufacturing: a new service-oriented networked manufacturing model. *Computer Integrated Manufacturing Systems* **16**(1), 1–7 (2010)
9. Leitão, P., Marik, V., Vrba, P.: Past, present, and future of industrial agent applications. *IEEE Transactions on Industrial Informatics* **9**(4), 2360–2372 (2013)
10. Hsieh, F.S., Chiang, C.Y.: Collaborative composition of processes in holonic manufacturing systems. *Computers in Industry* **62**(1), 51–64 (2011)
11. Obitko, M., Vrba, P., Marik, V., Radakovic, M., Kadera, P.: Applications of semantics in agent-based manufacturing system. *Informatika (Slovenia)* **34**(3), 315–330 (2010)
12. Sampath, M., Sengupta, R., Lafortune, S., Sinnamohideen, K., Teneketzis, D.C.: Failure diagnosis using discrete-event models. *IEEE Transactions on Control Systems Technology* **4**(2), 105–124 (1996)

PRIME as a Generic Agent Based Framework to Support Pluggability and Reconfigurability Using Different Technologies

André Dionísio Rocha^(✉), Diogo Barata, Giovanni Di Orio,
Tiago Santos, and José Barata

CTS - Uninova, Departamento de Engenharia Electrotécnica,
Faculdade de Ciências e Tecnologia, Universidade Nova de Lisboa,
2829-516 Caparica, Portugal
{andre.rocha,gido,jab}@uninova.pt,
{d.barata,tp.santos}@campus.fct.unl.pt

Abstract. Presently the manufacturers are facing a challenging and important period. The markets are very different comparatively to the past, with constant changes and facing a big crisis. Hence, with these new characteristics is very important for the companies quick adaptations in order to take advantage of new business opportunities. However on the shop floor is not easy reconfigure the production lines to perform new tasks. The PRIME framework presents an agent based solution capable to rapidly reconfigure and readapt the production line using standard technology. In this paper is demonstrated the usability of this framework with three completely different technologies. With this flexibility, using PRIME it is possible perform plug and produce, reconfigurability and monitoring for all kind of technologies, not obligating the companies to reform all components in the line, avoiding external costs and stoppages.

Keywords: Multiagent systems · Standard technology · Plug and Produce · Reconfigurability · Distributed systems · Evolvable production systems

1 Introduction

The world and consequently markets are facing a global financial crisis. This crisis is one of the most challenging era in the entire history. With this new challenges, the enterprises need to re-adapt the entire way as they face these new market needs, more specifically, competitiveness, new customer needs and requirements. So, it is important for all the manufacturers, in particular Small and Medium Enterprises (SME), an effective approach, capable to allow these companies higher levels of flexibility, dynamism, and reconfigurability on the shop-floor level. As result of this new world, the manufacturers are constantly trying to solve the problem of volatility.

Nowadays the product life cycle is constantly decreasing and in some cases the companies are not able to re-adapt their production lines to new business opportunities because of the time and costs required for this re-adaptation. In order to allow

SMEs to face this problem, recently a lot of production paradigms have been proposed and developed in academic environments. However, a real response for this problem was not acquired and the problem keeps present day-by-day inside companies. The PRIME architecture [1] developed in the scope of PRIME project, funded by the European FP7 program, proposes a new approach, this new approach results in a solution to perform plug and produce on the shop-floor using any kind of computational devices. This means that to run PRIME architecture as an agent based framework [2] performing plug and produce, in a production line, it is not necessary reformulate the entire system, introducing specific controllers with a minimum computational performance to run a framework capable to offer reconfigurability, adaptability and flexibility. In this document is presented a demonstration of how it is possible run this framework, using different controllers or PLCs, in the same production line, but using the same framework.

This document is divided by six sections. In the next sections is described the PRIME contribution to cloud-based engineering systems. In section three it is possible to see a literature review about this topic. In section four is described the PRIME Multiagent Framework and how this framework can detect and plug a new resource. Section five contains three different test cases, each test case represents a detection, in this case plug, of a specific resource, using different controllers (standard PLC, DPWS controller and Windows based controller). In the last section are compiled the conclusions and further works.

2 Contribution to Cloud-Based Engineering Systems

In the last few decades the computational systems has suffered a huge improvement and development. The IT area is not an exception and as result of those improvements several cloud based solutions have been proposed for all different problems. The manufacturing systems are not an exception and in the last years several solutions have been presented to improve the performance and analyses of the systems. However, the main contributions have not resulted in valid solutions for the most of the current systems, because of the specifications and restrictions of each system, obligating to implementations very rigid and specific for each system. Without a generic way it is impossible for most of the SMEs manufacturers dispend a huge effort to implement an entire collector of data infrastructure, for its specific system. In this document is presented three different test cases using PRIME as a generic framework, capable to work with standard technology to collect all relevant data and store it into a database. Hence, this information can be used to perform data analyses, understanding the evolution of the system and possible changes. With this generic approach, the SMEs are able to quick and without unnecessary effort collect and process relevant data for the entire line.

3 Related Work

Over the last decades, the way as academics and enterprises look to the production lines has changed a lot. In this section it is described a brief study about some approaches and paradigms designed and developed under these new visions.

3.1 Agile Manufacturing

Agile manufacturing (AM) has been first proposed during the 1990s [3]. During this decade many studies and developments were introduced in this topic. A non-consensual definition for this concept was achieved but all they are basically related to responsiveness.

In [4] “Agile Manufacturing can be defined as the capability of surviving and prospering in a competitive environment on continuous and unpredictable change by reacting quickly and effectively to changing markets, driven by customer-designed products and services”.

Agile Manufacturing is a top down approach that covers the entire firm, is not a new production paradigm itself, but is more a new way to do business. However, the agility on the shop-floor level is not so easy to achieve and some new paradigms to manage the shop-floor behaviours and deal with all complexity have been proposed, such as Holonic Manufacturing Systems [5], [6], Reconfigurable Manufacturing Systems [7], [8], Evolvable Assembly Systems [9], [10] and Evolvable Production Systems [11], [12]. Those approaches bring flexibility and responsiveness to the shop-floor. To implement those kind of production paradigms, the enterprises should re-adapt the hardware in order to run intelligent entities inside each module on the line.

3.2 Evolvable Production Systems

The Evolvable Production Systems (EPS) paradigm has been first presented in the scope of EUPASS project [13]. The main idea in an EPS is a re-usage of modules in different or in the same production line constituting different systems with different valences, without any reprogramming effort. First of all it is necessary that all components are abstracted by intelligent entities. Those entities should be inserted in a society of entities (production line) and re-adapt them behaviours accordingly to the existent entities and current physical positions and status.

With this approach, the system has not a central unit to control the entire system, but distributed entities responsible to specific tasks. With this approach, it is possible introduce the concept of plug and produce. This means, plug a new resource (module) in the production line without being necessary stop the line, reconfigure the entire line and reprogramming.

In the IDEAS project an architecture was proposed, based on CoBASA architecture [14], to perform those kind of behaviours on the shop-floor level [15]. This approach is constituted by generic entities responsible to abstract different modules on the system and manage the availability of functionalities and tasks to be executed.

Although some possibilities were presented, as was described in this section, with the current economic state and needs, it is impossible for the SMEs change the entire hardware of the line to be able to run this kind of system. PRIME proposes a new generic approach, capable to run in hardware with different characteristics, fulfilling the current needs, without obligating the SMEs to change and reform the lines in order to run the previously presented approaches.

4 PRIME Multiagent Framework

The PRIME Multiagent Framework has been developed under the framework of the FP7 PRIME project. This framework has as main goal provide, in an easy way, re-configuration, adaptation, plug-ability and monitoring in a shop-floor environment.

The framework provides these behaviours using different hardware and requirements. Hence, PRIME should provide all these behaviours in all possible production lines, such as production lines composed by standard technology or production lines constituted by intelligent devices. The framework is composed by generic agents and each one has a distinct task, as represented in Fig. 1.

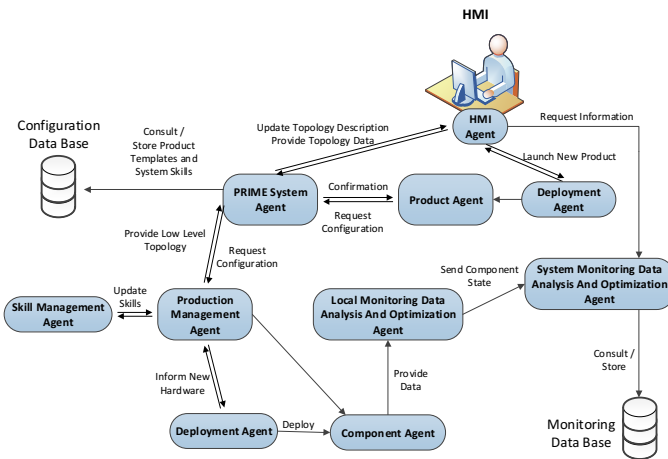


Fig. 1. PRIME Multiagent Framework

Two databases are used to store relevant information, such as performance and status data, used by the system to perform monitoring, and information related to possible configurations for the resources plugged in the system, according to the production needs, such as product variants and usage of different resources for the same tasks. More specifically, when the operator wants to produce a new variant of products, the system is able to get the most appropriated configurations that should be sent for each component and, in this way, reconfigure the entire line accordingly to the specifications of this new variant.

The proposed framework is composed by eight distinct agents with different responsibilities, some agents are responsible to abstract and monitoring the hardware

and other agents are more related to higher level actions, such as combination of different tasks that can be provided by the hardware, each task provided by each resource is described as skill that can be offered to the product. The product is described as a list of skills that must be performed by the system, in order to produce it. The PRIME Multiagent Framework is responsible to match those requested skills and reconfigure the entire line accordingly to those requirements. With this approach it is easier for the operator reconfigure the line, using the description of the necessary skills for a specific product.

- Prime System Agent (PSA) – The PSA is the higher entity in the entire framework. This agent is unique for each instantiation of PRIME, so is the central point of the entire framework. PSA is responsible to manage the PRIME Semantic Model where all the current state of the system, for example, topology and available functionalities, are stored.
- Production Management Agent (PMA) – The PMA is responsible to aggregate resources and responsibilities which are localized in the same space, allowing the aggregated area to provide higher tasks orchestrating these aggregated resources. This agent works as a tree, in order to constitute different layers of aggregations and increasing modularity and scalability of the entire systems.
- Skill Management Agent (SMA) – Each SMA works in pair with a specific PMA. The SMA is responsible to receive the existent skills in a PMA and combine, according to the defined rules, the higher level skills that the PMA can provide.
- Component Agent (CA) – The CA is the lower entity and it is responsible by abstract each physical hardware that constitutes the topology of the system. More specifically, the CA write and read data related to the execution of the entity abstracted by it. The resource has the possibility to be configured by this agent and the CA can extract relevant data as well.
- Local Monitoring and Data Analyses Optimization Agent (LMDAOA) – Similarly to the PMA and SMA, the LMDAOA works in pair with a CA. In this specific case, each CA has an associated entity of this type. This agent is responsible to receive the relevant extracted data from CA and pre-process it and analyses it, in order to define the first layer of monitoring.
- System Monitoring and Data Analyses Optimization Agent (SMDAOA) – Each instantiation of the PRIME Agent Framework runs one SMDAOA. This entity is responsible to collect all relevant data of the system. All this relevant data should be provided by each LMDAOA. With this data, it will compute all the information, store in a global database with all historical data of the system, and perform monitoring analyses. This agent provides this data to the HMIA when requested.
- Human Machine Interface Agent (HMIA) – The HMIA works as a gateway to external specific HMI. This agent as the capability to offer services which can be used by other entities to extract relevant information from the entire system. Hence, an external HMI to get relevant information, such as the current or older topologies of the system and data related to the execution of the entire sys-

tem or a specific resource, should call the service that starts the communications between the agents which provides that kind of information.

- Product Agent (PA) – When the operator wants to launch a new variant of a product or even a new product, a PA should be launched containing all information which describes this new product, such as process plan with the necessary skills. The PA triggers the configuration routines with the PSA, sending the list of necessary skills.
- Deployment Agent (DA) – In all the machines (controllers and computers), where one or more PRIME agents will be launched, is mandatory that a DA is already running in each machine and must be the first agent launched. The DA has the responsibility to deploy (launch) all the necessary PRIME agents as CAs, PMAs, Pas, among others. With this feature is possible to launch any type of PRIME agents, available, in the machines, remotely.

These classes enclose and abstracts all the generic interactions between the entities. However, the CA and DA should be extended to incorporate details about specific equipment, because these agents are directly connected to specific hardware.

4.1 Detection of New Resource (Hardware)

New physical devices, such as robots, grippers, etc. can be plugged, unplugged and re-plugged in runtime. In Fig. 2 is described all necessary interactions (messages which the agents should send and process) between the agents to provide pluggability.

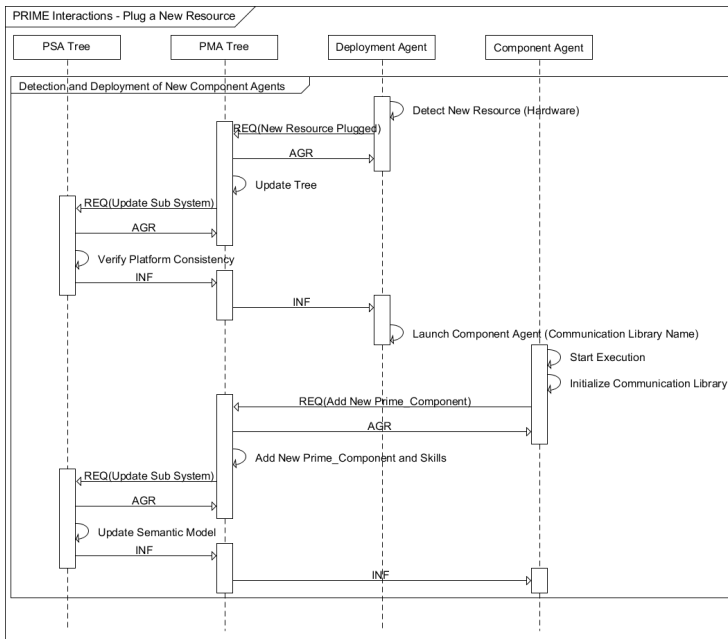


Fig. 1. PRIME Agent Interactions during a Plug

PRIME agents was developed using JADE framework [16] and all performed communications are FIPA compliant [17], more specifically is used the FIPA Request Protocol. Hence, with this functionality PRIME is able to provide plug and produce using all kind of technology.

5 Test Cases

PRIME, as was described in the previous section, is capable to detect and plug any kind of resource, with different scales of intelligence. Each device is described as one of these groups, accordingly to them capacities:

- Fully-intelligent resources: This type of resources are capable to autonomously run the necessary agents, such as CA, LMDAOA and DA. Usually this kind of resources are composed by Windows or Linux based controllers, capable to run Java environment.
- Semi-intelligent resources: These devices are able to autonomously announce the existence of new resources. The device offers the possibility to reconfigure itself but without running locally the agents.
- Passive resources: In this case, the device is a fully dummy resource, without any capacity of computation. To manage a device with these characteristics, another machine should run the necessary agents and monitoring the memory and connections with a standard PLC, responsible to control this hardware.

Three different demonstrations were created in order to test the detection of these three types of devices by the PRIME Multiagent Framework. The entities which interact with the hardware implement a generic interface that contains all specific interactions with the hardware. The CA and DA implement specific Detection and Communication libraries respectively, for each resource.

5.1 Detection and Configuration of Fully-Intelligent Resources

In this case, it has been used an intelligent device. Using a controller from Elrest, running Windows XP Pro for Embedded Systems (Fig. 3), was possible to prove that PRIME is able to manage resources controlled by such devices.

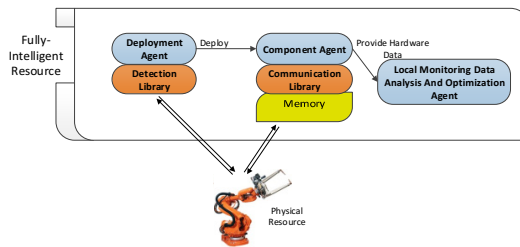


Fig. 2. PRIME Agent environment using a Fully-intelligent Resource

This kind of resources are the most suitable to integrate with PRIME, providing all the necessary information in an autonomous way. With a Windows based controller, PRIME agents can run locally, the DA, CA and LMDAOA. To detect resources controlled by these devices, when the controller executes the bootstrapping, automatically launches the DA which detects the current plugged hardware and starts the routines to launch the CA. The CA when launched, launches a LMDAOA. As the agents are running locally, when PRIME decides to configure a resource, the CA is able to write directly to the controller memory, changing the routines performed by it.

5.2 Detection and Configuration of Semi-Intelligent Resources

The second demonstration (Fig. 4) is responsible to prove the usability of Semi-intelligent resources to detect and reconfigure physical devices in a production environment by PRIME. In this was used an INICO S1000 PLC, running DPWS framework that offers services, capable to run specific routines, as reconfiguration or detection of new components.

To run this demonstration, a central machine such as a computer or a Windows / Linux based controller, should run the DPWS framework which is responsible to detect new INICO PLCs and call the services. The DA extends the libraries necessary to launch and run the DPWS framework, and in a cyclic way checks if in this local environment was detected new resources (INICO PLCs), if yes, the DA launches a new CA in this central machine and this new CA is capable to send new configurations to the PLC, calling available services for that proposes.

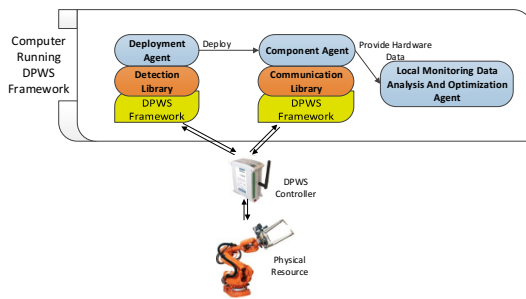


Fig. 3. PRIME Agent environment using a Semi-intelligent Resource

5.3 Detection and Configuration of Passive Resources

Although the usage of more powerful devices, as described in the previous sections, is important because of the natural evolution of manufacturing systems, standard technology still being the most common technology.

The last demonstrator, represented in Fig. 5, represents how the PRIME platform is able to manage and interact with this kind of technology.

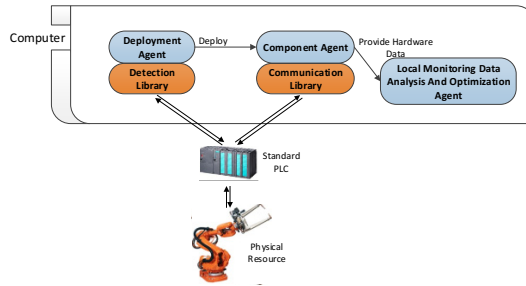


Fig. 4. PRIME Agent environment using a Passive Resource

Usually, a PLC is responsible to control a specific resource or a wrap of resources, such as robots or a conveyor belt. Hence, to integrate PRIME with the following structure of resources, it is necessary an external machine to run the agents. This external machine can be a computer or a Windows / Linux based controller, running a Java Virtual Machine and a JADE container. Inside this JADE container lives a DA responsible to detect the existence of new physical resources. In order to detect new resources, the DA extends a specific library for each case, for instance the DA can check the Ethernet ports in a local network or specific variables retrieved by the PLC. When detected a new device, a new CA will be launched to abstract the device. The CA, in this case with a standard PLC, extends a library capable to configure and consult the PLC memory, using standard protocols, such as an OPC connection.

6 Conclusions and Further Work

The PRIME Multiagent Framework was presented in previous works, with the capacity to perform reconfigurability and plug ability using standard technology. In this document was presented three different test cases that represents three different possibilities of abstractions made by the PRIME Multiagent Framework on the shop-floor using different technologies. The test cases were performed using resources controlled by Windows based controller, DPWS controller and standard PLC. In all the cases were possible to see the detection and reconfiguration of the resources using the different technologies.

With this demonstration, it is possible to say that PRIME effectively perform plug and produce, reconfigurability and monitoring using different technologies. This new proposal results in a new possibility for SMEs in a more flexible and re-configurable approach without wasting time and money adapting the entire line to the recent emerged production paradigms, which required machines with high performance.

In order to use this real advantage, it is now important to create all the tools that will be used by the operator to develop the lower level libraries, such as the detection and communication libraries. It is also important to define and create auxiliary software, capable to allow the operator an easy way to enable a module to run and to be detected by this framework.

Acknowledgments. This research was supported by the EU Frame Work 7 project PRIME (Plug and Produce Multi-agent Environment, Grant Agreement No. 314762).

References

1. Antzoulatos, N., Castro, E., Scrimieri, D., Ratchev, S.: A multi-agent architecture for plug and produce on an industrial assembly platform. *Prod. Eng.* **8**(6), 773–781 (2014)
2. Rocha, A., Di Orio, G., Barata, J., Ribeiro, L., Antzoulatos, N., Castro, E., Scrimieri, D., Ratchev, S.: An Agent Based Framework to Support Plug and Produce (2014)
3. Yusuf, Y.Y., Sarhadi, M., Gunasekaran, A.: Agile manufacturing: The drivers, concepts and attributes. *Int. J. Prod. Econ.* **62**(1–2), 33–43 (1999)
4. Gunasekaran, A.: Agile manufacturing: A framework for research and development. *Int. J. Prod. Econ.* **62**(1–2), 87–105 (1999)
5. Leitão, P., Restivo, F.: A holonic approach to dynamic manufacturing scheduling. *Robot. Comput.-Integr. Manuf.* **24**(5), 625–634 (2008)
6. Leitão, P., Restivo, F.: ADACOR: A holonic architecture for agile and adaptive manufacturing control. *Comput. Ind.* **57**(2), 121–130 (2006)
7. Koren, Y., Heisel, U., Jovane, F., Moriwaki, T., Pritschow, G., Ulsoy, G., Van Brussel, H.: Reconfigurable Manufacturing Systems. *CIRP Ann. - Manuf. Technol.* **48**(2), 527–540 (1999)
8. Koren, Y., Shpitalni, M.: Design of reconfigurable manufacturing systems. *J. Manuf. Syst.* **29**(4), 130–141 (2010)
9. Frei, R., Di Marzo Serugendo, G., Barata, J.: Designing self-organization for evolvable assembly systems. In: *Second IEEE International Conference on Self-Adaptive and Self-Organizing Systems, SASO 2008*, pp. 97–106 (2008)
10. Onori, M., Barata, J., Frei, R.: Evolvable assembly systems basic principles. In: *Information Technology for Balanced Manufacturing Systems. IFIP*, vol. 220, pp. 317–328. Springer, Boston (2006)
11. Neves, P., Barata, J.: Evolvable production systems. In: *IEEE International Symposium on Assembly and Manufacturing, ISAM 2009*, pp. 189–195 (2009)
12. Ribeiro, L., Barata, J.: Re-thinking diagnosis for future automation systems: An analysis of current diagnostic practices and their applicability in emerging IT based production paradigms. *Comput. Ind.* **62**(7), 639–659 (2011)
13. Onori, M., Alsterman, H., Barata, J.: An architecture development approach for evolvable assembly systems. In: *The 6th IEEE Int. Symposium on Assembly and Task Planning: From Nano to Macro Assembly and Manufacturing, ISATP 2005*, pp. 19–24 (2005)
14. de Oliveira, J.A.B.: Coalition based approach for shop floor agility – a multiagent approach (2003)
15. Ribeiro, L., Barata, J., Onori, M., Hanisch, C., Hoos, J., Rosa, R.: Self-organization in automation - the IDEAS pre-demonstrator. In: *IECON 2011 - 37th Annual Conference on IEEE Industrial Electronics Society*, pp. 2752–2757 (2011)
16. Bellifemine, F.L., Caire, G., Greenwood, D.: *Developing Multi-Agent Systems with JADE*. John Wiley & Sons (2007)
17. Bellifemine, F., Poggi, A., Rimassa, G.: JADE–A FIPA-compliant agent framework. In: *Proceedings of PAAM*, vol. 99, p. 33 (1999)

The Migration from Conventional Manufacturing Systems for Multi-agent Paradigm: The First Step

João Alvarez Peixoto¹(✉), José Antonio Barata Oliveira²,
André Dionísio Rocha², and Carlos Eduardo Pereira¹

¹ Universidade Federal do Rio Grande do Sul, Porto Alegre, Brazil
joao.alvarez@ufrgs.br, cpereira@ece.ufrgs.br

² Universidade Nova de Lisboa, Lisboa, Portugal
{jab, andre.rocha}@uninova.pt

Abstract. The consumer market ever more calls for diversified products in small batches and the industry lacks production systems that meet the demands with efficiency and ability to adapt quickly. Integrated manufacturing systems implemented have their management for programmable logic controllers and electrical interconnections, control logic and satisfactory robustness, but they do not attend the needs of diversity and flexibility in production. The solutions to these needs refer the company to migrate to the use of new technologies of control, circuit and logic. But, for an industry migrates is a very big and expensive step. Then, there is an urgent need for methods that implement the interface between logic controllers and multi-agent systems in order to evolve an integrated manufacturing system taking advantage of all electrical circuitry, control logic and the logic controller that installs itself, taking advantage of the self-adapting characteristics that the multi-agent systems provide.

Keywords: Multi-agent systems · Industrial manufacturing · Agility · Self-adaptive systems

1 Introduction

The modern consumer behavior is in constantly changing and the industry is facing the big challenge of accompanying these changes. On the one hand, consumers are seeking ever more customized products which represent their individuality, on the other hand, the industry, to remain competitive, needs to meet this demand of large-scale variety.

The study of James [1] has pointed out that the business environment in the future would be characterized by constant changes in market demand and the global competitiveness would push the entry of new products.

The high-volume production continues to be processed however, as pointed out [2], there is a tendency to mass production of highly customized product. And it leads to a large volume of small lots. And the speed that the market demands products highly customized to be delivered is important. The production line space to adapt to a new product is smaller and significant to the final cost. As stated in [3], to cope with this new reality and achieve a competitive advantage over competitors, future productions systems must provide solutions to: long time for system design, commissioning and

setup; complex variations requirements; inflexible implementations; scalability; fault-tolerance or redundancy; and incompatibility between different technologies.

But, what method it is necessary to industries will migrate to new paradigms that attend the market requisites? One cannot simply dismantle the existing production systems and build new ones, with new paradigms. This work will be discussing the steps to migrate from a conventional manufacturing to a system self-adaptive, making use of all existing infrastructure and local logical.

This work shows a study of manufacturing industrial and the possible solution for new necessities of market. In section 2 approach how could-based can be used for support to self-organized systems. The section 3 shows de concepts of industrial manufacturing management. The section 4 shows the approaches this problematic by academics and researches groups. The section 5 discusses a need of method to migrate of conventional system to self-organized systems. And section 6 shows the conclusion of this work.

2 Contribution to Cloud-Based Engineering Systems

The requirements of diversity in production lead the industry to need versatile systems that use shared resources. One way is to share resources through Cloud-based. This concept computing systems applied in manufacturing, such as multi-agent systems, recourse to cloud environments to seek methods, algorithms, and means for obtaining a skill required by a new production process that is presented. The multi-agent systems need not have all the variants of a production process to serve it with the diversity it needs, just to have these variants seek in a cloud environment, sharing resources with all agents in the system.

With the computing resources evolution available to the manufacturing management, solutions using the “cloud” concept have emerged as a good alternative to systems which have high power of communication, but do not have elevated power to local processing. In [4] the application of multi-agent solutions with cloud systems is approached and can be seen in Figure 1.

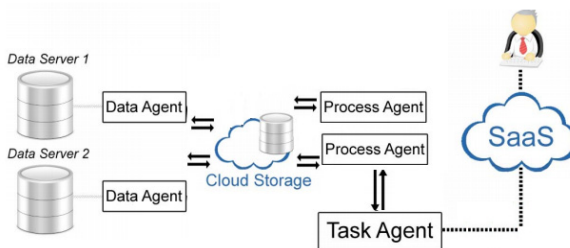


Fig. 1. Multi-agents using cloud concept, based on [4]

In Figure 1 the Process Agents resorting to the cloud environment (Cloud Storage) to obtain data on the process as well as the Task Agent resorting to cloud environment (SaaS) to learn skills with humans.

3 Manufacturing Systems Management

The management system has been constantly the subject of research and to every new demand that arises new paradigms are researched and implemented. This work mentions what it thinks to be the most significant in terms of solution presented to industry.

3.1 Management with Programmable Logic Controllers (PLC)

Manufacturing system has evolved from craft production with low volume, high variety and general purpose machines to production lines, dedicated machines and large enterprise, which enable the mass production [5]. Mass production brought the concept of a manufacturing with a viewpoint centered on Programmable Logical Controllers (PLC), which operates in a loop: (i) read all inputs; (ii) execute defined logic (the process) to generate the outputs from the inputs; (iii) trigger the outputs conform the processing logic;

3.2 Flexible Manufacturing Systems (FMS)

For the same equipment being able to perform more than one operation in manufacturing, it should be resourced to enable, through feeding device, change its functionality, providing distinct processes to be performed by the same equipment. A FMS is distinguished from other forms of automated manufacturing by considering the diversity of the products they want to produce (product flexibility) and adaptive characteristics of the machines (flexibility of the equipment) [6] e [7];

3.3 Computer Integrated Manufacturing (CIM)

CIM is a concept where the approach aims at integrating all process stages: sales, supplies, design and development, production and delivery. The paradigm is the integration of all the company activities through the use of information technology [8], such as databases, networks, etc., that allows the data exchange and sharing between business units and its applications. Computer integrated manufacturing is the efficient use of information technology in manufacturing to increase productivity and efficiency of businesses;

3.4 Evolvable Assembling Systems (EAS)

EAS are the integrated systems with equipment that allow modularity, adaptability and scalability of the product. They are modules who should provide open hardware and software architecture with plug and play functionality; the connection is made without the other equipment being disconnected or reconfigured. The reconfiguration of systems allows the manufacture to be evolvable. The mounting system of the evolution is based on simple systems, reconfigurable elements with specific tasks (system modules), which allow a continuous evolution of the system. An EAS can co-evolve with the product and assembly process [4]. The EAS can be implemented by Service Oriented Systems (SOA), that is the basic element in the abstraction of services which has properties of autonomy, interoperability, platform independence, encapsulation and availability [9], or by using Multi-agent Systems (MAS) defined as a paradigm derived from the distri-

buted artificial intelligence field, characterized by decentralization and parallel execution of activities based on autonomous entities, called agents [10].

The table 1 shows a comparison among the proposed manufacturing management system, linking the paradigm employed, the main feature and the ability to use cloud approach.

Table 1. Comparison among the systems of manufacturing management

Management system	Paradigm used	Main Feature	Cloud Solutions
Centralized	Logic control	All control of process	-
FMS	Logic control	Idle resources	-
CIM	Computer control	Require availability resources	Possible
EAS	SOA or MAS	Adaptation to manufacturing required	High

4 Approaches to New Paradigms for Manufacturing

4.1 Academic Approaches

The self-organizing systems researches are increasing, but there are still few studies with real industry application. But the fact the academics take care of this problem is a big step to find new forms of applying concepts and get new solutions. The table 2 shows some research in doctoral thesis that approaches the topic.

Table 2. Comparative approaches in academic research

Ref.	Problematic	Method	Application
[11]	Need for agility on the factory floor to handle disturbances and uncertainty	Multi-agent systems for interface between generic and physical environment	Integrated manufacturing plant with 2 robots
[12]	Properties of self-x to implement self-organizing systems	Product fits into modules, forming coalitions, generating optimized layouts	Plant with 3 robots, 5 conveyors, and 3 parts feeders
[13]	Diagnostics in complex industrial installations with a large number of components	Agents make the diagnosis of component failure and estimate its propagation	Manufacturing plant with 2 conveyors, 2 robots and pallets
[14]	Attending the diversity production requirements to market demands	Agents in layers, one for deliberation and one for rapid reaction	Manufacturing cell with axis of rotation and translation
[15]	Replace the component automation interconnected with distinctive technology	Converting the functionality of a device existing in a service offering	Plant with 2 dosage machine and 1 transport line
[16]	Necessity of use dynamic allocation of resources to changing production	Situation analysis, objectives and adaptation of system behavior	Implementation of power drives using MatLab
[17]	Production attend a series of small lots, sometimes a unique lot of one product	Defines a semantic link among the concepts of agent, environment and organization	Production line for small series of assembling boards
[18]	Attending to the rapidly changing needs of the consumer	Each agent met together in order to form a productive arrangement	Case study in industries to support decision making

Among the studies reported can be seen that the problems are similar, the methods are different and the results refer to the same path: industrial manufacturing. Thus, the academy has solutions by attend the need of industry to diversity of market demand.

4.2 Project Groups

The multi-agent paradigm systems used in industrial manufacturing has been the subject of research projects, sometimes there is in the group companies tendency to apply these concepts. This interest demonstrates this topic importance, and the fact of industry assumes that it finds solution to varieties of products required by the market. The table 3 cites some project groups who work among with companies and research institutes. These groups are predominating in Europe when the topic is more development in research and industries appliance.

Table 3. Groups of projects that approaches multi-agents systems in industrial manufacturing

Project	Referencies	Approach	Some Partners
SOPRO	[19]	Self-organizing systems	Fraunhofer IZM
COSMOS	[20]	Self-adapter of product variance	UNINOVA, Phoenix Contact, OST, EDAG
EUPASS	[21]	Self-integrated modules of flexible production	UNINOVA
IDEAS	[22]	Self-adapter to changing of technologies components	UNINOVA, Nottingham University, FESTO, KTH, MASMEC
XPRESS	[23]	Design of production based on self-organizing.	University of OULU, Fraunhofer, Airbus, KUKA.
PRIME	[24]	Plug-and-produce systems in self-organizing concepts	UNINOVA, Siemens, Nottingham University, Introsys, Asyrl, TQC, Simplan

Here it's possible to observe the importance of the self-organizing for central researches and manufacturing industries.

4.3 Gaps Among Approaches

The cited approaches, either in theses either for research groups indicate solutions to the need of quickly respond the change in the product industry, but they point the way to the deployment of a new technology. Considering the industry has controllers installed, mounted with their hardware and their defined logic locations, the proposed solutions do not take advantage of it, which is present on the factory floor.

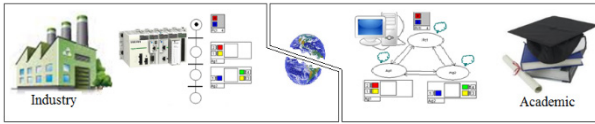


Fig. 2. Paradox between the current technologies installed in industry and solutions that academics offer, two would with different approaches

And this is a big gap in application terms, it is a fact that the industry does not want to eliminate the controllers they have and with known characteristics. But one needs to migrate to new concept, because of what not answers the new demands of the market. This is the paradox the academy is responding and has been a big gap to be studied and resolved.

5 Discussion of a Method to Migration

The solutions proposed by academy to attend the need of self-adaptation with multi-agent systems require computer systems with high capacity, which makes the controllers that manage machines today in the industry, do not support this technology. But abandoning these controllers seems, in the industry eyes of the something unacceptable face every investment already made in installation.

The Figure 3 shows the first step proposed for migration.

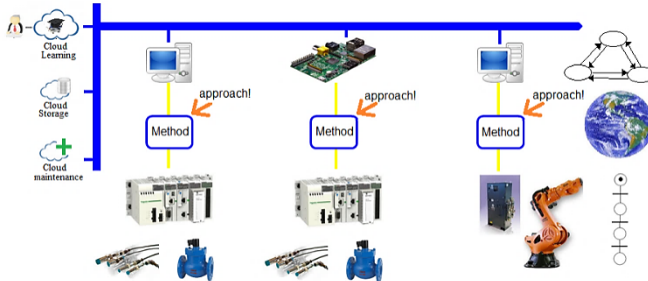


Fig. 3. Proposed migration from the existing system of automation to self-adaptive systems

For the industry to join the new paradigm will require several intermediate steps. And the first step is to develop a method that can migrate the conventional management system for managing a multi-agent system.

The method can be abstract the functionality of a controller existing in an envelope, disposing in the multi-agent system to supply and request services, beyond the capability of interaction and negotiation. The method will have to define how to access controller existing, which can be learned by agents assigned in the cloud (cloud learning).

Inspection requirements and the database can also be modeled in the cloud, in order to provide specifications of the items that should be targeted in specific manufacturing agents (cloud maintenance) and storage of knowledge about the colligations system to attend a specific demand (cloud storage).

The method under discussion must then be connected in a multi-agent platform and interfaced with the hardware controller by one communication form, translate the features of each station in services and their needs must be translated into requests.

6 Conclusions and Future Work

Market demand is a reality that the industry must attend and that this work has examined solutions that academic and research groups had presented and took part in proposing an intermediate method between the management of current and future manufacturing. A conclusive research that refers to a method that helps to evaluate a management system for logic controller to migrate to a multi-agent platform is something wanted by the industry as the first step to adherence to new paradigm.

Once the first step is given, more multi-agent systems begin to work in and more results will be reviewed and for directing the path. As future work this paper suggests the implementation of methods that interfacing existing controllers on the factory floor with management modules of the agent in order to abstract functionality. These methods may be validated and defined its comparison of efficacy. Also suggests the search of agents that act in the cloud and can support maintenance inspection.

References

1. James, F., Smit, H.: Service-oriented paradigms in industrial automation. *IEEE Transactions on Industrial Informatics*, Nova York **1**(1), 62–70 (2005)
2. Herrera, V., Bepperling, A., Lobov, A., Smit, H., Colombo, A., Lastra, J.: Integration of multi-agent systems and service-oriented architecture for industrial automation. In: 6th Proceedings of the IEEE International Conference on Industrial Informatics, INDIN 2008, Daejeon, pp. 768–773 (2008)
3. Cândido, G., Colombo, A., Barata, J., Jammes, F.: Service-oriented infrastructure to support the deployment of evolvable production systems. *Proceeding of the IEEE Transactions on Industrial Informatics* **7**, 759–767 (2011)
4. Othmane, B., Hebri, R.: Cloud computing & multi-agent systems: a new promising approach for distributed data mining. In: Proceedings of the 34th International Conference on Information Technology Interfaces, ITI 2012, pp. 111–116. IEEE: Oran., Algeria (2012)
5. ElMaraghy, H.: Flexible and reconfigurable manufacturing systems paradigms. *International Journal of Flexible Manufacturing Systems* **17**, 261–276 (2005)
6. Peixoto, J., Pereira, C., Cavalcante, A.: When agents meet manufacturing: paradigms and implemations. In: Proceedings of the XIX Brazilian Congress of Automatic, CBA 2012, Campina Grande, pp. 957–964 (2012)

7. Peixoto, J.A.: Development of manufacturing automation systems using service-oriented architectures and multi-agents systems. 134 f. Dissertation of Master Degree – Electrical Engineering Department, Federal University of Rio Grande do Sul - UFRGS, Porto Alegre (2012)
8. Leitão, P., Barata, J., Camarinha-Matos, L., Boissier, R.: Trends in agile and co-operative manufacturing. In: Proceedings of the Low Cost Automation Symposium – LCA, pp. 156–165. IFAC, Berlin (2001)
9. Ribeiro, L., Barata, J., Colombo, A.: MAS and SOA - a case study exploring principles and technologies to support self-properties in assembly systems. In: Second IEEE International Conference on Self-Adaptive and Self-Organizing Systems Workshops (SASOW), pp. 192–197 (2008)
10. Leitão, P.: Agent-Based Distributed Manufacturing Control: A State-of-the-Art Survey. *Engineering Applications of Artificial Intelligence* **22**(7), 979–991 (2009)
11. Oliveira, J.A.B.: Coalition based approach for shop floor agility—a multiagent approach. Dissertation for PhD degree in Electrical Engineering – Faculty of science and technology, University Nova de Lisboa, Lisboa (2004)
12. Frei, R.: Self-organisation in evolvable assembly systems, 250 f. Dissertation for PhD degree in Electrical Engineering – Faculty of science and technology, University Nova de Lisboa, Lisbon (2010)
13. Ribeiro, L.: Diagnosis in Evolvable Production Systems, 230 f. Dissertation submitted for a PhD degree in Electrical Engineering – Faculty of science and technology, University Nova de Lisboa, Lisbon (2012)
14. Cavalcante, A.L.D.: Agent-based and self-organizing architecture for manufacturing. Theses of Doctor Degree - Electrical Engineering Department, Federal University of Rio Grande do Sul - UFRGS, Porto Alegre (2012)
15. Cândido, G.M.: Service-oriented architecture for device lifecycle support in industrial automation. Dissertation for PhD degree in Electrical Engineering – Faculty of science and technology, University Nova de Lisboa, Lisbon (2013)
16. Oberthür, S.: Towards an RTOS for self-optimizing mechatronics systems. 147 f. Dissertation submitted for a PhD degree in Electrical Engineering, Paderborn University, Paderborn (2009)
17. Roloff, M.L.: A New Approach for Implementing Multiagent Systems for the Production Control in Small Series. 2014, 294 f. Thesis of Doctor Degree in Automation and Control Engineering, Federal University of Santa Catarina, Florianópolis (2014)
18. Peschl, M.: An architecture for flexible manufacturing systems based on task-driven agents. Thesis to Doctoral program – Faculty of Information Technology and Electrical Engineering, Oulu University, Finland (2014)
19. SOPRO Project - Self-Organizing Production. <http://www.izm.fraunhofer.de/en/abteilungen/>
20. COSMOS Project – Flexible Modular Automation. <http://www.cosmosproject.eu/>
21. EUPASS Project – Evolvable Ultra-Precision Assmby Systems. http://cordis.europa.eu/result/rcn/51017_en.html
22. IDEAS Project –Instantly Deployable Evolvable Assembly Systems. <http://www.ideas-project.eu/>
23. XPRESS Project - Flexible production experts for reconfigurable assembly technology. <http://www.xpress-project.eu/>
24. Prime Project - Plug and Produce Intelligent Multi Agent Environment based on Standard Technology. <http://www.prime-eu.com>

Distributed Computing

Experimental Assessment of Cloud Software Dependability Using Fault Injection

Lena Herscheid^(✉), Daniel Richter, and Andreas Polze

Hasso Plattner Institute, Potsdam, Germany

{lena.herscheid,daniel.richter,andreas.polze}@hpi.de

Abstract. In modern cloud software systems, the complexity arising from feature interaction, geographical distribution, security and configurability requirements increases the likelihood of faults. Additional influencing factors are the impact of different execution environments as well as human operation or configuration errors. Assuming that any non-trivial cloud software system contains faults, *robustness testing* is needed to ensure that such faults are discovered as early as possible, and that the overall service is resilient and fault tolerant. To this end, *fault injection* is a means for disrupting the software in ways that uncover bugs and test the fault tolerance mechanisms. In this paper, we discuss how to experimentally assess software dependability in two steps. First, a model of the software is constructed from different runtime observations and configuration information. Second, this model is used to orchestrate fault injection experiments with the running software system in order to quantify dependability attributes such as service availability. We propose the architecture of a fault injection service within the OpenStack project.

Keywords: Fault injection · Dependability · Distributed systems · Cloud systems · Availability

1 Introduction

Fault tolerance is an essential dependability requirement especially in distributed and cloud software systems, where components can fail in arbitrary ways, but a high availability or reliability of the service is nevertheless required.

To evaluate the dependability of complex software systems, a sufficiently realistic dependability model of the system needs to be built. Prominent dependability modeling languages such as fault trees or reliability block diagrams originally stem from the hardware domain. Designed for static systems consisting of thoroughly stress-tested hardware components with known error rates, they cannot reflect dynamic software traits [1]. Since the behaviour of cloud software largely depends on interaction, timing, and environment factors, we believe that experimentation and runtime data is needed to construct such a dependability model.

Runtime software fault injection is a technique for artificially introducing faults, or error states, into the application execution in order to uncover bugs. In contrast to compile-time injection, not the source code, but rather the running system, potentially

including its execution environment, is modified. Fault injection experiments are used to gain insights into the system's failure behaviour and its resiliency.

We propose to use a fault injection service for experimentally obtaining dependability data from OpenStack¹ applications. We intend to use such data for building more realistic quantitative dependability models from distributed and cloud software, where much of the failure behaviour depends on dynamic and environmental factors. Ultimately, the framework discussed in Sections 0 and 0 will serve to answer the following research questions:

- How does the unavailability of some nodes affect performance?
- How does availability and consistency degrade in the presence of faults? With the CAP theorem [2] in mind, how are availability and consistency related to network partitions?
- Which components suffer most from faults? Are there single points of failure?

2 Relationship to Cloud-Based Solutions

In the cloud computing community, the need for resiliency testing of production systems has been acknowledged recently [3]. There has been a paradigm shift -- from trying to avoid failures at all costs to embracing faults as opportunities for making the system more resilient. The rationale behind fault injection testing of deployed software can be summarized as follows [4]:

“It's better to prepare for failures in production and cause them to happen while we are watching, instead of relying on a strategy of hoping the system will behave correctly when we aren't watching.”

Even in the unlikely case that the software itself is bug-free, the infrastructure will eventually break, making resilience mechanisms necessary.

Fault injection can be viewed as the software equivalent to hardware stress testing. Based on the assumption that software systems will unavoidably suffer from external as well as internal faults, fault injection is a means for reducing uncertainty: The deployed system is observed under a realistic “worst case” faultload, and it should maintain a desired level of availability, performance, and service quality despite this faultload. Anecdotal evidence suggests that testing recovery mechanisms under faultload targets a relevant class of cloud software outages [5]:

“All these outages began with root events that led to supposedly tolerable failures, however, the broken recovery protocols gave rise to major outages.”

Such outages can be avoided by routine fault injection experiments.

The amount of effort put into the fault tolerance and resilience of cloud applications is often determined by Service Level Agreements (SLAs), and the trade-offs between development efforts, costs for redundancy, availability, and consistency are usually application-specific and based on management decisions. Fault injection can also serve as a tool for testing disaster recovery plans, which are necessary to avoid high losses in revenue in the case of failures. Gunavi et al. [5] therefore propose a new kind of (node) “Failure as a Service” (FaaS). This is what we aim at providing.

¹ www.openstack.org, 12/24/2014

3 Related Work

Table 1. Related work on distributed software fault injection. Work explicitly dealing with cloud platforms is printed bold

Name	Fault Types	Implementation
ChaosMonkey [6]	node crash, network latency, zone outage	AWS VM termination
Testing OpenStack	node crash, network partition	systemd, iptables
FATE [7]	programmable	instrumentation (AspectJ)
PreFail [8]	programmable, disk failures	based on FATE
AnarchyApe	node crash, network latency, kernel panic, permissions faults	distributed Java scripts
FSaaS for Hadoop [9]	node crash, network latency + partition, packet loss, fork bomb	based on AnarchyApe
Failure as a Service	machine crashes, network failures, disk failures, CPU overload	distributed failure agent scripts
GameDay [4]	application specific	manual
Orchestra [10]	message delay + byzantine incorrectness	message manipulation in the OS protocol stack
Grid-FIT	message delay + byzantine incorrectness	message manipulation in the grid middleware
NFTAPE [11]	bit-flips in registers + memory, communication + I/O errors	custom fault injecting execution environment
FIAT [12]	memory faults	custom fault injecting execution environment

Table 1 summarizes related work in the area of distributed software fault injection. [10], [11], [12], [13] discuss tools for injecting faults into distributed systems mainly at the operating system and middleware levels. More recent approaches specific to cloud software are printed bold in table 1. *Chaosmonkey* [6] is a widely used, Java-based tool for Amazon Web Services (AWS) application resilience testing. The approach of injecting faults into deployed systems was first successfully employed by Netflix and later on adapted by other companies offering cloud-based software².

Further approaches to providing resiliency testing services have been presented [14] [9] [5] [15] [15]. Their focus mainly lies on hardware fault models, namely network partitions and latency, as well as node crashes. There are also “fault model agnostic”, configurable solutions such as [7] [8] [4]. These solutions provide a framework for easily injecting faults, but the fault classes themselves have to be implemented to some extent by the user. Some fault injection testing for OpenStack has also been explored [14].

² E.g. StackExchange: <http://blog.codinghorror.com/working-with-the-chaos-monkey/>, 12/23/2014

The toolsets shown in Table 1 can be used with deployed applications with some additional integration effort. Our work is different from these approach in the sense that it aims at providing a standalone OpenStack service, and also targets a broader fault model which includes software faults.

When testing resiliency by means of fault injection, the *representativeness* of the emulated faults should be of major concern. A recent study [16] shows that state-of-the-art fault injectors do not inject faults according to realistic distributions, observed in real-world systems. Our fault injector will therefore inject software faults, based upon anecdotal evidence (e.g., as described in [5]), instead of hardware faults only.

4 Fault Injection as a Service

Figure 1 depicts the architecture we propose for integrating fault injection as a service into the existing OpenStack ecosystem. Providing an API similar to other OpenStack services will make the tool easy-to-use and accessible. The fault injection daemon, which obtains fault scenarios from a database containing “faultload”, should access the REST APIs of other OpenStack services in order to inject faults from different classes.

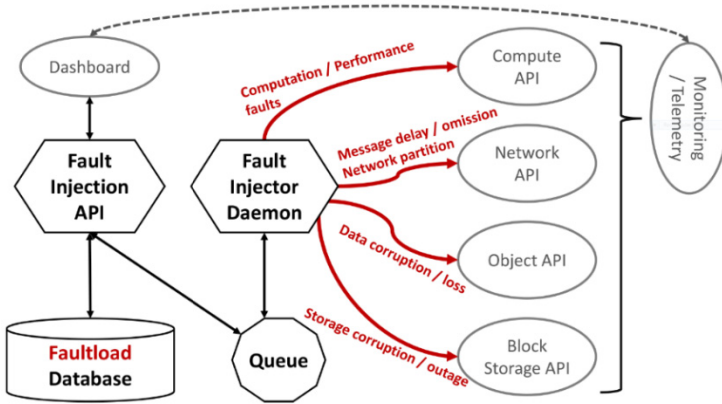


Fig. 1. Proposed architecture for “fault injection as a service”. The fault injection daemon accesses other OpenStack service APIs in order to inject different classes of faults. Monitoring and telemetry data should be gathered in order to evaluate how resilient the software is.

4.1 OpenStack

*OpenStack*³ is a prominent open source “cloud operating system”, or *cloud management stack*. Encompassing a number of independent software projects interacting with each other through REST APIs, OpenStack is frequently deployed as a modular and configurable Infrastructure as a Service (IaaS) solution for web applications.

³ www.openstack.org, 12/24/2014

With an increasing number of applications built on top of OpenStack, a tool for experimentally assessing the dependability of deployed software is desirable. Therefore, we suggest to integrate fault injection into the OpenStack ecosystem as its own REST service. Our approach is targeted at testing a wide range of software artifacts: OpenStack services themselves, as well as applications deployed on top of OpenStack IaaS, get tested.

4.2 Implementing Fault Classes

Faults from some classes can be injected by merely using API calls in a non-intrusive fashion, others would require the insertion of custom hooks. In the following paragraphs, we discuss the targeted fault classes at different levels in the software stack:

Physical Node Faults: Since hardware must be assumed to fail at random due to environmental stress or burn-in and wear-out phenomena, this fault class definitely has to be covered by an injection tool. The temporary or permanent outage of physical nodes can be simulated by cutting off messages from those nodes. In the case of compute nodes, API calls may also be used to shut them down. Furthermore, single nodes might suffer from increased CPU utilization (for instance because of other, compute-intensive jobs running on them). This fault class can be implemented either using per-node hooks, or by starting more compute jobs via the API.

Virtualization Level Faults: Relevant fault classes might be hypervisor service crashes or incorrectness (intrusive), or simply erroneous network configuration. Problems arising from the concurrent hosting of multiple VMs, over-commitment, or violated CPU quotas can be injected at the hypervisor level. Further, environment variables in VMs could be modified to assess their resilience against such robustness threats.

Service Level Faults: The interaction between different OpenStack services might be malfunctioning. For instance, the API might be used in unexpected or incorrect ways. Such faults can be introduced by the fault injector daemon directly. Exhausted rate limits can be simulated by re-configuring the compute API⁴.

Network Faults: Anecdotal evidence suggests that the assumption of a reliable, unpartitioned network does not hold in modern distributed systems⁵. To represent such network faults, message loss or delay, as well as partial or total network partitions can be introduced into the networking service.

5 Runtime Dependability Models

Figure 2 shows how we intend to use the fault injection service. The vision is a comprehensive framework which uses various sources to automatically run orchestrated fault injection experiments on a deployed cloud software system. From the observed runtime behaviour under faultload, dependability models, including quantitative data, shall be derived automatically.

⁴ <http://docs.openstack.org/trunk/config-reference/content/configuring-compute-API.html>, 12/24/2014

⁵ <https://github.com/aphyr/partitions-post>, 12/24/2014

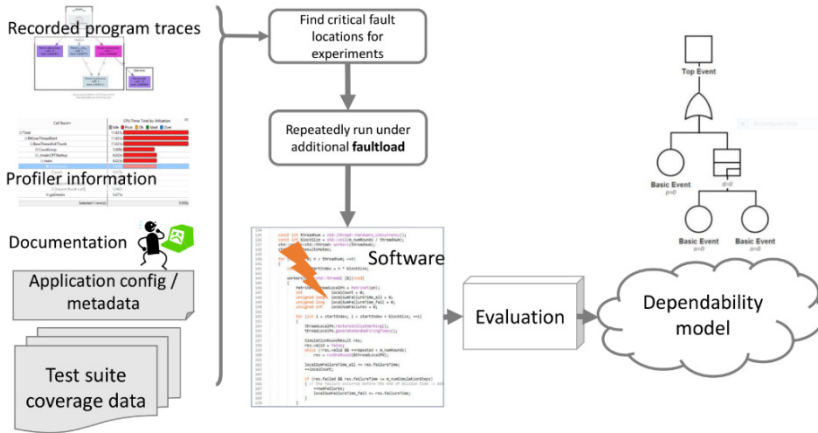


Fig. 2. Proposed experimental framework: Fault injection is used as a tool for getting runtime behaviour based dependability models. The faultload is designed according to application-specific information sources, such as profiler data, configuration, and documentation.

A platform-independent fault model, which takes into consideration dynamic information, is needed for cloud software. Such a fault model would answer the question of which faultload is adequate: *Which fault classes should be injected, and how often?*

There is a vast amount of related efforts in the quality assurance domain: literature such as the Orthogonal Defect Classification (ODC) [17], as well as online resources. A recent trend is mining data from bug trackers and using collaborative defect databases such as the Common Weaknesses Enumeration (CWE)⁶. Pretschner et al. [18] propose a fault model tailored for automatic testing. A literature study, with the goal of understanding state of the art software fault models, is currently in progress.

We believe that *fault activation* and *error propagation* patterns are of special interest for a broad class of distributed software failures. Understanding such environment-dependent patterns would enable the design of realistic faultloads and injection locations.

6 Conclusion and Future Work

As we have discussed, fault injection is a promising means for assessing the resilience of cloud software applications. Since the technique is used on deployed software, it yields more realistic failure data than static analysis approaches. We have proposed a draft architecture for “fault injection as a service” within the OpenStack ecosystem. The implementation of the service itself is work in progress.

In order to assess the system’s behaviour under faultload, it needs to be observed.

Running fault injection campaigns against a deployed system has the advantage that regular monitoring mechanisms can be used to observe how fault tolerant the system is. In the case of OpenStack, the in-built telemetry service *Ceilometer*⁷

⁶ <http://cwe.mitre.org/index.html>, 12/24/2014

⁷ <https://github.com/openstack/ceilometer>, 12/24/2014

provides information on the current state of the system. We still need to integrate monitoring into our architecture. Further approaches might be extracting dependability traits from logs, as demonstrated in [19].

A fault injection service would allow for non-intrusive resiliency tests, and can also be harnessed to experimentally assess the importance of single nodes with regard to overall application dependability. Ultimately, our goal is to use it for obtaining cloud software failure data, so that quantitative dependability models can be applied to make predictions.

References

1. Beizer, B.: Software is Different. *Ann. Softw. Eng.* **10**(1–4), 293–310 (2000)
2. Brewer, E.: CAP twelve years later: How the “rules” have changed. *Computer* **45**(2), 23–29 (2012)
3. Tseitlin, A.: The antifrangible organization. *Communications of the ACM* **56**(8) (2013)
4. Allspaw, J.: Fault Injection in Production. *Queue* **10**(8), 30:30–30:35 (2012)
5. Gunawi, H., Do, T., Hellerstein, J., Stoica, I., Borthakur, D., Robbins, J.: Failure as a service (faas): A cloud service for large-scale, online failure drills. University of California, Berkeley (2011)
6. Netflix: Chaos Monkey (accessed 2013). <https://github.com/Netflix/SimianArmy>
7. Gunawi, H., Do, T., Joshi, P., Alvaro, P., Hellerstein, J., Arpaci-Dusseau, A., Arpaci-Dusseau, R., Sen, K., Borthakur, D.: FATE and DESTINI: A framework for cloud recovery testing. In: *Proceedings of the 8th USENIX Conference on Networked Systems Design and Implementation*, Berkeley, CA, USA, pp. 238–252 (2011)
8. Joshi, P., Gunawi, H., Sen, K.: PREFAIL: A programmable tool for multiple-failure injection. In: *Proceedings of the 2011 ACM International Conference on Object Oriented Programming Systems Languages and Applications*, New York, NY, USA, pp. 171–188 (2011)
9. Faghri, F., Bazarbayev, S., Overholt, M., Farivar, R., Campbell, R., Sanders, W.: Failure scenario as a service (FSaaS) for hadoop clusters. In: *Proceedings of the Workshop on Secure and Dependable Middleware for Cloud Monitoring and Management*, New York, NY, USA, pp. 5:1–5:6 (2012)
10. Dawson, S., Jahanian, F., Mitton, T.: ORCHESTRA: A fault injection environment for distributed systems. Tech. rep. In: *26th International Symposium on Fault-Tolerant Computing (FTCS)* (1996)
11. Stott, D., Floering, B., Burke, D., Kalbarczpk, Z., Iyer, R.: NFTAPE: A framework for assessing dependability in distributed systems with lightweight fault injectors. In: *Proceedings of the IEEE International Computer Performance and Dependability Symposium, IPDS 2000*, pp. 91–100 (2000)
12. Segall, Z., Vrsalovic, D., Siewiorek, D., Yaskin, D., Kownacki, J., Barton, J., Dancey, R., Robinson, A., Lin, T.: FIAT-fault injection based automated testing environment. In: *Eighteenth International Symposium on Fault-Tolerant Computing, FTCS-18, Digest of Papers*, pp. 102–107 (June 1988)
13. Looker, N., Xu, J.: Dependability assessment of grid middleware. In: *37th Annual IEEE/IFIP International Conference on Dependable Systems and Networks, DSN 2007*, pp. 125–130 (2007)

14. Ju, X., Soares, L., Shin, K., Ryu, K., Da Silva, D.: On fault resilience of openstack. In: Proceedings of the 4th Annual Symposium on Cloud Computing, New York, NY, USA, pp. 2:1–2:16 (2013)
15. Yahoo: AnarchyApe (accessed 2012). <https://github.com/yahoo/anarchyape>
16. Natella, R., Cotroneo, D., Duraes, J.A., Madeira, H.S.: On Fault Representativeness of Software Fault Injection. *IEEE Transactions on Software Engineering* **39**(1), 80–96 (2013)
17. Chillarege, R., Bhandari, I., Chaar, J., Halliday, M., Moebus, D., Ray, B., Wong, M.-Y.: Orthogonal defect classification—a concept for in-process measurements. *IEEE Transactions on Software Engineering* **18**(11), 943–956 (1992)
18. Pretschner, A., Holling, D., Eschbach, R., Gemmar, M.: A generic fault model for quality assurance. In: Moreira, A., Schätz, B., Gray, J., Vallecillo, A., Clarke, P. (eds.) *MODELS 2013*. LNCS, vol. 8107, pp. 87–103. Springer, Heidelberg (2013)
19. Pecchia, A., Cotroneo, D., Kalbarczyk, Z., Iyer, R.K.: Improving log-based field failure data analysis of multi-node computing systems. In: 2011 IEEE/IFIP 41st International Conference on Dependable Systems Networks (DSN), pp. 97–108 (June 2011)
20. Grottke, M., Trivedi, K.: A classification of software faults. *Journal of Reliability Engineering Association of Japan* **27**(7), 425–438 (2005)

Usability of Scientific Workflow in Dynamically Changing Environment

Anna Bánáti¹(✉), Eszter Kail¹, Péter Kacsuk^{2,3}, and Miklos Kozlovsky^{1,2}

¹ John von Neumann Faculty of Informatics, Biotech Lab, Obuda University,
Bécsi str. 96/b., Budapest H-1034, Hungary

{banati.anna, kozlovsky.miklos}@nik.uni-obuda.hu

² LPDS, MTA SZTAKI, Kende str. 13-17, Budapest H-1111, Hungary

³ University of Westminster, 115 New Cavendish Street, London W1W 6UW, UK
kacsuk@sztaki.mta.hu

Abstract. Scientific workflow management systems are mainly data-flow oriented, which face several challenges due to the huge amount of data and the required computational capacity which cannot be predicted before enactment. Other problems may arise due to the dynamic access of the data storages or other data sources and the distributed nature of the scientific workflow computational infrastructures (cloud, cluster, grid, HPC), which status may change even during running of a single workflow instance. Many of these failures could be avoided with workflow management systems that provide provenance based dynamism and adaptivity to the unforeseen scenarios arising during enactment. In our work we summarize and categorize the failures that can arise in cloud environment during enactment and show the possibility of prediction and avoidance of failures with dynamic and provenance support.

Keywords: Scientific workflow · Dynamic workflow management system · Distributed computing · Cloud failures · Fault tolerance

1 Introduction

Over the last years the e-Science is gaining more and more ground. Existing e-Science experiments being (also called in silico experiments) really data and process intensive, it is inevitable to be executed in High Performance Computing (HPC) environments, such as clusters, grids and more recently clouds. Thanks to the virtualized environments, one of the main advantages of the clouds is the elasticity and the availability of resources. [1]

The enormous number of nodes, the complexity of the infrastructure and the high end computing resources needed to support scientific applications executed in the cloud, bring increased potential for failures and performance problems. On one hand due to the virtualization the resource management appears simpler from the applications' point of view and many of the system level failures are hidden from the users. However, on the other hand these failures could have significant impact on the execution of scientific workflows and because of their invisibility workflow monitoring,

analyzing or reproducibility is even more difficult, than in the case of other distributed systems [2]. Therefore it is even more crucial for the scientists to capture more and more parameters and data about the execution (provenance data) and about the environmental conditions since reproducibility and knowledge sharing in the scientists' community is one of the main challenges that scientific workflow management systems have to face with.

In our PhD research work we investigate provenance data analyses supporting dynamic executions of workflows and fault tolerance techniques. In this work we have summarized and classified the potential failures that may arise during the execution of scientific workflows in the cloud.

The contributions of this paper are:

1. Summarize and classify the emerging failures in the cloud during scientific workflow execution.
2. Examine the possibility of prediction and avoidance of failures with dynamic support.
3. Examine the possibility of prediction and avoidance of failures with provenance support.

The rest of the paper is organized as follows. The next section presents the contribution of our work to cloud based solutions, than we provide a short background and overview about works related to our research. Section 4 presents the dynamic requirements of scientific workflow management systems at different levels and in different phases of the workflow lifecycle. In section 5 we analyze the failures and give a solution to handle or avoid them. Finally we summarize our conclusions and reveal the potential future research directions.

2 Relationship to Cloud-Based Solutions

One of the main challenges in cloud systems is to ensure the reliability of job execution in the presence of failures. Cloud applications may span thousands of nodes and run for a long time before being aborted, which leads to the wastage of energy and other resources. [3, 4, 5]

In order to minimize failed execution and thus the multiple re-executions of the same workflow fault tolerance techniques must be investigated and supported. Since the numbers of failures are high and the types of them vary, general methods can hardly exist. In this work we have summarized and classified the most frequent failures that can arise during execution time on parallel and distributed environment focusing on cloud environment solely. We classified the potential failures into four different levels: cloud, workflow, task and user level. After categorizing the potential failures, we show how dynamic behavior and provenance support can give solutions for avoiding and preventing them or to recover from situations caused by failures and problems that cannot be foreseen or predicted.

3 Related Works

The analyses and recovery or avoidance strategies of failures arising during scientific workflow execution is a widely dealt research area. Many research works focus on different fault tolerance techniques and fault tolerance analyses of workflow management systems. However most of these works deal only with different hardware failures, but higher level failures are not mentioned or specified, in general only the states of jobs are differentiated (finished, failed, and killed). The cause of the failures is usually not investigated.

Vishwanath and Nagappan in their work [6] investigate the number and the cause of possible hardware failures in modern day data centers, which consist of thousands of network components, such as servers, routers and switches. These components have to communicate with each other to manage tasks in order to provide highly available cloud computing services. Consequently the number of hardware failures can be surprisingly high. Researchers in this work set up a hierarchical reliability model which helps analyzing the impact of server -, networking equipment and individual component failures in order to decrease hardware costs and to design a more fault tolerant system.

Bala and Chane in their work [7] present the existing proactive and reactive fault tolerant techniques that are used in the various cloud systems. They differentiate the reactive techniques into seven categories (Checkpointing/Restart, Replication, Job migration, SGuard, Retry, Task resubmission, user defined exception handling), while proactive techniques in three categories (Software rejuvenation, Proactive Fault Tolerance using Self- Healing and Proactive Fault Tolerance using Preemptive Migration).

Plankensteiner et al. [8] investigated the fault tolerance of Grid workflow management systems. They also give an overview of the existing fault tolerant techniques in different grid systems. The detection and avoidance of failures as well as recovery methods are also discussed in the paper. They give a deep and detailed taxonomy about the failures arising during enactment. This taxonomy grounds for our research work as well. To improve fault tolerance they suggest the use of light-weight and heavy-weight checkpoints, the storing of multiple instances of data and tasks and the use of alternate tasks.

4 Dynamic Scientific Workflow

The Lifecycle of scientific workflows can be partitioned into disjunctive phases (hypothesis generation, design, instantiation, execution, result analyses) [9 10, 11, 12] with the help of which the development, handling and enactment steps and requirements can be clearly defined and understood.

In one of our earlier work [13] we have summarized the requirements of a dynamic workflow management system regarding three phases (design, instantiation, execution) of the workflow lifecycle. In each phase (which can be interpreted as different abstract level as well) we have differentiated additional levels in order to have a deeper insight about this topic. [table 1.]

Table 1. The different levels of dynamism and the various solutions and methods that can be used according to the levels

design phase (abstract workflow level)	system level	composition level	task level	
	- black boxes - advance and late modelling technique	- language or graph structure	- modularity, reusability	
instantiation phase (concrete workflow level)	system level	task level	workflow level	
	- incremental compilation - various protocol support - provenance based sched. - multi instance activity	- task based sched. - late binding of data	- partitioning to sub workflows - parameter sweep appl. - wf based sched. - mapping adaptation	
execution phase (execution level)	system level	task level	workflow level	user level
	- exception handling - breakpoints - checkpoints - provenance based decisions - monitoring, logging - dynamic resource allocation	- dynamic resource allocation	- alternate task - change the model	- user intervention

5 Classifying Arising Failures in the Cloud and Analyzing Dynamic Solutions

As we mentioned earlier, during the different phases of the workflow lifecycle we have to face many types of failures, which lead unfinished task or workflow execution. In these cases the users, instead of getting the appropriate results of their experiment, the workflow process aborts and in general the scientist does not have knowledge about the cause of the failure.

The arising failures are examined at four abstract levels, namely the cloud level, task level, workflow level and user level. [Table 2.], [8, 15, 16, 17] The cloud level deals on the one hand with errors and problems related to the infrastructure (hardware or network failures), on the other hand with problems related to configuration parameters, which manage the execution.

In the table after the possible failures there is a „→” sign inserted and then the potential solutions that can be carried out by a dynamic system are presented.

5.1 Cloud Level

Virtualized resource management or “cloud” technologies can simplify the scientific application’s view of the resources, but do not remove the inherent complexity of large-scale applications. Thanks to the virtualized environments many levels of failures are hidden from the scientific application, and thus hard to monitor and analyze. [6] There are several issues related to computing, memory or storage resources, which are usual in grid, cluster or HPC systems, but thanks to the virtualization in cloud environment they become irrelevant. For example disk quota exceeded, out of memory, out of disk space and CPU time limit exceeded.

Cloud level is divided into two sublevels, namely the hardware level and the configuration level.

Hardware Level

The infrastructure is constructed from thousands of servers, routers and switches connected to each other. They communicate with each other to process the jobs. The servers consist of multiple hardware elements for example hard disks, memory modules, network cards, and processors etc., which are capable of failing. While the probability of seeing any such failure in the lifetime (typically 3-5 years in industry) of a server can be very small, the probability to meet failures in the datacenter, the number of components that could fail at any given instant is can be very high. At such a large scale, hardware component failure is rather normal than an exception. [6]

Cloud providers apply hardware redundancy and fault tolerance techniques to handle them transparently. The most popular fault tolerance technique is checkpointing and job migration or replication in order to prevent or to recover from failures. Some systems provide automatic and periodic checkpointing but a dynamic system should give the possibility of dynamic and user defined checkpointing techniques as well.

Configuration Level

At cloud level we have to face with not only hardware failures, but also task submission -, authentication -, service unreachable and file staging failures. At configuration level it is also true, that the checkpointing technique can decrease the waste derived from any failures. In addition, the execution of a task can be failed, if some configuration policy is not suitable. For example the system should periodically check the queues and guarantee, that all the jobs in the queues will be processed in a limited time. Another example can be the number of job resubmissions, which can influence the success of job executions, when it is a constant value. In order to be able to prevent these types of failures we can adjust the configuration parameters based on provenance information, and we can dynamically change the settings during workflow execution. [18]

5.2 Workflow Level

At workflow level we mention those failures, that have impact on the whole workflow and can corrupt the whole execution of the workflow. Independently from the type of failures, the scientists can reduce the severity of waste, if they can or they have the possibility to build the abstract workflow model from smaller modules or sub-workflows. In this way the effect of failures is isolated to a small piece of workflow.

At this level, unavailable input data, invalid input data and failed data transfer can lead to errors. To handle these faults, the common fault tolerance techniques, namely data and file replication is one of the best solutions.

Table 2. The failures at the different levels and their possible solution or optimization

design phase (abstract wf level)	cloud level failures	task level failures	user level	
				- infinite loop → advanced language and modeling support
instantiation level	cloud level failures	task level failures	workflow level failures	
	- HW failures - network failures - file not found - Network congestion - task submission failure → checkpoint - authentication failed → user intervention - file staging - Service not reachable	- Incorrect output data - Missing shared libraries	- Input data not available → data and file replication - Input error → data and file replication - Data movement failed → checkpoint	
Execution level	cloud level failures	task level failures	workflow level failures	user level failures
	- HW failures - network failures. - file not found - Job hanging in the queue of the local resource manager → dynamic resource brokering - Job lost before reaching the local resource manager → dynamic resource brokering + user intervention	- job crashed → user intervention, alternate task, checkpoint - deadlock/livelock → dynamic resource allocations, checkpoint - uncaught exception (numerical) → exception handling + user intervention	- Data movement failed → checkpoint	- User-definable exception

5.3 Task Level

The task level failures can influence the execution of only one task, and the impact of any failures does not cover the whole workflow. In generally it is true at this level (and at workflow level, too), that in the bulk of the cases the possibility of user intervention is the most helpful and efficient tools to handle the arising failures. On the one hand the user intervention can occur on the fly during execution, if it concerns to only one or a few threads of the whole workflow. On the other hand when a problem affects the entire execution than it has to be suspended and a checkpoint has to be inserted. If user intervention is supported, at these points [19] the user has the possibility to solve certain failures. In addition the scientist can make some changes, for example modify filtering criteria, change parameters or input data, restart a given task or a whole workflow or even do some time management actions.

In the instantiation phase incorrect output data or missing shared libraries can abort the execution.

6 Conclusion and Future Work

In order to minimize the effects of failures on the execution of scientific workflows, the failures should be discovered, handled or even predicted. In our work we have investigated the arising failures of scientific workflow execution in cloud environment at the different operation levels. We analyzed the possible solutions to prevent or to handle these failures transparently from the user. We have showed the methods and tools with which most of the problems can be solved. We have also highlighted that with provenance support the problems can be even more effectively handled or prevented. In our future work we would like to prove the effectiveness of the dynamic system and the provenance support with a mathematical model. and based on this model we would like to develop new proactive fault tolerance techniques.

References

1. da Cruz, S.M.S., Paulino, C.E., de Oliveira, D., Campos, M.L.M., Mattoso, M.: Capturing distributed provenance metadata from cloud-based scientific workflows. *Journal of Information and Data Management* 2(1), 43 (2011)
2. Samak, T., Gunter, D., Goode, M., Deelman, E., Juve, G., Silva, F., Vahi, K.: Failure analysis of distributed scientific workflows executing in the cloud. In: 2012 8th International Conference on Network and Service Management (CNSM) and 2012 Workshop on Systems Virtualization Management (SVM), pp. 46–54. IEEE (2012)
3. Liang, Y., Zhang, Y., Jette, M., Sivasubramaniam, A., Sahoo, R.: BlueGene/L failure analysis and prediction models. In: International Conference on Dependable Systems and Networks (DSN), pp. 425–434 (2006)
4. Pham, C., Cao, P., Kalbarczyk, Z., Iyer, R.K.: Toward a high availability cloud: Techniques and challenges. In: IEEE/IFIP 42nd International Conference on Dependable Systems and Networks Workshops (DSN-W), pp. 1–6. IEEE (2012)

5. Chen, X., Lu, C. D., Pattabiraman, K.: Failure analysis of jobs in compute clouds: A google cluster case study. In: *The International Symposium on Software Reliability Engineering (ISSRE)*. IEEE (2014)
6. Vishwanath, K.W., Nachiappan, N.: Characterizing cloud computing hardware reliability. In: *1st ACM Symposium on Cloud Computing*. ACM (2010)
7. Bala, A., Chana, I.: Fault tolerance-challenges, techniques and implementation in cloud computing. *IJCSI International Journal of Computer Science Issues* **9**(1) (2012) ISSN (Online): 1694-0814
8. Plankensteiner, K., Prodan, R., Fahringer, T., Kertesz, A., Kacsuk, P.: Fault-tolerant behavior in state-of-the-art grid workflow management systems (2007)
9. Bahsi, E.M.: *Dynamic Workflow Management For Large Scale Scientific Applications*, PhD Thesis, B.S., Fatih University (2006)
10. Deelman, E., Gil, Y., Ellisman, M., Fahringer, T., Fox, G., Gannon, D., Goble, C., Livny, M., Moreau, L., Myers, J.: Examining the challenges of scientific workflows. *IEEE Computer* **40**(12), 26–34 (2007)
11. Deelman, E., Gil, Y.: Managing large-scale scientific workflows in distributed environments: Experiences and challenges. In: *e-Science*, p. 144 (2006)
12. Ludäscher, B., Altintas, I., Bowers, S., Cummings, J., Critchlow, T., Deelman, E., Vouk, M.: Scientific process automation and workflow management. In: *Scientific Data Management: Challenges, Existing Technology, and Deployment*. Computational Science Series, pp. 476–508 (2009)
13. Kail, E., Bánáti, A., Karóczkai, K., Kacsuk, P., Kozlovsky, M.: Dynamic workflow support in gUSE. In: *Proceedings of the 37th International Convention, MIPRO* (2014)
14. Kail, E., Bánáti, A., Kacsuk, P., Kozlovsky, M.: Provenance based adaptive and dynamic workflows. In: *15th IEEE International Symposium on Computational Intelligence and Informatics*, pp 215–219. IEEE Press, Budapest (2014)
15. Das, A.: On Fault Tolerance of Resources in Computational Grids. *International Journal of Grid Computing & Applications* **3**, 1–10 (2012)
16. Mouallem, P.A., Vouk, M.: *A fault tolerance framework for kepler-based distributed scientific workflows*. North Carolina State University (2011)
17. Alsoghayer, R.A.: *Risk assessment models for resource failure in grid computing*. Thesis, University of Leeds (2011)
18. Bánáti, A., Kacsuk, P., Kozlovsky, M.: Towards flexible provenance and workflow manipulation in scientific workflows. In: *Proceedings of CGW 2014* (2014)
19. Kail, E., Kacsuk, P., Kozlovsky, M.: A novel approach to user-steering in scientific workflow. In: *Proceedings of CGW 2014* (2014)

Graph-Transformational Swarms with Stationary Members

Larbi Abdenebaoui^(✉), Hans-Jörg Kreowski, and Sabine Kuske

University of Bremen, P.O. Box 330440, D-28334 Bremen, Germany
{larbi, kreo, kuske}@informatik.uni-bremen.de

Abstract. The concept of graph-transformational swarms is a novel approach that offers a rule-based framework to model discrete swarm methods. This paper continues the research on graph-transformational swarms by focusing on a special type of members called stationary members. The stationary members are assigned to particular subgraphs of the considered environment graphs. Every stationary member is responsible for calculations and transformations on the assigned area, and the applicability of the member's rules depends only on this area and not on the whole environment. A further advantage of stationary members is that it is easier to guarantee that they can act in parallel than for moving members. Cloud computing is an engineering topic where swarms with stationary members can be applied in an adequate way, namely, by modeling the nodes of the server network that forms the cloud as stationary members. We illustrate the proposed concept by means of a case study.

Keywords: Swarm computation · Graph transformation · Stationary members · Cloud computing

1 Introduction

Swarms in the nature are fascinating phenomena that have inspired various concepts and algorithms in computer science (see, e.g., [3, 4]). However, there seems to be no framework unifying those concepts. Graph-transformational swarms have been proposed in [1] to partly fill this gap by providing a framework to model a variety of discrete swarm methods.

A graph-transformational swarm consists of members that act and interact simultaneously in an environment, which is represented by a graph. The members are all of the same kind or of different kinds. Kinds and members are modeled as graph transformation units [7] each consisting of a set of graph transformation rules specifying the capability of members and a control condition which regulates the application of rules. The basic framework is introduced in [1], where a simple ant colony, cellular automata and discrete particle systems are modeled to demonstrate the usefulness and flexibility of the approach.

This paper continues the research on graph-transformational swarms by focusing on a special type of members called stationary members. The stationary members are assigned to particular subgraphs of the considered environment graphs and stay there.

They are responsible for calculations and transformations at the assigned areas. The number of such members is proportional to the size of the underlying graph if parts of the members' subgraphs are exclusively assigned. The advantage of stationary members is that it is easier to establish the applicability of rules and to guarantee that the members can act in parallel than for moving members.

Graph-transformational swarms are related to other graph transformation approaches to parallelism and distribution as they are surveyed in [9] (see, particularly the contributions by Litovsky, Métivier and Sopena, by Janssens and by Taentzer et al.). These related approaches consider parallel and distributed computing on the level of rule application rather than on the level of units as in the case of swarms. One of the closest approaches seems to be the graph relabeling systems (see, e.g., [10,11]) where all node labels are changed simultaneously in every step implying massive parallelism and stationarity with respect to nodes.

The paper is organized as follows. Section 2 sketches how cloud-based systems can benefit from the concept of stationary members. In Section 3 we define the new notion of stationary members recalling for this purposes both the basic concepts of the underlying graph transformation approach and the notion of graph-transformational swarms. Section 4 demonstrates the notion of stationary members by means of a case study. The paper ends with the conclusion.

2 Contribution to Cloud-Based Engineering Systems

Cloud computing is an emerging technology with high promises, but also with various technical challenges. A cloud consists of a network of computer systems that have different tasks providing resources as services. Such a network can be modeled in a natural way as a graph. Every computer system in the cloud can be represented by a node and the connections between them via labeled edges. The labels can encode various technical information. Given such a graph, the graph-transformational swarms with stationary members can be applied to solve problems and to analyze the behavior of the cloud. The key connection of this paper to cloud systems is the assignment of the stationary members to the nodes of the cloud network so that the members can execute calculations locally and parallel to each other. Depending on the problem and the architecture of the chosen network, it is possible to define different kinds of stationary members that have different roles. The technical details about how this can be achieved follow in Sections 3 and 4.

Graph-transformational swarms with stationary members can contribute to cloud-based engineering systems at least by (1) offering a visual and mathematical basis for the analysis of cloud behavior, and (2) providing a framework to design distributed algorithms based on parallel rule applications able to be used directly in a cloud. The first claim is directly inherited from the advantages using graph transformation as basic method in the proposed framework. The second claim is illustrated by the example introduced in Section 4: a cycle freeness test. The proposed solution can be directly applied to a cloud system for detecting deadlocks.

3 Graph-Transformational Swarms and Stationary Members

In this section, we define the new notion of stationary members. To achieve this, we recall the concept of graph-transformational swarms starting with the basic components of the chosen graph transformation approach as far as needed in this paper (for more details, see, e.g. [2, 6, 7, 8]).

3.1 Basic Concepts of Graph Transformation

A (*directed edge-labeled*) graph consists of a set of unlabeled nodes and a set of labeled or unlabeled edges such that every edge is directed. If the target is equal to the source, then the edge is called a *loop*. A *match* of a graph G in a graph H is an image of G in H under a graph morphism. If G is a subgraph of H , we use the notation $G \subseteq H$.

A rule $r = (N, L, K, R)$ consists of four graphs: the *negative context* N , the *left-hand side* L , the *gluing graph* K , and the *right-hand side* R such that $N \supseteq L \supseteq K \subseteq R$. We depict a rule as $N \rightarrow R$ dashing the elements in N that do not belong to L and using different shapes for nodes so that K can be identified as the identical parts of L and R . Given the rules $r_i = (N_i, L_i, K_i, R_i)$ for $i = 1, \dots, n$, the *parallel rule* $p = \sum_{i=1}^n r_i$ is given by the disjoint unions of the respective components of each r_i .

The application of a rule $r = (N, L, K, R)$ to a graph G replaces a match of L in G by R such that the match of K is kept. If L is a proper subset of N the match of L must not be extendable to a match of N . A rule application is denoted by $G \xRightarrow[r]{}$ H where H is the resulting graph and called a *direct derivation* from G to H . A sequence $G = G_0 \xRightarrow[r_1]{}$ $G_1 \xRightarrow[r_2]{}$ $\dots \xRightarrow[r_n]{}$ $G_n = H$ is called a *derivation* from G to H . Such a derivation can also be denoted by $G \xRightarrow[*]{}$ H . Two direct derivations $G \xRightarrow[r]{}$ H_1 and $G \xRightarrow[r']{}$ H_2 of two rules r and r' are (*parallel*) *independent* if the corresponding matches intersect only in gluing items.

The following considerations are based on a parallelization theorem in [5]:

A parallel rule $p = \sum_{i=1}^n r_i$ can be applied to G if and only if the rules r_i for $i = 1, \dots, n$ can be applied to G and the matches are pairwise independent. Moreover the r_i can be applied one after the other in arbitrary order deriving in each case the same graph as the application of p to G .

This allows the use of massive parallelism in the context of graph transformation based on local matches of component rules which are much easier to find than matches of parallel rules.

A *control condition* C is defined over a finite set P of rules and specifies a set $SEM(C)$ of derivations. Typical control conditions are priorities and regular expressions over P . Other control conditions are the expressions $\|r\|$ and $[r]$. The first ex-

pression requires that a maximum number of the rule r be applied in parallel and the second one requires that the rule r may be applied or not.

A *graph class expression* X specifies a set of graphs denoted by $SEM(X)$. We use the graph class expression $id-looped(G)$ which adds to each node of the graph G a loop labeled with the name of the node. Another graph class expression is *forbidden*(H) for a graph H . $SEM(forbidden(H))$ contains all graphs without a subgraph isomorphic to H .

A *graph transformation unit* is a pair $gtu = (P, C)$ where P is a set of rules, and C is a *control condition* over P . The *semantics* of gtu consists of all derivations of the rules in P allowed by C . A unit gtu is *related* to a unit gtu_0 if gtu is obtained from gtu_0 by relabeling. The set of units related to gtu_0 is denoted by $RU(gt u_0)$.

3.2 Graph-Transformational Swarms

A graph-transformational swarm consists of members of the same kind or of different kinds to distinguish between different roles members can play. All members act simultaneously in a common environment represented by a graph. The number of members of each kind is given by the size of the kind. While a kind is a graph transformation unit, the members of this kind are modeled as units related to the kind so that all members of some kind are alike.

A swarm computation starts with an initial environment and consists of iterated rule applications requiring massive parallelism meaning that each member of the swarm applies one of its rules in every step. The choice of rules depends on their applicability and the control conditions of the members. We allow to provide a swarm with a cooperation condition. Moreover, a swarm may have a goal given by a graph class expression. A computation is considered to be successful if an environment is reached that meets the goal.

Definition 1 (Swarm). A *swarm* is a system $S = (in, K, size, M, coop, goal)$ where in is a graph class expression specifying the set of *initial environments*, K is a finite set of graph transformation units, called *kinds*, $size$ associates a *size* $size(k) \in \mathbb{N}_{>0}$ with each kind $k \in K$, M associates a family of *members* $(M(k)_i)_{i \in [size(k)]}$ with each kind $k \in K$ with $M(k)_i \in RU(k)$ for all $i \in [size(k)]$, $coop$ is a control condition called *cooperation condition*, and $goal$ is a graph class expression specifying the *goal*¹.

A swarm may be represented schematically depicting the components *initial*, *kinds*, *size*, *members*, *cooperation* and *goal* followed by their respective values.

Definition 2 (Swarm Computation). A *swarm computation* is a derivation $G_0 \xRightarrow{p_1} G_1 \xRightarrow{p_2} \dots \xRightarrow{p_q} G_q$ such that $G_0 \in SEM(in)$, $p_j = \sum_{k \in K} \sum_{i \in [size(k)]} r_{jki}$ with a rule r_{jki} of $M(k)_i$ for each $j \in [q]$, $k \in K$ and $i \in [size(k)]$, and $coop$ and the control conditions of all members are satisfied.

¹ $\mathbb{N}_{>0} = \mathbb{N} - \{0\}$ and $[n] = \{1, \dots, n\}$.

That all members must provide a rule to a computational step is a strong requirement because graph transformation rules may not be applicable. In particular, if no rule of a swarm member is applicable to some environment, no further computational step would be possible and the inability of a single member stops the whole swarm. To avoid this global effect of a local situation, we assume that each member has the empty rule $(\emptyset, \emptyset, \emptyset, \emptyset)$ in addition to its other rules. The empty rule gets the lowest priority. In this way, each member can always act and is no longer able to terminate the computation of the swarm. In this context, the empty rule is called sleeping rule. It can always be applied, is always parallel independent with each other rule application, but does not produce any effect. Hence, there is no difference between the application of the empty rule and no application within a parallel step.

3.3 Stationary Members

The basic idea of swarm computation is that the members of a swarm can solve problems by team work and massive parallelism better or faster than a single processing unit. In the general setting, there may be two obstacles to meet these advantages. (1) To compute which member can perform which action may take time proportional to n^k where n is the size of the environment and k is the size of the left-hand side of the rule to be applied. The latter one can often be chosen small enough, but the former can get very large. (2) To make sure that members can act in parallel, one must check independence for each pair of matches of rules to be applied which is quadratic in the number of members in general. Both obstacles can be avoided by stationary members. Their matches can be found locally in a small area rather than in the whole environment and independence of most pairs of matches is automatically guaranteed because they are always far away from each other.

Although the environment is changed in a swarm computation, there may be an invariant part. A member of a swarm may be considered as stationary if all left-hand sides of its rules can only match in the vicinity of a fixed subarea of the permanent part of the environment. Then the matches of the rules depend only on the size of this subarea and its vicinity and no longer on the size of the whole environment. Moreover, the independence of such a match from other matches must only be checked if the subareas and vicinities overlap which is never the case if the involved subareas are far enough away from each other. More formally, we get the following definition.

Definition 3 (Stationary Members). Let $S=(in,K,size,M,coop,goal)$ be a swarm. Then its members are called *stationary* if the following holds:

- (1) Each initial environment graph $G \in SEM(in)$ is associated with a set SUB of subgraphs which is kept invariant by swarm computations, i.e., SUB is a set of subgraphs of G' for each swarm computation $G \xRightarrow{*} G'$.
- (2) Each member $m \in M(k)$ for each $k \in K$ is associated with a subgraph $G(m) \in SUB$.

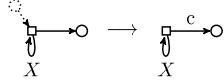
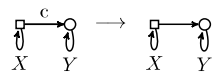
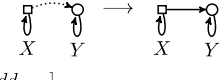
- (3) Each left-hand side of each rule of each member m contains a subgraph that matches only in $G(m)$ and the rest of the match can be found in the neighborhood of $G(m)$.

Here neighborhood is a generic notion and may consist of all nodes adjacent to $G(m)$ and the edges connecting them to $G(m)$ or all nodes reachable by paths from $G(m)$ of a bounded length.

4 A Case Study: Cycle Freeness Test

In this section, we illustrate the notion of stationary members by means of a simple and well-known decision problem. We provide a swarm with stationary members that tests an input graph for cycle freeness. Due to the massive parallelism of the swarm members' teamwork, the number of computational steps is linearly bounded. We have chosen this simple example because more sophisticated examples would need too much space. But to illustrate all the features of swarms, we solve the cycle freeness problem in a dynamic setting meaning that new edges can be added to the underlying graph from time to time so that after enough edge additions every initial graph ends up with cycles.

The swarm that tests a simple, unlabeled and directed graph G for cycle freeness is depicted below. It gets the graph G as a parameter and we assume that the nodes are numbered from 1 to n . G is turned into the initial environment by adding an i -loop to each node $i \in [n]$. There are three kinds: (1) *marker* with a single rule $mark_X$ which marks an edge outgoing of a node with an X -loop provided that there is no incoming unlabeled edge. The control condition $\|mark_X\|$ requires that the rule be applied with maximum parallelism. The size is the number n of nodes. The member $marker_i$ for $i \in [n]$ is obtained from *marker* by relabeling all occurring X with i . (2) *resetter* has a single rule that turns a marked edge into an unmarked one. The X - and Y -loop identify source and target yielding stationarity of the members $resetter_{i,j}$ where X and Y are relabeled by the node identifier $i, j \in [n]$. (3) *adder* has a rule that adds an edge between an X - and a Y -looped node. The control condition $[add_{X,Y}]$ requires that the rule may be applied or not. The cooperation condition requires that *marker* is applied as long as possible followed by an arbitrary number of repetitions of *resetter* followed by *adder* followed by *marker* and this again as long as possible. The goal is to reach a graph without unlabeled edges meaning that all unlabeled edges are changed into c -marked ones.

<p>$\text{cyclefree}(G)$</p> <p>initial: $\text{id-looped}(G)$</p> <p>kinds: $\text{marker}, \text{resetter}, \text{adder}$</p> <p>size: n, n^2-n, n^2-n</p> <p>members: marker_i for $i \in [n]$, $\text{resetter}_{i,j}$ for $i, j \in [n], i \neq j$, $\text{adder}_{i,j}$ for $i, j \in [n], i \neq j$</p> <p>coop: $\text{marker}!; (\text{resetter}, \text{adder}, \text{marker}!)*$</p> <p>goal: $\text{forbidden}(\text{O} \rightarrow \text{O})$</p>	<p>marker</p> <p>rules:</p> <p>mark_X: </p> <p>control: $\ \text{mark}_X\$</p>
<p>resetter</p> <p>rules:</p> <p>$\text{reset}_{X,Y}$: </p>	<p>adder</p> <p>rules:</p> <p>$\text{add}_{X,Y}$: </p> <p>control: $[\text{add}_{X,Y}]$</p>

As the rule applications of the swarm members of kind *marker* change unlabeled edges into *c*-marked ones, the nodes and their loops are kept invariant so that the members are stationary and the match of the rule mark_i is fixed by the unique *i*-loop and varies only in the outgoing edges. Two matches of mark_i are independent if they access different outgoing edges which can be checked locally. Matches of mark_i and mark_j for $i \neq j$ are always independent. Consequently, a maximum parallel step of the swarm marks simultaneously all edges outgoing from nodes without incoming unlabeled edges. As long as there are such edges, their number decreases in each computational step of the *marker*-members such that - by induction - we always end up with the unlabeled edges on cycles. In particular, the number of such steps is bounded by the length of the longest simple path and cycles are never broken. Summarizing, the following result is shown.

Theorem 1. The swarm $\text{cyclefree}(G)$ reaches its goal if and only if G is cycle-free. To decide this, the number of steps is bounded by the length of the longest simple path in G .

Moreover, the *resetter*-step returns the graph given before the *marker*-computations, and the *adder*-step adds new edges. The resulting graphs are tested by the *marker*-computations for cyclefreeness in the same way as the initial graph. Therefore, Theorem 1 holds for them, too.

5 Conclusion

In this paper, we have introduced the notion of graph-transformational swarms with stationary members, which establishes a connection between different areas of research: graph transformation, swarm computation and cloud computing. The idea is to model a cloud as a graph and to apply the concepts and results of graph-transformational swarms within the framework of cloud computing.

We have presented a case study that demonstrates how to apply the notion of stationary members to solve graph problems. The case study shows that such solutions take advantage of massive parallelism, can be visually represented and support correctness results. However, in order to prove the power of the concept, bigger and more difficult examples should be modeled in the future. In cloud computing specially, one can consider task scheduling problems which are in general NP-hard problems. Their solutions can profit from a combination of swarm heuristics and the massive parallelism within the proposed framework.

Acknowledgement. We are grateful to the anonymous reviewers for their valuable comments.

References

1. Abdenebaoui, L., Kreowski, H.-J., Kuske, S.: Graph-transformational swarms. In: Bensch, S., Drewes, F., Freund, R., Otto, F. (eds.) Proceedings of the Fifth Workshop on Non-Classical Models for Automata and Applications – NCMA 2013, Umea, Sweden, August 13–August 14, pp. 35–50. Österreichische Computer Gesellschaft (2013)
2. Ehrig, H., Ehrig, K., Prange, U., Taentzer, G.: Fundamentals of Algebraic Graph Transformation. Monographs in Theoretical Computer Science. An EATCS Series. Springer, Heidelberg (2006)
3. Engelbrecht, A.P.: Fundamentals of Computational Swarm Intelligence. John Wiley & Sons (2006)
4. Kennedy, J., Eberhart, R.C.: Swarm Intelligence. Evolutionary Computation Series. Morgan Kaufman, San Francisco (2001)
5. Kreowski, H.-J.: Manipulationen von Graphmanipulationen. PhD thesis, Technische Universität Berlin (1977)
6. Kreowski, H.-J., Klempien-Hinrichs, R., Kuske, S.: Some essentials of graph transformation. In: Esik, Z., Martin-Vide, C., Mitrana, V. (eds.) Recent Advances in Formal Languages and Applications. SCI, vol. 25, pp. 229–254. Springer, Heidelberg (2006)
7. Kreowski, H.-J., Kuske, S., Rozenberg, G.: Graph transformation units – an overview. In: Degano, P., De Nicola, R., Meseguer, J. (eds.) Concurrency, Graphs and Models. LNCS, vol. 5065, pp. 57–75. Springer, Heidelberg (2008)
8. Rozenberg, G. (ed.): Handbook of Graph Grammars and Computing by Graph Transformation. Foundations, vol. 1. World Scientific, Singapore (1997)
9. Ehrig, H., Kreowski, H.-J., Montanari, U., Rozenberg, G. (eds.): Handbook of Graph Grammars and Computing by Graph Transformation. Concurrency, Parallellism, and Distribution, vol. 3. World Scientific (1999)
10. Métivier, Y., Sopena, E.: Graph Relabelling Systems: A General Overview. Computers and Artificial Intelligence **16**(2) (1997)
11. Bauderon, M., Métivier, Y., Mosbah, M., Sellami, A.: Graph Relabelling Systems: A Tool for Encoding, Proving, Studying and Visualizing Distributed Algorithms. Electronic Notes in Theoretical Computer Science **51**, 93–107 (2002)

Embedded Systems

Analysis and Generation of Logical Signals for Discrete Events Behavioral Modeling

Rogério Campos-Rebello^{1,2(✉)}, Anikó Costa^{1,2}, and Luis Gomes^{1,2}

¹ Universidade Nova de Lisboa, Faculdade de Ciências e Tecnologia, Almada, Portugal

² UNINOVA – Centro de Tecnologias e Sistemas, Almada, Portugal
{rcr, akc, lugo}@uninova.pt

Abstract. This paper presents a proposal for structuring logical signals for discrete events behavioral modeling. Graphical formalisms will be used to illustrate applicability of the proposed techniques. Input logical signals are generated based on the analysis of physical signals coming from the environment and other input logical signals. Their analysis is introduced in the flow of the input signal analysis, defined as pre-processing when using a modeling formalism. Their analysis is done in the first step of pre-processing, allowing to put these signals at the same level of the physical ones, enabling its use in the rest of the signals' analysis, and also allowing the generation of events and conditions associated with these signals. Likewise, logical signals are also defined in the flow of post-processing, allowing the definition of output logical signals through analysis and composition of the output signals generated by the model execution. The output logical signals are analyzed in the last step of post-processing in order to allow the use of the signals affected by the events in its analysis. The usage of these signals allows improvements in terms of expressiveness and compactness of the resulted models, both directly due to its use as well as by the increase of the possibilities of analysis provided to the following parts of the development flow.

Keywords: Signal analysis · Modelling formalisms · Embedded systems

1 Introduction

During the last decades, computer systems have experienced an increase in their complexity. The main reasons are related with the development of hardware that supports new functionalities, increasing memory and processing capacity, as well as software frameworks supporting their development. Becoming possible to create more complex systems, it allows the creation of more robust and enjoyable systems with more capabilities. Furthermore, their development becomes more complex and susceptible to failures, both in increase of quantity and variety. To handle these complexity problems, several approaches have been proposed in order to decompose the system development. The Model Based Development approach, as the Model Driven Architecture (MDA) defined by the Object Management Group (OMG) [1], is an example, which uses specific languages for system specification.

There is a wide variety of modeling languages. Among them, graphical languages are distinguished by providing an easier reading by the human user. Some examples of these

type of languages are Statecharts [2], state-machines variants [3], and Petri nets [4][5][6]. They allow a graphical view of the behavioral model, providing a visual representation of the system behavior easily understandable (and analyzed) by a human user. Creation of quite large models makes them confuse and difficult to interpret. Therefore, decomposition of modeling techniques had been proposed, allowing creating less complex models.

Some of these techniques allow transferring the signal analysis for pre- and post-processing, removing them from an explicit representation within the model.

The growing development of the Service Oriented Architecture (SOA) and the Event-Driven Architecture (EDA) [7] combined with the reduction of cost in sensor technology have led, in the last years, to a big development in the use of events in the analysis of signals and system' behavior [8]. Use of event modeling allows the development of more complex systems expressed through a much more compact model, supporting the development of much more user friendly interfaces.

One of the most well-known examples is the Complex Event Processing (CEP). They were first presented by David Luckham in his book *The Power of Events: An Introduction to Complex Event Processing in Distributed Enterprise Systems* [9]. They are used in different areas, as an application based in RFID presented in [10]. Together with CEP was defined RAPIDE [11] [12], a computer language for definition and execution of models of system architectures with CEP.

This paper emphasizes introduction to the pre- and post-processing flows allowing putting the techniques of logical signals analysis within them. This addition allows the modeler to use these techniques to define new signals from which the analysis through events can take advantage.

2 Relationship to Cloud-Based Engineering Systems

Cloud-based engineering service-oriented systems are systems that allow the user to configure the system through services that are available online. In these systems, the software and hardware as services are reconfigured. Event-Driven Systems are similar, where the events are provided like services.

The work proposed in this paper presents the addition of logical signals to the signals analysis flow, in order to improve the detection of behaviors. The use of this flow with events makes it suitable for creation of event-driven systems, allowing an easier analysis of the signals. The use of the events like services in the model makes this proposal interesting to create cloud-based systems. We argue that the use of model-based development strategies within cloud-based systems will benefit from adopting the proposed signal analysis techniques.

3 Related Work

The analysis of input and output signals on pre- and post-processing is a solution that has been developed to solve the problem of increased complexity of the models. For this purpose, the entire analysis of signals from the environment is made outside the model, communicating with the model through the results of this analysis.

In terms of inputs, two forms are considered to analyze a signal:

Condition - the value of the signal is analyzed to verify that a certain equation holds. A condition checks the signal value at a specific point in time.

Event - the event analyzes the signal evolution in a time window (at least two points in time, associated with two execution steps) in order to verify if the signal evolution obeys to a specific defined behavior.

Previously, signal analysis was also presented in [13], considering not only the evolution of the signal values, but also variations of the signal at consecutive steps, as any difference level of variation of the signal (Δ). The first level of variation (Δ^1) is defined as a difference of the signal value in two consecutive instants. The second level of variation (Δ^2) is defined as a difference of Δ^1 in two consecutive instants. With these it is possible to define higher order of differences.

Table 1. Events and Conditions Definition

Conditions		Closed Events		Open Events	
>	$\Delta^m X_n > k$	\leq to >	$\Delta^m X^{n-1} < k \wedge \Delta^m X_n > k$	< to >	$\Delta^m X^{n-1} < k \wedge \Delta^m X_n > k$
\geq	$\Delta^m X_n \geq k$	< to \geq	$\Delta^m X_{n-1} < k \wedge \Delta^m X_n > k$	> to <	$\Delta^m X_{n-1} < k \wedge \Delta^m X_n > k$
<	$\Delta^m X_n < k$	> to \leq	$\Delta^m X^{n-1} < k \wedge \Delta^m X_n > k$	< to =	$\Delta^m X^{n-1} < k \wedge \Delta^m X_n > k$
\leq	$\Delta^m X_n \leq k$	\geq to <	$\Delta^m X_{n-1} < k \wedge \Delta^m X_n > k$	> to =	$\Delta^m X_{n-1} < k \wedge \Delta^m X_n > k$
=	$\Delta^m X_n = k$	\neq to =	$\Delta^m X^{n-1} < k \wedge \Delta^m X_n > k$	= to >	$\Delta^m X^{n-1} < k \wedge \Delta^m X_n > k$
\neq	$\Delta^m X_n \neq k$	= to \neq	$\Delta^m X_{n-1} < k \wedge \Delta^m X_n > k$	= to <	$\Delta^m X_{n-1} < k \wedge \Delta^m X_n > k$

In Table 1, the definitions are presented to an m-level variation. Given this set of assumptions, it is possible to define several ways to analyze a signal. The work presented in [14] defines a set of elementary events, allowing the definition of a set of behaviors that the signal can have.

In Table 1, these types of events, defined as in [14] as open and closed events, are presented, including the conditions that allow their determination. The various conditions are also presented, which allows analysis of a given signal value.

In a similar way, output signals can be affected by two different methods. They can be updated by an action directly over the signal or by creation of an event associated to the output signal that will determine the signal's behavior:

Action - it is an assignment action of the signal, at a certain moment, with a specific value, as in $\text{Signal_ID} = k$.

Event - the event is associated with an output signal; when the event is active, generates a defined behavior with which the signal will be affected.

The output events are defined in [15]. In this work, the behavior associated with the event, with which the signal will be affected are defined taking into account three variables: Evolution Function, Window, and Final Value.

The **Evolution Function** ($f(n)$) can be defined as any $f(n)$ function. This function will guide the evolution of the signal, giving, for each execution step, the contribution value of the event to the associated signal. Generically the contribution of the event to the associated signal to each step $n+p$ is equal to the value of $f(p)$.

The **Window** (w) is an integer value that defines the number of steps following the occurrence of the event where the event contributes to the value of the associated

output signal. For example, if the value of the window is 2, the event will contribute for the signal associated value in the execution steps $n+1$ and $n+2$.

The **Final Value (fv)** is the value that the associated signal should have at the end of the event contribution, which means at the end of the window.

To define the evolution behavior, it is necessary to define only two of these three variables (Evolution Function, Window, and Final Value). Therefore, three different types of output events, based on variables which are left free are defined.

Table 2. Output Events definitions

	Timed Assignment	Guided Assignment	Evolution
Evolution Example			

In Table 2 the three types of output events are presented. For each one, a graphical representation of a generic evolution is presented.

The **Timed Assignment** event is based on the definition of the window value and the value for the signal in the last step of the window. In this case, knowing previously the final value of the signal, the function needs to do the approximation to this value in the exact number of steps defined in the window.

The **Guided Assignment** event, as an assignment event defines the value for the signal in the last step of the contribution. The evolution function is defined as well with the final value of the signal. In this case, the window is not a priori defined. The window value is obtained as the number of steps needed to reach the final value guided by the defined function.

In an **Evolution** event, unlike the assignment events, the final value of the associated signal is not a priori known. The signal value evolves depending on the defined function associated to the event during the defined time window. The final value will be obtained accordingly, from the computation of the evolution function during the time window.

4 Signal Analysis

Input and output events, such as the conditions and the actions presented in the previous chapter, are defined as a way to analyze the signals in order to find or generate behaviors in the chosen input or output signal, respectively. As result of such definition the analysis of the input signal and the assignment of the output signals are transferred to pre- and post-processing, respectively. Consequently, the presented events are a result of the flow of pre- or post-processing.

This paper proposes to include, in the flow of pre- and post-processing, the analysis of logical signals, generated from the analysis of the physical signals and other logical signals.

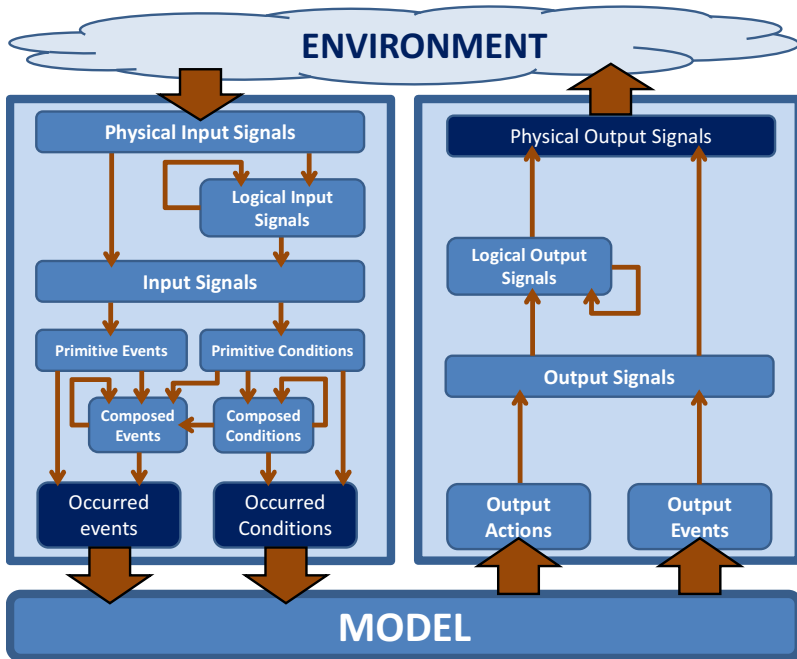


Fig. 1. Pre- and post-processing flow

These logical signals, after defined and calculated their values, will become available for analysis through events and conditions, such as the physical signals. Although they are placed at the same level for the subsequent analysis, the value of the logical signals may represent quite different amounts.

With this addition the pre- and post-processing of the system, in terms of signals, is defined by the diagram in Fig. 1.

In the pre-processing part (Fig. 1-left) the values of the physical signals from the environment are received at each execution step. Then, based on their values, logical signals are defined and analyzed. They can be used in the analysis of other logical signals. After the analysis of the logical signals, these, together with the physical signals, are provided as a set of input signals for further analysis. In the next step the primitive conditions and events associated to the signals are calculated. Finally, based on primitive events and conditions, the composition of events and conditions are computed. Similarly as for logical signals, the analysis of some composed events and conditions can depend on the analysis of other events or conditions. The results of those analyses are introduced to the system model.

In the post-processing part (Fig. 1-right), the execution of the model generates events and actions associated to the output signals. These actions and events update the output

signals by changing their values. Similarly to input signals, the analysis of a logical output signal can depend on the analysis of other logical output signals. After all the logic signals analyzed, the values of the signals generated by the events and actions in conjunction with logic signals are provided as outputs to the environment.

4.1 Physical Signals Analysis

Internal representation of a physical input signal is composed by the value received from the environment in the current time step and a series of values previously received during a time window. Associated with this window of values various levels of differences between values are also calculated. This list of values, as shown in Fig. 2, saves a set of consecutive values that the signal had in the past execution steps and the difference between them.

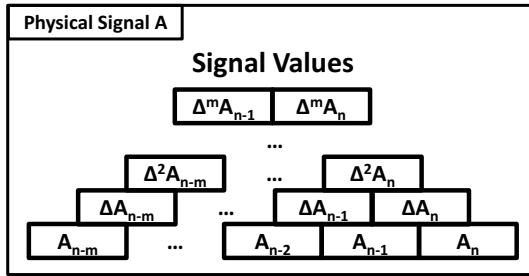


Fig. 2. Physical Signal Composition

This window with the history of values of the signal allows the analyses of events associated with the signal, and analyze logical signals. To calculate the size of this window is necessary to analyze all events and logical signals associated with that signal.

The number of deltas (steps) to be analyzed is given by the maximum of the largest deltas analyzed in each event associated with the signal.

Regarding the number of values to store in terms of Delta zero (d0), the value depends on delta (Δ). The maximum value is given by the results in the following equation for each event associated with signal:

$$\text{for } \Delta^n, d0 = n + 1$$

For instance, for an event that analyzes the Δ^2 of the signal, the signal needs to hold 3 values (from A_n to A_{n-2})

In terms of logical signals is necessary to find the oldest value being analyzed in the logical signal to determine how many values to hold.

Exemplifying, if the maximum value analyzed in a logical signal is $\Delta^3 A_{n-3}$, it will be needed to analyze values until the third delta and in the delta zero from A_n to A_{n-6} . The value is obtained by the following analysis: $\Delta^3 A_{n-3} = \Delta^2 A_{n-4} - \Delta^2 A_{n-5}$; $\Delta^2 A_{n-4} = \Delta A_{n-5} - \Delta A_{n-6}$; $\Delta A_{n-5} = A_{n-6} - A_{n-7}$.

4.2 Logical Signals Analysis

A logical signal can represent different things, for example the conversions of the value of a physical signal in radians to degrees, the average value, or even complex values resulting from complex functions, like the FFT of a signal.

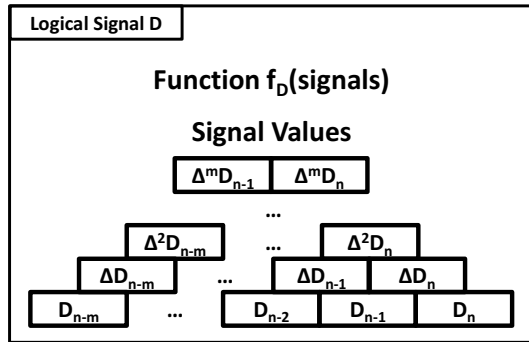


Fig. 3. Logical Signal Composition

In terms of its composition, the logical signal inherits all the characteristics of the associated physical signal. It also has a function (or set of functions) associated (Fig. 3). The values of the logical signal are the results of this function.

In the case of a logical signal, the values from n to $n-m$ may not represent time steps. Although the representation is equivalent, it depends of the following processing steps to know the meaning of the values.

Logical signals are present in both, pre- (Logical Input Signals) and post-processing (Logical Output Signals). Logical Input Signals are analyzed in the pre-processing step immediately following the acquisition of physical input signals. Their analysis depends on the values of the physical signals as well as other logical signals.

Fig. 4 presents the analysis process of the Logical Input Signals.

Once received and analyzed all physical input signals, the logical input signals that only depend on physical signals are computed. Next, all logical input signals also depending on recently computed logical signals are computed. This process is repeated until all the logical signals have been computed.

At the end of the analysis, physical and logical signals become available to the rest of the analysis at the same level. This means that for the continuation of the flow does not matter if these signals come from the environment or have been generated.

On the other hand, the output signal analysis flow is accomplished through post-processing, and the analysis of events and actions affecting the output signals is made in a similar way as for input signals.

After having analyzed all the events and executed all actions, a set of output signals is available. These signals are provided to the environment, but they are also used in the analysis of logical output signals.

The analysis of logical output signals is similar to the analysis of input logical signals. The flow is equivalent to the Fig. 4 where Input physical signals are replaced by Output Signals and Input Signals are replaced by physical output signals.

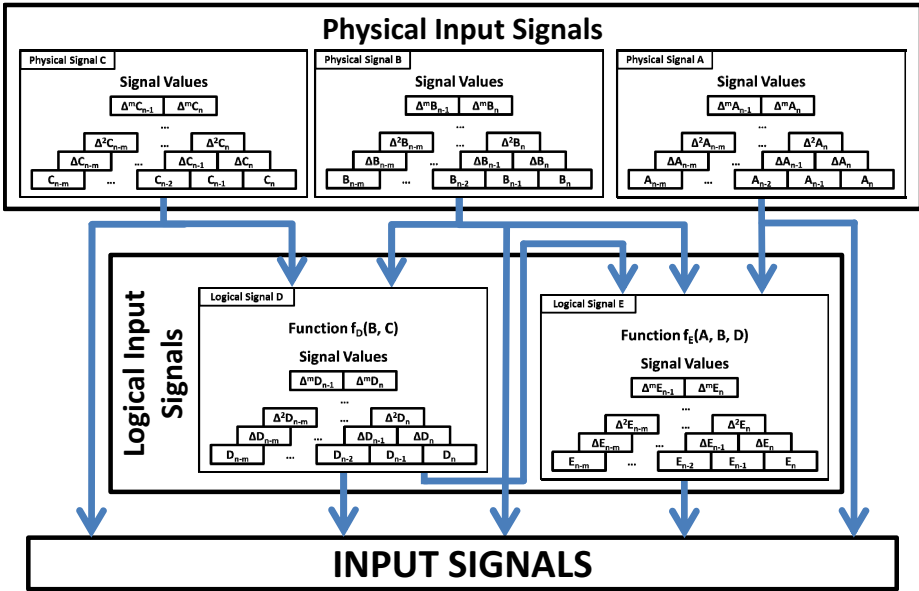


Fig. 4. Analysis of Input Logical Signals

Thus, the analysis of the logical output signals is performed in the final steps of post-processing immediately before the last step where the output physical signals are available for the environment. The steps of analysis between the Physical Output Signals and Output Signals are similar to those presented previously between Physical Input Signals and Input Signals.

5 Discussion

This work intends to take advantage from techniques of generation of logical signals in order to improve the performance of the flow presented before, contributing to the compactness of the representation of dependencies on signals, where the analysis of the signals is moved to pre- and post-processing of the model.

The addition of logical signals is intended to get smaller and more readable models, removing complexity from the model to pre- and post-processing, in order to exploit the benefits of graphical modeling formalism and its readability by humans.

The definition of the logical signals in this flow, being analyzed through functions, allows a wide number of applications. It is possible to define functions that only convert a physical signal value into some unit of interest. For example, if there are two temperature sensors, one measuring in Celsius and other one in Fahrenheit, in order to allow the further analysis depending on the measured temperature by both sensors, it is necessary to create at least one logical signal that convert one of the temperature unit into the other one. For example, one can create a logical signal T_c (equivalent value in Celsius) associated to the physical signal T_f (temperature value in Fahrenheit). The function associated to the logical signal T_c is the following:

$$T_c = (T_f - 32) * (5/9)$$

This conversion allows in the next processing steps the analysis of the two signals under the same conditions.

Other example is the average value of the signal in the last 5 time steps Ta , or the difference between the present value and the value 5 steps before Td obtained by associate the following functions:

$$Ta = (T0 + T1 + T2 + T3 + T4) / 5$$

$$Td = T5 - T0$$

It is also possible to present values resulting from the analysis of more than one signal, obtaining values of other quantities. For example, consider a vehicle inside a factory, controlled from a docking station where it must return to be recharged. It is possible to calculate the distance to the station (Ds), in order to know if it is still inside the control area, using the values that vehicle traveled in latitude (Lt) and longitude (Lg) associating the following function to a logical signal:

$$Ds = \text{sqrt}(Lt^2 + Lg^2)$$

In a more complex way, it is possible to calculate values in a transformed space (not analyzed in the time domain), obtaining analysis such as spectral distribution when calculating the FFT of a given signal or even the average value of a set of signals.

6 Conclusions and Further Work

Moving the analysis of Logical Signals into the pre- and post-processing phases of the modeling flow provides a set of new capabilities for the analysis of signals to be used by the model.

This addition allows acquiring extra information from the signals coming from the environment, so allowing a more detailed analysis and defining more input conditions and output actions.

Moreover, this addition can also allow obtaining certain values without the need to add new hardware that would measure them, since this value could be determined by analysis of other signals. In this way, the number of variables available for use by events and conditions previously defined improves.

Comparing with models produced without these logical signal techniques, these additions will potentially contribute to a significant reduction of the models. In some cases they may even allow a huge compression of models as, for example, complex behaviors can be encapsulated in an event that depends on logical signals.

Acknowledgments. The first author was supported by a Grant from project PTDC/EEI-AUT/2641/2012, financed by Portuguese Agency” FCT - Fundação para a Ciência e a Tecnologia”. This work was partially financed by Portuguese Agency” FCT - Fundação para a Ciência e a Tecnologia” in the framework of projects PEst-OE/EEI/UI0066/2011 and PTDC/EEI-AUT/2641/2012.

References

1. Object management group. <http://www.omg.org/>
2. Statecharts, H.D.: A visual formalism for complex systems. *Sci. Comput. Program.* **8**(3), 231–74 (1987)
3. Börger, E., Stärk, R.F.: *Abstract State Machines: A Method for High-level System Design and Analysis*. Springer, Heidelberg (2003). <http://books.google.pt/books?id=Am43BAC06L8C>
4. Jensen, K.: High-level petri nets. In: Pagnoni, A., Rozenberg, G. (eds.) *Appl. Theory Petri Nets SE – 12*, pp. 166–180. Springer, Heidelberg (1983). http://dx.doi.org/10.1007/978-3-642-69028-0_12
5. Reisig, W., Berlin, H.: *Distributed Algorithms: Modeling and Analysis with Petri Nets W*, pp. 38–43. Reising Institut für Informatik Humboldt-Universität (1998)
6. Zurawski, R., MengChu, Z.: Petri nets and industrial applications: A tutorial. *IEEE Trans. Ind. Electron.* **41**(6), 567–583 (1994)
7. Bruns, R., Dunkel, J.: *Event-Driven Architecture*. Springer London, Limited (2010). <http://books.google.pt/books?id=BtsfBAAAQBAJ>
8. Eckert, M., Bry, F.: Complex Event Processing (CEP). *Informatik-Spektrum* **32**(2), 163–167 (2009). <http://dx.doi.org/10.1007/s00287-009-0329-6>
9. Luckham, D.C.: The power of events: An introduction to complex event processing in distributed enterprise systems. In: Bassiliades, N., Governatori, G., Paschke, A. (eds.) *RuleML 2008*. LNCS, vol. 5321, p. 3. Springer, Heidelberg (2008). http://dx.doi.org/10.1007/978-3-540-88808-6_2
10. Zang, C., Fan, Y.: Complex event processing in enterprise information systems based on RFID. *Enterp. Inf. Syst.* **1**(1), 3–23 (2007). <http://dx.doi.org/10.1080/17517570601092127>
11. Luckham, D.C.: *Rapide: A language and toolset for simulation of distributed systems by partial orderings of events*. Computer Systems Laboratory (1996). <http://books.google.pt/books?id=AWamHAAACAAJ>
12. Luckham, D.C., Kenney, J.J., Augustin, L.M., Vera, J., Bryan, D., Mann, W.: Specification and analysis of system architecture using Rapide. *IEEE Trans. Softw. Eng.* **21**(4), 336–354 (1995)
13. Campos-Rebelo, R., Costa, A., Gomes, L.: Enhanced event modeling for human-system interactions using IOPT petri nets. In: Hippe, Z.S., Kulikowski, J.L., Mroczek, T., Wtorek, J. (eds.) *Human-Computer Systems Interaction: Backgrounds and Applications 3*. AISC, vol. 300, pp. 39–50. Springer, Heidelberg (2014)
14. Campos-Rebelo, R., Costa, A., Gomes, L.: Elementary events for modeling of human-system interactions with petri net models. In: Camarinha-Matos, L.M., Barrento, N.S., Mendonça, R. (eds.) *DoCEIS 2014*. IFIP AICT, vol. 423, pp. 219–226. Springer, Heidelberg (2014). http://dx.doi.org/10.1007/978-3-642-54734-8_25
15. Campos-Rebelo, R., Costa, A., Gomes, L.: Output events for human-system interaction modeling. In: *2014 7th Int. Conf. Hum. Syst. Interact. (HSI)*, pp. 261–266 (2014)

EmbedCloud – Design and Implementation Method of Distributed Embedded Systems

Kazimierz Krzywicki^(✉), Marian Adamski, and Grzegorz Andrzejewski

Department of Electrical Engineering, Computer Science and Telecommunications,
University of Zielona Gora,
ul. Licealna 9, 65-417 Zielona Gora, Poland
K.Krzywicki@weit.uz.zgora.pl,
{M.Adamski,G.Andrzejewski}@iee.uz.zgora.pl

Abstract. This paper presents a novel design and implementation methodology of the distributed embedded systems, called EmbedCloud. It defines structured implementation model for each module in the system. EmbedCloud forms the basis for the automatic code generation algorithm of the distributed embedded systems which accelerates and simplifies synthesis process of such systems. The EmbedCloud utilizes CloudBus protocol demonstrated in previous publications, which provides a process synchronization and control mechanism for a number of processing units distributed in a network. The CloudBus protocol allows to significant savings in the amount of transmitted data between end modules in the distributed embedded system, especially when compared with the other protocols used in the industry. To verify and evaluate the performance of the EmbedCloud, a concurrent process was described using Petri nets. Hardware tests and synthesis verification of the distributed embedded system was performed on the testing platform built with AVR, ATmega series microcontrollers. The tests confirmed the correctness of the developed source code and EmbedCloud method. Furthermore, resource requirements and reaction time analysis were performed.

Keywords: Distributed embedded systems · Embedded system design · Hardware synthesis · Process control · EmbedCloud method · CloudBus protocol

1 Introduction

The dynamic development of the automatic industrial process control has caused an increased complexity and size of embedded systems. Typically, they are composed of execution units that are connected together in a logical way and form a distributed embedded system. The design and implementation of such systems is often complicated and requires long time for a large number of end modules operating in a system [1, 4, 7]. Moreover, the operating costs of systems based on PLCs (Programmable Logic Controllers) networks is high.

Most of the currently available models and tools for automatic code generation provide synthesis to a single hardware execution unit without any internally implemented process synchronization and communication with external hardware units [2, 3, 5, 6].

For a large number of end modules it is necessary to design them separately, e.g. using GALS (Globally Asynchronous Locally Synchronous) architecture [7, 8, 10]. These problems have led us to develop a new method which significantly reduces the design and implementation time of distributed embedded systems.

This paper proposes a novel design and implementation method of the distributed embedded systems, called EmbedCloud. It allows a structured implementation for each module in a distributed embedded system. Furthermore, the EmbedCloud is the base for the automatic code generation algorithm which accelerates and simplifies synthesis process of such systems. The end module communication and process synchronization is achieved through the CloudBus protocol presented in [9].

In Section II relationship to Cloud-based Engineering System is described, Section III describes the CloudBus protocol. Section IV presents synthesis model and EmbedCloud method. Section V discuss verification and research results in the term of resource usage and reaction time. Section VI, concludes the paper.

2 Contribution to Cloud-Based Engineering Systems

Large and complex distributed embedded systems form a cloud-based systems, due to large number of modules that perform various tasks and exchange data. However, such system is presented to an end-user as a single, complex, global system.

The proposed EmbedCloud accelerates and simplifies synthesis process of such systems and through the use of the CloudBus protocol provides a process synchronization and control mechanism for a number of processing units distributed in a network. The CloudBus protocol allows fast reconfiguration of the implemented system and allows to form the distributed embedded system with devices based on a different architectures.

The distributed embedded systems are able to overcome the limitations of single-unit environments and scatter the system into a various number of processing units.

3 CloudBus Protocol

The CloudBus protocol is one of the methods of the data exchange and concurrent process synchronization in the distributed embedded systems. It realizes distributed control method with a various number of end modules, where all of them are equal to each other and each of them implements a functional part of designed concurrent process. The CloudBus communication model allows the significant savings of the transmitted data between end modules [9]. Schematic diagram of the CloudBus protocol network topology is shown in Fig. 1.

The data transfer between end modules, necessary for process synchronization is executed only when one of the end modules requires information (input or variable state) from outside their own native resource variables. The end module broadcasts question to the system (other end modules) about the state of the specified variable, e.g. *if p1 = 0?*.

The end module that natively controls this variable (e.g. *p1*) sends the answer to the system (other end modules) when it gets previously requested state.

Basic data frame of the CloudBus protocol is shown in Fig. 2.

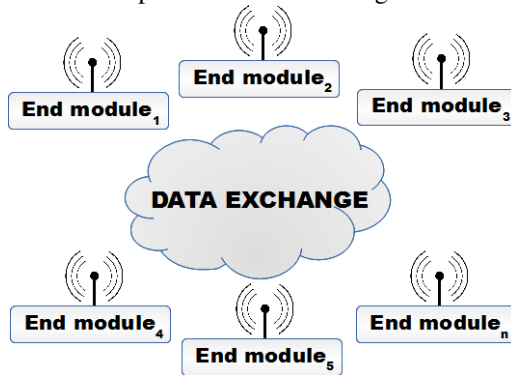


Fig. 1. Schematic diagram of the CloudBus protocol network topology



Fig. 2. Data frame structure of the CloudBus protocol

The fields of the protocol corresponds to: *CNT* – entire frame length; *FUNC* – command code (e.g. question/answer); *VARS* and *DATA* represents binary arrays of the variables and their states (values); *CRC* – the CRC error checksum.

In order to ensure safety and proper operation of the system, each module has a defined maximum time for receiving a response with requested variable. Alternatively, the CloudBus protocol allows to check presence of other end modules in the system.

The comparison of the CloudBus protocol with other protocols used in the industry (e.g. Modbus RTU, Profibus DP or DeviceNet protocol) showed significant savings in the amount of transmitted data between end modules in the distributed embedded system [9].

4 EmbedCloud – Design and Implementation Method

4.1 Hardware-Software Synthesis of Embedded Systems

The general requirements [1, 7] of the distributed embedded system are listed below:

- concurrency – concurrent process execution,
- openness, flexibility, scalability – fast reconfiguration and development,
- resource sharing – ability to share data between end modules,
- platform independent model architecture – end modules may have different hardware architecture.

Fig. 3 presents a comparison of two synthesis models of the embedded systems: (a) where one module performs the entire concurrent process, and (b) where the process has been decomposed into individual sub-processes and is implemented by three independent end modules.

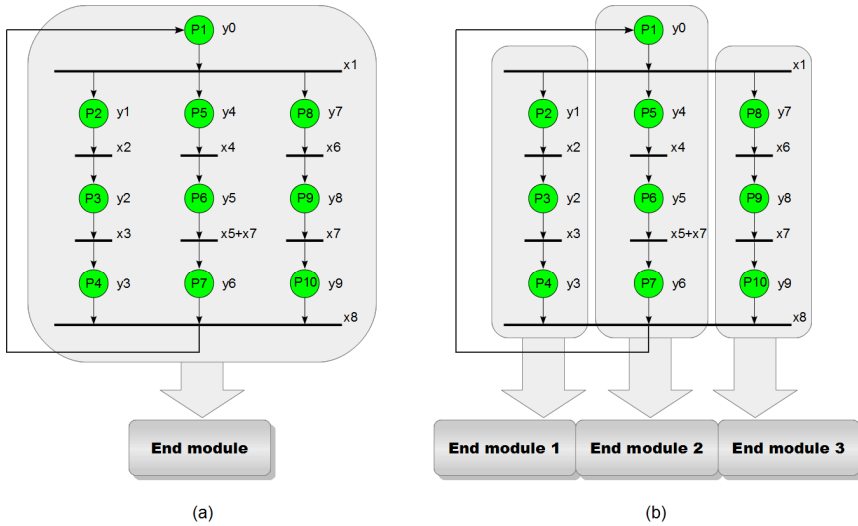


Fig. 3. Single module (a) embedded system vs. distributed (b) embedded system synthesis model

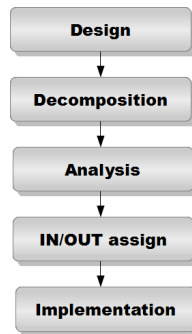


Fig. 4. General diagram of the concurrent process synthesis of the distributed embedded system

A general diagram of the concurrent process synthesis of distributed embedded system is shown in Fig. 4. The first step is to *Design* (describe) concurrent process using one of the models e.g. Petri nets. The next step is *Decomposition* into individual sub-processes. The decomposition can be realized by different criteria imposed by the designer such as: system reaction time, hardware resource usage or designer’s manual decomposition. After structural and behavioural *Analysis* of the decomposed process, *IN/OUT assign* is made – the designer assigns inputs/outputs for each end module. Finally, each module in the distributed embedded system is implemented.

4.2 EmbedCloud Structure

The proposed new design and implementation method (called EmbedCloud) of the distributed embedded system, defines an implementation model of ordered structure

for each end module, Fig. 5. Implementation structure is the same for all end modules of the distributed embedded system.

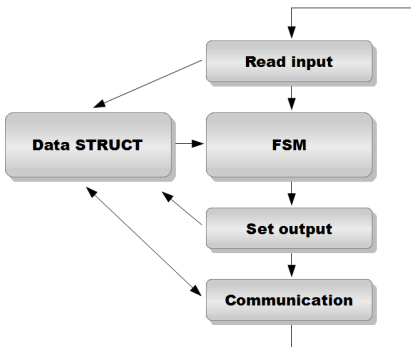


Fig. 5. General diagram of the EmbedCloud implementation method

The main step in the EmbedCloud implementation flow is *DATA STRUCT*. It is responsible for storing the information about the state of the native I/O and the state of shared variables in the system. In the *Read input* block native I/O states are read and stored in *DATA STRUCT*. Afterwards *FSM* (Finite State Machine) block using the data from *DATA STRUCT*, executes a selected control process or some of its parts. In the next step (*Set output*) the native I/O states are set. After performing all process operations, the information is exchanged (*Communication*) between end modules using the CloudBus protocol. The CloudBus and EmbedCloud method are closely related, because the CloudBus protocol is responsible for obtaining and making available the necessary data from other end modules. Moreover, it provides a process synchronization mechanism. In the *Communication* step, the end module broadcasts to the system (other modules) messages about the state of specific variables that were asked. The received responses are stored in the *DATA STRUCT* and algorithm returns to the *Read input* and starts again.

Such structure of the EmbedCloud allows to implement end modules, which differ only in the following elements: the native I/O and implemented control model (*FSM* block). This allows to use different architecture of each end module, such as micro-controller, FPGA or DSP devices. Furthermore, it forms the basis for the automatic code generation algorithm.

4.3 The Conception of the Automatic Code Generation Algorithm

The EmbedCloud structure allows to propose a simplified version of the algorithm for the automatic code generation for the end modules, Fig. 6.

After designing the concurrent model (*Model design*), the algorithm starts performing the decomposition. The *Decomposition* output are files in PNML or HPN format that contains divided sub-processes (represented by structured text) for each end module in the system. In the loop, files are parsed and processed for the structural

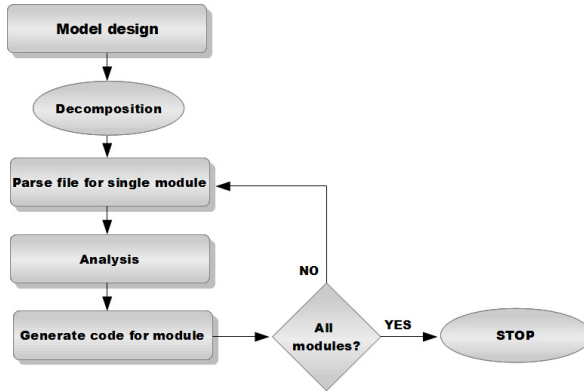


Fig. 6. Proposed algorithm for automatic code generation

and behavioural *Analysis*. After processing the code is generated using the Embed-Cloud method. The process stops, when all files have been processed. The output of the algorithm is source code for each end module.

5 Experimental Results

To verify and evaluate the performance of the EmbedCloud method a concurrent process was designed with interpreted 1-bounded Petri net model, Fig. 3 (a). Fig. 3 (b) presents Petri net model after manual decomposition to three individual sub-processes for each end module. For the *Module 1* and *Module 3* it was necessary to add resting places (*RP1*) to preserve the proper functioning and synchronization of the end modules. The *Module 2* executes the *P1* place with $y0$ output. The transitions and allowing arc are described by logic equations e.g. $x3 * P7M2$, which means: input $x3$ AND place *P7* from *Module 2*.

Hardware tests and synthesis verification of the distributed embedded system was performed on the testing platform built with AVR family, ATmega8 microcontrollers.

Table 1 presents a comparison of the synthesis results in the terms of memory usage and reaction time. The results were obtained with EmbedCloud method to generate a source code for ATmega8 microcontrollers. All of the end modules were transmitting data with the RFM12 transceiver (manufactured by Hope Microelectronics) using the CloudBus protocol. The results demonstrated following memory usage for the ATmega8 end module: 25% of total (8k bytes) program memory, 6% of total (1k byte) data memory. The maximum reaction time (CPU clock set to 16MHz) is 0,07ms for CPU processing and less then 2ms when external communication (at 115,2kbit/s) is also performed. Concluding, the hardware resource usage and reaction time is negligibly small.

It should be noted, that memory usage and reaction time depends on the concurrent model and its decomposition. Incorrectly performed decomposition may negatively affect the obtained results, hence it is necessary to make appropriate optimization and decomposition process.

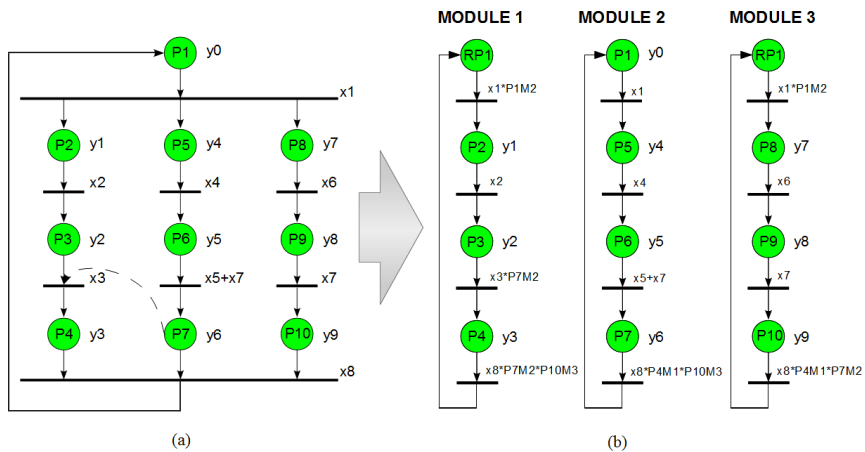


Fig. 7. Petri net model before (a) and after (b) decomposition

Table 1. Memory usage and reaction time for implemented distributed embedded system

End Module	Program Memory Usage [Bytes]	Data Memory Usage [Bytes]	Max. CloudBus Data Transmit [Bytes]	Max. CloudBus Reaction Time [ms]	Max. CPU Reaction Time [ms]	Max. Total Reaction Time [ms]
Module 1	1928	60	25	1,74	0,06	1,80
Module 2	2134	60	25	1,74	0,07	1,81
Module 3	1888	60	20	1,39	0,06	1,45

6 Conclusion

The paper presented the new EmbedCloud design and implementation methodology of the distributed embedded systems and formed the basis for the automatic code generation algorithm to accelerate and simplify the synthesis process of such systems.

Experimental results verified the proposed methodology and demonstrated a negligible memory usage (less than 2k bytes of program memory and 60 bytes of data memory usage) and minimal reaction time to the data requests (reaction time for CPU processing was 0,07ms; after including the data transmission to other modules – the result was less than 2ms for entire sub-process). However, it is necessary to implement and investigate various number of real distributed embedded systems with different wired and wireless network connections.

Current and further research focuses on developing the automatic code generation algorithm and graphic software tool where the embedded system designer, draws concurrent process model, assigns I/O and gets generated source code as output. Depending on the requirements, the software tool gives code in ANSI C language

or one of the HDL (Hardware Description Language), such as VHDL or Verilog. Using the automatic code generator and design tool, allows the significant time savings in the design and implementation of the distributed embedded systems.

References

1. Marwedel, P.: Embedded system design. Springer, New York (2011)
2. Nicolescu, G., Mosterman, P.J.: Model-Based Design for Embedded Systems. CRC Press, Boca Raton (2009)
3. Moreira, T.G., Wehrmeister, M.A., Pereira, C.E., Petin, J., Levrat, E.: Automatic code generation for embedded systems: From UML specifications to VHDL code. In: Industrial Informatics (INDIN), pp. 1085–1090. IEEE (2010)
4. Hsieh, W.H., Kao, S.P., Tan, K.H., Chen, J.L.: Energy-saving cloud computing platform based on micro-embedded system. In: Advanced Communication Technology (ICACT), pp. 739–743. IEEE (2014)
5. Raghav, G., Gopalswamy, S., Radhakrishnan, K., Hugues, J., Delange, J.: Model based code generation for distributed embedded systems (2010)
6. Babic, J., Marijan, S., Petrovic, I.: Introducing Model-Based Techniques into Development of Real-Time Embedded Applications. *Automatika* **52**(4), 329–338 (2011)
7. Adamski, M., Karatkevich, A., Wegrzyn, M.: Design of embedded control systems, vol. 267. Springer, New York (2005)
8. Bukowiec, A., Tkacz, J., Gratkowski, T., Gidlewicz, T.: Implementation of Algorithm of Petri Nets Distributed Synthesis into FPGA. *International Journal of Electronics and Telecommunications* **59**(4), 317–324 (2013)
9. Krzywicki, K., Andrzejewski, G.: Data exchange methods in distributed embedded systems. In: New Trends in Digital Systems Design, Fortschritt - Berichte VDI, Dusseldorf, vol. 836, pp. 126–141 (2014)
10. Bukowiec, A., Mroz, P.: An FPGA synthesis of the distributed control systems designed with Petri nets. In: Networked Embedded Systems for Every Application (NESEA). IEEE, London (2012)

Cloud Based IOPT Petri Net Simulator to Test and Debug Embedded System Controllers

Fernando Pereira^{1,2,3(✉)} and Luis Gomes^{1,3}

¹ Universidade Nova de Lisboa - Faculdade de Ciências e Tecnologia,
Lisboa, Portugal

`fjp@deea.isel.ipl.pt, lugo@fct.unl.pt`

² ISEL, Instituto Superior de Engenharia de Lisboa, Lisboa, Portugal

³ UNINOVA – CTS, Lisboa, Portugal

Abstract. IOPT-Tools is a cloud based integrated development environment to the design of embedded system controllers and other digital systems, employing the IOPT Petri net modeling formalism. The tools include a graphical editor, a state-space based model-checking subsystem and automatic code generators to deploy the controllers on the target hardware platforms. This paper presents a new Simulator tool that offers the capability to execute embedded system controllers based on IOPT models in a Web browser. To allow the test and debug of embedded system controllers, the Simulator provides options to manipulate the value of input signals, step by step execution, and continuous execution with programmed step frequency and breakpoint definition. Simulation history is recorded, continuously storing information about the entire system state, to enable playback and history navigation. History data can later be exported in spreadsheet format for analysis with external tools and waveform drawing. The tool can be accessed from <http://gres.uninova.pt>.

Keywords: Embedded systems · Cloud based tools · Petri nets

1 Introduction

The main goal of the IOPT-Tools integrated development environment [1] is to provide a rapid application development framework to the design of embedded system controllers and general purpose digital systems. In such framework, debug and simulation tools assume special importance, allowing the detection of mistakes during the early development phases, before reaching the prototype implementation, greatly contributing to reduce development time and cost and minimize the risk of prototype hardware damage due to controller design errors.

The tools offer a complete Cloud based tool-chain, including a graphical editor, a model-checking sub-system based on state-space computation, automatic code generation tools to produce software code or hardware descriptions, and the simulation and debug tool presented in this paper. All tools have a Web based user interface, with data storage and computing intensive operations executed on the Cloud, in the IOPT-Tools servers.

In this environment, embedded system controllers are modeled using IOPT nets [2], a subclass of Petri nets [3] specifically created for this purpose, with the addition

of the concepts of input and output signals and events to the traditional Petri net place and transition nodes. This way, controller behavior is expressed using the standard Petri net concepts, but the interface between the controllers, the controlled systems and the user interface is defined using input and output signals and events.

Figure 1 presents the typical IOPT-Tools development work-flow, including all development stages. The first steps, starting with the model edition, debug and simulation, model-checking and property verification are performed inside the tools using a pure software solution. This way, designers can test and debug controllers, focusing exclusively on the controller behavior without distractions from hardware details. The final development stages are also assisted by the automatic code generation tools, minimizing the risk of low level coding mistakes and simplifying the migration to different hardware platforms.

The simulator is usually employed in the second development stage, immediately after a model is designed or suffers changes, the typical use case situations must be simulated to check if the model exhibits the expected behavior. After successful completion of the typical use case sequences, development can progress to the next stages, including model checking and property verification, automatic code generation and prototype implementation.

To better analyze the debug and simulation results, a simulation history table is automatically recorded, containing all system data for every execution step, including the net marking, input and output signals and events and internal variables. The history can be visualized as a spreadsheet table, exported to create waveform drawings or used to replay a graphical animations of the stored execution steps. The user can also navigate through the history and restart the simulation from any saved history step, to test the system behavior under different input sequences.

The tools can be used from the IOPT-Tools web service, located at <http://gres.uninova.pt>, and do not require any software installation on the user's personal computer or tablet computer, running directly on the Web browser. New users can log-in using a guest account to experiment the tools, but can also create personal user accounts to store private models.

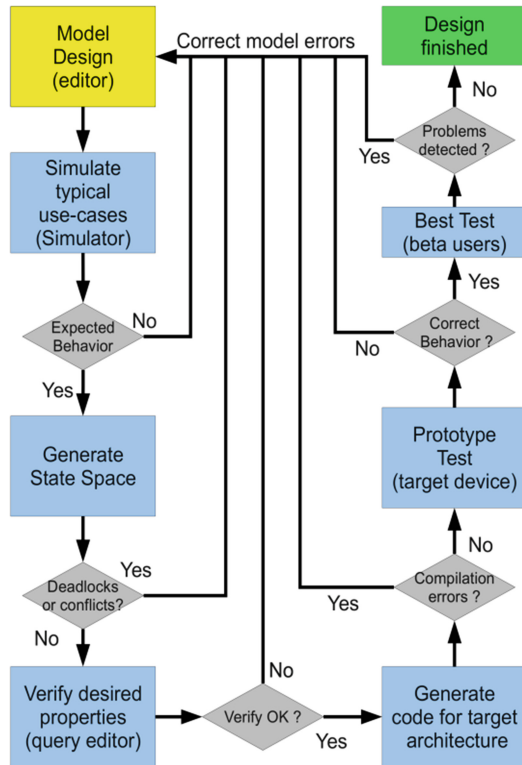


Fig. 1. The typical IOPT-tools workflow

For more information about the tools and IOPT nets, a detailed user manual is also available online at the tools Web site [4].

2 Relationship to Cloud-Based Solutions

The tools presented in this paper are a cloud-based solution. The simulator and the other tools run directly on the user's Web browser, using AJAX (Asynchronous Java-script and XML) principles [5]. All data files are stored on the cloud, in the IOPT-Tools servers, and all tasks requiring heavy duty computation, as state-space calculation and model-checking are also performed on the server, with a Web interface to display the results. This solution minimizes the computation requirements on the user's terminal equipment and can be used from low end personal computers, tablet computers or even smart-phones, as long as a W3C compliant Web browser is available.

On another way, the simulator is also a building block of a distributed architecture proposed in [6], intended to simplify the development of cloud-enabled embedded devices. This architecture minimizes the hardware resources required to implement embedded devices, greatly reducing costs, by storing all user interface data and code on the cloud and executing the user interface logic in the user's Web browser. The embedded device only needs to provide a minimal TCP/IP infrastructure to exchange data with the user interface code running on the browser, including information about the current system state and input and output signals, and receive feedback from the user interface logic.

3 Related Work

The simulator presented in this paper is integrated in a larger tool-chain, including a model editor [7], a model-checking infrastructure composed by a state-space generator and a query system [8] and automatic code generation tools [9]. Additional information about these tools has been published in [1] and a user manual in [4]. The underlying modeling formalism on which the tools are based, IOPT nets, has also been discussed in [2]. A direct connection to the HIPPO system [10] provides additional tools, including the calculation of incidence matrices and analysis of place invariants, concurrency relations and sequential relations.

Computer simulation is widely disseminated over most engineering and scientific fields, and simulators can be found in many development environments [11]. General purpose simulation software applications like Math-lab and Simulink [12] are often used to simulate diverse physical systems, covering a wide range of scientific fields. Among electrical and electronics engineers, simulators like SPICE are very popular for electrical circuit analysis. Like the tools presented in this paper, Matlab and Simulink are often used on the development of embedded system controllers, including automatic code generation tools to deploy models on hardware prototypes. IOPT nets are often used as a high level modeling formalism to the design of digital system circuits.

Simulators are usually employed to study the behavior of systems, in situations where it is not practical, costly or convenient to perform the corresponding experiments in the real world, like the effects of natural disasters, weather prediction, the behavior of sub-atomic particles, or the evolution of human demographics.

Traditionally, Petri nets have been used as a modeling language to run simulations. As the standard Petri net classes are autonomous and lack the capabilities to communicate with the external world, the purpose of these classes are the simulation by itself, and almost all Petri net tool-chains include a Simulator tool. For example, simulators can be found in CPN-Tools [13], CPN-AMI [14] and Renew [15].

Although existing simulators implemented in Java could be executed from Web browsers, the new simulator tool runs entirely inside the Web browser, without requiring any additional virtual machine. This way, simulator usage is not limited to PCs and can be executed on a wide range of hardware platforms and operating systems, from PCs and tablet computers to smart-phones, as long as a W3C compliant Web browser is available.

A previous Animator tool [16], could also be used to run animated simulations of Petri net models, but required the definition of a series of user interface «screens» containing graphic objects to visualize the system state and interact with the user. However, the tool and the simulations produced by this tool do not offer a Web interface and cannot be integrated in the IOPT-tools environment. The development of cloud-enabled version of the Animator tool is planned for the future and the new simulator tool already contains infrastructure code to interact with animated user interface windows build using the future Animator.

4 Research Innovation

The simulator presented in this paper should not be understood as a Petri net simulator, but as an embedded system controller simulator that uses IOPT Petri nets as the underlying modeling formalist. Due to the non-autonomous nature of IOPT nets, the new Simulator tool exhibits fundamental differences from the existing Petri net simulators for autonomous Petri net classes.

With traditional Petri net simulators, the user interaction with the simulator is limited to the definition of an initial marking before starting the simulation and during execution, the user can only choose the transitions that fire on each execution step, from a set of enabled transitions. In contrast, using the new embedded system controller simulator, the user interacts with the simulator by setting the value of input signals and autonomous input events. All enabled transitions will automatically fire in the next execution step, as IOPT nets use a maximal step semantics. In this regard, the IOPT simulator has more similarities with the tools found in the Ladder and Grafcet [17] programmable logic controller tool-chains for industrial automation, than with the autonomous Petri net simulators.

As the user does not have to manually choose which transitions will fire, the Simulator is typically used in continuous run mode, as opposed to the traditional Petri net simulators that are often used in step by step execution mode. As a consequence, the

concept of Breakpoints, popular in software development tools, has been introduced to the new Simulator, enabling the automatic interruption of continuous execution when selected transitions are fired.

As embedded system simulations typically run at very fast step rates, the user may not be able to notice all execution details in real time. To solve this problem, a simulation history mechanism has been added to enable the posterior analysis of the results and export data to draw waveform graphics. To help the user track the system evolution in real time, special attention was given to graphical feedback, dynamically changing the colors of input and output signals, triggered events, marked places, enabled transitions and transitions with guards ready.

From an implementation point of view, the new simulator also differs from traditional Petri net simulators, as it employs a compilation execution strategy instead of using a model interpreter: each time the simulator is called, the Javascript code responsible for implementing the model behavior is rewritten, according to the model in use. This strategy offers improved simulation performance, enabling simulations running at very fast step rates, comparable to the speeds employed in real embedded devices based in micro-controllers.

Finally, to reinforce the embedded system controller nature of the new simulator, it is important to notice that the tool was designed with an architecture ready to enable the implementation of a distributed IcE (In Circuit Emulator), to remotely debug embedded systems running on physical devices over the internet, using the same user interface of the simulator. To implement this solution, the code responsible for executing the IOPT semantics is replaced with proxy code that forwards execution-flow commands to the remote embedded systems using HTTP requests. The status of the embedded devices is also read in real time using HTTP. The communication protocol presented in [6], and back-end HTTP server to run on the embedded devices are currently under development.

5 IOPT Petri Nets

The IOPT Petri net class is a non-autonomous Petri net class derived from Place-Transition nets [3], with the addition of input and output signals and events. In the same way as the traditional Petri nets, system behavior is expressed using places and transitions. However, the new input and output capabilities allows the definition of an interface with the external world, used to establish the communication between the controllers (IOPT models) and the controlled systems.

Figure 2 displays an example IOPT model. IOPT models support the usual places and transitions from P/T nets, plus the following characteristics:

- 1 – Input and output signals, can hold Boolean or integer range values, suitable to represent digital or analog I/O signals, respectively.
- 2 – Input events, representing instantaneous changes in input signals.
- 3 – Output events cause instantaneous changes in the value of output signals. Output events associated with transition firing, can increment or decrement the value of output signals by a specific amount. The signals hold the last values.

- 4 – Autonomous input and output events, not associated with I/O signals, are used to instantaneously propagate events between different component models.
- 5 – Guard expressions may be associated with transitions, containing logic conditions to inhibit transition firing according to the value of input signals
- 6 – Input events may also be associated with transitions to synchronize firing.
- 7 – Output actions may be associated with places, to define the value of output signals, when the places are marked. When no actions are active, the signals revert to a default value.
- 8 – Output actions associated to transitions, define the value of output signals when the transition fires. The affected signals memorize the last values.
- 9 – Transition priorities solve conflict situations where multiple transitions are simultaneously enabled, but there are not enough tokens to fire all of them.
- 10 – Test Arcs prevent the firing of transitions in the same way as normal Arcs, but do not consume the tokens and thus, do not cause transition conflicts.
- 11 – Maximal step execution semantics to provide deterministic execution, ensuring that all transitions ready to fire, will fire in the next execution step. Single server semantics is used, which means that even if a transition is enabled for multiple firings, only one firing will be produced per execution step.

6 Simulator Functionality

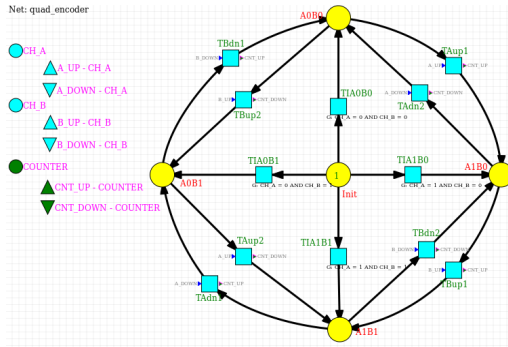


Fig. 2. IOPT Model - Quadrature decoder

Figure 3 presents the IOPT simulator user interface, composed by a toolbox on the left, a properties form on the right and a drawing of the model on the center. The toolbox contains icons for step-by-step execution, undo the last executed step, continuous execution, reset to initial marking, define a new forced marking, history navigation, history replay and history file export. The properties form contains the entire simulator status, including the current net marking, input signals, output signals and input and output events.

The model drawing reflects that status of the system, by changing the colors of the nodes. Places change colors according to the current marking: no tokens, one token or

many tokens. Transitions change color according to the readiness: autonomously enabled, ready to fire or both. Boolean input and output signals change color according to the value, and input and output events also flash when triggered. This color scheme helps the user interpret the current system status, resulting in much faster debug sessions. For example, instead of manually calculating the value of guard expressions to check if a transition is ready to fire in the next execution step, the user can simply observe the transition color.

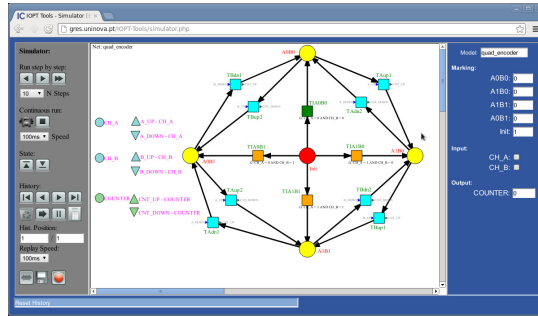


Fig. 3. Simulator / Debugger User Interface

The user can interact with the system both in the properties form and directly in the model drawing. For example, the value of an input signal can be changed on the corresponding item on the properties form, but it may also be changed by picking the corresponding signal on the graphic.

Continuous execution can be automatically interrupted with Breakpoints associated with transitions. Picking on a transition sets or resets a Breakpoint. A red border is drawn around transitions with Breakpoints. Execution stops immediately after a transition with a Breakpoint is fired, and the user interface reflects the system status after the firing. In case the user desires to inspect the status of the system prior to the firing, it is possible to undo the last executed step or move one position backwards in the recorded history.

The simulator maintains a complete record of the system status during entire simulation sessions. Whenever a new step is executed, the entire system status is recorded, including the value of input signals, events triggered, and information about transitions fired. The user can navigate through the saved history, and the user interface will change to reflect the status of the selected history step. This way, it is possible to inspect the past system evolution to detect flaws that may have not been noticed by the user during the original execution.

To simplify the inspection of the past system evolution, it is possible to replay the recorded history with programmable speed, starting on the current history step. In alternative, the simulator history can also be presented in the form of a spreadsheet table, as displayed in figure 4. To simplify inspection, repeated execution steps with identical status are compressed in a single table line with indication about the number of repetitions.

Finally, the history table can be exported in CSV (Comma Separated Values) text file, suitable for spreadsheet edition, or to be imported by other software. Taking advantage of the graphing functionality offered by most spreadsheet applications, it is very easy to create waveform diagrams of the input and output signals, as well as the internal system status variables.

For more detailed information about the simulator usage, tool options, interaction and color schemes, a user manual can be downloaded from the tools web interface [4].

7 Simulator Architecture

The core of the simulator is based on a new automatic code generator tool that produces Javascript code. Instead of relying on a model interpreter, the part of the simulator code that implements the model semantics is dynamically generated each time the simulator is executed, with code that implements the semantic rules of execution defined in each model.

Step	Rep.	Marking	Transitions	Input_signals	Output_signals	Input_events	Output_events
			Trans	CH_A	CH_B	COUNTER	
1	1	A0B0=1	TA0B0	0	0	0	
2	1	A0B1=1	TA0B0	0	0	0	
3	1	A0B0=1	TA0B0	0	0	0	
4	5	A0B0=1	TA0B0	0	0	0	
9	1	A1B0=1	TA0A1	1	0	1	A_UP
10	2	A1B0=1		1	0	1	
12	1	A1B1=1	TB0A1	1	1	2	B_UP
13	1	A1B1=1		1	1	2	
14	1	A0B1=1	TA0A1	0	1	3	A_DOWN
15	2	A0B1=1		0	1	3	
17	1	A1B1=1	TA0A2	1	1	2	A_UP
18	1	A1B1=1		1	1	2	
19	1	A1B0=1	TB0A2	1	0	1	B_DOWN
20	2	A1B0=1		1	0	1	
22	1	A0B0=1	TA0A2	0	0	0	A_DOWN
23	2	A0B0=1		0	0	0	
28	1	A0B1=1	TB0A2	0	1	1023	B_UP
29	2	A0B1=1		0	1	1023	
29	1	A1B1=1	TA0A2	1	1	1022	A_UP
29	2	A1B1=1		1	1	1022	
31	1	A1B0=1	TB0A2	1	0	1021	B_DOWN
32	1	A1B0=1		1	0	1021	

Fig. 4. Recorded history table

The automatic code generator itself, is implemented using a XSLT Transformation [18] applied to the model's PNML [19] files. The code generator uses the same principles as the VHDL and C code generators and detailed information about the code generation techniques can be found in [9]. The generated Javascript code contains the following items:

- A semantics execution function that runs a single execution step of the model being simulated
- Several functions that evaluate the state of each transition, to check if it is autonomously enabled or the associated input events and guard functions are ready (to provide animated graphical feedback)
- Several JSON [Javascript Object Notation] objects representing the net marking, the input signals, output signals, input events, output events and model arrays.

The user interface code calls another XLST transformation to create an SVG (Scalable Vector Graphics) [20] document containing the graphical representation of the model, that is displayed in the central area of the simulator window.

To process each execution step, the simulator executes the following tasks:

- a) Update the JSON objects representing input signals and autonomous input events
- b) Update the user interface color schemes, using the transition evaluation functions
- c) Call the Javascript function that executes a single execution step
- d) Update the user interface status form, according to the new values on the JSON objects
- e) Update the graphical model according to the new status and apply color schemes

This architecture is ready to implement an in-circuit emulator used to remotely debug embedded systems designed using IOPT tools. To achieve this, the Javascript execution function in c) is replaced by a proxy function that communicates with the remote system, sending and receiving the JSON objects used in a) and d).

8 Conclusions and Future Work

The simulator has been developed and integrated in the IOPT tools service and has been used to debug and simulate numerous models. The behavior of the simulated models has been compared with real world implementations of the same models running on embedded hardware boards, and also with the state-space graphs, with no inconsistencies detected. As a consequence, the simulator can be used effectively to detect design flaws before reaching the prototype implementation phase. As the typical development cycle takes only a few seconds after completing a model edition to start a new simulation session, development time can be enormously reduced. The alternative solution, debugging models using prototype boards, generally impose much longer development cycles, as the FPGA synthesis tools usually take many minutes to generate the bit-stream files necessary to reconfigure the hardware devices.

The rapid detection of design flaws often requires the simulation of the entire embedded systems. Although IOPT nets have been designed to the development of controllers, the user can build enhanced models containing both the controller and also the controlled systems. With this solution, the user can simulate the entire embedded systems, including controlled hardware and can even calculate the state-space graphs of the entire system.

Future work includes the addition of a waveform editor, to pre-program sequences of input signals and graphically visualize the resulting output signal waveforms. A database of signal waveforms can be stored in the cloud, and used as an automatic unit-test framework to perform regression tests and compare results with previous executions. An in-circuit emulator to debug remote systems is currently under development. Integration with an Animator tool is planned and the Simulator is currently ready to interact with other windows that present Animator generated screens. These screens will add new user interface windows, bringing additional user friendliness and the ability to be used by persons without knowledge about Petri nets.

Acknowledgments. This work was partially financed by Portuguese Agency” FCT - Fundação para a Ciência e a Tecnologia” in the framework of projects PEst-OE/EEI/UI0066/2011 and PTDC/EEI-AUT/2641/2012.

References

1. Pereira, F., Moutinho, F., Gomes, L.: IOPT-Tools - Towards cloud design automation of digital controllers with Petri nets. In: ICMC 2014 International Conference on Mechatronics and Control, July 3-5, Jinzhou, China (2014)
2. Gomes, L., Barros, J., Costa, A., Nunes, R.: The Input-Output Place-Transition Petri Net Class and Associated Tools. In: Proceedings of the 5th IEEE International Conference on Industrial Informatics (INDIN 2007), Vienna, Austria, July 2007
3. Reisig, W.: Petri nets: an introduction. Springer, New York (1985)
4. Pereira, F., Moutinho, F., Gomes, L.: IOPT Tools User Manual - Version 1.1. FCT/UNL, Lisbon (2014). <http://gres.uninova.pt>
5. Zakas, N.C., McPeak, J., Fawcett, J.: Professional Ajax, 2nd edn. Wiley (2007) ISBN 1-4571-0715-5
6. Pereira, F., Gomes, L.: Minimalist Architecture to Generate Embedded System Web User Interfaces. In: Camarinha-Matos, L.M., Tomic, S., Graça, P. (eds.) DoCEIS 2013. IFIP AICT, vol. 394, pp. 239–249. Springer, Heidelberg (2013)
7. Pereira, F., et al.: Web based IOPT Petri net Editor with an extensible plugin architecture to support generic net operations. In: IECON 2012-38th Annual Conference on IEEE Industrial Electronics Society. IEEE (2012)
8. Pereira, F., Moutinho, F., Gomes, L.: Model-checking framework for embedded systems controllers development using IOPT Petri nets. In: 2012 IEEE International Symposium on Industrial Electronics (ISIE), pp. 1399–1404. IEEE, May 2012
9. Pereira, F., Gomes, L.: Automatic synthesis of VHDL hardware components from IOPT Petri net models. In: IECON 2013-39th Annual Conference of the IEEE Industrial Electronics Society, pp. 2214–2219. IEEE, November 2013
10. Wiśniewski, R., Stefanowicz, Ł., Bukowiec, A., Lipiński, J.: Theoretical Aspects of Petri Nets Decomposition Based on Invariants and Hypergraphs. In: Park, J.J.H., Chen, S.-C., Gil, J.-M., Yen, N.Y. (eds.) Multimedia and Ubiquitous Engineering. LNEE, vol. 308, pp. 371–376. Springer, Heidelberg (2014)
11. Sadilek, D.A., Wachsmuth, G.: Prototyping Visual Interpreters and Debuggers for Domain-Specific Modelling Languages. In: Schieferdecker, I., Hartman, A. (eds.) ECMDA-FA 2008. LNCS, vol. 5095, pp. 63–78. Springer, Heidelberg (2008)
12. <http://www.mathworks.com/products/simulink/>
13. Jensen, K.: Coloured Petri Nets. Basic Concepts, Analysis Methods and Practical Use, vol. 1. Basic Concepts. Springer, Berlin (1997)
14. Hamez, A., Hillah, L., Kordon, F., Linard, A., Paviot-Adet, E., Renault, X., Thierry-Mieg, Y.: New features in CPN-AMI 3: focusing on the analysis of complex distributed systems. In: Sixth International Conference on Application of Concurrency to System Design, ACSD 2006, June 28–30, pp. 273–275 (2006). doi: 10.1109/ACSD.2006.15
15. Kummer, O., Wienberg, F., Duvigneau, M., Cabac, L.: Renew – User Guide, University of Hamburg, Dept for Informatics, Theoretical Foundations Group, Rel. 2(2) (August 28, 2009)
16. Gomes, L., Lourenco, J.: Rapid Prototyping of Graphical User Interfaces for Petri-Net-Based Controllers. IEEE Transactions on Industrial Electronics 57, 1806–1813 (2010)

17. Programmable controllers - Part 3: Programming languages. IEC International Standard 61131-3 ed3.0, 2013-02-20
18. Tidwell, D.: XSLT - Mastering XML Transformations, 2nd edn.. O'Reilly Media (June 2008) ISBN 978-0-596-52721-1
19. Billington, J., Christensen, S., van Hee, K.M., Kindler, E., Kummer, O., Petrucci, L., Post, R., Stehno, C., Weber, M.: The Petri Net Markup Language: Concepts, Technology, and Tools. In: van der Aalst, W.M., Best, E. (eds.) ICATPN 2003. LNCS, vol. 2679, pp. 483–505. Springer, Heidelberg (2003)
20. Scalable Vector Graphics (SVG) 1.1, 2nd edn., W3C Recommendation (August 16, 2011) <http://www.w3.org/TR/2011/REC-SVG11-20110816/>

Perception and Signal Processing

Improved Denoising with Robust Fitting in the Wavelet Transform Domain

Adrienn Dineva¹(✉), Annamária R. Várkonyi-Kóczy²,
and József K. Tar³

¹ Doctoral School of Applied Informatics and Applied Mathematics Óbuda
University, Budapest, Hungary

dineva.adrienn@bgk.uni-obuda.hu

² Bánki Donát Faculty of Mechanical and Safety Engineering,
Institute of Mechatronics and Vehicle Engineering Óbuda University, Budapest, Hungary
varkonyi-koczy@uni-obuda.hu

³ John von Neumann Faculty of Informatics, Óbuda University,
Budapest, Hungary
tar.jozsef@nik.uni-obuda.hu

Abstract. In this paper we present a new method for thresholding the coefficients in the wavelet transform domain based on the robust local polynomial regression technique. It is proven that the robust locally-weighted smoother excellently removes the outliers or extreme values by performing iterative reweighting. The proposed method combines the main advantages of multiresolution analysis and robust fitting. Simulation results show efficient denoising at low resolution levels. Besides, it provides simultaneously high density impulse noise removal in contrast to other adaptive shrinkage procedures. Performance has been determined by using quantitative measures, such as signal to noise ratio and root mean square error.

Keywords: Wavelet shrinkage · Robust fitting · Nonparametric regression

1 Introduction

Many applications of signal representation, adaptive coding, image enhancement, radio astronomy, etc., require the development of highly efficient data processing techniques. Traditional approaches, such as linear filtering, can smooth the corrupted signal, but with weak feature localization and incomplete noise suppression. Nonlinear filters have been proposed to overcome these limitations. Among the classical signal processing methods, wavelet-based noise reduction has been successfully applied to filter data, because it provides information at a level of detail, which is not available with Fourier-based methods [1]. The discrete wavelet transform analyses the signal at different frequency scales with different resolutions by reducing the signal into approximate and detail information [1][2]. For removing noise, wavelet shrinkage employs nonlinear soft thresholding functions in the wavelet domain [3]. The popularity of this nonparametric method is due to the excellent localization and feature extracting behavior. The fast signal transform algorithms provide significant

reduction in the computation time [1][2]. The effectiveness of wavelet shrinkage relies on that the wavelet transforms the additive white noise into white noise in the coefficient domain. Thus, fewer coefficients represent the signal which allows proper separation of the noise. Further, the wavelet-based technique requires only less assumption about the properties of the signal [3]. On the other hand, by using higher decomposition levels, the signal loses more of its important features which degrade the result significantly. The specific choice of the wavelet function, decomposition level, and thresholding rule allows to construct many different shrinkage procedures. A number of advanced concepts have been introduced on defining the threshold estimator rule (see, e.g. [3][4][5][6][7][8]). It is desirable to construct shrinkage procedures that are robust to impulse noises, which can lead to data loss. The main motivation for the work presented in this paper is to show that by applying robust fitting technique in the wavelet domain, highly efficient denoising effect can be achieved. The proposed method is robust to high density impulse-type noises and requires only low resolution levels.

1.1 Basics on Wavelet Shrinkage

The two major approaches of the noise removal task are the denoising in the time or space domain and the denoising in the transform domain. The transform-domain denoising procedures assume that the original signal can be well approximated by a linear combination of some basis functions. The wavelet transform preserves the true signal in few high-magnitude atoms and the others can be associated with noise. Consider the classical noise suppression problem:

$$y_i = f(t) + \epsilon_i, \quad i = 1, \dots, s \tag{1}$$

where y_i denotes the observed noisy data and ϵ_i represents the random noise, which is an independent and identically distributed (iid) process, and (t) stands for time. Let f denote the unknown function. The sampling points are equally spaced $s=2^n$ in order to allow to perform the discrete wavelet transform (DWT) [1]. The issue is to estimate f on $\underline{y}_i = [y_1, \dots, y_s]$ with minimum risk in least squares sense, i.e. to find

$$\hat{f} = \min \|f - \hat{f}\|^2 \tag{2}$$

The first step of wavelet shrinkage is the decomposition of Eq. (1), as follows

$$y_{ij} = \omega_{ij} + \epsilon_i, \quad j=1, \dots, n \tag{3}$$

where ω_{ij} are the wavelet (detail and approximate) coefficients on j^{th} scale. The general idea behind wavelet shrinkage is to replace the coefficients with small magnitude to zero (hard thresholding) [3],

$$\eta(\omega_{ij}, \lambda) = \begin{cases} \omega_{ij} & \text{if } \omega_{ij} > \lambda \\ 0 & \text{otherwise} \end{cases} \tag{4}$$

or set their value to the threshold level [3], the rule is given by

$$\eta(\omega_{ij}, \lambda) = \text{sgn}(\omega_{ij}), \max(|\omega_{ij}| - \lambda, 0) \quad (5)$$

where $\eta(\omega_{ij}, \lambda)$ is a soft thresholding function applied to the ω_{ij} transform coefficients and λ is the threshold value. Then, the reconstruction process performs the inverse discrete wavelet transform (IDWT).

1.2 Thresholding Operations in the Wavelet Domain

In this section we briefly summarize the prevalent shrinking concepts. The importance and advantages of wavelet shrinkage is discussed in several papers (see, e.g. [9]). Most of them construct nonlinear threshold functions based on statistical considerations. Shrinkage of empirical wavelet coefficient (RiskShrink) is firstly introduced in [3]. Another effective and widely used level-dependent and smoothness-adaptive method (SureShrink) is proposed to thresholds each dyadic resolution level using the principle of Stein's Unbiased Estimate of Risk [4][10]. The universal bound thresholding rule also provides good results with low computational complexity [5]; the rule is defined, as follows

$$\eta = \sigma_{\text{MAD}} \sqrt{2 \log s_j}, \quad (6)$$

where $\sigma_{\text{MAD}} = \frac{\text{median}(\omega_j)}{0.6745}$ denotes the absolute median deviation, and $\omega_j = [\omega_1, \dots, \omega_n]$. Later, the Heuristic Sure thresholding rule is introduced by a heuristic combination of the SureShrink and the universal bound [5];

$$\eta = \begin{cases} \eta_{\text{UB}} & \text{if } p \geq q \\ \min(\eta_{\text{Sure}}, \eta_{\text{UB}}) & \text{if } p < q \end{cases} \quad (7)$$

where $p = \frac{m-k}{k}$ and $q = (\log_2 k)^{\frac{3}{2}}$, $m = \sum_{i=1}^k \omega_i^2$. The Minimax estimator is also a preferred technique [6], the rule is given by

$$\eta = \begin{cases} \sigma_{\text{MAD}} (0.3936 + 0.1829 \log_2 s) & \text{if } s > 32 \\ 0 & \text{if } s < 32 \end{cases} \quad (8)$$

Regarding the shrinkage approaches concentrating on white noise modelling, another effective data-adaptive procedure for eliminating Gaussian noise from images is BayesShrink [7]. It performs the noise variance estimation on the sub-bands with median estimator. NeighShrink employs an overlapped window on the neighboring coefficients, thus this method takes into account the relation between the atoms [8]. The threshold value for each coefficient is determined by the principle, that when in the block the neighboring atoms represent the signal it is probable that the current element is also a part of the signal.

The other major approach in noise reducing applications is minimizing the effects of outliers (extreme values or elements that deviate from the observation pattern). Recent studies deal with eliminating the outliers during the signal pre-processing.

Several areas of engineering practice benefit from such algorithms, for instance monitoring and fault detection applications, data mining, feature identification in satellite images, etc., (see, e.g. [11][12]). It is proven, that the robust local polynomial regression technique detects outliers excellently [13]. With this in mind, the present paper proposes an improved denoising method based on robust fitting in wavelet domain.

2 Contribution to Cloud-Based Engineering

Cloud-based engineering has been a major discussion in the recent years [14]. The basic concept is that by sharing dynamic and quickly expandable resources among users more computational power, storage, etc., are available at lower cost. The challenges of outsourced applications involve the development of advanced signal processing techniques. On the other hand, the increasing amount of data, and transmission processes, generate a lot more noise. Typically, in a wider sense, collaborative or adaptive filtering solutions maintain big databases including many different kinds of data, such as sensing and monitoring data, signals of environmental sensing over large areas or multiple sensors. Additionally, several industrial processes depend on outsourced adaptive controllers [15]. In order to guarantee the proper performance, the signals need special care. Dealing with very sensitive data it is essential to ensure lossless processing even in nonstationary environments. The proposed denoising method can be applied in various scenarios where efficient noise removal is required especially when impulse-type disturbances may occur. Recent researches on cloud-based applications of multiple access communication highlight the construction of low probability of intercept signals [15][16]. Wavelet functions are proposed to employ as building blocks or atoms for the construction of communication signals. The theoretical and technical approaches and results presented in [17], show that the wavelet communication scheme satisfies the main objectives of secure, high throughput and low bit error. Based on the proposed robust thresholding method further improvements can be achieved, e.g. in energy threshold detection and recovery problems in the transformed domain.

3 Improved Denoising with Robust Fitting in the Wavelet Transform Domain

3.1 Local Polynomial Regression

The local polynomial regression (loess) procedure originally described in [18], is also called locally weighted running line smoother. Extensions of the original method can be found in, e.g [19]. The principle of the method can be summarized as follows. Lets consider Eq.(1). Function $f(t)$ can be approximated by fitting a regression surface to the data by determining a local neighbourhood of an arbitrary (t_0) . These neighbouring points are weighted depending on their distance from (t_0) . The closer points get larger w_i weights. The estimate \hat{f} is obtained by fitting a linear or quadratic polynomial using the weighted values from the neighbourhood. Detailed description of the procedure and the loess curve construction can be found in [13][18][20]. Loess relies

on least squares regression and it is known that this is vulnerable to outliers that can significantly degrade the result. In order to introduce robustness in the procedure an iterative reweighting is proposed with bisquare method [21]. The brief description of the simple bisquare method following the notation of [20], is the next. The residuals can be obtained $\hat{\varepsilon} = y_i - \hat{f}_i$ after fitting a linear regression. The weights are obtained by the bisquare function, the formula is given by

$$B(x) = \begin{cases} (1 - x_i^2)^2 & |x_i| < 1 \\ 0 & \text{otherwise} \end{cases} \quad (9)$$

and the robust weights are calculated as

$$r_i = B\left(\frac{\hat{\varepsilon}_i}{6\hat{q}_{0.5}}\right) \quad (10)$$

where $\hat{q}_{0.5}$ denotes the median of $|\hat{\varepsilon}_i|$.

3.2 Wavelet Shrinkage with Robust Fitting

The proposed shrinkage approach includes the following steps. Firstly, the corrupted signal is decomposed with orthogonal wavelet functions, which separates correctly the detail and approximate coefficients of the signal. Then, the robust fitting is applied on the coefficients on each level. Afterwards, the signal is reconstructed with inverse discrete wavelet transform. Thus, the realization of the new shrinkage procedure is the following: 1.) perform the discrete wavelet transform, 2.) fit the local polynomial regression curve on the coefficients with the w_i weights; 3.) get the residuals; 4.) get the median absolute value of the residuals; 5.) calculate the robust weights r_i with Eq. (20.); 6.) repeat step 1 with $r_i w_i$; 7.) repeat step 3 to 6 until it converges; 8.) perform the IDWT.

4 Simulation Results

The performance of the proposed procedure has been tested on a one-dimensional signal corrupted with additive white Gaussian noise and impulse noises (Fig.1.). The results have been compared with two other shrinkage algorithms. The simulation has been built by using Matlab7. The performance is measured by the root mean square error (RMSE) and the signal to noise ratio (SNR), calculated by the formula below

$$\text{SNR}_{\text{dB}} = 10 \times \log_{10} \frac{\sigma_s^2}{\sigma_n^2} \quad (11)$$

where σ_s^2 is the variation of the signal after denoising and σ_n^2 is the variation of the eliminated noise. For the decomposition an orthogonal wavelet has been chosen from the Symlet family [2]. The results are summarized in Table1.

Table 1. Simulation results

	Shrinkage with Robust Fitting	HeurSure	HeurSure	Minimax
SNR [dB] before	2.2294	2.2294	2.2294	2.2294
SNR [dB] after	23.5412	8.7601	3.6653	5.9276
RMSE	0.04159	0.5372	0.7621	0.3293
Level of decomposition	1	4	8	4
Abs. max error	0.2289	0.8621	0.9535	1.1107
Elapsed Time [s]	0.4196	0.0184	0.0127	0.0312

The performance of the robust fitting-based method can be seen in Fig. 2. The procedure precisely removes the noise and smoothes the signal. Though, the HeurSure and the Minimax rule are faster (see Table 1.) and eliminate additive noise, but can not cope with impulse noise (Figs. 3-4). Since the reconstruction is not sufficient, further smoothing and impulse-eliminating processes are desired, which increase the total elapsed time. With this in mind, the speed of the proposed procedure is acceptable. Fig. 5. shows the denoising effect of the HeurSure method at 8 decomposition levels. Comparing Fig. 4. with Fig 5. and the SNR and RMSE values, it can be seen, that in case of denoising with smoothness-adaptive shrinkage, the presence of impulse noises and the increase of resolution levels lead to data loss.

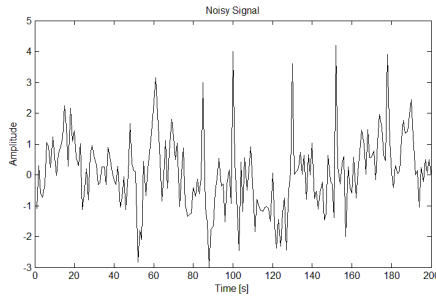


Fig. 1. The original signal corrupted with additive white Gaussian noise and impulse noises

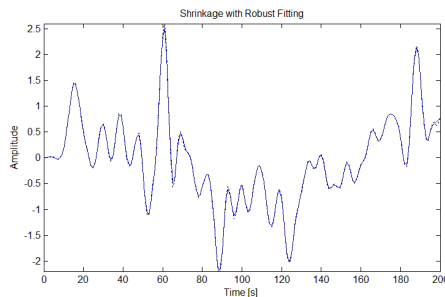


Fig. 2. Denoising effect of shrinkage with robust fitting. *black (dotted)* line –original signal, *blue (solid)* line –denoised signal

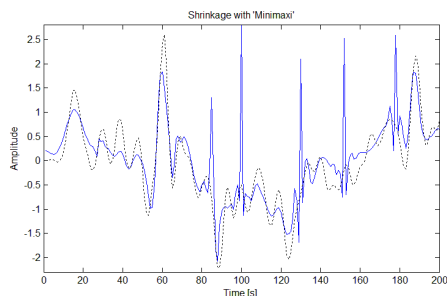


Fig. 3. Denoising effect of minimax method. *black (dotted)* line –original signal, *blue (solid)* line – denoised signal

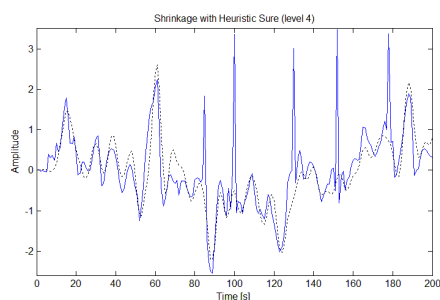


Fig. 4. Denoising effect of heuristic Sure method. *black (dotted)* line –original signal, *blue (solid)* line – denoised signal, level of decomposition: 4

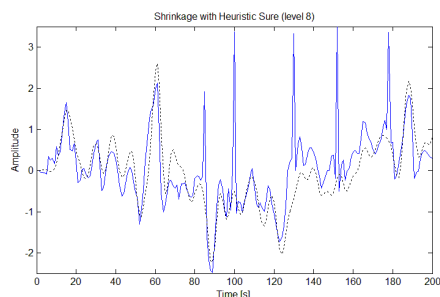


Fig. 5. Denoising effect of heuristic Sure method. *black (dotted)* line –original signal, *blue (solid)* line – denoised signal, level of decomposition: 8

5 Conclusions

In this paper a new approach is proposed for shrinking the wavelet coefficients. There are various sources of perturbations that may occur in the coefficient domain. This procedure excellently removes both additive noise and impulse noise with retaining the important parts of the signal. The method requires only low resolution levels and

is able to avoid data loss. Simulation results support, that the denoising efficiency can be significantly improved. Due to fitting a polynomial and calculating the robust weights on each point the performance is time-consuming. However, it is not necessary to use all the data points. Research into solving this limitation by introducing further data adaptive law in the proposed method is already underway. Future work also aims to reduce complexity, and to extend the procedure to nonorthogonal representation and investigate other types of signals.

Acknowledgments. This work was supported by the Hungarian National Scientific Research Fund (OTKA 105846).

References

1. Mallat, S.: Multiresolution Approximations and Wavelet Orthonormal Bases of L^2 . *Trans. Am. Math. Soc.* **315**, 69–78 (1989)
2. Daubechies, I.: The Wavelet Transform, Time Frequency Localization and Signal Analysis. *IEEE Trans. Inform. Theory* **36**, 961–1005 (1990)
3. Donoho, D.L.: De-noising by Soft-thresholding. *IEEE Trans. on Inf. Theory* **41**(3), 613–627 (1995)
4. Donoho, D.L., Johnstone, I.M.: Ideal Spatial Adaptation via Wavelet Shrinkage. *Biometrika* **81**, 425–445 (1994)
5. Donoho, D.L., Johnstone, I.M.: Adapting to Unknown Smoothness via Wavelet Shrinkage. *Journal of the American Statistical Association* **90**, 1200–1224 (1995)
6. Donoho, D., Johnstone, I.M.: Minimax Estimation via Wavelet Shrinkage. *Annals of Statistics* **26**, 879–921 (1998)
7. Chang, S.G., Yu, B., Vetterli, M.: Spatially Adaptive Wavelet Thresholding with Context Modeling for Image Designing. *IEEE Trans. on Image Processing* **9**(9), 1522–1531 (2000)
8. Cai, T.T., Silverman, B.W.: Incorporating Information on Neighboring Coefficients into Wavelet Estimation. *Sankhya: The Indian Journal of Statistics B*, 127–148 (2001)
9. Taswell, C.: The What, How, and Why of Wavelet Shrinkage Denoising. *IEEE Computing in Science and Engineering* **2**(3), 12–19 (2000)
10. Stein, C.M.: Estimation of the Mean of a Multivariate Normal Distribution. *The Annals of Statistics* **9**(6), 1135–1151 (1981)
11. Mastriani, M.: Fuzzy Thresholding in Wavelet Domain for Speckle Reduction in Synthetic Aperture Radar Images. *Int. Journal of Intelligent Technology* **1**(3), 252–265 (2006)
12. Ivera-Azcárate, A., et al.: Outlier Detection in Satellite Data Using Spatial Coherence. *Remote Sensing of Environment* **119**, 84–91 (2012)
13. Rousseeuw, P.J., Leroy, A.M.: *Robust Regression and Outlier Detection*. John Wiley & Sons (2005)
14. Rudas, I.J.: Cloud Computing in Intelligent Robotics, In: *IEEE 10th Jubilee International Symposium on Intelligent Systems and Informatics*, pp. 15–17. IEEE Press (2012)
15. Tronsco-Pastoriza, J.R., et al.: Secure Signal Processing in the Cloud: Enabling Technologies for Privacy-preserving Multimedia Cloud Processing. *IEEE Signal Processing Magazine* **30**(2), 29–41 (2013)

16. Valsan, S.P., Swarup, K.S.: Wavelet Transform Based Digital Protection for Transmission Lines. *Int. Journal of Electrical Power and Energy Systems* **31**(7–8), 379–388 (2009)
17. Teolis, A.: *Computational Signal Processing with Wavelets*. Birkhauser, Boston (1998)
18. Cleveland, W.S.: Robust Locally Weighted Regression and Smoothing Scatterplots. *Journal of the Am. Stat. Ass.* **74**, 829–836 (1979)
19. Cleveland, W.S., McGill, R.: The Many Faces of Scatterplot. *Journal of the Am. Stat. Ass.*, 829–836 (1984)
20. Martinez, W.L., Martinez, A.R.: *Computational Statistics Handbook with MATLAB*, Boca Raton. Chapman & Hall/CRC, FL (2008)
21. Fox, J.: *Nonparametric Simple Regression*. Sage Publication Inc., Thousand Oaks (2000)

Selection of Large-Scale 3D Point Cloud Data Using Gesture Recognition

Robin Burgess^(✉), António J. Falcão, Tiago Fernandes, Rita A. Ribeiro, Miguel Gomes, Alberto Krone-Martins, and André Moitinho de Almeida

UNINOVA / CTS, Campus FCT/UNL, Monte da Caparica,
2829-516 Caparica, Portugal

{rb,tmf}@ca3-uninova.org, {rar,ajf,mdg}@uninova.pt,
{algol,andre}sim.ul.pt

Abstract. An essential task when visualizing and analyzing large-scale 3D point cloud data is the selection of subsets of that data. This presents two challenges, the need for a selection method that is independent of the size of the dataset and how to interact with a 3D space effectively in a digital world still rooted in 2D interaction and visualization. We present an interface for defining volumes to select 3D point cloud data that uses hand gesture control with a Leap Motion device. The use of volumes is scalable to very large datasets, and the use of the Leap Motion gives the user access to the third dimension, facilitating interaction with the point cloud data. We illustrate with a large astronomical data archive hosted on the cloud that is retrieved on as-needed basis.

Keywords: Point cloud data · Gesture recognition · Large scale data

1 Introduction

In an age when automated massive data analysis is becoming a mainstream activity, the task of visualization is essential for the understanding and critical interpretation of data and results – for science and mission analysis and control alike [1][2][3]. Particularly, in Space related activities, most of the data leading to new scientific discoveries is expected to come from online archives collected through automatic instruments and all-sky surveys. Very few works address the topic [4]. Unfortunately, no adequate visualization solutions are available today for interactively visualizing and analyzing such amounts of complex datasets. Within this context we present an interface for defining volumes to select 3D point cloud data that uses hand gesture control with a Leap Motion. The use of volumes is scalable to large-scale datasets, and the use of the Leap Motion gives the user access to the third dimension, facilitating interaction with the point cloud data.

When working with any data, it is often of interest to analyze the particular properties of subsets of that data. It is therefore necessary to be able to select the subset of interest. When properties of that data are already known, it is possible to use

An erratum to this chapter is available at DOI: 10.1007/978-3-319-16766-4_55

automatic processes to select it. Otherwise, some form of manual selection is necessary. If the data visualized is in the form of 3D cloud points, such data can only be selected in relation to its position, and therefore it is necessary to have an effective method of spatial selection available. A challenge when designing such a method is how to define a 3D space easily when traditional interaction tools, such as a mouse or a touchpad are naturally geared towards 2D interaction. In cases where the point cloud dataset is too large to process in a single device and the data is stored on a distributed server, any solution must avoid the possibility of processing large chunks of the dataset.

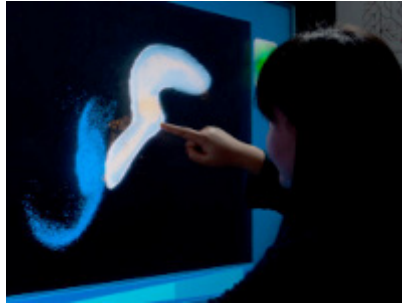


Fig. 1. 3D selection using a touch-based interface [5]

Our goal is to design an interactive spatial selection method for a large-scale 3D point cloud visualizer. The method had to provide the user with the ability to select areas of the point cloud of any size without requiring the processing of large amounts of data.

The existing work related to selection of 3D point cloud data is not very extensive, and as far as we have been able to ascertain, does not consider the size of the dataset used [2]. One solution is to manually select 3D point cloud data by using a lasso to define a 2D area, as seen in Fig. 1, which then selects all points visible through it. This results in selections as seen in Fig. 2. This solution can easily result in selecting points that the user did not intend to select, and which then must be deselected similarly. Therefore, the selection becomes a complex multi-step process.

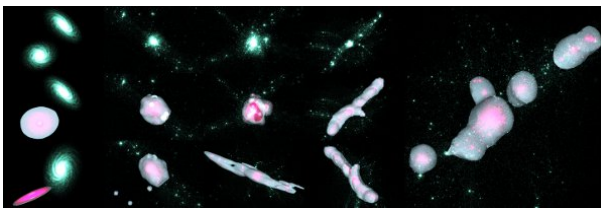


Fig. 2. 3D selection of galaxies using TeddySelection and CloudLasso techniques [5]

A paper by Lingyun Yu et al. [5] describes two solutions, TeddySelection and CloudLasso - two spatial, structure-aware selection techniques. They too rely on the use of a lasso, but they simplify the selection process by relying on algorithms to analyze the structure of the data and select a more limited area that is more likely to

correspond to the user's needs. The performance of both techniques will scale with the number of particles to be selected, or even with the size of the whole dataset.

Another solution that has been used is the creation of volumes that encapsulate the point cloud data that the user wishes to select. One example is the 3D Point Cloud Editor [6], illustrated in Fig. 3. The volumes can be modified and multiple volumes can be combined using Boolean operations. This solution has the advantage of not requiring the processing of data to define the boundaries of its selection.



Fig. 3. Selection of points from a point cloud using a cuboid [6]

The Slice-n-Swipe [7] solution uses a Leap Motion and has the user perform gestures to define cuts in the point cloud and select the desired half. It introduces a 3D element into the selection process but allows only fairly simple selections to be made.

Finally, another proposed solution [8] uses a PrimeSense sensor for gesture recognition and an Oculus Rift for visualization, and selection is achieved by using the hand as a virtual brush to select the desired area of the point cloud.

Our solution combines gesture recognition to solve the problem of interaction with a 3D space by using a Leap Motion [9], with the data-independence of creating 3D volumes for selection. The Leap Motion provides the user with direct access to the third dimension, which otherwise can only be managed with complex multi-step processes or with the aid of data processing. This work is being developed in the context of a project, financed by the European Space Agency (ESA), denoted IVELA-Intelligent Visualization [10]. The project's main objective is to develop tools to support astronomers and physicists performing scientific visual analytics studies on gathered data, such as the mission GAIA [11]. The GAIA mission aims to map about a billion of the Milky Way's stars, and gather information about each of those stars, including their speed and direction. With this data they hope to learn more about the composition, formation and evolution of our Galaxy.

This paper is structured as follows. This first section and section 2 provide an introduction to the topic of research and its relation with the theme of the conference. Section 3 presents the prototype developed. Section 4 discusses the solution presented and its virtues and flaws. Section 5 briefly concludes the paper.

2 Contribution to Cloud-Based Engineering Systems

As mentioned before, this work is being done as part of the development of an astronomical visualizer for large-scale stellar datasets [10]. Since a single computer cannot easily handle such large volumes of data, the data is stored in a cloud server and will be loaded as required. Scientists using the visualizer must be able to perform selections of clusters or regions of interest efficiently and effectively.

3 The Prototype

A prototype of the interaction system was created as a proof of concept of a tool for visual analytics. It was developed using the Unity game development system, developed by Unity Technologies [12] and programmed in C#. To allow interaction between the Unity application and the Leap Motion device [9], the Leap Motion C# API and Unity assets made by the Leap Motion company were used.

The prototype environment displays a randomly generated cluster of stars. Using both hands to interact with the prototype through the Leap Motion, the point cloud stars can be selected by creating spherical or cubic selection volumes.

3.1 Interaction

The prototype displays 3D models representing the hands, as seen in Fig. 4. The movements of these models mirror the movements of the hands and fingers detected by the Leap Motion. This allows the user to more easily relate the movements of their hands to the effects to the environment in the prototype. The 3D model and their movement scripts used were part of the functionalities provided by the Leap Motion team.

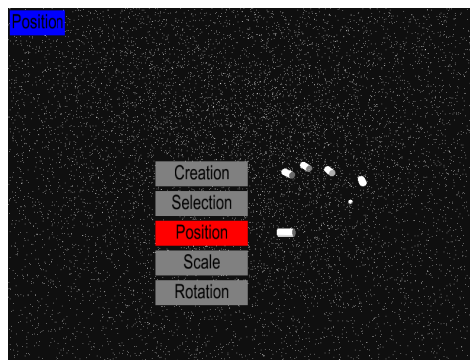


Fig. 4. The 3D representation of a hand

3.2 The Modes

The interface is separated into distinct interaction modes, as follows:

- Navigation Mode
- Selection Mode
- Creation Mode
- Position Mode
- Rotation Mode
- Scale Mode

The user can choose which mode is active via a menu in the bottom of the screen, as shown in Fig. 4. By separating the various activities into different modes, the user can more freely interact with less risk of their gestures being misinterpreted.

3.3 The Menu

Using a simple command gesture, users can activate the menu at any point. The menu is composed of submenus that the user can activate by swiping left or right. Each of the submenus consists of a vertical list of buttons. To pick a menu option the user must move their hand up and down, highlighting the corresponding option, and then pinch their fingers together. Using the menus, the user is allowed to pick the active mode (Navigation, Selection, Creation, Position, Rotation or Scale) as seen in Fig. 4, switch to a mouse-based interface, pick the shape of the 3D volume they wish to create and change the visualization mode of the dataset.

3.4 Navigation Mode

Navigation within the prototype is based on the flight analogy. The user can move the camera forwards, backwards, left, right, up and down by moving the hand accordingly relative to the center of the Leap Motion's interaction volume, as well as rotate it along the horizontal and vertical axis by tilting the hand similarly.

3.5 Creation Mode

In creation mode either a spherical, cubical or cylindrical selection volume can be created. Two opposite sides of the volume are locked to the palms of two hands so that the user can freely move the volume and scale it by moving their hands within the 3D space. The user then locks the volume in place by pinching their index and thumbs together. This automatically switches the mode to the position mode. Fig. 5 shows a volume after creation.

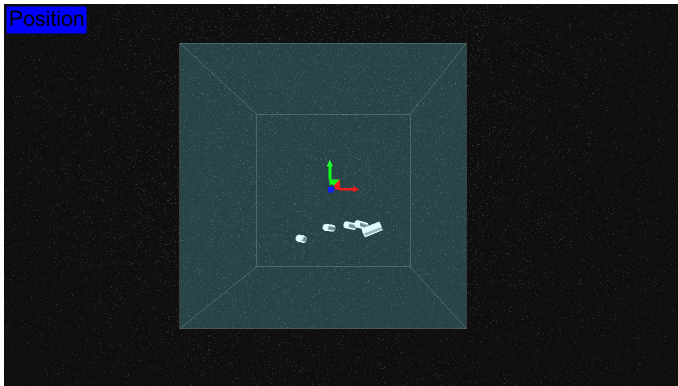


Fig. 5. A cubic selection volume after being created

3.6 Position Mode, Rotation Mode and Scale Mode

The position, rotation and scale modes allow the user to edit the active selection volume. In the position mode, the user can move the selection by making a grabbing gesture with their hand and moving it. The volume moves in whichever direction the hand is in relative to the center of the device's interaction volume.

In the rotation mode, the user can rotate the volume by holding a pinching gesture and dragging the hands around, causing the volume to rotate in a corresponding direction.

In the scale mode, the user can increase or decrease the size of the volume along one of three axes by holding one hand at a height above or below the other. Using a gesture command they can switch between the three axes.

3.7 Selection Mode

In the selection mode, the user can select volumes by pinching the index and thumb finger. The volume closest to the hand is selected. The selected volume can be deleted with a gesture command or it can be edited in the position, rotation or scale modes.

3.8 Visualization

When creating and editing a selection volume, one of the difficulties is to know which data points the volume is actually selecting. As such, visualization plays an important part in the process and several visualization modes were made available to the user:

- All: All data points are drawn.
- Only Selected: Only selected data points are drawn.
- Only Not Selected: Only non-selected data points are drawn.
- Colors: All points are drawn, but are given a different color depending on whether they are selected or not.

4 Discussion

While the Leap Motion can facilitate selection by giving the user the ability to interact with the software in three dimensions, there are still some limitations to its usage. The first problem is that the visualization is still two dimensional. The lack of depth perception associated with this means that it can be difficult to make a mental connection between the visualized space and the user's hands, rendering the advantages of 3D interaction far less effective. However, the available visualization modes help to solve this problem. For example, if the color visualization mode is active, then as the volume's position is changed, the effect on the selection is clearly visible.

The second problem is that the Leap Motion still has important limitations in its tracking ability. For example, it cannot keep track of a hand while it is occluded by another hand, limiting certain gestures in one axis. It also is limited in how many gestures it can easily identify. These problems raise many difficulties in designing sophisticated scientific visual analytics tool that users can understand intuitively and use effectively, and, therefore it remains a simple interaction system. Indeed, we have not come across any user interface that uses the Leap Motion in a way that is not either trivially simple or very hard to master. However, new developments are expected in the near future and these might solve part of the pointed problems for developing a truly scientific visual analytics tool.

Despite its limitations, the use of the Leap Motion remains a more effective way of modifying the position of a 3D volume than any 2D interaction system. Any such system would require the user to refine the volume's position while changing position of the camera.

5 Conclusion

The selection method described in this paper is scalable, and intuitively simple to understand. Despite the current limitations of gesture recognition hardware and software, it holds a distinct advantage over systems that work purely with 2D tools.

However, there is still a long way to go before it can be considered a useful tool for any serious scientific work. Future developments could include the use of the Oculus Rift for improved visualization and the refinement of the gesture interface.

References

1. Bowman, D.A., Kruijff, E., La Viola, J.J., Poupyrev, I.: 3D User Interfaces: Theory and Practice. Addison-Wesley (2004)
2. Fisher, D.: Animation for Visualization: Opportunities and Drawbacks. In: Steele, J., Iliinsky, N. (eds.) *Beautiful Visualisation*, p. 338. O'Reilly ed. (2010)
3. Hey, T., Tansley, S.: The Fourth Paradigm - Data intensive scientific discovery. In: Tolle, K. (ed.). *Microsoft Research, Redmond* (2009)

4. Becciani, U., Costa, A., Antonuccio-Delogu, V., Caniglia, G., Comparato, M., Gheller, C., Jin, Z., Krokos, M., Massimino, P.: VisIVO-Integrated Tools and Services for Large-Scale Astrophysical Visualization. In: Publications of the Astronomical Society of the Pacific, vol. 122(887), p. 119 (2010)
5. Yu, L., Efstathiou, K., Isenberg, P., Isenberg, T.: Efficient Structure-Aware Selection Techniques for 3D Point Cloud Visualizations with 2DOF Input. *IEEE Transactions on Visualization and Computer Graphics* **18**(12), 2245–2254 (2012)
6. Li, Y., Hielsberg, M.: 3D Point Cloud Editor (2012). <http://paradise.caltech.edu/~yli/software/pceditor.html>
7. Bacim, F., Nabiyouni, M., Bowman, D.A.: Slice-n-Swipe: A free-hand gesture user interface for 3D point cloud annotation. In: 2014 IEEE Symposium on 3D User Interfaces (3DUI), pp. 185–186, 29-30 (2014)
8. Lubos, P., Beimler, R., Lammers, M., Steinicke, F.: Touching the Cloud: Bimanual annotation of immersive point clouds. In: Proc. 3DUI, pp. 191–192 (2014)
9. Leap Motion, Inc. <https://www.leapmotion.com>
10. IVELA project. <http://www.ca3-uninova.org/projects>
11. European Space Agency. <http://www.esa.int>
12. Unity Technologies. <http://unity3d.com>

Context Classifier for Service Robots

Tiago Ferreira¹(✉), Fábio Miranda², Pedro Sousa²,
José Barata², and João Pimentão²

¹ Holos SA, Caparica, Portugal

tiago.ferreira@holos.pt

² Faculdade de Ciências e Tecnologia – UNL Caparica, Caparica, Portugal

f.miranda@campus.fct.unl.pt, jab@uninova.pt,

{pas,pim}@fct.unl.pt

Abstract. In this paper a context classifier for service robots is presented. Independently of the application, service robots need to have the notion of their context in order to behave appropriately. A context classification architecture that can be integrated in service robots reliability calculation is proposed. Sensorial information is used as input. This information is then fused (using Fuzzy Sets) in order to create a knowledge base that is used as an input to the classifier. The classification technique used is Bayes Networks, as the object of classification is partially observable, stochastic and has a sequential activity. Although the results presented refer to indoor/outdoor classification, the architecture is scalable in order to be used in much wider and detailed context classification. A community of service robots, contributing with their own contextual experience to dynamically improve the classification architecture, can use cloud-based technologies.

Keywords: Context · Service robots · Reliability · Fuzzy sets · Bayes networks

1 Introduction

Aside from our language and the common understanding of the world and its operation, what contributes to a much more efficient exchange of knowledge between human beings, is the notion of context [1]. Humans are able to add and take into account situational information (context) in a conversation to better understand the subject, retain more information in a more efficient way and to respond appropriately to it, in other words, to increase the conversational bandwidth as said in [1]. When interacting with machines or between machines, that awareness can be lost and so can the information richness [2].

As the matter of environment (as a subset of context) regards the physical world, there is also uncertainty associated with its sensing. That uncertainty can be caused, for example, by inaccuracy or incompleteness of sensed information [3]. There is a need for models that manage and take into account that uncertainty [4]. Fuzzy logic is used to set transitions of an element between membership and non-membership in linguistic terms and it involves ambiguity [5]. It can be used to describe subjective contexts and perform a multi-sensor fusion between those contexts.

Bayesian networks consist in nodes (that represent events) and arcs (representing relationships/conditional dependencies). Nodes not connected represent variables that

are conditionally independent. Bayesian networks are used to process data sets and to deduce high level information [4], assigning the most likely class to a given observation, described by a set of attributes. According to [6] this technique is best suitable for a factored state representation in which a state consists of a vector of attributes.

2 Relationship to Cloud-Based Solutions

The presented architecture was developed using Robotic Operating System (ROS)[7] on top of the Servrobot platform (servrobot.holos.pt). ROS allows for the exchange of information between software modules within the system using a messaging protocol. These software modules need not to be in the same machine or system and may send messages across the Internet. As the architecture is a software module itself it can receive and send information to other modules or robots. In this sense this architecture is scalable to receive inputs from several service robots. This is a typical application scenario for Cloud-based technologies use thus it can be used by a community of service robots contributing with their own contextual experience to dynamically improve the classification architecture and it's performance. Robotearth is an example of cloud-based technologies use in robotics[8].

3 State of the Art

Context has been used in the robotic field in many applications using several context models and or techniques [9]. A detailed review was made focusing on the application of context in the field. The most relevant results are presented in Table 1.

Table 1. Overview of context models in robotic systems their application purpose

Application Purpose	Context Model/Reasoning Technique
Object Recognition	Markov Random Field (probabilistic classifier)[10], Ontologies[11, 12]
Safety	Dempster-Shafer[14], Ontologies[15]
Human-machine interface	Polynomial classifiers[16], Hidden Markov Model[17]
Localization	Ontologies + Bayesian model[18]
Navigation	Ontologies[19]
Smart Environments	Ontologies + Logic[20], Ontologies[21]

As it can be understood from Table 1, ontologies seem to be the most used technique to support machine learning in the robotics field. Applications include several areas and reliability seems overlooked.

4 Implementation

4.1 Problem Approach

As it was stated before there are several applications for context analysis in the robotics field but context can be integrated in other applications as well. It is believed that the reliability field hasn't explored context in complete way. Context can and should be integrated in the reliability field allowing reliability calculation optimization.

A classification hierarchy is proposed, in which the context is first classified as indoor environment or outdoor environment and then there will be another computational model created to sub-classify in more detail the type of environment present.

4.2 Architecture Overview

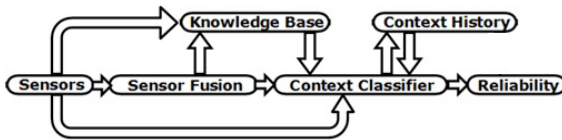


Fig. 1. Reliability context integration architecture

In Fig.1 the reliability context architecture is presented. It will first receive the sensor inputs and process its signals in order to reduce any noise and outlier values as well as to perform any necessary sensor fusion. In the knowledge base the information from sensors and sensor fusion are stored. A context classifier is created that will provide contextual information to the reliability calculation. Those classifications will be also stored in a context history module. This history can be re-fed to the classification module to improve performance. From that history the last state will be considered for the current classification.

It is believed that the environmental conditions will influence a great deal the reliability calculation and estimation. The key elements present in the surroundings may be crucial for optimizing reliability assessment, for example if a mobile robot is working under a very dusty outdoor environment it may be more prone to have mechanical failures thus reducing its reliability.

4.3 Architecture Implementation

Managing Input Sources.

The physical sensors taken into account in the architecture and their fuzzy linguistic terms are:

- Thermometer for temperature (“very hot”, “hot”, “comfortable” and “cold”);
- Hygrometer for humidity (“very high”, “high”, “comfortable” and “dry”);
- Photosensor for light (“very high”, “high”, “medium”, “low” and “very low”);

- GPS module for the number of satellites (“high”, “medium”, “low” and “none”);
- IMU for the soil type (“concrete”, “pavement” or “smooth”);
- GAS detector for gas level (“dangerous” or “non-dangerous” atmosphere);
- Time used to distinguish the “day” and “night” formalisms.

Fuzzy Logic Membership Functions.

Fuzzy logic was implemented to transform a sensed numeric value into a linguistic term (a qualitative semantic), therefore fuzzification was used to aggregate the sensor inputs. This will increase the flexibility and modularity of the overall algorithm over the slight changes in the sensor values (also decreasing its complexity and load).

The fuzzification was applied to temperature, humidity and light intensity. For each of them tests were conducted during various times of the day and weather conditions to achieve the necessary linguistic terms and membership functions. In this work the functions were chosen with no specific form, but there are many forms that can be assigned (triangular, trapezoidal, Gaussian, etc.).

Choosing the Classification Model.

Since ontologies are often specialized to some domain-specific applications (although they are used for many different purposes), it was preferred not to model the world around the robot “statically“ by describing its relations “manually“ in the beginning. Instead, the main interest is in one technique that could be taught and that can adapt to new situations.

The environment is partially observable because the robots sensors cannot give access to all the complete state of the environment at each point in time. Since its being dealt with a stochastic environment, the classification task is a sequential activity, a single classification at a time considering the previous state is performed, there is a dynamic environment and can be considered discrete, a factored representation is present the technique should support probabilities and uncertainty. Therefore the most suitable technique for classification is a Bayes classifier (Bayes network). It seemed to be a good start since it has good performances, even with less training data, is highly scalable, can adapt to a wide variety of classification tasks and is appropriate for a factored representation of data.

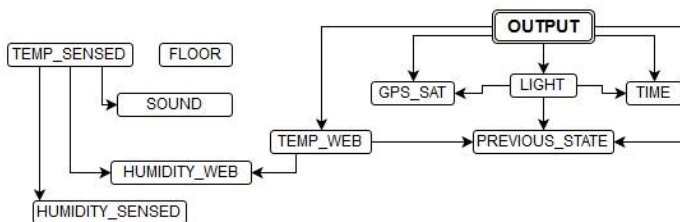


Fig. 2. Bayes Network

In this work the WEKA [22] framework was used to generate the Bayes network for this classification. In Fig.2 the Bayes network is represented with the different attributes and relations to the proposed output classification.

Reliability.

To integrate this work in reliability calculation a context factor must be added in the calculation.

$$R = e^{-\lambda \cdot \pi \cdot t} \quad (1)$$

Where R is the reliability, λ is the module hazard rate, π is the terrain factor and t is the time. The terrain factor can be calculated by:

$$\pi = \sum \pi_{tx} \times t_{tx} \quad (2)$$

Where π_{tx} is the terrain factor asserted to terrain x and t_{tx} is the total percentage of the operating time in terrain x . The proposed architecture results can be integrated in this factor by substituting the terrain concept by the context concept.

5 Field Tests and Experiment Results

From the first dataset collected, an 87.5% of correctly classified instances were obtained, using a 10-fold cross-validation evaluation on the training dataset. The confusion matrix represents TP (true positives), FP (false positives), FN (false negatives) and TN (true negatives). From Table 2 it can be understood that 119 instances were correctly classified as “indoor” out of a total of 121 indoor instances (true positives). A more detailed accuracy table is presented below (Table 3).

Table 2. Confusion Matrix

Indoor	Outdoor	Classified as
119	2	Indoor
17	14	Outdoor

Table 3. Detailed performance measures

TP Rate	FP Rate	Precision	Specificity	F-Measure	Class
0.983	0.548	0.875	0.452	0.926	INDOOR

TPR (True Positive Rate), also known as *sensitivity* or *recall* measures the proportion of positives that are correctly classified as such. FPR (False Positive Rate), also known as *false alarm rate* or *fallout* it’s the complementary with the specificity (1-specificity). Precision represents the positive predictive values. Specificity (also known as TNR – True Negative Rate) measures the proportion of negatives, which are correctly identified as such (complementary of FPR). F-measure a combined measure for precision and recall.

It was found that the number of GPS satellites is the most relevant attribute, although all other attributes are needed to increase systems consistency and accuracy.

A mixed environment test including the “previous state” attribute was done. In Fig.3, a mixed testing path is presented. The indoor path is represented in blue color, the outdoor path is represented in red color and the transition areas are represented in orange. In Table 4, the obtained confusion matrix is presented.

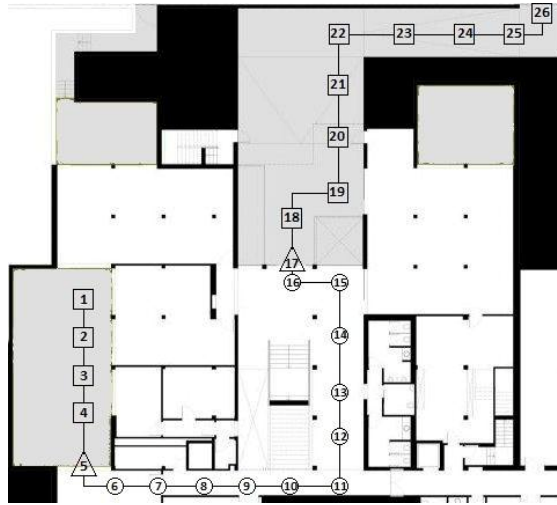


Fig. 3. Holos mixed testing path

Table 4. Confusion Matrix from the mixed testing path

Indoor	Outdoor	Classified as
119	19	Indoor
2	146	Outdoor

In this test the percentage of correctly classified instances was increased to 92.66% of overall accuracy. From the incorrectly classified instances, the 2 FP cases are located on step 6 of the Fig.3 and they occurred due to the presence of a glass wall in the room. Near the glass wall, the classifier can be deceived. Regarding the 19 false negative cases, 2 of them occurred on the step 5 of the path (Fig.3) which is the transition step, 6 of them occurred in step 18 due to the presence of a porch and the fact that the GPS attribute is slower to acquire satellites when moving from indoor to outdoor environments. The majority of the FN cases (11) occurred in step 17, which is another transition step.

Table 5. Detailed performance measures

TP Rate	FP Rate	Precision	Specificity	F-Measure	Class
0.862	0.014	0.885	0.986	0.873	INDOOR

It's now possible to remake all the calculations for the real application scenario. In Table 5, those calculations are presented. Very good results were achieved in specificity and sensitivity (a perfect classifier should be 100% specific and 100% sensitive) as well as a decrease in the FPR. Considering the “previous state” attribute in the classification, the most relevant attributes where: “light”, “GPS satellites”, “previous state” and “temperature web”.

As can be seen by these results this architecture is able to achieve similar results to those in [23] even without the previous state optimization (around 88%). When the previous state is included the results improve by approximately 5% in comparison.

6 Conclusions and Future Work

There are several context models, techniques and frameworks. From all of those possibilities the ones based on ontologies seem to be the ones with most widespread use. From all existing frameworks and for the intent of this architecture, machine-learning techniques, particularly Bayesian networks, seemed to be the more appropriate method for solving the systems classification problem. This is verified by the good results achieved by this system. One big reason for the good results in the system was the inclusion, in the architecture, of the previous state in the Bayes network. Future experiments should be considered with more linguistic terms in the fuzzy sets (for example, “morning”, “afternoon”, “late afternoon“ or “night” instead of just “day” or “night” for the time). Increasing the attribute quantity can add a valuable improvement in the overall performance. However, increasing the number of attributes doesn't necessarily improve the systems accuracy.

It is believed that a good base was created for a more complex and detailed classification. As knowing if the robot is indoor or outdoor with good accuracy allows a detailed context sub-classification.

References

1. Dey, A.K., Abowd, G.D.: Towards a Better Understanding of Context and Context-Awareness. *Handheld Ubiquitous Comput.* 304–307 (1999)
2. Dey, A.K.: Understanding and Using Context. *Pers. Ubiquitous Comput.* **5**, 4–7 (2001)
3. Haghghi, P., Krishnaswamy, S., Zaslavsky, A., Gaber, M.M.: Reasoning about context in uncertain pervasive computing environments. *Smart Sens. Context* **5279**, 112–125 (2008)
4. Bettini, C., Brdiczka, O., Henricksen, K., Indulska, J., Nicklas, D., Ranganathan, A., Riboni, D.: A survey of context modelling and reasoning techniques. *Pervasive Mob. Comput.* **6**, 161–180 (2010)
5. Zadeh, L.: Fuzzy Sets. *Inf. Control.* **8**, 338–353 (1965)

6. Russell, S., Norvig, P., Canny, J., Malik, J., Edwards, D.: *Artificial intelligence: a modern approach* (2009)
7. Quigley, M., Conley, K.: *ROS: an open-source Robot Operating System. ... open source* (2009)
8. Kehoe, B., Sachin, P.: *A Survey of Research on Cloud Robotics and Automation. IEEE Trans. Autom. Sci. Eng.* 1–11 (2010)
9. Miranda, F., Ferreira, T.: *Review on Context Classification in Robotics. Rough Sets Intell.* (2014)
10. Varvadoukas, T., Giannakidou, E., Gomez, J.V., Mavridis, N.: *Indoor Furniture and Room Recognition for a Robot Using Internet-Derived Models and Object Context. Front. Inf. Technol.* 122–128 (2012)
11. Wang, E., Kim, Y.S., Kim, H.S., Son, J.H., Lee, S., Suh, I.H.: *Ontology Modeling and Storage System for Robot Context Understanding. Knowledge-Based Intell. Inf. Eng. Syst.* **3683**, 922–929 (2005)
12. Choi, J., Park, Y., Lim, G., Lee, S.: *Ontology-Based Semantic Context Modeling for Object Recognition of Intelligent Mobile Robots. Recent Prog. Robot. Viable Robot. Serv. to Hum.* 370, 399–408 (2008)
13. Wibisono, W., Zaslavsky, A., Ling, S.: *Improving situation awareness for intelligent on-board vehicle management system using context middleware. IEEE Intell. Veh. Symp.* 1109–1114 (2009)
14. Nienhiiser, D., Gump, T., Zollner, J.M.: *A Situation Context Aware Dempster-Shafer Fusion of Digital Maps and a Road Sign Recognition System. Intell. Veh. Symp. 2009 IEEE.* 1401–1406 (2009)
15. Schlenoff, C., Messina, E.: *A robot ontology for urban search and rescue. In: Proc. 2005 ACM Work. Res. Knowl. Represent. Auton. Syst., KRAS 2005*, pp. 27–34 (2005)
16. Trovato, G., Zecca, M., Kishi, T., Endo, N., Hashimoto, K., Takanishi, A.: *Generation of Humanoid Robot's Facial Expressions for Context-Aware Communication. Int. J. Humanoid Robot.* **10**, 23 (2013)
17. Mou, W., Chang, M., Liao, C.: *Context-aware assisted interactive robotic walker for Parkinson's disease patients. Intell. Robot. Syst.* 329 – 334 (2012)
18. Yi, C., Suh, I.H., Lim, G.H., Choi, B.-U.: *Bayesian robot localization using spatial object contexts. In: 2009 IEEE/RSJ Int. Conf. Intell. Robot. Syst.*, pp. 3467–3473 (2009)
19. Provine, R., Uschold, M., Smith, S., Stephen, B., Schlenoff, C.: *Observations on the use of ontologies for autonomous vehicle navigation planning. Rob. Auton. Syst.* (2004)
20. Mastrogiovanni, F., Sgorbissa, A., Zaccaria, R.: *Context assessment strategies for Ubiquitous Robots. In: 2009 IEEE Int. Conf. Robot. Autom.* pp. 2717–2722 (2009)
21. Hristoskova, A.: E., C., Veloso, M., De, F.: *Heterogeneous Context-Aware Robots Providing a Personalized Building Tour. Int. J. Adv. Robot. Syst.* **10**, 13 (2013)
22. Bouckaert, R.R., Frank, E., Hall, M., Kirkby, R., Reutemann, P., Seewald, A., Scuse, D.: *WEKA Manual for Version 3-7-11.* (2014)
23. Zhou, P., Zheng, Y., Li, Z., Li, M., Shen, G.: *IODetector: A generic service for indoor outdoor detection. ... Embed. Netw. Sens.* (2012)

Distributed RSS-Based Localization in Wireless Sensor Networks with Node Selection Mechanism

Slavisa Tomic^{4(✉)}, Marko Beko^{1,3}, Rui Dinis^{2,5},
Goran Dimic⁶, and Milan Tuba⁷

¹ Universidade Lusófona de Humanidades e Tecnologias, Lisbon, Portugal

mbeko@uninova.pt

² DEE/FCT/UNL, Caparica, Portugal

rdinis@fct.unl.pt

³ UNINOVA – Campus FCT/UNL, Caparica, Portugal

⁴ ISR/ IST, Lisbon, Portugal

s.tomic@campus.fct.unl.pt

⁵ Instituto de Telecomunicações, Lisbon, Portugal

⁶ Institute Mihailo Pupin, University of Belgrade, Belgrade, Serbia

goran.dimic@pupin.rs

⁷ Faculty of Computer Science, Megatrend University, Belgrade, Serbia

tuba@ieee.org

Abstract. In this work, we address the target localization problem in large-scale cooperative wireless sensor networks (WSNs). Using the noisy range measurements, extracted from the received signal strength (RSS) information, we formulate the localization problem based on the maximum likelihood (ML) criterion. ML-based solutions are particularly important due to their asymptotically optimal performance, but the localization problem is highly non-convex. To overcome this difficulty, we propose a convex relaxation leading to second-order cone programming (SOCP), which can be efficiently solved by interior-point algorithms. Furthermore, we investigate the case where target nodes limit the number of cooperating nodes by selecting only those neighbors with the highest RSS measurements. This simple procedure may decrease the energy consumption of an algorithm in both communication and computation phase. Our simulation results show that the proposed approach outperforms the existing ones in terms of the estimation accuracy. Moreover, they show that the new approach does not suffer significant degradation in its performance when the number of cooperating nodes is reduced.

Keywords: Wireless localization · Wireless sensor network (WSN) · Received signal strength (RSS) · Second-order cone programming problem (SOCP) · Cooperative localization · Distributed localization

1 Introduction

Ad hoc wireless sensor networks (WSNs) composed of tiny and low-power sensor nodes scattered over a region of interest form a very useful tool for monitoring the environmental characteristics, such as temperature, sound levels, air pollution, etc. Low device costs and savings in the infrastructure permit deployment of tens,

hundreds, or even thousands of sensor nodes [1]. Besides sensing, nodes have a limited capability of processing and communicating the acquired data.

In many practical applications, data gathered inside a WSN are irrelevant if the locations of the reference nodes are not known. Hence, nodes' position information is a key requirement for many applications. Installing a global positioning system (GPS) device in each sensor node would be very expensive, and it would also restrict the network applicability [2]. An alternative and more cost-efficient solution is to equip only a small fraction of nodes with GPS, called anchor (or reference) nodes, and to determine the position of the remaining nodes, called target nodes, by employing the (noisy) ranging information between target and anchor nodes.

Ranging (distance) measurements are obtained between two sensor nodes which are in the communication range of each other, and are typically extracted from time-of-arrival (TOA), time-difference-of-arrival (TDOA), round-trip time (RTT), angle-of-arrival (AOA), received signal strength (RSS) information or a combination of them, depending on the available hardware [3]. Ranging based on RSS has the lowest implementation costs, since it does not require any special hardware [3], rendering it an attractive low-cost solution for the localization problem.

The required processing inherent to localization schemes can be executed in a centralized or a distributed fashion. The former approach assumes the existence of a fusion center which coordinates the network and performs all computational processing. Moreover, this approach is characterized by stability and fundamental optimality, but its computational complexity grows with the number of nodes in the network [2]. On the other hand, the main advantages of the latter approach are scalability and low-complexity. However, this approach is executed iteratively; thus, it is sensitive to error propagation and might require a long convergence time. Hence, the trade-off between the computational complexity and estimation accuracy is the main feature that determines which approach is more suitable to employ. In this work, we will focus exclusively on the distributed algorithms, since we deal with large-scale WSNs, and this approach is more likely to preserve energy.

Recently, RSS-based localization techniques have attracted much attention in the research society [4]-[11]. The approaches described in [4]-[8] consider centralized algorithms exclusively. In [9], a distributed algorithm based on an augmented Lagrangian approach using primal-dual decomposition was presented. However, the authors dealt only with a non-cooperative localization problem, where a single target node emits beacon frames to all anchor nodes in the network. A distributed cooperative algorithm characterized by a spatial constraint that limits the solution space to a region around the current position estimate was presented in [10]. Using discretization of the solution space, the authors in [10] found the position update of each node by minimizing a local objective function over the candidate set using direct substitution. Another distributed cooperative localization algorithm that dynamically estimates the path loss exponent (PLE) by using RSS measurements was introduced in [11]. This algorithm was based on gradient descent search which employs a circular Gauss-Seidel algorithm. Although the approaches in [10], [11] have excellent computational characteristics, their performance highly depends on good initialization, since the objective function is non-convex and the algorithm may get trapped into local minima or a saddle point, resulting in a large estimation error.

In this paper, we consider a large-scale RSS-based cooperative localization problem, and we propose a solution which is based entirely on a distributed approach. We derive a novel second-order cone programming (SOCP) estimator, which, in huge contrast to the existing methods, does not depend on initialization and requires much less iterations to converge. We also investigate the case where the target nodes limit the number of cooperating nodes (neighbors), discarding potentially bad links and reducing energy consumption in the network.

The remainder of this paper is structured as follows. In Section 2, a relationship of the research topic to cloud-based solutions is defined. In Section 3 the RSS measurement model is introduced and target localization problem is formulated. Section 4 provides details about the development of the proposed SOCP estimator and the node selection mechanism for reducing the number of cooperating nodes. The analysis of the computational complexity is summarized in Section 5. In Section 6 we provide the simulation results in order to compare the performance of the new approach and the existing ones. The main conclusions are summarized in Section 7.

2 Relationship to Cloud-Based Solutions

Sensor nodes in WSNs are deployed over a region of interest in order to obtain the desired information (such as temperature, noise pollution, etc.). Due to the limited power and computational potential of sensor nodes, one may consider connecting them to the “cloud”. This approach channels the effort towards providing connectivity and communication capabilities to each sensor node by connecting them to the “cloud”, rather than trying to increase local computational resources at each sensor node, which might be technically difficult for some cases. As a result, not only flexibility and more robust security mechanisms may be acquired, but also access to larger pools of resources available on the Internet can be enabled, allowing the development of higher value-added services, and faster and better decisions to each individual device to accompany the changes in the environment.

3 Measurement Model

We consider a WSN with $|\mathcal{T}| + |\mathcal{A}|$ nodes, where \mathcal{T} and \mathcal{A} are the sets of all target and anchor nodes, respectively, and $|\cdot|$ represents the cardinality of a set ($|\mathcal{T}| = T, |\mathcal{A}| = A$). The locations of the nodes are denoted as $\mathbf{x}_1, \dots, \mathbf{x}_T, \mathbf{x}_{T+1}, \dots, \mathbf{x}_{T+A}$, where $\mathbf{x}_i \in \mathbb{R}^q (q \geq 2)$. The considered network can also be seen as a connected graph, $\mathcal{G}(\mathcal{V}, \mathcal{E})$, where \mathcal{V} and \mathcal{E} are the set of vertices and edges, respectively. In order to preserve the energy and prolong the lifetime of the network, each node has a limited communication range, R . Hence, two nodes, i and j , can exchange information if and only if they are within the communication range of each other, i.e., $\mathcal{E} = \{(i, j) : \|\mathbf{x}_i - \mathbf{x}_j\| \leq R, i \neq j\}$. Target node i considers any neighboring node j (target or anchor) as an anchor node in the localization process. Set of neighbors of a target node i is defined as $\Omega_i = \{j : (i, j) \in \mathcal{E}\}$.

For ease of expression, we define $\mathbf{X} = [\mathbf{x}_1, \mathbf{x}_2, \dots, \mathbf{x}_T]$ as the $q \times T$ matrix of all target positions in the WSN. We assume that the anchor positions are known *a priori*, while each target node i is given an initial estimation of its position, $\hat{\mathbf{x}}_i^{(0)}$, $i = 1, \dots, T$; hence, $\hat{\mathbf{X}}^{(0)}$ contains all initial estimations of the target positions.

From the relationship $L_{ij} = 10 \log_{10} \frac{P_T}{P_{ij}}$, where P_T is the transmit power of a node, and P_{ij} is the received power at the i -th target node from the j -th neighboring node, the RSS localization problem can be formulated according to the path loss model (in dB) instead of RSS [12],[13]

$$L_{ij} = L_0 + 10\gamma \log_{10} \frac{\|\mathbf{x}_i - \mathbf{x}_j\|}{d_0} + n_{ij}, \forall (i, j) \in \mathcal{E}, \quad (1)$$

where L_0 is the path loss value at a short reference distance d_0 ($\|\mathbf{x}_i - \mathbf{x}_j\| \leq d_0$), γ is the path loss exponent, and n_{ij} is the log-normal shadowing term between nodes i and j , modeled as a zero-mean Gaussian random variable with variance σ_{ij}^2 , i.e., $n_{ij} \sim \mathcal{N}(0, \sigma_{ij}^2)$. We assume that all path loss measurements are symmetric, i.e., $L_{ij} = L_{ji}$, for $i \neq j$.

Based on the measurements from (1), we derive the maximum likelihood (ML) estimator as

$$\hat{\mathbf{X}} = \operatorname{argmin}_{\mathbf{X}} \sum_{(i,j):(i,j) \in \mathcal{E}} \frac{1}{\sigma_{ij}^2} \left[L_{ij} - L_0 - 10\gamma \log_{10} \frac{\|\mathbf{x}_i - \mathbf{x}_j\|}{d_0} \right]^2. \quad (2)$$

The least squares (LS) problem defined in (2) is non-linear and non-convex; hence, finding its globally optimal solution is difficult, since there may exist multiple local optima. In the following text we will show that the ML estimator in (2) can be approximated into a convex estimator, using SOCP relaxation, which can be solved efficiently by interior-point algorithms [14].

For the sake of simplicity (and without loss of generality), in the remainder of this work we assume that $\sigma_{ij}^2 = \sigma^2$, $\forall (i, j) \in \mathcal{E}$. Moreover, we assume that P_T of all nodes are identical, i.e., L_0 and R are equivalent for all nodes.

4 Distributed Algorithm

Observe that the objective function in (2) depends only on the positions and pairwise measurements between the incident nodes. Given that the initial guess of the targets' positions and the true anchors' positions are known, problem in (2) can be solved independently by each target node, using only local information from its neighbors. Breaking down the localization problem in (2) into smaller sub-problems is particularly suitable for large-scale and highly-dense networks, because this approach can significantly reduce the computational complexity of an algorithm.

Solving the localization problem in a distributed fashion implies using an iterative scheme, consisting of two phases:

- 1) *Communication phase* - each target node in the network transmits its position estimate to its neighbors.

- 2) *Computation phase* - each target node updates its position estimate. To update its position, target node i solves the following optimization problem:

$$\hat{\mathbf{x}}_i^{(k+1)} = \underset{\mathbf{x}_i}{\operatorname{argmin}} \sum_{(i,j) \in \mathcal{E}} \frac{1}{\sigma^2} \left[L_{ij} - L_0 - 10\gamma \log_{10} \frac{\|\mathbf{x}_i - \hat{\mathbf{x}}_j\|}{d_0} \right]^2, \quad (3)$$

Where $\hat{\mathbf{x}}_j$ denotes the last position estimate of the j -th neighboring target node (or the true node position, if j -th node is an anchor) received by i -th target node. In the following text, we will show that (3) can be approximated into a convex problem.

4.1 The Proposed SOCP Estimator

Given the measurements in (1), the ML estimate of distance between nodes i and j is derived as:

$$\hat{d}_{ij} = d_0 10^{\frac{L_{ij} - L_0}{10\gamma}}. \quad (4)$$

We can reformulate (4) as:

$$\mu_{ij} \hat{d}_{ij}^2 = \eta d_0^2, \quad (5)$$

where $\mu_{ij} = 10^{-\frac{L_{ij}}{5\gamma}}$, and $\eta = 10^{-\frac{L_0}{5\gamma}}$. Assuming that the initial target positions estimates are available, from (5), target node i updates its position estimate by minimizing the following LS problem:

$$\mathbf{x}_i^{(k+1)} = \underset{\mathbf{x}_i}{\operatorname{argmin}} \sum_{(i,j) \in \mathcal{E}} \left(\mu_{ij} \|\mathbf{x}_i - \hat{\mathbf{x}}_j\|^2 - \eta d_0^2 \right)^2. \quad (6)$$

Define auxiliary variables $\varphi_i = \|\mathbf{x}_i\|^2$ and $\boldsymbol{\alpha} = [\alpha_{ij}]$, where $\alpha_{ij} = \mu_{ij}(\varphi_i - 2\hat{\mathbf{x}}_j^T \mathbf{x}_i + \hat{\mathbf{x}}_j^T \hat{\mathbf{x}}_j) - \eta d_0^2, \forall (i, j) \in \mathcal{E}$. Introduce an epigraph variable e , and apply second-order cone constraint (SOCC) relaxation to obtain the following convex optimization problem:

$$\underset{\mathbf{x}_i, \boldsymbol{\varphi}, \boldsymbol{\alpha}, e}{\operatorname{minimize}} \quad e$$

subject to

$$\alpha_{ij} = \mu_{ij}(\varphi_i - 2\hat{\mathbf{x}}_j^T \mathbf{x}_i + \hat{\mathbf{x}}_j^T \hat{\mathbf{x}}_j) - \mu d_0^2, \forall (i, j) \in \mathcal{E},$$

$$\|2\boldsymbol{\alpha}; e - 1\| \leq e + 1, \quad \|2\mathbf{x}_i; \varphi_i - 1\| \leq \varphi_i + 1. \quad (7)$$

Problem defined in (7) is a SOCP problem, which can be efficiently solved by the CVX package [15] for specifying and solving convex programs. We will refer to (7) as ‘‘SOCP’’ in the further text.

4.2 The Proposed Node Selection Mechanism

Theoretically, it is possible that each target node communicates with every other node in the network, i.e., $|\Omega_i| = T + A - 1$, for $i = 1, \dots, T$. In practice however, the size of the neighborhood fragments is much smaller, due to limited energy resources. Since the RSS range errors are multiplicative, i.e., they have constant multiplicative factors with range [1], edges from distant nodes may negatively influence the performance. Hence, we intend to drop all potentially bad links in the network.

Here, we investigate two possible node selection mechanisms that are based on distance criterion. The basic idea is to exploit the information of only n_d closest neighbors at each target node, rather than the information from all $|\Omega_i|$ neighbors. Thus, our goal is to achieve a good trade-off between the estimation accuracy and energy consumption. The derivation of the optimal mechanism is not possible [11]; hence, we use a sub-optimal scheme that is based on distance estimates between nodes. The scheme is suboptimal, since we deal with noisy RSS measurements, and the measurements with the highest RSS are not necessarily the best ones.

Target node i estimates the distance between itself and its neighbor $j, j \in \Omega_i$, according to (4). We can sort these estimates of target node i as:

$$\hat{d}_{i_1} \leq \hat{d}_{i_2} \leq \dots \leq \hat{d}_{i_m}, \quad 1, \dots, m \in \Omega_i,$$

where \hat{d}_{i_1} and \hat{d}_{i_m} are the lowest and highest distance estimates, respectively. Target node i selects the new group of cooperating nodes, Ω'_i as follows:

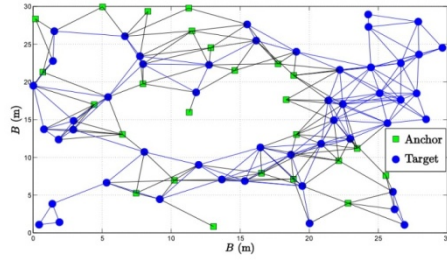
- 1) Choosing all anchors and n_d nearest target nodes, i.e., $\Omega'_i = \{j: j \in \mathcal{A}\} \cup \{i_1, i_2, \dots, i_{n_d}: i_m \in \mathcal{T}, \text{ for } m = 1, \dots, n_d\}$;
- 2) Choosing n_d nearest neighbors, i.e., $\Omega'_i = \{i_1, i_2, \dots, i_{n_d}\}$.

Applying the node selection mechanism is likely to reduce the energy consumption inside a WSN, as it can be seen in Fig. 1.

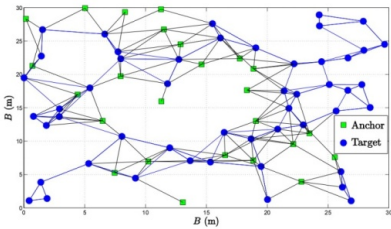
Table 1. Summary of the Considered Algorithms

Algorithm	Description	Complexity
DSCL	The spatially constrained algorithm in [10]	$K_{\max} \times T \times F \times \mathcal{O}(\max_i \{ \Omega_i \})$
LS	The least squares algorithm in [11]	$K_{\max} \times T \times t_{iter2} \times \mathcal{O}(\max_i \{ \Omega_i \})$
SOCP	The proposed algorithm in (7)	$K_{\max} \times T \times \mathcal{O}((\max_i \{ \Omega_i \})^3)$

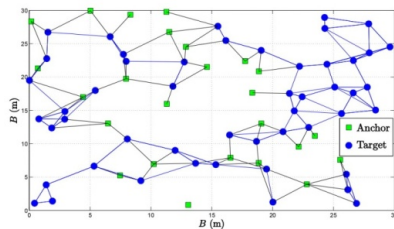
Fig. 1 illustrates a possible network layout when target nodes cooperate with (a) all nodes in their communication range, (b) all anchor neighbors and at most n_d nearest target neighbors, and (c) at most n_d nearest neighbors. One can see from Fig. 1 that the network is significantly skimmed when the node selection mechanism is applied. Although this procedure may degrade the estimation accuracy, it is likely to preserve energy in a WSN in both communication and computation phase of the algorithm.



a)



b)



c)

Fig. 1. A possible network layout of a WSN with $A=25$, $T=50$ nodes. Target nodes communicate with a) all nodes in their communication range, b) all anchor neighbors and at most $n_d = 3$ nearest target neighbors, and c) at most $n_d = 4$ nearest neighbors.

5 Analysis of Computational Complexity

The trade-off between the computational complexity and estimation accuracy determines the applicability potential of an algorithm; hence, it is the most important feature of a localization algorithm. For this reason, we are also interested in comparing the computational complexities of the proposed approach with the existing ones. Here, we investigate the worst case asymptotical complexity of the algorithms, i.e., we present only the dominating elements.

Table 1 gives an overview of the considered algorithms, together with their computational complexities. The worst case complexity of the proposed SOCP approach is calculated according to [16].

From Table 1 it can be seen that the worst case complexity of a distributed algorithm mainly depends on the neighborhood fragments (the biggest one). The size of the neighborhood fragments is not severely affected if the number of nodes in the network is increased, which makes the distributed algorithms a desirable solution in highly-dense or large-scale networks. Furthermore, we can see from Table I that the new approach is computationally the most demanding. This fact is justified by its superior performance in terms of the estimation accuracy and convergence, as we will see in the following section.

6 Performance Assessment

In this section, we present the computer simulation results in order to compare the performance of the proposed approach with the state-of-the-art. The new approach was solved by using the MATLAB package CVX [15], where the solver is SeDuMi [17].

To generate the RSS measurements, the propagation model (1) is used. We considered a random deployment of nodes inside a square region of length $B = 30$ m in each Monte Carlo (M_c) run. Random deployment of nodes is of practical interest, since the algorithms are tested against various network topologies. In order to make the comparison fair, we first obtained $M_c = 500$ nodes positions, and we run the considered algorithms for these scenarios. Furthermore, we made sure that the network graph was connected in each M_c run. The path loss exponent is $\gamma = 3$, the reference distance $d_0 = 1$ m, the reference path loss $L_0 = 40$ dB, and the communication range of a node $R = B / 5$ m. We assumed that the initial estimation of the target positions, $\hat{\mathbf{X}}^{(0)}$, is in the intersection of the diagonals of the square area, and the maximum number of iterations $K_{\max} = 100$. We assumed that the working sequence of the nodes is random, and that all target nodes use the last received position estimate of their neighbors. A iteration is completed when all T target nodes compute and transmit their position estimates. As the performance metric we used the normalized root mean square error (NRMSE), defined as

$$\text{NRMSE} = \sqrt{\frac{1}{T M_c} \sum_{i=1}^{M_c} \sum_{j=1}^T \|\mathbf{x}_{ij} - \hat{\mathbf{x}}_{ij}\|^2},$$

where $\hat{\mathbf{x}}_{ij}$ denotes the estimate of the true location of the j -th target in the i -th Monte Carlo run, \mathbf{x}_{ij} .

Fig. 2 illustrates the NRMSE versus k performance of the considered algorithms, when target nodes choose all neighboring anchor nodes and at most n_d nearest target nodes for cooperation. As the lower bound on the performance, we have provided the simulation results when the considered approaches use all nodes that are inside their communication range for cooperation. In Fig. 2, the average number of anchor neighbors was $\bar{n}_{ia} = 2.54$, and the average number of all neighbors was $\bar{n}_i = 7.48$. It is worth noting that the new approach outperforms the state-of-the-art for more than 1 m, in the case where no node selection mechanism was applied. From Fig. 2, we can see that the performance of all approaches improves when the number of cooperating target neighbors increases, as expected. Although the proposed approach does not converge for $n_d = 1$, it outperforms the existing ones in general. This can be seen from Fig. 2 (top), where the proposed approach reaches the lower bound for $n_d \geq 3$, while the existing ones show considerable gap for all choices of n_d in comparison to their lower bounds, Figs. 2 (middle and bottom).

Fig. 3 illustrates the NRMSE versus k performance of the considered algorithms, when target nodes choose at most n_d nearest neighboring nodes for cooperation. In Fig. 3, the average number of neighbors was $\bar{n}_i = 7.48$. From Fig. 3, it can be seen that the performance of all algorithms betters as the number of cooperating nodes is

increased. This result is anticipated, because when n_d is increased the collected information of each target node also increases, as well as the probability of having more anchor neighbors. Moreover, we can see that the new approach outperforms the existing ones for $n_d > 3$, requiring only $k = 30$ iterations to converge in general.

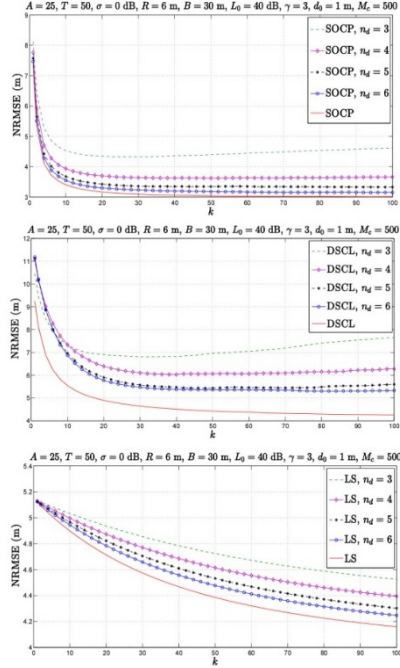
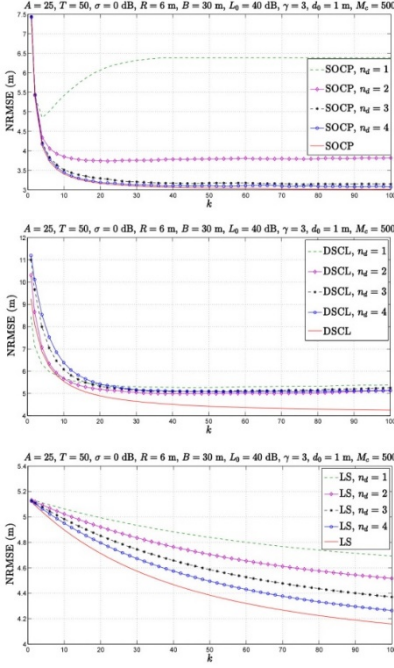


Fig. 2. NRMSE versus k comparison of the proposed SOCP (top), DSCL (middle), and LS (bottom) approach for different n_d nearest target neighbors, when $A = 25, T = 50, \sigma = 0$ dB, $R = 6$ m, $B = 30$ m, $L_0 = 40$ dB, $\gamma = 3, d_0 = 1$ m, $M_c = 500$.

Fig. 3. NRMSE versus k comparison of the proposed SOCP (top), DSCL (middle), and LS (bottom) approach for different n_d of the nearest neighbors, when $A = 25, T = 50, \sigma = 0$ dB, $R = 6$ m, $B = 30$ m, $L_0 = 40$ dB, $\gamma = 3, d_0 = 1$ m, $M_c = 500$.

7 Conclusions

In this work, we investigated the RSS-based target localization problem in large-scale cooperative WSN. We proposed a completely distributed algorithm based on SOCP relaxation technique. The simulation results confirm the superiority of the proposed approach in terms of the estimation accuracy and convergence. Furthermore, we have considered the case where the target nodes limit the number of cooperating nodes, by selecting only a certain number of neighbors with the highest RSS measurements. This simple procedure does not affect the computational complexity of an algorithm, and it can reduce the energy consumption inside the network. Unlike the existing

approaches, the simulation results show that the proposed method does not deteriorate significantly in the performance when the number of cooperating nodes is reduced.

In this paper, we have presented the results accumulated via computer simulations. The algorithm's implementation in a real WSN is yet to be done, and practical indoor scenarios will be of particular interest.

Acknowledgments. This work was partially supported by Fundação para a Ciência e a Tecnologia under Projects PEst-OE/EEI/UI0066/2014, EXPL/EEI-TEL/0969/2013–MANY2 COMWIN and EXPL/EEI-TEL/1582/2013 GLANC, PEst-OE/EEI/LA0008/2013 (IT pluriannual founding and HETNET), PEst-OE/EEI/UI0066/2011 (UNINOVA pluriannual founding), EnAcoMIMOCO EXPL/EEI-TEL/2408/2013, ADIN PTDC/EEI-TEL/2990/2012, and TR 32043, and the grant SFRH/BD/91126/2012 and Ciência 2008Post-Doctoral Research grant.

References

1. Patwari, N.: Location Estimation in Sensor Networks. PhD Thesis, University of Michigan, Ann Arbor, MI, USA (2005)
2. Destino, G.: Positioning in Wireless Networks: Noncooperative and Cooperative Algorithms. PhD Thesis, University of Oulu, Oulu, Finland (2012)
3. Patwari, N., Ash, J.N., Kyperountas, S., Hero III, A.O., Moses, R.L., Correal, N.S.: Locating the Nodes: Cooperative Localization in Wireless Sensor Networks. *IEEE Signal Process. Mag.* **22**(4), 54–69 (2005)
4. Ouyang, R.W., Wong, A.K.S., Lea, C.T.: Received Signal Strength-based Wireless Localization via Semidefinite Programming: Noncooperative and Cooperative Schemes. *IEEE Trans. Veh. Technol.* **59**(3), 1307–1318 (2010)
5. Wang, G., Yang, K.: A New Approach to Sensor Node Localization Using RSS Measurements in Wireless Sensor Networks. *IEEE Trans. Wirel. Commun.* **10**(5), 1389–1395 (2011)
6. Wang, G., Chen, H., Li, Y., Jin, M.: On Received-Signal-Strength Based Localization with Unknown Transmit Power and Path Loss Exponent. *IEEE Wirel. Commun. Lett.* **1**(5), 536–539 (2012)
7. Vaghefi, R.M., Gholami, M.R., Buehrer, R.M., Ström, E.G.: Cooperative Received Signal Strength-Based Sensor Localization With Unknown Transmit Powers. *IEEE Trans. Signal Process.* **61**(6), 1389–1403 (2013)
8. Salman, N., Ghogho, M., Kemp, A.: H: On the Joint Estimation of the RSS-based Location and Path-loss Exponent. *IEEE Wireless Commun. Lett.* **1**(1), 34–37 (2012)
9. Béjar, B., Zazo, S.: A Practical Approach for Outdoors Distributed Target Localization in Wireless Sensor Networks. *EURASIP J. Adv. Signal Process.* 1–11 (May 2012)
10. Cota-Ruiz, J., Rosiles, J.G., Rivas-Perea, P., Sifuentes, E.: A Distributed Localization Algorithm for Wireless Sensor Networks Based on the Solution of Spatially-Constrained Local Problems. *IEEE Sens. J.* **13**(6), 2181–2191 (2013)
11. Bel, A., Vicario, J.L., Seco-Granados, G.: Localization Algorithm with On-line Path Loss Estimation and Node Selection. *Sensors* **11**(7), 6905–6925 (2011)
12. Rappaport, T.S.: *Wireless Communications: Principles and Practice*. Prentice-Hall, Upper Saddle River (1996)

13. Sichitiu, M. L., Ramadurai, V.: Localization of wireless sensor networks with a mobile beacon. In: Proceedings of the IEEE International Conference on Mobile Ad-hoc and Sensor Systems (MASS), Fort Lauderdale, FL, USA, pp. 174–183 pp. 25–27, October 2004
14. Boyd, S., Vandenberghe, L.: Convex Optimization. Cambridge University Press, Cambridge (2004)
15. Grant, M., Boyd, S.: CVX: Matlab Software for Disciplined Convex Programming. Version 1.21 <http://cvxr.com/cvx> (accessed on April 15, 2010)
16. Pólik, I., Terlaky, T.: Interior Point Methods for Nonlinear Optimization. In: Di Pillo, G., Schoen, F. (eds.) Nonlinear Optimization, 1st ed. Springer, Heidelberg, Cetraro, Italy (2010)
17. Sturm, J.F.: Using SeDuMi 1.02, a MATLAB Toolbox for Optimization Over Symmetric Cones. Optim. Meth. Softw. 11, 625–653 (1999)

Signal Processing in Medicine

Continuous Speech Classification Systems for Voice Pathologies Identification

Hugo Cordeiro^{1,2(✉)}, Carlos Meneses², and José Fonseca¹

¹ Department of Electrical Engineering, Faculty of Sciences and
Technology of the New University of Lisbon, 2829-516 Caparica, Portugal
jmf@uninova.pt

² Department of Electronics and Telecommunications and Computers,
High Institute of Engineering of Lisbon, 1959-007 Lisbon, Portugal
{hcordeiro,cmeneses}@deetc.isel.ipl.pt

Abstract. Voice pathologies identification using speech processing methods can be used as a preliminary diagnostic. The aim of this study is to compare the performance of sustained vowel /a/ and continuous speech task in identification systems to diagnose voice pathologies. The system recognizes between three classes consisting of two different pathologies sets and healthy subjects. The signals are evaluated using MFCC (Mel Frequency Cepstral Coefficients) as speech signal features, applied to SVM (Support Vector Machines) and GMM (Gaussian Mixture Models) classifiers. For continuous speech, the GMM system reaches 74% accuracy rate while the SVM system obtains 72% accuracy rate. For the sustained vowel /a/, the accuracy achieved by the GMM and the SVM is 66% and 69% respectively, a lower result than with continuous speech.

Keywords: Voice pathologies identification · Continuous speech · Gaussian mixture models · Support vector machines

1 Introduction

Voice pathologies are caused by different factors such as the extensive or incorrect use of voice, stress, tobacco smoke inhalation, gastric reflux or hormonal problems. These pathologies typically affect the vocal folds and are detectable by direct laryngoscopy, which is the visualization of the vocal folds using a camera. However, this method is invasive, uncomfortable for the patient and may, depending on the equipment used, require a local anesthetic. The diagnostic equipment is also expensive and has high maintenance costs, requiring sterilization between diagnoses.

The use of an efficient, non-invasive, easy and fast method in pathologies recognition may be useful as an initial evaluation or as a complementary method for the diagnosis of voice pathologies. A method of voice pathologies diagnosis based in speech signals is especially useful in screening situations because it doesn't involve specialized equipment.

Several works in pathological voice identification discriminate between healthy and unhealthy subjects, without the identification of the pathology. Some works in pathological voice identification [1-4] use features like pitch jitter, shimmer,

harmonic-to-noise ratio (HNR) and energy spectrum to discriminate unhealthy subjects. Other works use features like MFCC [5] and wavelet analysis [6]. In [7] a comparison between different systems and features in pathological voice identification can be found.

There are few works in voice pathologies identification and all use the sustained vowel /a/ as speech signal. In this task, features like jitter and shimmer alone are not sufficient to discriminate pathologies [8]. In [9], spectral modulation and SVM are used to detect polyps pathology among three pathologies and healthy voices, using the vowel /a/ from the MEEI corpus [10]. The system achieves an average recognition rate of 90%. The features are obtained by spectral modulation where the discrete spectrum of the signal is modeled in sub-bands. The signal obtained from patients with polyps presents a higher energy in the pitch band. After feature extraction, an algorithm based on principal component analysis is used for dimensionality reduction. Finally, feature selection based on mutual information is used to sort only the most relevant characteristics.

In [11], the authors compare the results obtained in previous work [9] with those obtained with the MFCC as parameters. The results obtained are approximately 25% lower than the results obtained by spectral modulation.

In [12] five different pathologies are identified, assuming that the voice is pathological. Two Arabic vowels equivalent to /a/ and /i/, where tested from a corpus consisting of numbers from 1 to 10, with 72 patients, thus generating 720 speech signals, where 80% are used for training and 20% for testing. From each vowel the value of the first and second formant are extracted taking 4 or 5 frames in the middle of the speech signal (where it is more stable). Using these four features a neuronal network achieves a recognition rate of 67.8% for male patients and 52.5% for female patients. Tests were also conducted with a classifier based on vector quantization but the results were inferior to those obtained by the neural network. It is reported in that work that, in some diseases, a deviation in the formants mean values allows the discrimination of the pathologies. In [13] wavelets are used in a MLP (Multi Layer Perception) neural network for identification between nodules and Reinke's edema. The accuracy reaches 87% for Reinke's edema and 86% for nodules using 80% of the data for training and 20% for independent testing. In [14] the authors use jitter in the wavelets components with SVM (Support Vector Machines) to perform distinction between nodules and Reinke's edema. Using a similar dataset as in [13], 82% accuracy has been achieved. Also for this database SVM classifiers were used to evaluate the impact of the first peak bandwidth presented in [15], pitch jitter and pitch in Reinke's edema vs. nodules identification. With the vowel /a/ the results obtained using the first LPC spectral peak achieves an overall accuracy 84.6% and do not improve by using additional features like pitch jitter. The results obtained are in line and sometimes overlap the results reported in previous publications with the same corpus, but in this work the test uses 50% of the data.

In the previous referenced works the vowel /a/ speech signal was used in pathological voice classification. In [5], continuous speech signals were also used and the results are compared with the obtained with the vowel /a/. The classifiers use MFCC and HMM and show 99.5% accuracy for the vowel /a/ and 98.6% for continuous speech. In this work, it was found that pathological voice recognition can be done based on continuous speech. However, continuous speech signals analysis has never been tested for voice pathologies identification.

The main objective of this work is to evaluate which voice signal has higher potential for voice pathologies identification: the vowel /a/ or continuous speech. The latter assumes that voice pathology have speech characteristic that are phoneme independent. To inspect that, the two signals are evaluated using MFCC as speech signal features, applied to SVM and GMM classifiers.

2 Relationship to Cloud-Based Solutions

As mentioned in the previous section, the area of pathological voice recognition is growing but there are few works on pathologies identification. One of the reasons is the lack of a reference database for the area development. Pathological voice recognition has numerous advances and in many cases recognition rates over 90% are achieved. However, for pathologies identification there is a considerable lack of data, since it must be divided by pathologies. The data shared in the cloud make possible to have more data and more important provide the same data to define strategies for studies comparison. For that, it is possible to establish a criterion for the acquisition of speech signals from subjects with pathologies. This can be done in innumerable institutions that can disseminate and share this information in the cloud. The Research from this topic always involves multidisciplinary teams and sharing information in the cloud will certainly produce important advances in the automatic diagnostic of voice pathologies.

3 Database

For training and testing the systems the MEEI database [10] was used. It contains 53 healthy subjects and 724 subjects with voice disorders. For these two set of subjects, the sustained vowel /a/ and a continuous speech excerpt, "rainbow passage" are available. Of all subjects with pathologies, only 477 have the information about the pathologie. This work uses the nodules, edema, unilateral vocal folds paralysis pathologies diagnostics and healthy subjects. The signals were recorded with a sampling rate of 25 kHz or 50 kHz. For this work all the files were down sampled to 25 kHz. There are 17 files from healthy subjects from the "rainbow passage" (continuous speech) recorded at 10 kHz that have been removed, resulting in a total of 36 healthy subjects.

For this work, two sets of pathologies were defined. A first set with subjects diagnosed with the physiological disorders edema and nodules. A second set was created with subjects diagnosed with unilateral vocal fold paralysis, a neuromuscular disorder. Each of these sets contains 59 files. A third set have 36 healthy subjects. Table 1 shows the database distribution by gender.

Table 1. Database gender distribution

Pathology	Males	Females	Total
Healthy	14	22	36
Nodules	1	18	19
Vocal Fold Edema	9	31	40
Vocal Fold Unilateral Paralysis	29	30	59

3.1 Nodules

Vocal fold nodules are benign lesions that can occur in both vocal folds, in places where friction is higher. Its location is usually at the junction of the anterior third and the posterior two thirds. When the vocal folds vibrate, impact zones exist and it is precisely in these areas where the lesions that cause nodules appear. This disease is common in people who intensively use their voice, as politicians, teachers, singers and children that often yell. The nodules are small, about the size of a pinhead and can appear over a given area on groups. The main symptoms are dysphonia, with the change in the voice tone, via a variable hoarseness. In extreme cases it may be possible to achieve a complete aphonia. Nodules do not allow complete closure of the vocal folds thus adding noise to the speech signal. To compensate for this effect the subjects tend to increase the tension in the muscle, further increasing collision that forces the vocal folds.

3.2 Vocal Folds Edema

The vocal folds edema increases the volume of the vocal folds. Causal factors are the use and abuse of the voice in which in some cases the subject may suffers from nodules. This pathology can be also due to the use of tobacco or drugs, excessive coughing, menstruation, menopause or pregnancy. The increase in the volume of the vocal folds causes changes in its elasticity with the consequent change in the voice timbre.

3.3 Vocal Folds Paralysis

The vocal folds paralysis is a peripheral neurology disorder. The tension and position of the vocal cords are controlled by the laryngeal muscles, which in turn are controlled by the nervous system. The vocal cord paralysis arises when these muscles cannot perform its function. The paralysis is in the muscle although the vocal folds can continue to vibrate in a not controlled way. The paralysis can be caused by various phenomena, such as compression of muscles due to infections, tumors or intoxications. The paralysis typically affects only one vocal fold. This implies that each fold vibrates at a different frequency. In these cases, the voice has a bimodal sound and the patient cannot speak loudly losing the power of vocal amplification. In this work, only unilateral paralysis is evaluated.

4 Implemented Systems

In this section the systems implementation and the data organization used to perform the tests between the sustained vowel and continuous speech signals are described. In the end results are presented.

As previously mentioned, speech signals used on this study were acquired with a sampling frequencies of 25 kHz or 50 kHz. To normalize the training set, all samples were down sampled to 25 kHz.

The features extracted from the speech signal were MFCC, energy and delta-energy. MFCC coefficients were estimated using filter banks scale 25-mel in 20 ms frames with 10 ms overlap. Several tests were conducted from order 8th to 24th. All the data was normalized with zero mean and unit variance. In the vowel /a/, with a duration between 3 and 5 seconds, all frames are analyzed. In the continuous speech, the silence zones were removed using the endpoint algorithm proposed in [16].

4.1 Dataset Organization

Two classes of pathologies were created: physiological lesions composed of edema in the vocal folds in a total of 59 subjects; and neuromuscular disorder with 59 subjects with unilateral paralysis of vocal folds; a third class with 36 healthy subjects is used.

The systems were trained with 75% of the data and tested with the remaining 25%, resulting in approximately 15 test subjects in classes with pathologies and 8 speakers in the healthy subjects. The k -fold cross-validation method [17] was used. In total 4 systems were created in order to rotate the train and test set and evaluated all data set.

4.2 SVM System

Support Vector Machines (SVM) classifiers are typically used as a two class classifier. In order to have a multiclass classifier, three SVM models were trained. This approach is known as one-against-one [18] and in this technique for N classes $N(N-1)/2$ SVM classifiers are trained. In this case, classifier #1 compares physiological pathologies vs. healthy, classifier #2 computes neuromuscular pathologies vs. healthy and classifier #3 computes physiological pathologies vs. healthy.

The test is done by single frame classification with both classifiers #1 and #2 classifying all frames as healthy/unhealthy. If the percentage of frames classified as healthy by classifier #1 averaged with classifier #2 is higher than 50% the subject is classified as healthy. Otherwise, the subject is classified as unhealthy and the classifier #3 identifies the pathology.

4.3 Gaussians Mixtures Models

Gaussians Mixtures Models (GMM) allows the train of N independent models. These systems had great impact on solutions for speaker recognition [19]. The system implemented for this work consists in one model for each class. Each model is represented by M Gaussian mixtures with covariance diagonal matrix. In this case, it was

found that the best results are obtained with 16 Gaussian mixtures for each class. For each test segment the likelihood is computed in each class and classified in the class that maximizes this value.

4.4 Metrics and Results

As described above, tests with the sustained vowel /a/ and with continuous speech used SVM and GMM classifiers. The systems evaluation was performed by the overall system ACC (accuracy) (1), the class sensitivity TPR (True Positive Rate) (2) and the class precision PPV (Positive Predictive Rate) (3). These measures are computed using the TP (True Positive), FP (False Positive), FN (False Negative) and TN (True Negative) approach. Table 2 and 3 show the obtained results.

$$ACC = (TP + TN) / (TP + TN + FP + FN) \tag{1}$$

$$TPR = TP / (TP + FN) \tag{2}$$

$$PPV = TP / (TP + FP) \tag{3}$$

In general, the system implemented with continuous speech using GMM achieved better results (74% accuracy), as well as best average precision and sensitivity rates (76.2% and 77.9% respectively).

The systems that used the sustained vowel /a/ achieved about 20% in absolute value less precision rate for healthy subjects. These results are particularly important since the unhealthy subjects are not diagnosed with any of the pathologies what can be considered an important disadvantage of these systems.

Continuous speech based systems have typically better results than the vowel /a/ based systems. Only in two instances the results obtained with the sustained vowel are better. In the first case, in table 2, the sensitivity rate in unilateral paralysis using the SVM classifier is 69.4% against 56% for continuous speech. With the GMM classifier the precision rate is 61%. In the second case, the precision for nodules and edema is 66.6% when used the vowel /a/ in the SVM classifier. However, when using continuous speech in the GMM classifier this value is 66.2%, decreasing only 0.4%.

Table 2. SVM system best results for continuous speech and Vowel /a/ in parentheses. ACC: 72% (69%), both systems use MFCC 20th order.

Classification \ Original	Healthy	Nodules and Vocal Fold Edema	Unilateral Paralysis	Sensitivity (TPR)
Healthy	34 (33)	0 (1)	2 (2)	94.4% (91.6%)
Nodules and Vocal Fold Edema	1 (9)	44(32)	14 (18)	74.5% (54.2%)
Unilateral Paralysis	2 (3)	24 (15)	33 (41)	56% (69.4%)
Precision (PPV)	91.8% (73%)	64.7% (66.6%)	67.3% (67.2%)	

Table 3. GMM system best results for continuous speech and Vowel /a/ in parentheses. ACC: 74% (66%), systems use MFCC 12th order for continuous speech and 8th order for the vowel /a/.

Classification \ Original	Healthy	Nodules and Vocal Fold Edema	Unilateral Paralysis	Sensitivity (TPR)
Healthy	33 (30)	3 (2)	0 (4)	91.6% (83.3%)
Nodules and Vocal Fold Edema	1 (10)	45 (32)	13 (17)	76.2% (54.2%)
Unilateral Paralysis	1 (4)	20 (15)	36 (40)	61% (67.7%)
Precision (PPV)	94.2% (68%)	66.2% (65.3%)	73.4% (65.5%)	

5 Conclusions and Future Work

This work presents two voice pathologies identification systems using continuous speech and the sustained vowel /a/. Three classes were created: healthy subjects, subjects diagnosed with vocal fold edema and nodules (physiological disorders) and subjects diagnosed with unilateral vocal folds paralysis (neuromuscular disorder).

The main objective was to compare the performance of voice pathologies identification using continuous speech with the sustained vowel /a/ typically used in these applications. Two classifiers systems were created, using SVM and GMM, both using MFCC parameters as speech signal features. The results showed that continuous speech allows better results for the two systems and that GMM models classifier overcame the SVM classifier. In particular GMM and continuous speech have better precision values in the identification of healthy subjects. However, the sustained vowel /a/ has the best results in the sensitivity for unilateral vocal fold paralysis. Considering this fact, some research in system fusion will be done in the future to verify if, this way, it is possible to improve the overall performance. Continuous speech shows high potential for voice pathologies identification. In the future this performance may be improved using other speech signal features and different classifiers.

There are few studies in pathological voice identification. Different databases and pathologies studied make the comparison with other works inconsistent. For that a cloud sharing database approach certain will bring relevant improvements in this task.

Acknowledgments. The authors would like to thank Prof. Ana Mendes from Polytechnic Institute of Setúbal for sharing the database used in this study and the High Institute of Engineering of Lisbon by the scholarship that allowed the work progress.

References

1. Lieberman, P.: Some acoustic measures of the fundamental periodicity of normal and pathologic larynges. *J. Acoust. Soc. Amer.* **35**, 344–353 (1963)
2. Iwata, S.: Periodicities of pitch perturbations in normal and pathological larynges. *J. Acoust. Soc. Amer.* **45**, 344–353 (1972)

3. Shama, K., Krishna, A., Niranjan Cholayya, N.U.: Study of harmonics-to-noise ratio and critical-band energy spectrum of speech as acoustic indicators of laryngeal and voice pathology. *EURASIP Journal on Advances in Signal Processing* 1 (2007)
4. Cordeiro, H., Fonseca, J., Meneses C.: Spectral Envelope and Periodic Component in Classification Trees for Pathological Voice Diagnostic. In: 36th Annual International Conference of the IEEE Engineering in Medicine and Biology Society (EMBC), pp. 4607–4610 (2014)
5. Dibazar, A., Narayanan S.: A system for automatic detection of pathological speech. In: 36th Asilomar Conf., Signal, Systems & Computers (2002)
6. Fonseca, E.S., Guido, R.C., Scalassara, P.R., Maciel, C.D., Pereira, J.C.: Wavelet time–frequency analysis and least squares support vector machines for the identification of voice disorders. *Comput. Biol. Med.* **37**, 571–578 (2006)
7. Sáenz-Lechón, N., Godino-Llorente, J.I., Osma-Ruiz, V., Gómez-Vilda, P.: Methodological issues in the development of automatic systems for voice pathology detection. *Biomedical Signal Processing and Control* 1, 120–128 (2006)
8. Scalassara, P.R., Dajer, M.E., Maciel, C.D., Guido, R.C., Pereira, J.C.: Relative entropy measures applied to healthy and pathological voice characterization. *Applied Mathematics and Computation* **207**, 95–108 (2009)
9. Markaki M., Stylianou Y.: Using modulation spectra for voice pathology detection and classification. In: Proc. IEEE EMBC 2009, Minneapolis, pp. 2514–2517 (2009)
10. Key Elemetrics, Elemetrics Disordered Voice Database (1994)
11. Markaki, M., Stylianou, Y.: Voice Pathology Detection and Discrimination Based on Modulation Spectral Features. *IEEE Transactions on Audio, Speech, and Language Processing* **19**, 1938–1948 (2011)
12. Muhammad, G., Alsulaiman, M., Mahmood, A., Ali, Z.: Automatic voice disorder classification using vowel formants. In: IEEE Int. Conf. Multimedia and Expo (ICME) (2011)
13. Fonseca, E.S., Pereira, J.C.: Normal versus pathological voice signals. *IEEE Engineering in Medicine and Biology Magazine* **28**, 44–48 (2009)
14. Carvalho, R.T.S., Cavalcante, C.C., Cortez, P.C.: Wavelet transform and artificial neural networks applied to voice disorders identification. In: Third World Congress on Nature and Biologically Inspired Computing (NaBIC), pp. 371–376 (2011)
15. Cordeiro, H., Fonseca, J., Meneses, C.: Edema and Nodules Identification in vowels using spectral features and jitter. In: CETC 2013, Conference on Electronics, Telecommunications and Computers, Procedia Technology, vol. 17, pp. 202–208 (2014)
16. Lamel, L., Rabiner, L., Rosenberg, A., Wilpon, J.: An Improved Endpoint Detector for Isolated Word Recognition. *IEEE Transactions on Acoustics, Speech, and Signal Processing* **29**, 777–785 (1981)
17. Kohavi, R.: A study of cross-validation and bootstrap for accuracy estimation and model selection. *IJCAI* 14 (1995)
18. Chih-Wei, H., Chih-Jen, L.: A comparison of methods for multiclass support vector machines. *IEEE Transactions on Neural Networks* **13**, 415–425 (2002)
19. Reynolds, D.: Speaker identification and verification using Gaussian mixture speaker models. *Speech Communications* **17**, 91–108 (1995)

3D Human Scanning Solution for Medical Measurements

Balázs Sütő^{1(✉)}, Zsolt Könnyű¹, Zsolt Tölgyesi¹, Tibor Skala³,
Imre Rudas⁴, and Miklos Kozlovsky^{1,2}

¹ Biotech Laboratory, Óbuda University, Bécsi út 96/b, Budapest 1034, Hungary
{suto.balazs, konnyu.zsolt, tolgyesi.zsolt}@biotech.uni-obuda.hu,
kozlovsky.miklos@nik.uni-obuda.hu

² MTA SZTAKI, Pf. 63, Budapest H-1518, Hungary

³ Faculty of Graphic Arts, Zagreb, Croatia
tibor.skala@gmail.com

⁴ Óbuda University, Bécsi út 96/b, Budapest 1034, Hungary
rudas@uni-obuda.hu

Abstract. Today anthropometry can be performed with three-dimensional scanners. Our aim is to establish a low-cost, easy-to-use hardware and software solution, which is capable to do automatic, computer-based anthropometry and medical measurements for health care. We have designed and build a large, remote controlled turntable and a 3D scanner application, which can be used to digitalize 0.2-2,6 m tall real world objects into 3D models. With the turntable a 360° field of view can be reached even when using completely stationary, static sensors. Our software uses RGBD sensors for data acquisition, however it can be combined with other image sensors. With our solution prosthesis design can be more accurate and simplified, and we can provide for 3D modelers an efficient, real time method to scan and visualize human scale 3D objects. The scanned models can easily be used for rapid prototyping and 3D printing. The models can be exported into the most popular 3D modeling file formats for further analysis. Our solution decreases significantly the time, effort and cost of the clean up process of the 3D scanning. In this paper we provide information about our 3D scanning solution's design, and implementation, and we also describe its accuracy. The realized hardware and software solution provides a cheap and sufficiently reliable method to gather real time 3D depth and RGB data from human size objects for 3D reconstruction.

Keywords: 3D reconstruction · RGBD · 3D human scanning

1 Introduction

Today anthropometrical data is used in a great variety of projects. Examples include designing [1], somatotyping [2] and face measurement [3]. Traditionally data were collected using measure tapes and other measurement tools which was a physically exhausting task both for the subjects and for the staff. Since taking the measurements required physical contact with the subjects, obtaining data from many different geo-

graphical locations posed a problem and prolonged project time. With the appearance of 3D anthropometry these issues were solved but due to the additional hardware the cost of the projects increased significantly. Thanks to the popularity and evolution of RGBD sensors now they provide a cheap and reliable marker-less solution for 3D scanning. The scanned body models generated by 3D surface reconstruction based technologies can be used for anthropometrical data collection. The goal of our project is the design and development of a 3D anthropometrical scanner system which can be used to scan human bodies for medical purposes. The proposed solution must have a low implementation cost. The scanner system must support dynamic and static camera settings, therefore scanning with a moving and a fixed camera must both be possible. Initial versions of the scanner application have to be compatible with the Kinect for Windows V1 and V2 sensors while later versions should also support other RGBD cameras. To create a technology independent software an application layer which hides the differences between the mentioned frameworks must be developed.

2 Relationship to Cloud-Based Solutions

Data clouds can be used to store anthropometrical data and models collected by our software. By uploading the data to the cloud we are able to create a global database and share the data among a large group of users. A cloud-based database also enables the users to access the models and measurements without regard to their physical location.

The data cloud solves the problem of managing geographically distributed work. Due to the low priced nature of the solution, building huge networks with globally distributed measuring sites becomes a possibility.

3 Description of a Problem Solution

Our proposed solution for the problem is an anthropometrical scanner system based on a self-developed 3D body scanner application and an electronic hardware turntable.

Among the state of art algorithms we considered choosing the ICP algorithm due to its impressive speed, robustness and popularity. We selected two framework libraries which implement ICP, Kinect Fusion and the Point Cloud Library, because after some research they seemed to be the most suitable implementations to meet our goals.

The current version of our program uses the aforementioned frameworks, their data structures and algorithm implementations, but the whole process of 3D reconstruction can only be completed by using Kinect Fusion. The application builds a volumetric model from the RGB and depth data acquired from the sensor by integrating them into the model as sequence of frames. The model can be visualized in 2D using ray casting. Our program performs a 3D surface-reconstruction on the model, creating a triangle based polygon mesh, which can be exported into ply, stl or obj file formats. The RGB and depth frames can be saved with their associated camera pose and imported into Blender using a Blender script to create an UV mapped model.

Our system supports dynamic and static camera settings. To create a technology independent software we developed an application layer that hides the differences between the mentioned frameworks.

To automatize the scanning process we created an Arduino based scan turntable. The turntable can be accessed and controlled from the application by setting up a virtual COM port. By using the turntable, 360° scanning of objects becomes possible without actually moving the sensor around. Thanks to this possibility the scan process can be made more comfortable, faster and the number of possible errors due to manual scanning can be reduced.

It is also possible to use multiple stationary RGBD sensors for scanning [4], however this results in increased computation time and hardware costs. If this approach is used the sensors must be well placed around the subject so while providing the 360° FOV they would not interfere with each other. Compared to the turntable based method this solution is less mobile because if the scanning hardware are moved, the cameras always need to be recalibrated before scanning.

The application uses multiple threads, and is capable of vertex-color based color reconstruction. UV mapping and Infra camera support are currently in development. In later versions we would like to make other RGBD sensors compatible with our software. The 360° angle of view could also be provided by using multiple sensors.

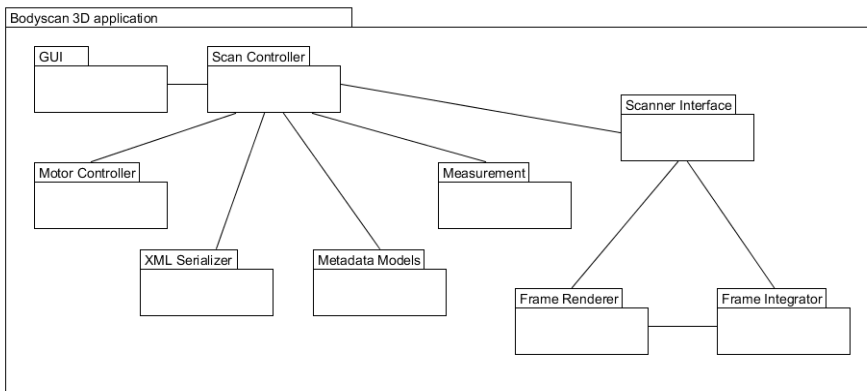


Fig. 1. The architecture of our application solution

The application itself consists of a modular backend and user friendly GUI. The backend supports the most popular 3D scanner software frameworks (Kinect Fusion [5], Point Cloud Library [6]) and a variety of 3D RGBD cameras. The aforementioned libraries provide the essential data types and algorithms for data acquisition and 3D surface reconstruction of 3D objects. Modularity means that in addition to being able to fine-tune the scanning settings, like the camera resolutions and properties of the 3D model, the data acquisition, data types, 3D modeling and reconstruction algorithms can also be changed if needed, to provide a highly customizable software.



Fig. 2. The Arduino based scan turntable designed and constructed at Biotech Laboratory for 3D body scanning

By using an additional HD camera it is also possible to obtain high definition RGB data for the scene which can be integrated into the 3D model by utilizing UV mapping to provide high definition textures. These HD textures can be stored with the exported surface-reconstructed body model and can later be used for a variety of medical purposes like automatic skin cancer detection. This technology is currently being implemented using Blender scripts.

The algorithm for projecting the HD texture on the 3D mesh:

1. Running a retopology script to normalize the mesh
2. Unwrapping of the mesh and generation of the UV map. This provides the coordinate mapping which transforms the acquired RGB values into the coordinate system of the mesh.
3. Iterating the camera poses (Each pose has an attached RGB frame.)
4. Using the 3D mesh to separate irrelevant data of the RGB frame, eroding it and applying a filter at the edge of the relevant area to prevent overlaps at the projecting process
5. Projecting the RGB data on the texture in the created UV system from every camera position.

4 Results

For testing we first measured certain body proportions of our test subjects like neck, hip and waist size by hand using a tape measure. After the scanning finished we exported the models from our software and measured the same proportions on the captured models using Meshlab. In the predefined scan space we managed to scan people in relatively good quality using a low-end desktop PC. By utilizing the maximum scanning precision and resolution of the Kinect sensor and choosing the correct parameters for the scan the errors of the scan were under 0.8 cm-s in all cases.

During testing we used a volumetric model constructed from $512 \times 512 \times 512$ voxels and a model resolution of 256 voxels/meter. Using the same settings on a high-end desktop PC we were able to process 30 depth frames/second allowing real-time reconstruction. We also tested different indoor lighting and camera setups, including stationary and dynamically moving Kinect sensors. While we found the reconstruction algorithms to be more robust by using a stationary sensor and the turntable, illumination only affected the quality of the RGB colors and captured textures, but not the quality of the mesh models.



Fig. 3. 3D scanned mesh model of man with a crutch

5 Conclusions and Future Work

While the RGBD based technologies and methods cannot produce the same quality models as other approaches, they provide an affordable alternative. From the list of currently available RGBD hardware sensors we chose the two versions of the Microsoft Kinect sensor due to their high compatibility rating with other systems. Compared to other RGBD devices the Microsoft Kinect is relatively cheap and reliable. After normalization it can provide the necessary precision for 3D body scanning.

The Arduino [7] based scan turntable in coordination with the well-placed RGBD sensors provide the 360° FOV which is necessary to scan the whole human body. The rotation speed and direction can be controlled from the scanner application. While it is also possible to scan without using the turntable, in that case the comfort and reliability of the scan process is reduced. Currently our system is fully compatible with the

Kinect for Windows V1 and V2 sensors and uses a single camera for RGBD data acquisition, but we have plans for using additional cameras in the future.

During testing using the aforementioned devices and technologies we managed to scan 3D human bodies, and we found that errors of the scan were always below 0.8 cm-s. Color and colorless reconstruction were also tested. While minor movement errors were mostly mitigated by the ICP algorithm, generally the subject had to stand still during the whole scanning process. This was due to the limitations of the ICP and Kinect Fusion based real-time scanning approach. [5]

In the future intelligent marker management could be used to increase tracking and reconstruction precision and performance. We are also planning to extend sensor compatibility to other RGBD devices and making a variety of medical sensors compatible with our system to increase sensor modality.

References

1. Niu, J., Li, Z.: Using Three-Dimensional (3D) Anthropometric Data in Design. In: Handbook of Anthropometry, V. R. Preedy, pp. 3001–3013. Springer, New York (2012)
2. Olds, T., Daniell, N., Petkov, J., David Stewart, A.: Somatotyping using 3D anthropometry: a cluster analysis., UniSA, Health Sciences, GPO Box 2471, Adelaide 5001, Australia tim.olds@unisa.edu.au
3. Loconsole, C., Barbosa, N., Frisoli, A., Costa Orvalho, V.: A New Marker-Less 3D Kinect-Based System for Facial Anthropometric Measurements. In: Perales, F.J., Fisher, R.B., Moeslund, T.B. (eds.) AMDO 2012. LNCS, vol. 7378, pp. 124–133. Springer, Heidelberg (2012)
4. Robinson, M., Parkinson, M.: Estimating Anthropometry with Microsoft Kinect. In: Digital Human Modeling Symposium (2013)
5. Izadi, S., Kim, D., Hilliges, O., Molyneaux, D., Newcombe, R., Kohli, P., Shotton, J., Hodges, S., Freeman, D., Davison, A., Fitzgibbon, A.: KinectFusion: Real-time 3D Reconstruction and Interaction Using a Moving Depth Camera. In: Proceedings of the 24th Annual ACM Symposium on User Interface Software and Technology, New York, NY, USA (2011)
6. Rusu, R.B., Cousins, S.: 3D is here: Point Cloud Library (PCL). In: IEEE International Conference on Robotics and Automation (ICRA), Shanghai, China (2011)
7. Arduino Uno. <http://arduino.cc/en/Main/ArduinoBoardUno>

Semi-Automated Quantitative Validation Tool for Medical Image Processing Algorithm Development

Viktor Zoltan Jonas^{1(✉)}, Miklos Kozlovsky^{2,3}, and Bela Molnar⁴

¹ Doctoral School of Applied Informatics, Óbuda University, Budapest, Hungary
viktor.jonas@3dhistech.com

² Biotech Knowledge Center, Óbuda University, Budapest, Hungary

³ MTA SZTAKI/Laboratory of Parallel and Distributed Computing,
Victor H. str. 18-22., Budapest H-1518, Hungary
kozlovsky.miklos@nik.uni-obuda.hu

⁴ Second Department of Internal Medicine, Semmelweis University, Budapest, Hungary
bela.molnar@3dhistech.com

Abstract. Cancer research and diagnostics is an important frontier to apply the power of computers. Researchers use image processing techniques for a few years now, but diagnostics only start to explore its possibilities. Pathologists specialized in this area usually diagnose by visual inspection, typically through a microscope, or more recently on a computer screen. They examine at tissue specimen or a sample consisting of a population cells extracted from it. The latter area is the area of cytometry that researchers started to support by creating image processing algorithms. The validation of an image processing approach like that is an expensive task both financially and time-wise. This paper aims to show a semi-automatized method to simplify this task, by reducing the amount of human interaction necessary.

Keywords: Validation tool · Automated validation · Medical image processing

1 Introduction

The project [1] we are currently participating in aims to reproduce a medical research and diagnostic method called ploidy analysis (PA) through image processing means. PA is a method to measure DNA content in cell nuclei as a basic cancer marker, and is considered as a segment of pathology, more closely image cytometry (ICM). In diagnostics PA is usually done by a machine called Flow Cytometer (and the family of assessments related to it flow cytometry (FCM)), an appliance that operates with a light beam directed at a transparent capillary, where objects are traveling in sheath fluid, facilitating laminar flow. The objects are measured through their optical properties like light scattering, but the result is more one-dimensional measurement functions of time. Image cytometry takes a different approach. Digital pathology is in the process of introduction into medical diagnostics. This new approach is based on the idea of taking traditional glass slide specimen to the computer screen through digitalization. This enables experts to use the monitor to evaluate the samples, and

also use software tools to achieve the task. Expectations are that this approach enhances objectivity reproducibility and traceability of forming diagnoses. Image cytometry is the sub-field where the software tools are used to process the digitized sample, enabling its users to analyze vastly more objects than the traditional visual-manual method using microscopes for inspection and clickers for counting. The project we are working on aims to reproduce a flow cytometry analysis by image processing means [2][3]. Is the ICM approach viable as a diagnostic approach? This is a twofold question in itself: is it possible, and is it capable of sufficient throughput (equivalent of FCM)? The hypothesis of course is that it is possible, but measurements have to be taken to confirm.

A crucial part in applying (image processing) algorithms in forming medical diagnoses, is validation. There are two possible routes: validation by comparison to a validated approach (in this case FCM result), or the method used for validating FCM in the first place: clinical a study. The clinical study approach was chosen to eliminate the inherent error accumulation, and the simpler procedure regarding laboratory access and overall expenses in human work. This approach is semi-automatic in the sense of needing manual input for the quantitative validation in the form of the planar coordinates of the reference objects. The novelty in our approach is to decrease the human interaction as much as possible. To achieve this validation process was separated into two steps, only the first needing direct expert interaction: marking the objects to detect on the sample. Something similar was done traditionally: using a clicker counter, while examining the sample with a microscope. This we named the quantitative part. It is possible to add a qualitative part that relies on the result of a quantitatively sound detection as reference, for measuring object detection quality.

This paper aims to present an algorithmic tool for first approach validation of the image cytometry algorithm described, and possibly other image segmentation projects. The tool is constructed to be also useful in image processing algorithm development, by enabling continuous comparison to results of pervious variants.

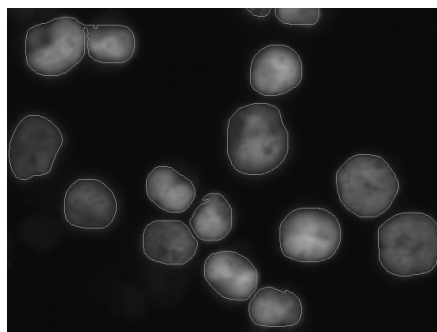


Fig. 1. Sample area with segmentation mask. On the top-left a merged pair of nuclei is visible. On the bottom left area a few (very) low-intensity objects are located.

2 Benefits from Cloud-Based Engineering Systems

The image processing of medical images regarding small objects usually entail tiled image processing. This, in itself is a problem that scales well in parallel processing. Comparing or validating the results of an above mentioned algorithm can also be organized for highly parallel processing. More importantly considering the amount of samples to analyze in a pathology lab (that are usually highly centralized facilities), that should be done more quickly, than manual/visual inspection of the sample, to have relevance in diagnostics. A glass slide has the useful area of roughly 15x25mm. The optics in the hardware our project used for sample digitization enables $\sim 0.2\mu\text{m}/\text{pixel}$ resolution. This means a bit more than 9GB of image data for each image channel. (Naturally for storage it can be compressed, but processing usually uses the uncompressed, full magnification data.) Though our project uses single channel images, but a medium sized diagnostic lab works with a few hundreds of these samples a day [4].

Recent papers discuss the role of cloud in medical image processing like [5]. Considering the amount of data accumulated in digitized glass slides the storage advantages of clouds seems also an option to explore. Creating the required storage capacity, the security issues and the problem of maintaining these may be easily solved through cloud. Taking a step back another dimension of clouds can also be valuable for this area and that is the consultation over medical cases, the possibility to easily share and inspect samples, or even cases (sets of samples corresponding to a patient) are already feasible, but with pre-cloud techniques his can be solved only in a less than ideal manner.

3 Related Literature

There is extensive literature on the evaluation of image segmentation quality and validation. We started with an earlier work in mind; that work was a case study of a clinical validation [6]. The categorizing approach of [7] was of great help to widen our field of view in this area. And other works like [8], which used the same supervised approach as we planned, were of great help to select the depth and scope of this paper.

4 Discussion

Image processing projects usually encounter at least two types of demand considering validation/comparison. One is the actual validation of the segmentation algorithm or the software solution, where segmentation result usually has to be compared to human “segmentation” results (as in a clinical study – supervised approach). The other case is during the development of the algorithm that compares the algorithm to its previous version or to a completely different approach to confirm or measure the change or difference, to be able to rank them, and improve the best one further. Accordingly the

proposed software application is constructed to compare two measurements. This enables us to consider it as an ordering relation of some sort between image processing algorithms and also as a validation tool, when comparing human validation as reference input. The analysis tries to find corresponding object pairs (or n-tuples) from both measurements (reference and the currently tested), compare them, and register their relation using result/error classes.

4.1 Data

A measurement to compare can be considered an array of records containing all measured morphometrical and colorimetric properties of each detected object (cell nucleus in the case of the actual study). This paper focuses on reproducing the process of a manual validation project, only the morphology and location information is analyzed, though a simple check is conducted on other properties of the measured objects for enabling automatic discovery of unanticipated changes. Samples of human blood (lymphocyte nuclei) were used in this case. A 1 mm² area was analyzed on each of the 17 digital slides. The images processed were 0.1625µm/per pixel resolution compressed (jpeg 80). This means roughly 6150*6150 pixels on each sample.

4.2 Analysis

The simplest case is when object shapes (as polygons) match, and also all their measured (non-geometrical) parameters match. (For optimization purposes all shape comparison is preceded by the comparison of their bounding boxes, to ensure quicker analysis.) This group is labelled *Perfect match*. If the criterion for parameters fails the cluster is labelled *Parameter mismatch*. These two groups are most significant in synthetic tests, where objects with known geometry are segmented and analyzed. It can also be helpful during algorithm development to detect unwanted changes in segmentation or parameter measurement, as a step of automated testing protocol. This is why these two cases are handled separately, if at the end of this step all objects are accounted for, the analysis is over, if not, the remaining are passed to the next stage of the test.

		Reference objects							Σ
		1	2	3	4	5	...	n	
Measurement objects	1	x							1
	2		x	x					2
	3				x				1
	4					x			1
	5								0
	6						x		1

m									
Σ		1	1	1	2	1	...		

Fig. 2. Illustration of the relation matrix. Rows represent the items of the gold standard, columns contain the elements of the compared measurement. X-es designate objects where overlap is possible.

This next stage leverages the idea of neighborhood matrices and object overlap. Both measurements are assigned to a dimension of the matrix, and relations are recorded to the cell addressed by the two interacting detected objects. If their bounding boxes intersect, and also the actual shapes intersect the interaction is marked in the corresponding matrix cell as a binary flag (as visible in Fig. 2). Shape overlap is detected by simply rendering the two objects to the same image additionally, and counting overlapping pixels. Intersecting ratio is defined as the intersection area over the area of the object with greater area. When this matrix is populated a simple analysis is conducted. For simplicity name the horizontal dimension reference and the vertical the measurement. Also generate column and row sums for the matrix.

1:0 and 0:1 Object Relation

These cases can be found by collecting entries, where either the column sum or the row sum equals to zero. When there is a reference object that has no corresponding measurement object it is marked as *false negative*. The complementary case is labelled *false positive* (measurement for no reference). These objects are registered, and removed from the matrix.

1:1 Object Relation

Where the column and the row sum is also equals to one means that to the reference object only one measurement object is assigned, and also to that measurement object corresponds only (this) one reference object. These objects are further grouped into two classes. Where the centroid of the objects is on the same location the object pair is labelled as *match*, where the centroid locations differ, the label assigned is *shifted*. (In our case instead of centroid simply the center of the bounding box was used.) A shifted (or not perfect) match can be observed on Fig. 3.



Fig. 3. Reference marker and detected object overlap test. Manually placed “reference” position marker on the left, segmented object mask on the right.

This classification may later be used for a few purposes:

When a measurement is run only on a smaller sub-area of the reference area, there is difference in coordinate systems of the two samples, but otherwise comparing two identical measurements. Similarly if the tissue sample is digitized twice, similar difference may be observed. A new digitization process may assign a new coordinate system for the digital sample, or the tiling can change the coordinate system locally, because of mechanical or parametric differences of the two attempts.

Naturally these analyzed pairs of objects are also removed from the matrix.

1:n and n:1 Object Relation

In the remaining set of objects where the column sum equals one (and the row sum is greater than one, otherwise it would have been processed earlier) is the class of *Merged*, meaning more reference objects to a single measurement object. Conversely where only row sum equals one is labelled *Split*, assigned to the case where to one reference there are multiple measurement objects.



Fig. 4. A segmentation object containing two markers. Image processing “merged” the two nuclei into one segmented object.

All remaining cases are labelled as *Residuum*. (n:m relations are not desirable in this setting, found no purpose in further analyzing them.)

For the validation of the above described method the results of the previously published manual assays were used. To be able to compare these results the result classes of the two methods have to be arbitrated. The resulting classification results are visible in **Table 1**.

Table 1. Results of the manual and the automatic assay. Reference column designates the count of nuclei the expert marked. FP (false positive), FN (false negative), Match and Other columns contain the count of objects in the named cluster.

Reference	Human rating				Algorithmic rating			
	FP	FN	Match	Other	FP	FN	Match	Other
1508	34	253	1223	24	30	264	1213	17
1937	41	450	1411	66	43	453	1401	46
1301	68	243	977	71	67	238	1001	26
1766	38	348	1381	32	47	464	912	97
1674	48	347	1257	61	44	345	1238	48
2040	19	434	1535	59	20	437	1514	47
977	51	115	850	12	51	123	829	19
1586	29	305	1242	32	27	312	1235	22
1259	32	170	1075	8	31	180	1065	8
2175	28	479	1606	81	24	482	1584	55
1677	20	383	1245	42	19	382	1224	36
1524	23	423	983	111	22	425	973	64
2175	40	551	1559	53	38	548	1535	47
2110	16	528	1512	64	10	532	1503	40
1776	32	413	1275	80	22	412	1246	64
1957	11	547	1352	47	170	361	1016	11
831	61	107	706	18	61	110	703	10

Definition of the Evaluation Classes

Match: reference marker corresponds with exactly one measurement. In the proposed method the “Match” and “Shifted” classes, and also the half of the count of the “Split” class¹

False positive: there is a measurement, but no corresponding reference object. Same in the proposed method and the other half of the “Split” class¹

False negative: to a reference there is no measurement object. Same in the proposed method

Other: all other cases, usually where one measurement corresponds to more reference objects. Merged, Residuum classes

The result classes of the assays can be considered categorical variables, the manual results as expected and the algorithmic results as measured values. The Chi-square goodness of fit test is used to confirm that the proportions the algorithm produced do not differ significantly from the ones the manual assay states.

The test was conducted using the significance level of 95% ($p = 0.05$). The column **h** in Table 2 contains whether the above null hypothesis stands, column **p_t** contains the p-value needed to reject the null hypothesis at the actual significance level.

Table 2. The result of the Chi-square goodness of fit test of concordance between the human and the algorithmic rating. Sample ID designates the glass slide containing the cell nuclei; the other columns contain the results of the statistical test.

sample ID	χ^2	p.	h	sample ID	χ^2	p.	h
1M01	1.7038	0.7900	1	1M13	5.1632	0.2710	1
1M02	3.5843	0.4652	1	1M14	0.5417	0.9693	1
1M03	21.0897	3.0e-04	0	1M15	12.1855	0.0160	0
1M04	731.7800	0	0	1M16	0.4652	0.9768	1
1M05	1.6605	0.7979	1	1M17	6.8198	0.1457	1
1M06	1.4359	0.8379	1	1M18	3.5227	0.4744	1
1M10	2.1032	0.7168	1	1M19	227.0211	0	0
1M11	1.9999	0.7358	1	1M20	2.3150	0.6780	1
1M12	0.3481	0.9865	1				

5 Conclusion

The results of the proposed comparator algorithm mostly concur with the results of the manual assay. In case of four samples the results seem to differ significantly. Further investigation is needed to uncover the cause in those cases. This may enable faster, more objective comparison of image segmentation. Being able to compare measurements in the magnitude of a few tens of thousands of objects automatically adds the possibility for some additional testing of similar image segmentation algorithms.

¹ In the manual assay the rule of thumb given to the expert was to mark the best fitting segmentation result as a Match all others as false positives.

A few weaknesses were discovered. Comparison processing time grows quickly with the number of measured objects. Analysis speed is inherently at least $O(n^2)$ because of the interaction-matrix. If the processing algorithm in itself is tile processing based (as in the case of our project), comparing the result subsets tile-wise seems a viable solution. In other cases by using spatial ordering of both the reference and the measurement is possible (like the storage or indexing the measurement in a quad tree manner), thus being able to construct interaction matrices for objects that possibly overlap in a distributed (and also quicker than $O(n^2)$) manner.

Comparison of larger objects is not efficient or even not possible; rendering them on single images in memory may not be an option. Overlap calculation in their case should be implemented by an entirely different approach.

The separate step of detecting complete matches and geometric matches for testing purposes makes this twice as slow, the two “modes” should probably be used separately, mode chosen explicitly. To add a module with the possibility of supplying image masks and/or text files with a strictly set format as comparison input is also our future goal. This is necessary to be able to use the tool more generally or in other projects. Extending the comparison capabilities to the level of detail of the segmented objects’ level is also a possibility.

References

1. Jonas, V.Z., Kozlovsky, M., Molnar, B.: Ploidy Analysis on Digital Slides. In: IEEE 14th International Symposium on Computational Intelligence and Informatics (CINTI 2013), Hungary, pp. 287–290 (2013). ISBN 978-1-4799-0194-4, doi:10.1109/CINTI.2013.6705207
2. Jonas, V.Z., Kozlovsky, M., Molnar, B.: Nucleus detection on propidium iodide stained digital slides. In: IEEE 9th International Symposium on Applied Computational Intelligence and Informatics (SACI 2014), Timisoara, Romania, pp. 139–143 (2014). doi:10.1109/SACI.2014.6840051
3. Jonas, V.Z., Kozlovsky, M., Molnar, B.: Separation enhanced nucleus detection on propidium iodide stained digital slides. In: IEEE 18th International Conference on Intelligent Engineering Systems (INES 2014), Tihany, Hungary, pp. 157–161 (2014). doi:10.1109/INES.2014.6909360
4. Stathonikos, N., Veta, M., Huisman, A., van Diest, P.J.: Going fully digital: Perspective of a Dutch academic pathology lab. *Journal of Pathology Informatics* (2013). doi:10.4103/2153-3539.114206
5. Kagadis, G.C., Kloukinas, C., Moore, K., Philbin, J., Papadimitroulas, P., Alexakos, C., Nagy, P.G., Visvikis, D., Hendee, W.R.: Cloud computing in medical imaging. *Medical Physics* 40 (2013). doi:10.1118/1.4811272
6. Krecsak, L., Micsik, T., Kiszler, G., Krenacs, T., Szabo, D., Jonas, V., Csaszar, G., Czuni, L., Gurzo, P., Ficsor, L., Molnar, B.: Technical note on the validation of a semi-automated image analysis software application for estrogen and progesterone receptor detection in breast cancer. *Diagnostic Pathology* 6, 6 (2011). doi:10.1186/1746-1596-6-6
7. Zhang, H., Fritts, J.E., Goldman, S.A.: Image segmentation evaluation: A survey of unsupervised methods. *Computer Vision and Image Understanding (CVIU)* 110(2), 260–280, (2008)
8. Ledig, C., Shi, W., Bai, W., Rueckert, D.: The IEEE Conference on Computer Vision and Pattern Recognition (CVPR), pp. 3065—3072 (2014)

High Resolution Digital Tissue Image Processing Using Texture Image Databases

Gábor Kiss¹(✉), Orsolya Eszter Cseri¹, Ádám Altsach¹,
István Imre Bándi¹, Levente Kovács¹, and Miklos Kozlovszky^{1,2}

¹ Óbuda University/Biotech Knowledge Center, Budapest, Hungary
{kiss.gabor, cseri.eszter, altsach.adam, bandi.istvan,
kovacs.levente, kozlovszky.miklos}@nik.uni-obuda.hu

² MTA SZTAKI/Laboratory of Parallel and Distributed Computing, Budapest, Hungary

Abstract. Texture based image databases integrated with effective searching algorithms are useful solutions for many scientific and industrial purposes. Medical image processing of high resolution tissue images is one of the areas, where the cell/tissue classification can rely on such solutions. In this paper we are describing the design, development and usage of a specialized medical texture image database. Our primary aim with this texture database is to provide Digital Imaging and Communication in Medicine (DICOM) compatible texture image dataset for cell, gland and epithelium classification in histology. Our solution includes a Picture Archiving and Communication System (PACS) subsystem, which is mainly provide a communication interface (texture image searching and retrieval) and enables image processing algorithms to work more effectively on high resolution tissue slide images. In this paper we describe how our Local Binary Pattern (LBP) based algorithm benefits texture database usage when solving image processing problems in histology and histopathology.

Keywords: PACS · DICOM · LBP · Texture based image database · Medical image processing · Digital microscopy

1 Introduction

With the development of high resolution scanning and informatics, the practitioner's workflow has changed, and high resolution digital microscopy becomes possible. Slide sharing, in digital world is just easy as forwarding images via Internet, also visualization and archiving the images become simple tasks. Unfortunately, the migration into digital world did not solve all problems, and slide assessment tasks still remain complex and time consuming in the workflow. Practitioners - independently of whether they use traditional methods or new digital slides-, are sharing the same level of difficulties to do cancer grading and determine efficient treatments. In many countries (due to the large amount of samples) patients are waiting in long queues for their diagnosis result. Such waiting queues need to be avoided, because during waiting time, health problems may get worse.

2 State of the Art

We have done a market screening of the available high resolution digital microscopy image assessment software solutions. Our evaluated systems were the followings: the TissuemorphDP [1] image analyzer from Visiopharm, which is designed mainly for the population of nuclei examination, HER2-CONNECT [2] targeting tumor cells detection, Virtuoso, DeveloperXD [3] and the MediaCybernetics [4] doing image of tissue analysis.

We have examined also some image databases namely: ASH Imagebank [13], Image After [14], TinEye [15], RevIMG [16]. The ASH Imagebank is a hematology database with key word search. ImageAfter is a texture based approach with the string-based search method. Finally TinEye and RevIMG are Content Based Image Retrieval systems (CBIR). All the examined systems support only full size images instead of plain texture images.

MorphCheck is our medical image analysis platform working on high resolution digital microscopy images. It enables the load of high resolution tissue images, automatically detects the basic structures of tissue (nuclei, glands, surface epithelium) and provides quantitative and qualitative parameter measurements. Recently we have added texture based image analysis to improve its object recognition accuracy. The users can do texture-base search and object recognition without manual selection.

Most of the image acquisition modalities are using the DICOM standard combined with PACS. We also have enabled the support of a DICOM/PACS based medical database system [5] in our system. DICOM and PACS technologies guarantee the standard storage for medical images and the software makes the additional extension of its abilities later. PACS server is being used by virtual servers in a cloud. We are using IaaS (Infrastructure as a Service), because we can scale to any amount of computer resources dynamically based on usage and other parameters. The scaling process is supported by the EC2 compatible cloud middleware.

The system measures a large number of morphological parameters on the detected image objects and store them in the database, all higher level analysis and decision is based on the archived database parameters. Image processing and classification tasks demand high computing capacity, thus the algorithms are able to run on various hardware architectures and support GPUs to enable higher performance [6], [7]. Our aim is to increase the efficiency of the software with new texture-based approaching.

3 Architecture

MorphCheck consists of two well separable parts. One of these parts is the plain algorithmic methods working on processing and detection. The other part is using the texture-based approach doing the image processing tasks (shown in Fig. 1.) The user may define workflows and freely use a combination of both parts of the image processing methods. A workflow contains tasks (e.g.: texture based and classifier algorithms) and can be arbitrary complex. The system also supports manual image annotation, where the pathologist makes the annotation of the tissue sample and uploads it into the database. The annotated images will be stored in the PACS system, and algorithms can reuse later on their data during classification processes.

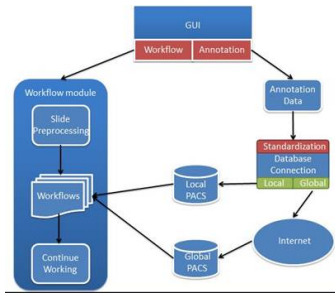


Fig. 1. High-level system architecture of MorphCheck

4 Texture Based Search Algorithm

Our implemented LBP algorithm is based on the Local Binary Pattern [9] (shown in Fig. 2. and Eq.1). The value of LBP code of a pixel is given by:

$$s(x) = \begin{cases} 1, & \text{if } x \geq 0; \\ 0, & \text{otherwise} \end{cases} \tag{1}$$

Fig. 2. part A shows a sample image with intensity pixels and the center pixel is being marked by blue color. Fig. 2. part B shows the differences between each pixels and the marked center pixel, and the differences are being written to the place of the original pixel. For example: The center pixel is 70 and the top left pixel is 47. The difference is -23, and it is written to the top left pixel place at the part B of the Figure 2. The last calculation is being based by Eq.1. Take each pixel on B image and if the current pixel greater than or equal 0, at C image the same pixel will be marked as 1. Otherwise it will be written 0. Finally the LBP code can be read by the clockwise direction.

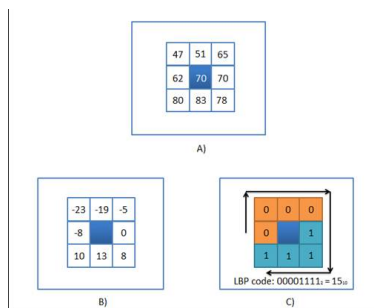


Fig. 2. Local Binary Pattern. A) Sample intensity pixels with center pixel, B) Differences from center pixel, C) LBP code in binary number and decimal system.

The task is to separate and classify the natural textures on the images. The input of the algorithm is the area where the examination happens, and those classes should be later identified on images (more pictures may belong to one class).

At first the Simple Linear Iterative Clustering (SLIC) algorithm slices images into pieces of texture [10], [11]. In the SLIC algorithm it is necessary to set two parameters: the size of the superpixel and how uniform it should be. The second parameter means how homogenous the colors should be in the superpixel. At high parameters we get inhomogeneous, compact and not random size superpixels (shown in Fig. 3.).

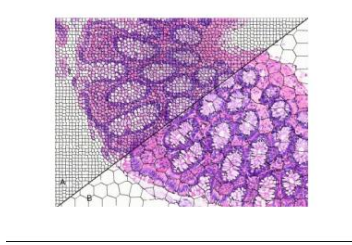


Fig. 3. A high resolution tissue image split into superpixels

After these steps we examine all superpixel in terms of belong in to a class. This process happens to the help of two parameters: Simple histogram and rotation invariant Local Binary Pattern histogram. With both parameters we calculate distance measure for all images. For the case of histogram we calculate the difference with the Earth Mover's Distance [4] metric. In the case of the LBP histogram we calculate the absolute difference of both histograms. Based on LBP to all superpixel we calculate a classification, after that we compare all superpixels classification with other. The robust classified superpixels are which superpixels classified same class, on the basis of both histograms (LBP and simple), all others are indeterminate superpixels. Currently, to avoid the false negative hits we classify them to the unclassified class, but later with the stable neighbors we will assign ranks to them.

5 Measurement and Test Environment

To measure image object classification efficiency, we have adapted some metrics from the literature. It is necessary to introduce some concepts to this:

- Reference result set: The pixels, which are marked in the reference image by a skilled expert.
 - Test result set: The pixels, which are marked by the algorithms.
- The selected pixel-based parameters from the literature are [12]:
- False negative (FN): Reference result set contains the current pixel, but the test result set does not.
 - False positive (FP): The test result set contains the currently pixel, but the expert is not marked it on the reference result set.

- True positive (TP): The pixel is contained in both reference result set and test result set.
- True Negative (TN): Neither set contains the current pixel.
- Accuracy $(TP+TN)/(TP+TN+FP+FN)$: This is the measure between 0% and 100%, where 100% means the reference result set and the test result set are equal. Thus the doctor and algorithms marked different pixels on the images.
- Recall $(TP/(TP+FN))$: This is a measure number indicates how much it found from the reference result set. If found all of them 1, else converge to zero.
- Precision $(TP/(TP+FP))$: Measurement of the hit. If the algorithm marked all pixels marked, the precision value is 1, else converge to zero.

6 Performance and Accuracy

In this section we show the performance of our LBP based algorithm, according to next aspects: runtime, accuracy, recall, precision. We use anonym tissue samples to do the efficiency measurements. To the tests we use 20 digital samples, which consist of 50 ROI (Region of Interest). From among these 32 ROI were healthy, 18 unhealthy. Table 1 contains all the data which has been produced by the tests.

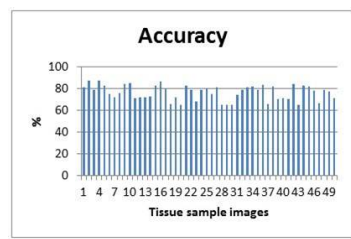


Fig. 4. Result of accuracy examination

We run the examined algorithms under the tests, then we have calculated on all images the defined metrics (TP,TN,FP,FN). The accuracy is being shown by the Fig. 4. and Table 1. This metric of our implemented algorithm is in the range of 64.3- 87,3% and the average is 75,99%.

The other important derived result is the so called “recall” (shown in Fig. 5.). Mixed results arise in the course of the tests. The LBP based algorithm tries to avoid the false positive hits. The area will be marked as undetermined if there is small confidence. This is the main reason of low recalls in the test result.

The third examined parameter was the precision (shown in Figure 6.). Our implemented algorithm is able to find pixels between 0,6 and 0,8 precision on all reference images. Among the examined 50 test, the founded pixels in 24 cases were correct, which means over 80% precision (which is very good if using such samples).

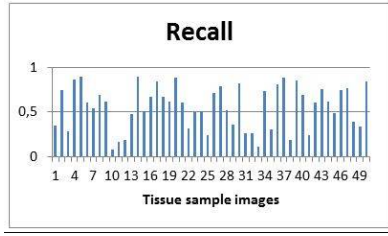


Fig. 5. Result of recall examination

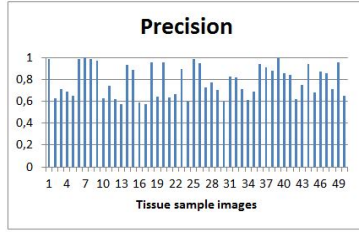


Fig. 6. Result of precision examination

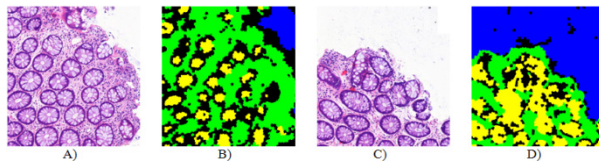
Table 1. Runtime, accuracy, recall and precision values of each image

Image	Runtime	Accuracy	Recall	Precision (0-1)
1.	48032 ms	80,5561 %	34,989983 %	0,987352781
2.	50503 ms	87,3210 %	74,7283407 %	0,627021984
3.	45815 ms	78,4133 %	27,5994314 %	0,707845967
4.	53523 ms	86,8289 %	86,2483716 %	0,69109668
5.	48907 ms	82,3787 %	89,4566917 %	0,652158323
6.	45962 ms	74,5288 %	60,1550501 %	0,98606324
7.	49185 ms	71,5572 %	54,2035412 %	0,997744071
8.	51919 ms	75,7369 %	68,6987809 %	0,984041932
9.	47646 ms	83,8932 %	61,719451 %	0,968283442
10.	46471 ms	84,8415 %	72,857387 %	0,626680672
11.	46991 ms	70,9533 %	16,0547004 %	0,739163416
12.	50978 ms	71,2926 %	18,0046956 %	0,621332388
13.	56035 ms	71,4357 %	47,9457611 %	0,571567614
14.	53736 ms	72,6450 %	89,063646 %	0,934838713
15.	45531 ms	82,1188 %	50,8651431 %	0,883274726
16.	51051 ms	85,9209 %	67,1163571 %	0,591183075
17.	45935 ms	79,3216 %	83,922605 %	0,574389702
18.	57948 ms	65,2986 %	66,5004848 %	0,956795831
19.	50487 ms	71,7855 %	61,324101 %	0,646012997
20.	46289 ms	64,3528 %	87,9682645 %	0,957433946
21.	55556 ms	82,6466 %	59,9626072 %	0,632806935
22.	42149 ms	78,7552 %	31,8393793 %	0,666676572
23.	42207 ms	68,0102 %	49,1480765 %	0,896028264
24.	53199 ms	78,2759 %	50,4916674 %	0,594485946
25.	48327 ms	79,9055 %	23,9523506 %	0,986024626

Table 1. (Continued)

26.	54416 ms	74,5399 %	70,6376023 %	0,948759786
27.	53046 ms	80,5891 %	78,4338479 %	0,722898764
28.	46335 ms	64,9316 %	52,0194195 %	0,775494037
29.	58761 ms	64,8349 %	36,1403908 %	0,705592692
30.	52995 ms	64,8009 %	82,1711576 %	0,593973493
31.	44834 ms	74,0871 %	26,2567997 %	0,824267399
32.	42018 ms	78,9241 %	25,8365777 %	0,819038487
33.	49489 ms	81,2256 %	10,4580788 %	0,710334421
34.	48039 ms	81,3128 %	72,8684392 %	0,609290772
35.	48893 ms	78,9584 %	30,04997 %	0,689207987
36.	51592 ms	83,4439 %	80,8248287 %	0,944038789
37.	43584 ms	65,4951 %	87,9658039 %	0,913664024
38.	53240 ms	81,6129 %	18,0776139 %	0,876442238
39.	49503 ms	70,2107 %	84,9993829 %	0,992048124
40.	52690 ms	71,1560 %	68,9798564 %	0,854984643
41.	43347 ms	70,2632 %	23,2500211 %	0,843804389
42.	56431 ms	84,0216 %	60,8157887 %	0,623285695
43.	54683 ms	64,8362 %	75,8693771 %	0,749807238
44.	56764 ms	82,4279 %	613156813 %	0,941009703
45.	58503 ms	81,9611 %	48,3010939 %	0,684079944
46.	44213 ms	77,9225 %	74,623875 %	0,874604003
47.	51478 ms	66,5134 %	76,3992459 %	0,856582055
48.	47767 ms	78,8671 %	39,228208 %	0,709422414
49.	46275 ms	76,8262 %	33,2365511 %	0,952316072
50.	43277 ms	71,0800 %	84,0721253 %	0,651843577

Fig. 7 shows some test images. During visualization we are using some false colors by our algorithm: Yellow is a correct hit, black is undetermined area, blue is a background and green is a not examined tissue type. On the sample images there are some tissue structure: purple circle are glands, pink area is the epithelium. In this test we are searching for glands. In the B and D images the avoidance of the false positive hits showed by black color. Finally there are lots of good hits in a gland, epithelium and the background, among the black undetermined areas.

**Fig. 7.** A) Test image 1, B) Results of test image 1, C) Test image 2, D) Results of test image 2

The key of the algorithm's accuracy is the closed distance measure technique. In the future we can probably enhance the accuracy by changing the current histogram based approach to the GLCM (Gray-Level Co-Occurance Matrix) based approach.

7 Summary

We have successfully implemented into the MorphCheck system an LBP-based texture classifier algorithm, which significantly provides more efficient object classification and segmentation than the previous solutions. After the integration we have done efficiency examination of our algorithm. We have used pre-defined metrics for the algorithm assessment. For the texture based algorithm we have combined MorphCheck with a DICOM/PACS based system and annotated a large number of tissue images. We used 1039 texture in PACS database and the LPB algorithm was working on these annotated textures. The new texture based algorithm and the combined PACS has been validated and facilitates diagnostic works significantly.

Acknowledgements. This work makes use some of the software results produced by the Hungarian National Technology Programme, A1, Life sciences, the "Development of integrated virtual microscopy technologies and reagents for diagnosing, therapeutical prediction and preventive screening of colon cancer "Hungarian National Technology Programme, A1, Life sciences, (3dhist08) project and the ÓE-RH 1104/2- 2011 project. Authors would like to thank Semmelweis University and Major & Co. to provide us annotated tissue samples for processing and classification.

References

1. Visiopharm for digital pathology. Visiopharm (March 2013). <http://www.visiopharm.com/pdf/visiomorphdp-factsheet.pdf>
2. Her2-connect. Visiopharm (March 2013). <http://ww1.prweb.com/prfiles/2010/11/18/4253634/Imageforpressrelease.bmp>
3. Developerxd. Definiens (March 2013). <http://www.definiens.com/tissue-diagnostics.html>
4. Bickel, E.L.P.: The earth mover's distance is the mallows distance: Some insights from statistics. In: ICCV 2001, IEEE 12th International Conference on Computer Vision, pp. 251–256 (2001)
5. Digital imaging and communications in medicine, National Electrical Manufacturers Association (2004). <http://dicom.nema.org>
6. Reményi, A., Szénási, S., Bándi, I., Vámosy, Z., Valcz, G., Bogdanov, P., Kozlovsky, M., Sergyán, S.: Parallel biomedical image processing with GPGPUs in cancer research. In: 3rd IEEE International Symposium on Logistics and Industrial Informatics, Budapest, Hungary, August 2011, pp. 225–248 (2011)
7. Kozlovsky, M., Szénási, S., Vámosy, Z.: GPGPU-based data parallel region growing algorithm for cell nuclei detection. In: CINTI 2011, 12th IEEE International Symposium on Computational Intelligence and Informatics, pp. 493–499 (2011)
8. Fugal, D.L.: Conceptual wavelets in digital signal processing. Space & Signals Technical (2009)

9. Xiaoyu Wang, S.Y., Han, T.X.: An hog-lbp human detector with partial occlusion handling. In: ICCV 2009, IEEE 12th International Conference on Computer Vision, pp. 1550–5499 (2009)
10. Achanta, R., Shaji, A., Smith, K., Lucchi, A., Fua, P., Süsstrunk, S.: Slicsuperpixels, Institute of Electrical and Electronics Engineers, Tech. Rep. (2010)
11. Achanta, R., Shaji, A., Smith, K., Lucchi, A., Fua, P., Süsstrunk, S.: Slic superpixels compared to state-of-the-art superpixel methods. *IEEE Transactions on Pattern Analysis and Machine Intelligence* **34**, 2274–2282 (2012)
12. Yasnoff, J.W.A., Mui, J.K.: Error measures for scene segmentation. *Pattern Recognition* **9**, 217–231 (1977)
13. ASH ImageBank, hematology imagebank. (March 2013). <http://imagebank.hematology.org/>
14. ImageAfter texture database (March 2013). <http://www.imageafter.com/index.php>
15. TinEye Reverse Image Search (March 2013). <https://www.tineye.com/>
16. RevIMG reverse visual search (March 2013). <http://www.revimg.net/>

Smart Monitoring Systems

Georeferenced Dynamic Event Handling

Sérgio Onofre¹✉, João Paulo Pimentão², and Pedro Sousa²

¹ Holos SA, Caparica, Portugal
onofre@holos.pt

² Department Engenharia Electrotécnica, FCT – UNL, Caparica, Portugal
{pim,pas}@fct.unl.pt

Abstract. A fast and efficient response to hazardous events can make the difference between life and death. Using this necessity as premise, surveillance systems are evolving, increasing the number of sensors used in event detection and developing new methods and algorithms for events handling. Nevertheless the timeliness and efficiency of response to events could be improved using new technologies, such as mobile devices with GPS capabilities, georeferenced location of events, and event classification. Having access to events and security agents' locations could improve event's handling in terms of responsiveness and appropriate distribution of work load per agent. Under the scope of a research project Advanced Surveillance System (DVA) a new approach to surveillance systems based in this geographic position of sensors, detected events and security agents was developed. DVA implements new algorithms for events' assignment and processing. This paper describes DVA's new approach to event handling.

Keywords: Multi-agents · Surveillance · Distributed systems · Geographic position · Mobile · Collective behavior · Human-machine cooperation · Task assignment

1 Introduction

The surveillance systems have been used as an important tool in protecting people and goods. These systems have evolved, from simple monitoring cameras to complex systems that detect different types of events automatically.

DVA's architecture is based in a multi-agent architecture, where events, sensors and human resources are georeferenced. The cooperation between these georeferenced components, allows the creation of a comprehensive surveillance system able to display collective intelligence, supported by the collective awareness in the performance of surveillance and security functions [1].

Event assignment to a human resource depends on several criteria, such as: proximity (distance and "time to"), type of event, workload and profile.

This paper begins by presenting some current approaches used to perform task's assignment, and then introduces a new approach to event assigning and processing, based in the new architecture for Surveillance Systems developed under the scope of the DVA project (<http://dva.holos.pt>).

2 Relationship to Cloud-Based Solutions

Using current technological innovations, DVA implements, as basis for its data repository, a Cloud storage system. The use of Cloud allows to recover events' data and status, actions history and latest agents' positions in order to minimize system failures in case of malfunctions.

All the actions executed, GPS positions, event status and agent assignments are saved in the cloud after its executions or when changes occur, storing in, real time, a snapshot of the system is current status. In case of failure of one software agent, the system will deploy another software agent to replace its task, using as reference data stored in the cloud.

3 Dynamic Task Assignment

There are several approaches to the problem of dynamic task allocation, especially when it involves different parameters such as tasks type or location and performing agents assigned types or locations. These parameters can encompass a large amount of data that needs to be correlated.

One of the approaches to visualize and interpret large high-dimensional data sets is Self Organizing Maps (SOM). SOM could be used to visualize process states or financial results, by representing the central dependencies within the data on the map [2]. There are several approaches to task assignment based in SOM using neural networks. One of the most recent is presented by Huan Huang et al [3], where a dynamic task assignment and path planning for Multi-AUV (autonomous underwater vehicles) systems in variable oceanic currents environment is proposed. In this work, the authors present two algorithms used to solve their problem: SOM-based algorithm - to assign targets to AUVs; velocity synthesis - to plan the path for each AUV in complex ocean current environment.

Another approach for AUV is presented by Sanem Sariel et al in "Naval Mine Countermeasure Missions" [4], where DEMiR-CF's distributed framework is presented for multirobot teams. This framework integrates incremental task selection schemes, distributed allocation methods, and several precaution routines. Also based in SOM, Anmin Zhu and Simon X. Yang [5], propose a dynamic task assignment for multi-robots in arbitrarily non stationary environments, where: initial neural weights of the network to select the winner, update of the weights, and neighborhood function are defined.

In "UAV Task Assignment", Brett Bethke et al [6], present a health-aware task assignment algorithm for control and coordination of actions of multiple autonomous vehicles in a dynamic environment, improving team's operational reliability and capabilities through better system self-awareness and adaptive mission planning.

A distributed market-based coordination algorithm for a team of robots is presented by Nathan Michael et al [7]. In this case agents will bid for task assignment, assuming that the agents have knowledge of all tasks as well as the maximum number of agents that can be assigned to every individual task. A distributed auction algorithm described

in "Distributed Task Assignment for Mobile Agents" by Brandon J. Moore and Kevin M. Passino [8], is used to assign mobile agents to spatially distributed tasks. This approach controls the motion of the agents during the algorithm's progress.

Finally in the "Dynamic Task Assignment in Robot Swarms" by James McLurkin and Daniel Yamins [9], four algorithms are described for dynamic assignment of tasks in multi-robot systems: Random-Choice, Extreme-Comm, Card-Dealer's and Tree-Recolor.

These approaches could be used in different systems as described, nevertheless all of them assume that agents have the same characteristics, not differentiating their suitability for a given task. Also these approaches are not assuming different types of tasks. These assumptions work on general systems, but not on systems that have different types of task to assignment and different types of agents to execute them. Another important issue is the fact that the full set of events is not known at the beginning, with events emerging during execution with different requirements such as agent profile or priority. Also, events' processing time (time used by agents to solve the event) is not the same for each event. This time constrains agent's action to the event, giving more relevance to the workload of each agent.

4 Georeferenced Dynamic Event Handling

Considering the weakness of current surveillance systems in terms of cooperation between humans and machines, this paper presents a new approach to events' assignment, improving the efficiency and time response to events. The next sections briefly describe the DVA, the dynamic georeferenced event assignment algorithm and the event handling process.

4.1 The DVA System

DVA's surveillance architecture is a multi-agent system, which allows a distributed approach to surveillance by assigning tasks among the agents. Each agent is responsible for very specific tasks according to its profile. The main types of agents present in DVA are: Sensors, Processors, Inference, Action, and Mobile [1]. In summary, Sensor Agents interact directly with the sensors (for example a camera or temperature sensor) and send the data to the Processor Agents. These agents transform raw data into parameters with: value, type of parameter, unit, timestamp and coordinates. The parameters are used by the Inference Agent that, with a set of rules, can infer the existence or not of a given event. If an event is detected, the system automatically creates an Action Agent, which will be responsible by its handling.

Events are described by: event type, priority, location, time of occurrence, status and associated parameters. Event statuses are: **To be checked**, **Confirmed**, **Concluded** and **Canceled**.

In DVA, associated to each status, different actions can be defined, such as:

- **Concluded and Cancelled:** Send email notification; Send SMS notification;
- **To be checked and Confirmed:** Send email notification; Send SMS notification;

- **To be checked:** Assign event for confirmation;
- **Confirmed:** Assign event for processing. Email and SMS notifications can be used to alert users of a new event occurrence, sending event's complementary information.

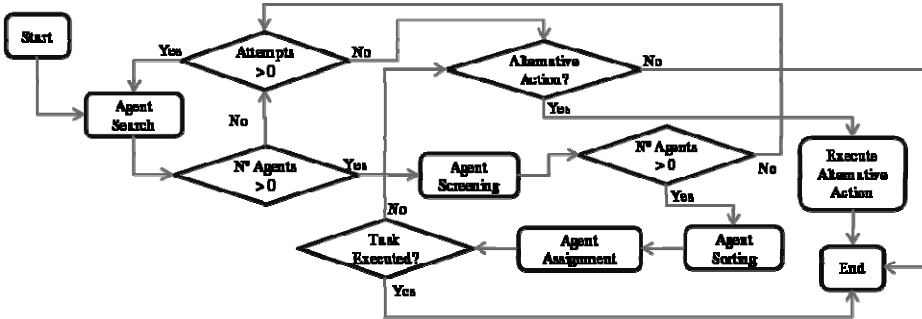


Fig. 1. Georeferenced assignment process

Event assignment process, illustrated in figure 3, uses different criteria (such as agent's types, location and workload) to search and assign an agent to event's confirmation and processing. The event assignment process, executed by the Action Agent, starts by identifying all the Mobile Agents presented in the system and then sorting them, using the algorithm described in the next section, to determine which must be selected.

4.2 Dynamic Georeferenced Event Assignment

As mentioned before, in DVA's system, events are typed, prioritized and georeferenced. Also, Mobile Agents (human agents) are typed, according with their function, locomotion mean, georeferenced and tagged with their current workload. This categorization, in terms of events and agents, provides information used to improve the assignment process. Resuming, in terms of categorization:

Events have a: Type (Fire, Earthquake, Flood, Intrusion and Gas); Priority/severity (High, Medium and Low); Location (GPS coordinates).

Agents have a: Type (Profile: Fire-fighter, Policeman, Security Agent or Civil Protection); Workload (Number of Event assigned); Location(GPS coordinates); Locomotion (on foot, by car).

Using these categorizations as criteria, the system can locate and select the most appropriated agent according with event's type, priority and location.

Distance and Time Criterion

DVA uses Google Maps services to calculate distance and time between two locations, on foot and by car, depending of agent's locomotion means. These values will be used as inputs to determine which agent is closest to event's location. Nevertheless, to ensure DVA's independence from external services, in case of service failure, DVA's

system uses Haversine's formula [10], to calculate the distance between locations. The formula used is:

$$D = 2r \arcsin \left(\sqrt{\sin^2 \left(\frac{\phi_2 - \phi_1}{2} \right) + \cos(\phi_1) \cos(\phi_2) \sin^2 \left(\frac{\lambda_2 - \lambda_1}{2} \right)} \right) \tag{1}$$

Where: D = Distance between two locations; r = Radius of earth (6371000); ϕ_1, ϕ_2 = Latitude of location 1 and location 2; λ_1, λ_2 = Longitude of location 1 and location 2;

Using the calculated distance, is possible to estimate the time to reach the location on foot, by car, or other type of vehicle, defining an average speed to each case.

For example, considering 5km/h for walking/running and 50km/h for car's use, to determine the time in minutes, the formula used is:

$$T_{walking} = \frac{D}{5000} \times 60 \text{ and } T_{car} = \frac{D}{50000} \times 60 + T_{traffic} \tag{2}$$

As mentioned before, the lowest calculated time (according with agent locomotion) will be used as a criterion to determine the event's assignment. Noteworthy that for the car's use the time delay in case of transit must also be considered, nevertheless in this paper will be considered zero for simplicity.

Workload Criterion

Each agent can have one or more events assigned and each represents a workload's increase. In addition, event's processing time is undetermined, being different for each event. For example, a small fire event could be solved in 5 minutes with a Fire extinguisher and large fire could last a morning or a day to be extinct. Given this fact, at this time, just the number of events is considered. Nevertheless as the system tested in practice, one may get further insight on how to deal with this issue. The workload criterion will represent, therefore, the number of events currently assigned to an agent.

Profile Criterion

Depending of the agent's profile, its capability to respond to a given event's type will be different. For example, a policeman will find it harder to respond to a fire than an intrusion, likewise fire-fighters respond better to fires than to intrusions. The next table shows an example of classification, identifying performances of each agent's profile according event's type. In this case, "1" represents the best performance and "5" the lowest.

Table 1. Profile vs event performance

	Police	Firefighter	Security	Civil protection
Fire	3	1	3	3
Flood	3	1	4	2
Intrusion	1	5	2	5
Earthquake	3	2	4	2
Gas	3	3	4	2

Priority and Events List Criteria

When a new event arises, an agent either be free, processing an event or on the way to an event. If the agent is not free, the new event's priority will be compared with current agent's events list priority. The result of this comparison will influence event's assignment, even changing its previous assignments. Current agent's events list could change distance and time to the new event, by adding to the route all current's events that have the same or higher priority than the new event.

For example, if an agent is underway to an event of highest criticality 10km away from its current position and the new event is on the opposite direction, the distance to consider to the new event is not the one from the current position, but the distance to the current event over a distance up to the new event. Nevertheless, if the current event has less criticality than the new one, the agent can interrupt its way, so the current position is considered to calculate the distance. This criterion will influence the distance and time criteria, changing time to reach event according agent's events list and events priority.

Winner Agent

To identify which agent is the most adequate for event's assignment, an adaptation of the Euclidean formula for three dimensions is used. The three dimensions to consider in the Euclidean formula will be: Time, Workload and Profile. In Euclidean 3D space formula, the distance between two points is defined as:

$$d = \sqrt{(x_2 - x_1)^2 + (y_2 - y_1)^2 + (z_2 - z_1)^2} \quad (3)$$

Where "d" is the calculated distance, and "x", "y", "z" represent the different dimensions. The direct application of this formula works when the three-dimensions are defined with same magnitudes i.e. normalized. In DVA, the three-dimensions have very different magnitudes (Time, Workload and profile), thus being necessary to rescale them. Considering this special case, the Euclidean formula was adapted to:

$$Sc_a = \sqrt{\left(\frac{t_a}{30}\right)^2 + \left(\frac{l_a}{5}\right)^2 + \left(\frac{p_a}{5}\right)^2} \quad (4)$$

Where "Sc_a" is agent "a" scores to new event, "t_a" the time to agent "a" reaches the event, "l_a" agent "a" workload and "p_a" agent "a" profile. In DVA 30 minutes is considered by our consultant security experts as the maximum allowable to reach a location, under duress 5 as the maximum workload by agent and 5 as the lowest adequate profile. These values were used to normalize the formula's parameters.

The winner agent will be the one that has the lowest score for the set of agents.

$$W_a = \arg \min_i \{Sc_1, Sc_2, \dots, Sc_n\} \quad (5)$$

Event Reassignment Procedure

If the assigned agent has to interrupt a previous event handling, caused by a new event (with higher priority) assignment, a new event assignment will be executed for the event whose handling was been interrupted. This procedure will be executed until all the events have an assigned agent.

5 Example

This section illustrates an example of DVA's Dynamic georeferenced event assignment application. This example will not use Google Maps services, but the formulas presented to calculate distance and time.

In this example's application, DVA has five agents available to handle events. As a start point, two events will be considered. These two events are already assigned to agents A4 and A2 respectively. Agent A2 is already in its event's location, processing it and agent A4 is on the way to event E1. When a new event arises, represented as E3, a new assignment process will start. Table 2 illustrates the current system's events list, with its values, and the current situation of agents are shown in table 3.

Table 2. System's events list

	Event 1	Event 2	Event 3
Latitude	38,64885	38,66601	38,63088
Longitude	-8,88107	-8,96553	-8,91523
Priority	High	High	Low
Type	Fire	Intrusion	Intrusion

Table 3. Agents current status

	Agent 1	Agent 2	Agent 3	Agent 4	Agent 5
Latitude	38,68316	38,66601	38,63195	38,64161	38,67807
Longitude	-8,91026	-8,96553	-8,94150	-8,90579	-8,94150
Workload	0	1	0	1	0
Event list	-	Event 2	-	Event 1	-
Status	Stooped	Handling	Stooped	On way	Stooped
Profile	Police	Security	Police	Police	Firefighter
Locomotion	Motorcycle	Walk	Walk	Car	Car

Using these two tables as inputs, all the criteria will be calculated, according to the agents' profiles setups and locations, its events list and workload. The next table presents the calculated values for each criterion, and the final score for each agent.

Table 4. Agents calculation and scoring

	Agent 1	Agent 2	Agent 3	Agent 4	Agent 5
Profile	5	4	5	5	2
Distance	5,83	9,57	2,28	5,87	5,72
Vehicle Time	7,00			7,04	6,87
Walking Time	69,95	114,87	27,41	70,44	68,65
Score	0,23	70,31	27,41	0,31	0,64

Comparing the calculated scores, Agent 1 will be the agent assigned to E3. In this case, it will not be necessary to perform any event reassignment.

6 Conclusions

DVA was developed to react geographically to events such as intrusion, fires, gas leakage, earthquakes or floods. This system can help prevent or minimize events that can compromise the safety of persons or property. The assignment process described in this paper aims to improve the current surveillance systems, reducing event's time response and increasing efficiency, by using geographical position of events and humans together with other functional characteristics.

This new approach, may also contribute to reduce the surveillance system dependency on humans, by automating event detection and assignment, thus minimizing human errors and personnel costs. Also, this approach could fulfill some of the gaps found in related work in the literature, such as use of agents with different characteristics, such as speed and profile, and different events types and priorities.

DVA is currently in test, being used as a support system to surveillance of Madan Parque (Science and Technology park). The current tests will allow us to validate the application of the assignment process. Some preliminary results of these tests allowed us to identify areas where the system can be improved. One of the already identified areas for improvement is the relation between agent profile and performance on event types. In fact, we found that the allocation of "hard" values to this relationship is not consensual and the performance could be improved by the use of fuzzy logic.

References

1. Onofre, S., Sousa, P., Pimentão, J.: Geo-referenced multi-agent Architecture for Surveillance. In: 16th PEMC (2014)
2. Kohonen, T.: The self-organizing map. *Proceedings of the IEEE* **78**(9), 1464–1480 (1990)
3. Huang, H., Zhu, D., Ding, F.: Dynamic Task Assignment and Path Planning for Multi-AUV System in Variable Ocean Current Environment. *Journal of Intelligent & Robotic Systems* (August 2013)
4. Sariel, S., Balch, T., Erdogan, N.: Naval Mine Countermeasure Missions. *IEEE Robotics & Automation Magazine* **15**(1), 45–52 (2008)
5. Zhu, A., Yang, S.X.: A neural network approach to dynamic task assignment of multirobots. *IEEE Transactions on Neural Networks / a Publication of the IEEE Neural Networks Council* **17**(5), 1278–87 (2006)
6. Bethke, B., Valenti, M., How, J.: UAV Task Assignment. *IEEE Robotics & Automation Magazine* **15**(1), 39–44 (2008)
7. Michael, N., Zavlanos, M.M., Kumar, V., Pappas, G.J.: Distributed multi-robot task assignment and formation control. In: 2008 IEEE International Conference on Robotics and Automation, pp. 128–133 (2008)
8. Moore, B.J., Passino, K.M.: Distributed Task Assignment for Mobile Agents. *IEEE Transactions on Automatic Control* **52**(4), 749–753 (2007)
9. Mclurkin, J., Yamins, D.: Dynamic Task Assignment in Robot Swarms. *Robotics: Science and Systems* (2005)
10. Sinnott, R.W.: Virtues of the Haversine. *Sky and Telescope* **68**(2), 159 (1984)
11. Claro, J., Dias, B., Rodrigues, B., Onofre, S., Pimentão, J.P., Sousa, P.: Autonomous robot integration in Surveillance System. In: PEMC 2014 (2014)

Implementation of User-Oriented Smart Services into an Innovative DC Low Voltage Net

Manja Görner^(✉), Thomas Göschel, Stephan Kassel^(✉),
Thomas Klein^(✉), and Sabrina Sander

Westfälische Hochschule Zwickau, University of Applied Sciences, 08056
Zwickau, Germany

{Manja.Goerner,Thomas.Goeschel,Stephan.Kassel,
Thomas.Klein,Sabrina.Sander}@fh-zwickau.de

Abstract. In this paper a concept of smart services implemented in an innovative DC net (direct current) is described. It shows how various components with different DC-energy-level-demands and user-based requirements can be connected interoperable. Thus smart services can be defined in that technical environment. The implemented system is able to remember the residents' individual preferences to provide a comfortable living situation.

Keywords: DC voltage · Services · Smart home · Interoperability

1 Introduction

In terms of smart homes and cyber-physical systems it is a general effort to provide house systems with more intelligence to achieve an enhanced usability. At the same time, in terms of scarcity of natural resources and increasing environmental awareness, energy and cost efficiency is indispensable for a profitable operation.

Today's households' demand for electricity is fulfilled either via the public energy network or internal measures. The most widespread system for generating own electricity are photo-voltaic (PV) systems. But in 2012, less than one percent of the German households supplied themselves with self-generated electricity on the basis of a PV system. [1] A PV system produces power with DC voltage. This is normally converted into AC voltage before it is fed into the home network. But many household appliances operate with DC voltage. Therefore, a rectifier is installed in the power supplies of the appliances. Both the inverter and the rectifier lead to conversion losses. [2]

In this paper a model room with an innovative DC net is presented. This DC net is supplying the electric and electronic devices in a residential unit directly with DC voltage. The necessary adaptation of the appliances is described. Based on these appliances a smart services environment is defined. The services build a platform for an interoperable connection between these appliances and, at the same time, serve as a gateway for individual user intervention.

The paper gives an overview about the projects main ideas and the project partners' contributions.

2 Relationship to Cloud-Based Solutions

In this paper, the preliminary results of a project are presented, which is igniting subsequent projects. Therefore it represents a fundamental conceptual basis. The actual prototypical model room includes a central local control. A following project will dissolve this restriction by shifting significant portions of the control into a cloud. Firstly this offers the user ubiquitous access to the system. Furthermore, by outsourcing of information the system would be less affected. It would handle only the information it needs at that moment. An expensive performance improvement of the components would not be necessary, yet strong functionality would be guaranteed.

3 Related Literature

Currently there are various ideas for services in a smart home, but most of them are based on an AC net with AC appliances. The differences in the approaches of provided services are resulting from their intentions. For example, one of the greatest German energy companies, RWE, is including into the definition of services the opening and closing from windows, blinds and heating as well as the lighting and consumer electronics. The target of these services is to provide home safety, by increasing the protection from burglary and fire, as well as to maximize comfort and convenience. [3]

Regarding the implementation of DC networks in buildings, many studies and approaches already exist, like the project “Stroomversnelling” from the Netherlands. The aim is to implement a DC system, with only one AC socket connection, within three steps. [4] There are more similar conceptions like in [5] and [6], but nearly all of them are only focusing on the implementation of a DC net, without a smart interconnection of the appliances. This situation is unsatisfactory, especially when, simultaneously, the number of devices in households is permanently increasing.

The problem is also mentioned by the Energy Information Agency (EIA). According to their studies, consumer electronics and small appliances are the fastest growing sectors of residential electricity use. Twenty years ago, in 1993, this category played no role in their investigations. But eight years later, they already counted more than ten devices in that category. Last year, some members of the IEEE listed all small appliances and consumer electronics devices in their houses. They counted to more than fifty. [7] This is an important argument to perform research how the small appliances and consumer electronics should be integrated in a smart home.

4 Research Contribution and Innovation

Based on these observations, the project EGNIAS was launched. The project team decided to combine a DC approach for the technical energy network with the ideas of the smart home, to let DC appliances interact with each other.

For defining the services, a technical base has been created. The system was built as a model room with an inside dimension of approximately 140x90x50 cm (WxDxH). The room is divided into an entrance area, a working area, a dining area, a lounge area and a reading area. The model has been populated with furniture built by the universities faculty of wood design.

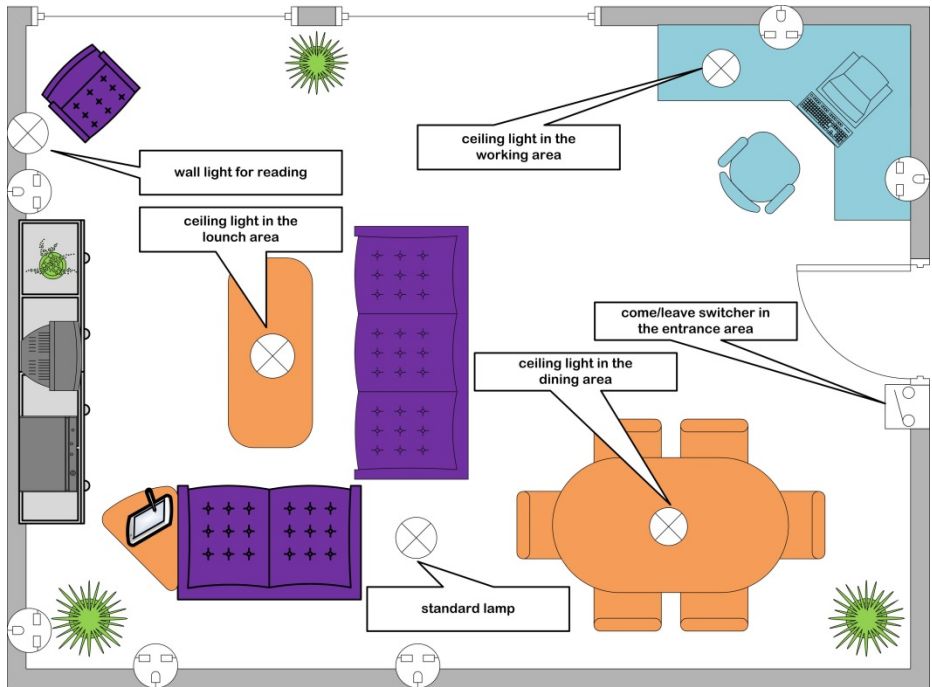


Fig. 1. The model room

Technically, the room controller is implemented with a PLC (Programmable Logic Controller). It is connected by an IO-unit with the model apartment. The power outlets are controlled by a digital output terminal; the lamps are connected to a dimmer with an analog output terminal. The feedbacks of the achieved luminosities come from light sensors, which are connected to the analog inputs of the PLC. The control button next to the door in the entrance area is connected with the system by a KNX-communication terminal.

The central PLC is responsible for the room observation and control as well as the residential unit's energetic supervision. This includes determining the energetic subscription and usage sizes which allows the determination of user-dependent power efficiencies, as well as the monitoring of the energy storage. Thus, power supply reliability can be achieved, combined with the possibility for an ex-post review of the power storage characteristic.

The model room was equipped with a DC voltage based power supply system. Therefore, a PV element and an energy storage have been connected to the room. With the PLC based room controller various components (sensors, actuators, power supply, operator controls ...) are interoperable connected via various transmission media (KNX, radio, etc.).

The challenge was set by configuring reasonable and suitable services for the inhabitants based on the DC low voltage appliances. The highest power supply voltage into the pattern room can maximum achieve 24 volt. The project team decided, according to the statement of the Energy Information Agency (EIA), to install in a first step only consumer electronics like a television, a radio, a personal computer, a tablet and a telephone as well as a standard lamp, three ceiling lights and one wall light. Including all of these components, a set of services should be designed.

The plugs from a number of these appliances have been changed, so that the appliances can be connected to the newly designed power supply system, requesting the suitable voltage level.

With these appliances, individualized settings for well-being should be created. Special attention is given to the creation of an intelligent interface between the deterministic system behavior and the complexity of human perception. (The same brightness can be perceived differently in various situations.) Furthermore, external influences, like sunlight, have to be taken into consideration for the models.

In these appliance settings, services have been defined. A service is defined as a process to influence physical environmental parameters selectively. Input variables of these processes are the actual values of the environmental parameters and planned activities of the users. The resulting values of the output parameters are derived from the planned activities (of the selected services).

Special attention was given to the matching of the provided services with the user's needs. They should provide an appropriate room climate. This concept has been implemented so far, that different room regions are differently illuminated and that the combination of services is restricted to reduce possible distractions. For example during the meal service the TV is turned off, so that the people are not distracted and the communication is encouraged at the table. A service is therefore not responsible for the control of one appliance. It provides a combination of control commands for a multitude of devices.

Because the environment is perceived differently by each person, the user can change the room situation as desired, and customize the services individually. Appliances can be turned on or off and the light intensity can be adjusted. These individual settings for the services can be stored for later replaying after a service change.

The built-in brightness sensors are considering the effects of external light sources as well. This guarantees that external influences are taken into account when controlling the illumination.

Overall, the system architecture includes three layers: the hardware layer, the abstract layer and the user-oriented layer.

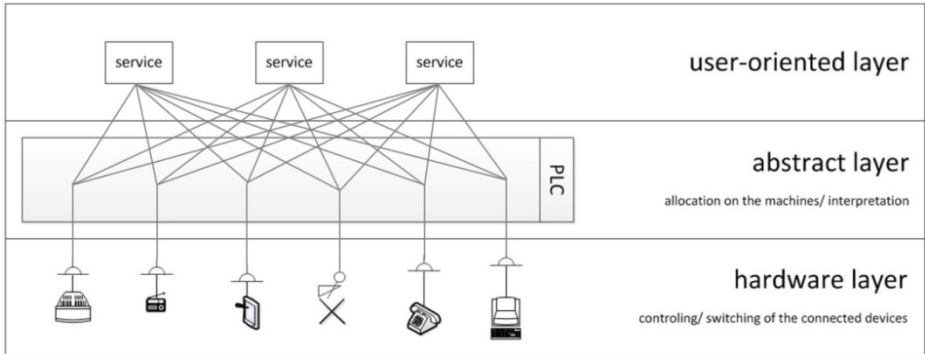


Fig. 2. The systems layer-based architecture

The user-oriented layer is the interface to the user. It provides the user's access to the system. In particular a tablet computer interface offers different views to the system, according to differing demands of several user groups. There are technically-skilled users, who want a detailed access, and technical-agnostic users who want a very simple and easy-to-use interface.

The hardware layer is the technical foundation. It is the layer, where the DC net is physically implemented and the appliances are connected and switched.

Between these two layers, there is an abstract layer. This layer serves as the translator between the other two layers. Here are the connection points established. It does not only interface with the two other layers. In this layer, all information and signals of the whole system are collected. The service processes, which were introduced earlier in this paper, are running here. This layer makes the system smart.

5 Discussion of Results and Critical View

It has been shown that different components with different DC-energy-level-demands and user-based requirements can be connected interoperable. In particular the appliances power slots are designed in a new and innovative way, so the appliances are directly provided with DC voltage. This makes the use of AC and DC converters unnecessary. It allows increasing the energy efficiency of the overall system.

The system is able to remember the resident's individual preferences of a feel-good atmosphere. The room is able to react on its environmental variables, for example the intensity of the solar radiation.

Because the appliances landscape is not yet very flexible, the implementation of services has to be classified as a static implementation. Each device has to be manually integrated into the system. This does not reflect the dynamics a user likes to have in his apartment. In fact, during the day he connects various appliances to the power supply and removes them again. This is not represented in the actual model.

6 Conclusions and Further Work

Within the built model it is shown how different voltage levels are provided to different consumers in a DC network. Using their specifically designed plugs the appliances get access to the relevant voltage level from the energy net, so no converter has to be used at this point. That increases the energy efficiency of the system significantly and user-side mistakes are prevented in advance.

In the next step, this interface should be made more intelligent, so that the appliances can tell the system what kind of devices they are (and what energy they need). Technically, this should be implemented by a NFC tag (near field communication) that is attached to the power plug of the appliance and behind the socket of the power outlet. By plugging the plug into the socket a data exchange connection is built like the universal plug&play method. So the information is exchanged, which voltage level must be provided to the appliances and how the devices may be integrated into the already existing services. This should be visualized for the user on his tablet-based user interface. If new room usage options are resulting from the enhanced appliances (like plugging in a media server), the definition of new high-level services will be possible. Technical alternative to the NFC technology may be a Bluetooth based technology.

In the basic model, the user accesses directly to the PLC program via the tablet's user interface or the control buttons in the room. The evolution plan of the project envisions the changing of this interface. Appropriate control variables should no longer be stored in the memory module of the PLC, but in a cloud. If the user wants to use a new service, the PLC gets a signal to download corresponding parameters from the cloud to be able to control the appliances. Thus, a continuous exchange of information is not necessary, limiting the information exchange. To manage his housing unit, the user does no longer need to be within the house. He only needs to be able to connect to the cloud and can control his home environment via a remote interface.

References

1. Institut der deutschen Wirtschaft Köln (IW) und Energiewirtschaftliches Institut an der Universität: Eigenerzeugung und Selbstverbrauch von Strom. Stand, Potentiale Trends. Köln (2014)
2. Hermanns, H., Wiechmann, H.: Demand-Response Management for Dependable Power Grids. In: Grimm, C., Neumann, P., Mahlke, S. (eds) *Embedded Systems for Smart Appliances and Energy Management*. pp. 1-22. Springer, Heidelberg (2013)
3. RWE. <http://www.rwe-smarthome.de/web/cms/en/457156/smarthome/information/what-is-rwe-smarthome/>
4. <http://www.directcurrent.eu/en/news/155-dc-grid-at-home-becomes-reality>
5. <http://www.directcurrent.eu/en/news/news-archive/159-dc-smart-grids-in-south-africa>
6. <http://www.cpes.vt.edu/public/showcase/d1.2FutureHome.php>
7. IEEE. <http://smartgrid.ieee.org/june-2013/881-is-dc-s-place-in-the-home>

Light Memory Operation Based on a Double Pin SiC Device

V. Silva^{1,2(✉)}, M. Barata^{1,2}, M.A. Vieira^{1,2}, P. Louro^{1,2}, and M. Vieira^{1,2,3}

¹ Electronics Telecommunication and Computer Department, ISEL, Lisboa, Portugal

² CTS-UNINOVA, Quinta da Torre, Monte da Caparica, 2829-516, Caparica, Portugal
vsilva@deetc.isel.ipl.pt

³ DEE-FCT-UNL, Quinta da Torre, Monte da Caparica, 2829-516, Caparica, Portugal

Abstract. Experimental optoelectronic characterization of a p-i'(a-SiC:H)-n/p-i(a-Si:H)-n heterostructure with low conductivity doped layers shows the feasibility of tailoring channel bandwidth and wavelength by optical bias through back and front side illumination. Front background enhances light-to-dark sensitivity of the long and medium wavelength range, and strongly quenches the others. Back violet background enhances the magnitude in short wavelength range and reduces the others. Experiments have three distinct programmed time slots: control, hibernation and data. Throughout the control time slot steady light wavelengths illuminate either or both sides of the device, followed by the hibernation without any background illumination. The third time slot allows a programmable sequence of different wavelengths with an impulse frequency of 6000Hz to shine upon the sensor. Results show that the control time slot illumination has an influence on the data time slot which is used as a volatile memory with the set, reset logical functions.

Keywords: Optoelectronics, Volatile memory, Set reset logical functions

1 Introduction

A volatile memory is a state variable that only maintains its value over a period of time and then its value changes without any intervention on the system. A decisive change of the state variable, at any time, will behave with the same manner. The time during which the state variable value is recoverable and the number of times it can be read without changing its value define the efficiency of the memory. Different memory technologies can be combined to produce innovative memories like one that uses light to read the state variable [1], or molecules [2].

The aim of this document is to answer the research question: how is it possible to build a memory using a pi'npin device?

The hypothesis, based on previous research of the characteristics of the pi'npin device [3], points out that charges are stored by illuminating the device in the front or back surfaces, and by using this characteristic it is possible to build a volatile memory. Experimental results have shown that different light sequences within a set of fixed tuples produce different outputs for the same tuples. This points out that there is a direct influence of the previous tuple upon the current one. Understanding this behavior will determine if the pi'npin presents itself as an effective volatile memory.

2 Contribution to Cloud-Based Engineering Systems

The cloud, an icon used to represent the Internet, is now a service provided by many enterprises that host data space and offer applications that virtualizes storage and data bases. The Cloud is used in many circumstances has a common spot where to different users share data. It is a valuable asset for research as a means of connecting and sharing experimental data among researchers, so that validation can be performed, or to distribute tasks. Cloud services are “services delivered over the network” [4].

Another appealing usage is the possibility that experimental setup can be linked in-to the Cloud, so that researchers use the same setup thus reducing costs and accessing instruments and devices that need skills which they do not necessarily have or need in their research. This would provide an out-of-the-lab research, especially to inaccessible areas or with hazard settings forbidden for researchers.

The experiments and device presented in this paper fits into that scenario; building an application that is hosted in the Cloud would connect an authorized researcher to our laboratory. The laboratory would have the necessary instruments switched on and controlled by a computer connected to the Cloud. The researcher would then set the inputs and expect the experimental results. Every experiment would be stored into a database in the Cloud where any researcher could see past experiments, comment results and suggest improvements.

3 Device Design, Characterization and Operation

The device consists of a 1cm^2 double pin/pin a-SiC:H photo detector with front and back optical bias shown in

Fig. 1. The device operates within the visible range and input channels of several wavelengths (R: 626nm), green (G: 524 nm), blue (B: 470 nm) and violet (V: 400 nm) transmitted together as different bit sequences shine on the front of the device.

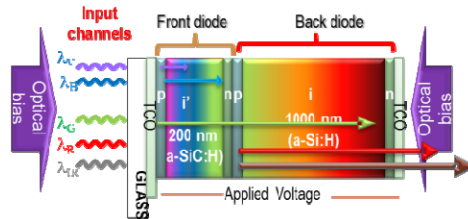


Fig. 1. Device configuration and operation

The combined optical signal is analyzed by reading out the photocurrent, under either front or back optical bias provided by constant illumination with (390 nm) LEDs [3].

In Fig. 2 the optical gain (α), defined as the ratio between the spectral photocurrent with and without applied optical bias, is displayed under front irradiation. The background intensity (ϕ) was changed between $5\mu\text{Wcm}^{-2}$ and $3800\mu\text{Wcm}^{-2}$. Results show that the optical gains have opposite behaviour under front and back irradiations. Under front irradiation and low flux, the gain is high in the infrared region, presents a well-defined peak at 750 nm and strongly quenches in the visible range, as shown in Fig. 2a).

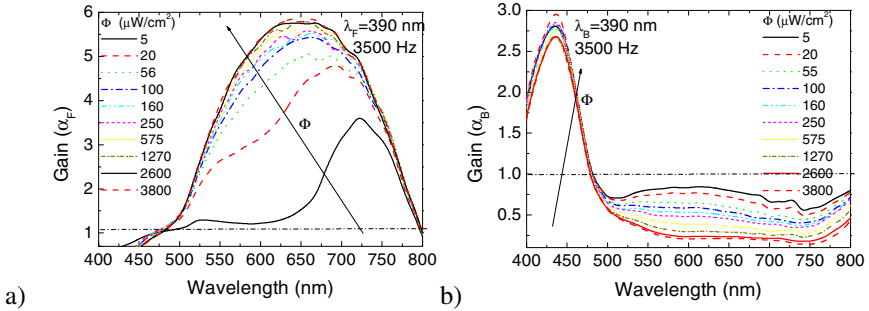


Fig. 2. Spectral gain (α_B) at $\lambda=390$ nm under a) front and b) back irradiation

As the power intensity increases the peak shifts to the visible range and the spectral sensitivity can be deconvoluted into two peaks, one in the red range that slightly increases with the background intensity and another, in the green range, that strongly increases with it. In the blue range the gain is much lower. This shows the controlled long-pass filtering properties of the device. Depending on the background intensity selects the infrared or the visible spectral ranges; low fluxes select the near infrared region and cuts the visible one, the reddish part of the spectrum is selected at medium fluxes, and high fluxes tune the red/green ranges [5]. Fig. 2b) shows the photocurrent gain under back irradiation. The background intensity (ϕ) was changed between $5\mu\text{Wcm}^{-2}$ and $3800\mu\text{Wcm}^{-2}$. Results show that under back irradiation, the gain is high in the blue region, presents a well-defined peak at 425 nm and strongly quenches above 500 nm [6].

4 Experimental Setup

The optical bias as a steady lighting is used in different applications of this device namely as a WDM communication element and digital light logical functions.

To use the device as a volatile memory the optical bias paradigm is changed and looked upon as two light Control signals; the Front Control and the Back Control. The operation has three phases, the Control, the Hibernation and the Data phase. During the Control phase only the Front Control and the Back Control signals may be presented to the sensor. The Hibernation phase has no illumination signals; the sensor is in complete darkness. During the Data phase the sensor is subjected to the Data Sense signal.

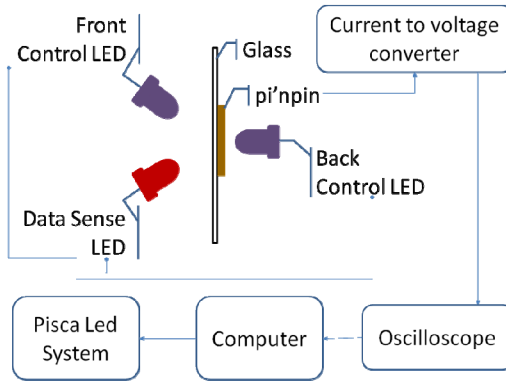


Fig. 3. LEDs, signals and the pi'npin device

The Front and Back Control signals use a 390 nm LED, set with an intensity current of 5 mA and 20 mA respectively. These values differ, so that the output of the pi'npin may be similar. The Data Sense signal is a single 626 nm LED channel pulsed at 6000Hz, set at an intensity current of 5 mA. These intensity current values were chosen so as to allow a clear visualization of the memory effect. The relative positioning of the LEDs and the pi'npin device can be visualized in Fig. 3.

A signal labeled as Dark is the photocurrent output when there are no Control signals and only the Data Sense signal is applied. It is used as a reference.

The double pi'npin sensor has a noise margin of 8nA [7].

5 Memory Effects

To introduce the memory theme a simple experiment is shown in Fig. 4a). On the top of the figure, there are the signals to guide the eyes.

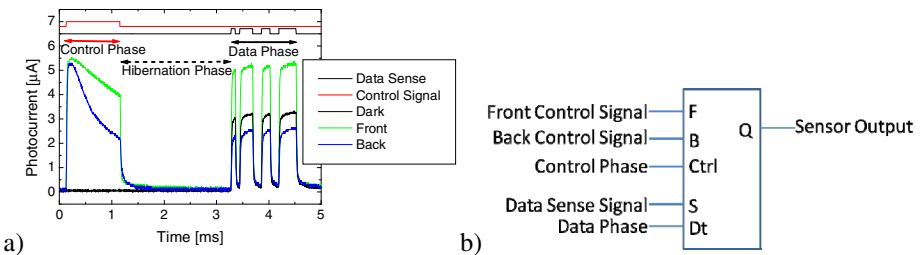


Fig. 4. a) Three outputs represented by the different conditions: Dark, Front Control and Back Control, on the same plot. b) Digital component of the equivalent pi'npin setup.

The experiment shown in Fig. 4a) is the result of the following sequential actions:

- 1- The Data Sense signal is applied and the pi'npin sensor's output is plotted and named Dark in Fig. 4a).

- 2- The Back Control signal is applied during 1 ms, followed by complete darkness during 2 ms, and then the Data Sense signal is applied. The output is plotted and named Back in Fig. 4a).
- 3- The Front Control signal is applied during 1 ms, followed by complete darkness during 2 ms, and then the Data Sense signal is applied. The output is plotted and named Front in Fig. 4a).

These sequential actions were spaced in time between them by more than 2 minutes. This to ensure that one action does not have a big influence on the next one.

Observing Fig. 4 between 3 and 5 ms it is notable the reduced output of the Back in relation to the Dark, and the enhanced output of the Front in relation to the Dark. There is an influence of the Control signal over the Data Sense signal. Let the output be represented by the function $f(control, sense)$.

To model this effect a digital component is presented in Fig. 4b). The digital component has all the input signals on the left hand side and the output signal on the right hand side.

The Control Phase input enables the Front Control and the Back Control signal, and the Data Phase input enables the Data Sense signal.

The operation of the digital component is better described with the aid of Table 1.

Table 1. Automata state variable table

Line	Inputs					Internal State		Output
	F	B	Ctrl	S	Dt	Store _{actual}	Store _{next}	Q
1	F	0	1	-	0	-	F	-
2	0	B	1	-	0	-	B	-
3	-	-	0	-	0	Store _{actual}	Store _{actual}	0
4	-	-	0	S	1	Store _{actual}	Store _{actual}	$f(\text{Store}_{\text{actual}}, S)$
5	-	-	1	-	1	-	-	-

Presented in Table 1 are the automata transition states of the digital component. In this table the (-) symbol represents a *don't care* value, which means that whatever the value that the variable has on that state, it does not interfere on the subsequent action. When used as an output it means that the output in that case should not be considered. The (1) symbol means that the signal is active, and the (0) symbol that the signal is not active. The internal state is defined by variable Store, which is represented as Store_{actual} indicating the value that it holds in the present state. Store_{next} represents the value that Store will hold due to the input values. Line 1 indicates that when the Control phase is active and the input Front Control as a value F the next state will be set with that value. Line 2 indicates that when the Control phase is active and the input Back Control as a value B the next state will be set with that value. Line 1 and 2 also imply that the Front and Back Control are not set simultaneously. Line 3 shows that when there is neither a Control phase nor a Data phase the internal state variable will hold the same value; i.e. during the Hibernation phase the stores value does not change, and that the output is inactive. Line 4 indicates that when the Data phase is active the sensor output is a function of the present value of the internal state variable

Store and of the Data Sense signal S ; output = $f(\text{control}, \text{sense})$. Line 5 indicates that if the Control phase and Data phase are set simultaneously the component will have unpredictable results.

The three phases, Control, Hibernation and Data have to be studied for the understanding of the memory effect. The approach used will focus on the duration in time of the three phases. Some time setting will be fixed and others vary to better observe and understand the results.

5.1 Control Signal Phase Duration

This study uses Control signals with different time duration, from 1 to 5ms. After each Control signal, follows a fixed Hibernation phase that lasts 3ms after which a Data Sense signal is applied. Fig. 5a) presents the results of the applied Front Control signals, and Fig. 5b) shows the results for the applied Back Control signals.

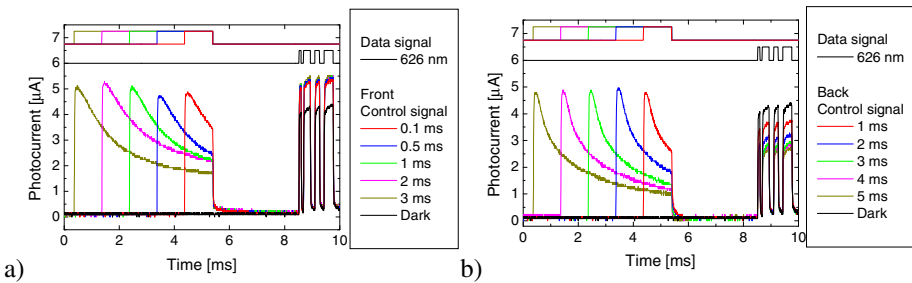


Fig. 5. a) Front Control signals and **b)** Back Control signals, with different lengths in time followed by a fixed Hibernation time and the same Data Sense signal.

Results show that there is almost no difference to the output produced by the applied Data Sense signal despite differences in the length of the applied Front Control signal. The Data Sense signal output is enhanced related to the Dark reference which is in conformance with the spectral gain presented in section 2. The results also show that higher duration of the Back Control signals reduces more the output of the applied signal when comparing it to the Dark reference. Comparing both Fig. 5 a) and b) on the Data Sense signal output, it is possible to infer the side on which a Control signal was set.

5.2 Constant Control Plus Hibernation Time

For visualization purposes the sum of the Control phase time plus the Hibernation phase time remains constant with a value of 3.1 ms. On successive experiments the focus will be on the Control signal duration, from 0.1 ms to 3 ms. The aim is to have the highest difference in photocurrent of the Data Sense signal output comparing the results of the applied Front Control or Back Control signal. The Data Sense signal is the same on all experiments, and is a random digital sequence.

Presented in Fig. 6a) is the experimental result of different Front Control signals followed by a short sequence of a Data Sense signal and in Fig. 6b) the experimental result of different Back Control signals followed by the same Data Sense signal.

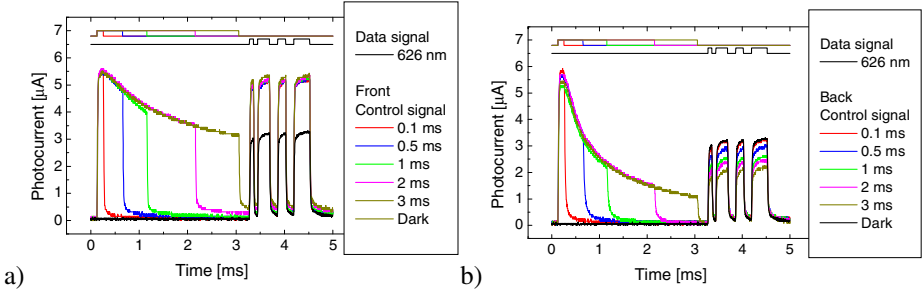


Fig. 6. a) Front Control signals and b) Back Control signals, with different lengths in time followed by the same Data Sense signal.

Results show that there is almost no difference to the output produced by the applied Data Sense signal despite differences in the length of the applied Front Control signal. The Data Sense signal output is enhanced related to the Dark reference which is in conformance with the spectral gain presented in section 2. Results also show that the output produced by the applied Data Sense signal reduces with the increase of the duration in time of the Back Control signal. The Data Sense signal output is quenched related to the Dark reference which is in conformance with the spectral gain presented in section 2. Observing both figures Fig. 6a) and b) it is clear that, the longer in time the Front and Back Control signals are the higher the photocurrent output difference between the Data Sense signals is.

5.3 Control Signal Current Intensity

The Control Signal is applied with different current intensities, 1mA to 30mA, followed by a fixed Hibernation time of 3ms, and then a Data Sense signal is applied.

Presented in Fig. 7a) is the result of each Front Control signal applied to the pi-npin and Fig. 7b) shows the results for the applied Back Control signals.

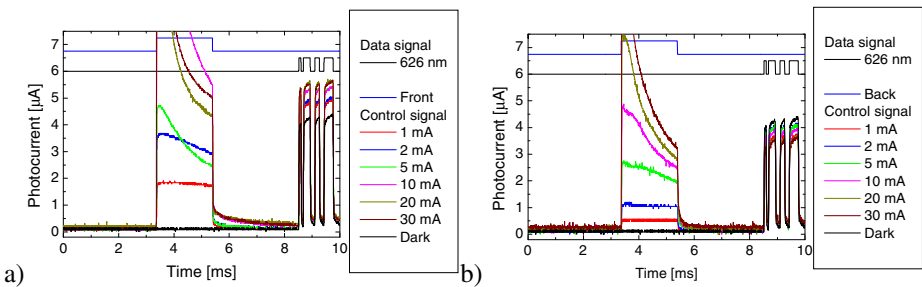


Fig. 7. a) Front Control and b) Back Control signals, with different current intensities followed by a fixed Hibernation time and the same Data Sense signal.

The figures are truncated for the higher currents because its representation does not concern the result discussion, and would otherwise prevent a better visualization of the results. The results show that the higher the Front Control signal current intensity is, the higher is the output signal, when comparing to the Dark reference. Results also show that the output of the Data Sense signal is slightly reduced, when compared to the Dark signal, for increasing current intensities of the Back Control signal.

Observing both figures Fig. 7 a) and b), and regarding the Dark reference, it is better to use the highest current possible for the Back and Front Control signals due to the fact that they provide Data Sense signal outputs with greater differences to the Dark reference.

6 Conclusions

By comparing the amplitudes of the Dark signal output to Data Sense signal output it is possible to know if the Control signal beforehand was a Control Front or a Control Back signal. The Control Front and Control Back signals are pulsed ultra-violet wavelengths. The Data Sense signal is a 626 nm wavelength signal. The memory stores which of the control signal was used last, either the Control Front signal or the Control Back signal. The memory is read by the Data Sense signal indicating if the Control Front signal was used or if the Control Back signal was used. A volatile memory can be built using a single pi'npin device.

Acknowledgments. This work was supported by FCT (CTS multi annual funding) through PIDDAC Program funds and PTDC/EEA-ELC/111854/2009 and PTDC/EEA-ELC/120539/2010.

References

1. Guo, R., You, L., Zhou, Y., Lim, Z.S., Zou, X., Chen, L., Ramesh, R., Wang, J.: Non-volatile memory based on the ferroelectric photovoltaic effect. *Nat. Commun.* **4**, 1990 (2013)
2. de Ruiter, G., Motiei, L., Choudhury, J., Oded, N., van der Boom, M.E.: Electrically Addressable Multistate Volatile Memory with Flip-Flop and Flip-Flap-Flop Logic Circuits on a Solid Support. *Angew. Chemie* **122**(28), 4890–4893 (2010)
3. Vieira, M.A., Vieira, M., Costa, J., Louro, P., Fernandes, M., Fantoni, A.: Double Pin Photodiodes with Two Optical Gate Connections for Light Triggering. *Sensors & Transducers* **10**, 96–120 (2011)
4. Software system engineering research group (SSERG). <http://www.sserg.org/>, https://tuhat.halvi.helsinki.fi/portal/files/28513674/cbse13_proceedings.pdf
5. Vieira, M., Vieira, M.A., Rodrigues, I., Silva, V., Louro, P.: Tuning optical a-SiC/a-Si active filters by UV bias light in the visible and infrared spectral ranges. *Phys. Status Solidi* **11**(11–12), 1674–1677 (2014)
6. Vieira, M., Vieira, M.A., Silva, V., Rodrigues, I., Louro, P.: Near-UV background as a bridge between visible and infrared communication (in Publ.)
7. Silva, V., Vieira, M.A., Louro, P., Barata, M., Vieira, M.: Simple and complex logical functions in a SiC tandem device. In: Camarinha-Matos, L.M., Barrento, N.S., Mendonça, R. (eds.) DoCEIS 2014. IFIP AICT, vol. 423, pp. 592–601. Springer, Heidelberg (2014)

Brain Inspired Health Monitoring Supported by the Cloud

Fernando Luis-Ferreira^{1,2(✉)}, Sudeep Ghimire^{1,2}, and Ricardo Jardim-Goncalves^{1,2}

¹ Departamento de Engenharia Electrotécnica, Faculdade de Ciências e Tecnologia, FCT, Universidade Nova de Lisboa, 2829-516 Caparica, Portugal

² Centre of Technology and Systems, CTS, UNINOVA, 2829-516 Caparica, Portugal
{flf, sud, rg}@uninova.pt

Abstract. The health status of a person can be assessed by specialized professionals with the help of medical devices. The assessment, in real-time, would be useful as most of the times a person is not in presence of health professionals. But own assessment lacks precision and reaction time that could be risky in critical conditions. The pervasiveness of Internet connections and ubiquity of smart devices makes it possible to overcome that limitation. By using sensing capabilities of portable/wearable devices in conjunction with medical knowledge and clinical history it is possible to monitor a person's health status in real-time with reaction mechanisms. The objective is to keep track of collected evidence, and relate with existing knowledge for better assessment. This paper proposes a framework, inspired by the brain and physiology, capturing real-time health related information, at a person's location, submitting that to the cloud for reasoning and decision and triggers advice or request medical assistance.

Keywords: Cloud · Health monitoring · Internet of things · Brain models

1 Introduction

A person living in modern societies is surrounded by an ever-growing number of technological devices [1]. The pervasiveness of computing and sensing devices offers different types of services that, ultimately, represent a source of data that can be used for the most different objectives and applications. As a person makes daily family or work activities, he/she is permanently exposed to an environment with which is necessary to properly interact and get valuable output for his/her life.

With the emerging developments of mobile devices and the Internet of Things becoming a reality, the offering of information provided by sensors or integrated services is growing fast. It would be desirable that a citizen could benefit from the best performance of all those systems, being supported by accurate context awareness thus improving quality of life, and security. In that direction, the information that devices and systems either portable or installed in surrounding environment (e.g. car, house, city, etc.) [2].

Most of animals have surveillance mechanisms, in which mammals stand out by the complexity of their sensorial organs and brain functions. Humans have, a sensorial

capacity and processing at brain that detect and identify dangerous (e.g. fire in the surroundings) or risky situations (e.g. if you step there you may fall). In fact much of these mechanisms rely on how the brain makes assessment of the environment and what are the present dangers and the risk of following actions. In the current environment, of applications in portable devices, (e.g. smartphones) such equipment should be empowered to identify the situations surrounding us and, eventually, warning us about identified risks in the proximities. That strategy is pursued by the emerging research area on context awareness [3]. Our current research, alike the brain, tries to identify our current physiological situation (e.g. temperature and heartbeat) and that of the surrounding environment (e.g. temperature, humidity) in order to evaluate our current health status and potential risks.

In the next section, the perspective of personal health monitoring powered by cloud with real-time data collection is explored. Section 3 provides research questions and hypothesis in close relation with the ongoing doctoral studies. Section 4 contains a discussion on methodology and concepts proposed by this research work and finally, section 5 presents conclusions and future work.

2 Personal Health Information Management Using the Cloud

Sensors and sensor networks are in expansion with the need to obtain data from persons or from the environment. Devices with the ability to capture data can have different capabilities; they can be standalone (e.g. RFID tags) or be part of a larger setup (e.g. data from meteorological stations). That range of devices includes devices that need to be small and cheaper so that they can be installed in many places (e.g. clothes) but also devices that must operate alone for long periods of time (e.g. car identifiers). That means the need to make those devices as simple as possible with low consumption with consequent constraints in their capabilities. The need for additional computational resources is an identified problem for small sensors and similar devices as they have small or inexistent computational power, they also may be passive, and must have low energy consumption.

The usage of small (and cheaper) low consumption devices, with limited or inexistent computational power, can be empowered by the usage of external resources. For that, the cloud can be a differentiating factor to overcome the limitation of small devices, either sensors or actuators, by providing storage capacity and computational power. The cloud can be used to ensure that sensors can generate data that is stored remotely at the cloud and processed remotely where computational power is available. In what refers to personal health information management, the usage of services at the cloud can provide reasoning over knowledge bases to evaluate a person's health and to generate evaluation reports in real-time [4]. For a person doing normal life, wearable or local sensors can permanently monitor generic activities or a specific exercise (e.g. jogging, playing sports). Data being permanently sent to the cloud can be remotely analyzed and, if dangerous events are identified, the adequate warnings will be issued and, eventually, request medical assistance.

3 Followed Research Method

The observation of the current fitness and eHealth oriented devices and how they are operating makes us to question about its potential usefulness, for users, and how it can be improved. The problems of real-time evaluation of a person and her circumstances lead to the following question.

Research Question: How to adopt lessons learned from the brain and neurophysiology to computing devices in order to monitor, inform and assist users for self-help when necessary?

Hypothesis: We propose, by hypothesis, that if we monitor bodily functions along with environmental condition, it will be possible to establish an overview of a person's health status and warn about potential risks by utilizing computation in cloud.

Background Observation

The brain and the nervous system permanently monitor a person's body. Information is acquired by our sensorial organs, is perceived and interpreted by the brain using existing knowledge, gained by learning and experience. The reasoning is based on a combination of different inputs, acquired by sensorial organs [5], which generate better assessment (e.g. I felt a spike on my feet, the sand is red so i have a cut and I am bleeding). Thus the brain uses multiple inputs to assess if there is danger for the person or if we only need to take care, avoiding multiple attendances to a doctor.

People use many devices that have computational power and embedded sensorial capacities. Smartphones have processing capacities, usually are equipped with a GPS, have a camera and can capture sound. They also have schedulers and planners where people can shape their foreseen activities for the day. Fitness devices provide information about physiological measurements (e.g. heartbeat) and are also capable of determining at what pace you are walking or running and in general the amount of calories being spent [6][7]. Based on all those capabilities, it is possible these days to determine if you are jogging (e.g. reading your electronic scheduler) and measuring your pace, or determine that you are in a work meeting. In those cases, an elevated heartbeat has different interpretations; in one case it is normal that you have higher heart frequency as you are running as in the other case you can be facing some disturbance, as a work meeting is not going as you would like. Using all this information it is possible to make an assessment on the health status of a person and, eventually, warn her to slow exercise or to control their reaction to a meeting.

In summary, with the existing devices and services, it is possible to monitor health status according to the context, and trigger events to inform or warn actions to be executed.

4 Methods and Associated Concepts

In this section we will first address the data processing flow to be followed in the proposed system, which starts with data acquisition from the real world until the actions to be performed in the real world.

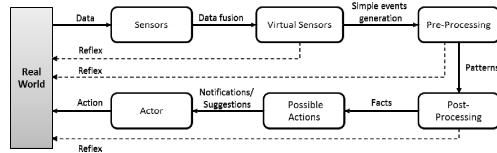


Fig. 1. Data processing flow

Figure 1 shows the data processing flow. In the first step data is captured from the real world by various types of sensors or from other service providers. Thus collected data act as measurement of the parameter under consideration like temperature, humidity etc. In the next step, data infusion is performed leading towards more meaningful state like the temperature and humidity of an object at a particular instant, which leads to the generation of virtual sensors (VS). VVs will have data infusion rules such as if the temperature $> x$ and humidity $< y$ then activate VS. These are useful for generating simple instances of events, with multiple parameters, thus allowing more understanding of the real world and may lead to reflex-like reactions as happens in the human body. The next step termed “Pre-Processing” is used for pattern extraction and will remove the unwanted data from the collected samples of instances thus providing filter over useful data. The patterns detected in this phase are passed to for post-processing, where domain knowledge and rules, are applied over the collected samples to generate facts. Interpretation of facts leads to generation of actions to be taken, over which actors can decide the follow-up procedures.

In the processing flow diagram, we also see that in each stage actions are generated, which we term as “reflex”- immediate response to the state of the real world. In order to act over the reflexes users should use their own knowledge and understanding of the overall scenario. The final actions are suggested based on wider processing of the scenario thus allowing users to respond with lower level of understanding. It is important to define some important concepts for further understanding of the methodology.

Sensor: Sensors are devices that are capable of reading physical and physiological parameters. A sensor S can be defined by a tuple $\langle D, C \rangle$ where D represents data-stream and C the context of the sensor. D will have a data-type and an ordered set of readings obtained at various time which can be represented as $D = \langle DataType, \{R_1, \dots, R_n\} \rangle$. C is used for understanding the contextual use of the sensor and can have an URI to an external Sensor Networks Ontology¹ or can also be linked with other instances of metadata resources.

Virtual Sensor (VS): VS are termed virtual because they don't have physical occurrence but are formed by logical infusion of various sensors. So, a VS can be defined

¹ <http://www.w3.org/2005/Incubator/ssn/ssnx/ssn>

by a relation \odot s.t. $VS = S_x \odot S_y$, where S_x and S_y are sensors as defined previously. The relation \odot can have different syntax and semantics as needed based on the type of data infusion that should be established between sensors. For instance if VS is used for taking into consideration humidity and temperature of a body part (e.g. arm, armpit) at the same time then a one to one union over the reading of the sensors for humidity and temperature will give an ordered set of reading for this new VS . And if the operator is to find the difference of the reading of two sensors (e.g. environment and body temperature) then the ordered difference between each element of the reading of two sensors will give the dataset for the VS . Note that the context of the VS can always be obtained by the union of the individual contexts of the sensors forming the VS .

Complex-Event Processing (CEP): CEP is a widely accepted term which is used to combine data from multiple sources (e.g. sensors or virtual) to infer events by observing specific patterns over observed data. This is important to identify meaningful events or threats by observing a series of patterns and an application of possible rules. For instance if it is observed that a person is having heartbeat above a given threshold and the difference between the outside and body temperature crossed a defined limit, then by comparing to similar patterns recorded as dangerous for that person, a warning is issue signalling that some immediate action has to be taken. Also note that based on the concept of adding context to the sensors and propagated to VS will be determinant for CEP to take into consideration the context of the environment. Same patterns can raise different scenarios in different contexts thus adding more value to the CEP.

For further understanding of the concepts of sensors and VS s, let us consider a simplified scenario in which body temperature, heartbeat and Scheduler is regularly monitored to detect critical situations. Table 1 shows a snapshot of some of the situations.

Table 1. – Data generated by the sensors and analyzed by the framework

Time [H]	9h00	9h30	10h00	10h30	11h00
T_body [°]	36	36.5	37	36.2	36.5
Heartbeat [BPM]	70	110	80	70	90
Scheduler	Jogging	Jogging	Showering	Work	Work
Result	0OK	1OK	2OK	3OK	4Warning

The data are read by individual sensor, which is infused to produce warnings by considering situations that can arise at a particular instance. This can be modelled with the definitions of sensors and VS s given before. Note that context of sensors (which can be position, data type, personal identity etc.) is not considered for simple understanding of the modelling process.

Sensors are:

$$S_{T_body} = \{36, 36.5, 37, 36.2, 36.5\},$$

$$S_{HeartBeat} = \{70, 110, 80, 70, 90\},$$

$$S_{Time} = \{9, 9.30, 10, 10.30, 11\},$$

$$S_{Scheduler} = \{(9, Jogging), (9.30, Jogging), (10, Showering), (10.30, Work), (11, Work)\}.$$

Now VS can be modelled as follows:

$VS_{T_BodyAndHeartBeat} = S_{T_body} \odot S_{HeartBeat}$, \odot is s.t. for $i=1\dots n$ $VS_{T_BodyAndHeartBeat} = \{(x_i, y_i)\}$ where $x_i \in S_{T_body}$ and $y_i \in S_{HeartBeat}$

In our example:

$VS_{T_BodyAndHeartBeat} = \{(36,70), (36.5,110), (37,80), (36.2,70), (36.5,90)\}$

$VS_{TimeAndScheduler} = S_{Time} \odot S_{Scheduler}$, \odot is s.t. for $i=1\dots n$ $VS_{TimeAndScheduler} = \{(z_i)\}$ where $x_i \in S_{Time}$, $(y_i, z_i) \in S_{Scheduler}$ and $x_i=y_i$

So we have: $VS_{TimeAndScheduler} = \{Jogging, Jogging, Showering, Work, Work\}$

We define: $VS_{Warning} = VS_{T_BodyAndHeartBeat} \odot VS_{TimeAndScheduler}$, \odot is s.t. for $i=1\dots n$ $VS_{Warning} = \{(x_i, y_i, z_i)\}$ where $(x_i, y_i) \in VS_{T_BodyAndHeartBeat}$ and $z_i \in VS_{TimeAndScheduler}$ and $x_i > 36$, $y_i > 80$ and $z_i = work$ or $y_i > 150$

Which gives us $VS_{Warning} = \{(36.5, 90, work)\}$

This model shows the fusion of data from sensors and VS to detect warning. The $VS_{Warning}$ thus detects the situation that the person is at work, has body temperature above 36 and heartbeat above 80 or if the heartbeat is above 150. In the scenario as shown in Table 1, this VS issues a warning for the last column, as expected.

4.1 Conceptual Architecture and Technology Adoption

This section will present the conceptual architecture that is being followed for the realization of the system. The system should have layered architecture with well-defined interfaces and clear distinction between the independent components to be implemented at each stage of data processing flow. Figure 2 shows the conceptual architecture with distinct layers divided, with components designated for specific functionality, and a clear demarcation on the cloud and private deployments.

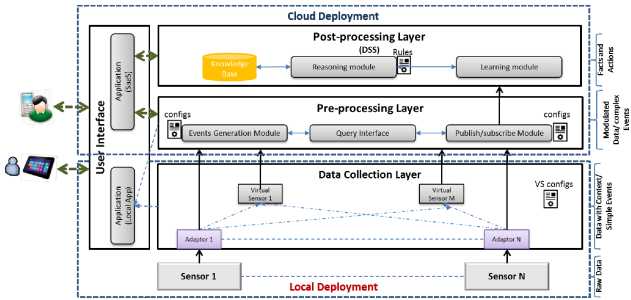


Fig. 2. Conceptual Architecture

Data Collection Layer: This layer is responsible for the collection of data via different sensors deployed in real world. Sensors interact with this layer through the adaptors. Adaptors are sensor specific implementations that act as sink for sensors, the output of which is data streams. The context of the sensor can be registered through admin configuration. This configuration will also define the adaptor for the particular type of sensor. This methodology allows easy integration of the sensor into the system with minimal changes for the new type of sensor. This layer also consists of VSs, which collect data

from the outputs of the adaptors. The operation to be performed on the data for generation of outputs for virtual sensors is defined in the configuration details assigned to the virtual sensor. *VS configs* are the configuration files (XMLs), which will generate a new set of outputs by selecting parameters from other sensors or VSS. Since VS can also be specified with constraints, some simple events (or reflexes) will be generated and notified to the user through local application within the reach of user even in the offline mode.

Pre-Processing Layers: This layer implements CEP functionality and provides a module for publication and subscription to data. It also provides interface to query over data, patterns and events that have been generated by this or lower layers. Events Generation Module is an implementation of CEP and is used for sampling and filtering of data, the rules for which are defined in the configuration file (configs). Publish/Subscribe module acts as a subscriber of events from the data collection layer and publisher for Post-Processing Layer. This module pulls data from the lower layer, passes it to modules for processing and pushes the pre-processed data towards post-processing layer for further treatment. The query interface is utilized by the application for providing notifications and statistics to the user.

Post-Processing Layer: This is a heavy-duty layer of the overall system, where critical processing of the data is performed such as reasoning and learning. This layer makes use of domain knowledge created by experts and reasoning algorithms based on logical reasoning, and/or probabilistic reasoning, to extract new facts for understanding of the overall situation. This layer also implements a learning mechanism to keep the knowledge base updated with new facts generated by automated reasoning. This layer thus acts like a decision support system (DSS) to help the responsible person to have better insight of the real-world scenario.

User-Interface: This layer is used for interaction with the users supported by local applications and applications deployed as SaaS. Local applications are for immediate response and notification of reflexes upon detected events. Other applications are provided as SaaS, in the cloud, and deliver detailed analysis of the scenario, historical data and suggested actions to be taken. The 'admin' functionality allows configuration changes of the sensors and virtual sensors. The applications can be configured to trigger alarms to the user, case an emergency situation is detected.

4.2 Technology Adoption

For the purpose of system implementation this research work adopts services and enablers, being developed by projects, under the European FI-PP program like FI-WARE² and FITMAN³, which provide enablers for data acquisition from the physical

² <http://www.fi-ware.org/>

³ <http://www.fitman-fi.eu/>

world, complex event processing, context aware data handling, data analysis etc. Shop-floor Data Collection⁴ (SFDC) is the implementation for data collection from various sensor networks (protocol agnostic methodology), and also for integration of tagged objects into the system. SFDC implements creation and configuration of the VSs and provides adaptors for some standard sensors with easy integration of new types of sensors. VSs are created by writing XML with defined schema. Complex Event Processing (CEP)⁵ and Publish/Subscribe Context Broker⁶ are configured and used in the data pre-processing layer. Both of these enablers are the important components, which are adapted for the realization of events generation and publish/subscribe modules respectively. In the implementation of post-processing layer it is very important to consider knowledge extraction over real time data, which we have adopted from some current research work as described in [8] and [9]. This module also makes use of ANN with semantics for implementing probabilistic learning algorithm, which have been inspired by some works as described in [10] and [11].

5 Concluding Remarks and Future Work

Research presented in this paper has potential impact in many societal and business aspects. New business models can be deployed to support real-time monitoring as proposed and, from the human side, a citizen can be monitored and assisted while performing a normal life. As by research presented in this paper, those objectives can be achieved by building computational methodology to integrate sensorial data and their interpretation, generating advice or asking for support as needed. This research work provides a framework for raw data collection from real world and multi-stage processing of data leading towards automated understanding of the surrounding. Proposed methodology will leverage cloud computing to utilize open linked data in the domain of health and big data processing for more reliable self-help health monitoring services. On-going validation and iterative testing of the implemented system in real scenarios is the most important task to be completed in a near future.

Acknowledgments. The research leading to these results has received funding from the EC 7th Framework Programme under grant agreement FITMAN nr 604674 (<http://www.fitman-fi.eu>).

⁴<http://catalogue.fitman.atosresearch.eu/enablers/shopfloor-data-collection>

⁵<http://catalogue.fi-ware.org/enablers/complex-event-processing-cep-ibm-proactive-technology-online>

⁶<http://catalogue.fi-ware.org/enablers/publishsubscribe-context-broker-orion-context-broker>

References

1. Sundmaecker, H., Guillemin, P., Fries, P., Woelfflé, S.: Vision and Challenges for realising the Internet of Things. European Commission (2010)
2. Luis-Ferreira, F., Jardim-Goncalves, R.: A behavioral framework for capturing emotional information in an internet of things environment. In: 11th International Conference of Numerical Analysis and Applied Mathematics, ICNAAM 2013, vol. 1558(1), pp. 1368–1371 (2013)
3. Abowd, G.D., Dey, A.K.: Towards a better understanding of context and context-awareness. In: Gellersen, H.-W. (ed.) HUC 1999. LNCS, vol. 1707, pp. 304–307. Springer, Heidelberg (1999)
4. Luis-Ferreira, F.: A pervasive computing framework supported by the cloud for personal health management. In: Proceedings of CE 2014 (2013)
5. Oie, K.S., Kiemel, T., Jeka, J.J.: Human multisensory fusion of vision and touch: detecting non-linearity with small changes in the sensory environment. *Neurosci. Lett.* **315**(3), 113–116 (2001)
6. Fitbit® Flex, One & Zip Wireless Activity & Sleep Trackers. <http://www.fitbit.com/> (accessed on June 30, 2013)
7. Nike+ FuelBand. Tracks your all-day activity and helps you do more.. Nike.com. http://www.nike.com/us/en_us/c/nikeplus-fuelband (accessed on June 29, 2013)
8. Angelov, P.: Nature-Inspired Methods for Knowledge Generation from Data in Real-Time (2006). <http://www.nisis.risk-technologies>
9. Gama, J., Rodrigues, P.: Knowledge discovery from data streams (2010)
10. Mikolov, T., Zweig, G.: Context dependent recurrent neural network language model. *SLT* (2012)
11. Bowman, S., Potts, C., Manning, C.: Recursive Neural Networks for Learning Logical Semantics, pp. 1–10. arXiv Prepr. arXiv1406.1827 (2014)

Renewable Energy

Optimal Generation Scheduling of Wind-CSP Systems in Day-Ahead Electricity Markets

H.M.I. Pousinho^{1,2(✉)}, P. Freire³, J. Esteves³, V.M.F. Mendes^{1,3},
C. Pereira Cabrita⁴, and M. Collares-Pereira¹

¹ University of Évora, Évora, Portugal,

hpousinho@gmail.com, collarespereira@uevora.pt

² IDMEC/LAETA, Instituto Superior Técnico, Universidade de Lisboa, Lisbon, Portugal

³ Instituto Superior of Engenharia de Lisboa, Lisbon, Portugal

vfmendes@deea.isel.pt

⁴ CISE, University of Beira Interior, R. Fonte do Lameiro, 6201-001 Covilhã, Portugal,
cabrita@ubi.pt

Abstract. This paper presents a coordination approach to maximize the total profit of wind power systems coordinated with concentrated solar power systems, having molten-salt thermal energy storage. Both systems are effectively handled by mixed-integer linear programming in the approach, allowing enhancement on the operational during non-insolation periods. Transmission grid constraints and technical operating constraints on both systems are modeled to enable a true management support for the integration of renewable energy sources in day-ahead electricity markets. A representative case study based on real systems is considered to demonstrate the effectiveness of the proposed approach.

Keywords: Concentrated solar power · Wind power · Mixed-integer linear programming · Transmission constraints

1 Introduction

Renewable energy grid integration increased in the E.U. to fulfill the Energy – 2020 initiative. Energy efficiency improvement, renewable technologies and lower emissions are priorities to ensure environmental sustainability [1]. Wind power systems and concentrated solar power (CSP) systems are engaged in the meeting of demand increase in the Southern Mediterranean, profiting from favorable renewable energy sources. But, the non-controllable variability and limited predictability of the energy source of these systems [2] conveys real-time uncertainty posing capacity planning challenges related to the tuning of ancillary services needed to ensure system stability and reliability [3]. Also, real-time uncertainty on renewable energy availability can increase costs if an unfitting prediction occurs. Hence, a coordination approach seems to be an adequate required option in order to reduce the uncertainty in power output. The wind-CSP systems coordination is a reliable option, enabling to accommodate energy integration into the power grid and day-ahead electricity markets [4], as well

as to increment the dispatchability attribute on the accommodation. The non-dispatchable characteristic of CSP systems is lessened with thermal energy storage (TES) systems, enabling plant base load support. TES not only allows offsetting generation deficit during non-insolation periods, reducing real-time net generation variability, but also allows shifting of generation towards appropriate periods [5]. TES has proved to be a reliable option [6], allowing control on the energy, improving the capacity value and profits. Moreover, TES further increments the dispatchability and can reduce the running of conventional thermal power plants in short-term ancillary services [7], reducing the need for spinning, implying a noted reduction in reserve costs. Also, TES allows reducing high marginal cost units when an unpredicted drop in renewable energy input occurs. Therefore, the line of research of coordination approach for wind-CSP having TES systems is regarded as an important promising one offering new technical challenges to the researchers and this paper presents a contribution on this regard.

The paper presents a mixed-integer linear programming (MILP) model for solving the generation scheduling problem of wind-CSP having TES systems. The aim is to achieve the optimal generation schedule that maximizes the profit of a power producer taking part in a day-ahead electricity market. The optimization approach considers not only transmission line constraints, but also technical operating constraints on wind power systems and on CSP systems to enable a true management support for the integration of renewable energy sources in day-ahead electricity markets.

2 Relationship to Cloud-Based Solutions

Cloud-based solutions can help the processing of approaches for helping trading in a day-ahead electricity market in order to take greater advantages of bids, requiring methodological approaches demanding computational effort not currently available to all power producers. Among these approaches the ones for the solution of the problems concerned with scheduling: energy management, unit commitment and energy offers are particular vital for upholding power producers. The approaches to solve these problems have been limited by the available computational resources, i.e., details concerning some reality are disregard in view of the excessive use of processing requirements. These limitations are evident for large systems and lead to solutions not addressed in convenient agreement with the reality, because the computational resources do not allow the usage of data or modeling for delivering more real adequate solutions.

Cloud-based solutions are able to contribute for upholding a power producer exploiting wind-CSP systems by setting out an adequate availability of computational resources needed to address scheduling problems in due time. Although of the uncertainty on the wind and solar power, i.e., intermittency and variability, cloud-based engineering systems will deal with problems having a better approach to the full reality in due time with gains in terms of profit. Cloud-based solutions will help on the smoothing of the electricity price due to the fact of having bids of wind power with higher level of energy and with more certainty in what regards the satisfaction on

delivering the electric energy accepted at the closing of the market. Also, environmental benefit is expected with mitigation of the deviation from the assumed compromises by a better finding of offers able of fulfillment, less spinning reserved is needed, less thermal units are needed and less fossil fuel is used. Eventually, cloud-based solutions will allow approaches in order that when a power producer exploiting a wind-CSP systems at site has renewable energy available is all captured to be converted into electric energy injected without concerns on dynamic stability into the power grid in due time.

3 State of the Art

The literature on optimal scheduling is still rapidly growing. Coordination strategies and optimization approaches for short-term scheduling have been are in research, for instances: a envisaged wind-thermal coordination via simulated annealing unveiled an improvement of smoothing the active power fluctuations [8], and one via MILP unveiled a reduction of the uncertainty in wind power output [9]; a envisaged coordination of wind power with compressed air energy storage unveiled an improvement due to the synergies between wind power and compressed air energy storage [10]; a envisaged wind and hydro power coordination, specially pumped-storage hydro power systems [11,12], unveiled an improvement on minimization of curtailment, energy imbalance and dispatchability. Furthermore, electrical vehicles connection to the power grid are expected to be used as controllable loads and a convenient operation with suitable market design may help in the accommodation more wind power [13].

Coordination strategies have unveiled progress in reducing of the uncertainty of wind power output by the use of different dispatchable resources or loads, even though resources may not be installed in the same region of wind power systems deployment. But, when the surrounding of the load centres has attractive conditions of wind speed and solar irradiation, wind-CSP is an option design to be considered. This option enables a better accommodation of energy integration into the power grid and day-head electricity markets [14], as well as to increase the dispatchability attribute on the accommodation. The scheduling proposed in this paper is based on a MILP approach, which has been a successful approach for solving scheduling problems in general. So, also is expected to be one to help support decisions in a day-head electricity market.

4 Problem Formulation

The scheduling is computed by the maximization of the objective function given by the profit subject to transmission and systems constraints.

4.1 Objective Function

The profit is equal to the revenues from day-ahead electricity market sales and wind production incentive rate minus the CSP variable costs during the time horizon of the schedule. The objective function to be maximized is given as follows:

$$F = \sum_{k \in K} \left[\pi_k^{da} (p_k^s - p_k^b) + \sum_{i \in I} \xi p_{i,k}^{Wind} - \sum_{c \in C} \beta_c p_{c,k}^{CSP} \right] \tag{1}$$

In (1), K is the set of hours in the time horizon, π_k^{da} is the forecasted day-ahead market price in hour k , p_k^s is the power sold to day-ahead electricity market in hour k , p_k^b is the power purchased from day-ahead electricity market in hour k , I is the set of wind turbines, ξ is the wind production incentive rate, $p_{i,k}^{Wind}$ is the power output of the wind turbine i , C is the set of CSP systems, β_c is the variable cost of the CSP system c and $p_{c,k}^{CSP}$ is the power output of the CSP system c in hour k .

4.2 Constraints

The constraints for the scheduling are due to the transmission grid, operation of wind systems, operation or minimum up/down time of CSP systems.

Transmission Grid

The transmission grid constraints are given as follows:

$$(1 - \psi)^{-1} p_k^s - (1 - \psi) p_k^b = \sum_{i \in I} p_{i,k}^{Wind} + \sum_{c \in C} p_{c,k}^{CSP} \quad \forall k \tag{2}$$

$$-\chi \leq (1 - \psi)^{-1} p_k^s - (1 - \psi) p_k^b \leq \chi \quad \forall k \tag{3}$$

$$0 \leq \sum_{i \in I} p_{i,k}^{Wind} + \sum_{c \in C} p_{c,k}^{CSP} \leq \chi \quad \forall k \tag{4}$$

$$0 \leq p_k^s \leq \chi y_k \quad \forall k \tag{5}$$

$$0 \leq p_k^b \leq \chi(1 - y_k) \quad \forall k \tag{6}$$

In (2) to (6), ψ is the transmission loss, χ is the transmission capacity, and y_k is a 0/1 variable. In (2), the electric power balance is enforced between the day-ahead electricity market trading with wind power systems and CSP systems. In (3) and (4), the electric power bounds are set for the transmission line. In (5) and (6), the energy flow in the line is set infeasible for simultaneously trading by selling and purchasing.

Operation of Wind Systems

The operational constraints of wind power system are given as follows:

$$0 \leq p_{i,k}^{Wind} \leq W_{i,k} \quad \forall i, k \tag{7}$$

$$0 \leq p_{i,k}^{Wind} \leq \overline{P}_i^{Wind} \quad \forall i, k \quad (8)$$

where $W_{i,k}$ is the scheduled of wind turbine i in hour k , and \overline{P}_i^{Wind} is the wind turbine i power bound. In (7), the operating limits for the scheduled wind power of each wind turbine i are set. In (8), the maximum power capacity of each wind turbine i is set.

Operation of CSP Systems

The operational constraints of CSP systems are given as follows:

$$p_{c,k}^{CSP} = p_{c,k}^{FE} + p_{c,k}^{SE} - X_c \quad \forall c, k \quad (9)$$

$$p_{c,k}^{FE} = \eta_1 q_{c,k}^{FE} \quad \forall c, k \quad (10)$$

$$p_{c,k}^{SE} = \eta_3 q_{c,k}^{SE} \quad \forall c, k \quad (11)$$

$$\underline{Q}_c^{PB} u_{c,k} \leq q_{c,k}^{FE} + q_{c,k}^{SE} \leq \overline{Q}_c^{PB} u_{c,k} \quad \forall c, k \quad (12)$$

$$q_{c,k}^{FE} + q_{c,k}^{FS} \leq S_{c,k} \quad \forall c, k \quad (13)$$

$$q_{c,k}^S = q_{c,k-1}^S + \eta_2 q_{c,k}^{FS} - q_{c,k}^{SE} \quad \forall c, k \quad (14)$$

$$\underline{Q}_c^S \leq q_{c,k}^S \leq \overline{Q}_c^S \quad \forall c, k \quad (15)$$

$$\underline{Q}_c^{FE} \leq q_{c,k}^{FE} \leq \overline{Q}_c^{FE} \quad \forall c, k \quad (16)$$

$$0 \leq p_{c,k}^{CSP} \leq \overline{P}_c^{CSP} \quad \forall c, k \quad (17)$$

$$p_{c,k}^{SE} - p_{c,k+1}^{SE} \leq RD_c^T \quad \forall c, k = 0, \dots, K-1 \quad (18)$$

$$\eta_2 (q_{c,k+1}^{FS} - q_{c,k}^{FS}) \leq RU_c^T \quad \forall c, k = 0, \dots, K-1 \quad (19)$$

$$0 \leq p_{c,k}^{SE} \leq M z_{c,k} \quad \forall c, k \quad (20)$$

$$0 \leq p_{c,k}^{FS} \leq M (1 - z_{c,k}) \quad \forall c, k \quad (21)$$

$$p_{c,k}^{FE}, p_{c,k}^{SE}, q_{c,k}^{FE}, q_{c,k}^{SE} \geq 0 \quad \forall c, k \quad (22)$$

In (9) to (21), $p_{c,k}^{FE}$ and $p_{c,k}^{SE}$ are the power produced by the solar field (SF) c and the TES c in hour k , X_c is the parasitic power of the CSP plant c , η_1 is the SF efficiency, $q_{c,k}^{FE}$ is the thermal power from the SF c in hour k , η_3 is the molten-salt tanks efficiency, $q_{c,k}^{SE}$ is the storage power in TES c to produce electricity in hour k , \underline{Q}_c^{PB} and \overline{Q}_c^{PB} are the thermal power bounds of the power block of CSP plant c , $u_{c,k}$ is the CSP plant c commitment in hour k , $q_{c,k}^{FS}$ is the thermal power from the SF c stored in hour k , $S_{c,k}$ is the thermal power produced by the SF c in hour k , $q_{c,k}^S$ is the thermal

energy stored in TES c at the end of hour k , η_2 is the TES efficiency, Q_c^S and \overline{Q}_c^S are the TES c thermal energy bounds, Q_c^{FE} and \overline{Q}_c^{FE} are the thermal power bounds from the SF c , \overline{P}_c^{CSP} is the CSP plant c power bound, RD_c^T and RU_c^T are the ramp-up and ramp-down limits for charging and discharging the stored energy of TES c , M is a sufficiently large constant $M \geq \overline{P}_c^{CSP}$, and $z_{c,k}$ is the 0/1 variable equal to 1 if TES c discharges power in hour k . In (9), the electric power balance is enforced between the power output of CSP system with the electric power produced from the SF, the storage and the parasitic power needed for maintaining the molten-salt fluid in operation conditions. This parasitic power occurs even if a CSP system is not operating, eventually implying that if the producer has not enough energy available, a small quantity of energy is soaked up from the grid, incurring on an associated cost. The parasitic power is assumed constant. In (10) and (11), the electric power from the SF and TES is considered dependent on the efficiencies associated with the thermal power of the SF and the storage power, respectively. In (12), the bounds for the sum of the power from the SF and TES are set. In (13) and (14), the balance of the thermal power in the SF and the energy stored in the TES is set, respectively. In (15), the bounds for the thermal power storage in the TES are set in order to avoid the solidification of salts and the maximum storage capacity to be exceeded. In (16), the bounds for the thermal power from the SF are set. In (17), the bounds for the power output of the CSP systems are set. In (18) and (19), the charge and the discharge ramp rates of the TES are set, respectively. In (20) and (21), power restrictions are set to prevent simultaneous discharging and charging of the TES in the same hour, imposed by the 0/1 variable, z_k .

Minimum Up/Down Time of CSP Systems

The minimum up/down time constraints of CSP systems are given as follows:

$$\sum_{r=k-UT_c^{SF+T}+1, r \geq 1}^k (u_{c,r} - u_{c,r-1}) \leq u_{c,k} \quad \forall c, k = L^{SF+T} + 1, \dots, K \quad (23)$$

$$\sum_{r=k-DT_c^{SF+T}+1, r \geq 1}^k (u_{c,r-1} - u_{c,r}) \leq 1 - u_{c,k} \quad \forall c, k = F^{SF+T} + 1, \dots, K \quad (24)$$

In (23) and (24), the minimum up/down times for the CSP system c are set based on [18], where $L_c^{SF+T} = \min[K, UT_c^{SF+T}]$ and $F_c^{SF+T} = \min[K, DT_c^{SF+T}]$.

5 Case Study

The case study is intended to show the advantages of the coordination between wind power systems and CSP systems having TES. These advantages are coming from the synergies between both systems and the adequate optimal mix of synergies is in favor of the proposed approach. The MILP for the approach has been solved using

CPLEX 12.1 solver under GAMS environment [15]. A computer with 8 GB RAM with 2.30 GHz of CPU is used for the simulations of realistic case studies based on a Iberian wind-CSP system with 40 wind turbines, $i = 1, \dots, 40$, and 2 CSP plants, $c = 1, 2$ and carried out with technical data shown in Table 1.

Table 1. Wind-CSP system data

$\underline{P}_i^{Wind} / \overline{P}_i^{Wind}$	$\underline{P}_c^{CSP} / \overline{P}_c^{CSP}$	$\underline{Q}_c^S / \overline{Q}_c^S$ (MWht)	$\underline{Q}_c^{FE} / \overline{Q}_c^{FE}$ (MWt)
0 / 2	0 / 50	45 / 700	0 / 150
$\underline{Q}_c^{PB} / \overline{Q}_c^{PB}$ (MWt)	$q_{c,0}^S$ (MWht)	RU_c^T / RD_c^T (MWe/h)	$UT_c^{SF+T} / DT_c^{SF+T}$ (h)
50 / 125	120	35 / 80	2 / 2

All wind power systems have the same data as well as CSP systems, respectively. The installed wind power capacity is 80 MW and for CSP is 100 MWe. The systems share a transmission line connecting to the power grid. This line has 3 % of losses and exported power is assumed to be between 50 MW and 130 MW. The module efficiencies for the CSP systems are respectively: 1) $\eta_1 = 0.40$; 2) $\eta_2 = 0.35$; 3) $\eta_3 = 0.80$. The parasitic power is 3.5 MWe and the wind production incentive rate is assumed to be of 35 €/MWh.

The time horizon in the simulations is a day on an hourly basis, corresponding to a participation in a day-ahead electricity market. Within the time horizon are considered as input data not only the solar and the wind power profiles, but also the day-ahead market prices profile. The solar irradiation profile derived from the System Advisor Model [16] was converted into available thermal power. The wind power profile is derived from the ANN forecaster designed in [17]. The wind power and thermal power output profiles respectively are assumed to be the same for each wind turbine and CSP systems as is shown in Fig. 1.

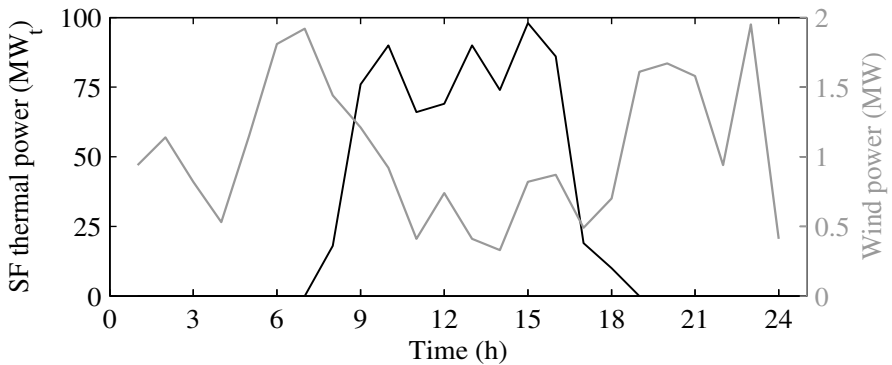


Fig. 1. SF thermal and wind power profiles

The scheduling problem for the wind-CSP coordination has a day-ahead time horizon, due to this short horizon, the energy market prices can be assumed as deterministic input data given by forecast average prices. The prices of the Iberian electricity market given in [18] are used in the case study and shown in Fig. 2.

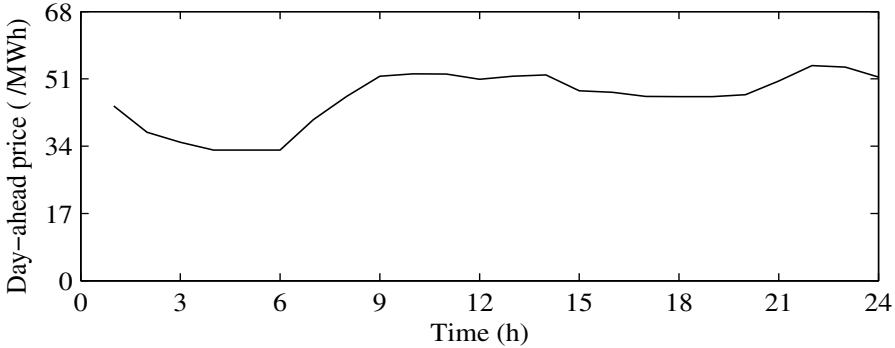


Fig. 2. Day-ahead energy market prices

A summary of the optimizing characteristics for processing the problem presented in the case study in what regards the number of constraints, continuous variables, binary variables and computation times is shown in Table 2.

Table 2. Optimizing characteristics of the case study

#	Constraints	Continuous variables	Binary variables	CPU time (s)
Case study	1,436	864	120	8

The number of installed wind turbines and CSP systems having TES are 20 and 2, respectively. The total installed capacities of wind power systems and CSP systems having TES are 80 MW and 100 MW_e, respectively. The energy and profit for the transmission line capacity of $\chi=60$ MW and $\chi=130$ MW associated with the enforced system are shown in Table 3.

Table 3. Energy and profit in function of transmission capacity

#	Transmission capacity (MW)	Energy stored (MWh)	Energy sold (MWh)	Profit (€)
Case study	60	6,405	1,259	83,527
	130	6,269	1,544	95,673

Table 3 allows a comparison between the profits, revealing a reduction of about 15% for $\chi=60$ MW. Table 3 shows that an increase in the transmission line capacity of the line allows to make a better use of the energy stored, allowing an augmented profit.

The optimal schedule for the wind-CSP coordination in what regards the assessing of the impact of transmission line constraints with $\chi = 60$ MW and with $\chi = 130$ MW are respectively shown in Fig. 3 (a) and (b).

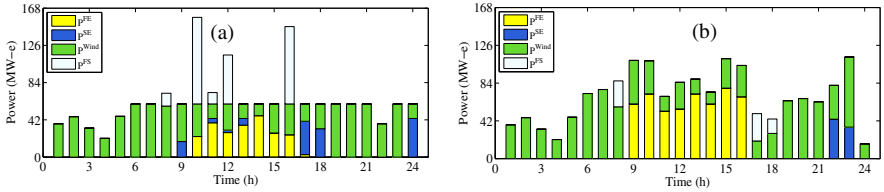


Fig. 3. Coordination for transmission capacities: (a) $\chi = 60$ MW; (b) $\chi = 130$ MW

Fig. 3 (a) shows for the high price hours a significant CSP production in comparison with low price hours. The benefit of TES shifting the production is revealed and the excess energy eventually overloading transmission from hours 8, 10 to 12 and 16 is able to be stored for a convenient discharge at hours 11 to 13, 17, 18 and 24. Additionally, the synergies between wind energy and solar energy allows for the possibility of enhancing the scheduling due to the negative correlation. Thus, an efficient energy schedule is obtained, illustrating the proficiency of the optimization approach for accommodating this deployment with different changing patterns of renewable energy in a power grid. The thermal energy storage shows the significance of the line capacity regarding the storage in the TES. For instance, the increase in the line capacity raises the level of the storage in the low prices hours with solar thermal power in order to be conveniently used during the other hours. If the capacity factor is incremented by downsizing the transmission capacity, then curtailment is to be expected and consequent decrease of the energy produced. The thermal energy storages in function of the transmission capacity and of the time are shown in Fig. 4.

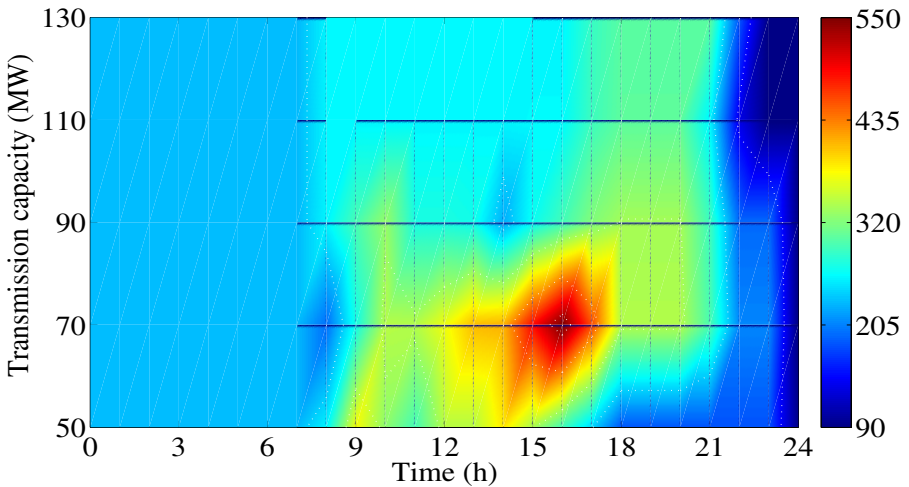


Fig. 4. Thermal energy storages in function of transmission capacity and over the time horizo

6 Conclusions

An approach based on MILP is proposed for the coordination problem of wind-CSP having TES systems and for supporting decisions of participating in day-ahead markets, taking into account transmission line constraints and prevailing technical operating ones for the wind power, CSP and TES. The approach reduces uncertainty and improves the integration of more energy into a grid due to the convenient optimal mix of synergies. The TES is effectively handled to improve the operational productivity. The case studies are in favour of the approach to support decisions in day-ahead markets.

Acknowledgements. This work was supported by Fundação para a Ciência e a Tecnologia (FCT), through IDMEC under LAETA, Instituto Superior Técnico, Universidade de Lisboa, Portugal.

References

1. Energy 2020 – A strategy for competitive, sustainable and secure energy (2011). <http://europa.eu>
2. Taylor, J.A., Callaway, D.S., Poolla, K.: Competitive energy storage in the presence of renewables. *IEEE Trans. Power Syst.* **28**, 985–996 (2013)
3. Lannoye, E., Flynn, D., O’Malley, M.: Evaluation of power system flexibility. *IEEE Trans. Power Syst.* **27**, 922–931 (2012)
4. Sioshansi, R., Denholm, P.: The value of concentrating solar power and thermal energy storage. *IEEE Trans. Sust. Energy* **1**, 173–183 (2010)
5. Dominguez, R., Baringo, L., Conejo, A.J.: Optimal offering strategy for a concentrating solar power plant. *Applied Energy* **98**, 316–325 (2012)
6. Madaeni, S.H., Sioshansi, R., Denholm, P.: How thermal energy storage enhances the economic viability of concentrating solar power. *Proc. IEEE* **100**, 335–347 (2012)
7. García-González, J., de la Muela, R.M.R., Santos, L.M., González, A.M.: Stochastic joint optimization of wind generation and pumped-storage units in an electricity market. *IEEE Trans. Power Syst.* **23**, 460–468 (2008)
8. Chen, C.-L.: Simulated annealing-based optimal wind-thermal coordination scheduling. *IET Gener. Transm. Distrib.* **1**, 447–455 (2007)
9. Kamalinia, S., Shahidehpour, M.: Generation expansion planning in wind-thermal power systems. *IET Gener. Transm. Distrib.* **4**, 940–951 (2010)
10. Daneshi, H., Srivastava, A.K.: Security-constrained unit commitment with wind generation and compressed air energy storage. *IET Gener. Transm. Distrib.* **6**, 167–175 (2012)
11. de la Nieta, A.A.S., Contreras, J., Munoz, J.I.: Optimal coordinated wind-hydro bidding strategies in day-ahead markets. *IEEE Trans. Power Syst.* **28**, 798–809 (2013)
12. Khodayar, M.E., Shahidehpour, M., Wu, L.: Enhancing the dispatchability of variable wind generation by coordination with pumped-storage hydro units in stochastic power systems. *IEEE Trans. Power Syst.* **28**, 2808–2818 (2013)
13. Li, Z., Guo, Q., Sun, H., Wang, Y., Xin, S.: Emission-concerned wind-EV coordination on the transmission grid side with network constraints: Concept and case study. *IEEE Trans. Smart Grid* **4**, 1692–1704 (2013)

14. Usaola, J.: Operation of concentrating solar power plants with storage in spot electricity markets. *IET Renew. Power Gener.* **6**, 59–66 (2012)
15. Cplex, Gams, Solver manuals. Gams/Cplex (2014). <http://www.gams.com>
16. Catalão, J.P.S., Pousinho, H.M.I., Mendes, V.M.F.: An artificial neural network approach for short-term wind power forecasting in Portugal. *Eng. Intell. Syst. Electr. Eng. Commun.* **17**, 5–11 (2009)
17. National Renewable Energy Laboratory, USA, Solar Advisor Model User Guide for Version 2.0 (2008) <http://www.nrel.gov/docs>
18. Market operator of the electricity market of the Iberian Peninsula, OMEL (2014). <http://www.omel.es>

Influence of Large Renewable Energy Integration on Insular Grid Code Compliance

Eduardo M.G. Rodrigues¹, Radu Godina¹, Tiago D.P. Mendes¹,
João C.O. Matias¹, and João P.S. Catalão^{1,2,3(✉)}

¹ University of Beira Interior (UBI), Covilha, Portugal

² INESC-ID, Lisbon, Portugal

³ Instituto Superior Técnico, Lisbon, Portugal
catalao@ubi.pt

Abstract. Large-scale deployment of renewables in island energy systems attracts local attention of grid operators as a way of reducing fuel fossil consumption. Planning a grid based on renewable power plants poses serious challenges to the normal operation of a power system, namely on frequency and voltage stability. In past grid code compliance, wind turbines did not require services for supporting grid operation. To shift to large renewable energy integration, the island grid code should incorporate a new set of requirements in order to regulate the inclusion of these services, which is the aim of this paper. The paper also discusses additional requirements such as “virtual” wind inertia.

Keywords: Grid codes · Renewables penetration · Insular energy systems · Smart grid · Cloud computing

1 Introduction

Renewable integration (especially wind energy) on mainland energy systems has been increasing significantly in the last decade [1]. However the penetration rate in insular energy systems is still low. Presently, high penetration of renewables is considered extremely challenging for normal grid operation by the local grid operators. Typically the islanded energy system has a small size, low interconnections and not a high short-circuit ratio (SCR). Therefore, it is more vulnerable to frequency and voltage stability issues [2] and since the generation units cannot be very large, its robustness is ensured by maintaining large reserve capacity, which raises electricity generation costs. Local grid operators are now aware that there is a significant potential for exploring renewable energy resources, which could reduce external dependency on imported fossil fuel [3]. However, it is well known that the intermittent nature of wind and solar energy cannot be controlled. This variability on seasonal and daily basis has been seen as a serious obstacle for large scale installation of renewable power plants. This paper discusses grid code requirements for large-scale integration of renewables in an island context as a new contribution to earlier studies.

2 Contribution to Cloud-Based Engineering Systems

Future insular power systems that rely on a heavy mix of distributed energy resources (DER) will require managing tools based on real-time monitoring, controlling and high computational power resources. Cloud computing proposes advances services which allow to use its massive computation power ability and the scalabilities relying on large scale servers that host the web services and web application. Similarly, cloud computing can provide physical or virtual resources on which the insular power system applications can run. On the DER point of view, local hardware facilities for executing specific software programs become practically residual. Thus, it reduces the installation and maintenance costs. Via a cloud structure each client can always access its respective applications or data, out from anyplace and by a connected device to the network. In addition, it provides a common platform for sharing data which drives increased cooperation between insular grid parties. On the other hand, for the network operator side, cloud-based grid management services create a unique framework for the design and implementation of a centralized structure for their distributed monitoring and control tasks. Therefore, by integrating cloud-based engineering systems in the insular power grid infrastructure, an efficient, reliable and secure energy distribution can be accomplished.

3 Island Power Generation System Overview

The island power generation infrastructure typically consists of diesel generators, small groups of thermal power plants, and may include natural hydro or thermal sources based production. Basically there are two types of units. One class of generators runs at constant output, known as base load units, while another group of generators has the function of adapting its output following the load needs. Wind and solar generators do not fit in any of these two groups because they are not flexible load following units. Generators like load following units are designed to operate with variable output. Moreover, this type of flexible generation must maintain a considerable amount of active power reserve for frequency regulation. In an island energy system this reserve is much more critical because conventional plants have a smaller size when compared to power installations in the mainland energy system. Replacing flexible load following units by renewable generating units implies that there will likely be less kinetic energy exchange to support grid power balance, resulting in a degradation of frequency regulation capability, which in turn may imply larger and faster frequency deviations [4]. Hence, the minimum level of conventional generation and concerns about grid stability creates a practical restriction on planning more renewables integration [5]. Even in low penetration scenarios, it is not uncommon to see power curtailment actions by the system operator to face renewable power excess on the grid, or even shutting down the wind farm due to a grid disturbance. However, the revenue lost due to curtailment or disconnection may be greater than the cost of maintaining conventional generation. To accelerate renewable integration, wind and solar farms should replicate conventional power plants during

and after network faults [6]. To become effective, island regulations must be updated to impose this strict operation profile. Grid code requirements have been studied for large wind farms integration in mainland systems [7]-[10]. Yet, technical literature focusing on island grid codes requirements is still very scarce and, therefore, this paper provides a new contribution to this issue. In essence, present insular regulations do not allow the grid operator to control distributed energy resources (DER). The coordination between transmission system operator (TSO) and distribution system operator (DSO) is insufficient for the effective DER integration. The lack of adequate regulation for DER systems connection is also a reality. Further, DER does not have any economic incentive to take part in the network operation. All these issues are taken into account in this paper.

4 Grid Code Requirements for DER

A grid code serves the mission of defining the physical connection point requirements to be followed by energy production equipment in order to connect to the grid. In addition it should provide rules for renewable power plants to support grid stability.

4.1 Regulations for Continuous Operation

A residual balance mismatch is fairly normal which may result in over-frequency as well as under-frequency. With intermittent generation at larger-scale, the balancing game becomes more complex and less predictable. A proactive attitude is required regarding DER system to cope with these issues through a well-defined specifications-based behavior.

Voltage and Frequency Operation. Renewable power plants must stay connected to the grid and able to withstand voltage and frequency variation limits established by the island grid system operator. Voltage range is related to the size of the transmission system, which is characterized by different voltage levels. Frequency nominal range is determined by the electrical characteristics of the insular energy system, such as overall inertia of the installed power generation infrastructure. Renewable power sources must also face voltage and frequency deviations outside the conventional range during a short time period and without being tripped.

Active Power Regulation. It is a set of power control strategies that gives freedom and flexibility to the system operator to manage the power output injected into the grid by renewable power plants. Wind and solar power plants should comply with this requirement. As the renewable generation is increased, active power regulation requirements become indispensable on island grid codes.

a) Maximum power limitation

This parameter has the purpose of setting the maximum power output of renewable generation below its power rating. By restricting the maximum amount of power injection, the system operator has a way to prevent more instabilities of active power balance due to the unpredictable nature of wind and solar resources.

b) Active power range control

Renewables cannot deliver dispatchable power on demand. The goal is to replicate traditional power sources that are fully controllable. Renewable generating units should be prepared to curtail artificially the power production to maintain power balance and also, if necessary, to contribute to the stabilization of grid frequency. Both requirements have different implementation scopes. The first one permits the TSO to introduce output power dispatch flexibility on wind power plants (WPP) and on solar power plants (SPP). The second is basically extending primary control function to the renewable plants.

c) Ramp rate limitation

Limiting the power gradient of renewable power through a set-point can be a very effective way to minimize the impact of a sudden rise of renewable generation. Ramp rate is defined as the power change from minute to minute (MW/min). The idea of this concept is to filter faster variations of wind power output by imposing a ramp rate according to the changes observed on power demand.

d) Delta control

It is a way of securing spinning reserve based on renewable power generation. Power output is artificially lowered, below the available power at the moment of generation. The difference is kept as reserve to be used like a conventional generation does (primary and secondary control). However, the curtailed power depends on available wind or solar power. Thus, the level of reserve is not constant. The curtailed power can be released not only for frequency regulation, but also to maintain the voltage of the overall system through the injection of reactive power to grid.

Power-Frequency Response. When an energy unbalance occurs the frequency deviates from its nominal value. As the unbalance grows a large deviation of frequency is expected to happen, threatening normal power network operation. In order to confine deviation extension to safe levels, frequency surveillance and corrective actions are performed by conventional generators (primary control) along with grid operator supervision and, if necessary, authorizes spinning reserve release (secondary control). For the specific case of European islands, frequency regulation capability compliance is not specified by local grid codes. Wind farms able to restore generation/demand balance are already required in some European countries. Typically, a mainland TSO imposes a frequency regulation strategy through a power frequency curve specification only addressing wind power plants operation. Nevertheless, no compliance is directly demanded for solar power plants on these regulations. Since insular grid codes in European space didn't yet evolved to require this behavior, formal analyses have to be carried out observing the most advanced specifications at non-insular territories. Fig. 1 shows power-frequency response curves required in Ireland, Germany and Denmark [11]-[13]. It is clear that frequency support behavior differs from country to country. The range for frequency correction is higher on Danish and Irish grids. Both regulations set a dead band range where active power production remains independent of frequency variation. Beyond this band both codes show different interpretations on how a wind farm should react to

frequency deviations. According to the German regulation, a renewable power plant has to curtail active power by starting at 50.2 Hz with a gradient of 40% of available generation at the moment per Hertz. As for the Irish code, when in the presence of over-frequency excursions, a renewable power plant reacts according to a power curtailment gradient set by the grid operator. Afterwards, if necessary, curtailment rate is updated to the grid operator needs. With respect to frequency events, the wind farms response in German networks is limited when compared to Danish and Irish requirements, because the regulations establish that energy production can be artificially kept lower to provide secondary control at lower frequencies. Furthermore, Danish rules also allow the grid operator to smooth wind power output of each wind power plant, adapting individually power frequency response to the needs. For this purpose, three curtailment gradients that reproduce a droop controller action can be configured over the Danish curve. In Fig. 1, droop regulation areas are identified as d1, d2 and d3. Similar flexibility is provided by Irish regulation.

Reactive Power Control. Traditionally, synchronous generators had the exclusive task of ensuring bulk system voltage regulation at transmission level. As for the distribution network, voltage regulation still remains under distribution substation control. Since their introduction, wind farms were built to generate only active power. Thus, they were operated to keep the power factor at unity. In the last decade this trend has changed. Most of the European grids on mainland context have introduced new regulatory conditions, extending reactive power capability along with active power generation to wind and solar power. Likewise, the growing dissemination of renewables-based DER systems in insular systems will force the incorporation of this ancillary service for security reasons as a result of strong technical constraints. Since an isolated power network is different from island to island, reactive power needs have to be addressed to meet local interconnection issues. This requirement comes in three different ways: by assuming a Q set-point, by power factor control or by managing power reactive flow as a function of grid voltage. The insular approach, for now, relies basically on power factor band specification that must be provided by the wind farm under normal operation. Again, instructions concerning solar power plants are completely absent in the regulations under analysis. Common range goes from 0.95 lag to lead at full active power, having voltage range within 90% to 110% of nominal value. Other ranges may be found, such as 0.86 inductive to unity power factor.

Given that the alternative ways to express reactive power support are not imposed by insular grid operators, it is necessary to conduct the analysis relying on mature standards, such as occurs in continental Europe. The Q set-point related to active power generation is one of the strategies adopted in Danish code. It distinguishes the support level according to the wind farm global rating power. Fig. 2 indicates that at power levels above 20% of the rated power, the wind farm whose rating exceeds 25MW has to provide an additional 33 % of reactive power, as maximum, to the instantaneously available active power output. Whereas, smaller wind power facilities have to provide an additional 23% of reactive power. The criterion for reactive range requirement must cover Q capability over the full output range through the specification of Q-P diagrams. However, it should be pointed out that during periods of reduced wind or solar production the reactive power capability is lower.

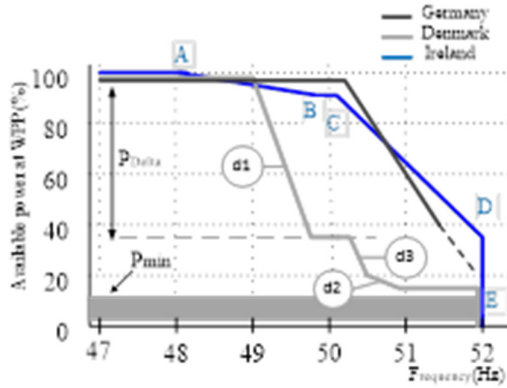


Fig. 1. Power-frequency response required by mature grid codes in mainland networks

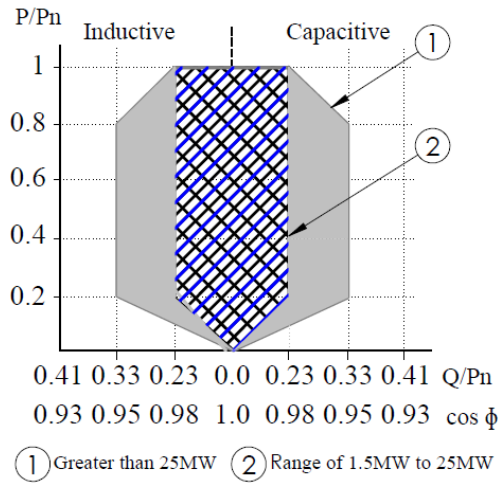


Fig. 2. Danish P-Q interconnection requirements for wind power plants

When the active power output is low and doesn't surpass a certain threshold, a less strict reactive power range could be imposed to solar or wind power plants under the grid code requirement. The third way of reactive power compensation is illustrated in Fig. 3, using as example the framework directives of the German regulator. The reactive power compensation range targets diverse voltage levels on the power system, from distribution to transmission networks. Renewable generation units must meet the reactive power capability within the area specified by the TSO, which is free to choose between three variants on the basis of relevant network requirements. In addition, the grid operator may alternate between the Q-V variants over time, whenever it is required. Reactive power compensation acting directly on grid voltage deviation has some merits when compared to the other reactive power compensation

approaches. The strongest argument relies on terminal voltage limitations that could affect reactive power generation of variable generators, including renewable power sources [14]. The criterion for reactive range requirement must cover Q capability over the full output range through a specification of Q-P diagrams. Since grid voltage level has a direct impact on renewable power source ability to provide reactive power, the Q-V diagram could also be required as a grid code specification in order to minimize its effect [15].

Emulating Inertia of Conventional Power Plants. “Virtual” wind inertia is a relatively new concept that can expand power-frequency response capability of a wind turbine to further improve grid frequency stability. The concept relies on using the kinetic energy stored in rotating masses of the wind turbine. Despite wind turbine technologies have different inertial response performances [16] a recent study has shown that “virtual” wind inertia can exceed the inertial power response of a synchronous generator with the same amount of inertia [17]. This requirement should be seen as an additional reinforcement of primary power-frequency response of a wind turbine.

4.2 Special Requirements under Network Disturbances

While conventional power plants, such as based on synchronous generators, have strong strength capabilities to resist to symmetrical and asymmetrical faults without being disconnected, wind power plants were not initially designed to handle grid faults. From an insular grid stability point of view, an unexpected shutdown of a wind farm may slow power system recovering because there is less generation to support it. For grid security reasons, renewable power plants should be tolerant to faults, at least during a short time, enough for fault clearance.

Fault Ride through Capability. It is the ability of a generator to survive a transient voltage dip without being tripped. Compliance with this requirement means the generator must be able to ride through all kinds of grid faults, including faults with very low remaining voltage levels and unsymmetrical (1-phase and 2-phase) faults. FRT capability is normally specified through a voltage-against-time profile, which establishes minimum phase-to-phase voltages at PCC for a maximum time frame. Typically a FRT requirement defines three main areas of response depending on voltage deviation severity and time duration of the anomaly. Voltage drop down to 90% of the voltage in the point of connection is not considered significant enough to damage the generator. Dropping below this value a generic FRT requirement establishes a maximum voltage drop at which a generator is forced to stay connected to the grid for a maximum exposure time, independently of the grid fault severity level and the number of faulty phases involved on the grid voltage anomaly. Between the maximum and minimum voltage drop, the exposure time to grid fault is extended as voltage deviation is lower. For voltage-time value pairs below the FRT line, the generator may be instructed to show a specific behavior before being tripped. Two grid codes were chosen to highlight a typical FRT curve. Fig. 4 shows mandatory

profiles described on Danish and German regulations. It should be noted that only the German regulatory framework aims to implement the requirement on a global sense, without targeting a specific renewable power source type. German grid code is in comparative terms the most demanding one. A full short-circuit at PCC must be supported by the wind turbine for a time window of 150 ms, which is a typical operation time of the protection relays while for the Danish network the anomaly tolerance is extended to 500 ms, but it is less severe in terms of voltage drop. It should be noticed that for the German case, wind farms may prolong their connection below the blue area upon agreement. As regards the insular European codes, low voltage ride-through compliance is already imposed in large insular systems such as the Canary archipelago (Spain) or the Crete Island (Greece), where renewable power penetration has grown over the last decade. Fig. 5 presents FRT specifications for Canary Islands, Crete and French Islands [18]-[21]. Comparatively to the mainland grid codes previously analyzed, insular voltage-time curves look very similar. Of the three codes analyzed, only in the Canary Islands wind power plants have to withstand instantaneous voltage drop down to zero for a time duration of 150ms. Extensive research concerning the ride-through control capability of wind turbine systems, and other DG systems as well, have showed that with adequate strategy control it is feasible.

Reactive Power Response. Since voltage recovering is a critical point, an additional effort is also required to the non-dispatchable power sources: a reactive current injection mechanism has to be activated as long as fault recovering is underway, followed by a progressive re-introduction of active power after the fault clearance. This capability is seen as crucial for a faster power system recover. This issue is even more critical if we consider that for an insular power network, due to its size and the absence of strong connections, any disturbed operating condition is immediately observed in every corner of the network.

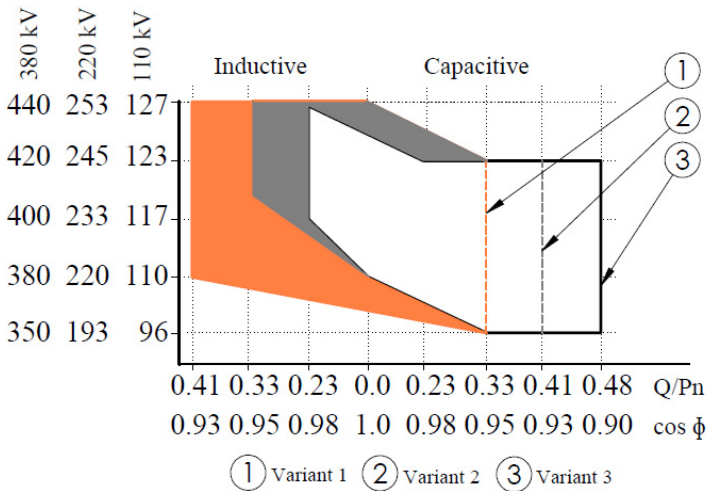


Fig. 3. Reactive power capability requirements for German case

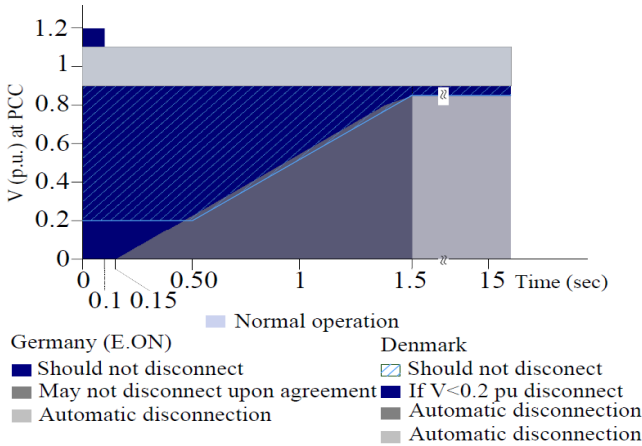


Fig. 4. FRT interconnection requirements for German and Danish codes

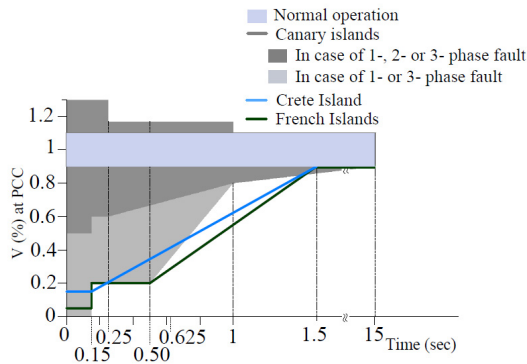


Fig. 5. FRT curve examples required in European insular power systems

Moreover, island grids are characterized by low short circuit power, which exacerbates the instability, contributing for example to a high variation of voltage when a defect appears. Therefore, a quick mitigation of the under-voltage phenomena is essential to normalize active power generation in order to ensure the power balance within the grid, consequently keeping the frequency in a normal range. Insular grid codes evolution on this topic is still scarce. However, the starting point for the introduction of this requirement has already been taken.

In Fig. 6, the rules in effect for the Canary Islands (Spain) are depicted, along with two non-insular equivalent specifications. For the insular Spanish grid code the wind turbine consumes reactive power as long as the voltage recover is underway. Also, for a drop voltage higher than 50% of the nominal voltage, reactive current does not surpass 90% of the global current injected on the grid. Moreover, the figure reveals that there is no reactive power absorption until full voltage recovery.

These constraints prevent additional instability on the voltage line. A visual comparison with the other two requirements leads to the conclusion that the German grid code is by far the most severe in terms of reactive power injection, forcing the wind power turbine to delivery only pure reactive current.

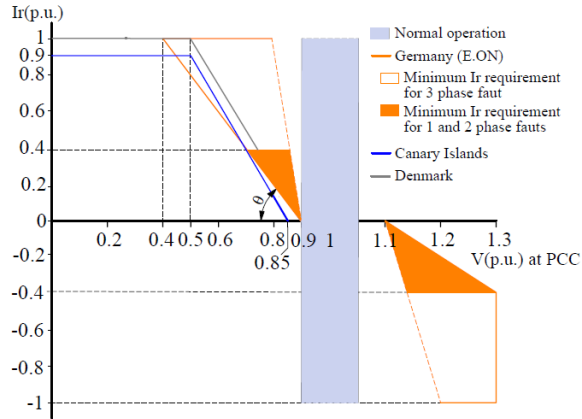


Fig. 6. Comparison of reactive power requirements during a voltage disturbance

5 Insular Smart Grid

A large renewable integration means a considerable dispersion of variable power production (VPP) of small scale, scattered across the island landscape. A complete change from a traditional organization to a network based on DER requires a new whole concept to operate the bulk electricity power. The smart grid concept embraces a set of advanced features, among them, monitoring and controlling of each grid element, whatever is the production entity or the physical distribution link, including real-time consumption tracking as well. Isolated networks being prone to stability issues are well suited to evaluate smart grid technologies. Smart grid operating strategies are today being studied in diverse insular regions in detriment of pilot projects on large interconnected systems. The successful implementation of insular Smart Grids implies meeting two key milestones: reinvention of grid operator’s role and the establishment of a reliable and efficient communication backbone.

5.1 Transmission/Distribution System Operators

Grid agents will have to evolve to adapt their role with the development of a Smart Grid related infrastructure, as well as their interactions with new players of the energy system, which are the renewable DER systems. The nature of the interactions can be described as key services to enable a reliable, secure and efficient exploration of the insular grid (Table 1).

Table 1. Grid agent’s role toward smart grid integration for an insular power system

<i>Power network optimizer</i>	<i>Contributor to system security</i>	<i>Data manager</i>	<i>Smart meter manager</i>	<i>Grid users / Suppliers relationship manager</i>	<i>Neutral market facilitator / Enabler</i>
Optimizing the development, operation, and maintenance of the distribution network by managing constraints, emergency situations and faults in a cost-efficient way, through planning, scheduling and forecasting tools.	Cooperate with the grid actors by offering new contributions to ensure the system security.	Gaining ability to manage large amounts of data and process them to produce relevant internal/external services.	Promote, operate and maintain smart meters in a cost-efficient way, while providing consumers with new services.	Respond to regulatory changes and expand the range of smart-related services offered to the actors of the energy system (grid users, local authorities, etc.) and other third parties.	On a short-term basis: comply with regulation and facilitate the exchange of information between the insular power grid players. On a medium-term basis: experiment and demonstrate the island system operator ability to play an active role in the proper functioning of market mechanisms, if applicable.

5.2 Communication and Supervisory Control

The information exchange between the VPP control center and the power plant is critical, promoting a successful change from centralized generation to distributed generation based paradigm. The link should be permanent, dependable and providing bi-directional communication capabilities. From system operator side through the control center, customized dispatch orders are sent to renewable power plants. On the other side, every distributed generation (DG) unit reports its operating conditions to the island operator system. Then, according to the received information, dispatch orders are updated to meet power demand and to stabilize grid electrical parameters.

6 Conclusions

In this paper, the technical requirements for large-scale integration of renewable energy sources were discussed regarding their incorporation in island grid codes, as a new contribution to earlier studies. By adding control and regulation capabilities to renewable systems, they change from a passive participation on the grid to an active role, providing services only normally found in conventional power plants. Insular power grid reform into a smart grid infrastructure was also addressed in this paper. Emphasis was given to the grid agents/operators new role and to the distributed communication network, as a catalyst of the renewable revolution alongside grid code evolution.

Acknowledgment. This work was supported by FEDER funds (European Union) through COMPETE and by Portuguese funds through FCT, under Projects FCOMP-01-0124-FEDER-020282 (PTDC/EEA-EEL/118519/2010) and PEst-OE/EEI/LA0021/2013. Also, the research leading to these results has received funding from the EU Seventh Framework Programme FP7/2007-2013 under grant agreement no. 309048.

References

1. Global Wind Energy Council, Global Wind Report (April 2011). <http://www.gwec.net>
2. Wang, P., Gao, Z., Tjernberg, L.B.: Operational adequacy studies of power systems with wind farms and energy storages. *IEEE Trans. Power Systems* **7**, 2377–2384 (2012)
3. Kavadias, K.A., Zafirakis, D., Kondili, E., Kaldellis, J.K.: The contribution of renewables on reducing the electricity generation cost in autonomous island networks. In: *Int. Conf. on Clean Electrical Power Proc. 2007*, pp. 777783 (2007)
4. Morren, J., et al.: Inertial response of variable speed wind turbines. *Electr. Pow. Syst. Res.* **76**, 980–87 (2006)
5. Papathanassiou, S.A., Boulaxis, N.G.: Power limitations and energy yield evaluation for wind farms operating in island systems. *Renewable Energy* **31**, 457–79 (2006)
6. Jauch, C.: Stability and control of wind farms in power systems. Ph.D. dissertation, Univ. Aalborg, Denmark (2006)
7. Iñigo, A.M., Jon, A., José, M.L., Pedro, I., José, V.L., Haritza, C.: Connection requirements for wind farms: A survey on technical requirements and regulation. *Renew. and Sust. Energy Reviews* **11**, 1858–1872 (2007)
8. Tsili, M., Papathanassiou, S.: A review of grid code technical requirements for wind farms. *IET Renewable Power Generation* **3**, 3008–3332 (2009)
9. Mohseni, M., Islam, S.M.: Review of international grid codes for wind power integration: Diversity, technology and a case for global standard. *Renew. Sust. Energy Rev.* **16**, 3876–90 (2012)
10. Díaz-González, F., Hau, M., Sumper, A., Gomis-Bellmunt, O.: Participation of wind power plants in system frequency control: Review of grid code requirements and control methods. *Renew. Sust. Energy Rev.* **34**, 551–564 (2014)
11. Verband der Netzbetreiber (VDN), Transmission Code 2007 - Network and System Rules of the German Transmission System Operators (August 2007). <http://www.vde.com>
12. Energinet.dk, Technical regulation 3.2.5 for wind power plants with a power output greater than 11 kW (2010)
13. EirGrid, EirGrid Grid Code – Version 5 (October 2013). <http://www.eirgrid.com>
14. Ellis, A., et al.: Reactive Power Performance Requirements for Wind and Solar Plant. In: *IEEE Power and Energy Society General Meeting Proc. 2012*, pp. 1–8 (2012)
15. Sandia National Laboratories, Reactive power interconnection requirements for PV and Wind plants (2012)
16. James, F., Rick, W.: Frequency Response Capability of Full Converter Wind Turbine Generators in Comparison to Conventional Generation. *IEEE Trans. Power Syst.* **23**, 649–656 (2008)
17. Keung, P.-K., Li, P., Banakar, H., Ooi, B.T.: Kinetic Energy of Wind-Turbine Generators for System Frequency Support. *IEEE Trans. Power Syst.* **24**, 279–287 (2009)
18. Électricité de France (EDF), Référentiel Technique SEI REF 04 (V5) – Protection de découplage pour le raccordement d’une production décentralisée en HTA et en BT dans les zones non interconnectées (May 2010) (in French)

19. Ministerio de Industria, Turismo y Comercio, P.O. 12.2 –SEIE: Instalaciones conectadas a la red de transporte de energía eléctrica: Requisitos mínimos de diseño, equipamiento, funcionamiento y seguridad y puesta en servicio, Boletín Oficial del Estado (2009) (in Spanish)
20. Red Eléctrica de España, Procedimientos de operación non peninsulares (April 2006) (in Spanish). <http://www.ree.es>
21. Red Eléctrica de España, P.O. 12.3. Requisitos de respuesta frente a huecos de tensión de las instalaciones eólicas (October 2006) (in Spanish)

Optimal Behavior of Demand Response Aggregators in Providing Balancing and Ancillary Services in Renewable-Based Power Systems

E. Heydarian-Forushani¹, M.E.H. Golshan¹,
M. Shafie-khah², and João P.S. Catalão^{2,3,4}(✉)

¹ Isfahan University of Technology, Isfahan, Iran

² University of Beira Interior, Covilhã, Portugal

³ INESC-ID, Lisbon, Portugal

⁴ Instituto Superior Técnico, Lisbon, Portugal
catalao@ubi.pt

Abstract. Due to the limited predictability and associated uncertainty of renewable energy resources, renewable-based electricity systems are confronted with instability problems. In such power systems, implementation of Demand Response (DR) programs not only can improve the system stability but also enhances market efficiency and system reliability. By implementing cloud-based engineering systems the utilization of DR will be increased and consequently DR will play a more crucial role in the future. Therefore, DR aggregators can efficiently take part in energy, balancing and ancillary services markets. In this paper, a model has been developed to optimize the behavior of a DR aggregator to simultaneously participate in the mentioned markets. To this end, the DR aggregator optimizes its offering/bidding strategies based on the contracts with its customers. In the proposed model, uncertainties of renewable energy resources and the prices of electricity markets are considered. Numerical studies show the effectiveness of the proposed model.

Keywords: DR aggregator · Demand response · Ancillary services markets · Renewable energy resources

1 Introduction

Increase of environmental conservation concerns and decrease of fossil fuel resources have caused penetration of renewable energy resources to be significantly augmented all over the world [1]. Due to the limited predictability and associated uncertainty of these resources, renewable-based electricity systems are confronted with instability problems [2]. In such power systems, implementation of Demand Response Programs (DRPs) not only can improve the system stability but also can enhance market efficiency, decrease peak demand, reduce price instability, and increase the system reliability [3]. The enhancement in market efficiency enables most of market participants, such as transmission system owner, distributors, and retailers to take advantages of implementing DR [4]-[6].

On the other hand, by implementing Cloud-based Engineering Systems (CES) the utilization of Demand Response (DR) will be increased and consequently DR will play a more crucial role in the future. Development of CES can significantly facilitate the aggregation of DR. Therefore, it can be an effective solution to increase the participation of electricity consumers to electricity markets [3]. To this end, both technology (e.g. CES) and policy (e.g. market rules and regulations) infrastructures are required to support implementation of DRPs in electricity markets [7], [8]. By developing the mentioned infrastructure, DR aggregators can efficiently take part in different electricity markets such as energy, balancing and ancillary services. In such situations, development of CES can definitely support DR aggregators to participate in the mentioned electricity markets as an important linking participant between Independent System Operator (ISO) and end users.

The literature covers many works regarding responsive demands who bid to the electricity markets [7]-[9]. However, DR aggregator performance has not been addressed in the reports. Although the participation of DR providers in the Demand Response eXchange (DRX) market has been presented in [10], the participation in energy and ancillary services markets has not been addressed. In [11], the DR aggregator has been considered as an agent in the electricity market modeled by multi-agent systems. However, the participation of the agent in ancillary services markets has not been modeled. It is noticeable that the simultaneous participation of DR aggregators in the energy, balancing and ancillary services markets has not been reported in the previous works, which is a new contribution this paper provides. In the renewable-based power systems, optimal behavior of these participants is complex due to many uncertainties. The major proportion of the energy is cleared in day-ahead session. Therefore, all market participants have to submit their offers for all hours of the day ahead, several hours in advance. Because of the unpredictable nature of renewable-based power systems in the future smart grid, the offers have a meaningful degree of uncertainty. Thus, employing the balancing markets and ancillary services market is crucial for market operators to supply the spinning reserve requirement. On this basis, the DR aggregators have the opportunity to participate in the mentioned markets and supply a proportion of required spinning reserve and regulation.

In this paper, a model has been developed to optimize the behavior of a DR aggregator to simultaneously participate in energy, balancing and ancillary services markets. To this end, the DR aggregator optimizes its offering/bidding strategies for the mentioned markets based on the contracts with its customers. In the proposed model, uncertainties of renewable energy resources and the prices of electricity markets are considered. Numerical studies show the effectiveness of the proposed model. In addition, Conditional Value at Risk (CVaR) is incorporated into the model to tackle the uncertainties of market prices and the behavior of consumers.

2 Contribution to Cloud-Based Engineering Systems

Due to significant growth of the importance of energy conservation and environmental protections, DR can favorably affect the future smart grid [12]-[13]. In this context, Cloud-based Engineering Systems (CES) certainly have meaningful impacts on the future smart grid by increasing the collaboration between market players from both electricity and information viewpoints.

In this context, since a large number of managing and controlling data in the network imposes market participants to employ new computational methods to mitigate the system operation time, the CES can have the most important application.

The CES strongly influences the developing network impact while it depends on the access to numerous computational resources (i.e. cloud) in order to tackle the environmental restrictions by using the scarce processing and information storage proficiency. On this basis, improvements in CES enable end-users to more efficiently behave in demand side programs. DR aggregators possess the technology to perform DR and they are responsible for the installation of the smart meters at the end-users' components. As a matter of fact, DR aggregators can provide connectivity communication capabilities to end-users' components in order to connect them to the cloud. This can reduce the technical complexity and the required efforts to increase the local computational resources at the level of each end-user's component. On the other hand, CES can improve the security of the mechanisms and consequently increase the robustness of collecting data by the aggregator. Since each aggregator represents a significant amount of total demand in the DR market, it can negotiate on behalf of the end-users with the operator more efficiently. Since these players are the link between customers and electricity markets, they have a critical role in moving towards the future smart grid. In the future smart grid, by developing the CES and consequently increasing the participation of customers in DRPs, the players will have a more important role in the electricity markets.

3 Modeling the Self-scheduling of DR Aggregators

DR aggregator aims to maximize its profit by participating in day-ahead energy, balancing and spinning reserve markets. A schematic of DR aggregator presence in the mentioned markets, including both renewable and thermal Generation Companies (Gencos) in the supply side and retailers and large customers in the demand side, is illustrated in Fig. 1.

3.1 Uncertainty Characterization

In this paper two major types of uncertainty have been considered: the uncertainties related to market prices and the uncertainties associated with the quantity of activated reserve by ISO. The modeling of these uncertainties is explained as follows.

Modeling the Uncertainty of Market Prices. In order to participate in the renewable-based electricity market, the DR aggregator has to forecast market prices. In this paper, three uncertain market prices are considered: day-ahead energy, balancing and spinning reserve. To this end, the Roulette Wheel Mechanism (RWM) technique [14] is applied for scenario generation. In order to develop an accurate and appropriate model, market prices have been characterized by log-normal distribution in each hour [15]. Thus, considering that μ and σ represent the mean value and standard-deviation, respectively, the Probability Distribution Function (PDF) of market prices can be formulated as follows:

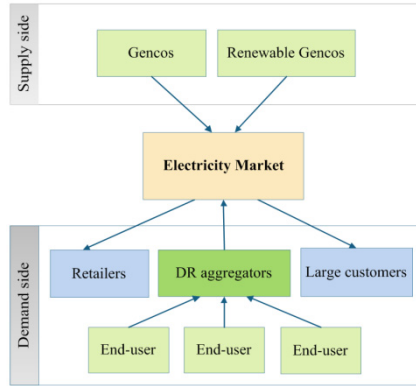


Fig. 1. Electricity market scheme

$$f_{Pr}(Pr, \mu, \sigma) = \frac{1}{Pr \sigma \sqrt{2\pi}} \exp \left[-\frac{(\ln Pr - \mu)^2}{2\sigma^2} \right] \tag{1}$$

Modeling the Uncertainty of Activated Reserve by ISO. In order to model the probability of quantity of activated reserve by ISO, Act_{is}^{Res} , it is considered to be uniformly distributed between 0 and the offered amount by the DR aggregator. On this basis, the PDF of quantity of reserve activated by the ISO can be formulated as follows:

$$f(x) = 1/P_{is}^{Res} \quad , \quad 0 \leq x \leq P_{is}^{Res} \tag{2}$$

Considering (2) different outcomes of ISO’s behavior for calling the DR aggregator and the activated quantity of reserve are taken into account by the RWM-based scenario generation process [14].

3.2 Incorporating Risk Management

The uncertain behavior of DR aggregator’s customers enforces the profit of this participant with a high risk. Based on this, the DR aggregator has to manage the mentioned risk. To this end, Conditional Value-at-Risk (CVaR) as an appropriate technique is employed to incorporate risk management into the problem. The CVaR can be formulated as follows:

$$Max : \quad \xi - \frac{1}{1-\alpha} \sum_{s=1}^{S_N} \rho_s \eta_s \quad , \quad \eta_s \geq 0 \tag{3}$$

$$-B_s + \xi - \eta_s \leq 0 \tag{4}$$

The parameter α is usually assigned within the interval of 0.90 to 0.99, and in this paper it is set to be equal to 0.95. If the profit of scenario s is higher than ξ , the value of η_s is set to 0. Otherwise, η_s is assigned to the difference between ξ and the related profit. The above constraints are employed to unify the risk-metrics CVaR.

3.3 Mathematical Model of the DR Aggregator

The DR aggregator offers a specified quantity in day-ahead energy and spinning reserve markets in order to obtain an accepted level of energy and ancillary services into day-ahead market for each hour. Then, it can submit new energy offers or update the previous ones in the balancing market. Moreover, in the proposed stochastic framework, risk aversion is implemented by restricting deviations of expected profit using the CVaR technique. According to the above mentioned description, the optimal offer of the DR aggregator at each hour can be obtained by solving the self-scheduling problem to maximize its profit. The objective function can be expressed as (5):

$$\text{Max } EP = \sum_{s=1}^{S_N} \rho_s \sum_{t=1}^T \left[\begin{array}{l} \pi_{ts}^{DA} \cdot P_{ts}^{DA} + \pi_{ts}^{Res} \cdot P_{ts}^{Res} + \pi_{ts}^{bal} \cdot P_{ts}^{bal} \\ + Act_{ts}^{Res} \cdot \pi_{ts}^{DA} \cdot \rho_{ts}^{call} \cdot \rho^{Response} \\ - Act_{ts}^{Res} \cdot \pi_{ts}^{bal} \cdot \rho_{ts}^{call} \cdot (1 - \rho^{Response}) \\ - D_t \cdot \pi_{ts}^{ariff} + \pi_{ts}^{DA} \cdot r_t^+ \cdot \Delta_{ts}^+ - \pi_{ts}^{DA} \cdot r_t^- \cdot \Delta_{ts}^- \end{array} \right] + \beta \left(\xi - \frac{1}{1-\alpha} \sum_{s=1}^{S_N} \rho_s \cdot \eta_s \right) \quad (5)$$

where, β is the weighting factor to achieve a trade-off between profit and CVaR.

The first term of (5) denotes the income of taking part in the day-ahead energy market. The next two terms represent the income resulting from spinning reserve and balancing markets. The fourth part represents the income resulting from delivering energy while it is called by the ISO. The fifth term denotes the purchase cost of energy from the balancing market that results from not delivering the activated reserve to the grid. The sixth term denotes the cost of responsive demands. The next two terms represent the positive and negative profit resulting from the balancing market and the last term indicates the CVaR multiplied by β .

The objective function is maximized considering the constraints described as follows:

$$P_{ts}^{DA} + Act_{ts}^{Res} + P_{ts}^{bal} \leq D_t \quad (6)$$

$$-\sum_{t=1}^T \left[\begin{array}{l} \pi_{ts}^{DA} \cdot P_{ts}^{DA} + \pi_{ts}^{Res} \cdot P_{ts}^{Res} + \pi_{ts}^{bal} \cdot P_{ts}^{bal} + Act_{ts}^{Res} \cdot \pi_{ts}^{DA} \cdot \rho_{ts}^{call} \cdot \rho^{Response} \\ - Act_{ts}^{Res} \cdot \pi_{ts}^{bal} \cdot \rho_{ts}^{call} \cdot (1 - \rho^{Response}) - D_t \cdot \pi_{ts}^{ariff} + \pi_{ts}^{DA} \cdot r_t^+ \cdot \Delta_{ts}^+ - \pi_{ts}^{DA} \cdot r_t^- \cdot \Delta_{ts}^- \end{array} \right] + \xi - \eta_b \leq 0 \quad (7)$$

$$0 \leq P_{ts}^{DA} \leq P^{\max} \quad (8)$$

$$0 \leq P_{ts}^{bal} \leq P^{\max} \quad (9)$$

$$0 \leq P_{ts}^{Res} \leq P^{\max} \quad (10)$$

$$\Delta_{t\omega} = P_t^{Act} - P_{ts}^{DA} \quad (11)$$

$$\Delta_{t\omega} = \Delta_{t\omega}^+ - \Delta_{t\omega}^- \quad (12)$$

The total capability of the aggregator in all day-ahead, balancing and ancillary services markets are given in (6). Eq. (7) represents the incorporation of risk into the problem. Constraints (8)-(10) are limits on the offer of DR aggregator, based on the

contribution in different markets. Equations (11) and (12) are employed to calculate the energy deviation using the actual injected energy.

4 Numerical Study

Some numerical studies are accomplished on the common load curve of a real-world system [16], in order to indicate the usefulness of the proposed model. It is assumed that the peak of the typical load curve is equal to 100MW. Various scenarios have been generated by means of the probability distribution function which is explained in Section 3. On this basis, all uncertainties of market prices and calling by ISO have been divided into the hours of the day. Changes in β have been accomplished to study the impact of being risk taker or risk averse. Considering $\beta=0$ means the DR aggregator takes no risk. The results are expressed in Table 1.

It can be concluded from Table 1 that, as the risk coefficient increases the total expected profit is reduced, but the violation from this profit value is also reduced. In other words, if a risk-averse DR aggregator makes a decision to mitigate the risk of violation of the obtained profit value it pays as a reduction in the expected profit value, while a risk-taker aggregator prefers to have a more expected profit but at the cost of more violation probability from that expected profit value. Moreover, as it can be seen in Table 1, DR aggregator participation in ancillary services and balancing markets increases its expected profit and manages its risk.

Table 1. Effect of different electricity markets on DR aggregator's profit and CVaR

Risk Level (β)	Electricity Market			Expected Profit (\$)	CVaR (\$)
	Day-ahead Energy	Balancing	Spinning Reserve		
0	✓			9421.5	8861.7
	✓	✓		9844.9	9420.5
	✓	✓	✓	11231.1	10783.3
0.5	✓			9278.6	8899.0
	✓	✓		9676.5	9458.7
	✓	✓	✓	11058.1	10897.2
1	✓			9159.4	8989.8
	✓	✓		9501.8	9492.2
	✓	✓	✓	11036.4	10962.0

Table 1 presents the effect of participation in the different markets on the DR aggregator's expected profit. As it can be seen in Table 1, an increase in DR aggregator's risk causes a reduction in its expected profits. Moreover, the participation in the balancing and spinning reserve markets can significantly improve the profit.

The hourly offers of a DR aggregator in the mentioned markets are indicated in Fig. 2. As it can be observed, the offers of the DR aggregator to the spinning reserve market are mostly more than the one to day-ahead energy market. In other words, DR aggregator prefers to participate in ancillary services more than energy markets. In

addition, the effect of participation in balancing and ancillary services markets on DR aggregator’s costs and incomes are presented in Table 2.

It should be mentioned that, in this paper the response probability of DR aggregator is considered to be equal to 0.05. According to Table 2, participation of a DR aggregator in ancillary services increases its expected profit. Moreover, participation in the balancing market can also augment the profit.

Table 2. Terms of costs and incomes of DR aggregator

Case	Participation in all day-ahead energy, balancing and ancillary services markets
Income from day-ahead energy market	5767.3
Income from balancing market	830.2
Income from spinning reserve market	7565.5
Positive imbalance income	243.3
Negative imbalance cost	454.2
Penalty resulted from not responding	295.1
Cost of responsive demands	2425.9
Expected profit (\$)	11231.1

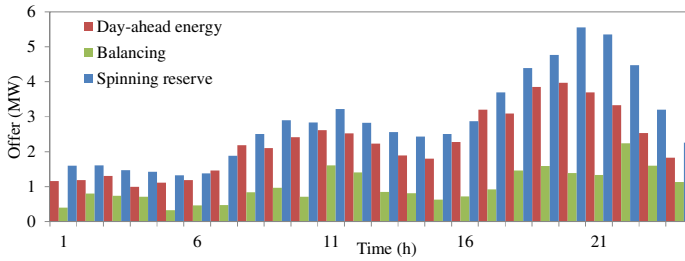


Fig. 2. Offers of the DR aggregator in day-ahead energy, balancing and ancillary markets

5 Conclusion

This paper investigated the impacts of different electricity markets on the optimal behavior of a DR aggregator in a renewable-based power system. In this regard, the DR aggregator can participate in day-ahead energy, balancing and spinning reserve markets in order to maximize its profit. In addition, the uncertain nature of market prices and quantity of activated reserve by ISO were modeled using RWM method. Furthermore, CVaR was applied as a risk measure for the DR aggregator, thus being able to specify the desirable weighting between expected profit and risk due to the uncertainty of customers’ behavior. The results showed that the participation in balancing and ancillary services markets can provide a significant opportunity for DR aggregators. These markets not only could increase the expected profit of DR aggregators, but also could reduce their risks.

Acknowledgment. The work of M. Shafie-khah and J.P.S. Catalão was supported by FEDER funds (European Union) through COMPETE and by Portuguese funds through FCT, under Projects FCOMP-01-0124-FEDER-020282 (Ref. PTDC/EEA-EEL/118519/2010) and PEst-OE/EEI/LA0021/2013. Also, the research leading to these results has received funding from the EU Seventh Framework Programme FP7/2007-2013 under grant agreement no. 309048.

References

1. Leão, R.P.S., et al.: The future of low voltage networks-moving from passive to active. *Int. J. Elect. Power Energy Syst.* **33**, 1506–1512 (2011)
2. Shao, S., Pipattanasomporn, M., Rahman, S.: Demand response as a load shaping tool in an intelligent grid with electric vehicles. *IEEE Trans. Smart Grid.* **2**, 624–631 (2011)
3. Palensky, P., Dietrich, D.: Demand side management: demand response, intelligent energy systems, and smart loads. *IEEE Trans. Ind. Informat.* **7**, 381–388 (2011)
4. Strbac, G.: Demand side management: Benefits and challenges. *Energy Policy* **36**, 4419–4426 (2008)
5. Nguyen, D.T., Negnevitsky, M., Groot, D.: Walrasian Market Clearing for Demand Response Exchange. *IEEE Trans. Power Sys.* **27**, 535–544 (2012)
6. Yousefi, S., Moghaddam, M.P., Majd, V.J.: Optimal real time pricing in an agent-based retail market using a comprehensive demand response model. *Energy* **36**, 5716–5727 (2011)
7. Goel, L., Aparna, V.P., Wang, P.: A framework to implement supply and demand side contingency management in reliability assessment of restructured power systems. *IEEE Trans. Power Sys.* **22**, 205–212 (2007)
8. Aalami, H.A., Moghaddam, M.P., Yousefi, G.R.: Demand response modeling considering interruptible/curtailable loads and capacity market programs. *Applied Energy* **87**, 243–250 (2010)
9. Moghaddam, M.P., Abdollahi, A., Rashidinejad, M.: Flexible demand response programs modeling in competitive electricity markets. *Applied Energy* **88**, 3257–3269 (2011)
10. Heydarian-Forushani, E., Parsa Moghaddam, M., Sheikh-El-Eslami, M.K., Shafie-khah, M., Catalao, J.P.S.: Risk-constrained offering strategy of wind power producers considering intraday demand response exchange. *IEEE Trans. Sust. Ener.* **5**, 1036–1047 (2014)
11. Shafie-khah, M., Catalao, J.P.S.: A stochastic multi-layer agent-based model to study electricity market participants behavior. *IEEE Trans. Power Sys.* (2014). doi:10.1109/TPWRS.2014.2335992
12. Hajati, M., Seifi, H., Sheikh-El-Eslami, M.K.: Optimal retailer bidding in a DA market e a new method considering risk and demand elasticity. *Energy* **36**, 1332–1339 (2011)
13. Aazami, R., Aflaki, K., Haghifam, M.R.: A demand response based solution for LMP management in power markets. *Elec. Power & Energy Sys.* **33**, 1125–1132 (2011)
14. Amjady, N., Aghaei, J., Shayanfar, H.A.: Stochastic multiobjective market clearing of joint energy and reserves auctions ensuring power system security. *IEEE Trans. Power Syst.* **24**, 1841–1854 (2009)
15. Conejo, A.J., Nogales, F.J., Arroyo, J.M.: Price-taker bidding strategy under price uncertainty. *IEEE Trans. Power Sys.* **17**, 1081–1088 (2002)
16. Shayesteh, E., Yousefi, A., Moghaddam, M.P.: A probabilistic risk-based approach for spinning reserve provision using day-ahead demand response program. *Energy* **35**, 1908–1915 (2010)

A Heuristic Approach for Economic Dispatch Problem in Insular Power Systems

G.J. Osório¹, J.M. Lujano-Rojas¹, João C.O. Matias¹, and João P.S. Catalão^{1,2,3(✉)}

¹ University of Beira Interior, Covilha, Portugal
catalao@ubi.pt

² INESC-ID, Lisbon, Portugal

³ University of Lisbon, Lisbon, Portugal

Abstract. Insular power systems are characterized by their isolated geographical location, which makes their interconnection with other power systems a challenging task. Moreover, these islands have important renewable resources that allow the reduction of generation costs and greenhouse gas emissions (GHE). To guaranty the quality, flexibility and robustness of the electrical framework, the representation of renewable power forecasting error by scenario generation or even the implementation of demand response tools have been adopted. In this paper, the failure events of a specific unit are considered according to its capacity. Then, using the forced outage rate, the probability of each failure event is computed. Results of energy not supplied and fuel consumption cost are determined by applying probabilistic concepts, while the final results are obtained by fitting and evaluating a nonlinear trend line carried out using the previous results, resulting in a proficient computational tool compared with classical ones.

Keywords: Insular power systems · Power system reliability · Probabilistic economic dispatch · Wind power forecasting error

1 Introduction

Isolated geographical location and good potential to develop renewable power generation systems are two of the important topics that have driven the integration of renewable energy sources into insular power systems. In fact, in insular power systems the major problem is the high generation cost related to the type of fossil fuel used and its transportation. However, in most of the cases, there are available endogenous resources that allow reducing the generation costs and GHE. Such concerns and characteristics have motivated the development and implementation of more renewable energy sources, such as wind energy, among others depending on the island location on the globe. Notwithstanding, one of the main obstacles is related to the legislation and administrative barriers [1], which can threaten the profitability of electric production.

One of the solutions that have been widely suggested is the penetration of energy storage systems (ESS) to face these problems, due to the fact that ESS can improve

the flexibility of the electrical system and allow more penetration of renewable energy sources. Nonetheless, several factors such as capacity tariffs, wind potential and investment costs affect the economic viability of those projects [2]. Other valid way is the implementation of demand response (DR) approaches, which allows also the manipulation of a system load curve.

One other option, which is the focus of this paper, consists in introducing the uncertainty of renewable power forecasts on economic dispatch (ED) problems. For several years now, wind power forecasting error has been represented by scenario generation as a flexible approach, which enables a representation of cross-temporal characteristics of the wind power time series, influencing the spinning reserve requirements [3].

In [4], a scheduling approach based on scenario generation was proposed. In this model, several scenarios of wind power production, load demand and forced unit outages are randomly generated considering the auto-correlated nature of each time series. Then, the optimal scheduling is determined by using a mixed integer stochastic optimization algorithm, where the main objective is to minimize the expected generation cost. In [5] and [6], the proposed approaches introduce the wind power generation in the ED problem as a restriction in the optimization problem. Based on the probabilistic infeasibility and using the Lagrange multiplier method, the influence of wind power behavior and penetration level on total generation cost is analyzed. In [7], the effects of wind power generation in the ED problem are studied introducing NO_x emissions modelled using an incomplete gamma function. In [8], a scheduling approach is presented as a dynamic programming problem, while wind power behavior is represented as a first-order Markov process. In [9] an ED approach based on fact that the aggregation of wind power generation reduces its forecasting error is presented, allowing the mitigation of the stochastic relations in the optimization problem.

In [10], an approach incorporating load forecasting error, forced outages of generation units and transmission systems by means of a Monte Carlo simulation (MCS) is presented, enabling the estimation of the optimal reserve required in the solution of unit scheduling problems taking into account a determined reliability level. In [11], a scheduling approach based on mixed-integer linear programming (MILP) to determine the optimal frequency-regulating reserve is proposed, while in [12] another approach based on mixed-integer programming (MIP) and MCS, considering N-1 contingencies is presented. In [13], a short-run ED approach is proposed, where the different states that take place during the contingency event are analyzed and represented as a linear programming problem.

In this paper, a new approach incorporating the renewable power forecasting error and the power system reliability in the analysis of generation cost, composed of fuel consumption cost (FCC) and energy not supplied (ENS), is developed and presented. In proposed approach, the failure events of a unit or multiple units are considered according to its generation capacity. Then, using the forced outage rate (FOR), the probability of each failure event is computed. Meanwhile, a transformation is applied to the probability of each event, and therefore the sum of the probability of all considered events is one. Initial results of ENS and FCC are determined by applying proba-

bilistic concepts, while the final results are obtained by fitting and evaluating a non-linear trend line carried out using the initial results.

2 Contribution to Cloud-Based Engineering Systems

Cloud-based solutions (CBS) can provide an easier and improved data connection with focus on remote tools, making suitable the concepts of the proposed study. CBS can enable a more efficient behavior of the computational resources and the information availability for the ED problem in an accurate time frame. Actually, CBS can provide an excellent interconnection to share in an efficient way the information between all electrical industry players'. A fast share of information is more and more required in the energy systems field, where data can be stored in a safe way to be ubiquitously accessed whenever needed, which is a valuable benefit of cloud-based engineering systems. Furthermore, the shared tools can improve the flexibility, accuracy and robustness of overall electrical framework, helping to improve the advent of electrical smart grids, namely in islanded location.

3 Insular Power System Characterization

Typically, insular power systems are characterized by a small number of conventional generation units, fewer than 26 units, and installed capacity lower than 2000 MW. Frequently, conventional generation units employed are steam turbines, combined cycle gas turbines, diesel engines, open cycle gas turbines and renewable energies [14]. In most cases, such units use heavy fuel oil and/or light fuel oil, although the integration of liquefied natural gas [15], [16]. Moreover, the cycling of power production as a consequence of integration of stochastic renewable power sources, such as wind power, produces an increment in the number of failure events and maintenance cost. Normally, in mainland power systems, units employed to supply peak loads could have a forced out rates (FOR) of 0.02%, cycling units could have 10.15%, while base load units could have 3.69%, on average [17]. The 5-unit system under study in this paper is described in Table 1 [18], representing minimum and maximum output power, curve consumption parameters of units, and down/up ramps.

Moreover, units 1 and 2 are considered as peak units, unit 3 is considered as cycle unit, and units 4 and 5 are considered as base load units, representing a real small insular electrical framework. The load demand to be supplied at time t is $450 \text{ MW} \pm 10\%$, while the number of intervals selected for discretization was ($B = 7$).

Table 1. Main characteristic of 5 units of insular power system

n	P_{min}^n (MW)	P_{max}^n (MW)	a_i (\$/h)	b_i (\$/MWh)	c_i (\$/MW ² h)	DR_n & UR_n (MW/h)	FOR
1	5	50	30	27.89	0.0143	48	0.01
2	10	50	27	19.00	0.0085	48	0.01
3	10	70	27	18.10	0.0081	114	0.12
4	20	120	25	12.69	0.0046	114	0.05
5	70	200	20	9.66	0.0014	150	0.05

4 Economic Dispatch Problem

The mathematical formulation of the ED problem is briefly described afterwards, where the uncertainty related with the integration of wind power forecasting (*WPF*) and the reliability of the power system are both incorporated in order to determine the expected value of ENS ($E\{ENS^t\}$) and FCC ($E\{FCC^t\}$) in a determined time instant t . The uncertainty of *WPF* is directly reflected on the value of net load (L^t). FCC could be modelled according to (1):

$$C_i^t = a_i + b_i(P_i^t) + c_i(P_i^t)^2 \quad (1)$$

where a_i , b_i and c_i are the coefficients of fuel consumption of each unit i , C_i^t is the FCC of unit i at time t . The definition of expected generation cost is expressed in (2):

$$E\{GC^t\} = E\left\{\sum_{n=1}^N C_n^t\right\} + VOLL \times E\{ENS^t\} \quad (2)$$

where *VOLL* is the value of lost load, $E\{\bullet\}$ is a function that represents the estimation of expected value of a determined variable. Also, the ED problem is constrained to the operational limitations of each unit, which typically are modelled according to their minimum and maximum power output operation, and up/down ramp constraints between the present state and previous state in time. Furthermore, it is important to note how $E\{GC^t\}$ is strongly dependent on FCC and ENS, so it is of the utmost importance to determine such values ($E\{FCC^t\}$ and $E\{ENS^t\}$) in an efficient and proficient way.

5 Proposed Approach

The proposed approach in this paper estimates the main components of the generation cost structure (FCC and ENS). The first step determines the order in which units are going to fail. This is carried out due to the number of possible combinations of failure events that increases exponentially until 2^N . In order to avoid this problem, a limited number of units to be failed (D) is selected according to a determined criterion. In the second step, the normal operation is modeled as 1 and the failure condition as 0, so all possible combinations of failure events are estimated only considering the first- D units. This approach allows all computational efforts to be concentrated only in the failure of units of interest. In the third step, for each combination of event failure, the ED problem is solved only incorporating the forecasting error, obtaining initial values of $E\{ENS^t\}$ and $E\{FCC^t\}$. Also, a transformation is introduced to deal with the sum of probabilities, obtaining the appropriate weights proportional to their corresponding probabilities. Then, initial values of $E\{ENS^t\}$ and $E\{FCC^t\}$ incorporating forecasting error and system reliability can be obtained by using traditional probabilistic theory. Figure 1 summarizes the proposed algorithm considering up to five points (initial values of $E\{ENS^t\}$ and $E\{FCC^t\}$).

5.1 Introducing Forecasting Error in the Proposed Approach

Assuming that the forecasting error and (L^t) are modelled using a Gaussian PDF, such PDF is incorporated in the optimization problem by dividing it in several intervals or power classes (B) [19]. A classical ED problem [20] could be solved for each element of the set of load values described above, obtaining the corresponding set of ENS values and FCC values.

Then, the part of $E\{ENS^t\}$ and $E\{FCC^t\}$ related to the forecasting error ($E\{ENS^t\}^{FE}$ and $E\{FCC^t\}^{FE}$) could be estimated using (3) and (4):

$$E\{ENS^t\}^{FE} = \sum_{b=1}^B (ens_b^t)(P_r\{l_b^t\}) \tag{3}$$

$$E\{FCC^t\}^{FE} = \sum_{b=1}^B (fcc_b^t)(P_r\{l_b^t\}) \tag{4}$$

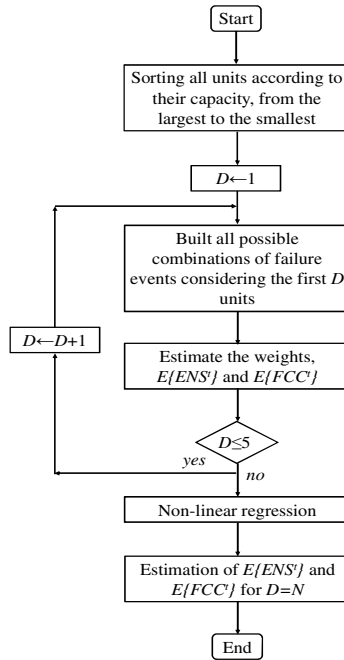


Fig. 1. Algorithm of proposed approach

5.2 Introducing Forced Outage Rate in the Proposed Approach

The power system reliability is incorporated by introducing a transformation applied to the probability of occurrence of a determined number of possible failure events, allowing the substitution of the probabilities of some determined failure events by weighted values whose addition is 1. Then, the ED problem is solved according to subsection 5.1 where the expected value of ENS and FCC that corresponds to a row j

considering only the forecasting error ($E\{ENS^t\}_j^{FE}$ and $E\{FCC^t\}_j^{FE}$) are obtained. Also, the values $E\{ENS^t\}$ and $E\{FCC^t\}$, which incorporate forecasting error and system reliability considering the failures of first- D units, are obtained by using (5) and (6):

$$E\{ENS^t\} = \sum_{j=1}^H (E\{ENS^t\}_j^{FE})(T_j) \tag{5}$$

$$E\{FCC^t\} = \sum_{j=1}^H (E\{FCC^t\}_j^{FE})(T_j) \tag{6}$$

6 Case Study

The 5-units case study has been presented and analyzed in order to illustrate the approach proposed in this paper, being adapted from other cases studies frequently used in the technical literature. Figure 2 shows the comparison of $E\{ENS^t\}$ between the results obtained from the MCS approach, considering 10,000 trials and the solution obtained from the application of probabilistic theory evaluating all possible combinations of event failures and the discretization of L' in nine intervals ($B = 9$), and the proposed approach for $D = 1, 2, \dots, 5$. It is possible to see how there is a small difference between MCS and the probabilistic solution due to the fact that MCS is not considering all possible combinations. Moreover, it is possible to see how the initial values of $E\{ENS^t\}$ converge to the probabilistic solution as the values of D tend towards N ; this is the most important effect of the transformation applied. Figure 3 presents a similar comparison for the estimation of $E\{FCC^t\}$, where the proposed approach has a tendency to lean towards the probabilistic solution.

In order to illustrate the approach to determine the optimal spinning reserve, the generation units presented in Table 1 have been sequentially committed according to their economic priority to supply a load demand of 60000 kW \pm 5%. The obtained results were used later to build the curves presented in Figure 4, which describes the behavior of ENS and FCC. The behavior of $E\{GC^t\}$ built according to equation (2) is shown in Figure 5 for a VOLL between 0.2 €/kWh and 6 €/kWh.

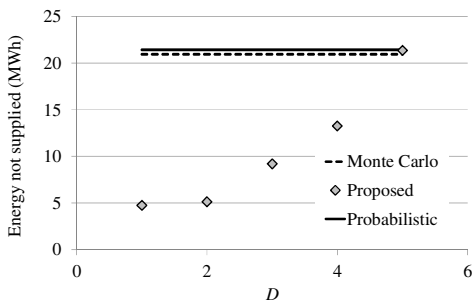


Fig. 2. Evolution of ENS comparison between MCS and the proposed approach

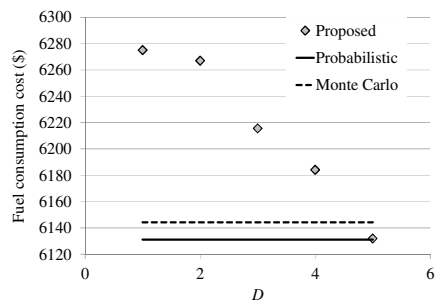


Fig. 3. Evolution of FCC cost comparison between MCS and the proposed approach

Table 2. Probabilistic Priority List Results

Variable	MCS	Proposed	Error	Error (%)
$E\{ENS\}$ (kWh)	8810.622	9797.0216	986.3992	11.19557
$E\{FCC\}$ (€)	11603.703	11593.558	10.145	0.087432
Time (s)	205.338	10.813	-----	-----

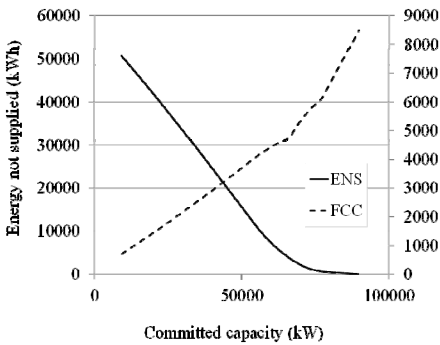


Fig. 4. Behavior of ENS and FCC with the committed capacity

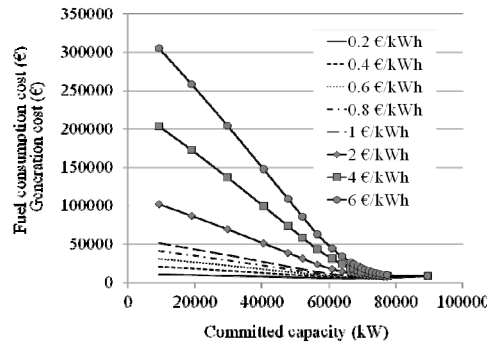


Fig. 5. Generation cost for several VOLL values

7 Conclusion

The integration of renewable energy sources in insular power systems is limited by their ability to accommodate and manage the variability of such stochastic sources. Moreover, determining the appropriate amount of spinning reserve considering the uncertainty of renewable power forecasting and system reliability is of the utmost importance. Hence, this paper has incorporated in ED problem such topics in order to determine FCC and ENS values in a proficient manner, taking advantage of the tendency of initial values towards the probabilistic solution that could be provided by the CBS system. The results obtained showed how the proposed approach allows the values of $E\{ENS^t\}$ and $E\{FCC^t\}$ to be obtained with a very reasonable error in just a few seconds, compared to the solution obtained from the MCS approach.

Acknowledgment. This work was supported by FEDER funds (European Union) through COMPETE and by Portuguese funds through FCT, under Projects FCOMP-01-0124-FEDER-020282 (PTDC/EEA-EEL/118519/2010) and PEst-OE/EEI/LA0021/2013. Also, the research leading to these results has received funding from the EU Seventh Framework Programme FP7/2007-2013 under grant agreement no. 309048.

References

1. Colmfenar-Santos, A., Monzón-Alejandro, O., Borge-Diez, D., Castro-Gil, M.: The impact of different grid regulatory scenarios on the development of renewable energy on islands: A comparative study and improvement proposals. *Renewable Energy* **60**, 302–312 (2013)
2. Papaefthymiou, S.V., Papathanassiou, S.A.: Optimum sizing of wind-pumped-storage hybrid power stations in island systems. *Renewable Energy* **64**, 187–196 (2014)
3. Wang, J., Botterud, A., Bessa, R., Keko, H., Carvalho, L., Issicaba, D., Sumaili, J., Miranda, V.: Wind power forecasting uncertainty and unit commitment. *Applied Energy* **88**, 4014–4023 (2011)
4. Tuohy, A., Meibom, P., Denny, E., O'Malley, M.: Unit commitment for systems with significant wind penetration. *IEEE Trans on Power Systems* **24**, 592–601 (2009)
5. Liu, X., Xu, W.: Economic load dispatch constrained by wind power availability: a here-and-now approach. *IEEE Transactions on Sustainable Energy* **1**, 2–9 (2010)
6. Liu, X.: Economic load dispatch constrained by wind power availability: a wait-and-see approach. *IEEE Transactions on Smart Grid* **1**, 347–355 (2010)
7. Hargreaves, J.J., Hobbs, B.F.: Commitment and dispatch with uncertain wind generation by dynamic programming. *IEEE Trans on Sustainable Energy* **3**, 724–734 (2012)
8. Liu, X., Xu, W.: Minimum emission dispatch constrained by stochastic wind power availability and cost. *IEEE Transactions on Power Systems* **25**, 1705–1713 (2010)
9. Roy, S.: Inclusion of short duration wind variations in economic load dispatch. *IEEE Transactions on Sustainable Energy* **3**, 265–273 (2012)
10. Wu, L., Shahidehpour, M., Li, T.: Cost of reliability analysis based on stochastic unit commitment. *IEEE Transactions on Power Systems* **23**, 1364–1374 (2008)
11. Chang, G.W., Chuang, C.-S., Lu, T.-K., Wu, C.-C.: Frequency-regulating reserve constrained unit commitment for an isolated power system. *IEEE Transactions on Power Systems* **28**, 578–586 (2013)
12. Sahin, C., Shahidehpour, M., Erkmén, I.: Allocation of hourly reserve versus demand response for security-constrained scheduling of stochastic wind energy. *IEEE Transactions on Sustainable Energy* **4**, 219–228 (2013)
13. Hesamzadeh, M.R., Galland, O., Biggar, D.R.: Short-run economic dispatch with mathematical modelling of the adjustment cost. *Electrical Power and Energy Systems* **58**, 9–18 (2014)
14. Monthly Report December 2013, Red Eléctrica de España, (Spanish Version) (2014)
15. Padrón, S., Medina, J.F., Rodríguez, A.: Analysis of a pumped storage system to increase the penetration level of renewable energy in isolated power systems. Gran Canaria: A case study, *Energy* **36**, 6753–6762 (2011)
16. Gitrakos, G.P., Tsoutsos, T.D., Zografakis, N.: Sustainable power planning for the island of Crete. *Energy Policy* **37**, 1222–1238 (2009)
17. Distributed generation operational reliability and availability database, Energy and Environmental Analysis, Inc. (2004)
18. Billinton, R., Allan, R.N.: Reliability evaluation of power systems, p. 56. Plenum Press, New York (1996)
19. Zhu, J.: Optimization of power system operation, p. 85. Wiley, Hoboken (2009)
20. Daneshi, H., Choobbari, A.L., Shahidehpour, M., Li, Z.: Mixed integer programming method to solve security constrained unit commitment with restricted operating zone limits. In: Proc. 2008 IEEE Int Conf on Electro/Information Technology, pp. 187–192 (2008)

Energy: Management

Experimental Wireless Wattmeter for Home Energy Management Systems

Eduardo M.G. Rodrigues¹, T. Caramelo¹, Tiago D.P. Mendes¹,
Radu Godina¹, and João P.S. Catalão^{1,2,3(✉)}

¹ University of Beira Interior, Covilhã, Portugal
catalao@ubi.pt

² INESC-ID, Lisbon, Portugal

³ Instituto Superior Técnico, Lisbon, Portugal

Abstract. This paper presents a novel prototype device for domestic load energy consumption monitoring. Zigbee-based wireless connectivity is included as a basic feature of the prototype. The proposed device allows individual tracking of major energy consumption loads. Real time energy data is acquired and transmitted through a RF link to a wireless terminal unit, which works as a data logger and as a human-machine interface. Both voltage and current measurements are implemented using Hall Effect principle based transducers, while C code is developed on two 16-bit RISC MCU. The experimental setup is described and tests are conducted in order to assess its performance.

Keywords: Power meter · Zigbee · MSP430 · Sensors · Cloud computing

1 Introduction

A growing appetite for energy is a worldwide trend observable not only on industrialized countries as well as in emerging economies. Despite being a signal of economic vitality of modern society, concerns are rising among governments on how to match the energy needs in medium and long term without pushing hard natural resources exploitation or at the expense of public debt [1]. Different levels of human activities contribute with distinguishable energy-related footprints. A large share of the world energy demand is related to domestic consumption [2]. In fact, in the building sector up to 30% of consumed energy comes from residential loads, which are also responsible for 25% of demand during on-peak [3]. Refrigerators, space heating/cooling systems, water heaters, cloth washers, dryers, lighting, dishwashers, and cooking ranges in the residential sector are normally classified as major energy consumption devices [4]. In medium term, significant energy savings may occur in the residential sector towards today's electrical networks evolution into smart grids [5]. Home located advanced metering systems will also enhance this trend by giving residential users an unprecedented freedom to organize their domestic appliances daily usage [6]. In addition, other additional rationalization efforts can be promoted by taking advantage of available present technology.

In this context, a 2.4GHz ZigBee based distributed power metering system is proposed as part of a wireless home network area. This paper reports the development of

an experimental wireless power meter device along with a wireless terminal unit to track and monitor individual energy consumption on domestic appliances. Practical development is supported on development boards equipped with microcontroller units. The power meter prototype is designed for electrical parameters measurement within AC low voltage systems. Energy related parameters calculations are root mean square (RMS) voltage or current, active and apparent power, along with load power factor.

This paper is organized as follows: Section 2 discusses the benefits of integrating home energy management services on a broad platform with cloud computing organization. Next, Section 3 presents the distributed metering system concept and unveils the wireless watt-meter prototype technical details, focusing on major engineering design steps. Afterwards, a set of experimental tests are analyzed on Section 4. Lastly, concluding remarks are made on Section 5.

2 Contribution to Cloud-Based Engineering Systems

An Advanced Metering System (AMS) for home application relies on specialized meters designed for recording electricity and gas consumption periodically – smart meter. In turn, consumers will also access to monitors called In-Home Displays, which in turn allow them to see how much power is used at any time and how much it is costing them. The collected data will inspire consumers to use less energy, reducing their bills and supporting the environment. They will also be able to perceive when it is cheaper to run appliances [7]. The rising deployment of smart meters to people's homes outcomes in great quantities of data that required to be processed by power utilities. Cloud computing platforms can offer great scalability and availability concerning network bandwidth, computational resources, and storage. On the other hand, with the installation at large scale of distributed power meter devices for individualized energy consumption control purposes, an unprecedented increase of data generation arriving to smart meters is expected, which could in turn give rise to severe issues on the quality service provided by the communication infrastructure between the utility and consumers [8]. Cloud computing could alleviate smart grid agents' concerns and home owners' apprehension by providing additional dependable services. This means greater scalability and availability resources concerning network bandwidth, computational resources, and storage. Benefits of introducing two-way communications of the AMS/HAN based power meters with a cloud-based system are related to the information of the house's expected electricity usage behavior being concentrated and made available to a utility, load serving entity or an aggregator, and with those entities being able to execute their optimization processes by ensuring precise information to their consumers. Furthermore, the end-user could remotely access with a smartphone data regarding electricity consumption or even set parameters to the HAN connected domestic appliances in real-time. In addition, from the home owner standpoint, domestic informatics resources may not be adequate to store long term data. Finally, there is always a risk of losing it or been corrupted by a defective computer [9].

Figure 1 presents an overview for a global energy management paradigm through the cloud computing link. As can be seen, the cloud computing infrastructure performs a crucial interface acting as virtual decoupler between smart grid universe and home users, while at same time offering highly interoperability concerning communication capabilities.

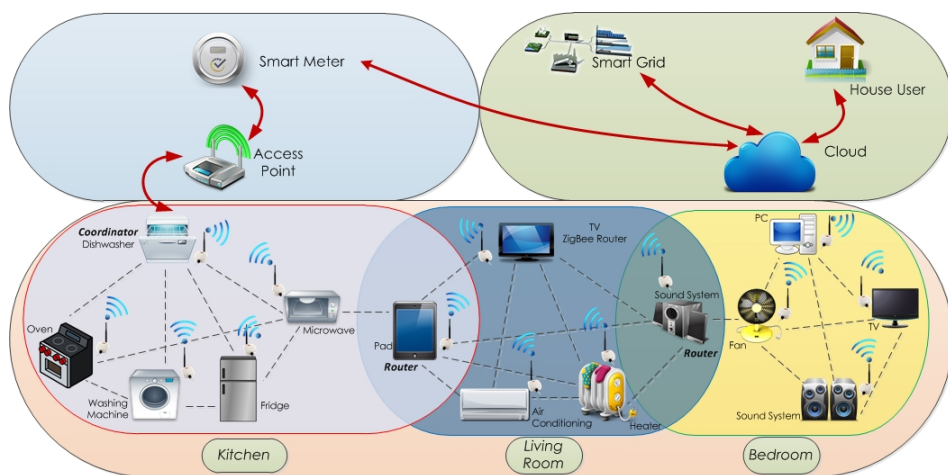


Fig. 1. Cloud services interoperability with AMS/HAN based home energy management system.

3 Wireless Watt-Meter Prototype

3.1 General Diagram

Figure 2 shows the minimum elements for the implementation of a home energy management system based on individual wireless metering systems. Three devices comprises the system: a smart meter, a metering unit that is in charge for the power and energy readings and a terminal unit prepared to receive real time energy consumption from each one of the domestic appliances plugged to a Zigbee network operated power meter. However, since a commercial smart meter is still expensive, the concept development and experimental tests have been conducted with the metering unit and terminal unit prototypes.

a) MSP430F5438A and MSP430F5529

Both models belong to MSP430 family of ultralow-power microcontrollers featuring a 16-bit RISC architecture. Major differences relay on flash and static ram memory, number of dedicated timer units, as well as serial bus interfaces (I2C, SPI and UART functionality) available. On the other hand, ADC specifications are exactly the same comprising a single module of 12-bit along with 16 channels (two are internally used) for conversion purposes. Sampling frequency is adjustable up to 200ksps in a single channel or in shared mode. For the metering unit, the MSP430F5438A MCU was chosen while the terminal unit was built on the MSP430F5529.

b) CC2530 radio

CC2530 radio is a mixed signal unit that comprises an IEEE 802.15.2 compliant RF transceiver along with an enhanced 8051 MCU supporting ZigBee, ZigBee PRO, and ZigBeeRF4CE standards. As the MCU side is equipped with up to 256kB of flash

memory, 8kB RAM memory, including 2 USARTs, 12-Bit ADC, and 21 general-purpose GPIO. It is well suited to cover small home areas and enables robust and flexible operation due to mesh networking capabilities offered by the Zigbee protocol. Zigbee based wireless applications are gaining increasing acceptance for smart grid and for improving HAN’s based AMS functionality [10], [11].

c) ACS712 Current Sensor

The Allegro ACS712 current sensor is based on the Hall-effect principle discovered by Edwin Hall. According to this principle, when a current carrying conductor is placed into a magnetic field, a voltage is generated across its edges perpendicular to the directions of both the current and the magnetic field. The sensor has the following main features: low noise analog signal, output sensitivity 66-185 mV/1A (+/-20 A), adjustable bandwidth up to 80 kHz and ratiometric linear output capability.

d) LV 25-400 Voltage Sensor

For voltage sensing the choice falls on the LV 25-400 voltage transducer manufactured by LEM. It is also based on Hall Effect principle. It allows maximum voltage RMS readings of 400V translated on reduced current mode output, allowing easy design of the analogue interface for instrumentation systems integration. It targets applications such as AC variable speed drives, servo-motor drives, DC motor drives static converters, as well as welding equipment’s power supplies.

3.2 Design Considerations and Specifications

Prototype implementation is followed by a functional block design approach, as can be seen in Figure 3.

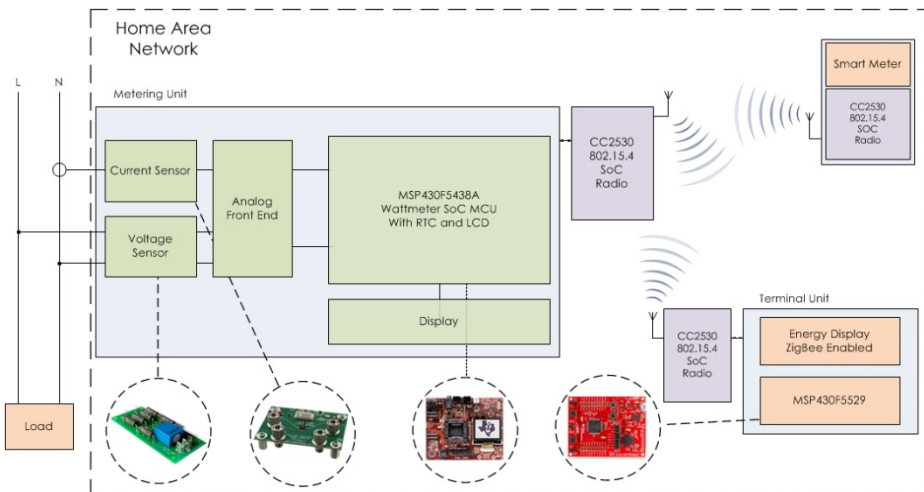


Fig. 2. Wireless power meter and terminal unit block diagram

a) Scaling of analog signal levels

Measures must also be appropriately handled to maximize metering system performance. Scaling is a set of procedures normally carried out to match physical signals with the ADC unit capabilities over its maximum conversion range.

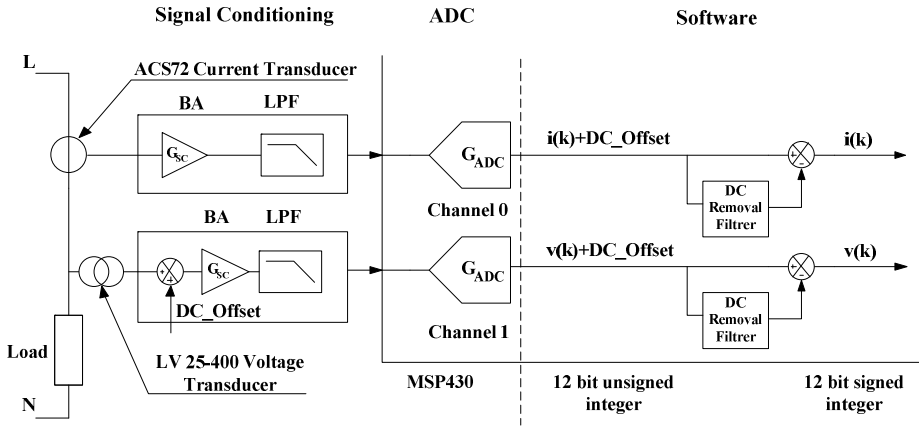


Fig. 3. Sensing, acquisition and post-filtering block diagram

Therefore, the signals before being acquired have to be scaled in the correct manner. Typically, real world signals are processed through an analog signal chain. ACS712 current sensor generates a unipolar voltage as output. The radiometric feature of the ACS712 means sensor gain and offsets are proportional to the supply voltage, V_{cc} . Thus, for 0 A load the sensor output is equal to $V_{cc}/2$, while sensitive range is proportional to its supply voltage. For the sake of simplicity, the ACS712 device is operated from a single power supply of 2.5 V that matches MSP430f5438A ADC internal voltage reference, which in turn reduces instrumentation chain complexity. The current transfer function is given by:

$$V_{IS} = K_{CT} I_{Load} + V_{OC} \quad (1)$$

where V_{IS} is the output voltage, K_{CT} is the gain coefficient of the transducer, I_{Load} is the sensed current and V_{OC} is the offset voltage related to the transducer zero current. Then, the ADC input voltage is expressed as:

$$V_{IS_ADC} = K_{CS}(K_{CS} I_{Load} + V_{OC}) \quad (2)$$

where K_{CS} is the gain of the signal conditioning circuit.

The transfer function of the 12-bit ADC is represented by the equation:

$$N_{12\ bit} = G_{ADC} V_{IS_ADC} = \frac{2^{12}}{2.5} V_{IS_ADC} \quad (3)$$

where $N_{12\ bit}$ is the 12-bit ADC code, G_{ADC} corresponds to the ADC equal to the ADC resolution divided by the input voltage range as indicated. The same formulation must be applied. Similar formulation can be applied to describe the instrumentation chain concerning grid voltage measurement. In digital power metering devices, the analog to digital converter unit has a key role on power meter performance. When it comes to commercial electricity metering equipment's most manufacturers opt for ADC's of

24-bit to digitize grid signals. The high level of quantization steps available is sufficient to guarantee an adequate resolution and precision in electrical measurements in order to fulfill international standards such as EN 50470-1:2006 or EN 50470-3:2006 [13]. However, the data acquisition capabilities available in the power meter prototype are modest in comparable terms. The MSP430F5438A has an internal ADC of lower word length configurable between 8-bit and 12-bit in steps of 2-bit. The resolution of the ADC determines the dynamic range of measured voltage and current. For voltage measurement, a maximum RMS reading of 300V is considered. Then, the voltage peak-to-peak range is given by:

$$U_{pk-to-pk} = 300 * \sqrt{2} * 2 = 848V \tag{4}$$

Considering that the accuracy of the MSP430F5438A’s 12 bit ADC is $\frac{1}{2^{12}}$, which is equivalent to 0.02% of the full scale ADC range, theoretical resolution is respectively:

$$U_{LSB:peak\ to\ peak} = 848V * 0,0002 = 0.17V \tag{5}$$

$$U_{LSB:RMS} = 300V * 0,0002 = 0.06V \tag{6}$$

b) Antialiasing filter requirements

For digitizing analog samples the minimum sampling rate f_s must be more than twice the signal maximum frequency, according to Shannon’s sampling theorem. On the contrary, if the rule is not respected the analog signal can’t be fully reconstructed from the input samples, posing an undesired effect know as aliasing. In view of the MSP430F5438A is not tailored for signal processing-intensive calculations, a performance and accuracy trade-off was decided. Thus, for power measurements the acquired electric quantities should be limited with a harmonic content up to 20th order. In practical terms, the prototype bandwidth is 1000Hz concerning a fundamental grid frequency of 50Hz. Therefore, a low pass filter has been designed to limit voltage and current signals bandwidth. A Bessel filter was chosen due to its good amplitude and transient behavior performance. In addition, the filter’s group delay is approximately constant across the entire pass-band, which is a mandatory design specification to limit distortion impacts on filtered signals. A cut-frequency of twice of the signal bandwidth specified can be observed from Bessel filter frequency response in Figure 4.

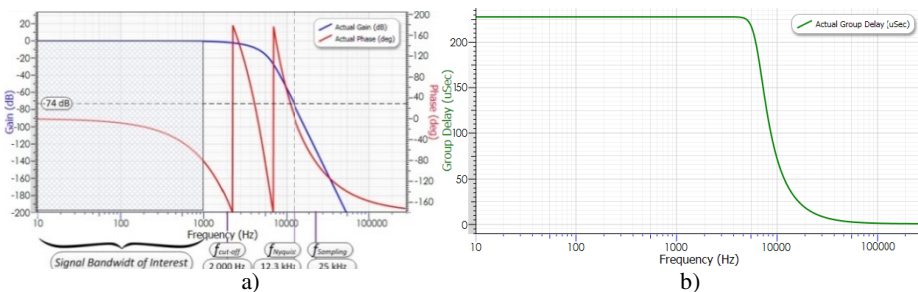


Fig. 4. 10th order Bessel filter frequency response: a) Magnitude and phase; b) Group delay

This is required to guarantee that the filter output attenuation at 1000Hz is virtually zero. High order Bessel filter and, consequently, higher sampling frequency selected have to do also with the ADC dynamic range, which in turn is related with its signal-to-noise ratio (SNR) [14]. For our study, it is assumed that the MSP430f5438A's 12-bit ADC is ideal. Hence, the SNR is 74 dB. Having this in mind, the Nyquist Frequency ($f_s/2$) is approximately 12.3 kHz. In order to comply with Shannon's theorem, the sampling rate has been selected slightly above the minimum recommended.

c) DC offset removal

Before moving to the energy transit related parameters calculation, the offset term must be eliminated from incoming signals. Instead of simply subtracting a fixed offset from the signals, a high pass filter was developed on Matlab. The first order IIR (Infinite Impulse Response) filter has a -3 dB cutoff frequency of 0.1Hz and sampling frequency of 25000s/sec.

The obtained digital filter can be expressed as:

$$y[n] = 0.996 * y[n - 1] + 0.996 * x[n] - 0.996 * x[n - 1] \quad (7)$$

Taking the z-transform of both sides and rearranging the terms, gives:

$$H(z) = \frac{0.996 - 0.996z^{-1}}{1 - 0.996z^{-1}} \quad (8)$$

To minimize the effects of binary word length on filter's outcome performance, especially when extracting the offset term on low voltage and current signals, filter's coefficients as well the result are handled in 32-bit arithmetic fixed point.

4 Experimental Tests and Results

A set of tests have been performed to verify the experimental watt-meter (Figure 5) implemented algorithms performance. For this purpose, a conventional electric heater has been chosen since it is a common domestic appliance. The domestic load offers two power regulation levels. The user can select between half and full power rated at 2000W. The tests focused on comparing current waveform acquisition by the device developed with the wave trace observed on an oscilloscope. In addition, a current clamp was employed to determine current RMS values at half and at full power. These measures made it possible to assess the prototype RMS estimation proximity to current clamp readings.

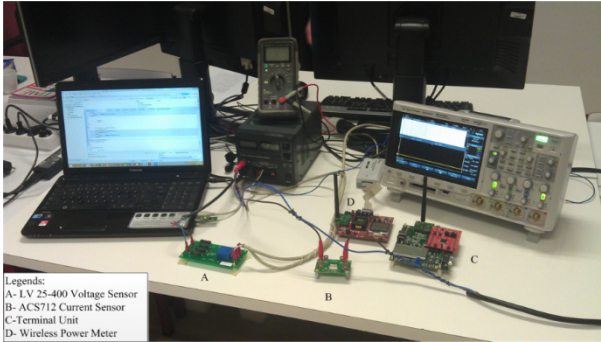
Figures 6 and 7 show that the current acquisition is relatively noisy; however, RMS estimation is not compromised.

In fact, on both load regimes the calculated values are very much in agreement within the current meter readings. Naturally the discrepancy found on prototype reading has to be confirmed with more tests covering a wider group of electric loads. This will be a future work of the authors. Moreover, a calibrated meter tool is mandatory to proceed to a metrological formal verification.

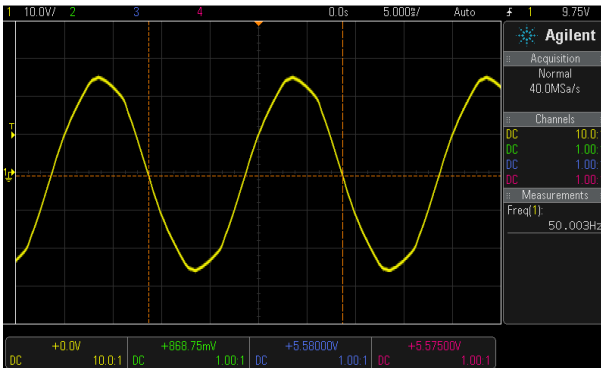
5 Conclusions

This paper presented a prototype device that allows individual tracking of major energy consumption loads. Energy data was acquired in real-time and transmitted through

the RF link to a wireless terminal unit, which works as a data logger and as a human-machine interface. Both current and voltage measurements were executed using Hall Effect principle based transducers, while C code was developed and loaded on two 16-bit RISC MCU. The experimental assembly was described and a set of tests were carried out in order to validate the prototype developed.

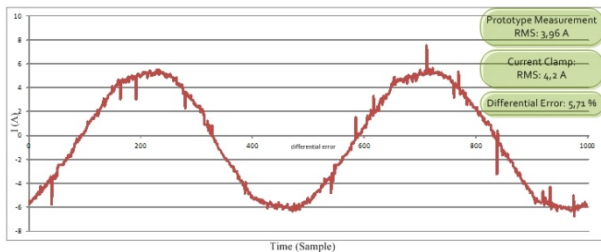


a)



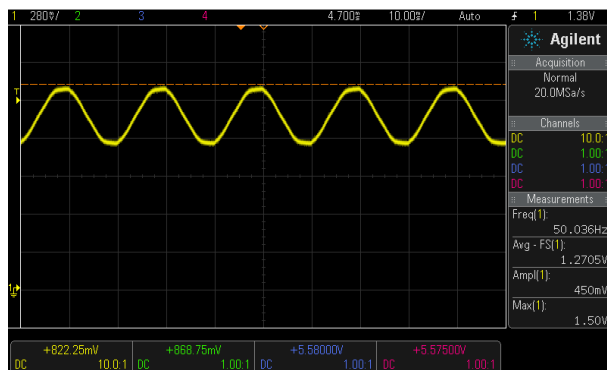
b)

Fig. 5. a) General view of the experimental test bench; b) Grid voltage reading



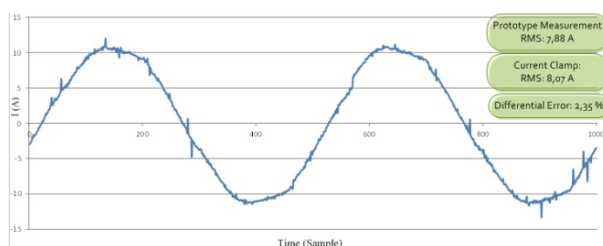
a)

Fig. 6. Half power operating electric space heater: a) Prototype acquired current profile; b) ACS712 output

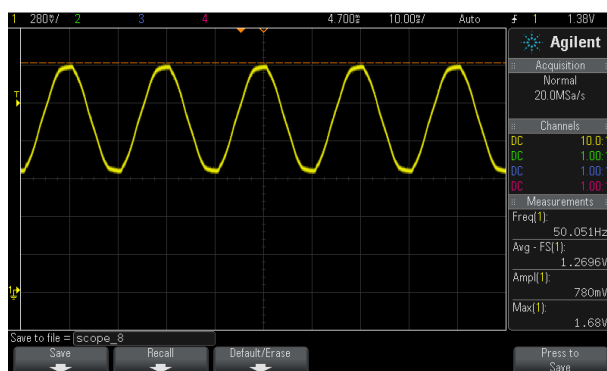


b)

Fig. 6. (continued)



a)



b)

Fig. 7. Full power operating electric space heater: a) Prototype acquired current profile; b) ACS712 output

Acknowledgment. This work was supported by FEDER funds (European Union) through COMPETE and by Portuguese funds through FCT, under Projects FCOMP-01-0124-FEDER-020282 (Ref. PTDC/EEA-EEL/118519/2010) and PEst-OE/EEI/LA0021/2013. Also, the research leading to these results has received funding from the EU Seventh Framework Programme FP7/2007-2013 under grant agreement no. 309048.

References

1. Byun, J., Hong, I., Kang, B., Park, S.: A smart energy distribution and management system for renewable energy distribution and context-aware services based on user patterns and load forecasting. *IEEE Transactions on Consumer Electronics* **57**(2), 436–444 (2011)
2. Nilsson, A., et al.: Effects of continuous feedback on households' electricity consumption: Potentials and barriers. *Applied Energy* **122**, 17–23 (2014)
3. Tadokoro, S., Jia, Q.-S., Zhao, Q., Darabi, H., Huang, G., Becerik-Gerber, B., Sandberg, H., Johansson, K.: Smart Building Technology [TC Spotlight]. *IEEE Robotics & Automation Magazine* **21**(2), 18–20 (2014)
4. Bozchalui, M., Hashmi, S., Hassen, H., Canizares, C., Bhattacharya, K.: Optimal Operation of Residential Energy Hubs in Smart Grids. *IEEE Transactions on Smart Grid* **3**(4), 1755–1766 (2012)
5. Koutitas, G.: Control of Flexible Smart Devices in the Smart Grid. *IEEE Transactions on Smart Grid* **3**(3), 1333–1343 (2012)
6. Georgievski, I., Degeler, V., Pagani, G., Nguyen, T.A., Lazovik, A., Aiello, M.: Optimizing Energy Costs for Offices Connected to the Smart Grid. *IEEE Transactions on Smart Grid* **3**(4), 2273–2285 (2012)
7. Rahman, M., Al-Shaer, E., Bera, P.: A Noninvasive Threat Analyzer for Advanced Metering Infrastructure in Smart Grid. *IEEE Transactions on Smart Grid* **4**(1), 273–287 (2013)
8. Green, R., Wang, L., Alam, M.: Applications and Trends of High Performance Computing for Electric Power Systems: Focusing on Smart Grid. *IEEE Transactions on Smart Grid* **4**(2), 922–931 (2013)
9. Fang, X., Misra, S., Xue, G., Yang, D.: Managing smart grid information in the cloud: opportunities, model, and applications. *IEEE Network* **26**(4), 32–38 (2012)
10. Kulkarni, P., Lewis, T., Dave, S.: Energy Monitoring in Residential Environments. *IEEE Technology and Society Magazine* **33**(3), 71–80 (2014)
11. Namboodiri, V., Aravinthan, V., Mohapatra, S., Karimi, B., Jewell, W.: Toward a Secure Wireless-Based Home Area Network for Metering in Smart Grids. *IEEE Systems Journal* **8**(2), 509–520 (2014)
12. Li, L., Chen, Y., Zhou, H., Ma, H., Liu, J.: The application of hall sensors ACS712 in the protection circuit of controller for humanoid robots. In: 2010 Int. Conf. Computer Application and System Modeling, Taiyuan (2010)
13. Holoubek, L.: Tauglich für das Smart Grid Elektrizitätszähler auf Basis eines Cortex-M4F-Mikrocontrollers, *Elektronik Industrie*, 30–32 (2012)
14. Analog Devices: Fundamentals of Sampled Data Systems AN-282 Application Note. Norwood, Massachusetts

Use of Web Based Meters to Improve Energy Efficiency and Power Quality in Buildings

Licínio Moreira^{1,2(✉)}, Sérgio Leitão², Zita Vale^{3,4}, and João Galvão^{1,5}

¹ School of Technology and Management, Polytechnic Institute of Leiria,
P-2411-901 Leiria, Portugal
licinio.moreira@ipleiria.pt

² INESC-TEC (UTAD pole) ECT, UTAD University, Vila Real, Portugal
sleitao@utad.pt

³ Department of Electrical Engineering, Polytechnic Institute of Porto (ISEP/IPP),
Porto, Portugal

⁴ GECAD (Knowledge Engineering and Decision Support Research Group),
Porto, Portugal

⁵ INESC Coimbra - Institute for Systems Engineering and Computers at Coimbra,
Coimbra, Portugal
jrgalvao@ipleiria.pt, zav@dee.isep.ipp.pt

Abstract. During the work conducted, several buildings were analysed, in terms of energy efficiency and power quality. Two case studies are here presented: an educational building and a museum. Most of the studies were conducted recurring to traditional measurement equipment, forcing the person to travel to the site to install equipment and every time he wanted to collect data. But one of the case studies, the museum, comprised the development of an analyser (hardware and software) able to measure electric energy, temperature and humidity. This analyser has the capability to register values on a database available in the internet and issue warnings to the building manager. This allows real-time information, supporting some energy efficiency actions. The objective is to improve this model and expand its use for several buildings, providing savings in terms of time and other resources, taking advantage of cloud-based systems.

Keywords: Energy efficiency · Cloud-based system · Energy management systems · Power quality · Smart city

1 Introduction

At present time, the availability of information on energy use for customers is, in most of the cases, limited to the monthly utility bills. The information provided by the utilities is generally limited to quantitative aspects, neglecting the qualitative issues. This diminutive information, along with the time gap between the effective consumption and the delivery of the bill constitute barriers to immediate actions. The widespread use of energy analysers, with metering and power quality analysis capabilities, connected to cloud-based systems would enable real-time knowledge and it could benefit the benchmarking of different building and processes.

The knowledge of individual data and the benchmarking of several similar processes or buildings, based on web systems, empowers the manager to the development of strategies for intervention to improve the energy efficiency of the building or process, within the concept of Smart City for sustainability.

This deals with a methodology shift in the energy auditing. It is intended to set off from the classic energy auditing, with individualized analysis requiring onsite data collection, to a more systematic approach, based on spread analysers dispatching data to a common database through the use of web-based systems.

2 Benefits from Cloud-Based Engineering Systems

Data and programs are part of the world of computing in the desktop PCs, but the current trend is to relocate them and integrate the usually server room to the cloud computing service or on-demand computing/software. The platform used is the Internet with exceptional growth and the common element is a shift in the geography of computation. For example, each time someone uses a search engine service, the main software is lodged computers on unseen to the user, possibly distributed across different continents. [1]

In a wider context we can say that cloud is a large-scale, distributed Information Technologies (IT) facilities available over the internet and is transforming the way intrinsic IT services are delivered and managed.

The use of cloud-based systems tends to reduce overall cost and increase efficiencies, especially when replacing an organization's locally operated system and supported with local servers. This detail is reflected in energy and environmental benefits. Also the cloud-based systems have a huge potential, improving efficiency and business agility, therefore contributing to a more sustainable world [2].

Industrial or services companies acting in energy audit, that use suitable equipment to collect energy consumption and/or power quality data variables will gather the inherent business benefits of this technology, mainly from the remote and possibly real-time data availability. The ease of data collection, data sharing and information delivery, boosted by the rising use of mobile devices, is another relevant benefit for users. Another impact of the use of this computing platform is the reduction of costs related to technical staff involvement in on-site data collection and system maintenance. All of this can play a crucial role in making IT more sustainable by significantly reducing energy consumption, raising levels of energy efficiency [3].

3 Motivation of the Work

The energy data from multiple sites, such as industrial, services and residential buildings has to date been collected on an individualized approach and on site, recurring to temporary placement of portable energy analysers. Although many installations are already fitted with smart meters for electric energy, they are only used in remote metering by the utility and the data isn't usually delivered to the customer in a timely way. Also, they only measure total energy at the point of common coupling, therefore

they don't allow the disaggregation of energy (electric and thermal) consumption by different sector or areas of the facility under study.

This high volume of data collected is related to main energy consumers in the buildings, highlighting the appliances, machinery, HVAC, lighting, compressed air. Also, data related with the activity in the building (production, occupation, building structure ...). Also some other data is linked with consumer behaviour, market and technologies, measurement methods, public procurement, market transformation programs, end-use metering, demand response, smart meters, smart homes and smart appliance, consumer electronics, ICT, residential lighting and home automation.

On this field, the disaggregation of energy variables, with several consumers and several parameters, is necessary. In each case study, sampling intervals of 5, 10 or 15 minutes are used, resulting in a large collection of data at the end of a campaign up to several weeks. This data requires to be treated and interpreted quickly, in order to promptly take actions, in terms of energy efficiency and/or power quality issues.

This individually collecting of data, along with individual data processing is time and resource consuming associated with the travelling to the site and losses of time due to computer media used and different software that perform the data processing. The main objective of this work is to demonstrate that the data management with resource to cloud-based systems can raise the performance in the analysis energy data.

Based on several case studies in urban and industrial environment, related with the researches developed on last years, to retrofit the energy systems and achieve better energy efficiency in these buildings and industrial activities, putting into practice the smart city concept. These studies are part of a set of actions to achieve the assimilation of the national programme which implements these requirements for greater energy efficiency (the 20/20/20 Plan) by the various economic and industrial players. This 20/20/20 Plan predicts a cut of 20% in GHG emissions for the EU by the year 2020, a share of 20% of energy from renewable sources and a 20% increase in energy efficiency and implementing smart grids and cities, for a low carbon and sustainability [4] and [5].

These case studies included, among others, plastic and mould industries, public library, sports hall, museum, comprising a vast diversity of data (numerical data; thermal images) to be processed. Here, the cloud technology can play an important role in data processing and in the dissemination of results [6], [7], [8] and [9].

4 Case Studies

The base of the studies consists of energy audits. The acquisition of existing energy consumption and other data was carried out with the use of various energy and power quality analysers, thermal camera and other equipment, aiming to characterize not only the energy consumptions, but in also the buildings structure and materials (walls, roof, warehouse and office). The energy audit consists of several aspects that will allow us to identify critical parts of this facility and that should be improved in order to achieve a higher level of performance. In this context, the energy facilities and activities associated with them were characterized according to the standard Energy Management Systems [10] and [11].

The energy audit of all sectors and all forms of energy, and its pursuance requires knowledge of the electrical, thermal, mechanical and environmental areas of the building. Thus, energy audits provide specific information and identify the actual energy savings, consisting primarily of a critical examination of how energy is used based on the available records of energy consumption and costs. An energy analysis was carried out, leading to the characterization of energy consumption in recent years. This consisted in the use of existing energy bills from the utility and the use of several energy analysers.

In several audits, especially the ones in industrial facilities, power quality issues were also addressed. In some cases, prior to the studies, the building manager didn't relate the malfunction of some equipment to power quality events, while others hold responsible the electricity distributor for every malfunction, even if it was not to blame. In general, one can conclude that the awareness of power quality issues is short. In most cases, this work contributed to the rise of awareness among industrial managers.

Given the diversity of buildings and activities analyzed, only two cases in the service area (library and museum) are presented here, being a sample of the objectives to increase energy efficiency, sustainability in the context of Smart City. One of them was conducted in the traditional manner and the other includes the development of a web-based meter.

4.1 Public Library

Approximately three quarters of the population in EU lives in cities or nearby. It is necessary to improve the energy efficiency of buildings, since about 40% of the primary energy consumed in the European Union, results from energy use in buildings [12] and [13]. Therefore, it is important to promote good practice in the application of renewable energy combined with energy efficiency measures. The EU has developing a long-term strategy to a low-carbon economy and to make better use of its energy systems and scarce resources. Urban areas consume 70% of the energy in the EU and emit about the same share of greenhouse gases. The Smart Cities Initiative is a new European task force, whose objective is to make Europe's cities more efficient and more sustainable in the area of energy.

This case study comes up with a new energy model that retrofits the present system in a public library building, as a way to the dissemination the Smart City concept and development of energy production based on a sustainable and autonomous process. Taking into account that to implement this concept, constant monitoring of energy data is essential and only installing measurement equipment, and consequent rapid dispatch data to be analyzed and stored in the cloud-based platform if able to achieve high levels of energy efficiency in buildings.

This work related to the ongoing research is based on an energy audit, comprising a survey on energy consumption by type: electrical and thermal (gas), recurring to portable energy analysers, as shown in Fig. 1, Another relevant aspect of this audit was the identification of anomalous situations in energy infrastructures: electrical and thermal, by means of a thermographic analysis of multiple parts of the installations, focused on electrical switchboards, as shown in Fig. 2, and thermal energy pinping.

This consists of gathering information for determine energy savings from a perspective of energy determination of equipment that can induce forced stops away the power supply, for wear and tear or malfunction resulting from higher operating temperatures and lead to a rapid degradation.



Fig. 1. Measuring Equipment - Power Analyzer in the Collection of Consumptions

This energy of the building library consists of a photovoltaic (PV) plant and a biomass energy source to replace the gas that is currently used.

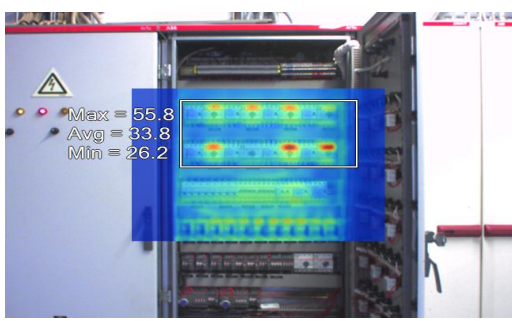


Fig. 2. Thermographic image of switchboard and temperatures (maximum; average; minimum)

As shown in Fig. 2, a spot with high temperature was detected on the bottom of a connection. This high temperature is due to a bad tightening and if this situation persists, the material would suffer a marked wear, leading to his destruction and possibly trigger a fire. The standards established by InterNational Electrical Testing Association (NETA) rule that a quick action is required, when the difference between electrical components exceeds 15°C or the difference between air temperature and the electrical component exceeds 40°C [14]. Besides bad electrical connections, thermal imaging can be used to detect the correct sizing of electrical components. An oversized (or underloaded) component would result in a low temperature, while an undersized (or overloaded) component would result in a high temperature. The innovative proposed model consists of a mix of energy production processes based on photovoltaic panels and biomass boilers. Economic analysis of the energy model al-

ready achieved some results regarding the payback of the investment, as well as to achieve decarbonisation of cities and a strategy for competitive and secure energy.

4.2 Museum

In the context of improvement of energy efficiency in public buildings, this case study comprised a small museum with an exhibition space of around 200 square meters and other areas (archive, administrative area, ...). This museum occupies a public building that was not built specifically for this purpose. The space underwent a minor retrofitting to receive the assets of the museum fifteen years ago. This implied some constraints on the use of the museum. Also, the energy bills were rising, becoming a major concern for the museum direction.

As a first approach, and after an energy audit conducted by the traditional method, the largest energy consumers were identified: lighting, dehumidifier and space heaters. The first step was the substitution of around 100 halogen spots (25, 35 and 50 W) by LEDs (4.4 W). The expected payback time is around 1.25 years, while increasing the light level in some spaces and minimizing the ultra-violet emission that fastens deterioration of some assets of the museum. Also, emissions of 1130 kgCO_{2e} per year were avoided due to energy consumption reduction. In addition, some motion detectors were installed in the museum, mainly improving the convenience of the museum staff and, in addition, enabling additional energy savings in the lighting system.

The next step in this case study was the development of a low cost web-based meter, primarily for temperature and humidity supervision, but energy measurement features were included in the first iteration. The basic configuration of the system is shown in Fig. 3. A module with a humidity and temperature sensor and signal conditioning communicates with the central processing unit (CPU) using the wireless technology *ZigBee*[®]. The energy measurement module is based on three current sensors and three 230/12 V and signal conditioning circuits that communicate with the CPU via a cable. The central unit, based on an *Arduino* processor, is responsible for processing the data received from the separate modules and record the data on a database. It is connected to the switch of the museum IT system via an Ethernet cable.

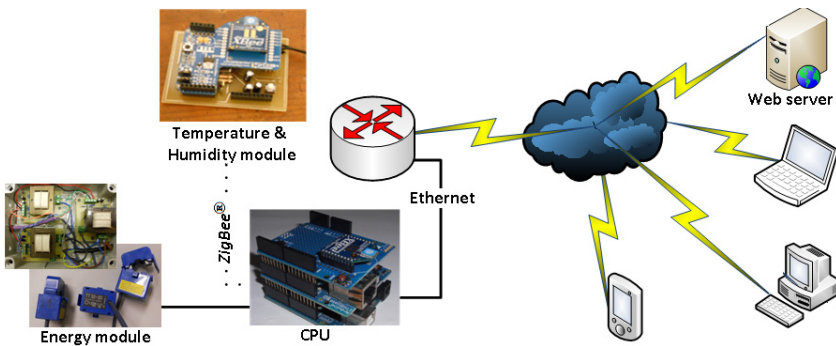


Fig. 3. Developed prototype of a web-based meter

The database created records the averaged values of temperature, humidity, voltage, current, active power, reactive power and power factor with an interval of 10 minutes. This data is available on an open web site. The system is also programmable with warning emission, by email, when the reference value of temperature and/or humidity is exceeded and anomalous energy consumption or power failures occur.

The central unit is scalable allowing to aggregate data from more temperatures and humidity modules or energy modules with slight changes in the software. Other changes, such as real-time power quality events recording are planned and possible without significant changes in the hardware of the meter.

The data recording and easy remote access to it, along with the warnings issued by the system, enables the manager of the building to take swift actions for a better energy efficiency.

5 Conclusions

With the increasing concerns for energy efficiency, a more efficient control of energy use is required. The timely availability of data, if possible in real time, constitutes a key factor in decision-making in all areas, including the energy management. Therefore, the traditional energy monitoring systems, sometimes limited to energy billing and periodic measures, constitute a barrier for the development of a proper energy management system focused on the best possible efficiency. Using the services provided by the cloud, the data could be attained more rapidly and the energy data handling can be simplified, using a common platform, optimizing processes for managing projects and opportunities. Also, with the use of cloud-based systems, the data may be available to different people wherever there is an internet connection.

As the efficiency of cloud computing increases, more services are developing, while each service or transaction tends to use less energy with several studies referring that cloud-based systems are more energy-efficient than on site IT systems. Bringing this energy saving together with the activity of energy auditing, further efficiency can be attained.

But sometimes the costs of buying and maintaining a system connected to the web can be an obstacle to the dissemination of these systems in buildings. The current work described here included the development of a low cost energy meter (including other parameter metering capabilities, such as power quality events, temperature and humidity). The dissemination of this kind of meters can play an important role in assisting the transition of locally available energy data to the web available data, allowing real-time information and benchmarking of different sites. These tools can play an important role in boosting the energy efficiency of buildings and processes.

Acknowledgment. This work has been partially supported by the Portuguese Foundation for Science and Technology under project grant PEst-OE/EEI/UI308/2014.

References

1. Hayes, B.: Cloud computing. *Commun. ACM* **51**(7), 9–11 July 2008. doi:10.1145/1364782.1364786 <http://doi.acm.org/10.1145/1364782.1364786>
2. Abood, D., et al.: Cloud Computing and Sustainability: The Environmental Benefits of Moving to the Cloud. Accenture Consulting (2010). www.accenture.com
3. Mann, K.: Cloud technology + mobile = a net positive impact on all businesses, Silicon Avenue. www.procisionplus.com
4. de Wilde, P., Coley, D.: The implications of a changing climate for buildings, *Building and Environment*, vol. 55, pp. 1–7, September 2012. ISSN 0360-1323. <http://dx.doi.org/10.1016/j.buildenv.2012.03.014>
5. Wada, K., Akimoto, K., Sano, F., Oda, J., Homma, T.: Energy efficiency opportunities in the residential sector and their feasibility, *Energy*, **48**(1), pp. 5–10, December 2012. ISSN 0360-5442. <http://dx.doi.org/10.1016/j.energy.2012.01.046>
6. Moreira, L., Leitão, S., Vale, Z.: Power Quality problems in the mould Industry. In: 11th Spanish Portuguese Congress on Electrical Engineering (11 CHLIE), Zaragoza (1–4 July 2009)
7. Galvão, J., Moreira, L., Leitão, S., Silva, E., Neto, M.: Sustainable energy for plastic industry plant. In: Proceedings of 4th International Youth Conference on Energy, IYCE/IEEE, Siófok, June 2013. doi:10.1109/IYCE.2013.6604193
8. Galvão, J., Moreira, L., Marques, P.: Smart City and Sustainable Renovation of Energy Systems for Efficiency; IN-TECH 2014 - International Conference on Innovative Technologies, September 10–13, Leiria, Portugal (2014)
9. Moreira, L., Leitão, S., Vale, Z., Galvão, J., Marques, P.: Analysis of Power Quality Disturbances in Industry in the Centre Region of Portugal. In: Camarinha-Matos, L., Barrento, N., Mendonça, R. (eds.) DoCEIS 2014. IFIP AICT, vol. 423, pp. 435–442. Springer, Heidelberg (2014)
10. EMS - Energy Management Systems - requirements with guidance for use. BSI Standards Publication - BS EN ISO 50001:2011
11. Galvão, J., Leitão, S., Malheiro, S., Gaio, T.: Hybrid Model for the Energy Efficiency of Building Services in Book: Energy Efficiency: Methods, Limitations and Challenges. Nova Science Publishers, USA (2012). see: https://www.novapublishers.com/catalog/product_info.php?products_id=30968
12. Carvalho, M.G.: Energy Policies in EU, Energy Conference Lisbon, 23 March 2012
13. European Commission, Report of the Public Consultation on the Smart Cities and Communities Initiative, Director General for energy, Brussels, 14 June 2011
14. NETA - InterNational Electrical Testing Association, Standards for Maintenance Testing Specifications, 2007. see <http://www.netaworld.com>

A Model-Based Approach for Resource Constrained Devices Energy Test and Simulation

Edgar M. Silva^{1(✉)}, Luis Gomes^{1,2}, João Rodrigues¹, and Pedro Maló^{1,2}

¹ Faculdade de Ciências e Tecnologia, Universidade Nova de Lisboa,
Lisbon, Portugal

{ems, jf.rodrigues}@campus.fct.unl.pt,
{pmm, lugo}@fct.unl.pt

² Centro de Tecnologia e Sistemas, UNINOVA, Lisbon, Portugal

Abstract. The constant evolution in communication technologies, has improved during the last decades the interaction between systems/devices/things/etc. Internet-of-Things (IoT) has become the last trend pushing forward in this direction, connecting all ‘things’, creating a sensing world around all of us. Although, IoT technologies, solutions, systems have to be proven/tested before deployment in the real settings. These decentralized systems normally use low power devices with small processing and storage capabilities, with roles mainly of sensing and data transmission. Until now, tests and energy simulation focus on wireless communications, since it has been identified as the main energy consuming module. This paper presents the acquisition and simulation of energy consumption by a single device, focused on all hardware components and not only in the communication, due to the new adopted solutions that do not rely so much in the communication (e.g. subscription). In this sense, a methodology capable of retrieving real and simulated energy consumption results from/for a single device is presented, relying on a model based approach (software, hardware, energy and simulation models) and on a precise energy consumption assessment system. It is also presented a Resource Constrained Device Model, capable of representing the available hardware in a device, and a circuit to retrieve more accurate energy consumption readings.

Keywords: Internet of Things (IoT) · Wireless Sensor Networks (WSN) · Power consumption · Simulation · Model Driven Engineering (MDE).

1 Introduction

Advances in microelectronic technologies have brought small and cheap devices, leading to highly heterogeneous environments. Manufacturers are engaged in developing devices for different purposes addressing different application domains and services to target different Internet-of-Things (IoT) deployments [1].

These deployments, such as Smart Cities, Domotics (Smart Buildings), etc., follow standards from Internet-of-Things (IoT), a global infrastructure for a more aware society, through advance services by interconnecting things, physical and virtually, based on existing and evolving interoperable information and communication technologies [2].

These systems normally use low power devices with small processing and storage capabilities, with roles mainly of sensing and data transmission, making full use of services to all kinds of applications, whilst ensuring fulfillment of all its requirements.

The major requirement for these devices is low-power operation, an extended life-time, which leads to the actual problem, energy consumption. This work aims to understand in which ways is possible to estimate the power consumption, going through some existent solutions performing both acquisition and simulation of energy consumption by a single device. Looking forward to improve these methods, a methodology capable of retrieving real and simulated energy consumption results from/for a single device is presented, relying on a model based approach.

2 Cloud-Based Engineering Solutions for Internet-of-Things

Nowadays, is possible to produce small and cheap devices, with computation, sensing and wireless communication capabilities. Thanks to advances made, Wireless Sensor Networks (WSN) offer technology support for a wide range of potential applications [3].

The relation with Cloud-based Engineering Systems can be established with base on the typical topology adopted in these systems. Considering a large number of nodes, and according to the type of sensing equipment, each device performs its task, collecting information and then, via subscription or periodically transmitting data, through a route to one or more collection points, called sink nodes. This unit gathers all data, making it available outside the WSN, exactly as other well-known Cloud-based systems [4].

One possibility is the paradigm expansion to a collaborative online platform, positioning itself on the cloud's information layer where all data is available to all interested entities. This will allow, for example, resource allocation strategies to reduce computational requirements for each user and also models exchange, creating a remote platform for energy testing [5].

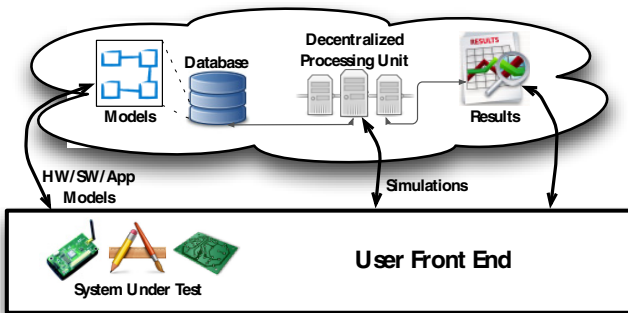


Fig. 1. Example of Cloud-based platform for collaborative simulation

A Model-based approach which allows users to share tailored models for each System Under Test and to request a remote simulation of such system is illustrated in Fig.

1. As simulations require high computational resources, remote effort allocation is the major advantage, saving local execution time while waiting for results.

3 Background Research

Over the last years Internet-of-Things (IoT) has moved from being a futuristic vision, to an increasing reality. It is a dynamic global network infrastructure, with self-configuring capabilities based on standards and interoperable communication protocols, where physical and virtual 'things' have identities, physical attributes and virtual personalities [1].

In order to realize the vision of the IoT, Wireless Sensor Networks (WSN) position themselves as a virtual layer where the information about the physical world can be accessed by any computational system [6]. On the physical side, WSN are formed by a number of devices, spatially distributed, in autonomous and cooperative monitoring of physical or environmental conditions [7].

One of the main challenges is to take into account the energy constraints of such devices, which aim to have a low-power operation, something that is difficult to predict during applications development [8]. For such task, power consumption analysis is a vital step to evaluate the performance of these devices. The following sections present a brief review of such approaches.

3.1 Power Consumption Analysis

The distributed nature of WSN, based on the interaction between software and hardware components, makes it less easy to correctly design and develop such systems. Power consumption is the main concern at this stage, with several methods proposed in a while, which aim to investigate this phenomenon. As a result, these strategies may help the prediction of the expected lifetime, just before deployment, providing to application developers useful recommendations to optimize energy consumption [7].

The two most common approaches for power consumption analysis are based on direct measurement, and on usage of simulation models. While measurement is a more accurate strategy for power consumption evaluation, it is known to have some limitations, as it turns to be very costly, tedious or even not practical, considering the typical topology of a network, with a large number of devices [4]. Due to this complexity, measurements taken on a single node are often generalized to the entire network when considering similar tasks and performed by homogeneous platforms. A common solution is measuring and monitoring the absorbed current, using a single resistor setup, placed between the power supply unit and the Device Under Test (DUT). Applying Ohm's law for the voltage drop across the resistor, current is measured. As this is an indirect measuring method, some of its accuracy limitations may put the process results at risk. Moreover, this also restricts the general consumption measurement on the device, making impossible to understand which components are draining current [3].

It is known that in comparison with other peripherals, radio modules are the source for greatest usage of energy so a way to understand the current drainage is by running applications that make use of a single component at a time, in order to generate its own energy profile. Combining the data collected for each application, simulation models may be generated for future testing, turning the scenario a little less complex.

3.2 Simulators

Simulation is the quickest way to test code and systems, before running it on the target hardware. Some simulation tools provide power consumption estimation, becoming a useful resource for performance analysis, when coupled with proper measurement techniques, keeping into account possible limitations on data acquisition [3]. There are several simulators, each with its own features and limitations. Avrora is widely used for WSN specific simulation, providing discrete-event simulation up to thousands of nodes. Although, it does not provide extensions besides from AVRMCU cores [8]. With the addition of an energy model, power profiling and lifetime prediction are enabled [9]. Bundled with Contiki OS, Cooja (<http://contiki-os.org>) is a useful tool to simulate such architecture, supporting emulation of platforms with TI-MSP430 or AtmelAVR micro-controllers, allowing heterogeneous networks emulation, supporting power consumption estimation [10]. MSPSim [11] can emulate TI-MSP430 micro-controller based devices from the instruction level, optimizing applications debugging process, and offering power consumption estimation, compatible with Contiki OS and TinyOS (<http://tinycos.net>). NS-2, from Network Simulator (<http://nsnam.org>), is a discrete-event simulator for general purpose, running up to 100 nodes. However, NS-2 cannot simulate power consumption in WSN [8]. PowerTossim (<http://eecs.harvard.edu>) is an extension to TOSSIM, which is a simulation environment included in TinyOS's framework. However, as TOSSIM only supports MICAz (<http://moog-crossbow.net>) hardware platform, the applying scope is reduced. Somov is the less tailored simulator as it offers power estimation of WSN applications for arbitrary hardware platforms, by separately defining the possible states of each component, having its performance and energy consumption data associated [4].

3.3 Model Driven Engineering (MDE) Approaches

With the sustained increase of technology, models are becoming more and more attractive to manage systems complexity, by simplifying design processes and formalization [12]. MDE's vision follows a unification principle, "everything is a model" (i.e. all can be modelled, programs, services, etc.), similar to the object technology basic principle, "everything is an object".

Another key initiative in MDE approaches is the Model Driven Architecture (MDA), an Object Management Group (OMG) initiative, which offers modelling support at different levels of abstraction [13]. MDA specifies a standard-based architecture for models, organized around three different abstraction levels, providing guidelines to structure the specifications [13][14]: Computation Independent Model (CIM), Platform Independent Model (PIM) and Platform Specific Model (PSM).

The CIM is a level for the domain practitioners, in which systems requirements as well as the environment are specified with specific domain vocabulary, bridging the gap between domain experts and the development experts [13].

The PIM level deals with system formal specification, structural as functional. Abstracts technical details, focusing on system operation itself rather on how operations will be carried out. PSM level gathers technical and engineering details from a specific platform, combining it with the system specification from PIM level.

4 Hypothesis

From the early background research, some of the most important features and constraints of WSN devices were identified. It was possible to understand some weaknesses in existent solutions for behavior emulation and power consumption analysis (via simulation and direct measuring). As a result, the main question of this paper is: *Would a model-based approach, combined with precise measuring and simulation, provide more accurate results, being able to solve the known weaknesses on other previous attempts to assess the power consumption?*

This is the starting point for the proposed solution, which will make use of the presented concepts, such as simulation, direct measuring and model driven engineering.

5 Proposed Solution

Starting with an overview of the developed architecture, in terms of direct measuring, a fine tuned reading circuit coupled to a processing unit aiming to output reliable data will be use. The circuit supplies the processing unit with the voltage and current readings, while this block, through oversampling [15], outputs what we call real lab tests. This approach leads to a precise result, since the oversampling method adds bits of resolution to the typical 12bit result.

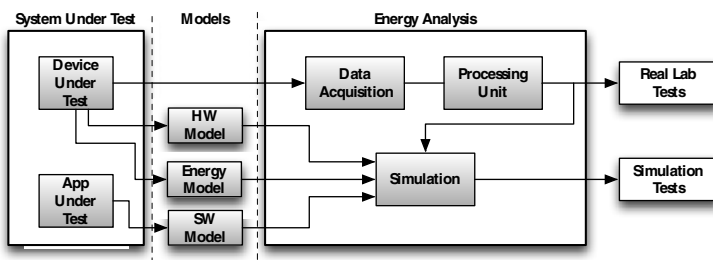


Fig. 2. Complete Architecture for Model-based Energy Testing/Simulation

With the precise feedback result, a model-based simulator can emulate the device behavior by using its meta-models, representing the hardware, software and energy specifications. In the end, is argued that this architecture will generate accurate results, since it is supplied with reliable information.

5.1 Energy Analysis

To perform realistic tests (real laboratory tests) a circuit was design to simultaneous retrieve the current and power consumed by the Device Under Test (DUT). This circuit (in principle) is not much different from other proposals found in the scientific community, as presented previously in Chapter 3.3.

Although, some changes were added to allow a more precise analysis of the current and power consumed. When looking to the power ranges needed to maintain an IoT device running (battery case) is possible to guarantee that a device will not work with half of the maximum supplied power, i.e. if the maximum power is 3.3V the device will not work with less than 1.65V, normally the range is between 3.3V and 2.6V. In the case of the DUT has an infinite capacity power supply, power provided to the device is almost constant with small fluctuations. Therefore the capability to change the power value passed to the processing unit was added, allowing the analysis of the total power supplied (maintaining the U_{ref} equals to zero) or, for instance, half of the power supplied (maintaining $U_{ref} = U/2$) which increases the precision in one bit (by hardware).

In the current case a very common Rsense arrangement is used (built with very small resistors in terms of value to not interfere with current consumed), but with two particularities. First, is possible to change Rsense resistor value (through a jumper's settlement to a better Rsense accommodation regarding the current consumed by the DUT). Second, the analyzed Rsense current is divided into two different signals that then will go to the processing unit. The first signal called CurrentDown is the current with a gain of two, and the second called CurrentTop is the current minus a U_{ref} also with a gain of two. This separation increases the current signal precision in one more bit (by hardware).

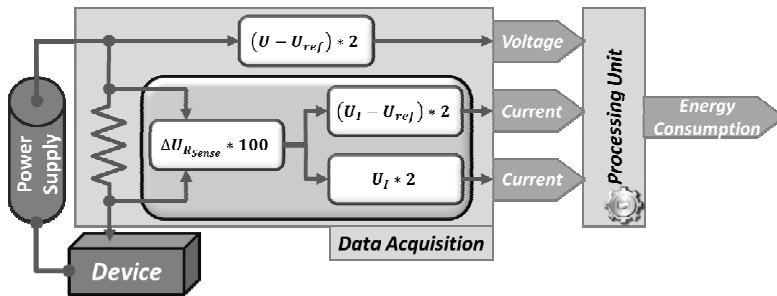


Fig. 3. Energy Measuring Circuit

5.2 Resource Constrained Device Meta-Model

As previously seen, the presented architecture follows a model based approach, in which a set of models (software, hardware and real lab energy consumption) is provided to the simulation module, so an automatic simulation can be performed based on all the information provided. Regarding the software Meta-Model which defines the software model, is basically dependent of the programming language used. At this

point the architecture uses the C and nesC Meta-Model since they are the more common programming languages used by the IoT development community [16].

Unlike the programming languages, that presents well defined Meta-Models or grammars, a hardware Meta-Model capable of representing a device is still missing. In this sense, and based in the work developed in [17] a Resource Constrained Device Meta-Model (RCDM) is proposed to describe the hardware components available in a device, see Fig 4.

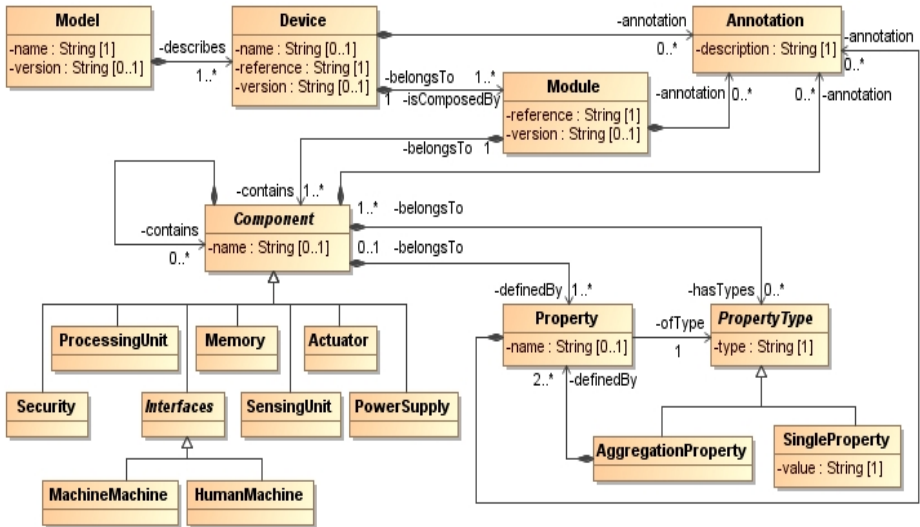


Fig. 4. Resource Constrained Device Meta-Model (RCDM)

RCDM provides a way to formally describe a device in terms of its hardware components. A device is composed by at least one module, that module can contain one or several components, e.g. a microcontroller as a processing unit, memory, AD/DA converters, etc. Each component is defined by one or more properties, identified by a name and with a type. The property type can be of two kinds, single or an aggregation of properties. A single property is used for instance when referring to a microcontroller architecture type (e.g. RISC, CISC). An aggregation property is used when referring to a combination of several properties, for example a radio transmission range which can be defined through, out or indoor environment, maximum range, distance unit.

6 Experiments (Definition)

The experiment definition starts with a selection of the devices to be tested. As most of the available products on the market share the same operating specifications, in terms of power supply, we were able to design and build a printed circuit board with the measuring circuit, capable of measure and monitor the power consumption.

Following the architecture presented in section 5, each system under test will be coupled with this circuit for data collection and analysis. By running a series of tests, we expect to achieve solid results to validate the supporting theory of this approach.

6.1 Device Selection

By reviewing the market share for IoT solutions, a survey was accomplished regarding complete devices specifications, identifying a set of hardware platforms as a good starting point for energy testing.

Being compatible with both TinyOS and Contiki operating systems, the adopted designs are TelosB (<http://tinyos.stanford.edu>) based devices by AdvanticsSYS (<http://advanticsys.com>) and IRIS based devices by MEMSIC (<http://memsic.com>). The main goal of this survey is to gather multiple combinations of the most relevant parts, such as microcontrollers, memory, transceivers and sensing units. Including devices with similar features, we aim to set a solid platform for further comparison, as it will include results from a wider group of hardware.

The following table presents the first devices to be tested.

Table 1. Selected Devices for Energy Test/Simulation

	Platform		Microcontroller		Memory		Radio	Sensors		
	Design	OS's	Ref.	Prog. Flash	Data RAM	Ext. Flash	RF Chip	Light	Temp. & Hum.	
XM1000	TelosB	TinyOS	Contiki	MSP430 @16MHz	116KB	8KB	1MB	TI-CC2420	S1087	SHT11
CM5000				MSP430 @8MHz	48KB	10KB	1MB		S1087	SHT11
CM3300				MSP430 @8MHz	48KB	10KB	1MB		External	
XM2110CA	IRIS			ATmega1281 @8MHz	128KB	8KB	-	Atmel-RF230	External	

Similar tasks will be performed on each device, as tailored applications will run on them. This will allow tracing the energy consumption, helping to confirm the effects of different clock speeds, program flash, memory, and radio units in the final consumption. Devices featuring external sensing units will be coupled with sensor boards in order to perform the tests. The selection consists in AdvanticsSYS EM1000, SE1000 and MEMSIC MTS400. We decided to include this hardware in order to estimate a wider range of hardware and to study the external sensing power consumption phenomena.

6.2 Device Testing

With the previous devices selection, is completed the System Under Test definition to be tested by developing a group of simple applications with a common objective – collect and analyze, at each time, the energy consumption from a single component. The combination of these applications with the chosen platforms is expected to allow the creation of the respective energy models for each device, improving the further model-based approaches for energy testing on the proposed solution.

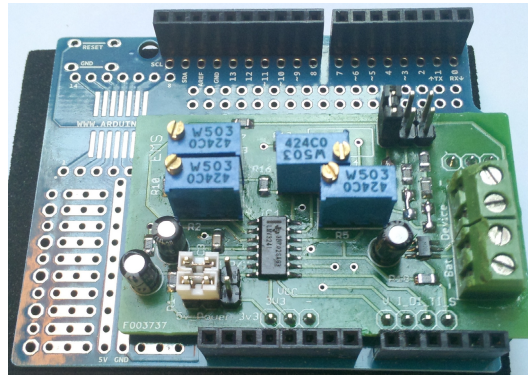


Fig. 5. Energy Measuring Board

7 Conclusion

The Internet-of-Things is here to stay: IoT deployments abound, more IoT-related technologies appear and new IoT centralized apps are launched each day. With this new paradigm, decentralized systems benefit from resource constrained devices sensing capabilities, improving the overall system with environment awareness.

To engineer such systems, some concerns should be considered regarding energy consumption. The hardware selection has to be made wisely but also the applications code development has to be analyzed to achieve better efficiency results, locally (device/system) as well as globally (network/overall system).

This work proposes an architecture capable of retrieving real and simulated energy consumption results from/for a single device, relying on a model based approach (software, hardware, energy and simulation models) and on a precise energy consumption assessment system. It is also presented a Resource Constrained Device Model, capable of representing the available hardware in a device, and a circuit to retrieve more precise energy consumption readings.

With this methodology is possible to analyze the performance of a certain application in several hardware platforms and using different programming language. Provides important information regarding energy consumption, and consequently allows the developer to make a more conscious choice on how to implement his solution and/or improvements.

As future work, exhaustive energy consumption tests will be carry out on the selected devices, using different applications to allow the development of precise simulation models.

References

1. Silva, E.M., Maló, P.: IoT Testbed Business Model. *Advances in Internet of Things* **4**, 37–45 (2014). doi:10.4236/ait.2014.44006

2. Vermesan, O., Friess, P.: *Internet of Things - From Research and Innovation to Market Deployment* (2014) ISBN: 978-87-93102-94-1
3. Moschitta, A., Neri, I.: Power consumption assessment in wireless sensor networks. In: Fagas, G. (ed.) *ICT - Energy - Concepts Towards Zero - Power Information and Communication Technology* (2014) ISBN: 978-953-51-1218-1
4. Dâmaso, A., Freitas, D., Rosa, N., Silva, B., Maciel, P.: Evaluating the Power Consumption of Wireless Sensor Network Applications Using Models. *Sensors* **13**, 3473–3500 (2013)
5. Wei, G., Vasilakos, A.V., Zheng, Y., Xiong, N.: A game-theoretic method of fair resource allocation for cloud computing services. *The Journal of Supercomputing* (2010)
6. Alcaraz, C., Najera, P., Lopez, J., Roman, R.: Wireless sensor networks and the internet of things: do we need a complete integration? In: *1st International Workshop on the Security of the Internet of Things*, Malaga (2010)
7. Asorey-Cacheda, R., García-Sánchez, A.J., Garcia-Sánchez, F., García-Haro, J., González-Castaño, F.J.: On Maximizing the Lifetime of Wireless Sensor Networks by Optimally Assigning Energy Supplies. *Sensors* **2013**(13), 10219–10244 (2013)
8. Somov, A., Minakov, I., Simalatsar, A., Fontana, G., Passerone, R.: A methodology for power consumption evaluation of wireless sensor networks. In: *IEEE Emerging Technologies & Factory Automation* (2009) ISBN: 978-1-4244-2728-4
9. Landsiedel, O., Wehrle, K., Rieche, S., Gotz, S., Petrak, L.: Accurate prediction of power consumption in sensor networks (2004)
10. Eriksson, J., Osterlind, F., Finne, N., Tsiftes, N., Dunkels, A., Voigt, T.: Cooja/MSPSim: interoperability testing for wireless sensor networks. In: *Proceedings of the 2nd International Conference on Simulation Tools and Techniques* (2009)
11. Eriksson, J., Dunkels, A., Finne, N., Osterlind, F., Voigt, T.: MSPsim - an extensible simulator for MSP430-equipped sensor boards. In: *European Conference on Wireless Sensor Networks*, Delft (2007)
12. Hausmann, J.H., Heckel, R., Lohmann, M.: Model-based discovery of Web services. In: *Proceedings of the IEEE Int. Conf. Web Serv.* (2004)
13. Object Management Group, M.D.A.G., Version, A.K., Carter, K., Technologies, W.F.X.: *MDA Guide Version 1.0.1*, Object Manag. Gr., vol. 234, p. 51 (2003)
14. Berre, A.-J., Liu, F.L.F., Xu, J.X.J., Elvesaeter, B.: Model driven service interoperability through use of semantic annotations. In: *2009 Int. Conf. Interoperability Enterp. Softw. Appl.*, China (2009)
15. Atmel Corporation, Enhancing ADC resolution by oversampling. In: *8-bit AVR Microcontrollers Application Note*. <http://www.atmel.com>
16. Lajara, R., Pelegrí-Sebastiá, J., Solano, P.: Power Consumption Analysis of Operating Systems for Wireless Sensor Networks. *Sensors* **10**, 5809–5826 (2010)
17. Cuteloop Consortium, Deliverable D1.3.2 Cuteloop Concept, FP7-216420 Cuteloop “Customer in the Loop: Using Networked Devices enabled Intelligence for Proactive Customers Integration as Drivers of Integrated Enterprise” (2009)

Energy: Improvement

Analysis of Causes and Effects of Harmonic Distortion in Electric Power Systems and Solutions to Comply with International Standards Regarding Power Quality

Mercedes Ruiz-Cortés^(✉), María Isabel Milanés-Montero,
Fermín Barrero-González, and Enrique Romero-Cadaval

Power Electrical and Electronic Systems, Escuela de Ingenierías Industriales,
University of Extremadura, Avda. de Elvas. s/n,
06006 Badajoz, Spain
meruizc@alumnos.unex.es
<http://peandes.unex.es>

Abstract. In recent years, power quality has gained importance due to increasing pollution in the electric system as a consequence of the proliferation of non-linear loads connected to the grid. For this reason, research has been intensified on this issue to improve power quality; especially through simulation models development using software tools, which allow studying the possible causes and effects of disturbances on the electric system and testing solutions to mitigate these power quality events. This paper focuses on analyzing by simulation a possible cause, effect and solution of harmonic distortion, as an example of using cloud-based platforms in order to get the power quality requirements of the future Smart Grid.

Keywords: Power quality · Disturbances · Simulation models · Harmonics

1 Introduction

Nowadays, there are countless loads which need power supply to work both in industries and in the tertiary and domestic sector. This fact has turned the electric power system into a fundamental cornerstone for economic and social development. For this reason, it is essential that power quality is as adequate as possible and keeps the voltage waveform within acceptable limits in terms of RMS value and frequency.

These parameters do not remain indefinitely in their nominal values because the electric system is not ideal. It may be affected in its normal operation unintentionally by electromagnetic signals called disturbances. These disturbances can be external to the power grid (due to lightning, natural disasters, accidents, etc) or internal to it, like large industrial receptors and even small power loads. In addition, the proliferation of electronic devices connected to the grid in recent years has made this problem worse.

These facts explain why power quality has gained relevance in the last decades. As a result, standards and regulations regarding power quality have been developed in order to establish acceptable values which guarantee a suitable electric supply.

An interesting approach to move forward in research about disturbances which affect the electric power system is based on examining their possible causes. In this way, this paper focuses on analyzing by simulation the implications of the presence of harmonic disturbances in the electric power system. Moreover, among the solutions to improve power quality, this paper exposes the importance, in the context of future Smart Grids, of designing cloud-based devices which enable consumers to monitor power quality parameters locally in their household, and upload that data to an Internet service to produce a crowdsourced perspective on power quality.

2 Contribution to Cloud-Based Engineering Systems

Cloud computing, considered as the real-time delivery of IT infrastructure, services and software over the Internet or an internal web-based infrastructure, is an important tool for improving the power quality from a global perspective. Monitoring and collecting data allows determining the presence of disturbances, analyzing their causes and measuring their effects. But above all, cloud computing enables to make decisions about which solutions to implement to minimize the effects regarding poor power quality or reliability. In addition, stored data allows having information for predicting the occurrence of disturbances, in order to anticipate the causes.

One of the challenges of the future Smart Grid is to enable the active participation of consumers to modify electricity purchasing patterns and behaviours. It can be achieved via power quality monitoring in their household. These data would allow having cloud-based information of consumptions and the data processing will provide information as the interaction with neighbors regarding power quality. It will also help to make decisions to reduce power quality problems. In this way, the Open Power Quality research project carried out in the University of Hawaii [1] has demonstrated how the combination of a low-cost hardware and cloud-based software allows the consumers to monitor some parameters regarding power quality in their homes and upload that data to an Internet service. This project proposes a crowdsourced approach in which collection of data is made by consumers and is analyzed oriented toward the needs of consumers.

Another feature of the Smart Grid is to meet user demand for power quality and provide users with an optimal variety of power quality and price program. According to it, power quality monitoring and the development of a power quality information platform to manage the collected data and evaluate results is an important issue. Besides, another challenge of Smart Grid is the user-friendly and intelligent interaction between the customers and the power provider, trying to meet user needs with the best power quality and reliability. Trying to fulfill these challenges, a power quality unified information platform based on cloud computing Software-as-a-Service (SaaS) model is proposed in [2]. It promotes information sharing and friendly interaction between both power provider and consumers.

As an example of usable collaboration and interaction between consumers, in this paper a solution to eliminate the effect of harmonic distortion and the appearance of

parallel resonance is proposed. The solution is as simple as using transformers of specific vector groups by consumers connected to the same Point of Common Coupling (PCC). However, this solution is impossible to implement without monitoring locally and exchanging that information between users. It shows the importance of developing cloud-based platforms in order to get the power quality requirements of the future Smart Grid.

3 State of the Art

The use of simulation tools has become an interesting method to analyze disturbances which affect the electric power system and contribute to the study of power quality. In [3] a set of five simulation models is presented to simulate various power quality events in a distribution system using the SimPowerSystems blockset, like voltage sag, transient, notches and harmonics.

The operation of some industrial loads that cause pollution on the electric power system is also simulated in the literature. In [4] a steel plant and an underground traction system are simulated and an active filter is installed in order to mitigate the voltage harmonic distortion. In [5] the authors propose a steel plant using induction furnaces model and present a Unified Power Quality Conditioner (UPQC) to compensate possible voltage problems. Meanwhile, in [6] the electric arc furnace is modelled with a Static Compensator (STATCOM) to improve the power quality, while in [7], a composite filter is employed in order to reduce harmonics, voltage flicker and imbalance. Electrified railway is another industrial non-linear load simulated in [8], with a STATCOM with PSO-implemented controller to suppress harmonic distortion, voltage fluctuations and to compensate reactive power. In [9], electrified railway systems are analyzed too using several types of Flexible AC Transmission Systems (FACTS) for power quality improvements.

In the same way, in [10] harmonic currents demanded by some non-linear household devices are simulated and different kind of faults and harmonic pollution brought by power electronic devices in power system are also simulated in [11]. The authors of [12] expose a categorization of power quality events and show a simulation model to validate the impact of power quality on sensitive equipment. Finally, the purpose of [13] is to present a solution to voltage sags/swell, harmonic distortion and low power factor using Distribution Static Compensator (D-STATCOM), showing its effectiveness through a simulation model.

4 Simulation Case Studied

This paper focuses on simulating a cause of harmonic distortion in an electric power system, checking one of its worst effects and proposing a solution based on exchanging information about harmonic consumption between users. The simulation model is shown in Fig. 1 and the parameters are collected in Table 1. It is a three-phase low voltage electric power system modeled as a voltage source and a series grid impedance. In the PCC it is connected a linear resistive-inductive load with a capacitor bank

in parallel in order to improve locally the power factor. At the same point, there are two non-linear loads, which are non-controlled three-phase rectifiers connected to the PCC via isolation transformers. The capacitor bank and non-linear loads have breakers in series in order to be able to simulate the behavior of the system when these devices are connected or not.

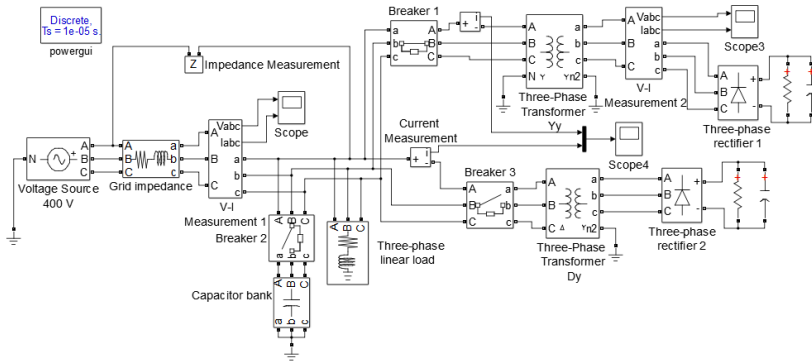


Fig. 1. Simulink model used to simulate causes, effects and solutions of harmonics

Table 1. Parameters values used in the simulation model

Parameter	Value	Parameter	Value
System voltage (V)	400	Linear load reactive power (kVAr)	40
Nominal frequency (Hz)	50	Transformers nominal power (kVA)	250
Grid resistance (mΩ)	25	Transformers transformation ratio (V)	400/400
Grid inductance (μH)	520	Three-phase rectifier dc voltage (V)	900
Capacitor bank capacitance (mF)	0.779	Three-phase rectifier resistive load P (kW)	500
Linear load active power (kW)	60	Three-phase rectifier capacitive load C (mF)	0.1

4.1 Causes

The main cause of harmonic distortion is the use of power electronic devices. The simulation model shown in Fig. 1 includes two three-phase rectifiers, demanding a current (downstream the transformers) with the waveform displayed in Fig. 2(a) with THD of 16.94% and dominant harmonics 5th and 7th (see harmonic spectrum in Fig. 2(b)).

4.2 Effects

Harmonics are responsible of many problems in electric power systems. The simulation model developed in this paper (Fig. 1) allows observing one of the effects caused by harmonics: resonance between capacitor banks for power factor correction and grid inductances, which amplifies the existing harmonics.

Fig. 1 represents a distribution power system that feeds a linear load connected to the same PCC as the three-phase rectifiers. In this case, breaker 1 is on and breaker 3

is off, so only the upper rectifier is considered. The linear load has a capacitor bank that is connected to the system after 0.5 seconds, in order to correct the power factor.

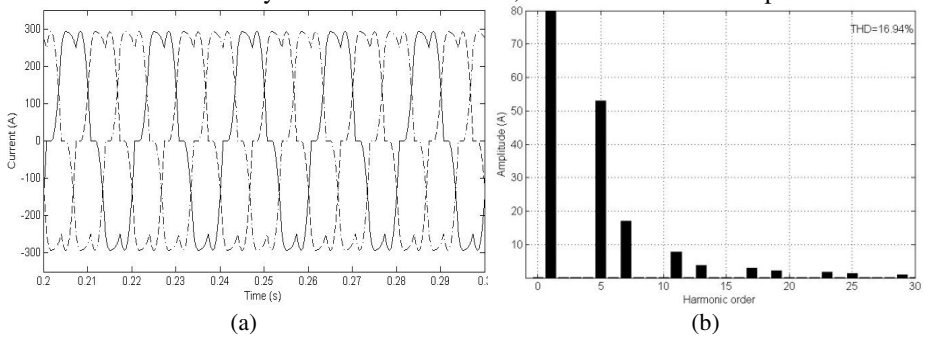


Fig. 2. Simulation results of the current demanded by three-phase rectifier: (a) waveform; (b) harmonic spectrum

Simulation results are exposed in Fig. 3 and Fig. 4. These figures show the waveforms of PCC voltage in Fig. 3(a) and network current in Fig. 3(b), and how their distortion gets worse when the capacitor bank is connected to the system. As it can be seen, Fig. 4(a) indicates that the voltage has a THD of 14.59% before the connection of the capacitor bank. This fact is a consequence of the harmonic emission caused by the rectifier, distorting the waveform of the current to a THD=10.48% (Fig. 4(a)). However, after the connection of the capacitor bank, voltage THD grows up to 25.44% and current THD to 20.67%, as Fig. 4(b) shows. This increase of THD is due to the remarkable rise of the value of 5th harmonic, because a parallel resonance occurs at a frequency near 250 Hz. In this way, 5th harmonic rises from 27.19 V to 52.73 V in the case of PCC voltage and from 33.26 A to 64.51 A in the case of grid current. The 7th harmonic is also modified by parallel resonance, although less than 5th harmonic; it grows up to 12.12 V to 32.04 V for PCC voltage and from 10.59 A to 28 A in the grid current.

4.3 Solutions

The problems caused by harmonics can be mitigated by different solutions. This paper presents a solution to eliminate the dominant harmonics in the modeled system, that is, 5th and 7th harmonics. In case of two similar non-linear loads at the same PCC, instead of connecting them directly to the grid, they are connected via transformers with different connections. The implemented solution consists of the association in parallel of a Dy transformer with the Yy transformer that feeds the three-phase rectifier previously analyzed, as it can be noted in Fig. 1.

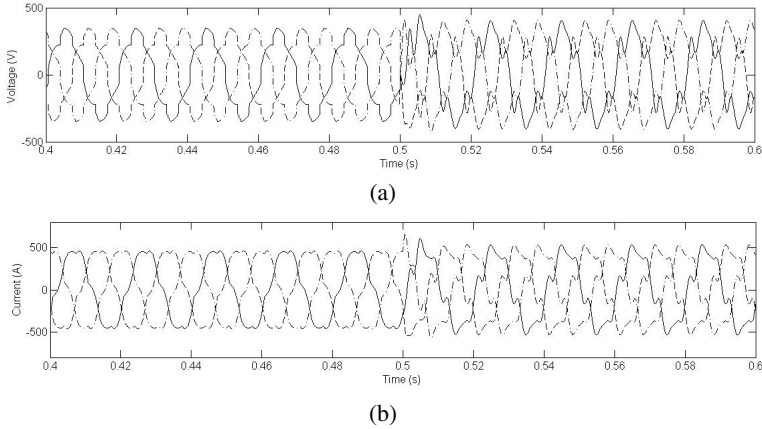


Fig. 3. Simulation results before and after resonance effect: (a) waveform of voltage in PCC; (b) waveform of network current

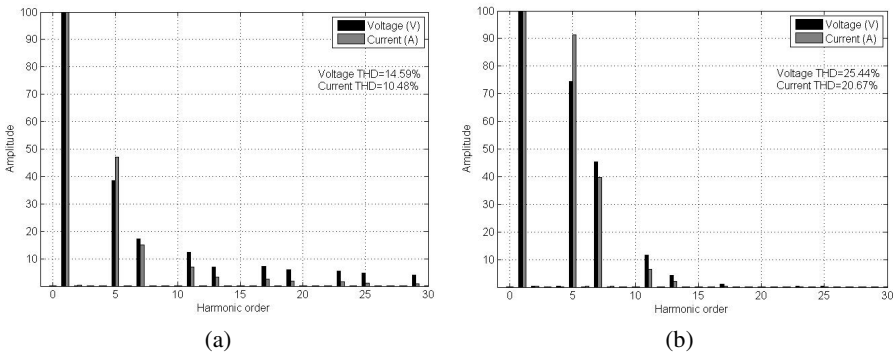


Fig. 4. Harmonic spectrum of voltage and current: (a) before capacitor bank connection; (b) after capacitor bank connection

The Dy transformer feeds another three-phase rectifier with an identical load than the first rectifier, and introduces a phase difference of 30° in the demanded current by the second rectifier. Therefore, the demanded currents by both rectifiers upstream the transformers are 30° out of phase between them, as Fig. 5(a) shows. Thus, the sum of both currents makes 5th and 7th harmonics to be cancelled; hence the current that flows in the system under these conditions (after 1 second of simulation) is much more similar to a sine wave (Fig. 5(b)). As a result, the waveform of voltage in PCC has been improved too (Fig. 5(c)). The harmonic spectra of both signals demonstrate the elimination of 5th and 7th harmonics and how their THD have been reduced to 7.07% in the case of the voltage and to 1.57% in the case of the network current, as Fig. 6(a) and Fig. 6(b) expose respectively.

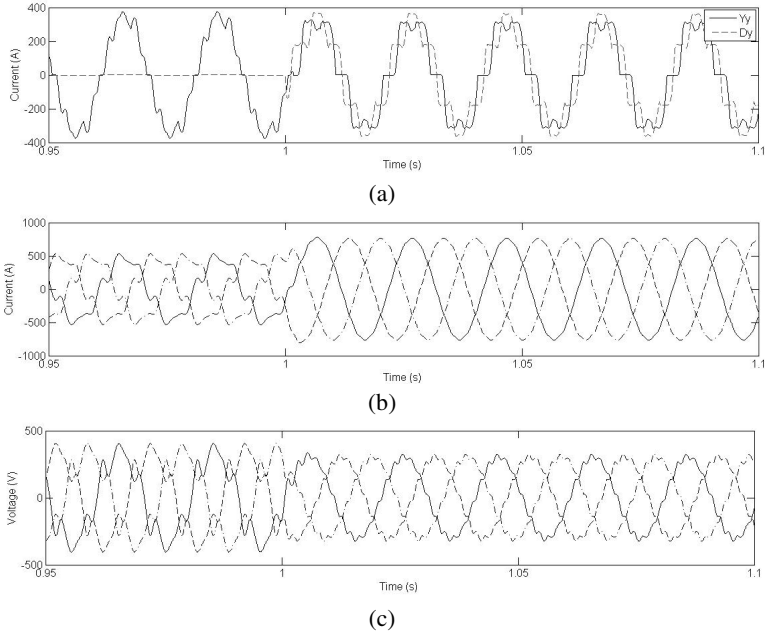


Fig. 5. Simulation results after implementing the solution: (a) waveform of current upstream in each transformer; (b) waveform of network current; (c) waveform of voltage in PCC

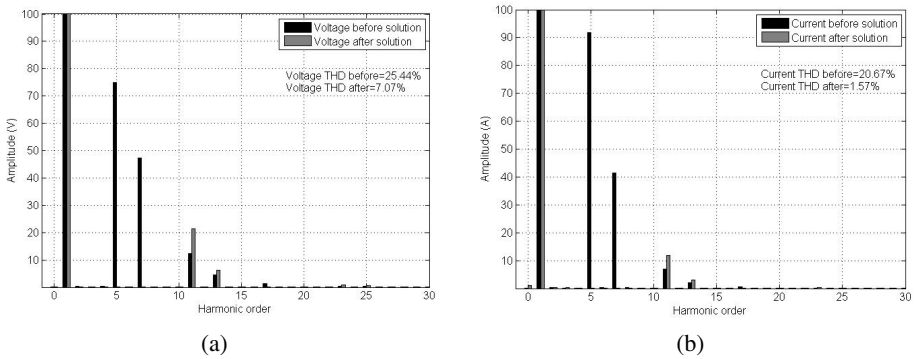


Fig. 6. Simulation results after implementing the solution compared with the previous results: (a) harmonic spectrum of voltage in PCC; (b) harmonic spectrum of network current

5 Conclusions and Further Work

The development of simulation models to analyze disturbances in the electric power system has become an interesting research method for improving power quality. In this paper, a simulation model has been proposed to confirm a cause of harmonics, the use of rectifiers connected to the network, and one of its effects, the appearance of

parallel resonance between capacitor banks and the grid impedance. In addition, it has been simulated a possible solution to eliminate the 5th and 7th harmonics through a special coupling of transformers, as an example of collaboration between consumers through cloud-based computing. As further work, it is proposed to develop a prototype to validate experimentally the results obtained by simulation and to implement more simulation models to analyze causes, effects and solutions of other type of disturbances.

References

1. Johnson, P.M.: Enabling active participation in the Smart Grid through crowdsourced power quality data, pp. 1–14, April 2014
2. Liu, L., He, W., Zhang, X., Zhang, Y.: Research and implementation of power quality unified information platform based on SaaS model. In: 2012 China International Conference on Electricity Distribution (CICED), pp.1–6, 10–14 September 2012
3. Tan, R.H.G., Ramachandramurthy, V.K.: Simulation of power quality events using Simulink model. In: IEEE 7th International Power Engineering and Optimization Conference (PEOCO), pp. 277–281 (2013)
4. Zamora, I., Mazon, A., Eguia, P., Albizu, I., Sagastabeitia, K.J., Fernández, E.: Simulation by MATLAB/Simulink of active filters for reducing THD created by industrial systems. In: IEEE Bologna Power Tech Conference Proceedings 3, pp. 8–16, Bologna (2003)
5. Vahabzadeh, A., Vadizadeh, H., Asl, F.A., Kadkhoda, F.: Use of unified power quality conditioner in khoozestan-iran steel complex network, a case study. In: 31st International Telecommunications Energy Conference (INTELEC 2009), pp. 1–6 (2009)
6. Tavakkoli, A., Ehsan, M., Batahiee, S., Marzband, M.: A simulink study of electric arc furnace power quality improvement by using STATCOM. In: IEEE International Conference on Industrial Technology (ICIT), pp. 1–6 (2008)
7. Bhonsle, D.C., Kelkar, R.B.: Design and analysis of composite filter for power quality improvement of electric arc furnace. In: 3rd International Conference on Electric Power and Energy Conversion Systems (EPECS), pp. 1–10 (2013)
8. Zaeim, R., Khoshkholgh, A.: Gain-scheduling adaptive control of the STATCOM for electrified railway systems using PSO. In: International Congress on Ultra Modern Telecommunications and Control Systems and Workshops (ICUMT), pp. 478–484 (2010)
9. Baseri, M.A., Nezhad, M.N., Sandidzadeh, M.A.: Compensating procedures for power quality amplification of AC electrified railway systems using FACTS. In: Power Electronics, Drive Systems and Technologies Conference (PEDSTC), pp. 518–521 (2011)
10. Suárez, J.A., di Mauro, G., Anaut, D., Agüero, C.: Analysis of the Harmonic Distortion and the Effects of Attenuation and Diversity in Residential Areas. *IEEE Latin America Transactions* 3(5), 53–59 (2005)
11. Zhu, W., Ma, W.Y., Gui, Y., Zhang, H. F.: Modelling and Simulation of PQ Disturbance Based on Matlab. *International Journal of Smart Grid and Clean Energy* 2(1) (2013)
12. Thapar, A., Saha, T.K., Dong, Z.Y.: Investigation of power quality categorization and simulating its impact on sensitive electronic equipment. *Power Engineering Society General Meeting* 1, 528–533 (2004)
13. Sivakoti, S.K.K., Naveen Kumar, Y., Archana, D.: Power Quality Improvement in Distribution System Using D-Statcom in Transmission Lines. *International Journal of Engineering Research and Applications (IJERA)* 1(3), 748–752 (2011)

Risk Analysis and Behavior of Electricity Portfolio Aggregator

Eduardo Eusébio¹(✉), Jorge de Sousa¹, and Mário Ventim Neves²

¹ Instituto Politécnico de Lisboa Rua Conselheiro Emidio Navaro, 1,
Instituto Superior de Engenharia de Lisboa, 1959-007 Lisboa, Portugal
{eaeusbio, jsousa}@deea.isel.ipl.pt

² Faculdade de Ciências e Tecnologia, Universidade Nova de Lisboa
2829-516 Costa de Caparica, Portugal
ventim@uninova.pt

Abstract. The scope of this paper is to adapt the standard mean-variance model of Henry Markowitz theory, creating a simulation tool to find the optimal configuration of the portfolio aggregator, calculate its profitability and risk. Currently, there is a deep discussion going on among the power system society about the structure and architecture of the future electric system. In this environment, policy makers and electric utilities find new approaches to access the electricity market; this configures new challenging positions in order to find innovative strategies and methodologies. Decentralized power generation is gaining relevance in liberalized markets, and small and medium size electricity consumers are also become producers (“prosumers”). In this scenario an electric aggregator is an entity that joins a group of electric clients, customers, producers, “prosumers” together as a single purchasing unit to negotiate the purchase and sale of electricity. The aggregator conducts research on electricity prices, contract terms and conditions in order to promote better energy prices for their clients and allows small and medium customers to benefit improved market prices.

Keywords: Aggregation · Risk analysis · Portfolio optimization · Load profiles

1 Introduction

Electricity generation nowadays presents a greater number of challenges related to reliability, sustainability and security of supply. The use of renewable resources in power generation has been adopted in most OECD countries as an answer to the climate change problems originated by the burning of fossil fuels in the traditional thermal plants to supply the ongoing increase in electricity demand. Portugal has been considered a pioneer country in electricity production from renewable sources and, in 2010, 52% of the electricity consumed came from renewable sources [1].

In terms of the economic model, the electricity industry has evolved from a vertically integrated state-owned monopoly company (not subjected to the normal rules of competition) to a liberalized market where generators and consumers have the opportunity to freely negotiate the purchase and sale of electricity. The liberalization of the

electricity market in Portugal to allow entry of independent power producers with long term contracts and the creation of active wholesale and retail markets came in a later stage.

The importance of reducing the level of consumption is very strong. Nowadays the actual economic situation affects all the participants in the sector [2], consumers, producers and “prosumers”, many hypotheses to decrease the bill to pay for electricity are considered, such as different energy suppliers, control load programs, load forecasting, smart-grid, smart-metering and smart-box.

This new electrical concepts allows the medium, small consumers and producers to integrate the satisfaction of the power system because they adopted the new distributed generation paradigm, opposed to the traditional power system, composed by medium and large power plants [1]

The small passive consumer evolves to an active player, participating in the generation of electricity and the provision of network services. In this context, both aggregators and companies can bring their customers, consumers, producers, consumers and traders to market [3] [4].

In a future with the smart-grids and smart-metering, the development of a new challenge in electric system has occurred, how to integrate these new consumers/producers, known as “prosumers”, in this contest a new partner arises in the aggregator company.

1.1 Purpose

The scope of this paper is to show how an aggregator company with a portfolio of customers, consumers, producers and “prosumers”, can adequately manage its selection of customers in terms of risk and profitability, computing his values. To achieve this purpose presents an adaptation of the theory of investment portfolios introduced in 1952 by Harry Markowitz.

The module CAEM-PA- Commercial Agents in the Electricity Market – Portfolio Aggregator, was created especially to deal with this type of non-financial assets. CAEM-PA gives the values of profitability and portfolio risk for the current portfolio, minimum variance point of portfolio and the layout of the efficient frontier where the optimal portfolios are located. Finally, the simulator computes the best optimum directions, in case the aggregator intends to increase the number of assets, thus allowing him, under negotiation conditions with an hypothetical future customer, to elaborate an adequate price proposal for energy sell.

The module CAEM-PA, also allows to view the matrix of variance-covariance between the assets in the portfolio, and the electrical interpretations that can be done.

1.2 Outline

This paper is organized as follows; Section I, provides an introduction on power systems, expected developments and presents the new concepts of aggregators and

“prosumers”. The second section relates to the topic under study, “Technological Innovation for Cloud-based Engineering Systems”. In Section III, following a literature study is made. Some techniques for portfolio evaluation are presented as well as a vision of the future in electrical distribution, regarding in particular the distributed energy resources. Section IV, Presents the methodologies applied to the study and characterizes the assets of the portfolio, consumers, producers and “prosumers”, an explanation of the mathematical treatment used to obtain the behavior, risk and profitability, of the aggregator company is also included. Section V, a case study of the portfolio aggregator is developed with the help of the CAEM-PA module. Finally in section VI, the paper ends with some conclusions.

2 Benefits from Cloud-based Engineering Systems

The new business relationship in the market presented in this study is based in a contractual relationship established between the aggregator and their customers.

Aggregator companies can use the cloud in their businesses as a way to help them expand their current commercial offerings without major investments.

Another important aspect is the effect of the cloud on small and medium size enterprises, the cloud allows them to have unrestricted access to certain geographic locations, which due to cost limitations would not have access, giving them an ability to act globally with a significant reduction in overhead cost.

The cloud also allows overcoming language barriers through centralized translation services and increases entrepreneurship, providing businesses and their collaborators the opportunity to exchange ideas, develop products quickly and economically.

3 Background

3.1 Portfolio Theory

The Portfolio Theory has its origins in the scientific article Portfolio Selection of Nobel Economy Harry Markowitz, a result of his doctoral dissertation [5]. In this article, Markowitz addresses the choice of portfolios of financial assets with uncertain future value, following a criterion completely new at the time: the expected return criterion, variance of returns.

The return was considered to be the only important aspect on an investment without taking account their variability. But in fact, we observe in financial markets that investors consider different portfolios with a variety of assets portfolio without considering only the return that was suggested.

Markowitz intuited that different choices of investors and diversification were based on two notions distinct: the notion of trade-off between return and risk of investments and the notion of interaction between the returns of different assets.

Markowitz then suggests that the return of asset must have two reference measures: its expected value and its risk [6].

3.2 Commercial Agents, Aggregators

Networks of the future based on smart-grids concept evolution have great flexibility, and assume an involvement of the end users known by active demand [7] [8]. This new concept of dealing with energy level consumption, decreasing his level because the aggregator tries to optimize the load diagrams of its customers in order to create an aggregator global load diagram more smooth, more friendly to the systems operation. Charges like water heaters, electric radiators, heat pumps, battery EV's, can be controlled, via communication with "energy box" installed in the customers home.[9][10][11].

An aggregator provides its customers with energy marketing services, see Fig. 2, giving them access to market prices by adding a significant number of loads, at the same time grants the aggregator power negotiation in the electricity market [12] [13].

The aggregator makes an energy balance at the level of customers, who have contract with him, including forecasting consumption to meet energy produced and introduced into the distribution system, performing a service of high value to the system operator [14].

The action of the aggregator between his customers (consumers, producers and "prosumers"), and the grid operator, can reduce or adequate the consumption to the production in an active way, that contributes to decrease the dependence from imported electricity and increases the participation of the renewable energy in the local energy mix [14]. The cooperation between aggregator and customers promotes environmental benefits.

4 Modeling Methodology

The customer portfolio module simulator, that includes several consumers, producers and "prosumers", with aggregator contract for energy supply and purchase, consists in three modules the CAEM-PA (portfolio evaluation), the EMT (energy negotiated) and the FLPP (energy and price forecast).

The CAEM-PA, main inputs are the historical data series of the customer, the contracted prices for sale and/or energy purchase predefined in the contract terms are indispensable; all this information is available (input) allowing, with appropriate treatment, obtain the output (risk, profitability, efficient frontier...), as depicted in Fig. 1.

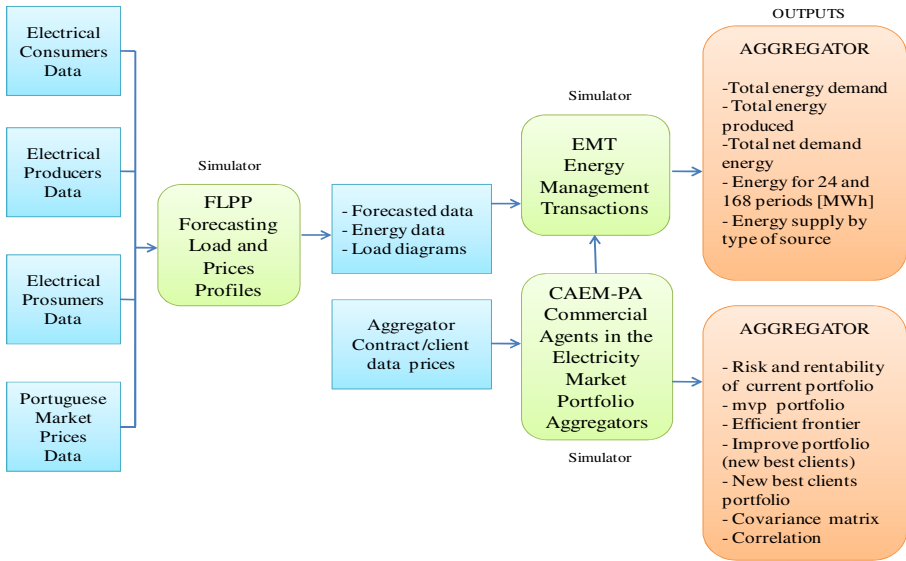


Fig. 1. Simulator scheme, main inputs, intermediate data, outputs, for portfolio aggregator, risk and profitability estimation

In this paper the principal module of the complete scheme simulator is presented in Fig.2, with the inputs and outputs of the module CAEM-PA.

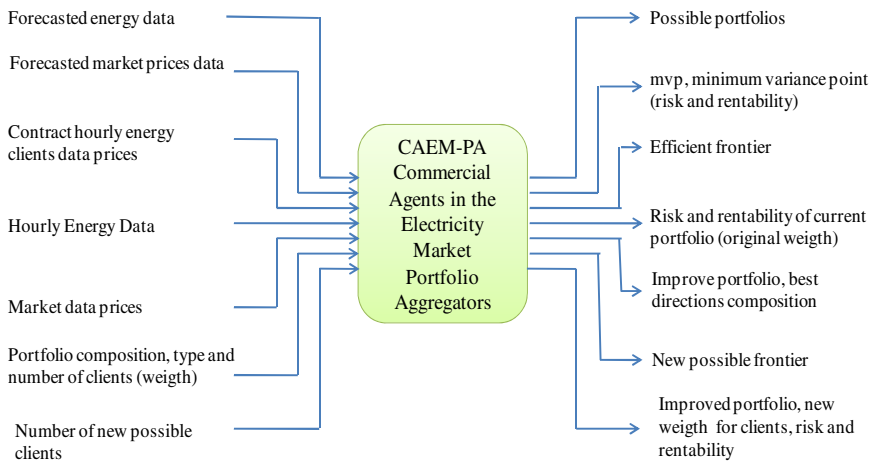


Fig. 2. Commercial Agents Electricity Market – Portfolio Aggregator, inputs and outputs

The profitability and risk of the portfolio for one entire week, 168 periods (hours), are computed, according to equation 1, and for its calculation a set of different scenarios of energy and prices are considered.

$$E(R_p) = \sum_{i=1}^n E(R_i) \times w_i \tag{1}$$

Where $E(R_p)$ profitability of portfolio P , $E(R_i)$ profitability of customer i , in the set of scenarios, and w_i the weight of customer in portfolio P , n is the number of customers in portfolio P , finally, i is the type of customers in portfolio.

$$\sigma_p = \sqrt{\sigma_p^2} \tag{2}$$

Where σ_p is the risk or volatility of the portfolio P .

$$\sigma_p^2 = \sum_{i=1}^n w_i^2 \sigma_i^2 + \sum_{i=1}^{n-1} \sum_{j=i+1}^n w_i w_j \sigma_{i,j} \tag{3}$$

Where σ_p^2 is the variance of the portfolio P , σ_i^2 is the variance of client i , w_i and w_j are the weights of the customers in the portfolio and $\sigma_{i,j}$ the covariance between the customers i and j , and n the total number of different type of customers. The efficient frontier of the portfolio is obtained with equations 4 and 5.

$$\begin{aligned} \min \quad & \sigma_p^2 = \sum_{i=1}^n w_i^2 \sigma_i^2 + \sum_{i=1}^{n-1} \sum_{j=i+1}^n w_i w_j \sigma_{i,j} \\ \text{s.a} \quad & \sum_{i=1}^n E(R_i) w_i \geq E(R_c) \\ & \sum_{i=1}^n w_i = 1 \\ & 0 \leq w_i \leq 1 \quad i = 1, 2, 3, \dots, n \end{aligned} \tag{4}$$

$$\begin{aligned} \max \quad & E(R_p) = \sum_{i=1}^n E(R_i) w_i \\ \text{s.a} \quad & \sum_{i=1}^n w_i^2 \sigma_i^2 + \sum_{i=1}^{n-1} \sum_{j=i+1}^n w_i w_j \sigma_{i,j} \leq \sigma_v^2 \\ & \sum_{i=1}^n w_i = 1 \\ & 0 \leq w_i \leq 1 \quad i = 1, 2, 3, \dots, n \end{aligned} \tag{5}$$

5 Case Study

The case study presented in this research is based on a set of customers as shown on Table 1. Different customer profiles, in one week time horizon, are considered, an example as depicted in Fig.3.

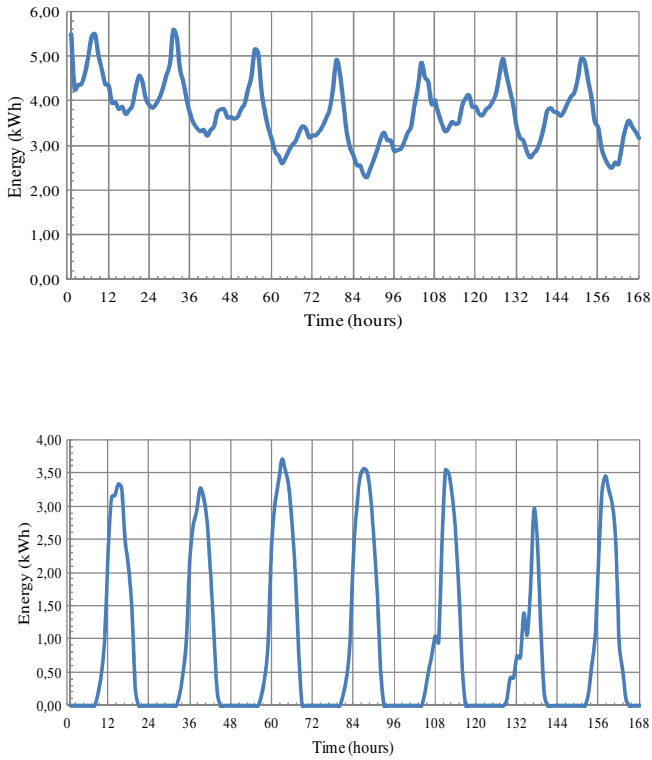


Fig. 3. Load diagrams: a) Small photovoltaic producer and b) Small residential consumer

Table 1. Type of customer’s portfolio and individual, weight, profitability and risk

	Type	Weight	Profitability	Risk
Customer A	Consumer	10	42,51	0,47
Customer B	Consumer	1	39,98	0,46
Customer C	Consumer	2	39,45	0,48
Customer D	Consumer	5	39,99	0,46
Customer E	Consumer	5	32,51	0,55
Customer F	Consumer	5	39,37	0,47
Customer G	Consumer	2	37,48	0,52
Customer H	Consumer	1	39,78	0,47
Customer I	Producer	1	13,55	0,66
Customer J	Producer	5	39,74	0,50
Customer K	Prosumer	10	1,00	1,10
Customer L	Prosumer	10	22,14	2,09
Customer M	Prosumer	5	27,37	0,76

Fig. 4 shows the risk and profitability for the minimum variance point of the customer’s portfolio, with risk and profitability value in the left side. The efficient frontier to the customer’s portfolio is depicted on the right side.

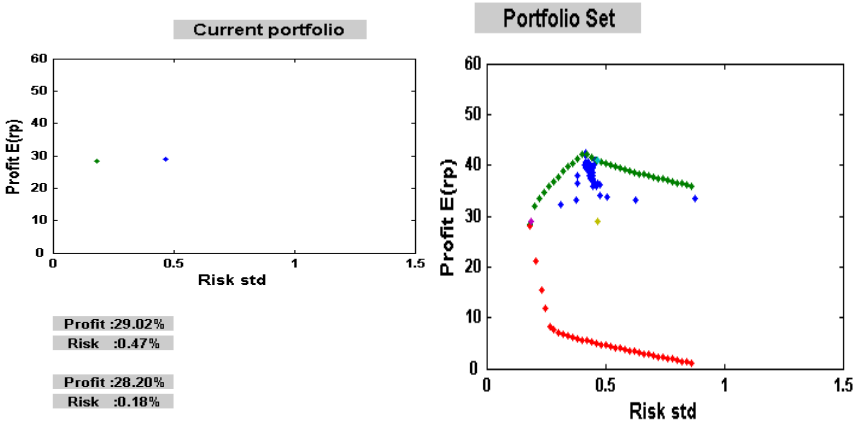


Fig. 4. Outputs of the module CAEM-PA, a) Minimum variance point with risk/ profitability, b) Efficient frontier of customer portfolio

Fig. 5 shows the risk and profitability for optimum points of customers portfolio, as well as the possible evolution points of customers portfolio when new customers are included, depicted in the left side. A global vision with indication of the composition, weights of the assets, in percentage of the total for the new customer’s portfolio composition, is depicted on the right side.

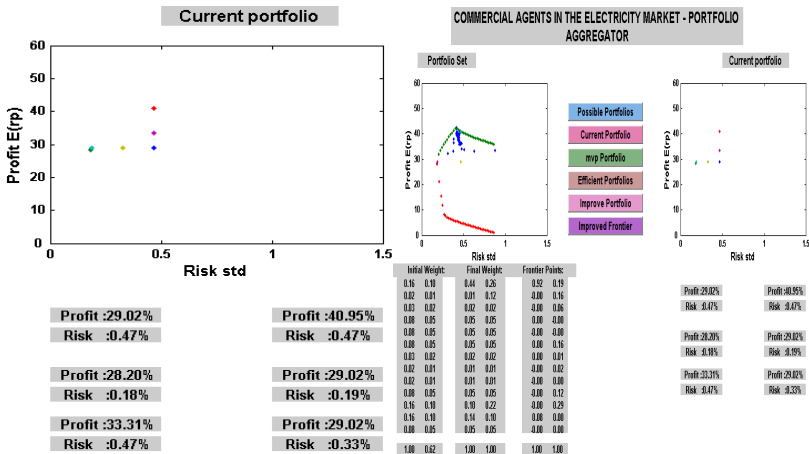


Fig. 5. a) Risk and profitability for the optimum points in the frontier and best points without discard any customer, b) Customers portfolio composition, and weights, for the referred best points

6 Conclusions

The module CAEM-PA, of the simulator, is able to deal and model an aggregator customer's portfolio; this tool computes profitability, risk, draws the efficient frontier, localization of the minimum variance point, position on the risk and profitability plan of customer's current portfolio. Besides, for all the significant points it is given the weight of the specific customer type on customer's portfolio composition.

The CAEM-PA, also discusses the increase of the customers number portfolio without any initial client. The aggregator achieves with this tool an important knowledge to create price proposals for negotiation process with potential new customers. In further works, the importance of the variance-covariance matrix is discussed, and the simulator allows to create an historical data with risk and profitability which is useful for VaR (value at risk) computation, as well as the energy quantities traded are developed by the Energy Management Transactions module.

References

1. Hossain, M.R., Than Oo, A.M., Ali, A.B.M.S.: Evolution of Smart Grid and Some Pertinent Issues. In: Universities Power Engineering Conference, AUPEC (2010)
2. UNRIC, <http://www.unric.org/pt/actualidade/30866-relatorio-da-onu-a-crise-da-divida-da-zona-euro-continua-a-ser-maior-ameaca-a-economia-mundial-e-preciso-inverter-politicad-austeridade> (last time accessed October 11, 2013)
3. Lampopoulos, I., Vanalme, G.M.A., Kling, W.L.: A methodology for modeling the behavior of electricity prosumers within the smart grid. IEEE ISGT Europe 2010 (2010)
4. Stern, P.C.: Information, Incentives, and Proenvironmental Consumer Behavior. *Journal of Consumer Policy* **22**, 461–478 (1999)
5. Markovitz, H., Sharpe, W.F., Miller, M.: Founders of modern finance: their Portfolio Selection. *Journal of Finance* **VII**(1) (1952)
6. Markovitz, H.: *Portfolio Efficient: Efficient Diversification of Investments*. Wiley & Sons, New York (1959)
7. Badano, A.: Regelverk Intelligentia Elnat och Smarta Matsystem. Energy Markets Inspectorate, EI R2011:03 (2011)
8. ADDRESS. <http://www.adressfp7.org/> EC FP7 project ADDRESS (ECGA no. 207643) (last time accessed October 10, 2013)
9. Piette, M.A., et al.: Development and Evaluation of Fully Automated Demand Response in Large Facilities. Demand Response Research Center (January 2005)
10. Camus, C., Farias, T., Esteves, J.: Potential impacts assessment of Plug-in electric vehicles on the Portuguese energy market. Elsevier, *Energy Policy Journal* **39**(10) 5883–5897 (2011)
11. Hadley, S.W., Tsvetkova, A.: Potential Impacts of Plug-in Hybrid Electric Vehicles on Regional Power Generation. Oak Ridge National Laboratory (2008) http://www.ornl.gov/info/ornlreview/v41_1_08/regional_phev_analysis.pdf (last time accessed September 14, 2012)
12. Eusébio, E., Sousa, J., Ventim Neves, M.: Commercial agent's portfolio optimization in electricity markets. *European Electricity Markets – EEM 2012* (April 2012)
13. Bollen, M.: Adapting Electricity Networks to a Sustainable Energy System. Energy Markets Inspectorate, EI R2011:03 (2011)
14. Lambert, Q.: Business Models for an Aggregator-Is an aggregator economically sustainable on Gotland?, MSc thesis, XR – EE – ICS 2012:003, Sthockholm, Sweden (2012)

Combined Operation of an Unified Power Quality Conditioner and a Superconducting Magnetic Energy Storage System for Power Quality Improvement

Nuno Amaro¹(✉), Luís Casimiro¹, João Murta Pina¹,
João Martins¹, and José M. Ceballos²

¹ Centre of Technology and Systems, Faculdade de Ciências e Tecnologia,
Universidade Nova de Lisboa, 2829-516 Caparica, Portugal

nma19730@campus.fct.unl.pt, {jmmp,jf.martins}@fct.unl.pt,

² “Benito Mahedero” Group of electrical Applications of Superconductors,
Escuela de Ingenierías Industriales, Universidad de Extremadura, Avenida de Elvas s/n,
06006 Badajoz, Spain
jmceba@unex.es

Abstract. Superconducting Magnetic Energy Storage (SMES) is a class of promising superconducting devices, considering its possible applications in power systems. This paper describes a combination of a SMES with a Unified Power Quality Conditioner (UPQC) for power quality improvement in an electric grid. The SMES device is used to improve the UPQC performance by increasing the stored energy in the DC link. Several power quality faults including voltage sags and current harmonics are simulated and the system behavior is demonstrated. This hybrid system has the advantage of being able to overcome different kinds of power quality faults with higher performance than as a set of individual systems, thus increasing power quality in electric grids.

Keywords: SMES · UPQC · Power quality

1 Introduction

In modern electric grids, power quality is a very important topic, considering the high dissemination of microprocessors and electronic devices, which require a highly stable power connection. In this context, power quality faults like voltage sags/swells, frequency oscillations and harmonic distortion, amongst others, must be minimized or, if possible, eliminated [1]. Amongst the several classes of devices that overcome power quality issues, active power filters already play an important role and are expected to be the main contributor to deal with such problems in the future, due to their flexibility [2]. The Unified Power Quality Conditioner (UPQC) is one of the most flexible devices because it consists of a combination of a series and a shunt active power filters, allowing a simultaneous compensation of voltage and current [3]. The two filters (series and shunt) are connected by means of a DC link with a capacitor. The capacitor is a very important element because it stores energy allowing the DC

voltage to maintain a required level, which is determinant in the overall system performance [4].

Superconducting Magnetic Energy Storage (SMES) systems are one class of devices based on the phenomena of superconductivity that are expected to have more applications in power systems [5][6]. By means of a superconducting coil it is possible to store energy and use it whenever it is necessary. Although these devices have a lower energy density when compared to other energy storage systems (like batteries), their power density is very high and the device can be fully discharged in a few milliseconds. This characteristic makes the SMES a power device instead of an energy device [7]. SMES can thus be used to address power quality issues and several projects are already running in this area, including voltage sags/swells compensation [8], mitigation of frequency oscillations [9] and UPS applications [10, 11].

The integration of SMES and FACTS (Flexible AC Transmission System) devices has already been discussed and there are several possible advantages in doing it [12]. The main advantage resides in the fact that with an SMES it is possible to add real energy storage capabilities to the whole system (SMES + FACTS device), which will increase its performance and applicability [13]. Since FACTS devices already contain a DC link, the overall cost of the SMES unit becomes lower because its Power Converter System (PCS) becomes simpler. In fact, the PCS becomes only a chopper converter connected to the DC link, eliminating the necessity to have a bidirectional power converter (rectifier and inverter) in the SMES. Some studies also indicate that through the addition of a SMES unit, it is possible to decrease the power rating of the FACTS device, also decreasing its costs [14].

Considering the various advantages in adding a SMES unit to a FACTS device, a system consisting of an UPQC with a SMES unit connected to its DC link is presented in this work. The system was designed to overcome two different power quality issues: voltage sags and harmonic distortion. Matlab/Simulink simulations are presented to mitigate the aforementioned power quality issues.

2 Relation to Cloud-based Engineering Systems

The evolution in power systems through the last years is leading to the creation of a new intelligent power grid usually known as Smart Grid [15]. In this new concept of power grid, both energy and information are expected to flow up- and downstream. With the increasing penetration of microprocessors and electronics the requirements for energy quality are also increasing and it is necessary to have full monitoring and control of the grid [16]. In such context, devices that increase power quality acquire great importance in power systems. This paper aims to contribute to the application of such devices, by presenting a hybrid device, which not only has power quality enhancement capabilities but also provides the possibility to storage energy. Such devices must be fully controllable and their successful dissemination also depends on the success of cloud-based software for security and operation control [17]. In this sense, and considering that all devices present in future power systems are expected to communicate with each other, cloud-based engineering systems are of great importance if smart grids are to be successfully implemented [18, 19].

3 System Description

The studied system is schematized in Fig. 1. The series active filter is connected close to the power source and the shunt filter close to the load. Although a different configuration could be chosen, this one allows a better controllability of the DC link voltage [20], which in this case is beneficial because there is the SMES unit connected to this link. The shunt filter converter must be bidirectional in order to allow a full controllability of the DC voltage.

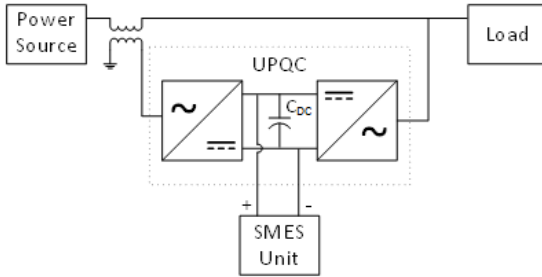


Fig. 1. Implemented system

3.1 UPQC

The UPQC is a very complete device, regarding its ability to deal with power quality issues. The combination of a series and a shunt active filters allows control of current and voltage. Both filters are connected through a DC link that contains a capacitor. The DC voltage in this link must be maintained at a certain level in order to allow full controllability of the system, and to charge the superconducting coil of the SMES unit. The implemented UPQC and its controller are shown in Fig. 2.

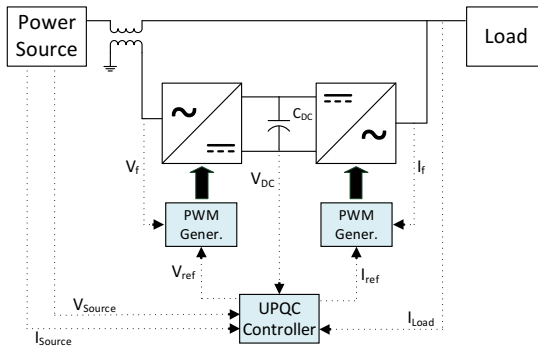


Fig. 2. Implemented UPQC

The pulse width modulation (PWM) signals for the two converters in the series and shunt active power filters are generated according to voltage and current reference

signals, respectively. The reference signal for the current in the shunt active power filter is generated following a Synchronous Reference Frame method [4]. The reference signal (used to generate the PWM signal) of the voltage in the series power filter is generated by a “feedforward” control method, comparing the voltage of the filter to a defined reference value. The DC link capacitor, C_{DC} , has a value of 20 μF , calculated following the formulation presented in [21].

3.2 SMES

A SMES system is composed of three main sub-systems: a superconducting coil, which stores energy in its magnetic field, a Power Converter System (PCS) responsible for the exchange of energy between the coil and the grid where it connects and a Control System (CS) that manages energy exchanges. Fig. 3 depicts the usual system configuration.

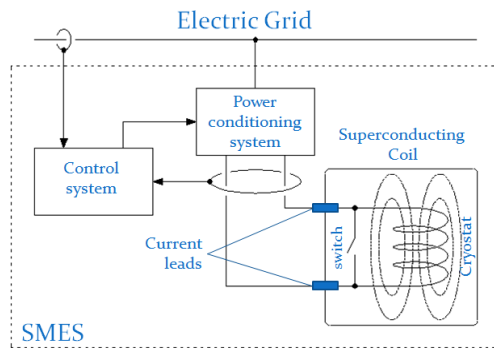


Fig. 3. SMES system constitution

The PCS system usually consist of a bidirectional power electronics interface (with rectifying and inverting capabilities). However, in this specific case, because the SMES is connected to a DC link, only a DC/DC converter is necessary (a chopper converter). The used SMES configuration is depicted in Fig. 4. The superconducting coil was simulated as simple inductance. In a real system, the total resistance of the system might be non-negligible (due to e.g. current leads or resistive contacts), but as a first approach it is not necessary to consider this resistance.

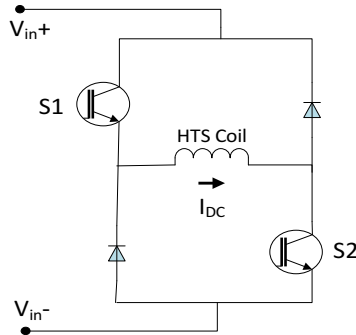


Fig. 4. SMES unit

Since the PCS of the implemented SMES is rather simple when compared to a PCS when the SMES is connected to an AC grid, the control system also becomes simpler because it is only necessary to control the two power electronic switches (in this case IGBTs) that form the chopper converter. The control must allow three different operation modes: charge, discharge and persistent. Charge and discharge mode correspond to charging and discharging the superconducting coil, respectively, and the persistent mode corresponds to a situation where the coil is already fully charged and current flow is maintained in a continuous mode. The control of the switches S1 and S2 defines the operating mode:

- S1 and S2 closed: charging mode;
- S1 open and S2 closed: persistent mode;
- S1 and S2 open: discharging mode.

In a system where the SMES is operating alone, the control of the chopper is very straightforward. The system enters a charging mode till the current in the coil reaches the desired value and then the persistent mode is activated. The discharge mode is used when there is a fault in the grid. However, in the case of a joint operation with an UPQC, the control must take care of other situations as well. The UPQC has a DC link in which the DC value cannot decrease under a certain value, otherwise the shunt filter enters a non-controllable situation [21]. This means that the charging process of the SMES must take into account the DC voltage value. The persistent and discharging modes operate in the same way as in a regular SMES system.

The main characteristics from the SMES unit simulated in this work are presented in table 1. Such characteristics were obtained following the method presented in [22].

Table 1. Characteristics of the simulated SMES unit.

Characteristic	Value
Number of pancake coils	4
Total inductance (H)	0.28
Rated current value (A)	70
Total length of SC tape (m)	800

The maximum stored energy using this coil is 686 J. Using only the capacitor in the DC link of the UPQC, the maximum stored energy was 4.9 J, which strongly limits applications of this system. The addition of a SMES unit allowed greatly increasing stored energy, which means that the system can overcome different kinds (with longer duration) of power quality faults.

4 Simulation Results

To evaluate the UPQC+SMES system performance, Matlab/Simulink simulations were performed, considering two different kinds of power quality problems: voltage sags and harmonic distortion (addition of 5th order harmonics). The simulated system is the one already depicted in Fig. 1.

4.1 Voltage Sags/Swells Compensation

Voltage sags of different levels were simulated using a three phase programmable voltage source in Simulink. Fig. 5 shows source and load voltages for a voltage sag of 50%, during two and a half cycles (50 ms). It is possible to see that the system successfully compensate the voltage sag, allowing maintaining voltage at the load during the whole period of the fault.

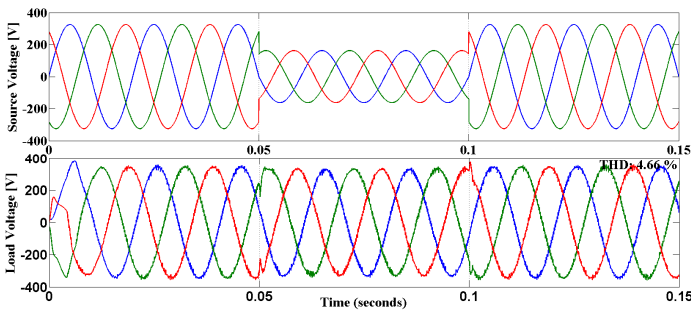


Fig. 5. Voltage sag compensation

The voltage in the DC link of the UPQC, which is used to charge the SMES coil, is shown in Fig. 6. The SMES is charged guaranteeing that voltage does not drops below a specific value, namely 700 V. This was chosen in order to have always a DC voltage above the minimum value that allows full controllability of the power filters, which in this case was calculated as 648 V, following the formulation presented in [21]. The consecutive voltage drops shown in the figure correspond to the charging process of the SMES. During the charging process, current flows to the superconducting coil, decreasing the amount of power at the DC link, thus forcing the DC link voltage to go down. Fig. 6 also shows the evolution of the current in the SMES system, which decreases around 13 A in order to compensate the voltage sag (the SMES is in discharge mode during this time).

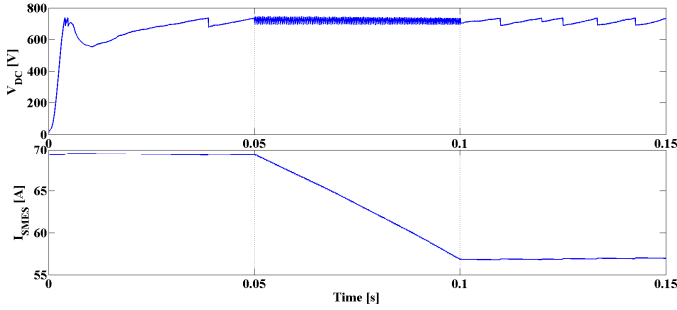


Fig. 6. Voltage in the DC link and current at the SMES coil during a voltage sag

4.2 Harmonic Distortion Mitigation

Another important fault that can occur in a power grid is harmonic distortion. The programmable three phase voltage source from Simulink was again used to add a 5th order harmonic with 0.25 pu content to the voltage signal. This corresponds to a THD of 14.92%. Voltages at source and load for this scenario can be seen in Fig. 7. The system can compensate the harmonic distortion and the load is barely affected by it. The THD at the load is 4.82% during the fault.

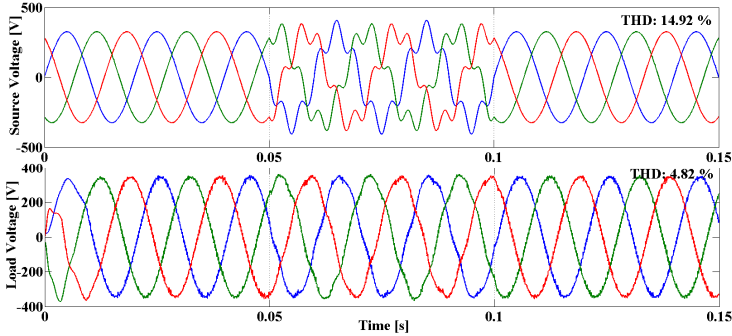


Fig. 7. Compensation of harmonic distortion in the system

5 Conclusion

A combination of an UPQC and a SMES device was presented in this paper and simulation results indicate that the hybrid system can be used to overcome power quality issues in an electric grid. The addition of an SMES unit to the UPQC has several advantages: by adding energy store capabilities, the SMES increases the application range of the UPQC (in this example, the stored energy increased from 4.9 to 686 J). The overall cost of the UPQC device becomes lower because with the combination of a SMES its power rating decreases. Since the SMES is connected to a DC link, the PCS becomes less costly and the control system also becomes simpler. The control

scheme of the full system is very similar to those of the two systems operating alone, with only the additional requirement on the DC voltage when charging the SMES coil.

Two different power quality faults (voltage sags and harmonic distortion of the 5th order) were simulated and results indicate that the system can overcome those faults, without any noticeable change of voltage and current at the load. Such system can improve power quality in electric grids and thus has a very large spectrum of applications.

References

1. EURELECTRIC: Power Quality in European Electricity Supply Networks (2003)
2. Akagi, H.: New trends in active filters for power conditioning. *IEEE Trans. Ind. Appl.* **32**, 1312–1322 (1996)
3. Akagi, H., Watanabe, E.H., Aredes, M.: *Instantaneous Power Theory and Applications to Power Conditioning*. John Wiley & Sons Inc., Hoboken (2007)
4. Rashid, M.H. (ed.) *Power Electronics Handbook*. Elsevier (2011)
5. Amaro, N., Murta Pina, J., Martins, J., Ceballos, J.M.: SUPERCONDUCTING MAGNETIC ENERGY STORAGE - A Technological Contribute to Smart Grid Concept Implementation. In: *Proceedings of the 1st International Conference on Smart Grids and Green IT Systems*, pp. 113–120. SciTePress - Science and and Technology Publications (2012)
6. Xiao, L., Dai, S., Lin, L., Zhang, J., Guo, W., Zhang, D., Gao, Z., Song, N., Teng, Y., Zhu, Z., Zhang, Z., Zhang, G., Zhang, F., Xu, X., Zhou, W.: Development of the World's First HTS Power Substation. *IEEE Trans. Appl. Supercond.* **22**, 5000104–5000104 (2012)
7. Tixador, P., Deleglise, M., Badel, A., Berger, K., Bellin, B., Vallier, J.C., Allais, A., Bruzek, C.E.: First Tests of a 800 kJ HTS SMES. *IEEE Trans. Appl. Supercond.* **18**, 774–778 (2008)
8. Kim, H.J., Seong, K.C., Cho, J.W., Bae, J.H., Sim, K.D., Kim, S., Lee, E.Y., Ryu, K., Kim, S.H.: 3 MJ/750 kVA SMES System for Improving Power Quality. *IEEE Trans. Appl. Supercond.* **16**, 574–577 (2006)
9. Xian, W., Yuan, W., Yan, Y., Coombs, T. A.: Minimize frequency fluctuations of isolated power system with wind farm by using superconducting magnetic energy storage. In: *PEDS Conference*, pp. 1329–1332. IEEE (2009)
10. Aware, M., Sutanto, D.: SMES for Protection of Distributed Critical Loads. *IEEE Trans. Power Deliv.* **19**, 1267–1275 (2004)
11. Tixador, P., Bellin, B., Deleglise, M., Vallier, J.C., Bruzek, C.E., Allais, A., Saugrain, J.M.: Design and First Tests of a 800 kJ HTS SMES. *IEEE Trans. Appl. Supercond.* **17**, 1967–1972 (2007)
12. Torre, W., Eckroad, S.: Improving power delivery through the application of superconducting magnetic energy storage (SMES). In: *2001 IEEE Power Engineering Society Winter Meeting, Conference Proceedings (Cat. No.01CH37194)*, pp. 81–87. IEEE (2001)
13. Chen, L., Liu, Y., Arsoy, A.B., Ribeiro, P.F., Steurer, M., Irvani, M.R.: Detailed Modeling of Superconducting Magnetic Energy Storage (SMES) System. *IEEE Trans. Power Deliv.* **21**, 699–710 (2006)
14. EPRI: *West Coast Utility Transmission Benefits Of Superconducting Magnetic Energy Storage* (1996)

15. IEA, (International Energy Agency): Smart Grids - Technology Roadmap (2011)
16. Ipakchi, A., Albuyeh, F.: Grid of the future. *IEEE Power Energy Mag.* **7**, 52–62 (2009)
17. Zhang, P., Li, F., Bhatt, N.: Next-Generation Monitoring, Analysis, and Control for the Future Smart Control Center. *IEEE Trans. Smart Grid.* **1**, 186–192 (2010)
18. Markovic, D.S., Zivkovic, D., Branovic, I., Popovic, R., Cvetkovic, D.: Smart power grid and cloud computing. *Renew. Sustain. Energy Rev.* **24**, 566–577 (2013)
19. Yigit, M., Gungor, V.C., Baktir, S.: Cloud Computing for Smart Grid applications. *Comput. Networks* **70**, 312–329 (2014)
20. Nielsen, J.G., Blaabjerg, F.: A Detailed Comparison of System Topologies for Dynamic Voltage Restorers. *IEEE Trans. Ind. Appl.* **41**, 1272–1280 (2005)
21. Teke, A.: Unified Power Quality Conditioner: Design, Simulation and Experimental Analysis (2011)
22. Amaro, N., Pina, J.M., Martins, J., Ceballos, J.M., Alvarez, A.: A Fast Algorithm for Initial Design of HTS Coils for SMES Applications. *IEEE Trans. Appl. Supercond.* **23**, 4900104–4900104 (2013)

Energy: Decision Support

Offering Strategies of Wind Power Producers in a Day-Ahead Electricity Market

R. Laia^{1,2}, H.M.I. Pousinho^{1,2}, R. Melício^{1,2(✉)}, V.M.F. Mendes^{1,3},
and M. Collares-Pereira¹

¹ University of Évora, Évora, Portugal
{rui.j.laia, hpousinho}@gmail.com,

{ruimelicio, collarespereira}@uevora.pt

² IDMEC/LAETA, Instituto Superior Técnico, Universidade de Lisboa, Lisbon, Portugal

³ Instituto Superior of Engenharia de Lisboa, Lisbon, Portugal
vfmendes@deea.isel.pt

Abstract. This paper presents a stochastic optimization-based approach applied to offer strategies of a wind power producer in a day-ahead electricity market. Further from facing the uncertainty on the wind power the market forces wind power producers to face the uncertainty of the market-clearing electricity price. Also, the producer faces penalties in case of being unable to fulfill the offer. An efficient mixed-integer linear program is presented to develop the offering strategies, having as a goal the maximization of profit. A case study with data from the Iberian Electricity Market is presented and results are discussed to show the effectiveness of the proposed approach.

Keywords: Mixed-integer linear programming · Stochastic optimization · Wind power · Offering strategies

1 Introduction

Renewable energy sources are viewed as of crucial usage for a sustainable society development [1] and the industry of conversion into electric energy is already exploiting these sources. Renewable energy sources can partly replace fossil fuel sources, avowing carbon emissions and reducing the fuel-import dependency on countries with rich fossil fuel stocks. Countries promote the usage of renewable energy sources by supporting mechanisms and policies to provide incentive or subsidy for renewable energy capturing [2]. Nowadays wind power is integrated into the electric power grid and there are encouragements by extra-market actions, involving, for instances, legislation, directives, feed-in tariffs, encouraging penalty pricing and guaranteed electric grid access [3]. These actions runs at modest penetration levels in nowadays, but will become flawed as wind power penetration increases [3]. This will force wind power producers (WPPs) to face the challenges of a day-ahead electricity market and bilateral contracting. For instance: in Portugal, WPPs are rewarded with a feed-in tariff in conditions of a limited amount of time or energy delivered, if one of these conditions fails, energy is sold either in the day-ahead electricity market or by bilateral contracts

[4]; in United Kingdom, large WPPs are forced to participate in whole-sales markets and subjected to financial penalties in case of deviation from contracts in forward markets [5]. Intermittency and variability of wind power are WPP concerns of uncertainty in what regards imbalance penalties due to imbalance on the electric power delivered [6]. This paper is a contribution to deal with these concerns of uncertainty by using an approach based on stochastic optimization MILP to enable WPPs to optimize their offers having as a goal the maximization of profit in a day-ahead electricity market.

2 Relationship to Cloud-Based Solutions

Cloud-based solutions can help the processing of approaches for helping trading in a day-ahead electricity market in order to take greater advantages of bids, requiring methodological approaches demanding computational effort not currently available to the WPP. Among these approaches the ones for the solution of the problems concerning with energy management, unit commitment and energy offers are particular vital for upholding a WPP business. The approaches to solve these problems have been limited by the available computational resources, i.e., details concerning some reality are disregard in view of the excessive use of computational requirements. These limitations are evident for large systems and lead to solutions not conveniently addressed in agreement with the reality, because the computational resources do not allow the usage of data or modeling for delivering more adequate solutions. Particularly, in what regards the fact that for WPP the market brings uncertainty and paying penalties due to uncertainty on wind power exploitation: the stochastic concern with scenarios data implies the processing of large sets of data requiring the use of reduction techniques to avoid the use of significant computational requirements.

Cloud-based solutions are able to contribute for upholding a WPP by setting out an adequate availability of computational resources needed to address those problems in due time. Although of the uncertainty on the wind power, i.e., intermittency and variability, cloud-based engineering systems will deal with problems approaching the full reality with gains in terms of profits for WPP's. Cloud-based solutions will help out smoothing the market-clearing electricity price due to the fact of having bids of wind power with higher level of energy and with more certainty in what regards the satisfaction on delivering the electric power accepted at the market-closing. Also, environmental benefits are expected with the increment in the ability of finding offers able to be fulfilled with a high level of being satisfied, i.e., integrating renewable energy into the electric grid with less deviation from the assumed compromises: less spinning reserved is needed, less thermal units are needed and less fossil fuel is used. Eventually, cloud-based solutions will allow processing approaches in order that when at a WPP site the renewable energy is available is all captured to be converted in electric energy to be injected without concerns on dynamic stability into the electric grid in due time.

3 State of the Art

Wind power and the market-clearing electricity price uncertainties are passed on the variables of the problems [7,8] to be addressed by the WPP in order to know how much to produce in order to formulate realistic bids, because in case of excessive or moderate bids, other producers must reduce or increase production to fill the so-called deviation, implying penalties causing economic losses [1]. In order for upholding a WPP in a competitive environment, three main lines of action have been proposed in the technical literature: One of them is based on the use of wind power with energy storage technologies [9]–[11]; another one is the use of financial options as a tool for WPP to hedge against wind power uncertainty [12]; and the final one focuses on designing stochastic models intended to produce optimal offer strategies for WPP participating in an electricity market [13]–[15], without depending on third-parties or governmental regulations. The third line of action is a stochastic formulation explicitly modeling the uncertainties faced by the scheduling activities of a WPP [16], using uncertain measures and multiple scenarios built by wind power forecast [17]–[19] and market-clearing electricity price forecast [20]–[22] applications. Mixed integer linear programming (MILP) is one of the most successful explored methods for scheduling activities because of rigorousness, flexibility and extensive modeling capability [23]. Hence, MILP is expected to be also a successful method for solving WPP problems in the context of the day-head electricity market and this paper aims at show the usefulness of this method for WPPs.

4 Problem Formulation

Wind energy conversion into electric energy for trading in a day-head market involves facing up uncertainties that must be taken into account in devising of the offer strategy. The uncertainties are due to the intermittence and variability on the available wind power and due to the market-clearing electricity price. These uncertainties if not conveniently addressed are capable of losses on profit due to the incurred imbalance penalties. The problem formulation in this paper is an addressing in a convenient way.

System imbalance is defined as a non-null difference on the trading between the delivered energy and the offered energy. If there is an excess of delivered energy in the power system, the system imbalance is positive; otherwise, the system imbalance is negative. The system operator seeks to minimize the absolute value of the imbalance in a power system through a mechanism based on prices penalization for the deviation of the delivered energy from the one offered by a producer in the day-ahead market. If the system imbalance is negative, the system operator keeps the price for the energy in excess for the producers with excess of offers, and pays a premium price for the energy produced above the offer. The prices are as follow

$$\lambda_t^+ = \lambda_t^D \quad (1)$$

$$\lambda_t^- = \max(\lambda_t^D, \lambda_t^{UP}) \quad (2)$$

In (1) and (2), λ_t^+ and λ_t^- , are applied in the balancing market to the energy deviations, λ_t^D is the day-ahead market-clearing price and λ_t^{UP} is the price of the energy that needs to be added to the system. If the system imbalance is positive, the prices are as follow

$$\lambda_t^+ = \min(\lambda_t^D, \lambda_t^{DN}) \tag{3}$$

$$\lambda_t^- = \lambda_t^D \tag{4}$$

In (3), λ_t^{DN} is the price of the energy of offers in exceeds. The uncertainties in the available wind power may result in differences between the energy offered by a WPP and the actual energy delivered. The revenue R_t of the WPP for hour t is as follows

$$R_t = \lambda_t^D P_t^D + I_t \tag{5}$$

In (5), P_t^D is the power traded by the WPP in the day-ahead market and I_t is the imbalance income resulting from the balancing penalty.

Since the total deviation for hour t is as follows

$$\Delta_t = P_t - P_t^D \tag{6}$$

where P_t is the actual power for hour t . I_t is given as follows

$$I_t = \lambda_t^+ \Delta_t, \Delta_t \geq 0 \tag{7}$$

$$I_t = \lambda_t^- \Delta_t, \Delta_t < 0 \tag{8}$$

In (6), a positive deviation means the actual production is higher than the traded in the day-ahead market and a negative deviation means an actual production lower than the traded, this way λ_t^+ is the price paid to the WPP for its excess of generation and λ_t^- the price to be charged for the deficit. Let

$$r_t^+ = \frac{\lambda_t^+}{\lambda_t^D}, r_t^+ \leq 1 \tag{9}$$

$$r_t^- = \frac{\lambda_t^-}{\lambda_t^D}, r_t^- \geq 1 \tag{10}$$

Then

$$I_t = \lambda_t^D r_t^+ \Delta_t, \Delta_t \geq 0 \quad (11)$$

$$I_t = \lambda_t^D r_t^- \Delta_t, \Delta_t < 0 \quad (12)$$

A WPP that needs to correct the energy deviations in the balancing market incurs an opportunity cost because in the day-ahead market energy is traded at a more competitive price. Equation (5) can be rewritten to reflect the opportunity cost. Two cases have to be considered. If the energy deviation is positive, $\Delta_t > 0$, the revenue is given as follows

$$R_t = \lambda_t^D P_t^D + \lambda_t^D r_t^+ \Delta_t \quad (13)$$

Using the total deviation expressed in equation (6), the revenue is given as follows

$$R_t = \lambda_t^D P_t^D - \lambda_t^D (1 - r_t^+) \Delta_t, \Delta_t \geq 0 \quad (14)$$

Similarly, if the energy deviation is negative, the revenue is given as follows

$$R_t = \lambda_t^D P_t^D + \lambda_t^D (r_t^- - 1) \Delta_t, \Delta_t < 0 \quad (15)$$

Equations (14) and (15) can be expressed in a general form as follows

$$R_t = \lambda_t^D P_t^D - C_t \quad (16)$$

where

$$C_t = \lambda_t^D (1 - r_t^+) \Delta_t, \Delta_t \geq 0 \quad (17)$$

$$C_t = -\lambda_t^D (r_t^- - 1) \Delta_t, \Delta_t < 0 \quad (18)$$

In (16), the term $\lambda_t^D P_t^D$ is the maximum revenue that the WPP can collect from trading the energy in a situation without wind power uncertainty. With wind power uncertainty a set of scenarios Ω is considered for wind power and system imbalances. Each scenario ω is weighted with a probability of occurrence π . The expected optimal revenue of the WPP over a time horizon is obtained by the maximization of the objective function given as follows

$$\sum_{\omega=1}^{N_\Omega} \sum_{t=1}^{N_T} \pi_\omega \left(\lambda_{t\omega}^D P_t^D + \lambda_{t\omega}^D r_{t\omega}^+ \Delta_{t\omega}^+ - \lambda_{t\omega}^D r_{t\omega}^- \Delta_{t\omega}^- \right) \quad (19)$$

The maximization is subjected to constraints as follow

$$0 \leq P_t^D \leq P^{\max}, \forall t \quad (20)$$

$$\Delta_{t\omega} = (P_{t\omega} - P_t^D), \forall t, \forall \omega \quad (21)$$

$$\Delta_{t\omega} = \Delta_{t\omega}^+ - \Delta_{t\omega}^-, \forall t, \forall \omega \tag{22}$$

$$0 \leq \Delta_{t\omega}^+ \leq P_{t\omega} d_t, \forall t, \forall \omega \tag{23}$$

In (20) the limit of offers to the maximum power installed in the wind farm is set. In (21) to (23) is imposed $\Delta_{t\omega}^+ = 0$ when $\Delta_{t\omega}^+$ is negative, $P_{t\omega} < P_t^D$, and imposed $\Delta_{t\omega}^- = 0$ when $\Delta_{t\omega}^-$ is negative, $P_t^D < P_{t\omega}$. When the system balance is negative, the WPP is penalized for the deficit of energy generated below the energy traded in the day-ahead market, so the term $\lambda_{t\omega}^D r_{t\omega}^+ \Delta_{t\omega}^+$ is null and the term $\lambda_{t\omega}^D r_{t\omega}^- \Delta_{t\omega}^-$ is subtracted from the revenue in the situation of no deviation, $\lambda_{t\omega}^D P_t^D$. When the system balance is positive, the WPP is penalized for the energy generated above the energy traded in the day-ahead market, so the term $\lambda_{t\omega}^D r_{t\omega}^- \Delta_{t\omega}^-$ is null and the term $\lambda_{t\omega}^D r_{t\omega}^+ \Delta_{t\omega}^+$ is subtracted from the revenue in the situation of no deviation.

5 Case Study

The effectiveness of the proposed stochastic MILP approach is illustrated by a case study using two sets of data from the Iberian electricity market [24]. The first data set comprises 10 days of November 2013 and the second 10 days of June 2014 as are respectively shown in Fig. 1.

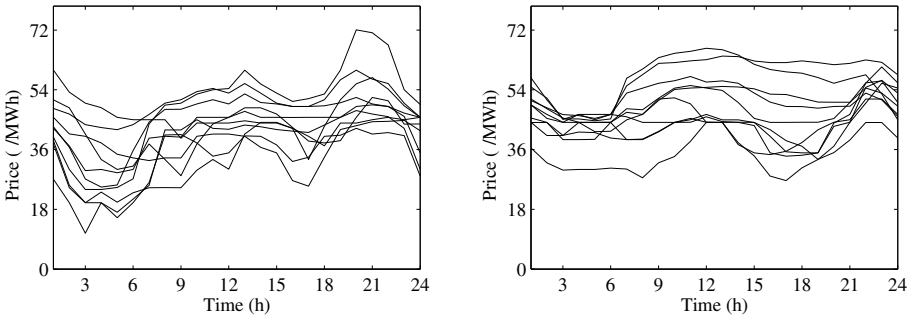


Fig. 1. Price scenarios; left: November 2013, right: June 2014

The total energy produced in 2013 and 2014 are respectively shown in Fig. 2.

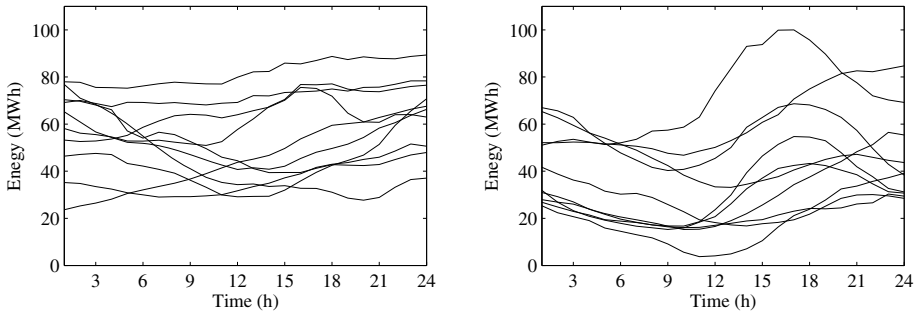


Fig. 2. Energy from wind; left: November 2013, right: June 2014

The energy produced is obtained using the total energy produced from wind scaled to the maximum power, $P^{\max} = 120MW$. The system operator matches the total energy production to the system needs. This is achieved by defining the price multipliers r_i^+ and r_i^- given by (9) and (10). The r_i^+ and r_i^- in 2013 are respectively shown in Fig. 3.

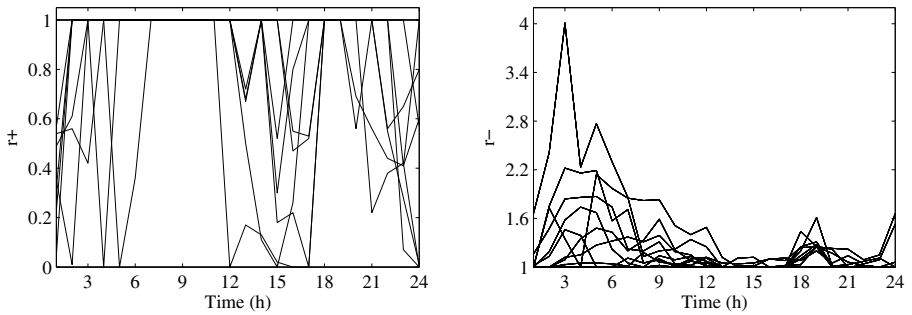


Fig. 3. Imbalance price multipliers 2013; left: r_i^+ , right: r_i^-

The r_i^+ and r_i^- in 2014 are shown in Fig. 4.

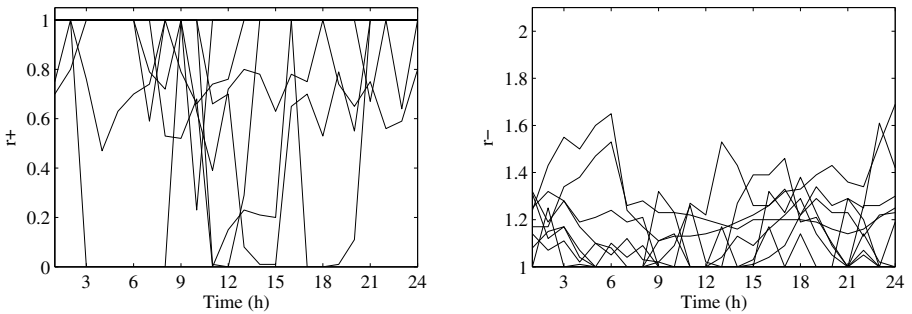


Fig. 4. Imbalance price multipliers 2014; left: r_i^+ , right: r_i^-

The optimal energy offer in conditions of maximizing a WPP revenue is determined by (19) to (23). The optimal energy offer and the expected hourly revenue are respectively shown in Fig. 5 and Fig. 6.

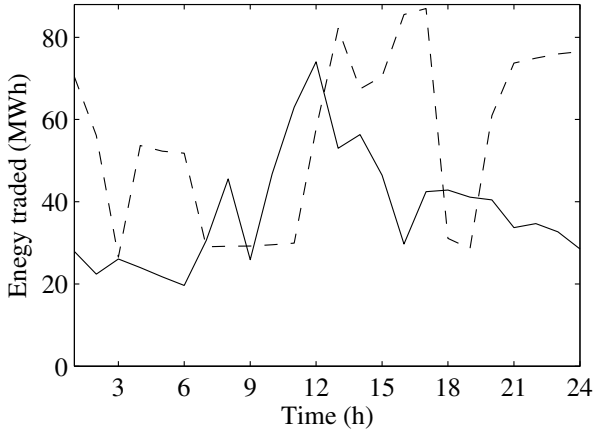


Fig. 5. Energy traded day-ahead market; dashed-line: 2013, solid line: 2014

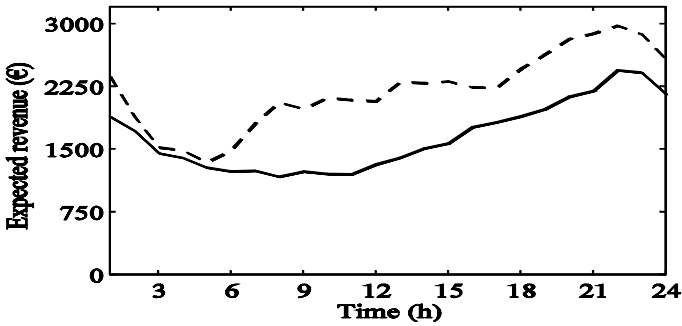


Fig. 6. Expected hourly revenue; dashed-line: 2013, solid line: 2014

The forecasted revenue for the 24 hours is 52,861 € in 2013 and 39,656 € in 2014. The difference between the expected revenue and the revenue for each scenario, assuming that the 24 hours will behave exactly the same in each scenario is shown in Fig. 7.

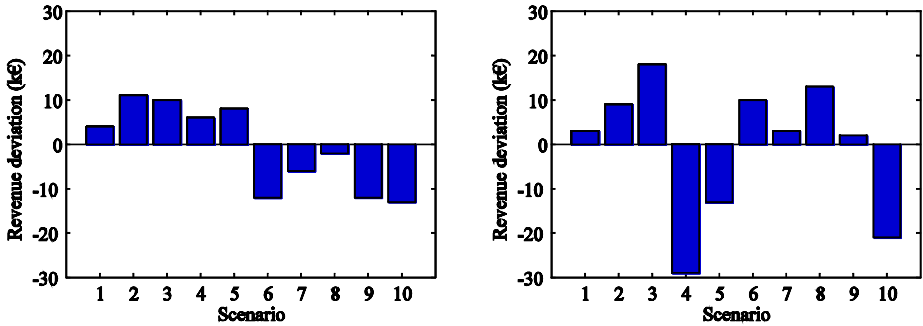


Fig. 7. Revenue deviation; left: 2013, right: 2014

In each year, the deviation for the worst case scenario is lower than the expected revenue, which means that if the condition during the day matches any one of the scenarios, the result would be always positive.

6 Conclusion

A stochastic MILP approach for solving the offering strategy of a WPP in a deregulated market is discussed in this paper and envisaged as potential convenient for the producers with the help of cloud-based solutions. The main result is the bidding strategy for a WPP facing the wind power and price uncertainties, as well the system imbalances which affect the price in case of deviations between the energy traded in the day-ahead market and the actual energy produced by the WPP.

Stochastic programming is a suitable approach to address parameter uncertainty in modeling via scenarios. The proposed stochastic MILP approach proved both to be accurate and computationally acceptable, since the computation time scales up linearly with number of price scenarios, units and hours over the time horizon. Since the bids in the pool-based electricity market are made one day before, this approach is a helpful tool for the decision-maker.

References

1. Pousinho, H.M.I., Catalão, J.P.S., Mendes, V.M.F.: Offering strategies for a wind power producer considering uncertainty through a stochastic model. In: Proceedings of PMAPS 2012 (2012)
2. Kongnam, C., Nuchprayoon, S.: Feed-in tariff scheme for promoting wind energy generation. In: IEEE Bucharest Power Tech Conference (2009)
3. Bitar, E.Y., Poolla, K.: Selling wind power in electricity markets: the status today, the opportunities tomorrow. In: 2012 American Control Conference, June 27-June 29, Canada (2012)
4. Barros, J., Leite, H.: Feed-in tariffs for wind energy in Portugal: current status and prospective future. Electrical Power Quality and Utilisation (EPQU) (2011)

5. Barros, J., Leite, H.: Feed-in tariffs for wind energy in Portugal: current status and prospective future. *Electrical Power Quality and Utilisation (EPQU)* (2011)
6. Al-Awami, A.T., El-Sharkawi, M.A.: Coordinated trading of wind and thermal energy. *IEEE Transactions on Sustainable Energy* 2(3) (2011)
7. Cena, A.: The impact of wind energy on the electricity price and on the balancing power costs: the Spanish case. In: *The European Wind Energy Conference (EWEC)*, Marseille, France, March 2009
8. El-Fouly, T.H.M., Zeineldin, H.H., El-Saadany, E.F., Salama, M.M.A.: Impact of wind generation control strategies, penetration level and installation location on electricity market prices. *IET Renewable Power Generation* 2(3), 162–169 (2008)
9. Angarita, J.L., Usaola, J., Martinez-Crespo, J.: Combined hydro wind generation bids in a pool-based electricity market. *Energy Policy* 79(7), 1038–1046 (2009)
10. Bathurst, G.N., Strbac, G.: Value of combining energy storage and wind in short-term energy and balancing markets. *Electric Power Systems Research* 67(1), 1–8 (2003)
11. Gonzalez, J.G., Muela, R.M.R., Santos, L.M., Gonzalez, A.M.: Stochastic joint optimization of wind generation and pumped-storage units in an electricity market. *IEEE Transactions on Power Systems* 23(2), 460–468 (2008)
12. Hedman, K., Sheble, G.: Comparing hedging methods for wind power: using pumped storage hydro units vs options purchasing. In: *International Conference on Probabilistic Methods Applied to Power Systems PMAPS*, pp. 61–66, Stockholm, Sweden (2006)
13. Bathurst, G.N., Weatherill, J., Strbac, G.: Trading wind generation in short term energy markets. *IEEE Transactions on Power Systems* 17(3), 782–789 (2002)
14. Matevosyan, J., Soder, L.: Minimization of imbalance cost trading wind power on the short-term power market. *IEEE Transactions on Power Systems* 21(3), 1396–1404 (2006)
15. Pinson, P., Chevallier, C., Kariniotakis, G.N.: Trading wind generation from short-term probabilistic forecasts of wind power. *IEEE Transactions on Power Systems* 22(3), 1148–1156 (2007)
16. Ruiz, P.A., Philbrick, C.R., Sauer, P.W.: Wind power day-ahead uncertainty management through stochastic unit commitment policies. In: *Proc. IEEE/PES 2009 Power Syst. Conf. Expo. (PSC 2009)*, pp.1–9 (2009)
17. Fan, S., Liao, J.R., Yokoyama, R., Chen, L.N., Lee, W. J.: Forecasting the wind generation using a two-stage network based on meteorological information. *IEEE Trans. Energy Convers.* 24, 474–482 (2009)
18. Kusiak, A., Zheng, H.Y., Song, Z.: Wind farm power prediction: A data-mining approach. *Wind Energy* 12, 275–293 (2009)
19. Catalão, J.P.S., Pousinho, H.M.I., Mendes, V.M.F.: An artificial neural network approach for short-term wind power forecasting in Portugal. *Eng. Int. Syst.* 17, 5–11 (2009)
20. Catalão, J.P.S., Mariano, S.J.P.S., Mendes, V. M. F., Ferreira, L. A. F. M.: Short-term electricity prices forecasting in a competitive market: a neural network approach. *Electr. Power Syst. Res.* 77, 1297–1304 (2007)
21. Coelho, L.D., Santos, A.A.P.: A RBF neural network model with GARCH errors: Application to electricity price forecasting. *Electr. Power Syst. Res.* 81, 74–83 (2011)
22. Amjady, N., Daraeepour, A.: Mixed price and load forecasting of electricity markets by a new iterative prediction method. *Electr. Power Syst. Res.* 79, 1329–1336 (2009)
23. Floudas, C.A., Xiaoxia, L.: Mixed integer linear programming in process scheduling: modeling, algorithms, and applications. *Annals of Operations Research* 139, 131–162 (2005)
24. <http://www.esios.ree.es/web-publica/>

New Multi-Objective Decision Support Methodology to Solve Problems of Reconfiguration in the Electric Distribution Systems

Sérgio F. Santos¹, Nikolaos G. Paterakis¹, and João P.S. Catalão^{1,2,3(✉)}

¹ University of Beira Interior, Covilhã, Portugal

² INESC-ID, Lisbon, Portugal

³ Instituto Superior Técnico, Lisbon, Portugal

catalao@ubi.pt

Abstract. The distribution systems (DS) reconfiguration problem is formulated in this paper as a multi-objective mixed-integer linear programming (MILP) multi-period problem, enforcing that the obtained topology is radial in order to exploit several advantages those configurations offer. The effects of distributed generation (DG) and energy storage systems (ESS) are also investigated. To address the multi-objective problem, an improved implementation of the ε -constraint method (AUGMECON-2) is used, providing an adequate representation of the Pareto set. The objective functions considered stand for the minimization of active power losses and the minimization of switching operations. The proposed methodology is tested using a real system based on the S. Miguel Island, Azores, Portugal. The potential uses of cloud-based engineering systems, both in terms of exploiting the enhanced decentralized computational opportunities they offer and of utilizing them in order to achieve communication and coordination between several entities that are engaged in DS, are thoroughly discussed.

Keywords: Distribution system reconfiguration · ε -constraint method · Switching cost · Multi-objective optimization

1 Introduction

The reconfiguration of power distribution systems (DS) is the process of opening and closing switches, changing the network topology, in order to achieve several operating advantages. The problem is to find a configuration that presents the least amount of active power losses, subject to the following restrictions: voltage levels, power transfer capability of branches, the rated power of transformers and often the radial configuration of the obtained system. A classification of the DS problems together with a literature survey can be found in [1].

Systems with meshed structures are not recommended for power distribution networks, because their protection schemes are more complex in comparison with radial distribution systems. The reconfiguration problem is typically a nonlinear, multi-objective, combinatorial problem, subject to operational constraints of loads. Some of these configurations are not allowed, or because they lead to a disconnected

system (with several islands) or non-radial systems. Others are not feasible, because they violate operational and load restrictions. Various objective functions have been used, but the most common one is the minimization of the active power losses [2].

Multi-objective approaches try to optimize a combination of the previous objective functions [3], [4]. In the emerging Smart Grid scheme, Distributed Generation (DG) and Energy Storage Systems (ESS) play a key role and pose new challenges in the operation of the DS [5], [6].

The majority of the related studies in the literature treat the problems using solution techniques based on meta-heuristics, mainly because they are easily applicable to the problem and offer computational advantages, especially in the case of the multi-objective formulations. There are also studies that try to solve the DS reconfiguration problem through the linearization of the AC power flow constraints [7], formulating it as a Mixed-Integer Linear Programming (MILP) problem.

However, treating the DS reconfiguration with a Multi-Objective Mathematical Programming (MOMP) approach poses difficulties, mainly due to the computational effort that is required and the need to guarantee that the obtained solution is the best possible [8]. Although solving a Single-Objective Mathematical Programming problem is a procedure that will return the maximum or the minimum solution among the feasible ones, the solution of a MOMP problem is not a trivial task, since there is not, in general, a single solution that optimizes every objective function simultaneously. In MOMP, the required result is the set of the relatively optimal solutions, called the Pareto set.

The aim of this work is to develop tools that contribute to the quality of service to the end-users at a minimal cost to the companies responsible for power distribution. Therefore, the novel contributions of this work are twofold. The first contribution is the formulation of the radial DS reconfiguration as a multi-period MOMP problem, considering the effects of DG and ESS with two objective functions: minimization of the active power losses and minimization of the total switching cost. The second contribution comes from the solution of the problem using an improved version of the ϵ -constraint method, namely the Augmented ϵ -constraint Method (AUGMECON-2), a state-of-the-art methodology introduced by Mavrotas in [8] and further improved in [9], in order to generate an adequate representation of the Pareto optimal solutions of the problem.

2 Contribution to Cloud-Based Engineering Systems

The DS reconfiguration (DSR) problem has been a topic of intensive research that has led to several applications during the past decades. Nevertheless, recent changes in the characteristics of the DS, such as the introduction of DG, ESS and flexible demand, as well as the introduction of various stakeholders that utilize the DS, require the reevaluation of the DSR problem using innovative solutions.

In this respect, cloud-based engineering solutions may prove invaluable in several ways. Illustratively, several applications that can immediately benefit the distribution system operator with respect to the DSR problem are:

1. Optimal DSR is formulated as a complex optimization problem. Given emerging elements that have to be considered in optimization procedures, the complexity of the DSR problem dramatically increases. The high computational burden, especially for a large-scale DS, may force distribution system operators to upgrade the informatics infrastructure, incurring high investment costs. A cloud-based engineering system could be used in order to solve the problem in a de-centralized fashion using cloud computing.
2. The introduction of several entities (e.g. load aggregators and DG unit's owners) that utilize the DS to materialize their purposes, imposes the need of transparency regarding the DSR decisions. The configuration of the DS affects several DS operating parameters, such as losses and quality of service, which in turn may affect the allocation of operating costs. A cloud-based engineering system (e.g. an on-line portal) may be used in order to allow stakeholders to access relevant information, promoting the fair allocation of costs.
3. Internet is a utility that is available virtually everywhere since there are many wired and wireless options to access the internet. A cloud-based engineering system may be utilized in order to monitor data, even at remote nodes of the DS at an affordable cost. In this way, better analytics may be obtained and exploited in the development of more accurate optimization problems and real-time operation (e.g. fault detection). Also, commands such as switching actions may be given remotely, eliminating constraints such as crew availability. Finally, advanced control schemes may be performed automatically (e.g. automated reconfiguration after the detection of a fault).

3 Methodology

3.1 Overview of Augmented ϵ -constraint Method

The ϵ -constraint method is a “generation method” that is used to construct an adequate representation of the Pareto-optimal set of solutions, and does not consider the Decision Maker's preferences a priori. Among the different objective functions, one is used as the objective function of the problem, while the others are treated as inequality constraints. Their bounding values are varied parametrically in order to produce the Pareto-optimal set of solutions. The application of the ϵ -constraint method requires the knowledge of the range of objective functions that are used as constraints. The range is usually calculated using the pay-off table that contains the values of the objective functions, resulting from the individual optimization of each single objective function [10]. The pay-off table alone does not guarantee that the range always provides the efficient set. AUGMECON addresses this issue through the utilization of lexicographic optimization. Lexicographic optimization is performed by optimizing the objective functions according to their priority. The highest priority objective function is optimized first and its optimal value is incorporated as an equality constraint in the optimization of all the less priority objective functions.

This procedure is repeated for all the objective functions. After lexicographic optimization, the ranges of the objective functions are divided in n equal intervals and $n + 1$ grid points are used to parametrically vary the bound of the objective functions used as inequality constraints in the classical ε -constraint method.

This method is guaranteed to provide only efficient solutions [8]. The number of grid points is adjustable and is directly linked to the density of the Pareto-optimal set representation. It also allows determining the desired trade-off between quality of the representation and computational burden. To reduce the computational burden, power flow equations are not incorporated as constraints of the optimization problem. Through a linear approximation of the active power flow losses (using Special Ordered Sets of Type 2- SOS2) a least-losses equivalent topology may be obtained. If required, branch currents, node voltages and the exact amount of losses may be calculated afterwards for the obtained topology using any available power-flow algorithms. The linearization through SOS2 variables offers computational advantages when using Branch-and-Bound based solution algorithms (e.g. CPLEX).

3.2 Mathematical Formulation

In this section, the proposed mathematical formulation is presented. To simplify the application of the aforementioned multi-objective optimization method and in order to reduce the computational burden, constraints that typically appear in DS reconfiguration problems in the literature, such as node voltage limits, line currents, reactive power, etc. are not considered, assuming that sufficient reactive power compensation is available locally (at the nodes) and that an advanced metering infrastructure (AMI) provides enough information regarding the state of voltage magnitude and angle. The nomenclature used in the formulation is presented in the Nomenclature at the end of the paper.

1) Objective Function

a) Minimization of the Total Operating Costs

Objective function (1) stands for the minimization of the total power losses over the total time period.

$$TL = \sum_t \sum_b P_{b,t}^{loss} \quad (1)$$

b) Minimization of the Total Switching Costs

Objective function (2) stands for the total cost emerging from the switching operations required throughout the horizon in order to change the DS configuration.

$$TSC = \sum_t \sum_b C_{b,t}^{sw} \quad (2)$$

The two objective functions are conflicting. As the load at the different nodes of the DS varies with time, the flows through the branches change, so do the losses. Thus, by reconfiguring the DS in order to minimize the losses at a specific time period, switching operations are contributing in the total switching-cost.

2) **Constraints**

a) *Radiality Constraints*

The radial configuration of the system is ensured by (3)-(5). Constraints (4) and (5) consider transfer nodes, i.e. nodes without production or consumption.

$$\sum_{b \in B} x_{b,t} = N - N^f - \sum_{i \in I: i \in (\Omega_i^t \cup \Omega_b^j)} (1 - y_{i,t}) \quad (3)$$

$$x_{b,t} \leq y_{i,t} \quad \forall b \in B, i \in (\Omega_i^t \cup \Omega_b^j), t \in T \quad (4)$$

$$\sum_{b \in B: i \in \Omega_b^j \cup \Omega_b^i} x_{b,t} \geq 2 \cdot y_{i,t} \quad \forall i \in \Omega_i^t, t \in T \quad (5)$$

A DS topology is radial if and only if it constitutes a tree-graph (no loops) and all the nodes are connected.

b) *Constraints ensuring the Connection of Nodes with Distributed Elements*

The following constraints prevent islanding. Thus, they do not allow a part of the network to be fed from distributed elements (i.e. storage systems, DG). For intentional islanding (e.g. for back-up reasons) these constraints could be handled in order to allow some nodes to play the role of a substation.

$$\sum_{b \in B: i \in \Omega_b^j} k_{b,t} - \sum_{b \in B: i \in \Omega_b^i} k_{b,t} + k_{i,t}^g = k_i^d \quad \forall i \in I, t \in T \quad (6)$$

$$-N^{de} \cdot x_{b,t} \leq k_{b,t} \leq N^{de} \cdot x_{b,t} \quad \forall b \in B, t \in T \quad (7)$$

$$k_{i,t}^g \geq 0 \quad \forall i \in \Omega_i^f, t \in T \quad (8)$$

$$k_{i,t}^g = 0 \quad \forall i \notin \Omega_i^f, t \in T \quad (9)$$

$$k_i^d = 1 \quad \forall i \in \Omega_i^{de} \quad (10)$$

$$k_i^d = 0 \quad \forall i \notin \Omega_i^{de} \quad (11)$$

c) *Node Power Balance, Branch Flow Limits, Substation Limits and Distributed Generation Limits*

Constraints (12)-(15) stand for the power equilibrium at each node of the distribution system and set the appropriate values for the respective decision variables.

$$\sum_{b \in B: i \in \Omega_b^j} f_{b,t} - \sum_{b \in B: i \in \Omega_b^i} f_{b,t} + P_{i,t}^f + P_{i,t}^{dg} + P_{i,t}^{dis} = D_{i,t} + P_{i,t}^{ch} \quad \forall i \in I, t \in T \quad (12)$$

$$-f_b^{max} \cdot x_{b,t} \leq f_{b,t} \leq f_b^{max} \cdot x_{b,t} \quad \forall b \in B, t \in T \quad (13)$$

$$0 \leq P_{i,t}^f \leq P_{i,t}^{f,max} \quad \forall i \in I \in \Omega_i^f, t \in T \quad (14)$$

$$0 \leq P_{i,t}^{dg} \leq P_{i,t}^{dg,max} \quad \forall i \in \Omega_i^{dg}, t \in T \quad (15)$$

d) *Linear Approximation of the losses*

The power losses on a branch are approximated using a quadratic function of the power that flows through the branch. The units of the coefficients b and c are $[.]$ and $[MW^{-1}]$, respectively.

$$P_{b,t}^{loss} = b \cdot |f_{b,t}| + c \cdot f_{b,t}^2 \quad \forall b \in B, \forall t \in T \quad (16)$$

The expression of the losses can be linearized using the concept of Special Order Sets of Type 2 (SOS2). This is described by (17)-(19). It should be noted that variables z are positive and continuous.

$$\sum_{p \in P} z_{b,t,p} = 1 \quad \forall b \in B, \forall t \in T \quad (17)$$

$$f_{b,t} = \sum_{p \in P} X_p \cdot z_{b,t,p} \quad \forall b \in B, \forall t \in T \quad (18)$$

$$F_{b,t} = \sum_{p \in P} Y_p \cdot z_{b,t,p} \quad \forall b \in B, \forall t \in T \quad (19)$$

By the definition of SOS2, it is also stipulated that no more than two adjacent values of z can be greater than zero. The accuracy of the approximation depends on the sampling of the non-linear function, i.e. the number of samples and the intervals that are used.

It is also reported that the linearization of a function using this method has computational advantages when using the Branch-And-Bound algorithm that is implemented in many commercial solvers.

e) *Switching Cost*

Equations (20)-(22) define the switching cost by following the change of status of every line. Through the parameter SC_b a different switching cost can be attached to every branch representing the cost emerging from this operation, considering several factors such as equipment degradation costs and crew constraints.

$$C_{b,t}^{sw} = (x_{b,t} - x_{b,t-1}) \cdot SC_b \quad \forall b \in B, t \in T | t > 1 \quad \text{if } x_{b,t} = 1 \quad (20)$$

$$C_{b,t}^{sw} = (x_{b,t-1} - x_{b,t}) \cdot SC_b \quad \forall b \in B, t \in T | t > 1 \quad \text{if } x_{b,t} = 0 \quad (21)$$

$$C_{b,t}^{sw} = 0 \quad \forall b \in B \quad \text{if } t = 1 \quad (22)$$

f) *Energy Storage System Constraints*

Energy Storage Systems (ESS) are an important asset of the smart-grid. Promising technologies such as Sodium-Sulfur batteries (NAS) have been already used in practice and can efficiently store large amounts of energy. Their primary goal is to support demand response activities, balancing volatile renewable energy sources production and offer back-up and other ancillary services. In this study, a general formulation of an ESS is considered through (23) to (28), in order to investigate their ability to facilitate the operating goals of the DS.

$$SOE_{i,t} = SOE_{i,t-1} + P_{i,t}^{ch} \cdot CE_i - \frac{P_{i,t}^{dis}}{DE_i} \quad \forall i \in \Omega_i^S, t \in T \quad (23)$$

$$P_{i,t}^{ch} \leq CR_i \cdot y_{i,t}^S \quad \forall i \in \Omega_i^S, t \in T \quad (24)$$

$$P_{i,t}^{dis} \leq DR_i \cdot z_{i,t}^S \quad \forall i \in \Omega_i^S, t \in T \quad (25)$$

$$SOE_{i,t} \leq SOE_i^{max} \quad \forall i \in \Omega_i^S, t \in T \tag{26}$$

$$SOE_{i,t} \geq SOE_i^{min} \quad \forall i \in \Omega_i^S, t \in T \tag{27}$$

$$y_{i,t}^S + z_{i,t}^S \leq 1 \quad \forall i \in \Omega_i^S, t \in T \tag{28}$$

4 Tests and Results

The proposed methodology has been coded using General Algebraic Modeling System (GAMS) and the solver CPLEX. The system used to illustrate the presented methodology is adapted from [11] and is presented in Fig. 1. All the branches are considered switchable except for branches L01, L06, L08, L12, L20, L21, L22, L23, L30, L31 and L32. Active power limits for all branches are considered as 500kW and the switching cost for a single open or close operation is 10€. To approximate the losses, 51 pairs of (X_i, Y_i) are used, one for every 5kW in the range [-500kW, 500kW], and constants a and b are 0.001 and 0.0003 MW⁻¹, respectively. The operation of the system is studied over a 7-hour horizon. An ESS is considered at node 27. Its capacity is 16 kWh, having a charging/discharging rate equal to 4 kW and charging/discharging efficiencies of 90%. Its minimum state-of-energy in order to avoid deep discharge is 8 kWh. Its initial state-of-energy is 9 kWh. Two DG units with maximum capacity as 15 kW and 10 kW are considered at nodes 21 and 45, respectively. Substations at Lagoa 1, Lagoa 2 and Lagoa 3 can provide 1136 kW, 480 kW and 2657 kW, respectively, and 11811 kW at the São Roque power node. The Pareto efficient set of solutions obtained by the AUGMECON method is shown in Fig. 2.

Five grid points are used and the CPU time needed is 54.8 seconds on a laptop with an 8-core processor and 4GB of RAM, running a windows 64-bit distribution. Using more grid points, no more efficient solutions are discovered, thus Fig. 2 provides the complete Pareto efficient solution set. After acquiring an adequate representation of the Pareto efficient solution set, a decision making procedure should be applied, such as the Analytic Hierarchy Process (AHP) or the Technique for Order of Preference by Similarity to Ideal Solution (TOPSIS), in order to make the final decision.

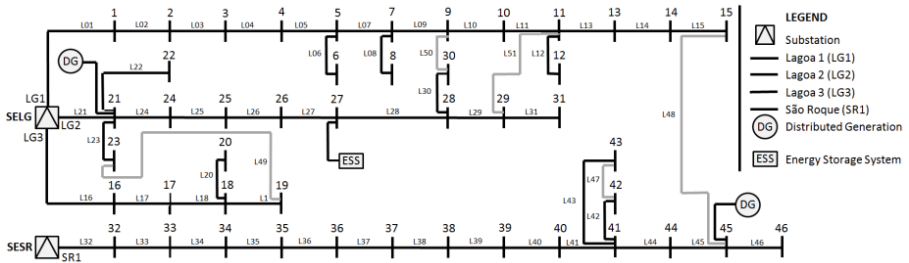


Fig. 1. Single-line diagram of Test System Network MT 10kV Interconnection São Roque - Lagoa adapted [11]

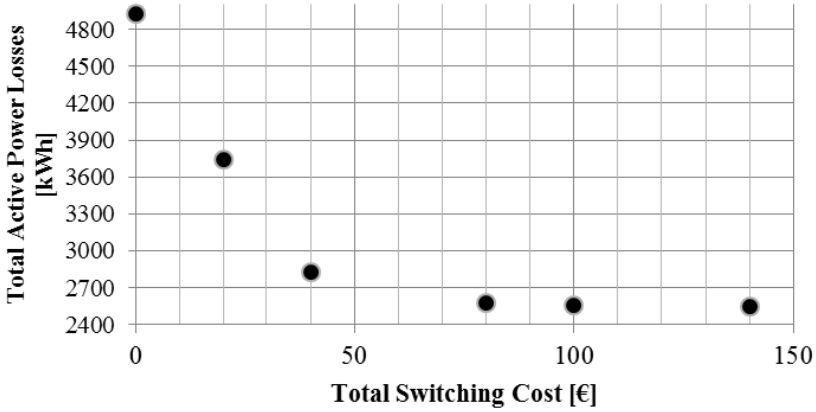


Fig. 2. The Pareto efficient solution set

However, at this point, an assumption is made about the decision maker’s final selection. It can be noticed that, as the switching cost decreases, the active power losses increase. Furthermore, it can be noticed that the first four solutions slightly increase the active power losses, while the switching cost is significantly decreased. Thus, the final selection considered is the 4-th efficient solution.

The configurations for this solution during the horizon are shown in Figs. 3 and 4. The first reconfiguration occurs at the beginning of period T4-T3 and T7 where the branches L49, L50, L51 and L45 open. At the beginning of period T4 the branch L50 and L45 closes and the branch L10 and L27 opens. The DG units provide power at their maximum capacity during all the periods. In Fig. 5 the ESS state-of-energy is presented. During period T4 the ESS is charging. This stored energy is used during periods T5 and T6 in order to serve the increased demand needs.

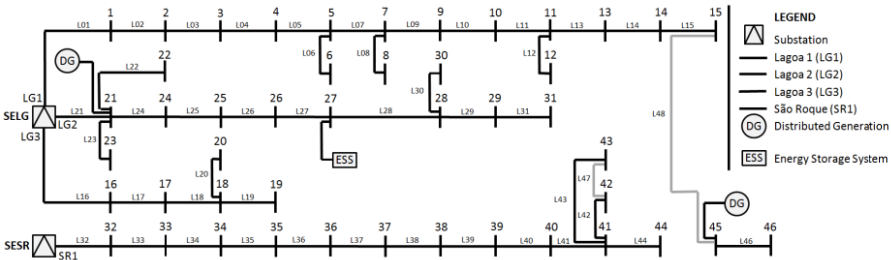


Fig. 3. Configuration of the distribution system during periods T1-T3 and T7

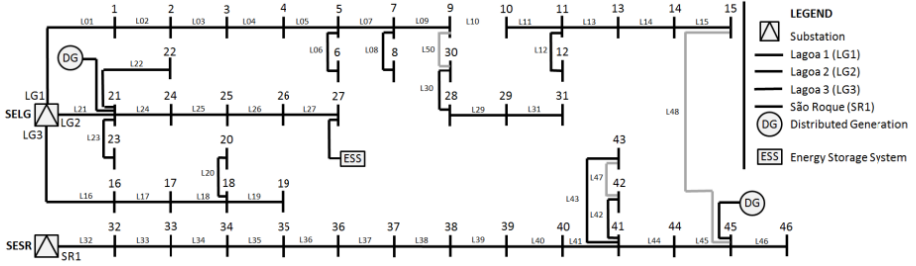


Fig. 4. Configuration of the distribution system during period T4-T6

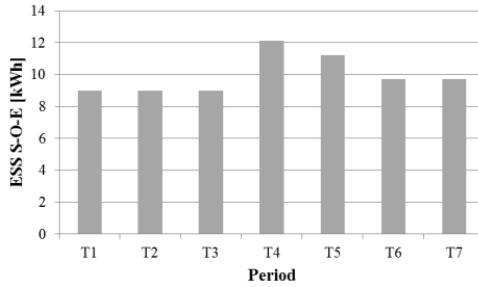


Fig. 5. ESS State-of-energy during the time horizon

5 Conclusions

In this work the application of a new method to handle the DS reconfiguration problem was presented. The problem was formulated as a multi-period multi-objective mixed-integer linear problem, solved using the augmented ϵ -constraint method in order to produce an adequate representation of Pareto efficient solutions set. The objective of the proposed formulation was to find the DS configuration that has as a result the minimum losses and switching operations. DG and ESS have also been considered in the proposed mathematical formulation. Applying the ϵ -constraint method in order to solve multi-objective problems related to the DS, considering also power flow equations, such as optimal placement and sizing of DG units and ESS, reliability and other quality of distribution issues, will be the subject of future works by the authors.

Acknowledgment. This work was supported by FEDER funds (European Union) through COMPETE and by Portuguese funds through FCT, under Projects FCOMP-01-0124-FEDER-020282 (Ref. PTDC/EEA-EEL/118519/2010) and PEst-OE/EEI/LA0021/2013. Also, the research leading to these results has received funding from the EU Seventh Framework Programme FP7/2007-2013 under grant agreement no. 309048.

Nomenclature: $i (I)$ - index (set) of nodes; $b (B)$ - index (set) of branches; $t (T)$ - index (set) of time intervals; $p (P)$ - index (set) of points that are used to approximate the non-linear function of losses; Ω_i^f - subset of nodes that are substations; Ω_i^{dg} - subset of nodes that have DG; Ω_i^s - subset of nodes that have ESS; Ω_i^{de} - subset of nodes with DG or ESS ($\Omega_i^{dg} \cup \Omega_i^s$); Ω_i^t - subset of transfer

nodes; Ω_b^i, Ω_b^j - mapping of nodes and branches defined as (i, j) . PARAMETERS: N - number of nodes; N^f - number of substation nodes; N^{de} - number of nodes that have DG or ESS; k_i^d - fictitious demand of node i ; $D_{i,t}$ - demand of node i during period t [kW]; f_b^{max} - flow limit of branch b [kW]; $P_i^{f,max}$ - max. power that substation of node i can provide [kW]; X_p - X-coordinate of point p that is used for approximation; DE_i - discharging efficiency of the ESS of node i ; CR_i - charging rate of node i [kW]; DR_i - discharging rate of node i [kW]; SOE_i^{max} - max. state-of-energy of ESS of node i [kWh]; SOC_i^{min} - minimum state-of-energy ESS of node i [kWh]; DE_i - discharging efficiency of the ESS of node i . VARIABLES: $P_{b,t}^{loss}$ - power losses of branch b during period t [kW]; $C_{b,t}^{sw}$ - switching cost of branch b during period t [€]; $x_{b,t}$ - binary variable- 1 if branch b is closed during period t , else 0; $y_{i,t}$ - auxiliary binary variable that is used to properly handle transfer nodes; $k_{b,t}$ - fictitious flow through branch b during period t ; $k_{i,t}^g$ - fictitious generation of node i during period t ; $f_{b,t}$ - flow through branch b during period t [kW]; $P_{i,t}^f$ - power provided by substation of node i during period t [kW]; $P_{i,t}^{dg}$ - power provided by DG of node i during period t [kW]; $P_{i,t}^{dis}$ - power provided by DG of node i during period t [kW]; $P_{i,t}^{ch}$ - charging power of the ESS of node i during period t [kW]; $z_{b,t,p}$ - SOS2 variables that are used to approximate the power loss.

References

1. Thakur, T., Jaswanti, T.: Study and Characterization of Power Distribution Network Reconfiguration. In: IEEE/PES T&D Conference and Exposition, Latin America, pp. 1–6 (2006)
2. Jabr, R., Singh, R., Pal, B.C.: Minimum Loss Network Reconfiguration Using Mixed-Integer Convex Programming. *IEEE Trans. Power Systems* **27**, 1106–1115 (2012)
3. Zidan, A., Shaaban, M.F., El-Saadany, E.F.: Long-term multi-objective distribution network planning by DG allocation and feeders' reconfiguration. *Electric Power Syst. Res.* **105**, 95–102 (2013)
4. Amanulla, B., Chakrabarti, S., Singh, S.N.: Reconfiguration of Power Distribution Systems Considering Reliability and Power Loss. *IEEE Trans. Power Delivery* **27**, 918–926 (2012)
5. Wu, Y., Lee, C., Liu, L., Tsai, S.: Study of Reconfiguration for the Distribution System With Distributed Generators. *IEEE Trans. Power Delivery* **25**, 1678–1684 (2010)
6. Malekpour, A.R., Niknam, T., Pahwa, A., Kabousi Fard, A.: Multi-Objective Stochastic Distribution Feeder Reconfiguration in Systems With Wind Power Generators and Fuel Cells Using the Point Estimate Method. *IEEE Trans. Power Systems* **28**, 1483–1492 (2013)
7. Franco, J.F., Rider, M.J., Lavorato, M., Romero, R.: A mixed-integer LP model for the reconfiguration of radial electric distribution systems considering distributed generation. *Electric Power Systems Research* **97**, 51–60 (2013)
8. Mavrotas, G.: Effective implementation of the ϵ -constraint method in Multi-Objective Mathematical Programming problems. *Applied Mathematics and Computation* **213**, 455–465 (2009)
9. Mavrotas, G., Florios, K.: An improved version of the augmented ϵ -constraint method (AUGMECON2) for finding the exact pareto set in multi-objective integer programming problems. *Applied Mathematics and Computation* **219**, 9652–9669 (2013)
10. Cohon, J.L.: *Multiobjective Programming and Planning*. Academic Press, New York (1978)
11. EDA - Electricidade dos Açores, "Caracterização das redes de transporte e distribuição da Região Autónoma dos Açores." S. Miguel (2014)

Cloud-Based Decision Support Ecosystem for Renewable Energy Providers

Ioana Andreea Stănescu¹(✉), Antoniu Ştefan¹,
and Florin Gheorghe Filip²

¹ Advanced Technology Systems, 1 Tineretului Street, 130029, Targoviste, Romania
{Ioana.Stanescu,Antoniu.Stefan}@ats.com.ro

² Romanian Academy-INCE, 125 Calea Victoriei, 010071, Bucharest, Romania
ffilip@acad.ro

Abstract. The increasing complexity of decision making environments requires new approaches that can improve the efficiency, the effectiveness and the quality of the decision making processes. Cloud-based Decision Support Ecosystems (DSE) create the premises for the next generation of DSS, by modeling dynamic system architectures and customizable decision layers that instantiate a new level of independence at end-user level. End-users are able to connect new data sources to the decision making processes without assistance from software developers, while maintain consistency, to build more relevant decision environments. The authors discuss key challenges associated with the DSE and present the design premises of a cloud-based DSE for renewable energy providers. The paper builds upon the PhD research carried out within the INDESEN Project, funded by Unitatea Executiva pentru Finantarea Invatamantului Superior, a Cercetării, Dezvoltării si Inovarii (UEFISCDI) through the Romanian Partnership Program.

Keywords: Dynamic architecture · Cloud computing · Renewable energy

1 Introduction

A Decision Support System (DSS) should enable decision makers to efficiently manage the increasing complexity, rapid changes and emergent risks of today's business environments. However, while it is easy to highlight the potential benefits of DSSs, it is often harder to deliver them in practice. Technology and knowledge advance at a rapid pace, but the complexity of the decision making environments also increases. The speed and the quality of decision making processes have to be enhanced at a faster rate. Beside context specific issues, decision makers also have to overcome collateral challenges associated with information overload and information distortion.

Nowadays, decision making does not rely on a single tool, but on a heterogeneous mix of systems of systems that support decision making processes. However, even if these systems are integrated and interoperable, they still reply on a static architecture that end-users cannot customize according to their needs. The unified management of all these DSSs coupled with the reduction of redundancies and end-user development

represent a significant challenge. *How can existing decision support technologies be improved considering emerging technologies and practices?*

Web technologies and mobile communication, increased processing power, cloud infrastructures, and intelligent devices have created the premises for DSSs that enable decision makers better their performance. There are many opportunities to employ new information technologies to improve decision making processes.

In this context, the authors advance the notion of Decision Support Ecosystems (DSE) that fundament the design and development of dynamic system architectures, and that introduces for end-users a new level of independence from system developers. The design premises of a cloud-based DSE for renewable energy providers are presented, and related challenges are discussed.

2 Cloud-Based Decision Support Ecosystems

The approach proposed in this paper builds upon cloud computing developments that enables the delivery of computing resources as a service. Cloud solutions implement horizontal scalable architectures, dynamic sizing (automatically adding and removing server instances), zero downtime architectures, dynamic failure detection and recovery architecture, etc [1], [2]. Cloud capabilities, especially dynamic sizing, answer to a critical issue that concern the use of the term “ecosystem” in connection to software: absence of intention [3]. Cloud services are key to building auto-adaptable software ecosystems. Because cloud environments are able to use as many servers as necessary to optimally respond to the cost and the timing constraints of an application [4], they are able to nurture the natural evolution of DSEs.

In the case of a dynamic system architecture, end-users are able to integrate their own data sources and they are able to customize the decision flows to integrate them. The authors have considered an Intelligent Decision Support and Control System for Low Voltage Grids with Distributed Power Generation from Renewable Energy Sources (INDESEN) to validate their premises.

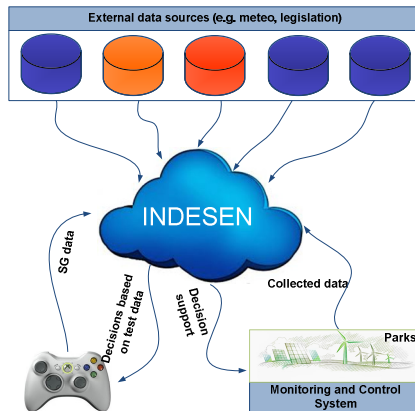


Fig. 1. Cloud-centric data flow

INDESEN is offered as a cloud based service. The service is open and it can interconnect several data sources with the actors that take the decisions based on the analyses carried out by the system. Data communication is based on open Web services standards SOAP (Simple Object Access Protocol), REST (Representational State Transfer).

The system is designed as a cloud centric solution that stores and processed data centrally. This approach increases the adoption by lowering upfront costs and overall Total Cost of Ownership. Another contributing factor in choosing a cloud based solution is the large geographical distribution of renewable energy power plants which can only be efficiently managed through a centralized solution.

For data collection purposes, the system defined a set of API functions that can be used by third-party developers, as well as a set of standard software agents that can be deployed on site and feed data from proprietary hardware to the cloud.

3 State-of-the-Art

Decision capabilities have been supported by a large range of systems ranging from Executive Information Systems, Expert Systems and Decision Support Systems to Business Intelligence, Business Analytics, Business Activity Monitoring, Business Performance Monitoring [5], Knowledge Based Systems [6], Creativity Enhancing Systems [7], etc.

Advances in Information Technology (IT) have brought solutions to many DSS issues and at the same time they also generated new opportunities and challenges for DSS developers. System integration and interoperability have significantly enhanced the performance, efficiency and quality of decision processes [8].

For the purpose of this paper, decision support tools used in the electrical energy field have been considered. In this context, Supervisory Control and Data Acquisition (SCADA) based solutions have been the first to be designed and developed to monitor and control renewable energy plants [9]. The early developments of such systems offered a friendly interface for controlling systems that contain Programmable Logic Controllers (PLC) and mainly aimed to assist the human operators in routine processes [10]. More complex solutions have followed providing functions that were able to provide monitoring and operational evaluation of remote Renewable Energy Sources [11].

Considering the specific requirements related to renewable energy production, storage, and distribution, research efforts in recent years have focuses on more advanced solutions able to facilitate renewable energy management and decision-making for independent or connected to public supply networks. Research has been carried out on renewable energy monitoring [12]; interoperability issues [8]; algorithms for fast oscillation detection [13]; environmental monitoring [14], linear and non-linear optimization algorithms used in renewable energy sources [15]; production of scientific knowledge on renewable energy [16]. Research addressing decision-making concerned energy availability for consumers, safety power supplying; reducing costs and maximizing generation [17].

4 Decision Support Ecosystems

4.1 Perspectives on Ecosystems

In recent years, ecosystems have gained momentum as an important field of research fueled by new business models [18]. A wide variety of ecosystems ranging from software to business and social ecosystems have been modeled. For the purpose of this research software and business ecosystems have been considered.

Software ecosystems are defined as a set of software solutions that enable, support and automate the activities and the transactions of the actors that operate in a business environment [19]. Considering the multitude of devices and applications that are used in a renewable energy plant, the adoption of an ecosystem approach has the potential to provide the prerequisites for better decision-making processes.

Companies have changed the focus from rear-view mirror analysis (studying data from the past) to looking through the windshield practices (using data to predict future patterns) because the ability to anticipate can bring significant advantages [20]. For renewable energy providers the ability to predict is even more relevant, as based on prediction they can better estimate energy prediction (based on more accurate weather patterns), deploy resources more effectively, reduce downtime, adjust staff levels, etc. Building business analytics ecosystems stands out as an essential component of future applications.

4.2 Key Challenges for DSE End-Users

The complexity of the decision-making environments has increased due to information overload, distortion of information, the need for faster, more accurate decisions, the challenging business environments, increased costs, etc. The capacity to access the right information at the right time, to retrieve knowledge, to analyse data and documents, as well as the ability to anticipate have become crucial for managers.

The premises for the DSE design have emerged from a set of challenges associated with existing DSSs. Power [5] has identified that:

- 1) DSS employ complex hardware and software technologies, and decision makers need computing and software knowledge to be able to operate such systems;
- 2) Decision makers need to manage rapidly changing environments, including changes associated with context environments and technology evolution;
- 3) There is a growing need for end-user development of DSS.
- 4) Decision makers need to understand the upside benefits, the downside risks, and the possibilities of further development.

Currently, DSS have a static architecture that translates into a limited flexibility at end user level. End users cannot perform changes in the system without assistance from developers even if they have advanced IT skills. Even if end users are able to connect to external data sources, the system logic is not customizable and the new sources cannot be integrated into decisional flows.

4.3 DSE for Renewable Energy Providers

The decision-making processes in the renewable energy field are extremely challenging as they are based on masses of details concerning many different issues that require analysis and management. Therefore, decision makers use different tools to monitor and control, to carry out diagnosis and prediction, and to make decisions. They also rely on a wide range of data sources to fundament their decisions. These data sources are difficult to predict when the decision support tool is developed. Even if initial, generic data sources exist, for better decisions DSE end users need to connect to more data sources.

The research reported in this paper addresses the above-mentioned challenge and documents the decision-making processes associated with the management of renewable energy plants with the purpose of supporting the design of a cloud- and knowledge-based Intelligent Decision Support and Control System for Low Voltage Grids with Distributed Power Generation from Renewable Energy Sources (INDESEN) where end users can integrate into decision flows any data sources that comply to accepted formats (Fig. 2).

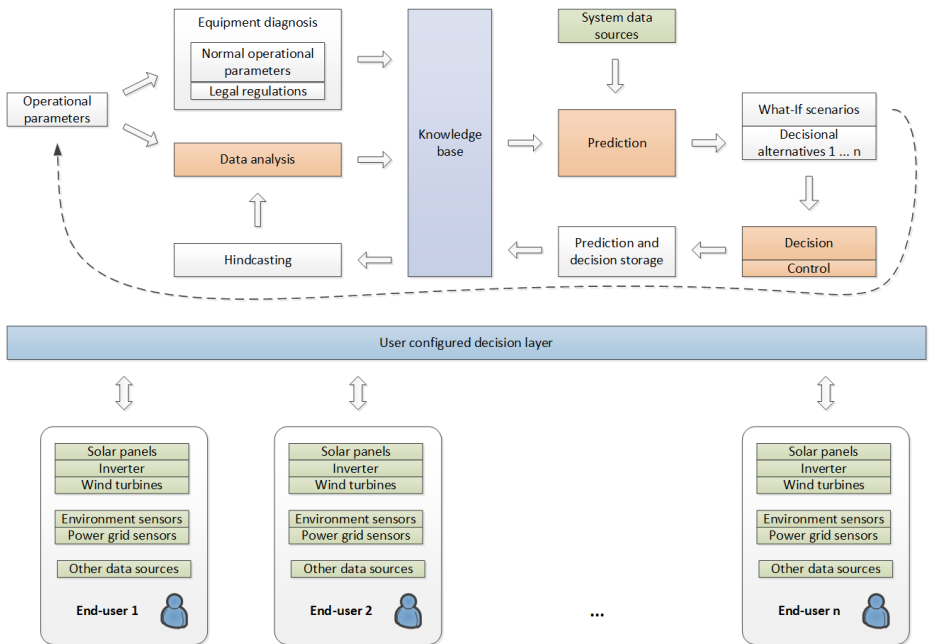


Fig. 2. INDESEN end user customizable decision layer

INDESEN is designed to integrate the following modules:

- The Monitoring Module. Enables real-time tracking of the parameters that monitor the electric energy quality and the environmental factors. The data will be stored in the INDESEN database and will fundament the development of the knowledge base and the diagnosis of the hardware equipment.

- The Diagnosis Module. The diagnosis of the equipment and of the causes that led to dysfunctions is carried out in the Diagnoses Module against reference standard values collected from the equipment specifications, the regulatory requirements issued by competent authorities, standards, national and European legislation, etc.
- The Prediction Module. The short-, medium, and long-term prediction is based on internal and external data sources. Data are constantly collected from the equipment and sensors installed in the renewable energy parks and from external weather services. The analysis takes into account the historical data and expert knowledge collected in the system. The capacity to produce electric energy is determined based on factors such as: the periodicity (day/ night; summer/ winter) of the environmental factors (solar radiation, temperature, wind speed), the equipment wear in time, etc.
- The Decision Module. The system will generate alternative decision scenarios that the decision-makers can choose from. For each scenario the system will present a synthesis of the rationale behind it build on historical data, current state of the equipment, weather prediction services, expert knowledge, etc.
- The Control Module. The system will allow real-time control of the equipment, in order to increase their efficiency. Decision-makers can intervene to optimize the energy supply/ storage ratio.

End users are able to integrate their own data sources in any of the above mentioned modules of INDESEN. The customizable decision layer maintains the consistency across the system, as end users can define correlations between the new data sources and the decision flows supported by the system. As INDESEN is designed as a cloud-based system, this enables the solution to scale according to the demands. End users will not encounter hardware or software capabilities issues when connected to a large number of new data sources.

5 Discussion and Conclusion

The increasing complexity of the decision-making processes in a globalized economy created the need for advanced computerized decision-support ecosystems that enable fact-based decisions, improve decision quality, enhance the efficiency and effectiveness of decision processes, and are able to provide competitive advantage while addresses rapid changes, and emerging risks. Wide access to knowledge management architectures, worldwide real-time access, increased performance and quality, user friendliness, standardized structures, and an easily administered controlling system represent key requirements for DSS. However, without an ecosystem perspective that is based on dynamic software architectures and that integrates cloud-based solutions and end user customizable decision support tools, decision support remain limited.

The authors present the key challenges of current DSS and the premises for the design of an end user customizable cloud- and knowledge-based Intelligent Decision Support and Control System for Low Voltage Grids with Distributed Power Generation from Renewable Energy Sources that is able to enhance decision-making processes within future enterprises.

This approach implements a new level of flexibility as end users can integrate data and knowledge sources independently from the system developers and they can re-configure decision making process to accommodate the sources also without support from developers.

Future work includes the development and testing of the customization features of the DSE at end user level.

Acknowledgments. This research has been carried out within the INDESEN Project “Intelligent decision support and control system for low voltage grids with distributed power generation from renewable energy resources”, Contract No. 42/2011, funded through the Romanian Partnership Program.

References

1. Gregg, B.: *Systems Performance: Enterprise and the Cloud*. Prentice Hall, New Jersey (2013)
2. Mahmood, Z., Erl, T., Puttini, R.: *Cloud Computing: Concepts, Technology & Architecture*. Prentice Hall, Westford (2013)
3. Stallman, R.M.: *Free Software, Free Society: The Selected Essays of Richard M. Stallman*. <http://www.gnu.org/philosophy/words-to-avoid.html#Ecosystem>
4. Marinescu, D.C.: *Cloud Computing*. Elsevier Science, Morgan Kaufmann, Waltham (2013)
5. Power, D.J.: *Decision Support Basics*. Business Expert Press, New York (2009)
6. Zaraté, P.: *Integrated and Strategic Advancements in Decision Making Support Systems*. IGI Global, Hershey (2012)
7. Delen, D.: *Real-World Data Mining: Applied Business Analytics and Decision Making*. Pearson FT Press, New Jersey (2014)
8. Stanescu, I.A., Stefan, A., Filip, F.G., Kittl, C., Lim, T.: Interoperability Scenarios in Serious Games Ecosystems: The Impact on FinES. In: 7th IFAC Conference on Manufacturing Modelling, Management, and Control, vol. 7 pt. 1, pp. 1334–1339. Elsevier, St. Petersburg (2013)
9. McCrady, S.G.: Practical Procedures for SCADA Software Development. In: Software, A., McCrady, S.G. (eds.) *Designing SCADA*, pp. 25–39. Elsevier, Oxford (2013)
10. Khedkar, M.K., Katti, P.K., George, M.: SCADA based Integrated Operation of Renewable Energy Sources. In: *Intl. Conf. of Energy and Informatics, Florida* (2008)
11. Papadakis, K., Koutroulis, E., Kalaitzakis, K.: A server database system for remote monitoring and operational evaluation of renewable energy sources plants. *Renewable Energy* 30(11), 1649–1669 (2005)
12. Villasevil, F.X., Vígara, J.E., Chiarle, L.: Plug-in driven architecture for renewable energy generation monitoring. *Renewable and Sustainable Energy Reviews* 27, 401–406 (2013)
13. Vanfretti, L., Baudette, M., White, A.: Monitoring and Control of Renewable Energy Sources using Synchronized Phasor Measurements. *Renewable Energy Integration*, 413–428 (2014)
14. Garel, E., Rey, C.C., Ferreira, O., van Koningsveld, M.: Applicability of the “Frame of Reference” approach for environmental monitoring of offshore renewable energy projects. *Journal of Environmental Management* 141, 16–28 (2014)

15. Iqbal, M., Azam, M., Naeem, M., Khwaja, A.S., Anpalagan, A.: Optimization classification, algorithms and tools for renewable energy: A review. *Renewable and Sustainable Energy Reviews* 39, 640–654 (2014)
16. Rizzi, F., van Eck, N.J., Frey, M.: The production of scientific knowledge on renewable energies: Worldwide trends, dynamics and challenges and implications for management. *Renewable Energy* 62, 657–671 (2014)
17. Dumitru, C.D., Gligor, A.: SCADA Based Software for Renewable Energy Management System. *Procedia Economics and Finance* 3, 262–267 (2012)
18. Hanssen, G.K., Dyba, T.: Theoretical foundations of software ecosystems. In: *Workshop on Software Ecosystems*, Cambridge, pp. 6–17 (2012)
19. Bosch, J.: From Software Product Lines to Software Ecosystems. In: *13th International Software Product Line Conference*, San Francisco (2009)
20. Pring, B., Roehrig, P., Frank, M.: *Code Halos: How the Digital Lives of People, Things, and Organizations are Changing the Rules of Business*. John Wiley & Sons, New Jersey (2014)

Energy: Simulation

Development of a Simulink Model of a Saturated Cores Superconducting Fault Current Limiter

Nuno Vilhena¹(✉), Pedro Arsénio¹, João Murta-Pina¹, Anabela Gonçalves Pronto¹,
and Alfredo Álvarez²

¹ CTS, Uninova, Departamento de Engenharia Electrotécnica, Faculdade de Ciências e Tecnologia, FCT, Universidade Nova de Lisboa, 2829-516 Caparica, Portugal
{n.vilhena,p.arsenio}@campus.fct.unl.pt, {jmmp,amg1}@fct.unl.pt

² “Benito Mahedero” Group of Electrical Applications of Superconductors,
Escuela de Ingenierías Industriales, Universidad de Extremadura, Avenida de Elvas s/n,
06006 Badajoz, Spain
aalvarez@unex.es

Abstract. Superconducting fault current limiters are considered as emerging devices for the advent of modern power grids. Those limiters as well as other electric power grid applications have been developed in the last years in order to support the increased penetration of dispersed generation. The development of such limiters requires new design tools that allows to simulate those devices in electrical power grids with different voltage ratings and characteristics. This work presents a methodology to simulate the behaviour of saturated core type limiters based on its characteristic curves. A prototype is tested to obtain its characteristic and then the methodology is implemented in Simulink. The simulation carried out by the proposed methodology is compared with a real test.

Keywords: Fault current limiters · Saturated-core fault current limiters · Modern power grids · Smart grids · Short-circuit currents · Superconductivity

1 Introduction

Superconducting Fault Current Limiters (SFCL) have been considering as emerging and attractive devices enabling an increased integration of distributed generation sources in modern power grids, due to their ability to limit fault currents and thus helping to mitigate several operation problems that such grids can experience [1].

Amongst all different topologies of inductive SFCL, the saturated cores topology [2], originally proposed in [3], involves the use of highly saturated iron cores that can be achieved by a high DC current flowing in a high temperature superconducting (HTS) coil. When the line current exceeds normal operation limits, e.g. due to a fault, the inductance increases abruptly, limiting the current through an inductive voltage drop. In this situation, the cores of the limiter alternate between saturated and unsaturated states.

In the last years, several projects were carried out using this topology. Zenergy Power Company operated a 15 kV three-phase limiter in the Southern California

Edison substation and an 11 kV in CE Electric UK substation [4]. Other company, InnoPower, developed a 35 kV/ 90 MVA device [5]. InnoPower has also been testing a 220 kV/300 MVA [6].

Finite elements method (FEM) software packages are often used to simulate the performance of these devices [7]. However, simulating a SFCL with FEM software can take a considerable amount of time, from several hours to days or weeks, even when considering simple devices in very simple grids.

In order to reduce the simulation time and to simulate those devices in more complex grids, a numerical method that can be applied to perform fast dynamic simulations of saturated cores SFCL is proposed in this work and is implemented in Matlab/Simulink. This methodology is based on the relationship between the linked flux with the primary of the device ψ_{FCL} and the line current i_{line} . The dynamic behaviour of the SFCL is thus simulated based on this ψ_{FCL} - i_{line} characteristic. This is an extension of the methodology proposed for transformer type SFCL [8–10] and presented in [11] for saturated cores SFCL.

This work also constitutes one of several studies that needs to be addressed in order to answer the following research question:

Are there development methodologies and simulation tools of Saturated Cores Fault Current Limiters, allowing analysing its performance in power grids with different degrees of complexity, and thus contributing to sustained advent of technologies based on superconducting materials?

Integration of SFCL devices in power grids depends also on developing tools to simulate them under different conditions, such as PSCAD or others. This work provides a contribution for such developments.

2 Contribution for Technological Innovation for Cloud-Based Engineering Systems

Electric energy demand has grown yearly, which means that there is a significant increase in the penetration of distributed generation (DG) to satisfy this increase in demand. To make a grid “smart” is essential to manage the future power grids especially from the usage of networked power devices. Smart Grids (SG) offer deep monitoring and controls of the grid but needs advanced analytics to analyse, to process and to storage the considerably big amount of data for safety efficient and reliable operational decisions. In order to project an efficient and scalable SG, solutions and services based on Cloud Computing must be incorporated [12].

In the energy domain, fail-safe power grids are foreseen, ensuring safety and power quality, supporting the coexistence of central and distributed generation, energy storage and bidirectional energy flow. SFCL exhibits several features that make them attractive in protecting network equipment as well as allowing improving network availability, contributing to assure fail-safe grids and thus robust and efficient SG [13].

3 Proposed Methodology Based on SFCL Characteristic

The proposed methodology is based on the magnetic characteristic of the limiter which relates line current i_{line} and linked flux with the primary ψ_{FCL} . This characteristic is able to describe the electromagnetic behaviour of the limiter. Equation 1 shows the developed voltage drop at the terminals of the SFCL that is directly related with the SFCL characteristic.

$$u_{SFCL}(t) = r_{SFCL} \cdot i_{line}(t) + \frac{d\psi_{SFCL}(t)}{dt} = r_{SFCL} \cdot i_{line}(t) + \frac{d\psi_{SFCL}(t)}{di} \cdot \frac{di_{line}(t)}{dt}. \quad (1)$$

Knowing the characteristic of the SFCL, it is possible to develop an adequate computational model for power system simulation software (such as PSCAD or SimPowerSystems/Simulink), that do not rely on knowledge of circuit equations, which is practically unfeasible.

The first step of the methodology consists of determining the magnetic characteristic of the limiter ψ_{FCL} - i_{line} . This characteristic may be determined by real tests. Using the characteristic obtained it is possible to implement the SFCL in Simulink, as a variable inductance. Thus, the limiter may be simulated in grids with different complexities and faster than recurring to FEM software.

3.1 Operation Principle of the Saturated Cores Fault Current Limiter

Several different geometries of this type of SFCL have been proposed. However the operation principle of the limiter remain the same [3]. Fig. 1 shows the basic elements of single-phase saturated cores SFCL.

Under normal operation, AC current in the AC coils creates a magnetic flux that is lower than the DC bias flux, remaining the iron cores highly saturated and making the impedance of the limiter negligible. However, when a fault occurs, the AC current increases abruptly, leading the cores out of magnetic saturation alternately. The line impedance is increased and the fault current is limited.

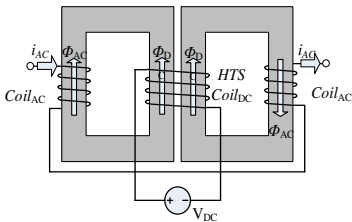


Fig. 1. Single-phase saturated cores SFCL conceptual diagram. It is composed of a HTS DC coil embracing the cores and two conventional AC coils connected in series with the line under protection wound on the outer limbs.

4 Experimental Test to Determination of the Characteristic of the SFCL

In order to determine the characteristic of the limiter, experimental measurements were carried out.

4.1 Topology of the Limiter and Experimental Apparatus

Fig. 2 shows the dimensions of the laboratory scale limiter used to develop the presented methodology. The core used for the tests was an EI iron core (instead of two separated cores). The AC coils are placed on the outer limbs and the DC biasing coil is placed in the inner limb (which has round cross section) of the core. The magnetic core provides closed magnetic paths for each outer limb. Therefore to assure that both outer limbs are driven into deep saturation, their cross sections must be less than 50% of the inner limb core section. In the present case, the outer limbs cross section are 40% of the inner limb cross section.

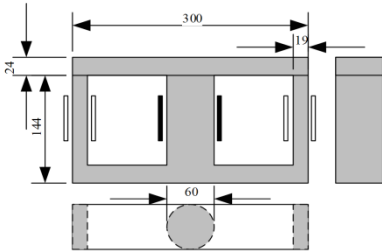


Fig. 2. Dimensions of the iron core of the limiter. All dimensions are in millimetres.

The test circuit comprises a voltage source u_g , a line resistor R_{Line} , a load R_{Load} , a circuit breaker S_f (used to simulate faults) and the SFCL. The AC coils are made of copper wire with 1.3 mm^2 cross section, 100 turns each. A 60 turns DC coil is built from 4 mm-wide first generation superconducting tape. Table 1 shows the parameters of the test grid. More detailed information can be found in [11].

The core must be highly saturated in order to make the impedance of the limiter negligible in normal operation and, at the same time, can not be saturated too deeply since it can go out the saturation, limiting the fault current. Thus, it is necessary to choose an adequate magneto motive force (MMF) value ensuring that all limbs of the core are saturated. Therefore, 35 A were chosen as DC current, corresponding to a MMF of 2100 A·turn.

Table 1. Characteristics of the test grid

Grid	Description	Value
u_g (V)	Voltage source	100
f (Hz)	Frequency of the electrical grid	50
R_{Line} (Ω)	Line resistance	1
R_{Load} (Ω)	Load resistance	20
I_{DC} (A)	DC bias current	35

4.2 Determination of the Characteristic of the SFCL

A test was carried out considering the parameters shown in Table 1. A fault was applied on the test circuit and data was acquired with a data acquisition board to a computer.

Fig. 3 shows the individual characteristic $\psi_{FCL}-i_{line}$, associated to each AC coil and the equivalent characteristic of the limiter, obtained by combining the previous ones. When line current is low, $d\psi_{FCL}/di_{line}$ is also low, thus the line current flows with any limitation. In fault condition, a high $d\psi_{FCL}/di_{line}$ is reached and an inductive voltage drop at the terminals of the limiter limits the line current.

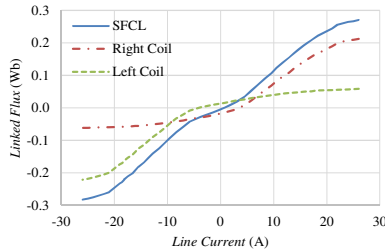


Fig. 3. Measured $\psi_{FCL}-i_{line}$ characteristic of each AC coil and calculated SFCL characteristic

5 Simulation of the FCL by the Developed Methodology

The presented methodology is based on the measured characteristic of the SFCL. A Simulink model of the SFCL was built based on its characteristic.

5.1 Model for the Dynamic Simulation of SFCL

To simulate the SFCL in Simulink was necessary to build a model that describes the SFCL behaviour according to Equation 1. The model may be built with a dependent current source that imposes a specific current in the line depending on the characteristic of the SFCL. The characteristic of the SFCL is function of linked flux and line current, thus if the linked flux is known the current that the SFCL should impose is also known. Equation 2 shows how the linked flux may be calculated, by the integration of the voltage drop over the SFCL u_{FCL} and subtraction of the resistive voltage drop over the SFCL $r_{FCL} \cdot i_{line}$. Fig. 4 shows the model in Simulink. The model is composed of a set of blocks that compute the linked flux according to Equation 2, a lookup table block (so-called Psi-i) that computes the current according to the linked flux with the primary of the SFCL, and a dependent current source block (so-called Inject SFCL current) which provides the current in the line.

$$u_{FCL}(t) = r_{FCL} \cdot i_{line}(t) + \frac{d\psi_{FCL}(t)}{dt} \Leftrightarrow \frac{d\psi_{FCL}(t)}{dt} = u_{FCL}(t) - r_{FCL} \cdot i_{line}(t) \Leftrightarrow \psi_{FCL}(t) = \int (u_{FCL}(t) - r_{FCL} \cdot i_{line}(t)) \cdot dt \quad (2)$$

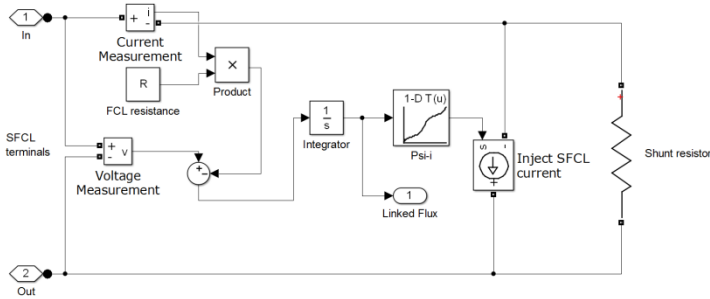


Fig. 4. Simulink model for the SFCL implementation

5.2 Evaluation of the Dynamic Behaviour of SFCL

To evaluate the behaviour of the SFCL using Simulink software, an electrical diagram was built. Fig. 5 shows this circuit, in the Simulink environment, which is composed of a voltage source, a line impedance, a load impedance, a circuit breaker and the SFCL.

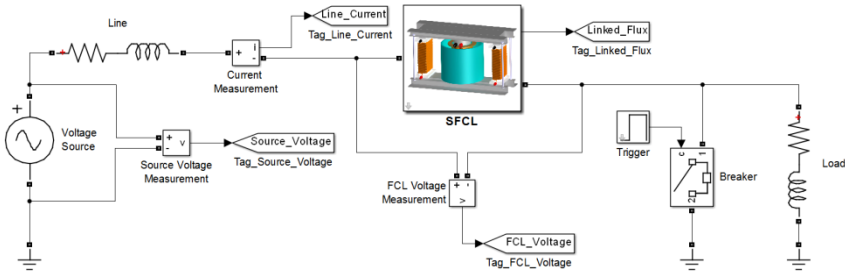


Fig. 5. Test grid implemented in Simulink

The achieved results from the proposed methodology were compared with real tests. Therefore, a simulation using this methodology and a real test were carried out considering $u_g=50 \text{ V}_{rms}$, $R_{line}=1 \Omega$ and $R_{load}=20 \Omega$ (to compare the simulation with the real test the line and load are considered purely resistive). The internal resistance of the SFCL is $R_{SFCL}=0.4 \Omega$. A short-circuit was applied around $t=1.49 \text{ s}$ and cleared around $t=2.49 \text{ s}$.

Fig. 6 shows the evolution of the line current as a function time, measured and predicted by the proposed methodology. Both curves show similar behaviour and good agreement. The fault current was limited to around 75% of the prospective current.

Fig. 7 shows the voltage drop of the SFCL as a function of time. As depicted, when a fault occurs the voltage drop increases and the fault current is thus limited. At normal operation, the voltage drop is less than 10% of the voltage power source.

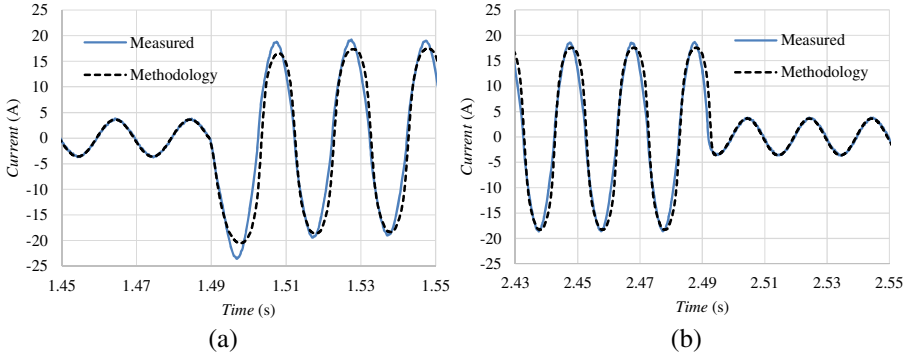


Fig. 6. Comparison between measured and predicted currents in the circuit under a fault. (a) At the moment the fault occurs (b) At the moment the fault is removed.

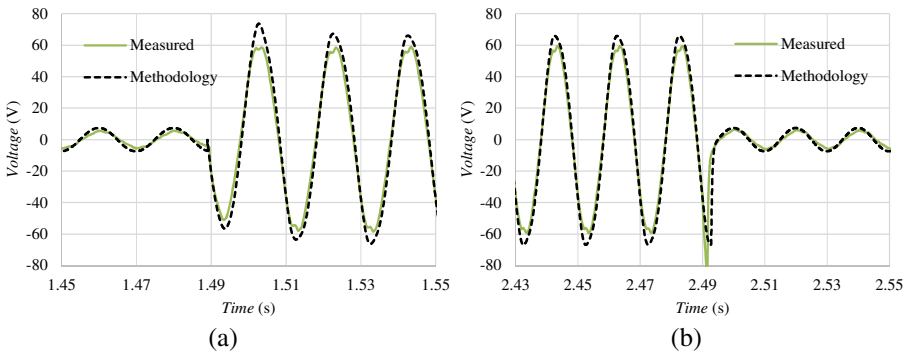


Fig. 7. Comparison between measured and predicted voltages drop in the SFCL under a fault. (a) At the moment the fault occurs (b) At the moment the fault is removed.

6 Conclusions

A methodology to simulate the dynamic behaviour of the saturated cores SFCL in an electrical grid was presented in this paper. The methodology shows good agreement with experimental measurements. Its main advantage is a drastic decrease in simulation times when compared with FEM software. This allows simulating these devices in complex grids, which is one requisite of utilities. Future work passes by including DC current explicitly in the $\psi_{FCL}-i_{line}$ curve expression.

References

1. Moon, W., Won, J., Huh, J., Kim, J.: A Study on the Application of a Superconducting Fault Current Limiter for Energy Storage Protection in a Power Distribution System. *IEEE Trans. Appl. Supercond.* **23**, 5603404 (2013)
2. Lee, P.J.: Applications and Related Technology. *Engineering superconductivity*, p. 391. John Wiley & Sons, Inc. (2001)
3. Raju, B.P., Parton, K.C., Bartram, T.C.: A Current Limiting Device Using Superconducting D.C. Bias Applications and Prospects. *IEEE Power Eng. Rev.* **PER-2**, 34–35 (1982)
4. Moriconi, F., De La Rosa, F., Darmann, F., Nelson, A., Masur, L.: Development and Deployment of Saturated-Core Fault Current Limiters in Distribution and Transmission Substations. *IEEE Trans. Appl. Supercond.* **21**, 1288–1293 (2011)
5. Xin, Y., Gong, W., Niu, X., Cao, Z., Zhang, J., Tian, B., Xi, H., Wang, Y.: Development of Saturated Iron Core HTS Fault Current Limiters. *IEEE Trans. Appl. Supercond.* **17**, 1760–1763 (2007)
6. Xin, Y., Gong, W.Z., Sun, Y.W., Cui, J.B., Hong, H., Niu, X.Y., Wang, H.Z., Wang, L.Z., Li, Q., Zhang, J.Y., Wei, Z.Q., Liu, L., Yang, H., Zhu, X.H.: Factory and Field Tests of a 220 kV/300 MVA Saturated Iron-Core Superconducting Fault Current Limiter. *IEEE Trans. Appl. Supercond.* **23**, 5602305 (2013)
7. Shahbazi, Y., Niayesh, K., Mohseni, H.: Finite element method analysis of performance of inductive saturable-core fault current limiter. In: 2011 1st International Conference on Electric Power Equipment - Switching Technology, pp. 352–355. IEEE (2011)
8. Pina, J.M., Suárez, P., Neves, M.V., Álvarez, A., Rodrigues, A.L.: Reverse engineering of inductive fault current limiters. *J. Phys. Conf. Ser.* **234**, 032047 (2010)
9. Pina, J.M., Pereira, P., Pronto, A., Arsénio, P., Silva, T.: Modelling and Simulation of Inductive Fault Current Limiters. *Phys. Procedia.* **36**, 1248–1253 (2012)
10. Arsenio, P., Silva, T., Vilhena, N., Pina, J.M., Pronto, A.: Analysis of Characteristic Hysteresis Loops of Magnetic Shielding Inductive Fault Current Limiters. *IEEE Trans. Appl. Supercond.* **23**, 5601004 (2013)
11. Vilhena, N., Arsenio, P., Pina, J., Pronto, A., Alvarez, A.: A methodology for modelling and simulation of saturated cores fault current limiters. *IEEE Trans. Appl. Supercond.*, 1–1 (2014)
12. Bitzer, B., Gebretsadik, E.S.: Cloud computing framework for smart grid applications. In: 2013 48th International Universities' Power Engineering Conference (UPEC), pp. 1–5. IEEE (2013)
13. Behzadifari, S., Salehfar, H.: Using superconducting fault current limiters to enhance the reliability of power transmission systems. In: IEEE PES General Meeting, pp. 1–8. IEEE (2010)

Simulation of a-Si PV System Linked to the Grid by DC Boost and Three-Level Inverter Under Cloud Scope

L. Fialho^{1,2}, R. Melício^{1,2(✉)}, V.M.F. Mendes^{2,3}, and M. Collares-Pereira²

¹IDMEC/LAETA, Instituto Superior Técnico, Universidade de Lisboa, Portugal

²Universidade de Évora, Évora, Portugal

ruimelicio@gmail.com

³Instituto Superior of Engenharia de Lisboa, Lisbon, Portugal

Abstract. This paper is about a PV system linked to the electric grid through power converters under cloud scope. The PV system is modeled by the five parameters equivalent circuit and a MPPT procedure is integrated into the modeling. The modeling for the converters models the association of a DC-DC boost with a three-level inverter. PI controllers are used with PWM by sliding mode control associated with space vector modulation controlling the booster and the inverter. A case study addresses a simulation to assess the performance of a PV system linked to the electric grid. Conclusions regarding the integration of the PV system into the electric grid are presented.

Keywords: PV system · DC-DC boost · Three-level inverter · Simulation

1 Introduction

The increment on the use of scarce fossil-fuel sources, the society wariness about the anthropogenic gas emissions and the increasing energy demand have strongly impelled the development of the use of renewable energy sources during the last decades [1]. For instance, the growth of the annual market regarding exploitation of solar energy is an evidentiary fact during the last decade. Particularly, a growing expansion is to be expected over the coming decade in what regards the deployment of photovoltaic (PV) systems.

The European Commission has launched a line of attack for the Europe to become a highly energy-efficient and a low-carbon economy with a set of proposals to create a new Energy Policy for Europe, reducing the anthropogenic gas emissions by 20% by 2020 and 50% until 2050, raising the overall share of conversion from renewable energy sources. Solar energy exploitation is expected to be significant on the European Energy Policy. Also, European Commission points out a future significant advance towards a more active role of the consumer by the implementation of the concept of smart grid (SG), improving integration into the grid for renewable energy sources and increasing energy efficiency. An advance thought to have a significant impact on mitigation of anthropogenic gas emissions, job and technology development [2].

A PV system directly converts solar energy into electric energy. The main device of a PV system is the solar cell. Solar cells are grouped to form PV arrays. An array is either a panel or a set of panels connected in series or parallel to form large PV systems. Simulation of PV systems is vital to assist in exporting energy, anticipating

bad performances and deciding convenient measures to avoid malfunctions and my significant benefit in real-time application from cloud-based solutions.

Power electronic converters have been developed for assisting in the integration of renewable energy conversion into the electric grid. Historically, low power PV systems use single-phase inverters, but in three-phase grid linking the use of only one single-phase inverter produces unwanted imbalance between the phase currents due to the injection of energy into only one phase of the grid. As reported in [3] a maximum power of 4.6 kW with 10 % of tolerance is possible to link to only one phase of a three-phase grid. Three single-phase inverters are needed for linking power greater than 5 kW to ensure a convenient balanced energy distribution between the phases.

2 Relationship to Cloud-Based Solutions

A Cloud-based solution is significant support for launching a line of attack for a future highly energy-efficient management of energy conversion and usage. As the global energy demand increases with the growing world population, alternative sources of energy turn out to be attractive for exploitation in what regards a sustainable society's development. Within this attractive exploitation, the renewable energy from PV systems exploitation is considered one promising and reliable energy source for distributed generation (DG). DG and the increase usage of electric energy, for instances, the expected significant usage of electrical vehicles, will drive upcoming concerns on nowadays electrical grid about the ability to encompass with the future. So, a hatching thought about the electric grid is needed and the SG conception is on the way. A SG will benefit from cloud-based solutions allowing data interchange between end users and producers for transparency on energy consumption and on energy conversion of other forms of energy into electric energy. A Cloud-based solution allows the wanted consumer commitment in the management within the SG scope. The SG will be a source of information able to interact with other kinds of data, not only monitoring the flow of electric energy, but also an entire set of environments, leading to a foreseen increase data to be processed by SG management systems. So, the SG architecture has to be implemented with ensured security and reliability. A layered framework is one option gathering information about the SG components offering an awareness of the behavior, enabling people or machines to act accordingly over a services platform. The engineered software framework can be transposed to a Cloud architecture system, taking advantages of the existing internet cloud services to process with reduced operational costs the data storage and data transfer in real-time with reduced operational costs. For instance, as depicted in Fig. 1 for the PV system in study in this paper. This framework facilitates the integration of sensors and actuators with bidirectional data exchange [4], [5], [6], allowing real-time simulations speeding up the integration PV system energy into Smart Grid.

3 Modeling

The solar cell is modeled by the five parameter equivalent circuit: a photo electric current controlled source giving I_s , a shunt single-diode D draining the current i_{Dj} ,

a shunt resistance R_p draining the leakage current I_p , a series resistances R_s delivering the output current I_j of the cell having the output voltage V_j . As a normal assumption, assume that the cells associated within the module are equally subjected to the same irradiance and the junctions are at the same temperature, then the equivalent circuit for the PV module is same of the cell, but with a suitable numerical transformation in the values for the parameters. The PV system under study is formed by a PV module, a DC-DC boost and a three-level power inverter linking the system to an electric grid. The PV system is shown in Fig. 1.

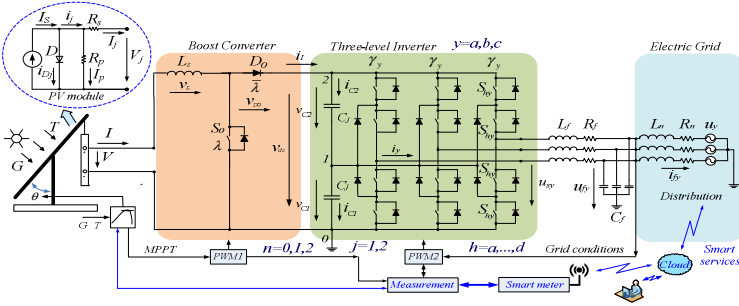


Fig. 1. PV system linked to the electric grid through power converters

In Fig. 1, G is the solar irradiance, T is the cell p-n junction temperature in [K] and the current i_j [2] is given by:

$$i_j \equiv I_j + (V_j + R_s I_j) / R_p \tag{1}$$

where j is a condition index: $j = oc$ identifies open circuit condition; $j = sc$, short circuit condition, $j = mx$, maximum power point (MPP) condition. From (1), finding R_s at short circuit and at MPP conditions, holds the equations [2] given by:

$$V_{oc} \frac{i_{mx} - I_{mx}}{I_{mx}} - \frac{V_{mx} i_{oc}}{I_{mx}} - V_{oc} \frac{i_{sc} - I_{sc}}{I_{sc}} = 0 \tag{2}$$

The MPP of a PV system depends on G and T , at the MPP the conversion is at the highest efficiency and satisfies the relation [2] given by:

$$\gamma R_p i_{mx}^{sc} (V_{mx} - R_s I_{mx}) (e_{mx} + I) + V_{mx} - I_{mx} (R_s + R_p) e_{sc}^{mx} = 0 \tag{3}$$

The input parameters for the MPPT algorithm are the values of the voltage and the current of the PV system. The condition to be satisfied is given by $\partial P / \partial V = 0$, i.e., if the condition is met, then the algorithm has found the MPP point. But typically in practice the algorithm iterates around that condition until eventually converges. The iteration procedures are as follows; if $\partial P / \partial V > 0$, an incremental adjustment is set in order to increase the out voltage, i.e., in the direction of the MPP; if $\partial P / \partial V < 0$, an adjustment is set in order to decrease the out voltage in the direction of the MPP [7].

The General Algebraic Modeling System (GAMS) is used to code a mathematical programming problem to identify the five parameters for the equivalent circuit of the PV system, using data information from the tests of open circuit, short circuit, maximum power point (MPP) conditions. The free solver COUENNE–Convex Over and Under Envelopes for Nonlinear Estimation for global optimization is used as a convenient option, due to the involvedness on the problem of identification of parameters [2]. The DC-DC boost converter has one unidirectional commanded IGBT, S_0 . This converter is linked between the PV module and capacity banks, which in turn is linked to a three-level inverter. The modeling for the DC-DC boost converter is given by the switching variable λ used to identify the state of S_0 and the switching variable $\bar{\lambda}$ used to identify the state of the diode D_0 . These variables have to satisfy the switching condition [8] given by:

$$\begin{cases} \lambda = 1 \text{ and } \bar{\lambda} = 0 \text{ (} S_0 = 1 \text{ and } D_0 = 0 \text{)} \\ \lambda = 0 \text{ and } \bar{\lambda} = 1 \text{ (} S_0 = 0 \text{ and } D_0 = 1 \text{)} \end{cases} \tag{4}$$

The module current I is modeled by the state equation given by:

$$dI/dt = 1/L_s [V - \bar{\lambda} (v_{D0} + v_{dc})] \tag{5}$$

where v_{D0} is the diode forward voltage at direct current and v_{dc} is the voltage at the capacity banks.

The three-level inverter is linked between capacity banks and a second order filter, which in turn is linked to the electric grid, modeled by a three-phase active symmetrical circuit. The DC-AC inverter is a three-level inverter, having twelve unidirectional commanded IGBT identified by S_{hy} , used as an inverter. The groups of four IGBT’s linked to the same phase constitute the leg y of the inverter with $y \in \{a, b, c\}$ [9]. The converter has $p = 3$ levels. For the balance control strategy, the switching voltage level variable n_y which ranges from 0 to $(p-1)$ is used to identify the state of the IGBT h in the leg y of the inverter establishing the switching function of each IGBT. The index h with $h \in \{a, b, c, d\}$ identifies the IGBT. The three conditions to be satisfied for the switching voltage level variable of a leg y , at each level [9], are given by:

$$n_y = \begin{cases} 2, & (S_{ay} \text{ and } S_{by}) = 1 \text{ and } (S_{cy} \text{ or } S_{dy}) = 0 \\ 1, & (S_{by} \text{ and } S_{cy}) = 1 \text{ and } (S_{ay} \text{ or } S_{dy}) = 0 \\ 0, & (S_{cy} \text{ and } S_{dy}) = 1 \text{ and } (S_{ay} \text{ or } S_{by}) = 0 \end{cases} \quad y \in \{a, b, c\} \tag{6}$$

The inverter output voltage u_{sy} in function of v_{dc} [9] is given by:

$$u_{sy} = \frac{1}{6} (2n_y - \sum_{\substack{j=a \\ j \neq y}}^c n_j) v_{dc} \quad y \in \{a, b, c\}; \quad n \in \{0, 1, 2\} \tag{7}$$

The voltage at the capacity banks v_{dc} appearing in (5) is a function of the electric charge stored or discharged from the capacitors by the action of the control of the converters. Hence, the state equation for this voltage is a function of the currents each capacitor i_{cj} [9] and is given by:

$$\frac{dv_{dc}}{dt} = \sum_{j=1}^{p-1} \frac{1}{C_j} i_{cj} \quad j \in \{1, \dots, p-1\} \tag{8}$$

The current i_{cj} [9] is given by:

$$i_{cj} = i_I - \sum_{y=a}^c \delta_{ny} i_y \quad j \in \{1, \dots, p-1\} \tag{9}$$

where the auxiliary variable δ_{ny} [9] is given by:

$$\delta_{ny} = \begin{cases} 0 & j > n_y \\ 1 & j \leq n_y \end{cases} \quad n \in \{0, 1, 2\}; \quad j \in \{1, \dots, p-1\} \tag{10}$$

The electric grid is modeled by an equivalent three-phase active symmetrical circuit, having a resistance and an inductance in series. Hence, for the electric current injected into the electric grid the state equation is given by:

$$\frac{di_{fy}}{dt} = \frac{1}{L_n} (u_{fy} - R_n i_{fy} - u_y) \tag{11}$$

where L_n and R_n are the electrical grid inductance and resistance, respectively, u_{fy} is the voltage at the filter, u_y is the voltage at the electric grid.

4 Control Method

The three-level inverter is a variable structure due to on/off switching states of the IGBT's. PI control and PWM by space vector modulation associated with sliding mode is used for controlling the inverter with the output vectors levels 0, 1 and 2 in the $\alpha\beta$ plane [9] shown in Fig. 2.

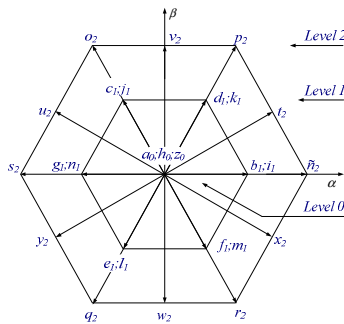


Fig. 2. Output space vectors for modeling of the three-level inverter

The sliding mode control strategy is an option known by the advantage of having attractive considerable robustness to parametric uncertainties [9] due to partial shading or electric grid disturbances. Sliding mode control is particularly attractive in systems with variable structure, such as inverters, ensuring the choice of space vectors. The aim is to let the system slide along a predefined sliding surface $A(e_{\alpha\beta}, t)$ by changing the system structure. All transistors have a physical limitation due to the switch of finite frequency. So, an error exists between the control and the reference $e_{\alpha\beta}$ values. The sliding along the surface $A(e_{\alpha\beta}, t)$ is ensured by a state trajectory near the surfaces satisfying the condition [9] given by:

$$A(e_{\alpha\beta}, t) \frac{dA(e_{\alpha\beta}, t)}{dt} < 0 \tag{12}$$

The control for the MPPT is a simple adjustments over the DC-DC boost converter in order to follow the condition given by $\partial P/\partial V = 0$.

5 Case Study

The mathematical modeling for the solar cell with single-diode, shunt and series resistances, for the MPPT algorithm and for the PV system with the DC-DC boost and the three-level topology is implemented in Matlab/Simulink without the use of Power System Blockset. This case study presents a simulation concerned with the data measured [11] from PV a-Si solar modules Kaneka KA58 provided in [10]. The irradiation is 800 W/m^2 , module temperature is $13 \text{ }^\circ\text{C}$ and nominal AC power is 6 kW . The data for the a-Si solar module Kaneka KA58 at STC [12] are shown in Table 1. Table 2 shows the data results for the PV modelling simulation.

Table 1. Data for the Kaneka KA58 solar module at STC

Technology	V_m^*	I_m^*	V_{oc}^*	I_{sc}^*	β_{oc}	α_{sc}
Amorphous	63 V	0.92 A	85 V	1.12 A	-206 mV/ $^\circ\text{C}$	1.3 mA/ $^\circ\text{C}$

The current injected into the grid is shown in Fig. 3.

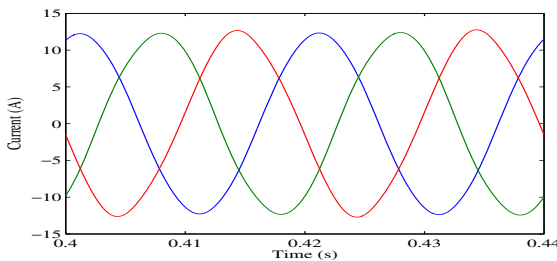


Fig. 3. Current injected into the electric grid

The total harmonic distortion (THD) given by the DFT for the current injected into the electric grid is shown in Fig. 4.

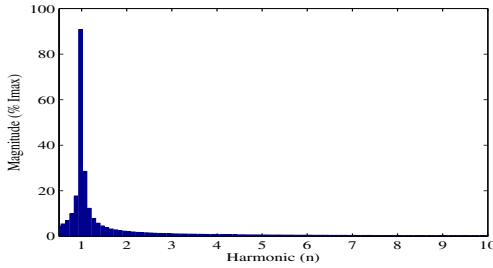


Fig. 4. Harmonics and interharmonics for the current injected into the electric grid

Fig. 4 allows concluding that the percentage of the fundamental harmonic component calculated by the DFT for the current injected into the grid has a very favorable result, about 93 %. Additionally, the observation of Fig. 4 is in favor that the current injected into the electric grid for the PV system with classical PI control presents a content of interharmonics relatively low and the higher order harmonics of the output current are filtered out by the second order filter.

Table 2. Data results for the Kaneka KA58 solar module

Parameter	R_s	R_p	m	I_{PV}	I_0
Kaneka KA58	6.28 Ω	976.02 Ω	243.08	1.11 A	1.18×10^{-6} A

The THD of the current injected into the electric grid has a very favorable result, about 2.4 %. Hence, the PV system with DC-DC boost and three-level power inverter topology has an adequate performance in what regards the fact that the THD of the output current is being lower than 5% limit imposed by IEEE-519 standard.

6 Conclusions

Simulation studies of PV systems are essential to assist engineers not only in the design phase, but also in real-time operation where cloud-base solutions may allow enough computer resources for a better management in what regards extracting of energy, anticipating performance and deciding convenient measures to avoid malfunctions. The increased integration of PV system into the electric grids leads to technical challenges implying research for more realistic physical models able of giving a better understanding of what concerns the eventually disturbance caused by PV systems, allowing to circumvent loss of energy quality and undesirable instability problems.

The paper proposes an integrated model for PV systems linked to the electric grid through power converters. The integrated model allows a more accurate description of the dynamic of the system. The model includes a maximum power point tracking and

power-electronic modeling for the power converters: DC-DC boost converter and the three-level convert linked to the electric grid. The control strategy used in the simulation is based on the use of classical PI controllers, PWM by SVM associated with sliding mode control and power factor control is introduced at the output of the inverter. Although more complex, this integrated model is justified for more realistic results. The application of this modeling to a case study on a-Si solar modules Kaneka KA 58 with a convenient filtering allows to anticipate that the THD for the output current is lower than the 5% limit imposed by IEEE-519 standard for this PV system with DC-DC boost and three-level power inverter topology.

Acknowledgments. This work was partially supported by Fundação para a Ciência e a Tecnologia, through IDMEC/LAETA, Instituto Superior Técnico, University of Lisbon and by Universidade of Évora.

References

1. López, M.E.A., Mantiñan, F.J.G., Molina, M.G.: Implementation of wireless remote monitoring and control of solar photovoltaic (PV) system. In: 6th IEEE/PES Transmission and Distribution: Latin America Conference and Exposition, pp.1–6 (2012)
2. Fialho, L., Melício, R., Mendes, V.M.F.: PV system modeling by five parameters and in situ test. In: 22th SPEEDAM, pp. 577–582 (2014)
3. Rampinelli, G.A., Krenzinger, A., Chenlo Romero, F.: Mathematical Models for Efficiency of Inverters Used in Grid Connected Photovoltaic Systems. *Renewable and Sustainable Energy Reviews* **34**, 578–587 (2014)
4. Batista, N.C., Melício, R., Mendes, V.M.F.: Layered Smart Grid Architecture Approach and Field Tests by ZigBee Technology. *Energy Conversion and Management* **79**, 721–730 (2014)
5. Papageorgas, P., Piromalis, D., Antonakoglou, K., Vokas, G., Tseles, D., Arvanitis, K.G.: Smart Solar Panels: In-situ monitoring of photovoltaic panels based on wired and wireless sensor networks. *Energy Procedia* **36**, 535–545 (2013)
6. Ayodele, T.R., Jimoh, A.A., Munda, J.L., Agee, J.T.: Challenges of Grid Integration of Wind Power on Power System Grid Integrity: a Review. *International Journal of Renewable Energy Research* **2**, 618–626 (2012)
7. Raj, J.S.C.M., Jeyakumar, A.E.: A Two Stage Successive Estimation Based Maximum Power Point Tracking Technique for Photovoltaic Modules. *Solar Energy* **103**, 43–61 (2014)
8. Fialho, L., Melício, R., Mendes, V.M.F., Rodrigues, L., Viana, S., Estanqueiro, A.: Simulation of a-Si PV system linked to the grid by DC-DC boost and two-level converter. In: 16th PEMC, pp. 934–938 (2014)
9. Seixas, M., Melício, R., Mendes, V.M.F.: Fifth Harmonic and Sag Impact with a Balancing New Strategy for Capacitor Voltages. *Energy Conversion and Management* **79**, 721–730 (2014)
10. Giacobbe, L.: Validação de Modelos Matemáticos de Componentes de Sistemas Fotovoltaicos. Master Thesis, DEEC/IST (2005) (in Portuguese)
11. IEC 60904-1: Photovoltaic devices - Part 1: Measurement of Photovoltaic (PV) Current-Voltage Characteristics (2006)
12. Kaneka Photovoltaic Products Information. <http://www.pv.kaneka.co.jp>

Modeling Reserve Ancillary Service as Virtual Energy Carrier in Multi-Energy Systems

M.Y. Damavandi^{1,2}, Mohsen Parsa Moghaddam¹, M.-R. Haghifam¹,
M. Shafie-khah², and João P.S. Catalão^{2,3,4}(✉)

¹Tarbiat Modares University (TMU), Tehran, Iran

²University of Beira Interior, Covilhã, Portugal

³INESC-ID, Lisbon, Portugal

⁴Instituto Superior Técnico, Lisbon, Portugal
catalao@ubi.pt

Abstract. Multi-energy systems (MES) are considered various energy carriers and energy players in an integrated energy model. Vast amount of decision making data is gathered in these systems that cannot be processed by conventional methods. Cloud-based computing is an opportunity to develop these kinds of integrated and efficient approaches. Developing mathematical models that can be compatible with cloud-based engineering systems will help decision makers to enhance the system agendas in short to long term studies. In this paper, the energy hub approach is developed to consider electric reserve ancillary service in MES. The reserve is modeled as a virtual energy output that can be injected into the upstream network. The reserve service is defined for electric energy converters and storages, comprehensively. Therefore, the energy hub mathematical model is developed and new elements are added to the input and output vectors and system conversion matrix. For energy converters, reserve is defined as the capability of the converter to increase its output service to its maximum operational limits. Moreover, for electric storages this capability is also restricted by storages' state of charges. The numerical results demonstrate the importance of reserve considerations in MESs and allow assessing the proficiency of the proposed model.

Keywords: Energy hub model · Multi-energy system · Reserve ancillary service

1 Introduction

Increasing the share of distributed energy resources (DER) in the energy service provision confronts policy makers with new challenges and opportunities in energy system studies. These new facilities introduce a dependency in both energy carriers and time domains [1]. Moreover, new independent decision makers enforce a high level of operational data to the energy system managers. In this situation, cloud-based engineering systems facilitate cooperation among independent decision makers and increase the utilization of inherent flexibility in the multi-energy systems (MES).

MES is an integrated energy system that considers the energy and information interaction between energy players and carriers simultaneously [2]. These interactions have

been modeled by “*Energy hub system*” and “*matrix modeling*” approaches ([3] and [4]). In these models, MES is divided into some super-nodes that can interact with various energy carriers via interconnectors. Each super-node (energy hubs in energy hub system and distributed multi-generations in matrix modeling) consists of energy converters and energy storages, delivering the required energy service by transforming input energy carriers.

The proposed models have been developed in [5]-[7] and new considerations such as renewable energy resources, demand side management, and demand response have been included in MES’s mathematical modeling. Moreover, in other power system studies, such as reliability index assessment and cascading failure mitigation, MES economic evaluation have been considered [8]-[11].

In [12] the energy hub model has been developed to consider integration of plug-in electric vehicles (PEV) in grid to vehicle (G2V) modes as a manageable load for ancillary service provision (frequency control). Moreover, the capability of MES to serve ancillary services has been discussed in [13] and the new concept of multi-energy/power arbitrage has been developed to consider reserve of distributed multi-generation.

In this paper, the reserve ancillary service is modeled on an energy hub approach as virtual output energy carriers that can be injected to the macro-MES level. The spinning reserve is provided from combined heat and power (CHP) units and electric storages. For CHP units, reserve provision is defined as the capability of the unit to increase its output electric power to its operational limits.

In addition, for electric storages this capability is restricted by power interaction with the system and stored energy. The energy hub model is developed to consider both storage and converter reserve provision in the mathematical model. Some rows are added to the output energy vector to model reserve energy as a virtual port, and consequently the system coupling matrix will be changed to consider the share of each energy element in the reserve provision. The numerical results demonstrate the proficiency of the proposed model and the energy scheduling adjustment of micro-MES in the operation time horizon.

2 Contribution to Cloud-Based Engineering Systems

By increasing the dependency among energy carriers, conventional methods for system management are no longer effective. Thus, decision makers in the energy sector try to propose multi-dimensional models for energy systems that can cover technical, economic and environmental aspects of these systems. In this way, MES can be considered as a cloud-based engineering system consisting of various energy players and carriers.

This cloud-based perspective of the energy system increases collaboration among energy players from both energy and information points of view. Moreover, the huge amount of management data enforces energy players to develop novel computational methods to decrease system operation time and manage unwanted contingencies. The cloud-based engineering system may entail two integrated data and energy layers in such a way that energy players share information with each other for increasing their operational flexibility in both normal and contingency conditions.

In this regard, proposing standard models for system players can enable energy and information interactions among players. Since energy hub approach as a modular model has these capabilities, nowadays; researchers in energy studies try to develop new models to include more characteristics of the energy system.

In this paper, the energy hub model is developed from a mathematical point of view to consider reserve ancillary services for a micro-MES energy player. The proposed model accelerates cooperation of the micro-MES in the cloud-based engineering system by increasing their profit from two individual energy markets. Moreover, the energy hub presentation of the reserve service as a modular approach helps system managers to exchange data among energy players more efficiently.

3 Energy Hub Modeling

The energy hub model consists of a conversion matrix (C) that transforms input energy carriers (p) to the required energy services (l). For assessing the impact of energy storages in MES, ref. [14] added a new vector (ê) to the input energy vector that demonstrates the changes in stored storages' state of charge (SOC). Matrix S determines the share of energy storages in the output energy vector. Moreover, one of the main energy hub approach assumptions is unidirectional energy flow. Therefore, ref. [5] has added the vector k in the output of the energy hub to inject the surplus energy in the system to the upstream energy network.

$$[C][p] = [l] \tag{1}$$

$$[C \quad S] \begin{bmatrix} p \\ \hat{e} \end{bmatrix} = [l] + [k] \tag{2}$$

In this paper, the electric reserve in MES is defined as the capability of MES to increase its injected electric energy to the upstream network. In the mathematical approach, this capability is considered as virtual energy output port that injected the required service to the upstream network. Therefore, new rows (r^{inj}) are added to the vector k to determine the supplied reserve services. In addition, corresponded zero rows are added to the vector l.

$$k^{new} = \begin{bmatrix} k^{old} \\ r^{inj} \end{bmatrix}, \quad l^{new} = \begin{bmatrix} l^{old} \\ 0 \end{bmatrix} \tag{3}$$

By adding new rows in the output, the matrices C and S will be modified to determine the share of each element of the new output energy service (electric reserve). For the energy converters, the reserve service is defined as the capability of the energy converter to increase its output energy to its operational limits. Furthermore, for energy storages this capability is restricted by their output power and stored energy in each hour. Therefore, determining the reserve service for electric energy storages needs new rows in p to show the share of electric energy storage for serving reserve to the MES as an input virtual energy carrier (rSt).

$$p^{new} = \begin{bmatrix} p^{old} \\ r^{St} \end{bmatrix} \tag{4}$$

$$C^{new} = \begin{bmatrix} C^{old} & \mathbf{0} \\ C^{EC} & C^{St} \end{bmatrix}, S^{new} = \begin{bmatrix} S^{old} \\ 0 \end{bmatrix} \quad (5)$$

where:

C^{old} : coupling matrix that states the conversion of inputs energy carriers into outputs energy services.

C^{EC} : coupling matrix to show the share of energy converters in output reserve which is based on the efficiency of energy converters.

C^{St} : coupling matrix to show the share of storage in output reserve which is based on the discharge efficiency of storage.

S^{old} : storage coupling matrix that shows the changes of output energy service versus changes in the stored energy.

M : matrix of vacant capacity of energy converters

U : decision making matrix with binary arrays which determines the participation of each converter in output reserve.

In order to produce C^{EC} , each array of M is divided by the corresponding array of P^{old} and after that are multiplied by array of U (6).

$$C^{EC} = (M/P^{old}).U \quad (6)$$

By substituting the modified terms in(1),the system new equation is as (7) and (8).

$$\begin{bmatrix} C^{new} & S^{new} \end{bmatrix} \begin{bmatrix} P^{new} \\ \dot{e} \end{bmatrix} = \begin{bmatrix} I^{new} \end{bmatrix} + \begin{bmatrix} K^{new} \end{bmatrix} \quad (7)$$

$$\begin{bmatrix} C^{old} & \mathbf{0} & S^{old} \\ C^{EC} & C^{St} & \mathbf{0} \end{bmatrix} \begin{bmatrix} P^{old} \\ r^{St} \\ \dot{e} \end{bmatrix} = \begin{bmatrix} I^{old} \\ \mathbf{0} \end{bmatrix} + \begin{bmatrix} K^{old} \\ r^{inj} \end{bmatrix} \quad (8)$$

4 MES’s Operational Framework

In this paper the MES is divided into three layers, namely as macro-MES, micro-MES and multi-energy demand (MED). Fig. 1 demonstrates a micro-MES that receives input energy carriers from macro-MES and serves required energy services to the MED. Furthermore, the micro-MES is equipped by energy converters (e.g. CHP units and auxiliary boilers (AB)) and energy storages (e.g. heat storage (HS) and electric storage (ES)). These facilities enable micro-MES to participate in both energy and ancillary service markets to increase its profit. Micro-MES operator maximizes its profit by participating in energy and reserve markets and interacting energy with MED (9).

$$Maximizing \left\{ \sum_t \left[(w_t^{inj} - w_t^{in}) \pi_{e,t}^{MaMES} - g_t^{in} \pi_{g,t}^{MaMES} + r_t^{inj} \pi_{r,t}^{MaMES} + W_t^{MED} \pi_{e,t}^{MED} + Q_t^{MED} \pi_{h,t}^{MED} + r_t^{inj} \rho_{r,t} \pi_{e,t}^{MaMES} - r_t^{inj} \rho_{r,t} FOR^{MES} \pi_{e,t}^{con} - (r_t^{CHP} \rho_{r,t} / \eta_e^{CHP}) \pi_{g,t}^{MaMES} \right] \right\} \quad (9)$$

The operational constraints for micro-MES are described as follows:

Input energy carrier: micro-MES energy interaction with macro-MES is restricted by the interconnectors’ capability to transfer energy flow.

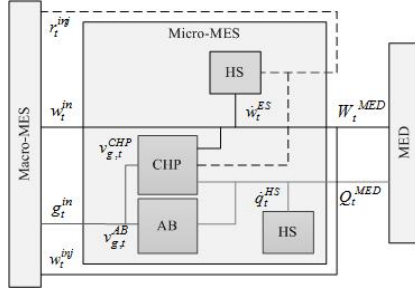


Fig. 1. MES schematic considering reserve ancillary service as virtual port

$$-\bar{W}^{in} \leq w_t^{in} - w_t^{inj} - r_t^{inj} \leq \bar{W}^{in} \quad (10)$$

$$0 \leq g_t^{in} \leq \bar{G}^{in} \quad (11)$$

CHP unit: The CHP unit converts input gas to the required heat and electric power. The heat and power output should be lower than units' maximum operational limits and their ratio should be equal to a predetermined parameter (λ^{CHP}).

$$0 \leq w_t^{CHP} + r_t^{CHP} \leq \bar{W}^{CHP}, \quad 0 \leq q_t^{CHP} \leq \bar{Q}^{CHP} \quad (12)$$

$$\lambda^{CHP} = q_t^{CHP} / w_t^{CHP} \quad (13)$$

AB operational constraints: The output heat of AB should be lower than its operational bound.

$$\underline{Q}^{AB} \leq q_t^{AB} \leq \bar{Q}^{AB} \quad (14)$$

Storages interaction limit: Rate of HS and ES interactions with Micro-MES should be in its operational zone.

$$|\dot{q}_t^{HS}| \leq \Gamma^{HS}, \quad |\dot{w}_t^{ES}| \leq \Gamma^{ES} \quad (15)$$

Decision variable constraint: v is dispatch factor and shows the share of each energy element of input energy and its amount should be between zero and 1.

$$0 \leq v_{g,t}^{CHP}, v_{g,t}^{AB} \leq 1 \quad (16)$$

$$v_{g,t}^{CHP} + v_{g,t}^{AB} = 1 \quad (17)$$

General energy hub conversion matrix: energy hub conversion matrix is represented in (18), transforming input energy carriers to the required energy services.

$$\begin{bmatrix} 1 & v_{g,t}^{CHP} \eta_e^{CHP} & 0 & 0 & 1/\eta_e^{ES} \\ 0 & v_{g,t}^{CHP} \eta_h^{CHP} + v_{g,t}^{AB} \eta_h^{AB} & 0 & 1/\eta_h^{HS} & 0 \\ 0 & (\bar{G}^{in} - v_{g,t}^{CHP} g_t^{in}) \eta_e^{CHP} / g_t^{in} & 1/\eta_e^{ES, dcha} & 0 & 0 \end{bmatrix} \begin{bmatrix} w_t^{in} \\ g_t^{in} \\ r_t^{PL} \\ q_t^{HS} \\ w_t^{ES} \end{bmatrix} = \begin{bmatrix} W_t^{MED} \\ Q_t^{MED} \\ 0 \end{bmatrix} + \begin{bmatrix} w_t^{inj} \\ 0 \\ r_t^{inj} \end{bmatrix} \quad (18)$$

5 Numerical Results

The micro-MES operator receives gas and electricity from macro-MES and delivers MED's required heat and electricity.

Figs.2 and 3 depict the MED’s consumption and price signals for input and output energy carriers.

Three cases are prepared to determine the operational behavior of micro-MES’s elements in various system operating conditions. In cases I and II, micro-MES is equipped with CHP, AB, and ES, while in Case III the system also has a HS.

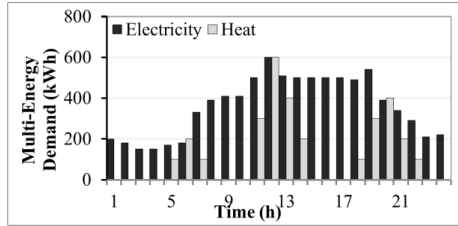


Fig. 2. Electricity and heat consumption of MED

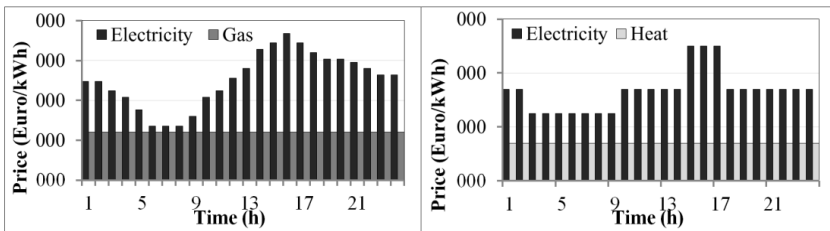


Fig. 3. Left side: Input energy price. Right side: output energy price

Case I: In this case, the micro-MES operator does not participate in the reserve ancillary service. Figs. 4 and 5 demonstrate the share of each element in electricity and heat balance of micro-MES. The CHP unit produces energy in hours 5, 11-14, and 18-22, while MED consumes heat and the energy price is almost high. Moreover, ES stores energy in hours 6-8 and provides a part of electricity demand in hours 16 and 17, when the maximum electricity price in the operation time horizon occurs.

Case II: In this case, besides participating in energy trade, the micro-MES sells reserve service to the macro-MES. Fig. 6 shows the CHP unit and ES reserve provision in micro-MES. In most of the operation period the ES reserve provision is restricted by its discharge rate, while for CHP unit the reserve provision restriction is more related to the share of CHP unit in electricity demand satisfaction. Moreover, Fig. 7 compares the ES behavior in Cases I and II. In Case II, ES is more eager to maintain its SOC level after hour 6 since the reserve price is acceptable for reserve provision to participate in the reserve ancillary service, instead of energy provision.

Case III: In this case, HS is added to the micro-MES’s equipment. Fig. 8 depicts the share of each element in micro-MES electricity balance. The CHP unit can be operated during hours 2, 3 and 15-17 when there is no heat demand, but the surplus heat can be stored in HS. Furthermore, Fig. 9 determines that in Case III the Micro-MES prefers to utilize its equipment to provide energy to maximize its profit, instead of participating in the reserve service provision. It means that reserve service and HS are two sources to increase the degree of freedom of the micro-MES operator. Adding both of these resources decreases the impact of each independent source.

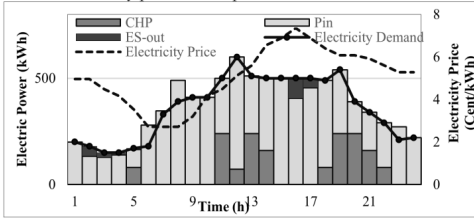


Fig. 4. Electricity operation scheduling of micro-MES in Case I

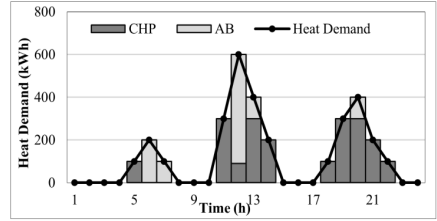


Fig. 5. Heat operation scheduling of micro-MES in Case I

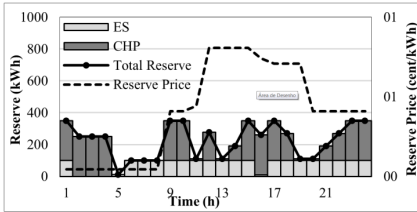


Fig. 6. Reserve provision in micro-MES in Case II

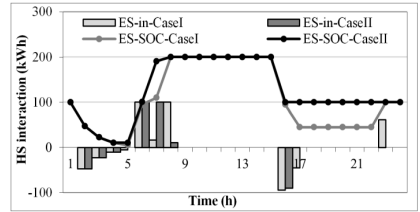


Fig. 7. ES behavior in Case I and Case II

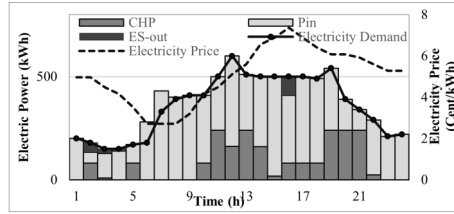


Fig. 8. Electricity operation scheduling of micro-MES in Case III

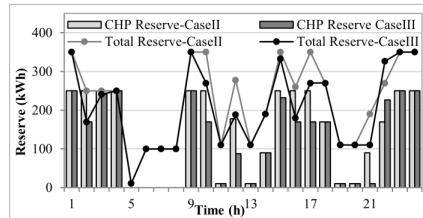


Fig. 9. CHP and total reserve provision comparisons in Case II and Case III

6 Conclusions

In this paper, reserve ancillary service has been modeled in MES. The energy hub mathematical model was developed to consider reserve for both electric energy converters and storages. The numerical results have determined that the micro-MES operator for electric energy converters prefers to participate in energy trade instead of reserve opera-

tion. On the contrary, for electric storage it was more profitable for the operator to maintain its SOC to participate in reserve provision service, instead of the energy trade. As a matter of fact, ES behaves like a converter that consumes in the off peak of electricity as primary resources and delivers electricity in the peak hours of price and its operation restricted by its capacity. Therefore, it is less efficient than conventional energy converters (e.g. micro-turbines and gas engines) to produce electricity and deliver to the energy market. On the other hand, its characteristics (e.g. fast ramp) make it suitable to participate in ancillary services. Moreover, in Case III it was shown that each system has various sources of flexibility for the operator (e.g. storage and participation in various markets), having cross impacts that influence each other performance.

Acknowledgment. This work was supported by FEDER funds (European Union) through COMPETE and by Portuguese funds through FCT, under Projects FCOMP-01-0124-FEDER-020282 (Ref. PTDC/EEA-EEL/118519/2010) and PEst-OE/EEI/LA0021/2013. Also, the research leading to these results has received funding from the EU Seventh Framework Programme FP7/2007-2013 under grant agreement no. 309048

References

1. Mancarella, P.: MES (multi-energy systems): An overview of concepts and evaluation models. *Energy* **65**, 1–17 (2014)
2. Mancarella, P., Chicco, G.: Real-Time Demand Response From Energy Shifting in Distributed Multi-Generation. *IEEE Trans. Smart Grid* **4**, 1928–1938 (2013)
3. Geidl, M., Koepfel, G., Favre-Perrod, P., Klockvl, B., Andersson, G., Frohlich, K.: Energy hubs for the future. *IEEE Power and Energy Magazine* **5**(1), 24–30 (2007)
4. Chicco, G., Mancarella, P.: Matrix modelling of small-scale trigeneration systems and application to operational optimization. *Energy* **34**, 261–273 (2009)
5. Schulze, M., Friedrich, L., Gautschi, M.: Modeling and optimization of renewables: Applying the energy hub approach. In: *Proc. ICSET Conf.* (2008)
6. Kienzle, F., Ahcin, P., Andersson, G.: Valuing Investments in Multi-Energy Conversion, Storage, and Demand-Side Management Systems Under Uncertainty. *IEEE Trans. Sustainable Energy* **2**, 194–202 (2011)
7. Mancarella, P., Chicco, G.: Real-Time Demand Response From Energy Shifting in Distributed Multi-Generation. *IEEE Trans. Smart Grid* **4**, 1928–1938 (2013)
8. Bozchalui, M.C., Hashmi, S.A., Hassen, H., Canizares, C.A., Bhattacharya, K.: Optimal Operation of Residential Energy Hubs in Smart Grids. *IEEE Transactions on Smart Grid* **3**, 1755–1766 (2012)
9. Houwing, M., Negenborn, R.R., De Schutter, B.: Demand Response with Micro-CHP Systems. *Proceedings of the IEEE* **99**(1), 200–213 (2011)
10. Almassalkhi, M., Hiskens, I.: Impact of energy storage on cascade mitigation in multi-energy systems. In: *Proc. IEEE Power and Energy Society General Meeting*, pp. 1–8. San Diego (July 2012)
11. Haghifam, M.R., Manbachi, M.: Reliability and availability modeling of combined heat and power (CHP) systems. *International Journal of Electrical Power & Energy Systems* **33**(3), 385–393 (2011)

12. Galus, M.D., Koch, S., Andersson, G.: Provision of Load Frequency Control by PHEVs, Controllable Loads, and a Cogeneration Unit. *IEEE Trans. Industrial Electronics* **58**, 4568–4582 (2011)
13. Mancarella, P., Chicco, G.: Integrated energy and ancillary services provision in multi-energy systems. In: *Proc. IREP Symposium* (2013)
14. Adamek, F., Arnold, M., Andersson, G.: On Decisive Storage Parameters for Minimizing Energy Supply Costs in Multicarrier Energy Systems. *IEEE Trans. Sustainable Energy* **5**, 102–109 (2014)

Simulation of Offshore Wind System with Three-Level Converters: HVDC Power Transmission in Cloud Scope

M. Seixas^{1,2,3}, R. Melício^{1,2(✉)}, V.M.F. Mendes^{2,3},
M. Collares-Pereira², and M.P. dos Santos²

¹IDMEC/LAETA, Instituto Superior Técnico, Universidade de Lisboa, Lisbon, Portugal

²Universidade de Évora, Évora, Portugal

ruimelicio@gmail.com

³Instituto Superior of Engenharia de Lisboa, Lisbon, Portugal

Abstract. This paper is on a simulation for offshore wind systems in deep water under cloud scope. The system is equipped with a permanent magnet synchronous generator and a full-power three-level converter, converting the electric energy at variable frequency in one at constant frequency. The control strategies for the three-level are based on proportional integral controllers. The electric energy is injected through a HVDC transmission submarine cable into the grid. The drive train is modeled by a three-mass model taking into account the resistant stiffness torque, structure and tower in the deep water due to the moving surface elevation. Conclusions are taken on the influence of the moving surface on the energy conversion.

Keywords: Offshore wind turbine · HVDC · Three-level converter · Simulation

1 Introduction

Over the last decades, the energy primary sources like oil, coal, nuclear and natural gas have been used as the main source of energy for conversion into electric energy [1]. Nonetheless, disadvantageous circumstances are pointed out in the use of these sources, for instances: for fossil-fuel, the harmful on the environment and the cost subject to market instability and tending to increase in the long run. Forecasts for non-nuclear and non-renewable energy sources are in support of an envisaged scarcity pointing to the exhaustion on those sources in less than a century [2]. Exploitation on renewable energy sources have emerged by support of country polices or by more in-depth protocols such as the Kyoto Protocol as a response to harmful on the environment, instability and increasing fuel costs.

The wind energy source is the one within the exploitation of renewable energy sources that has experienced a greater development [3]. This development has achieved such a level that there is an increasing difficulty in new deployment, i.e., a difficulty to find new appropriate places for onshore wind farms. Particularly, a considerable exhaustion on convenient places is reported for Europe [4]. Thus, there is an interest in the exploitation of offshore wind energy, which has the benefits of available vast sea areas and of more favorable wind conditions, than those on land. Higher values of wind speed with less variation, because of the non existence of obstacles are

encouraging offshore deployment [5]. Deployment of offshore wind energy has a power transmission technology depending on the distance from the floating platform to onshore: for distances less than 60 km is proposed to use high-voltage ac (HVAC); for longer distances is proposed high voltage dc (HVDC) [6].

Deployment of offshore wind energy has a less concern with visual and noise impact, allowing the use of wind turbines with larger rotors, allowing a higher value for the installed power. The increase in size of the wind turbines implies particular design. As fact the blades are larger, more flexible and tend to bend. Therefore, the model for the drive train has to capture this fact and this paper proposes a three-mass (TM) model to take into account the concern with the dynamic of the blades, the structure and the moving floating platform.

2 Relationship to Cloud-Based Solutions

The global growing demand for energy led to the deployment of new energy conversion called distributed energy located closely to the electric load to be served. A variety of small grid-connected devices referred to as distributed energy resources (DER) are introduced to allow the flow of distributed energy. DER systems typically use renewable energy sources, and increasingly play an important role for the electric grid. With the increasing demand for electricity and the growth of distributed generation (DG) there is a concern with the ability of the existing electric grid to accommodate the needed transformation. Thus, new insight into the electric grid is required and the concept of Smart Grid (SG) is on the way. SG conception includes the area of smart technologies able to quantify in real time the energy consumption, the power quality and ability to avoid or pre-detect eventual faults [7]. Vital for the SG conception is an architecture that guaranties safety and reliability. A layered processing system seems a good option, gathering information about the SG components delivering an insight into the behavior of the system, which allows operators or machines to take action accordingly, over a services platform. The designed software and hardware structure can be transferred to a cloud architecture system, benefiting of existing Internet Cloud Services, as in Fig. 1, to process the data storage and data transfer in real-time with cheap processing costs [7]. Due to safety issues, one expects that the best approach to the deployment of the cloud architecture in electrical grids will be a private cloud. Private clouds are projected and built exclusively for a single organization, which has full control over how applications and data are deployed in the cloud [8]. Every step in the project raises security issues that must be addressed to prevent vulnerability [9]. Due to the vulnerability, the SG approach advocates the use of a layered system that supports the integration of sensors and actuators, acting in a bidirectional data exchange, thus providing an introduction in the accelerating integration of SG services [10].

3 Modeling

The wind speed intermittence and variability stochastic character are possible to model by a deterministic sum of harmonics ranging 0.1–10 Hz as is indicated in [11] given by

$$u(t) = u_o [1 + \sum_k A_k \sin(\omega_k t)] \tag{1}$$

where u is the wind speed with perturbation, u_o is the average wind speed, A_k is the magnitude of the k eigenswing, ω_k is the eigenfrequency of the k eigenswing.

Offshore structures are influenced by marine wind and wave dynamics. The marine wave model [12] is given by

$$\eta(x, y, t) = \sum_{i=1}^n \eta_a(i) \cos[\vartheta(i)t + \varepsilon(i) - \phi(i)(x \cos(\psi(i)) + y \sin(\psi(i)))] \tag{2}$$

where $\eta(x, y, t)$ is the wave elevation for (x, y) position as a function of time, η_a is the vector of harmonic wave, ϑ is the vector of harmonic wave frequencies, ε is the vector of harmonic wave phases (random), ϕ is the vector of harmonic wave numbers and ψ is the vector of harmonic wave directions.

The offshore wind system (OWS) apart from the wind turbine has a rectifier linking a permanent magnet synchronous generator (PMSG) to a first set of two capacity banks. A high voltage DC transmission submarine cable links the first set of two capacity banks to a second one connected to an inverter, injecting the energy into an electric grid through a second order filter. The OWS is shown in Fig. 1.

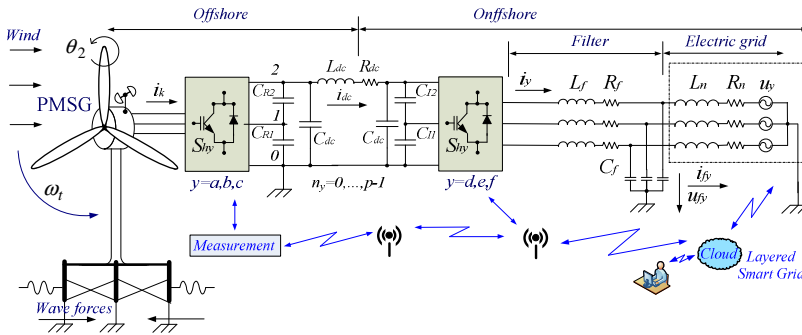


Fig. 1. Offshore wind system with three-level converter, HVDC

The drive train is modeled by a three-mass model. The first mass concentrates the inertia of the flexible part of the blades; the second mass concentrates the rigid part of the blades, hub, tower and platform, discarding the movement between the different elements, but including the floating motion influence on the second mass; the third mass concentrates the inertia of the generator. The equations for modeling the motion of the drive train are based on the torsional version of the second law of Newton and are given by

$$\frac{d\omega_t}{dt} = \frac{1}{J_b} (T_t - T_{db} - T_{bs}) \tag{3}$$

$$\frac{d\omega_h}{dt} = \frac{1}{J_h} (T_{th} + T_{bs} + T_{sm} - T_{dh} - T_{hs}) \quad (4)$$

$$\frac{d\omega_g}{dt} = \frac{1}{J_g} (T_{hs} - T_{dg} - T_g) \quad (5)$$

where ω_i is the rotor angular speed at the flexible blades part, J_b is the moment of the inertia of the rotating parts at the flexible blades part, T_t is the mechanical torque, T_{db} is the resistant bearing torque due to the damping at the flexible blades part, T_{bs} is the resistant shaft stiffness torque between the flexible blades part and hub, ω_h is the rotor angular speed at the hub plus rigid blades part, J_h is the moment of the inertia of the rotating parts of hub plus the rigid blades part, T_{th} is the mechanical torque of the rigid blades part, T_{sm} is the tower and platform stiffness torque due to floating surface motion, T_{dh} is the hub bearing resistant torque, T_{hs} is the shaft stiffness torque between hub and generator, ω_g is the rotor angular speed at the generator, J_g is the moment of inertia of the rotating parts of the generator, T_{dg} is the generator bearing resistant torque, T_g is the electric torque.

The equations for the PMSG modeling can be retrieved in diverse texts [13]. In the PMSG to avoid demagnetization of permanent magnet a null reference stator direct component current $i_{sd}^* = 0$ is imposed [14]. The three-level converter has twenty-four unidirectional commanded insulated gate bipolar transistors (IGBTs) to implement the rectifier or the inverter functionality [15]. The group of four IGBTs associated in the same phase is said to be the converter's y leg. The switching variable n_y with $n_y \in \{0,1,2\}$ is used to identify the IGBT i state in the leg y of the three-level converter. The switching variable n_y is given by the switching function of the IGBT. The switching variable as shown in [15] is given by

$$n_y = \begin{cases} 2, & (S_{cy} e S_{dy}) = 1 \text{ e } (S_{ay} e S_{by}) = 0 \\ 1, & (S_{by} e S_{cy}) = 1 \text{ e } (S_{ay} e S_{dy}) = 0 \\ 0, & (S_{ay} e S_{by}) = 1 \text{ e } (S_{cy} e S_{dy}) = 0 \end{cases} \quad (6)$$

The level variable δ_{jny} with $j \in \{1,2\}$ used to establish the charging state of the capacitor banks [15] is given by

$$\delta_{jny} = \begin{cases} 0 & j > n_y \\ 1 & j \leq n_y \end{cases} \quad (7)$$

The rectifier output voltage is given by

$$u_{sy} = \frac{1}{3} \sum_{j=1}^2 (2\delta_{jn_y} - \sum_{\substack{l=a \\ l \neq y}}^c \delta_{jn_l}) U_{CRj} \quad y \in \{a, b, c\} \tag{8}$$

The DC voltage at the first set of capacity banks U_{dcRj} rectifier side is given by

$$\frac{dU_{dcR}}{dt} = \sum_{j=1}^2 \frac{1}{C_{Rj} + C_{dc}} i_{CRj} \tag{9}$$

The linking between the first set of two capacity banks on offshore to a second one on onshore is assumed to be by a high voltage DC transmission submarine cable. The submarine cable is modeled by a π equivalent circuit [13]. The current i_{dc} in the cable is given by

$$\frac{di_{dc}}{dt} = \frac{1}{L_{dc}} (U_{dcR} - U_{dcI} - R_{dc} i_{dc}) \tag{10}$$

The DC voltage at the second set of capacity bank U_{dcI} , inverter side, is given by

$$\frac{dU_{dcI}}{dt} = \sum_{j=1}^2 \frac{1}{C_{Ij} + C_{dc}} i_{CIj} \tag{11}$$

The electric grid is modeled by an equivalent three-phase active symmetrical circuit given by a series of a resistance and an inductance. Hence, the electric current injected, into the electric grid is given by

$$\frac{di_{fy}}{dt} = \frac{1}{L_n} (u_{fy} - R_n i_{fy} - u_y) \quad y = \{d, e, f\} \tag{12}$$

This model is normally used in transient simulations and corresponds to what is said to be an infinite grid model linked by the equivalent series impedance.

4 Control Method

A classical PI controller is used to acquire the current references. IGBTs on/off switching states imply that the three-level converter is a time variant system. Therefore the sliding mode (SM) control strategy is crucial to alter the three-level converter, assuring the assortment of the proper space vectors. Additionally, PWM by space vector modulation (SVM) associated with SM is used for triggering the IGBTs. The SM strategy's aim is to

let the system slide along a predefined dynamic, also known as sliding surface $A(e_{\alpha\beta}, t)$, by changing the system structure, i.e., by changing the IGBTs on/off state. The IGBTs can only switch at finite frequency, due to physical limitations causing the control current not to be able to follow exactly the reference current, thus creating an error $e_{\alpha\beta}$. Hence, to maintain the system within the neighboring of the sliding surface, the state trajectory must comply with the conditions [15] given by

$$A(e_{\alpha\beta}, t) \frac{dA(e_{\alpha\beta}, t)}{dt} < 0 \tag{13}$$

A small error is acceptable in practice and a convenient achievement of this strategy is accomplished with hysteresis comparators [15]. If the current error, given by the comparators hysteresis output $\sigma_{\alpha\beta}$ is quantified in five levels is possible to relate the space vectors with the current error. So $\sigma_{\alpha\beta}$ are integers numbers taking values in the set $\{-2, -1, 0, 1, 2\}$. There are redundant vectors which correspond to different voltage level selection. The control strategy carries out a reduction on the capacitors banks unbalancing voltage by considering three vector tables [15], which take in account the voltage level of each capacitor bank by the defining the vector to be used. The output vectors for the level 0, level 1 and level 2 in the $\alpha\beta$ plane for the three-level converter are shown in Fig. 2.

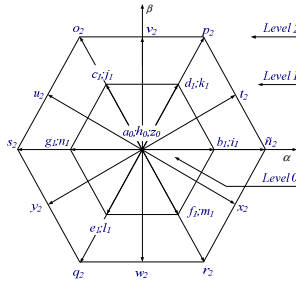


Fig. 2. Three-level inverter, output space vectors

5 Case Study

The OWS has a nominal power of 2 MW. The capacity banks have a value of 65 mF. The filter have a R_f of 8Ω a L_f of $500 \mu\text{H}$ and a C_f of 50 mF. The IGBTs switching frequency is 10 KHz. The mathematical model for the OWS with the three-level converter is implemented in Matlab/Simulink without the use of Power System Blockset. The wind speed considered has a profile defined by having an average speed starting with a value of 10 m/s followed by a ramp increase stabilizing after 1.5 s with an average speed of the 20 m/s, i.e., between 1.5 s and 4 s the wind average speed is constant. The significant wave height and the frequency are respectively 10 m and 0.25 Hz. The reference voltage and the DC voltages on the capacitor banks with the control strategy for selection of the vectors without unbalancing at the rectifier side are shown in Fig. 3. The DC current at the submarine cable is shown in Fig. 4.

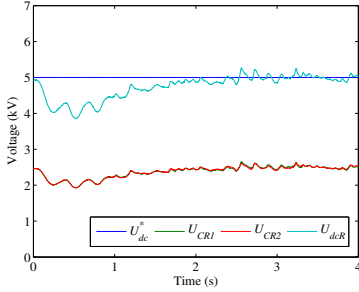


Fig. 3. DC voltages at the capacitor banks rectifier side

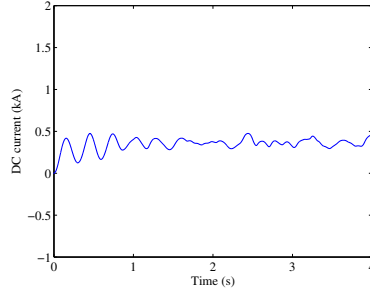


Fig. 4. DC current at the submarine cable rectifier side

The instantaneous current injected into the electric grid is shown in Fig. 5.

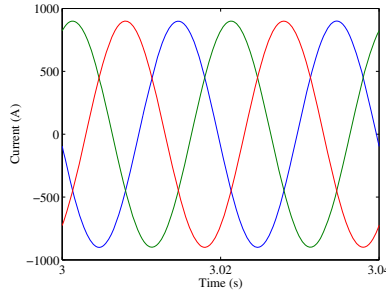


Fig. 5. Current injected into the electric grid

The average THD for the current injected into the electric grid is 0.53%. Hence, the THD of the output current is lower than the 5% limit imposed by IEEE-519 standard.

6 Conclusions

Increased wind power penetration leads to new technical challenges, transient stability and power quality. In this paper, a model for a simulation study is presented for offshore wind system equipped with a PMSG with a back-to-back neutral point clamp three-level power converter with HVDC transmission. The case study presented is intended to evaluate the offshore wind system behavior, taking into account the wind and the marine wave perturbations. The simulation carried out is in favor that the perturbation due to the marine wave has a negligible effect on the system performance. This fact is due to two situations: first the wave frequency is smaller when compared to the frequency of the wind gust; and second the floating platform is stable. So, the system feels little mechanical vibrations due to the marine waves. The simulation study revealed a good performance of the proposed offshore wind system with the three-level power converter and HVDC link. Although, there are effects on the current output of the power converter, the average value for the THD of the current injected into the electric grid is lower than 5% limit referred as to be imposed by IEEE-519 standard.

Acknowledgments. This work was partially supported by Fundação para a Ciência e a Tecnologia, through IDMEC under LAETA, Instituto Superior Técnico, Universidade de Lisboa, Portugal.

References

1. Tao, M., Hongxing, Y., Lin, L.: A feasibility study of a stand-alone hybrid solar–wind–battery system for a remote island. *Applied Energy* **121**, 149–158 (2014)
2. Ishugaha, T.F., Li, Y., Wang, R.Z., Kiplagat, J.K.: Advances in wind energy resource exploitation in urban environment: A review. *Renewable and Sustainable Energy Reviews* **37**, 613–626 (2014)
3. McKenna, R., Hollnaicher, S., Fichtner, W.: Cost-potential curves for onshore wind energy: A high-resolution analysis for Germany. *Applied Energy* **115**, 103–115 (2014)
4. Soukissian, T.: Use of Multi-Parameter Distributions for Offshore Wind Speed Modeling: the Johnson S_B Distribution. *Applied Energy* **111**, 982–1000 (2013)
5. Lange, B., Larsen, S., Højstrup, J., Barthelmie, R.: Importance of thermal effects and sea surface roughness for offshore wind resource assessment. *Journal of Wind Engineering and Industrial Aerodynamics* **92**, 959–988 (2004)
6. Gil, M.P., Gomis-Bellmunt, O., Sumper, A., Bergas-Jané, J.: Power generation efficiency analysis of offshore wind farms connected to a SLPC (single large power converter) operated with variable frequencies considering wake effects. *Energy* **37**, 455–468 (2012)
7. Ayodele, T.R., Jimoh, A.A., Munda, J.L., Agee, J.T.: Challenges of Grid Integration of Wind Power on Power System Grid Integrity: A Review. *International Journal of Renewable Energy Research* **2**, 618–626 (2012)
8. Mell, P., Grance, T.: The NIST Definition of Cloud Computing. Recommendations of the National Institute of Standards and Technology, NIST (2011)
9. Is a private cloud really more secure? <http://cloudandcompute.com/private-cloud/private-cloud-more-secure/>
10. Batista, N.C., Melício, R., Mendes, V.M.F.: Layered Smart Grid Architecture Approach and Field Tests by ZigBee Technology. *Energy Conversion and Manag.* **79**, 721–730 (2014)
11. Akhmatov, V., Knudsen, H., Nielsen, A.H.: Advanced Simulation of Windmills in the Electric Power Supply. *Int. J. Electr. Power Energy Systems* **22**, 421–434 (2000)
12. Eikeland, F.N.: Compensation of wave-induced motion for marine crane operations. MSc. Thesis, Norwegian University of Science, 16–26 (2008)
13. Ong, C.-M.: *Dynamic Simulation of Electric Machinery: Using Matlab/Simulink*, pp. 259–350. Prentice-Hall, New Jersey (1998)
14. Senjyu, T., Tamaki, S., Urasaki, N., Uezato, K.: Wind velocity and position sensorless operation for pmsg wind generator. In: 5th Int. Conf. on Power Electronics and Drive Systems, pp. 787–792 (2003)
15. Seixas, M., Melício, R., Mendes, V.M.F.: Fifth Harmonic and Sag Impact on PMSG Wind Turbines with a Balancing New Strategy for Capacitor Voltages. *Energy Conversion and Management* **79**, 721–730 (2014)

Energy: Power Conversion I

Disc Motor with Rotor Made of Aluminium or Polycrystalline High Temperature Superconductor

David Inácio¹, João Murta Pina¹, Mário Ventim Neves¹, and Alfredo Álvarez²

¹ CTS, Uninova, Departamento de Engenharia Electrotécnica, Faculdade de Ciências e Tecnologia, FCT, Universidade Nova de Lisboa, 2829-516 Caparica, Portugal
ddi@campus.fct.unl.p

² Department of Electrical Engineering, Escuela de Ingenierías Industriales, Universidad de Extremadura, E-06006 Badajoz, Spain

Abstract. The discovery of the superconductivity and the understanding of electromagnetic properties of high temperature superconducting (HTS) materials allowed the optimization and development of several applications, such as electrical machines and drives. Electromechanical conversion devices based in HTS materials potentially allows for reduction in devices dimensions or performance improvement for the same active volume, when compared with their conventional ones. An axial disc motor with high temperature superconductor (HTS) material or conventional aluminium in the rotor and conventional armature has been designed and developed. This paper describes simulations and laboratory experiments performed at liquid nitrogen temperature (77 K) in order to analyze the motor's behaviour and its electromechanical characteristics and to define an electric equivalent circuit that allows describing its operation. From the obtained results it was observed that the tested HTS behaves as a conventional hysteresis motor even though with a different nature. On the other hand, the motor with aluminium rotor behaves as a conventional induction motor. In asynchronous regime, the HTS motor exhibits a constant torque, higher than the conventional aluminium one.

Keywords: High temperature superconducting motor · Polycrystalline YBCO · Axial flux disc motor

1 Introduction

In 1911, Kamerling Onnes found a new state of matter in mercury, which exhibited electric resistance when cooled below 4.2 K. This was named Superconductivity [1]. The interest in these materials was accentuated by the discovery of High Temperature Superconductors (HTS) possible to cool by relatively cheap liquid nitrogen (77 K). Research on these materials have led to the optimization and development of several power systems. HTS material have been used e.g. in machines, both as tapes or bulk. The HTS YBCO compound (with a current density up to 10^7 A·cm⁻² at liquid nitrogen temperature) has been applied in electrical machines, such as hysteresis [2], reluctance [3], or trapped flux motors [4]. The former present a complex behaviour,

showing both synchronous and asynchronous regimes, similar to hysteresis conventional motors, although the operation principle is different [2]. The ability of trapping high magnetic flux, transporting high current densities, and its diamagnetism phenomena and hysteretic ability made HTS materials attractive, presenting reduced size and losses, for the same power, relatively to its conventional counterpart [5]. This lead to the research question "does polycrystalline HTS hysteresis motors show better electromagnetic characteristics than aluminium ones?".

2 Relationship to Cloud-Based Solutions

The study of an axial flux disc motor with the rotor in HTS polycrystalline material or aluminium , for several poles pairs configurations is preformed in this paper . All the obtained results could be shared in a cloud-based system allowing other researchers to perform analysis, and providing data backup an on-time data monitoring.

3 Developed Motor

Typically, the output power of rotating machine, P_{out} , may be expressed according to (1) [7], where $B_{g,max}$ is the maximum airgap flux density, $A_{g,max}$ is the maximum stator linear current, N_{mec} is the rotor speed and V is the active volume. The use of superconducting materials allows a higher flux density in the airgap, increasing the developed power.

$$P_{out} \propto B_{g,max} \cdot A_{s,max} \cdot N_{mec} \cdot V \quad (1)$$

3.1 Topology

The built disc motor, is composed by two 20 cm diameter conventional semi-stators with 24 slots, a coil pitch of 4 slots, 24 conventional cooper windings each one, a steel shaft, a 20 cm diameter rotor disc, which can be aluminium or YBCO, two support bearings and fixing screws. The mechanical transmission is carried by conventional bearings dried by ultrasounds. Further details are given in [8].

3.2 Electromagnetic Characteristics

When stator is energized, it produces rotating magnetic field. This field magnetizes the rotor. For the aluminium rotor, the behaviour is known. For the HTS rotor, the field magnetizes the HTS material, which is penetrated with magnetic flux that is trapped in the pinning centres, inducing the same stator's poles number. Due to this, the superconductors' rotor rotates synchronous with stator field, acting as a magnet. For load values lower than the maximum motor's torque, it runs with synchronous

velocity. In steady state, there is a constant relative angle between the stator's and the rotor's magnetic field, which origins a constant motor torque proportional to the product of the amplitudes of two fields with the phase between them. For values of load higher than the maximum motor's torque, flux flow is present, and the motor runs with slip. The torque is proportional to the HTS materials losses.

3.3 Simulations

The motor was simulated with a commercial 2D finite elements program (Flux2D from Cedrat). The 2D limitation implied the simulation of a linearized version of the motor, considering longitudinal infinite continuous periodicity to avoid edge effects. All the non-HTS materials, (copper, aluminium and steel) were defined using Flux2D libraries. The HTS material was parameterized based in the E-J power law, with the parameters indicated in Table 1. HTS motor was analysed for 1, 2 and 4 pole pairs.

Table 1. Measured and predicted electrical parameters from experimental tests

Critical Electrical Field	E_c	$10^{-4} \text{ V}\cdot\text{m}^{-1}$
Critical Current Density	J_{c0}	$4,4 \times 10^7 \text{ A}\cdot\text{m}^{-2}$
Induction	$B_0 = B_1$	10^6 T
Exponent	n	15
Additional Resistivity	ρ_0	$10^{-13} \text{ }\Omega\cdot\text{m}^{-1}$

Transient dynamic simulations were performed. Motor startup is shown in Fig. 1 a), and force dependence on imposed velocity in Fig. 1 b), for no load conditions. From Fig. 1 a), it is possible to confirm that the motor with aluminium rotor exhibits an asynchronous behaviour while the motor with YBCO rotor presents synchronous behaviour. From Fig. 1 b) it is possible to conclude that both motor's developed a linear force proportional to the pole pairs, being higher for the YBCO motor, when compared with the aluminium. In YBCO motor, for synchronous speed the linear force tends to zero, due to the no-load assumed conditions.

3.4 Experimental Tests

In order to develop a model for the motor blocked-rotor, no-load and load tests were performed for aluminium motor while for the HTS rotor only blocked-rotor and load tests were performed, as this is a synchronous motor. The experimental apparatus consisted in a 3-phase power transformer; electrical and mechanical power measuring modules; and a DC machine, load cells and optical sensors for mechanical torque and speed measurements using the mechanical power module. During tests only the disc motor was immersed in liquid nitrogen inside a styrofoam box. All the apparatus are shown in Fig. 2.

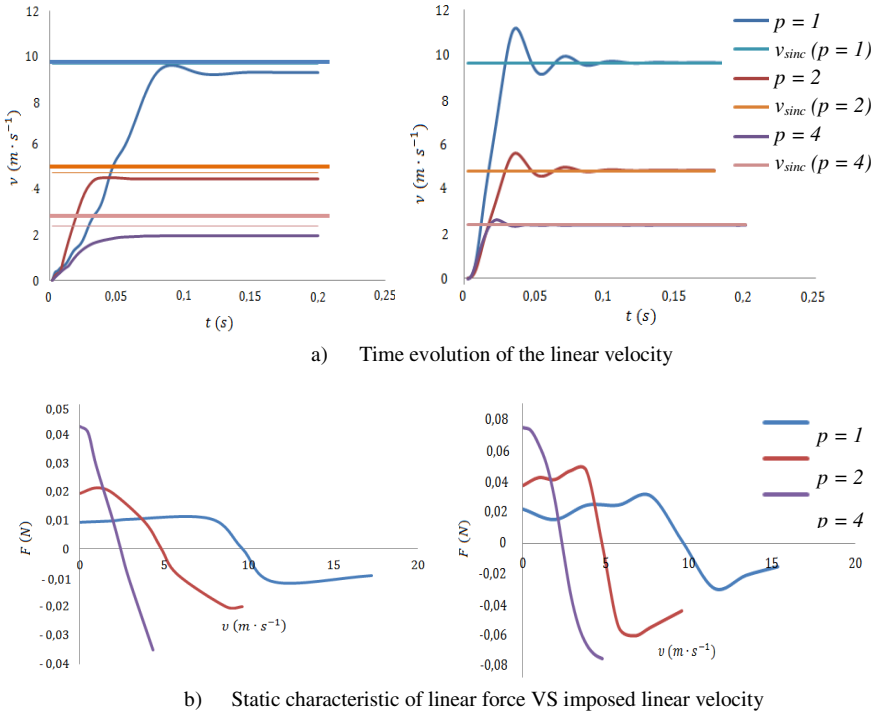


Fig. 1. Obtained FEM simulations for a) transitory dynamic and b) permanent regime conditions, for 1, 2 and 4 poles pairs in linear HTS and Aluminium motor, no load conditions

The motor was supplied by a wye connected 23 V, 50 Hz source for 1, 2 and 4 pair poles configuration. The mechanical load was based in a DC generator (controlled by two DC power supplies and a control resistor) driven by the motors’ shaft and feeding a resistive load.

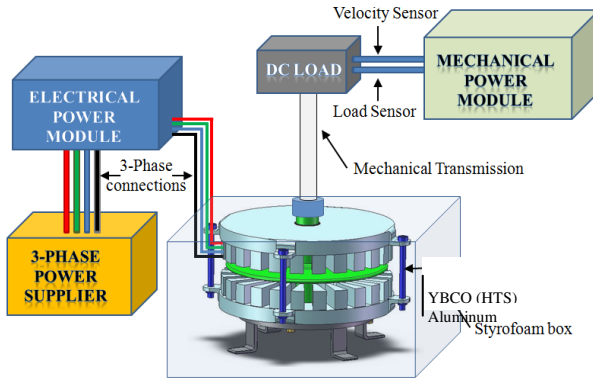


Fig. 2. Experimental apparatus for axial flux disc motor’s tests

The classic equivalent electrical circuit of the motor with aluminium rotor is shown in Fig. 3. From [9], the HTS rotor's motor can be described using the equivalent electrical circuit present in Fig. 3, where r_s , r_r and r_{fe} are the semi-stator's winding, the rotor's equivalent and the equivalent iron losses resistances while X_s , X_r and X_m are the semi-stator's, equivalent rotor's and magnetizing reactance's.

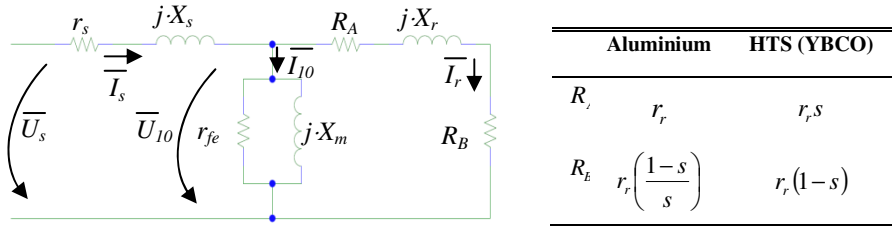


Fig. 3. Equivalent circuit for Aluminium motor and HTS (YBCO) polycrystalline bulk motor

Results from the blocked-rotor, no-load and load tests of the aluminium rotor (line current, I , line tension, U_c , the 3-phase electric power supplied, P_{ele} , the measured torque, T , and the mechanical rotor's velocity, N ,) were used to determine the parameters of the equivalent electrical circuit, and are synthesized in Table 2.

Concerning the HTS motor, parameters derivation was based in the parameters of aluminium motor since the HTS motor has the same semi-stators and supply system. The value of the magnetic losses, r_{fe} , was calculated based upon a similar induction motor case and considered the same for the both cases.

Table 2. Measured and predicted electrical parameters from experimental tests

Parameter	Aluminium			YBCO (HTS)	
	2	4	8	2	4
<i>Polar Configuration</i>					
r_s [Ω]	0.25	0.25	0.25	0.25	0.25
X_s [Ω]	0.317	0.346	0.325	0.317	0.346
X_r [Ω]	0.317	0.346	0.325	0.348	0.004
r_r [Ω]	0.038	0.045	0.039	0.371	0.134
r_{fe} [Ω]	40.2	41.7	46.1	40.2	41.7
X_m [Ω]	52.79	12.95	3.26	52.02	13.01
μ_r	--	--	--	0.0098	0.0103
δ	--	--	--	46.85	88.29

The theoretical analysis of the HTS motor, allowed defining the magnetization reactance, X_m , rotor's resistance, r_r , and rotor's dispersion reactance, X_r , as indicated in (3) – (5). The parameters used in (3) – (5) are detailed in Table 3.

$$X_m = \frac{(k_w \cdot N_{ph})^2 \cdot \omega \cdot m \cdot (r_o^2 - r_i^2) \cdot \mu_0}{l_g \cdot \pi \cdot p^2} \tag{3}$$

$$r_r = \frac{2 \cdot (k_w \cdot N_{ph})^2 \cdot \omega \cdot m \cdot (r_o^2 - r_i^2) \cdot \mu_0 \cdot \mu_r \sin(\delta)}{t_r \cdot \pi \cdot p^2} \tag{4}$$

$$X_r = \frac{2 \cdot (k_w \cdot N_{ph})^2 \cdot \omega \cdot m \cdot (r_o^2 - r_i^2) \cdot \mu_0 \cdot \mu_r \cos(\delta)}{t_r \cdot \pi \cdot p^2} \tag{5}$$

The analysis of equivalent circuit present in Fig. 3, allows conclude that the input impedance, \bar{Z}_{in} , is given in (6), being \bar{Z}_s the stator’s impedance, \bar{Z}_T the transversal impedance and \bar{Z}_r the rotor’s impedance.

$$\bar{Z}_{in} = \bar{Z}_s + \bar{Z}_T // \bar{Z}_r, \begin{cases} \bar{Z}_s = r_s + jX_s \\ \bar{Z}_T = r_{fe} // jX_m \\ \bar{Z}_r = (r_r \cdot s + (1-s) \cdot r_r) + jX_r \end{cases} \tag{6}$$

From the blocked rotor test, it’s possible to obtain \bar{Z}_{in} . Solving (5) in order to \bar{Z}_r it’s possible to obtain the values of μ_r and δ , which are present in Table 1. Using the values indicated in Table 3 and equations (3) – (5) it’s possible to predict the values of X_m , r_r , and X_r . They are indicated in Table 2 for 2 and 4 poles. As is possible to observe, the impedance is inversely proportional to the square of the number of pair poles. For 8 poles the current “asked” to the power supply exceeds the maximum available (25 A). For that reason, we only perform the experimental tests for 2 and 4 poles.

Table 3. Parameters of axial flux disc motor

Parameter		Value	Units
Outer rotor’s radius	r_o	100	mm
Inner rotor’s radius	r_i	10	mm
Airgap	l_g	5	mm
Rotor’s thickness	t_r	10	mm
Winding factor	k_w	0.5	-
Number of turns, per phase	N_{ph}	528	turns
Frequency	f	50	Hz
Number of phases	m	3	-

The theoretical electromechanical characteristics were computed, based on the experimentally obtained parameters and using the theoretical analysis above described, and compared with the experimentally obtained characteristics in tests. In Fig. 4 is shoed the comparison between the torque produced in the aluminium rotor’s motor and YBCO rotor’s motor. As is possible to observe, the experimental characteristics tend to evolutes coherent with the theoretically predicted ones.

Comparing with the simulated results, it's possible to conclude that the studied motor behaves as expected, however with lower values of torque. It is also important refer that the predicted quantities are related with the torque electrodynamically developed, or internal power, while the measured ones refer to the available quantities in the motor's shaft, which differ from the first ones by the mechanical losses. The main mechanical losses are the viscosity friction in the liquid nitrogen and the friction in the conventional bearings working at low temperature that should be included in the theoretical prediction.

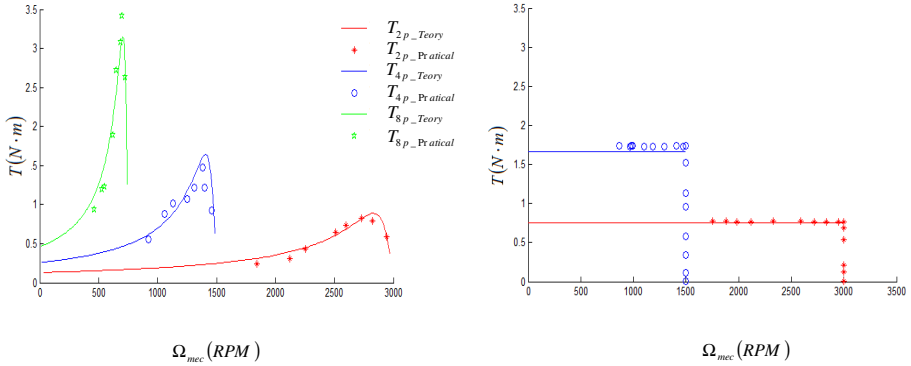


Fig. 4. Comparison between theoretical and experimental developed torque for aluminium rotor's motor (left side) and YBCO rotor's motor (right side)

4 Conclusions

Flux2D simulations allowed confirming that, for different configurations of poles, the HTS motor exhibits a synchronous behaviour in steady state and the developed force increase with the poles pair, inversely to synchronous speed.

The comparison of simulated, experimental and theoretical results allows conclude that all the characteristics are consistent each them, being possible to observe both synchronous and asynchronous regimes of the HTS motor. The comparison of the developed torques between the aluminium and HTS rotors showed that even for insufficient operating conditions, due to current supply limitation, the motor in bipolar configuration with the HTS rotor a has a higher torque developed compared with the aluminium one. Nevertheless, in tetrapolar configuration, the developed torque in the former is lower when compared to the conventional motor.

Acknowledgments. The authors thank to CTS - UNINOVA and FCT (CTS multiannual funding - PIDDAC Program funds) for the financial support for the work.

References

1. Kamerlingh-Onnes: The Superconductivity of Mercury, *Comm. Phys. Lab. Univ. Leiden*, Nos. 122 and 124 (1911)
2. Barnes, G.J., Dew-Hughes, D., McCulloch, M.D.: Finite difference modelling of bulk high temperature superconducting cylindrical hysteresis machines. *IOP Science: Superconductor Science and Technology* 13, 229 (2000)
3. Kovalev, L.K., Ilushin, K.V., Kovalev, K.L., Penkin, V.T., Poltavets, V.N., Koneev, S.M.-A., et al.: High output power electric motors with bulk HTS elements. *Physica C: Superconductivity* **386**, 419–423 (2003)
4. Miki, M., Felder, B., Tsuzuki, K., Deng, Z., Shinohara, N., Izumi, M., et al.: Influence of AC Magnetic Field on a Rotating Machine With Gd-Bulk HTS Field-Pole Magnets. *IEEE Transactions on Applied Superconductivity* **21**(3), 1185–1189 (2011)
5. Inácio, D., Pina, J., Gonçalves, A., Ventim-Neves, M., Rodrigues, A.L.: Numerical and Experimental Comparison of Electromechanical Properties and Efficiency of HTS and Ferromagnetic Hysteresis Motors, In: 8th European Conference on Applied Superconductivity (EUCAS 2007), Belgium (2007)
6. Tinkham, M.: *Introduction to Superconductivity*. McGraw-Hill (1996)
7. Vajda, I., Szalay, A., Gobl, N., Meerovich, V., Sokolovsky, V.: Requirements for the industrial application of superconducting rotating electrical machines. *IEEE Transactions on Applied Superconductivity* **9**(2), 1225–1228 (1999)
8. Inácio, D., Inácio, S. Pina, J., Valtchev, S., Ventim-Neves, M., Martins, J., Rodrigues, A.L.: Conventional and HTS disc motor with pole variation control, In: International Conference on Power Engineering, Energy and Electrical Drives, POWERENG 2009, Portugal, pp. 513–518 (2009)
9. Jung, H., Nakamura, T., Tanaka, N., Muta, I., Hoshino, T.: Characteristic analysis of hysteresis-type Bi-2223 bulk motor with the use of equivalent circuit. *Physica C* **405**, 117–126 (2004)

Investigation of the Tesla Transformer as a Device for One-Wire Power and Signaling and as a Device for Power and Signaling Through the Ground

Kaloyan Mihaylov¹, Rui Neves-Medeiros², Rumen Arnaudov^{1(✉)},
and Stanimir Valtchev²

¹Department of Telecommunications, Technical University of Sofia, Sofia, Bulgaria
kaloyan.mihaylov@gmail.com, ra@tu-sofia.bg

²Department of Electrical Engineering, UNINOVA,
Nova University of Lisbon, Caparica, Portugal
ssv@fct.unl.pt, rnm@uninova.pt

Abstract. A new method for power and communications through single wire or the ground as a medium is investigated. The focus of the research is based on the proper construction and operation of a Tesla Transformer, so as to be able to transmit power and/or signals through one wire or the ground. The conclusions are based upon experimental data. There are successful results for single wire power supply with efficiency of about 20%. There is room for improvement of the circuits, so better efficiency is expected. The utilization of the soil as a medium for currents propagation didn't give any useful results. Due to its complex properties, the ground transmission requires lower working frequency, hence bigger and more complicated coils, special drive circuit and good grounding.

Keywords: Single wire power · Single wire signalling · Power through the ground · Ground communications · Tesla coil · Tesla transformer · Quarter wave resonator

1 Introduction

The idea for wireless electricity is not new. The first experiments in this field began in the end of the 19th century. The most fascinating proposal was the Tesla's idea to send electrical power to every point on the globe by utilizing a giant low-frequency transmitter [1]. Most of his experiments are associated with the production of very high voltages for fun, although this is not the case. As it will be seen below, the electrical discharge or sparking is an unwanted side effect of his famous transformer. However, the scale of the Tesla's construction doesn't permit easy reproduction of those effects. Scaled-down models could be used to investigate the working principle of the transformer.

The main topics presented in the paper are the transformers construction, single wire experiments and ground experiments. Chapters 3, 4 and 5 describe the basic principles that we have obeyed during the building of the coils and conducting the experiments, and in chapters 6 and 7 there are the results.

In chapter 3 it is stressed that the secondary coil of the transformer behaves like a distributed-elements circuit, not as lumped elements one.

In chapter 4 is represented the method to find the resonant frequency of the coil. It is the starting point for energy transmission, because other frequencies doesn't work.

Due to its nature, in chapter 5 we have suggested the most useful methods to calculate the secondary coil of a Tesla transformer. The fully theoretical approach isn't precise enough, therefore we have focused our attention on more robust methods.

In chapter 6 we have shown the results of single wire power transfer. There are successful results.

Chapter 7 is dedicated to ground transmission experiments. We haven't got any measurable result for ground transmission. Because there are some successful attempts for ground transmission by other researches, some directions were given.

2 Relationship to Cloud-Based Solutions

The focus of cloud computing is usually computational performance, storage, network connectivity and collaboration. In order to deeply influence everyday life, a lot of small devices are brought in the network. Remote data acquisition and control techniques require a good network connectivity and power supply. However, there is no "one for all" solution. A lot of different tools exist for data or power transmission, like low-power wireless transceivers, optical transceivers and energy harvesting devices of different kind.

The aim of our experiments is to discover new methods for data transmission together with secure power supply. The single wire solution has shown its potentialities. Small portions of power were successfully transmitted over short distances. The true utilization of only one wire could enable further development and introduction of sensor nodes or electronic devices of other choice.

This method could be used in places where energy harvesting modules cannot bring the power needed to operate a device. Another advantage is the more robust communication between the devices (for example in noisy wireless environment).

Drawback of the system is the need of a conductor. However there are some developments that investigate the possibilities to use the ground instead of single wire. The circuits require much higher power levels and the propagation of the power is different from the single wire system, but the resonator coil and the principles are the same. Despite the lower frequencies, the ground is another medium that could be added to the existing communication solutions.

The results in this area of research give us conviction, that these methods will soon be ready to take place in the civil and industrial development, hence ensuring wider connectivity of different devices to the cloud.

3 Common Construction Mistakes

As it was stated above, the most common mistake is the consideration of the Tesla's resonator as a lumped element system [4]. Solution of the inductance and the capaci-

tance for a lumped element would not reveal any useful information for the constructor. The most common formulas of Wheeler and Nagaoka are valid for low-frequency designs.

In fig. 1 there is a typical example of poorly designed secondary. It consists of 5550 turns of 0.18 mm solid copper wire. Height of the coil is 1 m, and the diameter of the coil is 2 cm. The use of very thin wire leads to higher pure resistance, hence lower Q factor of the coil.



Fig. 1. Example of poorly constructed quarter-wave resonator coil

Another problem of such a coil is its height to diameter ratio. The higher length to diameter ratio increases the self-capacitance of the coil [6.3, p. 452]. It was found that the coil shown in fig. 1 has great amount of variable capacitance, dependent on the objects near the test setup. Therefore it has also low Q factor and weakly detected resonant frequency. According to [3, p. 452, table 1] the single-layer solenoids have lowest capacitance when their height to diameter ratio is about $0.5 \div 2$. Due to its high self-capacitance, the coil could be used as a sensor.

4 Experimental Approach for Detecting the Coil's Resonant Frequency

Since the secondary of a typical Tesla Transformer is described by the distributed element approach, it should be indicated what current/voltage distribution is expected. In fig. 2 there is the general case of a typical secondary coil.

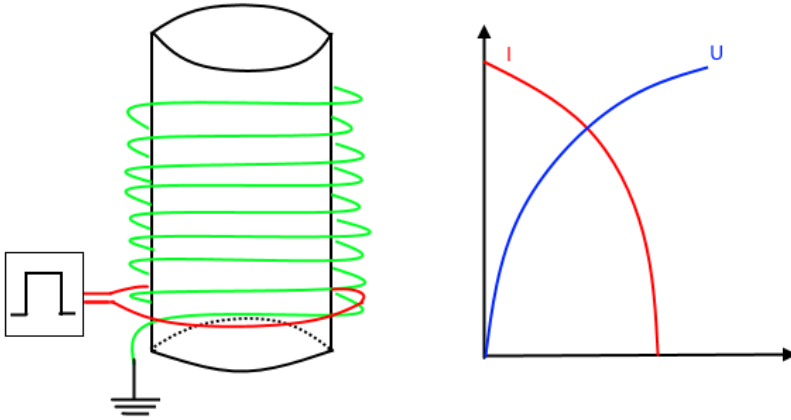


Fig. 2. Representation of the voltage-current distribution along a resonator coil

The current in the base of the coil is high and diminishes along the height of the coil. The voltage in the base is small, but increases along the coil height.

If the primary coil is impulse-fed, then the secondary oscillates on its natural resonance. The output voltage is measured with a scope's probe on top of the coil, without direct connection. The grounding pinch of the probe should be removed for accuracy. Ordinary signal generator could be used, even simple PWM circuit as SG3525 or TL494 to drive the primary, but only to find the resonant frequency of the secondary.



Fig. 3. Oscillogram of one of the driving channels of SG3525 and the response of the resonator

In fig. 3 the oscilloscope probe #1 is connected to one of the SG3525 outputs. The drive frequency is about 60 kHz. The second output is connected to a 1-turn primary of an arbitrary chosen air-core coil. *Note: the phase difference between channel 1 and channel 2 is because of the second output used to monitor the drive frequency. The actual voltage waveform of the first output (connected to the primary) does not correspond to the waveform of channel 1, due to the loading. The drive impulse exact time is marked with a red line on the oscillogram.*

The resonant frequency of the secondary coil is about 250 kHz. The experimenter should tune the drive frequency and duty cycle to achieve maximum amplitude. Also one must be careful of nearby objects around the coil. The human body strongly influences the parameters of the secondary, especially if it has a lot of turns and bigger self-capacitance.

5 Calculation of the Secondary Self-Resonant Frequency

In section 3 the most critical mistakes were given. To summarize, they are the use of thin wire and the high height to diameter ratio. Solid copper is preferred. The authors of the paper have the view that multistranded wire could be more suitable for the purpose if the separate strands are not insulated from each other. The insulation of the strands leads to higher inter-strands capacitance, hence lower frequency and Q of the coil.

The best method for coil calculation that we found suitable for our purposes is the GeoTC JavaScript library by the Tesla Secondary Simulation Project [2]. We have found that the calculations of the non-loaded bare (without top-load) secondary are within the pointed error limit. Other programs like E-Tesla6 (by Terry Fritz) could be more suitable if better accuracy is sought. A mixed Java/JavaScript web application based on GeoTC is FanTC (<http://www.classictesla.com/fantc/fantc.html>) which is used in our experiments.

6 Experimental Results for One-Wire Transmission

To conduct the experiments two pieces of plane PCB transformers were used.

The characteristics of the two types of transformers are given in table 1. In each of the cases the shorter coil (primary) is the exciting or load coil, and the longer coil (the secondary) is the resonator coil. The outer ends of the two secondaries are connected via 70 cm multistranded wire. The inner end of each secondary is connected to a 20 cm bolt used for capacitive loading of the resonator.

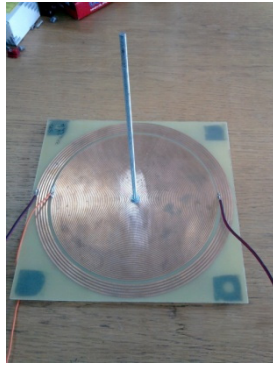


Fig. 4. Example of one of the transformers used in the experiments

Table 1. Characteristics of the transformers

Parameter	Transformer 1	Transformer 2
Number of turns (secondary)	60	100
Wire width	0.882 mm	0.353 mm
Turn spacing	0.482 mm	0.635 mm
Inner diameter	0	0
Outer diameter	163.7 mm	197.6 mm
Length of wire	15.426 m	31.038 m
Inductance	193.3	648.3

The circuit schematic is shown in fig. 5. R1 has the value of 10 Ohms and is used to measure the input current. R2 has variable resistance and it is used to measure the maximum power point. The diode bridge is compound of 4 BAT754 Schottky diodes with 200mV of voltage drop for each diode.

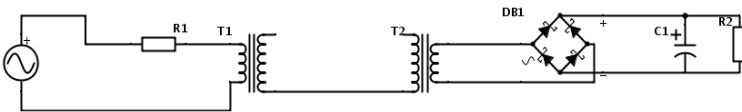


Fig. 5. Schematic of the connection of the transmitter and the receiver

Part of the data for a test setup which utilizes Transformer 1 is shown in Table 2.

Table 2. Input and output power

Frequency	Input power	Output power	Efficiency	Note
5.19E6	11.5 mW	0.87 mW	8%	Loading - bare bolt
3.87E6	12.16 mW	1.54 mW	13%	Loading - aluminium can

In the “Note” column there is a remark of how the secondary coil is loaded. In order to achieve maximum Q of the coil, minimum capacitance should be introduced. However, it was found that some capacitance should be added for better energy transmission. The details of how exactly the capacitive loading influences the power transmission are not deeply studied yet.

Also it should be noted, that in the power balance there is a big amount of loss in the R1 resistor, which is used to measure the current in the primary coil and great voltage drop at the receiver’s diode bridge. In table 3 the values of the experiments with “Transformer 2” styled coils are given.

Table 3. Values of experiments with Transformer 2

Frequency	Input power	Output power	Efficiency	Note
2.58E6	10.6 mW	1.3 mW	12.3%	Loading - bare
1.96E6	11.7 mW	1.05 mW	8.95%	Loading - can
1.93E6	8.09 mW	1.8 mW	22%	Loading - can

7 Experimental Results for Ground Transmission

30 cm long, 8 mm diameter copper pipes were used for grounding the transmitter and the receiver coils. The test setup is shown in fig. 7.

There was no measurable output power. The diode bridge DB1 was removed so as the secondary of T2 to be open circuit. Then a measurement on both ends of the circuit was conducted with digital oscilloscope, but no signal was detected.

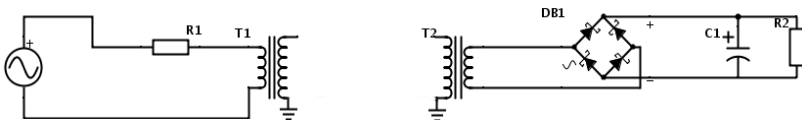


Fig. 6. Test setup of the ground transmission system

At a distance of up to 3 m there was mutual inductance between the coils. Any presence of power cords pushes an error in the measurements. The human body and movements around the transformers does influence the working conditions of the system.

8 Conclusions

The objectives of the experiments were examination of the possibilities to use a quarter-wave transformer as a power source for single wire power cord or power transmission through the ground. Two types of plane PCB transformers were used. To minimize RF interference and EM radiation from the system, the lower frequencies were preferred. Power levels of about 1 mW at the receiver’s side were obtained, which satisfies some of the modern low-power electronic devices (such as the STM32L-

series MCUs). These power levels are DC values after a bridge rectifier, so there is room for improvements.

The utilization of the system with ground as a medium for power transmission didn't give measurable results. The measurements included bare oscilloscope connection to the receiver's secondary without amplifier. However, there are promising results of utilization of a 136 kHz Tesla Coil transmitter with detectable signal at 5.5 km distance. [5]. Due to the properties of the soil, a different type of resonators should be used. The working frequency should be lower, hence bigger coils. The drive circuit should be optimized for higher power levels.

It should be noted that the aim of the experiments isn't maximum efficiency, but prove of the effect. Hence the system's performance is highly influenced by a lot of factors. The coupling between the primary and the secondary, mutual inductance, rectifier's efficiency, matching and other important factors are left out of consideration.

References

1. Tesla, N.: Patent #787412: Art of transmitting electrical energy through the natural mediums (1905)
2. Nicholson, P.: Tesla Secondary Simulation Project: Document pn2511
3. Langford-Smith: Radiotron Designer's Handbook, p. 452 (1957)
4. Corum, K.L., Corum, J.F.: Tesla Coils and the Failure of Lumped-Element Circuit Theory (1999)
5. Peterson, G.L.: Yahoo! Group "wireless_energy_transmission", post #2083

Experimental Magnetic Field Mapping of a Polycrystalline Superconducting YBCO Disc for an Axial Flux Motor

David Inácio¹(✉), João Murta Pina¹, José Maria Ceballos²,
Mário Ventim Neves¹, and Alfredo Álvarez²

¹CTS, Uninova, Departamento de Engenharia Electrotécnica, Faculdade de Ciências e Tecnologia, FCT, Universidade Nova de Lisboa, 2829-516 Caparica, Portugal
ddi@campus.fct.unl.pt

²Department of Electrical Engineering, Escuela de Ingenierias Industriales, Universidad de Extremadura, E-06006 Badajoz, Spain

Abstract. The method of creating large and complex-shaped melt-textured YBCO bulks based in artificial welding seeds opens the door to the study of applications with polycrystalline superconductor samples. In order to evaluate the superconducting quality of the bulks, Hall probe mapping can be applied in order to measure trapped flux field profiles after magnetisation. This paper describes the magnetic field mapping of an axial flux motor with a polycrystalline high temperature superconductor (YBCO) disc rotor at liquid nitrogen temperature (77 K). An axial flux hall probe is used and magnetic field profiles have been obtained for different polar configurations of a three-phase stator winding which will be operated at 50Hz. After the magnetization of the HTS disc trapped flux is measured, and its magnitude depends on the polar configuration and magnitude of the applied field.

Keywords: High temperature superconducting motor · Polycrystalline YBCO · Axial flux disc motor · Magnetic field mapping

1 Introduction

The application of melt-textured YBCO in power applications (motors, transformers, current limiters, etc.) requires manufacturing complex-shaped pieces, some with large sizes. Such large bulks are usually build using artificial welding of separate mono-grains from it, grown by the Top-Seeding technique. Different joining techniques have been proposed, based on the use of low-melting point welding agents like oxides [1] or YBCO/Ag composites [2]. Recently, new methodologies based on surface melting have been developed, leading to high quality welds [3]. The need to evaluate the quality of the superconducting joins has stimulated the development of different experimental characterization methods, as Hall probe mapping magnetometry [4].

The operation of the HTS disc motor is based in the vortex's dynamics within the HTS material due to the magnetic field variations imposed by the three-phase supply. The field in the HTS material depends on its magnetic history, exhibiting several

magnetic excursion that defines the operation regimes of the motor: in the synchronous regime, the rotor is synchronous with the stator rotating magnetic field due to trapped flux; however, in the asynchronous regime the rotor’s magnetic field slides over it and flux flow is present, leading to losses and, consequently, torque. For the asynchronous regime, the torque is given by (1) [5], and is maximum when the rotor is all magnetized.

$$T = \frac{p^2}{2\pi} P_{H / cycle} \tag{1}$$

Since torque proportional to the losses in the HTS material, it is useful that as much HTS material as possible gets penetrated by flux in order to take advantage of the disc size. For that reason, a research question is defined, namely "Is it possible to magnetise all the HTS material?".

2 Relationship to Cloud-Based Solutions

Mapping of trapped flux in an HTS disc material is showed in this paper. In order to observe if all the material is magnetized, several mappings were obtained for different poles configurations. All the obtained results could be shared in a cloud-based system allowing other researchers to perform analysis, and providing data backup an on-time data monitoring.

3 Hall Measurement System

In order to observe the magnetization of the rotor, a Hall probe magnetic mapping system was developed allowing obtaining field profile in a matrix of points. It consists in a three-dimensional computer-controlled positioner connected to an axial flux hall probe attached to a mechanical arm which, after the rotor’s magnetization, collects the magnetic field data. The system is showed in Fig. 1.

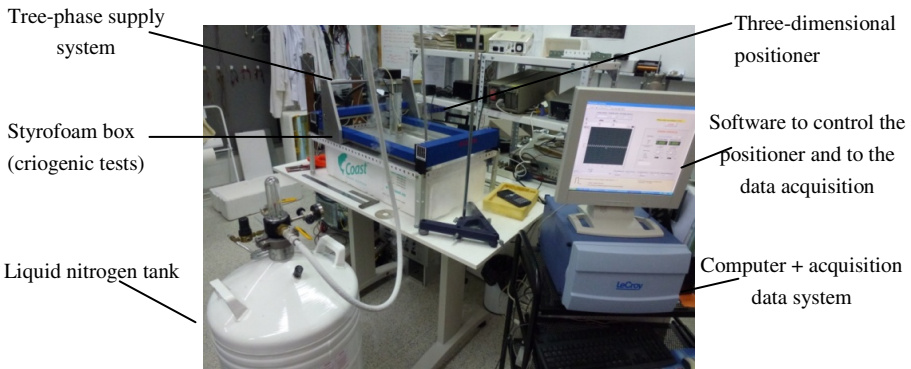


Fig. 1. Experimental apparatus for the static test of the HTS rotor

4 Topology of the Motor

The built disc motor is composed by two 20 cm diameter semi-stators with 24 slots and 24 conventional cooper windings each one, a steel shaft, a rotor consisting of a 20 cm diameter YBCO disc, two support bearings and fixing screws. Fig. 2 shows the device.

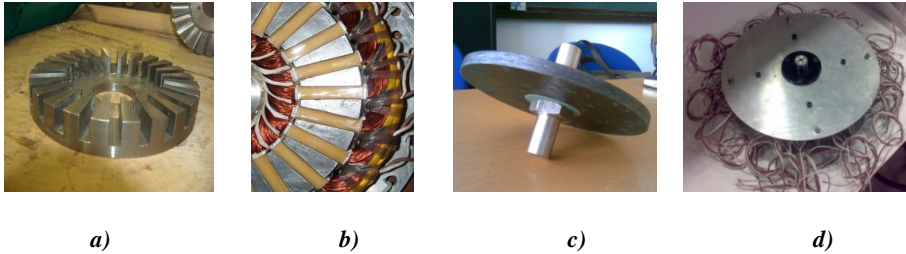


Fig. 2. Built motor: *a)* steel semi-stator; *b)* double cooper layer slot stator winding, *c)* polycrystalline YBCO rotor and *d)* full motor with two semi-stators

Spacing between the semi-stators and the rotor is regulated using adjustment nuts to ensure an airgap as small as possible. Dry bearings were used, after ultrasound treatment. The HTS material considered (YBCO) has a critical temperature of 90-92 K. For that reason, liquid nitrogen was chosen to cool the system due to its boiling temperature of 77 K.

5 Supply System

All the motor is submersed in liquid nitrogen during its operation. For that reason, the stator's cooper winding exhibit an electrical resistance significantly smaller when compared to room temperature, decreasing impedance. The input current was controlled by a 6 kVA DC power supply (0-15 V/0-400 A). The stators were wound with copper conductors with a 0.8 mm^2 cross section, allowing a maximum current of 8 A at room temperature. However, at liquid nitrogen temperature, this limit was considered superior.

As referred before, the rotor's magnetization was achieved using two semi-stators and a three-phase supply source, in bipolar and tetrapolar configurations, as showed in Fig. 3. In this figure a linear visualization of one semi-stator is illustrated.

Under normal operation the motor is supplied with a symmetric three-phase system as indicated in (2). In order to verify trapped flux capability of the rotor, only a static magnetization with three DC currents was applied.

$$\begin{aligned}
 I_1(t) &= I_m \sin(\omega \cdot t) \\
 I_2(t) &= I_m \sin(\omega \cdot t - 120^\circ) \\
 I_3(t) &= I_m \sin(\omega \cdot t - 240^\circ)
 \end{aligned}
 \tag{2}$$

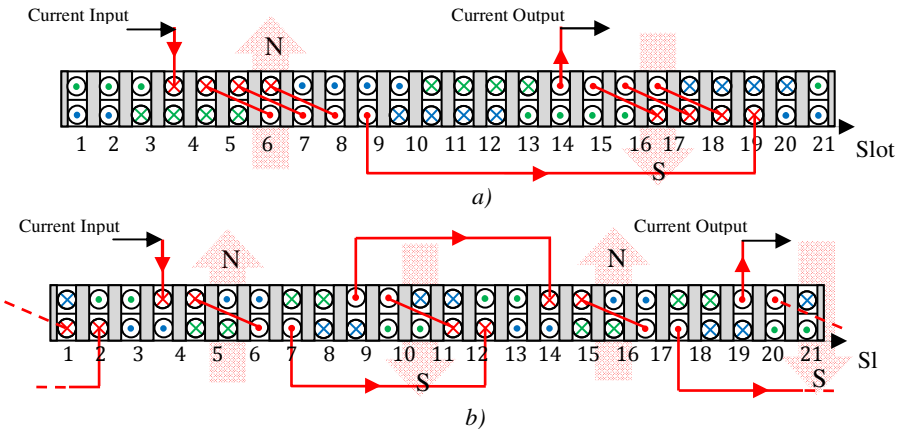


Fig. 3. Linear visualization of electrical connections, considering only phase 1, for a) bipolar configuration and b) tetrapolar configuration

Considering $t = 0$ s, the DC current in phase 1 is zero, in phase 2 is $-I_m \cdot (\sqrt{3}/2)$ and in phase 3 is $I_m \cdot \sqrt{(3/2)}$, where I_m is the magnitude of the current.

6 Data Acquisition System

The necessity of operation in cryogenic environment implies a specific support system made of bakelite to fix the Hall probe. Bakelite was chosen due to its low linear expansion coefficient. The probe supply was performed using a double layer cooper plate connected to an electronic module that allows probe calibration and data acquisition. The system is illustrated in Fig. 4.

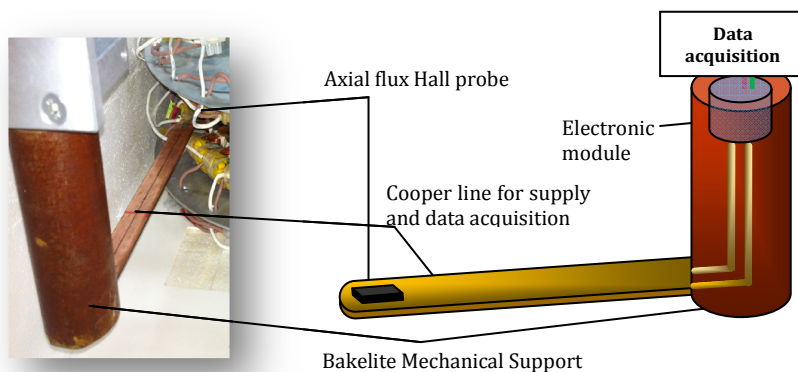


Fig. 4. Detail of the bakelite mechanical support for data acquisition

In order to obtain the matrix of magnetic field measurements, a three-dimensional computer-controlled positioner was used, allowing defining the xyz displacement and acquisition time. The data acquisition was performed as close as possible to the HTS disc, as detailed in Fig. 5. A data acquisition system was also used.

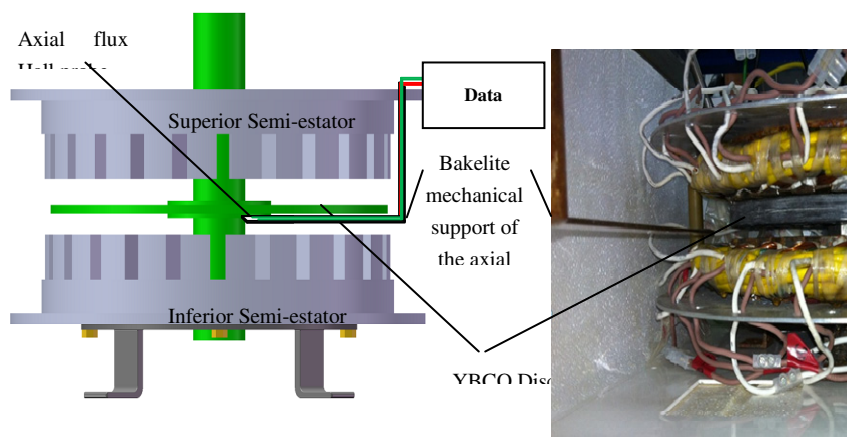


Fig. 5. Data acquisition system for recording data of the magnetic field mapping

Due to symmetry, measurements were performed only in half disc. In order to ensure a constant and secure distance to the probe, the disc was shimmed between the semi-stators. All the system for data acquisition (Hall probe + calibration) was connected to a magnetometer that allowed determining deviations between the beginning and the end of the recording data. The xy displacement step was 1.5 mm with an acquisition time of 0.5 seconds, to ensure the field stabilization. Thus, each measurement run took approximately two hours, allowing obtaining about 4500 points of field.

7 Obtained Magnetic Field Characteristic

The goal of the measurements was determining flux density distribution due to semi-stators excitation, at room temperature, as well as in rotor (trapped flux), at cryogenic temperature.

7.1 Magnetic Field Characteristic of Semi-Stators

These measurements were performed with a tetrapolar configuration and a maximum current of 11.5 A. From (2), for $t = 0$ s, the DC currents in phases 2 and 3 was -10 A and 10 A. These values were chosen in order to explore maximum current density of cooper windings, as the airgap was significantly increased to ensure scanning along the disc. Flux density measurements of semi-stators excitation at room temperature are showed in Fig. 6 *a*) for the entire disc, where it is possible to observe that it exhibits a maximum of 0.04 T. Two poles pairs configuration are observed, as expected.

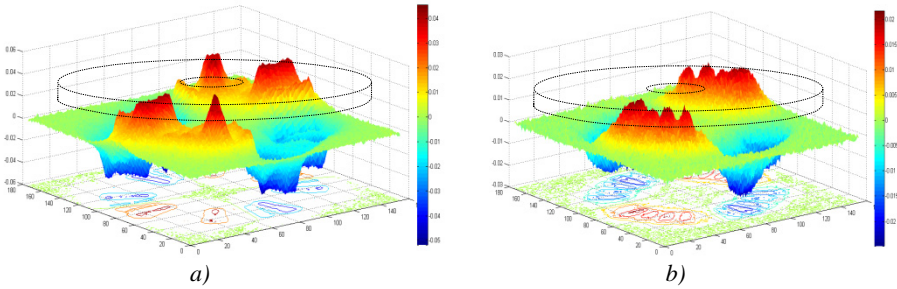


Fig. 6. Magnetic induction distribution, for tetrapolar configuration, *a*) due semi-stators supply, at room temperature and *b*) trapped in the rotor, after magnetization, at cryogenic temperature

7.2 Magnetic Field Characteristic of Rotor

As in previous measurements, this was performed using the tetrapolar configuration but at cryogenic temperature. Since the motor is submerged in liquid nitrogen, the stator's windings allow higher currents. The maximum current considered in this test was 34.6 A, leading to DC currents in phases 2 and 3 of -30 A and 30 A. The axial flux hall probe was calibrated for liquid nitrogen temperature.

After the magnetization, the supply system was turned off. Trapped flux mapping is showed in Fig.6 *b*). As it is possible to observe, profile is similar to Fig. 6 *a*), however, with different magnitudes, due to pinning characteristics of the material and since different currents were used in both measurements. From the comparison of Fig. 6 *a*) and Fig. 6 *b*) it is clear that the entire rotor is magnetized.

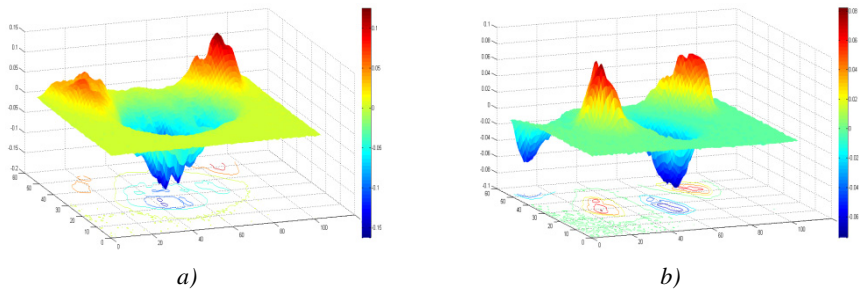


Fig. 7. Magnetic induction in half disc for *a)* tetrapolar *e b)* octopolar configurations, at liquid nitrogen temperature for $I_m = 127$ A

As described in (1), the developed torque is proportional to the rotor's trapped flux. Thereby, higher values of current in the stators imply higher trapped flux, up to a certain limit. Magnetic induction is showed in Fig. 7 *a)* (trapped flux) in the rotor, in half the disc, for tetrapolar configuration and $I_m = 127$ A. As is possible to observe, for a current 3.7 times higher, the trapped flux is, approximately, ten times higher. Measurements for the same current amplitude, but in octopolar configuration are showed in Fig. 7 *b)*. It is possible to observe, in half disc, four poles, which means that in full disc eight poles are present, as expected. Nevertheless, for these values of current amplitude, magnetic saturation is present in the ferromagnetic circuit, which must be taken into account in a detailed analysis.

8 Conclusions

In this paper a preliminary study is presented, describing experimental mapping of the magnetic induction characteristics of axial flux disc motor with the rotor composed by polycrystalline high temperature superconductor. As torque is proportional to the number of pole pairs, these were changed by means of electrical connections in the armatures. Field profiles from rotor and stator were obtained at room and liquid nitrogen temperatures.

Flux profiles allow verifying number of poles. Moreover, it is possible to conclude that entire disc rotor is magnetized. Thus, it is expected that, when the motor operate in asynchronous regime, a maximum "theoretical" torque may be achieved, since this is proportional to the losses in the superconducting material.

Acknowledgments. The authors thank to CTS - UNINOVA and FCT (CTS multiannual funding - PIDDAC Program funds) for the financial support for the work.

References

1. Salama, K., Selvamanickan, V.: Joining of high current bulk YBaCuO superconductors. *Appl. Phys. Lett.* **60**, 898–900 (1992)
2. Lo, W., Cardwell, D.A., Bradley, A.D., Doyle, R.A., Shi, Y.H., Lloyd, S.: Development of nonweak link bulk YBCO grain boundaries for high magnetic field engineering applications. *IEEE Trans. Appl. Supercond.* **9**, 2042–2045 (1999)
3. Puig, F.T., et al.: Self-seeded YBCO welding induced by Ag additives. *Physica C* **363**, 75–79 (2001)
4. Chen, C.L., Claus, H., Paulikas, A.P., Zheng, H., Veal, B.W.: Joining of melt-textured YBCO: A direct contact method. *Supercond. Sci. Technol.* **15**, 1–3 (2002)
5. Inacio, D., Pina, J.M., Luis, G., Martins, J.F., Ventim-Neves, M., Alvarez, A.: Experimental Characterization of a Conventional (Aluminum) and of a Superconducting (YBCO) Axial Flux Disc Motor. *IEEE Transactions on Applied Superconductivity* **21**(3), 1146–1150 (2011)

Energy: Power Conversion II

Analysis of a Multi-Ratio Switched Capacitor DC-DC Converter for a Supercapacitor Power Supply

Hugo Serra^(✉), Ricardo Madeira, and Nuno Paulino

Centre for Technologies and Systems (CTS) – UNINOVA
Department of Electrical Engineering (DEE), Universidade Nova de Lisboa (UNL)
2829-516 Caparica, Portugal
{has14926,r.madeira}@campus.fct.unl.pt, nunop@uninova.pt

Abstract. An energy harvesting system can use a supercapacitor in order to store energy; however, a voltage regulator is required to obtain a constant output voltage as the supercapacitor discharges. A Switched-Capacitor DC-DC converter allows for complete integration in CMOS technology, but requires several topologies in order to obtain a high efficiency. This paper presents the complete analysis of these topologies in order to determine expressions that allow to design and determine the optimum input voltage ranges for each topology. These expressions are verified using electrical simulations.

Keywords: DC-DC power converters · Switched capacitor circuits · Supercapacitors · Performance analyses · Design optimization · Efficiency

1 Introduction

In order to achieve infinite operation, electronic systems must obtain their energy directly from the surrounding environment [1]. This kind of procedure is commonly known as energy harvesting. Depending on the environment where the system is located at there are different energy sources that can be harvested [2]. In the case of systems with small size, the available energy is necessarily reduced, typically only providing a fraction of the necessary power needed for the operation of the system. Therefore, such a system has to be powered down while it harvests enough energy in order to work during a short time and then this cycle is repeated. This type of operation is useful for wireless sensor nodes, where the node only needs to report data periodically. This operation requires an energy storing device, which can be either a rechargeable battery or a supercapacitor. A rechargeable battery has the advantage of having a larger energy storing capacity, but its lifetime is seriously reduced by the number of charge/discharge cycles (typically the maximum number is around 1000 cycles). A supercapacitor has the advantage of having limitless charge/discharge cycles and being less expensive than a battery, but it stores much less energy than a battery for the same volume [3]. Depending on the mode of operation of the energy harvesting system, a battery, a supercapacitor or both can be used as the energy storing device. In the case of low power remote sensor that uses a power-down power-up cycle, it makes more sense to use a supercapacitor as the energy storage.

The energy stored in a capacitor is given by $E_c = 1/2 \cdot C \cdot V_c^2$, this means that as the capacitor supplies energy to the circuit its output voltage drops. As an example a 1 F supercapacitor charged to its maximum voltage (usually 2.3 V) can store 2.645 J, if this capacitor supplies energy for a circuit with a supply current of 20 mA during 10s, its output voltage would drop $\Delta V_c = I \cdot C = 200$ mV. Since the power supply voltage of the circuit should be constant it is necessary to have a voltage regulator between the supercapacitor and the circuit. In order to maximize the energy retrieved from the supercapacitor it is necessary for the voltage regulator circuit be able to both down-convert and up-convert the input voltage with an efficiency as high as possible. This prevents the use of a linear voltage converter because it can only step-down the voltage and its efficiency is reduced when the input voltage is much larger than the output voltage. The voltage regulator can be implemented using either an inductor based or a capacitor based DC-DC converter. The first option requires an inductor which is not feasible to implement in a CMOS integrated circuit. The second option can be fully integrated in a CMOS integrated circuit; however, switched-capacitor (SC) based DC-DC converters have maximum efficiency for a specific input output voltage ratio. This means that in order to maintain a high efficiency the SC voltage converter circuit has to change its topology as the input supercapacitor voltages decreases [4]. Therefore a careful analysis of each converter topology should be carried out in order to determine its efficiency as a function of the input voltage and the different parasitic capacitance of the circuit. This analysis will determine the voltages values that will result in a change in the voltage conversion factor.

2 Relationship to Cloud-Based Solutions

Cloud-based solutions rely on several servers, which are connected together through specialized connections, to distribute data processing tasks among them to overcome limitations in environments where the processing and information storage capability is lacking.

Wireless sensor networks which are integrated into cloud services, e.g. wireless sensor networks for real-time data collection, usually rely on batteries to supply energy to the nodes of the network. Due to the limited lifecycle of batteries, the long term sustainability of the wireless sensor network is compromised. An alternative is to use supercapacitors that acquire energy through energy harvesting systems. Unlike a battery, supercapacitors can charge/discharge an unlimited amount of times, however, a voltage regulator is needed to obtain a constant output voltage as the supercapacitor discharges. This paper analyses several SC DC-DC converters topologies in order to determine the optimum input voltage ranges for each topology.

3 Analysis of the SC DC-DC Converter Topologies

As previously mentioned, a SC based DC-DC converter has maximum efficiency for a given conversion factor between its input and output voltage. This means that as the supercapacitor discharges and its output voltage drops while the output voltage re-

mains constant, it is necessary to use different topologies for the SC converter circuit in order to maintain high efficiency. There is a compromise between the number of different topologies and the complexity of the circuit. In this case the input voltage can vary from 2.3V to 0 V and the output voltage should be held constant around 1 V. Assuming that a supercapacitor with 1F is used, the available energy, for the maximum voltage, will be 2.645 J. When the capacitor voltage is equal to 1 V the energy remaining in the capacitor is still 0.5 J and when it is equal to 0.7 V the remaining energy is only 0.245 J. This means that there is a small payoff in trying to up-convert input voltages smaller than 0.7 V, which would require a circuit with a voltage conversion factor larger than 2. After analyzing the efficiency of several voltage conversion circuits for the different input voltages, it was decided to use only 4 SC capacitor voltage converter circuits. These are depicted in Fig. 1 and correspond to the voltage conversion factors of $1/2$, $2/3$, 1 and $3/2$ [4]. Each of these converters is responsible for a given range of the input voltage (where its efficiency is maximized) and its clock frequency is adjusted in order to obtain an output voltage of 1 V at its output, independently of the input voltage and of the load. These 4 topologies can be combined into a single circuit with 3 capacitors that can be configured to any of the 4 topology using switches. In order to determine what are the input voltage ranges that maximize the efficiency for the different topologies it is necessary to analyze the behavior of each SC converter circuit to determine its operating parameters (efficiency and output voltage) as function of the different design parameters (capacitance values, clock frequency, etc) and the different non-ideal effects (e.g. parasitic capacitance, switch ON resistance).

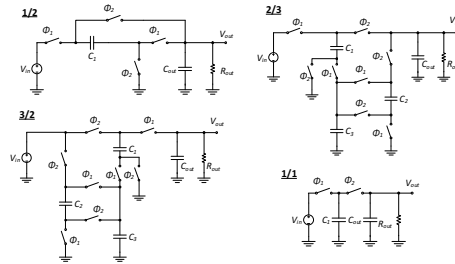


Fig. 1. Simplified schematics of the selected topologies for the SC converters

3.1 Analysis of the Efficiency of the $1/2$ SC Converter

Assuming that the clock frequency is adjusted in order to have the desired output voltage (e.g. $V_{out} = 1$ V) and that output decoupling capacitor C_{out} is large enough, it is reasonable to assume that the output voltage value is constant. In this case, the schematics of the $1/2$ SC converter circuit during phase ϕ_1 and ϕ_2 are shown in Fig. 2 and Fig. 3 respectively. In these schematics, C_B and C_T represents the bottom and top plate parasitic capacitances of C_1 and C_G represents the gate capacitance of all the

CMOS switches in the circuit. In each clock cycle, the switches drain a charge (ΔQ_{in2}) from V_{in} through the clock buffers. Using conventional switched-capacitor circuit analysis techniques [5] (Chapter 5) it is possible to determine the charge in each capacitor at the end of each clock phase. The resulting equations are shown in (1) and these allow to determine ΔQ_{in1} , ΔQ_{in2} , ΔQ_1 , and ΔQ_2 .

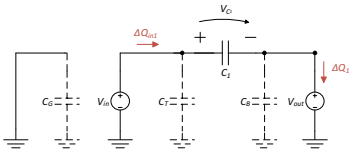


Fig. 2. Simplified schematic of the 1/2 SC converter during phase ϕ_1

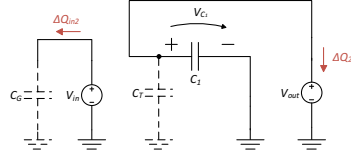


Fig. 3. Simplified schematic of the 1/2 SC converter during phase ϕ_2

$$\begin{cases} (V_{in} - V_{out}) C_1 + V_{in} C_T = V_{out} (C_1 + C_T) + \Delta Q_2, \\ 0 = V_{in} C_G + \Delta Q_{in2}, \\ -V_{out} C_1 = (V_{out} - V_{in}) C_1 + V_{out} C_B + \Delta Q_1, \\ V_{out} (C_1 + C_T) = (V_{in} - V_{out}) C_1 + V_{in} C_T + \Delta Q_{in1}. \end{cases} \quad (1)$$

The input (P_{in}) and output (P_{out}) power are calculated using ΔQ_{in1} , ΔQ_{in2} , ΔQ_1 , and ΔQ_2 and the values of V_{in} and V_{out} and are given by

$$\begin{cases} P_{in} = I_{in} V_{in} = V_{in} (\Delta Q_{in1} + \Delta Q_{in2}) F_{CLK}, \\ P_{out} = I_{out} V_{out} = V_{out} (\Delta Q_1 + \Delta Q_2) F_{CLK}. \end{cases} \quad (2)$$

The efficiency (η) is defined as the ratio between P_{out} and P_{in} , with $V_{out} = 1$ V, it is given by.

$$\eta_{1/2} = \frac{C_B + C_T - C_T V_{in} - 2 C_1 (V_{in} - 2)}{V_{in} (-V_{in} (C_1 + C_G + C_T) + 2 C_1 + C_T)} \quad (3)$$

The 1/2 SC converter circuit was simulated in Spectre with ideal switches and capacitors for different input voltages between 2 to 2.5 V and with V_{out} fixed at 1 V. From these transient simulations its efficiency was calculated and compared to the efficiency calculated using (3) for different parasitic capacitance values. The resulting efficiency values as a function of V_{in} and of the parasitic capacitance ($C_G = C_T = C_B$) assuming 0%, 1%, 5% and 10% are plotted in Fig. 4. These simulation results prove that (3) accurately describes the behavior of the efficiency of the converter and validates the theoretical analysis.

3.2 Analysis of the Output Voltage of the 1/2 SC Converter

A similar analysis can be performed in order to determine the output voltage of the SC converter, assuming that its output is connected to a load resistor (R_{out}) and a decoupling capacitor (C_{out}) with a very large time constant compared to the clock period ($C_{out} \times R_{out} \gg T_{CLK}$). In this case V_{out} is constant during each clock cycle.

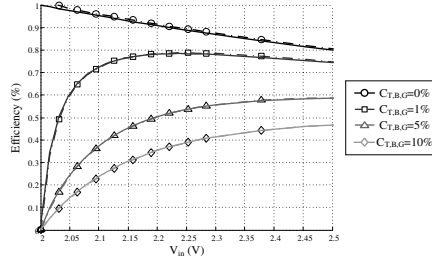


Fig. 4. Efficiency of the 1/2 SC converter circuit as a function of V_{in} and of $C_G = C_T = C_B$

$$\left\{ \begin{array}{l} (V_{in} - V_{out}[n-1]) C_1 + V_{in} C_T + V_{out}[n-1] C_{out} = \\ \quad = V_{out} \left[n - \frac{1}{2} \right] \left(C_1 + C_T + C_{out} + \frac{T_{CLK}}{2 R_{out}} \right) \\ -V_{out} \left[n - \frac{1}{2} \right] C_1 + V_{out} \left[n - \frac{1}{2} \right] C_{out} = \\ \quad = (V_{out}[n] - V_{in}) C_1 + V_{out}[n] \left(C_B + C_{out} + \frac{T_{CLK}}{2 R_{out}} \right) \end{array} \right. \quad (4)$$

The resulting equations are shown in (4). Solving in order to $V_{out}[n]$ and then considering the steady state condition ($V_{out}[n] = V_{out}[n-1] = V_{out}$), allows to calculate V_{out} (5). In order to simplify (5) it is possible to assume that $C_{out} \gg C_1$ resulting in (6).

Fig. 5 represents V_{out} as a function of the frequency for $V_{in} = 1V$: the solid lines are the plot of (6) and the marks correspond to the simulation results. These validate expression (6). This graph shows that it is possible to control the value of V_{out} by adjusting the clock frequency.

$$V_{out} = \frac{2 V_{in} F_{CLK} R_{out} (C_1 + 2 C_{out} F_{CLK} R_{out} (2 C_1 + C_T))}{1 + 2 F_{CLK} R_{out} (2 C_1 + C_B + 2 C_{out} + C_T + 2 F_{out} R_{out} (C_{out} C_T + C_B (C_{out} + C_T) + C_1 (C_B + 4 C_{out} + C_T))} \quad (5)$$

$$V_{out} = \frac{(2 C_1 + C_T) F_{CLK} R_{out} V_{in}}{1 + (4 C_1 + C_B + C_T) F_{CLK} R_{out}} \quad (6)$$

Using (6) to calculate the clock frequency for a given V_{out} results in

$$F_{CLK} = \frac{V_{out}}{R_{out} (2 C_1 (V_{in} - 2 V_{out}) + C_T (V_{in} - V_{out}) - C_B V_{out})} \quad (7)$$

Fig. 6 shows the plot of (7) for $V_{out} = 1V$, $P_{out} = 10 \text{ mW}$ ($R_{out} = 10 \Omega$) and $P_{out} = 100 \mu\text{W}$ ($R_{out} = 10 \text{ K}\Omega$). As V_{in} approaches the conversion ratio ($V_{in} = 2V$), the clock frequency becomes infinite.

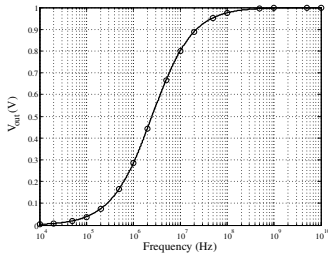


Fig. 5. V_{out} as function of the clock frequency

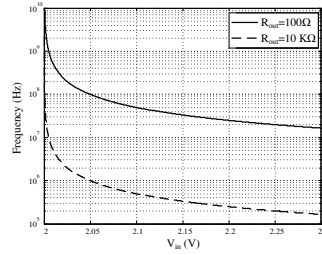


Fig. 6. Clock frequency as function of V_{in} for $V_{out} = 1V$

4 Circuit Design

In the previous section a theoretical study of the 1/2 converter was carried out. The behavior of the other three converters was determined using the same methodology.

The 1/1 converter, C_1 is only affected by the top plate parasitic capacitance (C_T), because the bottom plate capacitance is shorted to ground in both phases. Since C_T is charged and discharged in parallel with C_1 , there is no charge lost to ground through C_T . This means that the efficiency of this converter is not degraded by C_T . Only the gate capacitance from the switches causes a decrease in the efficiency.

The 2/3 and 3/2 converters have a similar topology except for the switches that connect to V_{in} and to V_{out} . In these converters, there are five parasitic capacitances: C_{T1} , C_{B1} , C_{T2} , C_{B2} and C_{T3} . Where the number 1, 2 and 3 refers to C_1 , C_2 and C_3 , respectively. The analysis showed that C_{T3} has no impact on the efficiency. Similarly to the 1/2 converter, this is because C_{T3} charges and discharges in parallel with C_3 in both phases. The other four capacitances result in a decrease in η .

In order to better understand the design constraints of the circuit, the circuit will be designed using a 130nm CMOS technology and the capacitors are implemented using MIMCAP including parasitics. Limiting the total area for the capacitors to 1 mm^2 results in a maximum capacitance value of 1 nF this means that 1/2 and 1/1 converters will have a capacitor of 1 nF; and the 2/3 and 3/2 converters will have 3 capacitors with 0.33 nF. This type of capacitors have a top and bottom plate parasitic capacitance of, approximately, 0.4% and 0.6% of the nominal value, respectively.

Equivalent equations to (6) were obtained for the remaining 3 converters using the same methodology. These equations are used to calculate V_{out} for the 4 converters for $P_{out} = 10 \text{ mV}$ ($R_{out} = 100 \Omega$), V_{in} is 2, 3/2, 1 and 2/3, according to the converter ratio. V_{out} is plotted in Fig. 7 using the parasitic capacitances values of the selected technology. This plot shows that the 2/3 and 3/2 converters need a higher clock frequency to have $V_{out} = 1V$, these higher frequencies will lead to lower efficiency due to the power needed to drive the larger switches.

The analysis described in section 3.1 was applied to the remaining 3 converters and their efficiency was calculated. Fig. 8 shows the plot of η in function of V_{in} . The solid lines are obtained from the equations and the shapes are simulation results. These plots were obtained for $C_G = 0$. The efficiency graph of Fig. 8 was calculated independently of the clock frequency and ignoring the charge lost through the gate capacitance of the switches. Since the gate capacitance increases with the CMOS switch size, which increases with the clock frequency value, the efficiency also depends on the clock frequency. The clock frequency value for each converter in order to have $V_{out} = 1\text{ V}$ is shown in Fig. 9. This graph was obtained using similar expressions to (7) calculated for all the converters.

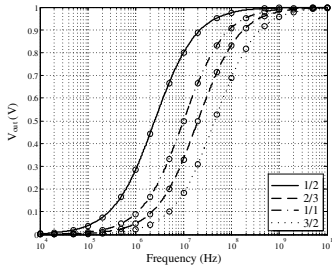


Fig. 7. V_{out} as function of the frequency clock, with $C_B = 0.6\% C_1$, $C_T = 0.3\% C_1$, $R_{out} = 100\ \Omega$ and $V_{in} = \{2, 1.5, 1, 0.67\}$ according to the converter ratio.

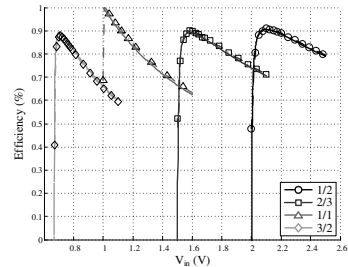


Fig. 8. η as function of V_{in} for the four converters with $C_B = 0.6\% C_1$ and $C_T = 0.3\% C_1$

The CMOS switches are constituted by NMOS and PMOS devices in parallel. These transistors are sized in order to have an ON resistance (R_{ON}) value that results in a time constant compatible with the clock frequency value. In [6] it is shown that R_{ON} and C_G for a settling error (*error*) and a frequency clock (F_{CLK}) and the capacitance coupled to the switch (C_1) are given by:

$$R_{ON} = \frac{1}{2 C_1 F_{CLK} \ln \left[\frac{1}{error} \right]} \quad (8)$$

$$C_G = 2 k_R k_C \ln \left[\frac{1}{error} \right] F_{CLK} C_1 \quad (9)$$

Where $k_R = 806.24\ \Omega \cdot \mu\text{m}$ and $k_C = 7.1\ \text{fF}/\mu\text{m}$ are coefficients derived by simulation Spectre [6]. Replacing (9) in (3) results η as function of V_{in} , V_{out} , *error*, R_{out} and F_{CLK} . This now takes into account the effect of the frequency in the parasitic capacitances of the switches. Replacing (7) in this new expression results in η in function of V_{in} , V_{out} , *error*, R_{out} . This final equation describes the efficiency with the frequency adjusting to the value necessary to maintain $V_{out} = 1\text{ V}$ and the

extra power consumed by the switches due to this adjustment. Fig. 10 shows the plot of η as function of V_{in} with $P_{out} = 10$ mW ($R_{out} = 100 \Omega$), $V_{out} = 1$ V, settling error of 1%, $C_B = 0.6\% C_1$ and $C_T = 0.3\% C_1$, for the 1/1 and 1/2 $C_1 = 1$ nF; and for the 2/3 and 3/2 $C_1 = 0.33$ nF. The plot shows the maximum achievable efficiency and the corresponding value of V_{in} . Through this it is possible to determine the range of operation for each converter. For example, in this case the 1/2 converter works from 2.3 to 2.07 V, with a maximum of 84% and a minimum of 64% efficiency. The 2/3 converter works from 2.07 to 1.76 V, with a maximum of 65% and a minimum efficiency of 57%. The 1/1 converter works from 1.76 to 1.05V, with a maximum of 83% and a minimum efficiency of 57%. Finally, the 3/2 converter works from 1.04 to 0.67 V, with a maximum efficiency of 84%.

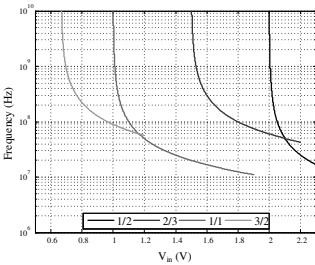


Fig. 9. Frequency clock as function of V_{in} , for a $P_{out} = 10$ mW ($R_{out} = 100 \Omega$) with $V_{out} = 1$ V

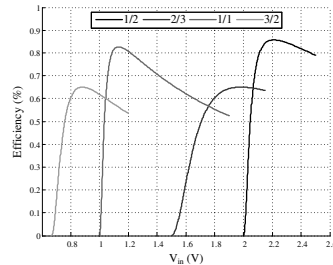


Fig. 10. η as function of V_{in} for a $P_{out} = 10$ mW ($R_{out} = 100 \Omega$), $V_{out} = 1$ V, settling error of 1%, $C_B = 0.6\% C_1$, $C_T = 0.3\% C_1$, for the 1/1 and 1/2 $C_1 = 1$ nF; and for the 2/3 and 3/2 $C_1 = 0.33$ nF

5 Conclusion

This paper presented a theoretical analysis of a multi ratio SC DC-DC converter for a supercapacitor power supply of an energy harvesting system. The different SC circuits of the converter were analyzed in order to obtain expressions that allow computing their efficiency as a function of the input voltage. These expressions were verified using electrical simulations and then used to design the circuit for a 130 nm CMOS technology and determine the optimum input voltage ranges for each topology.

References

1. Paradiso, J.A., Starner, T.: Energy Scavenging for Mobile and Wireless Electronics. *IEEE Pervasive Computing* **4**(1), 18–27 (2005)
2. Chalasani, S., Conrad, J.M.: A survey of energy harvesting sources for embedded systems. In: *IEEE Southeastcon*, April 3-6, pp. 442–447 (2008)

3. Simjee, F., Chou, P.H.: Everlast: long-life, supercapacitor-operated wireless sensor node. In: Proceedings of the 2006 International Symposium on Low Power Electronics and Design, ISLPED 2006, October 4-6, pp. 197–202 (2006)
4. Ramadass, Y.K., Chandrakasan, A.P.: Voltage scalable switched capacitor DC-DC converter for ultra-low-power on-chip applications. In: IEEE Power Electronics Specialists Conference, PESC 2007, June 17-21, pp. 2353–2359 (2007)
5. Gregorian, R., Temes, G.: Analog MOS Integrated Circuits for Signal Processing. Wiley, New York (1986)
6. Carvalho, C.: CMOS Indoor Light Energy Harvesting System for Wireless Sensing. Phd Thesis Faculdade de Ciências e Tecnologias, Monte da Caparica (2014)

A Piezoelectric Device for Measurement and Power Harvesting Applications

M. Alves¹, J.M. Dias Pereira^{1,3(✉)}, and J.M. Fonseca²

¹ ESTSetúbal-LabIM/IPS, R. Vale de Chaves, Estefanilha,
2910-761 Setúbal, Portugal

{mario.alves,dias.pereira}@estsetubal.ips.pt

² Faculdade de Ciências e Tecnologia, Universidade Nova de Lisboa,
2829-516 Caparica, Portugal

jmrff@fct.unl.pt

³ Instituto de Telecomunicações, Instituto Superior Técnico,
Av. Rovisco Pais 1, 1049-001 Lisbon, Portugal

Abstract. With the fast growth of wireless communications between nodes/sensor units, devices installed in remote places require power energy supply solutions to assure their functionality and data communication capabilities. For these applications energy harvesting takes place as a good solution, to increase the availability of energy, in opposition to the conventional systems of energy supply. Regenerative energy sources like thermoelectric, magnetic, piezoelectric, and/or renewable sources such as photovoltaic, wind, among others, allowed the development of different powering solutions for sensor units. The purpose of this work is to characterize a piezoelectric device to measure and capture mechanical vibrations from equipments, structures and piping vibrations, as well as from other sources. The study is carried out taking into account the power supply capabilities of piezoelectric devices as a function of the amplitude and frequency of the vibration stimulus, as well as, the electrical characteristics of the load circuit.

Keywords: Regenerative energy sources · Energy harvesting · Mechanical vibration energy · Stand-alone systems · Sensor applications

1 Introduction

Nowadays, with electronics becoming smaller and requiring less power, the energy harvesting has began to be a topic of great importance to self-powering systems. The energy available in the surrounding environment of an application can be a viable option to allow the development of energy autonomous systems or to extend the autonomy of systems supplied by storage elements, usually batteries.

Different sources that capture the energy of the environment, like solar, wind, vibration and temperature gradients, have been target of recent developments to improve their performances and efficiency.

A type of environmental source as a global solution to supply a wide range of applications is not feasible, since the requisites of power/energy can be completely different in amplitude or frequency/time.

Many energy harvesting systems are oversized, either because there is no controller to manage and optimize the energy flow or because they are designed for worst-case scenarios [1]. Create a dedicated harvesting solution with low power electronic internal consumption, is crucial to improve the performance of energy harvesting systems.

The main problem of autonomous and self-powered devices is related with energy storage solutions. The energy that is not consumed by the system is generally requested when the source cannot deliver the amount of energy that guarantees the consumption needs. Two main storage solutions can be used: batteries and supercapacitors. The use of supercapacitors has the following advantages: life cycle, which is at least two orders of magnitude higher than the corresponding one of lead acid batteries; long operation time in a temperature range of -40°C to $+60^{\circ}\text{C}$; higher power capability; ability to deliver for short time intervals electrical energy at significantly higher power than batteries [2]. Batteries are usually indicated for long time supplies (energy) without requisites of instantaneous high consumption (power).

The scaled solution purposed here aims to verifying the possibility of suppling enough energy for monitorization of physic variables in instrumentation applications. This energy must also be sufficient to assure the wireless communication of data.

A. Piezoelectric Elements

Piezoelectric material produces mechanical strain under the influence of an externally applied electrical field, and conversely produces electrical potential in response to an applied mechanical strain.

The goal of this work is to characterize a piezoelectric device to convert vibration mechanical energy to electrical voltage, not only as a measurement signal, but as low-power energy source. In the instrumentation field it is possible to use this principle for energy harvesting in the measure of force and wind, and in some type of flowmeters (Figure 1). At the same time, they give the information about the wind speed, it is possible to use the range of voltage generated for supplying the integrated application.

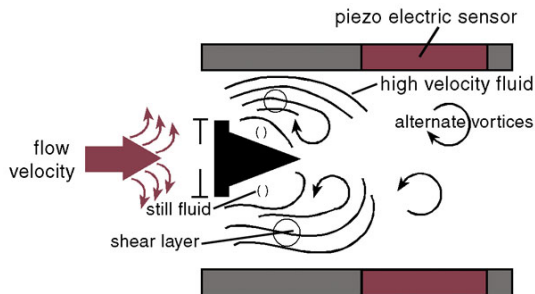


Fig. 1. Vortex flowmeter principle using piezoelectric elements

The measuring principle is based on development of Karmen Vortex shedding street in the wake of a body built into the pipeline. Vortex shedding creates alternate pressure conditions whose frequency is directly related with flow velocity, being the relationship, between these variables, given by:

$$V = \frac{1}{S_{th}} \times f \times d. \quad (1)$$

$0,2 < S_{th} < 0,21$ to $300 < R < 150000$
 Sth – Strouhal number
 R – Reynolds number

B. Cantilevered-beam Configuration

Solutions for piezoelectric energy harvesting are typically based on a cantilevered-beam configuration (Figure 2). The piezoelectric beam is clamped at one end and the other end is allowed to oscillate freely in response to vibration normal to the flat surface of the beam, converting these vibrations to in-plane material strain. It is extremely important that the natural frequency of harvester configuration is tuned to match the vibration source. Vibration sources vary considerably in amplitude and dominant frequency. In most of environments, vibration is not made up of a single frequency but is typically made up of a set of main fundamental frequencies and associated harmonics. [3]

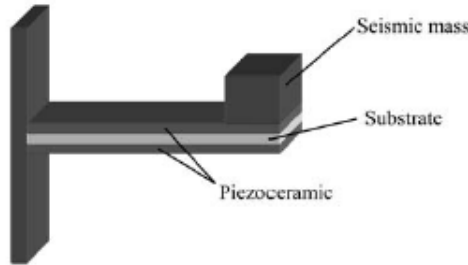


Fig. 2. Model of a cantilever-beam with piezoelectric ceramic layers

A cantilevered-beam piezoelectric energy harvester is a complex electromechanical system in which the electrical and mechanical loading of the beam are interrelated. The beam dimensions and tip mass determine the resonant frequency of the beam, which is tuned to match the dominant vibration frequency of its environment. These typically small vibrations are mechanically amplified. A development and fabrication process of a cantilever-beam with a thin film piezoelectric power generator is presented by Jeon et al. [4]

2 Main Contributions - Relationship to Cloud-Based Engineering

This work focuses a technological solution for power harvesting, with the aim at increasing the autonomy of low-power consumption applications. The present contribution intends to characterize a piezoelectric device as a solution to increase the energy sustainability and performance of instrumentation systems with wireless communication capabilities. These systems located in remote places have the ability to actualize information located in cloud data base computing systems. Particularly important for systems located in places where the viability of conventional energy supply is very expensive or technically difficult and it is crucial to minimize maintenance requirements. Figure 3 represents the block diagram of a sensing node with power harvesting and wireless communication capabilities.

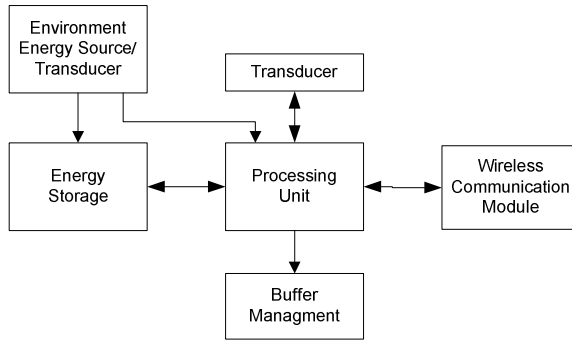


Fig. 3. Sensing node with power harvesting

3 Methodology

In this work two electrically isolated piezoelectric elements were used, whether independently or bridged for increased voltage (series configuration) or current output (parallel configuration). Series connection will double the open-circuit voltage compared to a single element, and the effective capacitance will be $1/2$ of the single capacitance. Parallel connection will double the current compared to a single element configuration, and doubling the effective capacitance. The option was to use the parallel connection in order to increase the power harvesting capability. However, the single element configuration was also tested and the results are presented as a reference for analyses facility. Each solution (single and parallel connection) was assembled in a cantilever-beam configuration.

The AC voltage at terminals of piezoelectric generator is in a first stage converted to DC voltage (Figure 4). The DC Voltage connected to a load permits defining the capability of generating power for instantaneous consumption, or for energy storage when connected to a supercapacitor.

The open circuit voltage (V_{OC}) and the short circuit current (I_{SC}) are the two main parameters to start this system characterization (Figure 5). Furthermore, achieving the Maximum Power Point (MPP) in function of load for different amplitude and frequency vibration is important to optimize the performance of this type of energy harvesting. To maximize transfer efficiency, the load must be matched to the piezo's equivalent impedance. Theoretically, the piezo impedance at a given amplitude and frequency, as well as the load impedance, can be thought as a pair of simple (but unknown) impedances which make up an impedance divider. The power transfer between the two impedances is optimized when their resistive and reactive values match. This corresponds to the point at which the piezo's loaded voltage is equal to half its open-circuit voltage.

The simplicity of the solution that is proposed intends to represent an advantage in terms of internal power consumption.

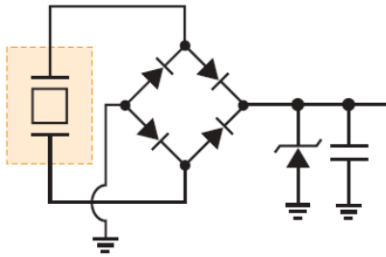


Fig. 4. Equivalent electric circuit AC-DC converter

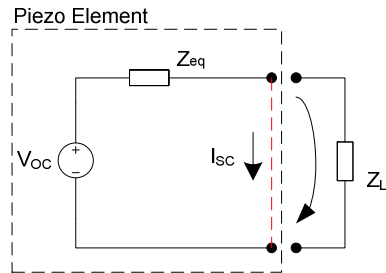


Fig. 5. Equivalent Thevenin circuit

This circuit (Figure 4) is ideal for directly powering small sensors that can perform their function (e.g. record or transmit a measurement). It could also be used to extend battery life, of devices with their own battery/capacitor power source.

4 Results and Critical View

The cantilever-beam configuration tested with piezoelectric elements is strongly dependent on the environment frequency vibration, and not only on vibration amplitude. The system can be mounted in a large number of applications, but if for some reason the frequency of vibration change, the performance as harvester source will be very poor. This can be an important limitation for harvest energy from environments that do not have a constant vibration but depends of external factors like ambient conditions. However in some applications the vibration frequency is well know, like for instance, the structure of an AC motor working at 230V/50Hz. In this case the natural frequency of the piezoelectric harvester element must be tuned to 50hz to match the vibration source. In a cantilever configuration the frequency tuning is performed by adding mass to the end of the cantilever solution. The tuning mass can be adjusted until the vibration frequency and the natural frequency of the piezoelectric device are equal. The beam dimension associated with the mass is also determinant to achieve

the resonant frequency of cantilever, and consequently the maximum power that will be possible to capture. In most applications it is very important, to characterize the frequency of the environment vibration in which the element will be operating.

In this work the results were obtained for a established frequency of 50Hz. This frequency matches the vibration of an AC motor structure. We have also tested frequencies out of the tuned cantilever configuration, and it could confirm that, in this condition, the voltage level, and consequently the power harvesting, was extremely low. This short band wide of the cantilever with piezo elements is limitative as harvesting source and also as transducer for variables measurement. One solution to solve this problem, could be using different cantilever assembled in parallel each one tuned at a different frequency.

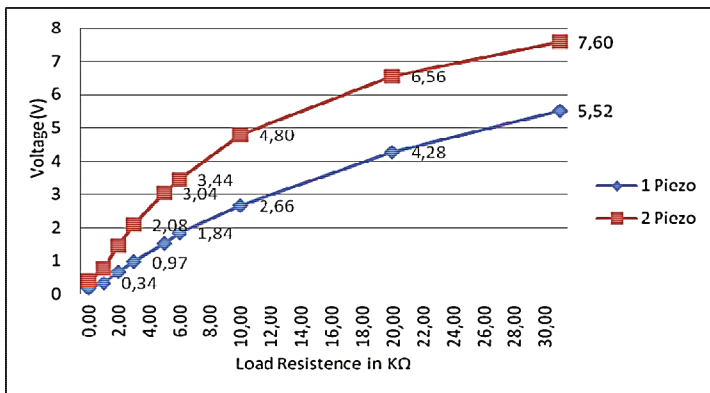


Fig. 6. Output Voltage in function of Load value

The DC output voltage (V_{out}) shown in figure 6 is lower than expected, due to the voltage drop in each diode (0,7V). Since low power consumption is involved, it is possible the use of Schottky diodes with voltage drops as low as 0,15V.

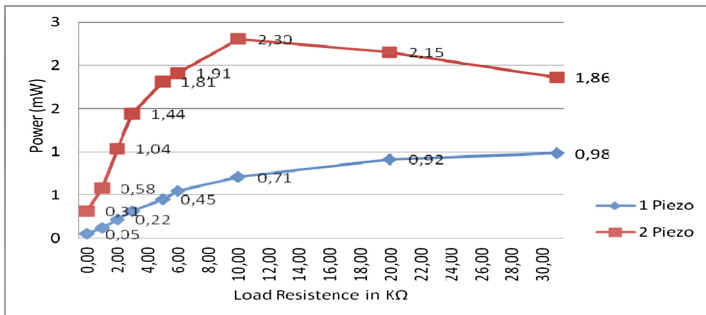


Fig. 7. Power harvesting in function of Load

Figure 7 shows the power harvesting behavior as a function of different load impedance, keeping the amplitude vibration constant. A clear difference was observed depending on the assembly in beam of a single or double piezoelectric elements. The power harvesting increased 3 fold for the majority of loads tested and MPP it was obtained for lower load impedances. This is significant to determine the load connected and also for the level and period necessary for charging the storage element. By comparing figure 6 and 7 it is possible to conclude that the power increase obtained corresponds to only a small increase in the output voltage. This is mainly due to the increase in current owed to parallel configuration.

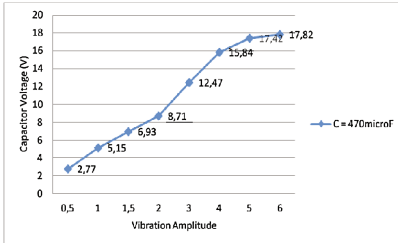


Fig. 8. Capacitor Voltage in function of Vibration Amplitude with $f=50\text{Hz}$

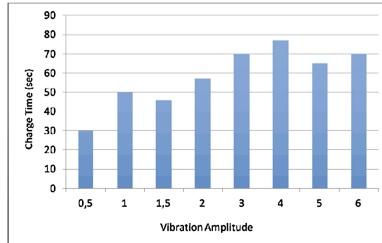


Fig. 9. Time of capacitor charging in function of Vibration Amplitude with $f=50\text{Hz}$

The results presented in figure 8 and 9 correspond to a established frequency of 50Hz and 2 piezoelectric elements connected in parallel. The piezoelectric elements output was rectified and connected to a capacitive storage of 470 μF . The voltage at the terminals of the capacitor and the time necessary for charging are represented for different amplitudes of vibration. We can observe that the storage element subjected to the highest vibration amplitude could charge 6 times higher level of voltage during only the double-time to charge. Tests with capacitors of higher value and the same configuration of two piezo elements were done as well. Lower levels of voltage and higher period of charging were observed in this case, showing that the power harvesting is very low for storage elements with higher capacity.

Taken together these results allowed to verify that good levels of power harvesting are possible when several piezoelectric elements assembled in parallel, which may have a promising application.

5 Conclusion and Further Work

The piezoelectric materials are very sensitive to the surrounding vibration, producing easily very good levels of voltage. This characteristic is undoubtedly very important for vibration measurement. The use of these elements for power harvesting are however limited by the fact that the levels of voltage are not followed by good values of power supplies capabilities, exhibiting low current values. One hypothesis to solve the problem is the use of several piezoelectric elements connected in parallel. By using

this method the power harvesting by piezoelectric elements can be a promising solution for low power consumption applications. Since this method can only be used in application where the environment vibration frequency has a low bandwidth, the best approach is to start by characterizing the vibration variation and the levels of power harvesting required.

New type of materials and ceramics are now being tested and developed to improve the piezoelectric characteristics. This will enable new values and facilities for power harvesting and measurement solutions and will probably greatly improve the efficiency and application of this method.

References

1. Kimball, J.W., Kuhn, B.T., Balog, R.S.: A System Design Approach for Unattended Solar Energy Harvesting Supply. *IEEE Transactions on Power Electronics* 24(3-4), 952–962 (2009)
2. Obreja, V.V.N.: On the performance of commercial supercapacitors as storage devices for renewable electrical energy sources. In: *ICREPQ 2007, Sevilla, Spain (March 2007)*
3. Gilbert, J.M., Farooq, B.: Comparison of Energy Harvesting Systems for Wireless Sensor Networks. *International Journal of Automation and Computing*, 334–347, October 2008
4. Jeon, Y.B., Sood, R., Jeong, J.-H., Kim, S.-G.: MEMS power generator with transverse mode thin film PZT. *Sensors and Actuators A Physical*, 16–22 (2005)

Design of High Voltage Full-Bridge Inverter Using Marx Derived Switches

Nelson Santos¹(✉), J. Fernando Silva², Vasco Soares¹, Sónia F. Pinto²,
and Duarte Sousa²

¹ Instituto Superior de Engenharia de Lisboa, INESC-ID
R. Conselheiro Emídio Navarro, 1959-007 Lisboa, Portugal
{nsantos, vesoares}@deea.isel.ipl.pt

² Instituto Superior Técnico, Universidade de Lisboa, INESC-ID,
DEEC, AC Energia Av. Rovisco Pais, 1049-001 Lisboa, Portugal
{fernando.alves, soniafp, duarte.sousa}@tecnico.ulisboa.pt

Abstract. This paper presents a high-voltage (HV) inverter to generate bipolar voltages with variable duty-cycle and frequency for HV pulsed power or HV electrical network applications. Each one of the four HV inverter switches is built with a series stack of semiconductor devices, derived from the Marx generator concept, using small capacitors to equally share the voltage among the individual series stacked semiconductors. A sliding mode control is used to control the output voltage and a delay technique is used to reduce dU/dt at the HV inverter output and to balance the capacitor voltages. The design and structure of the HV inverter switches is described together with the delay technique. Steady-state and dynamic behavior is evaluated. Simulation results are presented (using MATLAB/Simulink software) and discussed.

Keywords: Pulsed power systems · Marx generator · Bipolar pulses · High voltage inverter · Smart-grids

1 Introduction

In power electronic applications solid state power semiconductor devices are used to transfer large amounts of power and energy, in a controlled way, sometimes for very short times, as in the case of pulsed power. In HV applications solid-state semiconductor devices are sought because they have lower power losses compared to older devices like spark gaps or vacuum tubes. However, for HV applications, a single power semiconductor device is still not able to hold-off the tens or hundreds of kV or allow the kA currents needed. Connecting power semiconductor devices in series or/and in parallel is a way to avoid these limitations [1], although issues like voltage sharing and pulse synchronization remain.

For kV applications, such as switches, inverters in smart-grids, choppers or pulsed power, the semiconductor devices like MOSFET (Metal Oxide Semiconductor Field Effect Transistor), GTO (Gate turn-OFF Thyristor) or IGBT (Insulated Gate Bipolar Transistor) can be connected in series and operated synchronously as a single

switch device. To ensure proper operation of the switch it is crucial to balance the voltage between all the series connected semiconductor devices by dividing the voltage equally between them, both in steady-state and during transients.

However, even small variations of devices static and dynamic parameters, the imperfect synchronization or delay of the gate drive voltages, thermal impedance variations and asymmetrical parameters in the snubber circuits for voltage sharing [2], can impair the voltage balance among series semiconductor devices.

There are techniques to minimize the unbalanced voltages by using passive snubber circuits, active gate control circuits and voltage clamping circuits. Snubber circuits usually are RC (Resistor-Capacitor) or RCD (Resistor-Capacitor-Diode) in parallel with the collector-emitter of each IGBT of the stack, minimizing device switching losses while increasing the global losses and limiting the switching frequency. The active gate control proposes individual control of the signal gate of each device to dynamically balance the collector-emitter voltage. While this technique may not increase the switching loss or switching times, it presents some complexity in the drive circuit and may require additional small passive snubbers. Another approach, active voltage clamping, balances the voltage collector-emitter by using optimized snubbers (with low losses) and auxiliary circuits using usually extra semiconductor devices to improve the switching frequency restrictions [1].

This paper proposes a full-bridge inverter with four HV switches using IGBT, each one made of switching cells derived from the Marx generator concept [3], able to balance the voltages in the series cell stacks of each HV switch with efficiency. Performance evaluation is done using a typical inductive load at the output of the HV inverter and the voltage balancing is maintained, even with 10 % tolerance in the capacitor cells. Unsynchronized gate drive signals are used advantageously to reduce the output dU/dt , decreasing the load voltage stress and the electromagnetic interference problems [4].

2 Relationship to Cloud-Based Solutions

Research works, like the described in paper, need computers to perform numerical calculations and simulations. Sometimes, one computer is not enough as it takes too long to finish the simulations. Cloud technology can help and increase the productivity of research teams that locally do not have powerful enough resources due to budget constraints and strict control on the distribution of funds. Additionally, the physical implementation of prototypes can benefit from cloud-based solutions by connecting several teams in real time for development, analysis and sharing in the community. In return, HV full-bridge inverters will be key players in the supply systems sustainability of cloud data centers, its integration with renewable energy resources and power quality control in smart-grids.

3 Proposed Topology

3.1 Marx Derived Switch

The original Marx generator topology charges n capacitors in parallel and discharges them in series to obtain the HV U_{HV} approximately equal to n times the charging power

source U_{LV} voltage $U_{HV} = nU_{LV}$, without using step-up transformers. Figure 1(a) shows an example of Marx generator for positive HV pulses where the capacitors C_1, \dots, C_n are charged in parallel through the impedances Z_1, \dots, Z_n (resistive and/or inductive) when switches S_1, \dots, S_n are turned OFF and discharged in series into the load, when switches S_1, \dots, S_n are turned ON.

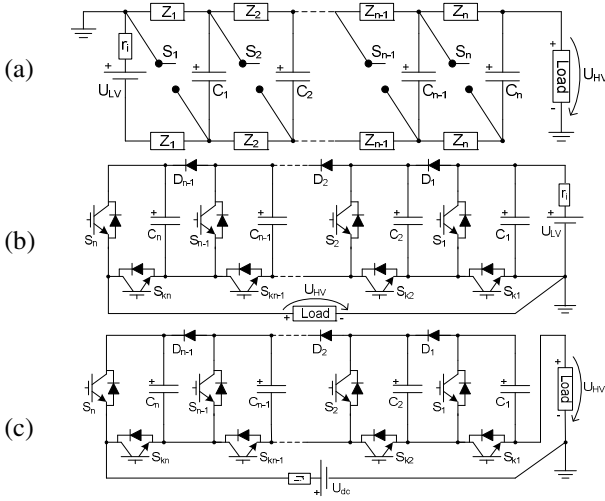


Fig. 1. Marx derived topology; (a) Marx generator topology; (b) Solid-state HV positive pulse generator; (c) series switch for positive voltages

To reduce the losses, the impedances and spark gaps are replaced by power semi-conductors, as depicted in Fig. 1(b), increasing the efficiency, the performance and the pulse frequency. To use the Marx generator concept as a switch, it is necessary to charge the capacitors in series (diodes of S_1 to S_n), to hold-off the HV, and to balance the capacitor voltage connecting them in parallel (diodes D_1 to D_{n-1}). Therefore, in the Fig. 1(b) circuit load and HV source are interchanged (Fig. 1(c)) to obtain a series stack of switching cells for positive HV pulses. This technique provides HV handling using U_{LV} (kV) rated semiconductor devices [3].

3.2 Full-Bridge Inverter Topology

The full-bridge inverter uses four HV Marx generator based switches Fig. 1(c), each switch denoted by S_{Mk} with $k \in \{1, \dots, 4\}$. The inverter outputs bipolar HV pulses from a single HV source U_{dc} (Fig. 2(a)). Each HV switch is composed by n series connected cells $n > U_{HV}/U_{LV}$. Each cell contains two IGBT S_{kn} , S_{Cn} with anti-parallel diodes (Fig. 2(b)). IGBT/diode hold-off voltages are imposed by capacitor C_n . The inter-cell diode D_n balances the C_n voltages.

Assuming the IGBTs S_{k1}, \dots, S_{kn} at each switch S_{Mk} are driven simultaneously, the inverter output voltage U_L depends on the states of S_{M1}, S_{M2}, S_{M3} and S_{M4} , obtaining three voltage levels, according to (1).

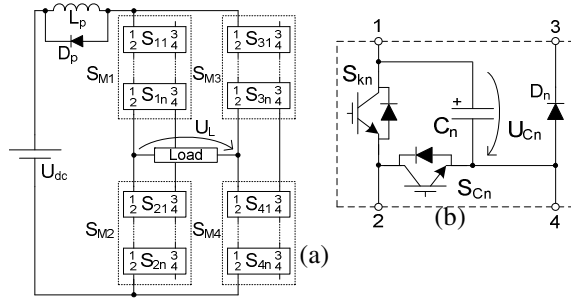


Fig. 2. Proposed Circuit; (a) HV Inverter; (b) single cell based in Marx generator

$$U_L = \delta(t)U_{dc} = \begin{cases} U_L = U_{dc} & \text{for } \delta(t) = +1 (S_{M1}, S_{M4} \text{ ON}) \\ U_L = 0 & \text{for } \delta(t) = 0 (S_{M1}, S_{M3} \text{ ON or } S_{M2}, S_{M4} \text{ ON}) \\ U_L = -U_{dc} & \text{for } \delta(t) = -1 (S_{M2}, S_{M3} \text{ ON}) \end{cases} \quad (1)$$

A sliding mode modulator [6], [7], [8] and [9] will be used to obtain the gate drive signals for the IGBT stacks S_{M1}, \dots, S_{M4} in order to control the output voltage U_0 .

3.3 Operation of the Switch

Each switch S_{Mk} has two modes of operation, charging mode, if S_{kn} are OFF and S_{Cn} are ON, and balancing mode, if S_{kn} are ON and S_{Cn} are OFF. In the charging mode, the S_{Mk} switch is OFF and all capacitors C_1 to C_n are charged in series through the S_{C1} to S_{Cn} by HV source U_{dc} . Series charging leads to some voltage imbalance. Under the balancing mode operation (the S_{Mk} switch is ON) all the capacitors are connect in parallel through S_{k1} to S_{kn} and D_1 to D_n , therefore equal voltage sharing is achieved. Assuming that an upper stack capacitor exhibits a voltage higher than those on the bottom, a current path is established that balances the voltages among the capacitors on the switch S_{Mk} (Fig. 3(a)). However, under opposite conditions, a lower stack capacitor cannot discharge to the remaining ones. This issue can be avoided by the replacement of diodes D_1 to D_n by IGBTs (thus increasing the cost and control system complexity). Other options include the use of balancing resistors (which decrease the efficiency) or using, as in the present paper, an unsynchronized gate drive signal technique approach. A sequential gate driver delay ($5 \mu\text{s}$) on each one of the cells (S_{k1}, S_{C1} to S_{kn}, S_{Cn}) is used on every transition mode operation, similar to the technique adopted on multilevel inverters, but for a short period of time. Figure 3 exemplifies the sequence delay technique adopted for one arm of the inverter to turn OFF S_{M1} and turn ON S_{M2} with $I_L > 0$ and $n = 3$.

The sequence delay technique begins at Stage 1 (St1) where the capacitors C_1, C_2 and C_3 of S_{M2} are linked in series with U_{dc} , and at same time C_1, C_2, C_3 of S_{M1} and C_1 of S_{M2} are connected in parallel for voltage balancing. Sequentially, follows the St2, then the St3 and finishes with St4 where the capacitors C_1, C_2 and C_3 of S_{M1} are linked in series with U_{dc} and C_1, C_2 and C_3 of S_{M2} are connected in parallel for voltage balancing purposes. All the states for S_{M1} and S_{M2} for $I_L > 0$ are resumed in Tab. 1.

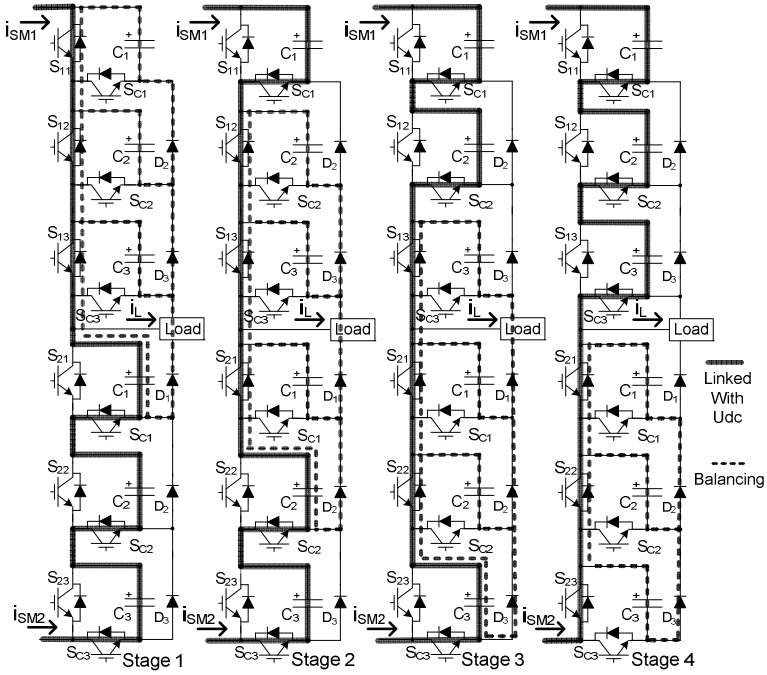


Fig. 3. Sequence delay technique for turn OFF S_{M1} and turn ON S_{M2} for $n = 3$ and $I_L > 0$

Table 1. Stages transition for S_{M1} and S_{M2} for $I_L > 0$

Stage	ON at S_{M1}	OFF at S_{M1}	ON at S_{M2}	OFF at S_{M2}	i_{SM1}	i_{SM2}
1	S_{11}, S_{12}, S_{13}	S_{C1}, S_{C2}, S_{C3}	S_{C1}, S_{C2}, S_{C3}	S_{21}, S_{22}, S_{23}	I_L	0
2	S_{12}, S_{13}, S_{C1}	S_{11}, S_{C2}, S_{C3}	S_{21}, S_{C2}, S_{C3}	S_{22}, S_{23}, S_{C1}	$2/3 I_L$	$-1/3 I_L$
3	S_{13}, S_{C1}, S_{C2}	S_{11}, S_{12}, S_{C3}	S_{21}, S_{22}, S_{C3}	S_{23}, S_{C1}, S_{C2}	$1/3 I_L$	$-2/3 I_L$
4	S_{C1}, S_{C2}, S_{C3}	S_{11}, S_{12}, S_{13}	S_{21}, S_{22}, S_{13}	S_{C1}, S_{C2}, S_{C3}	0	$-I_L$

To turn ON S_{M1} and turn OFF S_{M2} for $I_L > 0$ there is the need to invert the initial sequence, that is, to operate the stages from St4 to St1. If $I_L < 0$ it is necessary to change the drive sequence, leaving a slightly higher voltage on the C_1 of S_{M1} and S_{M2} in order to guaranty the proper equalization.

3.4 Design Parameters

It is considered that the HV inverter provides energy to a resistive load through one low-pass filter (LC). Also, the system is design for a specific efficiency parameter η_T by assuming P_0 as the nominal output power, P_{LC} the filter power losses and P_{CS} the switches power losses. Since the majority of the losses are due to IGBT switching effects, its relationship with maximum switching frequency and goal efficiency is (2).

$$\frac{1 - \eta_T}{\eta_T} = \frac{P_{LC}}{P_0} + \frac{P_{CS}}{P_0} \quad (2)$$

a) The filter is designed to reduce harmonic voltage content. Its contribution to the overall losses shouldn't be greater than 0.3 % of the nominal output power. For a cut-off frequency f_c and a damping ratio ξ the filter parameters are $\omega_0 = 2\pi f_c$, $Z = \frac{2\xi U_0^2}{P_0}$, $C = \frac{1}{Z\omega_0}$, where the ω_0 is the angular frequency and Z is the characteristic impedance of the load output. The corresponding filter parameters for the inductance and capacitor values are $L = \frac{\xi U_0^2}{\pi f_c P_0}$, $C = \frac{P_0}{4\xi \pi f_c U_0^2}$. It is considered that the losses in capacitor are negligible because most of them are due to the output current ripple Δi_L [10]. With r_C and r_L as the equivalent serial resistance of the capacitor and the inductor the power ratio can be calculated (3).

$$\frac{P_{LC}}{P_0} = \frac{r_L P_0}{U_0^2} + \frac{r_C \Delta i_L^2}{12 P_0} \quad (3)$$

To achieve a specific performance losses criteria r_L should obey the relationship presented in (4).

$$r_L < \frac{P_{LC} U_0^2}{P_0^2} \quad (4)$$

b) The efficiency of the IGBT is related to the semiconductor ON state and switching losses. The ON state losses P_{C1} are a function of the device ON state voltage U_{ce} , the anti-parallel diode voltage drop U_f and the maximum current output I_0 . Assuming one single IGBT and the duty cycle δ' , it can be written $P_{C1} = U_{ce} I_0 \delta' + U_f I_0 (1 - \delta')$. Considering $\delta' = 1/2$ the total ON losses P_C for the four switches with n cells each is (5).

$$P_C = 2n I_0 (U_{ce} + U_f) \quad (5)$$

The switching losses P_{S1} are related with the rise time t_r , the fall time t_f , and the switching frequency f_s . Since the IGBT voltage is $U_c = U_{dc}/n$ and I_0 represents its current, in a single device the switching losses are $P_{S1} = U_c I_0 f_s \frac{(t_r + t_f)}{2}$. Taking into account the voltage U_{dc} and the previous equation the total switching losses P_S for the four switches with n cell each are (6).

$$P_S = 2U_{dc} I_0 f_s (t_r + t_f) \quad (6)$$

Since P_{CS} should be no more than 1.7 % of P_0 , so (7).

$$\frac{P_{CS}}{P_0} = \frac{2U_{dc} I_0 f_s (t_r - t_f) + 2n I_0 (U_{ce} + U_f)}{P_0} \quad (7)$$

For a specific target efficiency the average switching frequency f_s must obey (8).

$$f_s < \frac{\frac{P_{CS}}{P_0} - \frac{2n I_0 (U_{ce} + U_f)}{P_0}}{\frac{2U_{dc} (t_r - t_f)}{P_0}} \quad (8)$$

c) The C_n value on each cell is important to the proper operation of the stack and voltage protection purposes by limiting the dU/dt . Additionally, the inductance L_p must consider the di/dt IGBT limitations. Assuming variations of ΔU_C (%) on capacitor nominal voltages, on C_1 to C_n , equations (9) and (10) can be presented. Equation (10) is also function of time delay t_d .

$$L_p = \frac{\Delta U_C \frac{U_{dc}}{n} t_r}{2I_0} \tag{9}$$

$$C_n = \left(\frac{(n-1)!}{n} \right) \frac{t_d I_0}{\Delta U_C \frac{U_{dc}}{n}} \tag{10}$$

It should be noted that the energy stored in L_p boosts the voltage in capacitors C_1 to C_n so a freewheel diode was added.

4 Simulation Results

The circuit presented in Fig. 2(a) was simulated using MATLAB/Simulink considering four HV switches with five cells each, $n = 5$. On the HV inverter output there is a LC filter with a cut-off frequency of $f_c = 500$ Hz. For other general parameters it is considered $P_0 = 1$ MW, $U_0 = 10$ kV, $R_0 = 100 \Omega$, $\eta_T = 98 \%$ and $\Delta U_C = 2 \%$. Figure 4(a) presents the inverter output voltage U_L and the voltage U_0 applied to the output resistor R_0 .

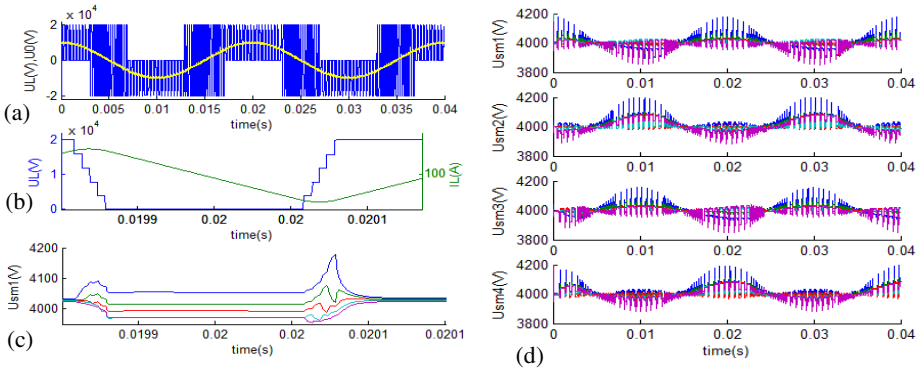


Fig. 4. Temporal evolution; (a) voltage output inverter U_L and voltage U_0 ; (b) voltage U_L and current I_L at output of inverter; (c) voltages cell of switch S_{M1} ; (d) voltages present in each cell in all four switches S_{M1} , S_{M2} , S_{M3} and S_{M4}

The capacitor voltages (Fig. 4(d)) are very similar and balanced around 4 kV, even using randomly chosen capacitor values within the typical tolerance of 10 %. In Fig. 4(b) it is shown an improvement of 80 % (for $n = 5$) reduction in the inverter output dU/dt regarding the synchronized gate driver technique. The output filter current exhibits smooth transitions around 100 A.

The voltage variation at Fig. 4(c) is higher at C_1 of S_{M1} . At turn OFF there is a voltage increase of 2.5 % relative to its nominal value. At turn ON the voltage in C_1 is 4.5 % higher to the same nominal value. Besides all the voltages sharing is achieved.

5 Conclusion

The full-bridge inverter proposed in this paper uses HV switches based on the Marx generator concept. Marx topology well-known toughness is suited for HV pulsed power or electrical network applications. A good voltage balancing was attained on each switch, with just 5 % difference even using 10 % of tolerance for the capacitors due to the use of just one extra diode (D_n) per cell. This is advantageous as the absence of resistors for balancing or capacitor discharging purposes means an improved efficiency. The inverter output dU/dt was also reduced and controlled using the proposed delay time unsynchronized gate drive technique.

Acknowledgments. This work supported by Portuguese national funds through FCT - Fundação para a Ciência e Tecnologia, under Project PEst-OE/EEI/LA0021/2013.

References

1. R. Withanage, R., Crookes, W., Shammas, N.: Novel voltage balancing technique for series connection of IGBTs. In: 2007 European Conference on Power Electronics and Applications, pp. 1–10 (September 2007)
2. Robinson, F.V., Hamidi, V.: Series connecting devices for high-voltage power conversion. In: Universities Power Engineering Conference, UPEC 2007, pp. 1134–1139 (2007)
3. Redondo, L.M., Silva, J.F.: Solid state pulsed power electronics. In: Rashid, M.H.(ed.) Power Electronics Handbook, 3rd edn., ch. 26, pp. 669–710. Butterworth-Heinemann Publishing, Elsevier (2011)
4. Redondo, L.M., Margato, E., Silva, J.F.: Rise time reduction in high-voltage pulse transformers using auxiliary windings. *IEEE Transactions on Power Electronics* **17**(2), 196–206 (2007)
5. Redondo, L.M., Canacsinh, H., Silva, J.F.: New technique for uniform voltage sharing in series stacked semiconductor. *IEEE Transactions on Dielectrics and Electrical Insulation* **18**(4), 1130–1136 (2011)
6. Santos, N., Silva, J.A., Santana, J.: Sliding mode control of unified power quality conditioner for 3 phase 4 wire systems. In: Camarinha-Matos, L.M., Barrento, N.S., Mendonça, R. (eds.) DoCEIS 2014. IFIP AICT, vol. 423, pp. 443–450. Springer, Heidelberg (2014)
7. Fernando Silva, J.: PWM audio power amplifiers: sigma delta versus sliding mode control. In: Proc. IEEE/ICECS 1998, Lisboa, Portugal, Setembro, vol. 1, pp. 359–362 (1998) ISBN 0-7803-5008-1
8. Fernando Silva, J.: Sliding mode control of voltage sourced boost-type reversible rectifiers. In: Proc. IEEE/ISIE 1997 Conference, Guimarães, Portugal, Julho, vol. 2, pp 329–334 (1997) ISBN 0-7803-3937-1
9. Fernando Silva, J., Pires, V.F., Pinto, S., Barros, J.D.: Advanced control methods for power electronics systems. special issue on Modelling and simulation of Electrical Machines, Converters and Systems of the Transactions on Mathematics and Computers in Simulation, IMACS 63(3-5), 281–295 (2003) ISSN 0378-4754
10. Silva, J.F.: *Electrónica Industrial – Semicondutores e Conversores de Potência*, Fundação Calouste Gulbenkian, 2a edição (2013)

Stable Integration of Power Electronics-Based DG Links to the Utility Grid with Interfacing Impedance Uncertainties

S. Kazem Hoseini¹, Edris Pouresmaeil², Jafar Adabi¹,
and João P.S. Catalão^{3(✉)}

¹ Faculty of Electrical and Computer Engineering, Babol (Noshirvani)
University of Technology, PO Box 484, Babol, Iran

² Centre for Energy Informatics, University of Southern Denmark (SDU),
Odense, Denmark

³ University Beira Interior, Covilhã, INESC-ID and IST, University Lisbon,
Lisbon, Portugal
catalao@ubi.pt

Abstract. For the integration of distributed generation (DG) units to the utility grid, voltage source converter (VSC) is the key technology. In order to realize high quality power injection, different control techniques have been adopted. However, the converter-based DG interface is subject to inevitable uncertainties, which adversely influence the performance of the controller. The interfacing impedance seen by the VSC may considerably vary in real distribution networks. It can be observed that the stability of the DG interface is highly sensitive to the impacts of interfacing impedance changes so that the controller cannot inject appropriate currents. To deal with the instability problem, this paper proposes an enhanced fractional order active sliding mode control scheme for integration of DG units to the utility grid, which is much less sensitive to interfacing impedance variations. A fractional sliding surface which demonstrates the desired dynamics of the system is developed and then the controller is designed in two phases: sliding phase and reaching phase to keep the control loop stable. The proposed controller takes a role to provide high quality power injection and ensures precise current tracking and fast response despite uncertainties. Theoretical analyses and simulation results are verified to study the performance and feasibility of the proposed control scheme.

Keywords: Voltage source converter · Distributed generation · Interfacing impedance · Fractional order control · Active sliding mode control

1 Introduction

The power network is experiencing structural changes due to increasing concerns about greenhouse gas emissions, energy cost, and security of conventional power generations as more distributed generations (DGs) are integrated to the utility grid [1]. These DG technologies are mainly used to deliver clean energy from renewable energy sources such as solar power, wind power, micro turbine generation plants and fuel cell plants, through power electronic voltage source converters (VSCs) [2].

Stable operation of the control loop in DG system is an important aspect; an unstable control loop cannot inject desired power from DG source to the grid. The interfacing impedance seen by the VSC may noticeably change depending on the configuration of the utility grid (as DG units are commonly installed in weak grids), output filter design, and grid synchronization techniques. Also some phenomena such as cable overload, temperature effect, and saturation often further aggravate the problem.

Uncertainties in the impedance seen by the VSC leads to instability in the control of DG interfacing system since the stability is so sensitive to the interfacing impedance variations. As a result of instable controller, the DG system cannot inject the expected currents or persistent oscillations may exist in the injected currents. Hence, it seems crucial to design a control structure for the DG system, which is insensitive to the variations of interfacing impedance.

Several control methods and studies have been reported for integration of DG sources into the power grid, however, few works have addressed instability problems of interfaced converters in DG technology. Influence of grid impedance on current control loop have been investigated in [3] and a control technique based on adjusting the controller gain was proposed to stabilize interfaced VSC; however, it needs problematic online measurement of interfacing impedance; moreover, changing controller gain may deteriorate other capabilities such as disturbance rejection. An adaptive grid-voltage sensorless control method has been presented in [4] for converter-based DG units, which needs an additional interfacing parameter estimator in a parallel structure to deal with the stability problem. Reference [5] proposed a model reference adaptive control to connect DG units to utility grid through a LCL filter; nevertheless, it uses converter output current as the feedback signal to the controller, which may result in the resonance of the grid current due to the interaction of converter output harmonic current and the resonant circuit formed by the grid inductor and filter capacitor. An impedance-based stability criterion has been verified in [6], which discusses the condition in which a grid-connected converter is stable, but it does not present a proper control solution for the instability problem. Effects of grid impedance variations on the stability of the interfaced converter have been investigated in [7]. It has been demonstrated that when either the inductance of the grid increases or the inductance and resistance of the grid increase together, the system stability is adversely affected. Also, [7] proposes an H_∞ controller to deal with the instability problem; however, its implementation and obtaining weighting-functions in such systems are very hard.

Hence, an effective control method is proposed in this paper, which combines fractional order control (FOC) with an active sliding mode control (ASMC). FOC, which is the use of non-integer order derivatives and integrals, has been realized as an alternative scheme for solving control problems [8,9]. Applying the notion of fractional order for managing control problems is a step closer to the practical situations since the real world processes are mostly fractional. Some models of fractional order and fractional calculus have been developed to solve different control problems [10,11]. Sliding mode control is a particular type of variable structure control systems designed to drive and then maintain the system states within a close neighborhood of the decision rule, and is well-known for its robustness to parameter variations and disturbances [12,13]. Therefore, combining fractional order approaches together with sliding mode control has attracted significant interest [14-16].

The objective of this study is to extend a fractional order active sliding mode controller (F_r ASMC) to the current control of a grid-connected three-phase VSC for possessing small steady-state tracking error and fast response of the grid current while

maintaining the system insensitive to interfacing impedance variations. In this control method, the system states are limited to lie on the fractional sliding surface where the dynamics of the system are only specified by the dynamics of the switching surface. The system is invariant in the control design, and the motion of the states trajectory is much less sensitive to disturbances and parameter variations. The control method is easy to implement and only needs nominal values of model parameters.

2 Contribution to Cloud-Based Engineering Systems

Over the past two decades, declines in the costs of small-scale power generations increases in the reliability needs of many customers, and the partial deregulation of electricity markets have made DG technology more attractive to businesses and households as a supplement to utility-supplied power. Moreover, the environmental advantages can also be considered as a key-driving element accelerating the development of DG technology in power system. However, the increasing numbers of DG units in power system require new and intelligent control techniques for the operation and management of electric networks in order to maintain or even to improve the power supply reliability and quality in the future. As a consequence, DG system can be considered as a cloud-based system, consisting of an intelligent control technique for integration of DG sources to the power grid. This cloud-based aspect of energy technology will concentrate on several issues in design of future power grids based on Smart Grids technology during the presence and cooperation of suitable energy storage devices in the distribution grid. The main goal in this research area is design of a control technique for integration of DG sources into the power grid. In the proposed model, load behavioral patterns can be monitored and the huge amount of data can be harvested from utility and load sides. Its processing is being carried out using algorithms established for signal processing. The proposed control technique confirms the role of DG technology in cloud-based energy system by creating a safe operating region for operation of DG units and injection of power from DG sources into the power grid.

3 Modeling of a Grid-Connected DG Interface

This section focuses on a three-phase DG model with a current-controlled VSC. To form a grid-connected DG model, the VSC is integrated to the utility grid with an inductive filter and an isolation transformer. The filter is responsible for filtering out the high frequency harmonics generated by VSC switching actions, and the transformer works as an interfacing reactor. Fig. 1 shows the equivalent circuit diagram of the grid-connected DG unit with three-phase two-level VSC. The VSC synthesizes the AC voltage using space vector modulation (SVM) technique with the available DC voltage. Control signals for the SVM are generated from an appropriate controller, and switching pulses are applied to the VSC switches for power injection from DG source into the power grid. The utility grid is modeled as a three-phase AC source with internal impedance using Thevenin's Theorem. $Z = R + j\omega L$ is the equivalent interfacing impedance seen by the VSC; i_x is the converter output current; v_{gx} is the grid voltage; and i_{dc} is the input DC current ($x=a, b$ and c).

3.1 Dynamic Analysis of the Proposed Model

To inject high quality power to the utility grid, a current control technique is usually adopted to form the output voltage so that minimum current error is achieved. A VSC controls the magnitude and frequency of the output voltage. The output voltage at each leg of the VSC can be expressed as

$$v_{xN} = D_{xN} \cdot v_{dc} \quad (1)$$

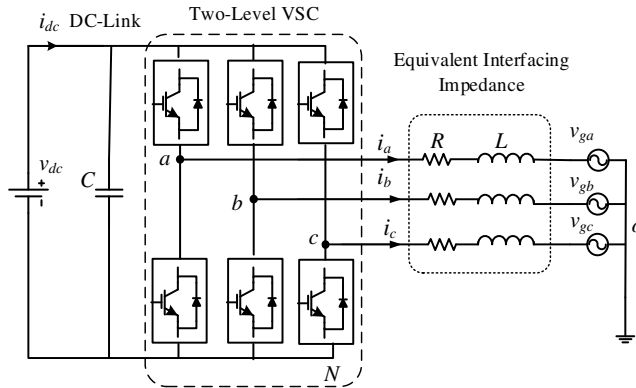


Fig. 1. Equivalent circuit diagram of a generic grid-connected DG unit using three-phase VSC

where v_{xN} is the converter output leg voltage, and the switching variable D_{xN} determines the switching state of interfaced converter, and can be defined as 1 or 0 when the upper (or lower) switch of the leg is switched on or off. Dynamic equations of the proposed model can be calculated by applying Kirchhoff's law in AC-side of the interfaced converter as,

$$L \frac{di_x}{dt} + Ri_x - v_{xo} + v_{gx} = 0 \quad (2)$$

where v_{xo} is the converter output phase voltage. By defining the switching state function of the VSC as,

$$U_x = \left(D_{xN} - \frac{1}{3} \sum_{x=a}^{b,c} D_{xN} \right) \quad (3)$$

and substituting (3) in (2), the dynamic equations of the proposed model can be re-written as,

$$L \frac{di_x}{dt} + Ri_x - U_x v_{dc} + v_{gx} = 0. \quad (4)$$

3.2 Steady-State Analysis of the Proposed Model

In synchronous reference-frame, a rotating reference-frame is utilized so that all fundamental positive sequence alternating variables become DC quantities in $dq0$ -coordinate system; then, objectives of controlling and filtering in the control loop of the system can be achieved easier. By Park transformation matrix, dynamic equations of the proposed model in (4) can transfer into the synchronous reference-frame with angular speed ω as,

$$L \frac{di_d}{dt} - L\omega i_q + Ri_d - U_a v_{dc} + v_{gd} = 0 \quad (5)$$

$$L \frac{di_q}{dt} + L\omega i_d + Ri_q - U_q v_{dc} + v_{gq} = 0. \quad (6)$$

It should be mentioned that zero components of line currents and grid voltages are zero since balanced operation and symmetric abc voltages are considered. Substituting time-varying components by the steady-state quantities and forcing time derivatives to zero, the steady-state expressions of the proposed model in equations (5) and (6) can be calculated as,

$$U_{ds} = \frac{-L\omega i_{qref} + Ri_{dref} + v_{gd}}{V_{dc}^*} \quad (7)$$

$$U_{qs} = \frac{L\omega i_{dref} + Ri_{qref}}{V_{dc}^*}. \quad (8)$$

4 Proposed FrASMC Design of Integrated DG Model

The current control structure of a three-phase VSC is the key element in the control design of a converter-based DG system. When the interfacing impedance seen by the VSC becomes highly inductive, the bandwidth of the controller is considerably decreased, which degrades the dynamic performance of the controller [7]. This leads the system to be oscillatory or even unstable. In this section, to deal with the instability problem a FrASMC is designed for the integration of DG units to the power grid with a three-phase framework. The proposed control scheme has the properties of fast response and small steady-state tracking error of the grid current while keeping the performance of the model insensitive to the interfacing impedance uncertainties.

The current dynamics of the proposed model in the synchronous reference frame (5) and (6) can be represented by the following state-space equations,

$$\begin{aligned} \frac{di_z}{dt} &= Ai_z + BU_z + Tv_{gz} \\ &= (A_o + \Delta A)i_z + (B_o + \Delta B)U_z + (T_o + \Delta T)v_{gz} \\ &= A_o i_z + B_o U_z + T_o v_{gz} + r, \end{aligned} \quad (9)$$

where, $i_z = [i_d \ i_q]^T$, $U_z = [U_d \ U_q]^T$, $v_{gz} = [v_{gd} \ v_{gq}]^T$,
 $A_o = \begin{bmatrix} -R_o/L_o & \omega \\ -\omega & -R_o/L_o \end{bmatrix}$, $B_o = \begin{bmatrix} 1/L_o & 0 \\ 0 & 1/L_o \end{bmatrix}$, v_{dc} , $T_o = \begin{bmatrix} -1/L_o & 0 \\ 0 & -1/L_o \end{bmatrix}$, and

$$r = \Delta A i_z + \Delta B U_z + \Delta T v_{gz}, \tag{10}$$

where, $z=d$ and q ; A , B and T are the system matrices; A_o , B_o , and T_o represent the nominal values of A , B and T ; ΔA , ΔB , and ΔT denote the system parameter variations; and r expresses the lump of uncertainties caused by parameter variations, which is assumed to be bounded by δ ,

$$|r| < \delta, \tag{11}$$

where, δ is a specified positive constant.

Considering the described model, the errors dynamics can be defined as follows,

$$e = x_{ref} - x = i_{zref} - i_z, \tag{12}$$

where, i_{zref} ($=x_{ref}$) is the reference current. The objective of the F_rASMC is to design the controller U_z such that the model state ($x=i_z$) precisely tracks the reference output current.

Output of the PID controllers is a linear combination of the input, the integral of the input, and the derivative of the input. Fractional order PID controllers are generalizations of PID controllers. Output of the fractional order PID controllers is a linear combination of the input, a fractional integral of the input, and a fractional derivative of the input. The proportional-integral equation, which defines the fractional order PI (F_rPI) [8,14] control action can be written as,

$$v(t) = k_p e + k_i D^{-\lambda} e \tag{13}$$

where k_p , k_i , and λ are design parameters of the fractional order PI control. If λ is 1, the result is a usual PI (called as *integer PI*). A switching surface is developed for interfaced converter based on FOC in order to design the F_rASMC. In this sense, a fractional form of the linear compensation PI networks is used to achieve fractional sliding surface of the form PI^λ . Based on the generalized (fractional) PI^λ structure, a candidate for fractional sliding surface, which represents a dynamic of desired model can be obtained of the form as,

$$S = k_p(x_{ref} - x) + k_i D^{-\lambda}(x_{ref} - x); 0 < \lambda < 2, \tag{14}$$

Sliding mode control forces the system state space trajectories to reach the sliding surface in a finite time and to stay on the surface for all future time. The main function of the sliding mode controller is to switch between two different structures of the system so that a new type of system motion (sliding mode) exists on the surface. Therefore, the proposed F_rASMC is designed in two phases as,

- 1- The sliding phase by $S = 0$
- 2- The reaching phase when $S \neq 0$.

In the first phase ($S = 0$), which shows the model operates in desired condition and there are no parameter variations, the active controller can be designed as follows,

$$U_{zeq} = -B_o^{-1}(A_o x + T_o v_{gz} + C_o S), \quad (15)$$

where C_o is a positive definite matrix for placing poles of the nominal system in its desired values. The active controller works properly when there are no uncertainties; however, the sensitivity of the dominant poles of the current controller is very high to system uncertainties mainly due to parameter variations, which lead to drive harmonic currents through the converter or even the controller may become unstable, i.e. $S \neq 0$. In this phase, in order to drive any states outside the surface to reach the surface in a finite time, a switching control law is developed to construct the F_r ASMC as,

$$U_z = U_{zeq} + \gamma sgn(S), \quad (16)$$

where γ is the switching factor, which can be tuned in order to eliminate the effects of parameter variations. As can be seen from (15) and (16), the nominal values of the model parameters are only required to design the controller.

5 Simulation Results

To investigate the performance of the proposed control strategy, the simulation models have been developed under Matlab/Simulink environment.

The rated rms grid phase voltage is 120 V at 60 Hz, and the nominal values of interfacing resistance and inductance are $R_o = 0.2 \Omega$ and $L_o = 0.1 \text{ mH}$, respectively. The dc-link voltage is set to 400 V and the switching frequency of the VSC is 10 kHz. To inject the desired active power P_{ref} to the grid, d -component of the reference current can be obtained as,

$$i_{dref} = \frac{2 P_{ref}}{3 v_{gd}}. \quad (17)$$

By setting a zero value for the q -component of reference current in the current control loop of DG unit, only active power will be injected by integration of DG sources into the power grid and power factor between the injected current from DG unit and load voltage will be obtained a unity value. The reference active power is set to 3 kW.

The stability and dynamic response of the DG model will now be analyzed, and the effectiveness of the designed controller will be evaluated and compared with conventional PI synchronous-frame current controller to validate the proposed procedure. To illustrate the effect of interfacing impedance variations on the current controller performance of a VSC-based DG system, the interfacing resistance and inductance seen by the VSC (R and L) change from [$R = 0.2 \Omega$ and $L = 0.1 \text{ mH}$] to [$R = 0.5 \Omega$ and $L = 0.6 \text{ mH}$] at the instant $t = 0.05 \text{ s}$ in simulations.

The performance of the PI current controller under above mentioned condition is depicted in Fig. 2. As can be seen, the current response cannot track the reference current properly when the interfacing impedance changes, which is consequence of the nonrobust PI current controller. Tuning the PI gains can bring the system into stability; however, it leads to degradation of disturbance rejection capability and increase in steady-state tracking error.

Fig. 3 shows the output current of the VSC and utility grid voltage with the proposed F_r ASMC. It can be observed that the current controller remains stable and injects high quality currents in phase with the utility grid voltage when the interfacing impedance changes. From Fig. 3 the grid-connected power factor is 1.

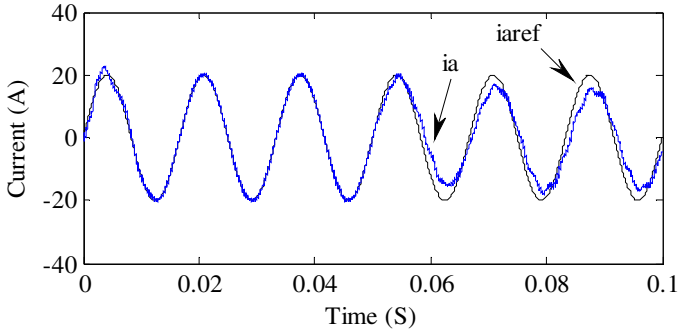


Fig. 2. DG current and its reference with conventional PI controller under interfacing impedance variation at $t = 0.05$ s

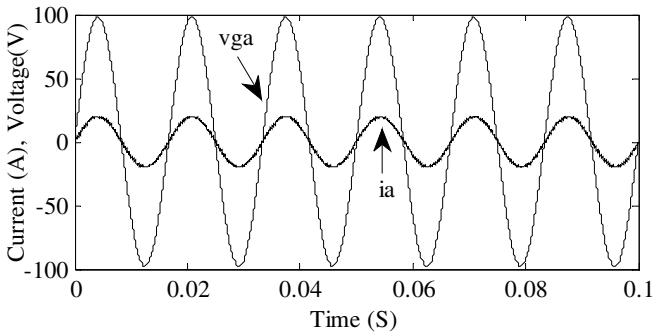


Fig. 3. DG current and grid voltage under interfacing impedance variation at the instant $t = 0.05$ s

By drawing harmonic spectra of current response of conventional PI and proposed F_r ASMC before and after interfacing impedance change (with $P_{ref} = 3$ kW), following results have been observed. THD of output current of the conventional PI current controller before impedance change is 1.08%. However, the THD after impedance change is 6.27%, which does not meet the THD requirement of the IEEE standard 1547 (that is below 5%) [17]. Furthermore, significant low order harmonics can be observed in the harmonic spectra. THD of VSC output current of proposed F_r ASMC before and after impedance change are 0.96% and 1.12%, respectively, which demonstrates the proposed controller successfully meets the standard requirement and has a better performance than conventional PI.

6 Conclusions

DG units are commonly integrated to the utility grid by VSCs for better controllability, reliability, and efficiency. The VSC transfers the generated power to the utility grid using a current controller that has the mission of injecting high quality currents. However, the stability of the current controller is often destroyed by the variations on the interfacing impedance seen by the VSC, such that the system becomes oscillatory or even unstable. In this paper, a F_r ASMC has been proposed for integration of DG units to the utility grid. The main aim of the proposed current controller is to deliver the desired power to the grid with low harmonic current, fast response, and high power factor while maintaining the system insensitive to the interfacing impedance variations. To validate the performance of the proposed F_r ASMC, simulation verification results have been presented and compared with the conventional PI current controller. The results show that high quality current injection is achieved with the proposed F_r ASMC for grid integration of VSC-based DG units.

Acknowledgment. This work was supported by FEDER funds (European Union) through COMPETE and by Portuguese funds through FCT, under Projects FCOMP-01-0124-FEDER-020282 (Ref. PTDC/EEA-EEL/118519/2010) and PEst-OE/EEI/LA0021/2013. Also, the research leading to these results has received funding from the EU Seventh Framework Programme FP7/2007-2013 under grant agreement no. 309048.

References

1. Akorede, M.F., Hizam, H., Poursmaeil, E.: Distributed energy resources and benefits to the environment. *Renewable Sustainable Energy Rev.* **14**(2), 724–734 (2010)
2. Blaabjerg, F., Teodorescu, R., Liserre, M., Timbus, V.A.: Overview of control and grid synchronization for distributed power generation systems. *IEEE Trans. Ind. Electron.* **53**(5), 1398–1409 (2006)
3. Liserre, M., Teodorescu, R., Blaabjerg, F.: Stability of photovoltaic and wind turbine grid-connected inverters for a large set of grid impedance values. *IEEE Trans. Power Electron.* **21**(1), 263–272 (2006)
4. Mohamed, Y.A.I., El-Saadany, E.F., Salama, M.M.A.: Adaptive grid-voltage sensorless control scheme for inverter-based distribution generation. *IEEE Trans. Energy Convers.* **24**(3), 683–694 (2009)
5. Mao, X., Ayyanar, R.: An adaptive controller for inverter-interfaced DGs connected to grids with a wide range of unknown impedances. In: *Energy Conversion Congress and Exposition (ECCE)*, pp. 2871–2877 (2010)
6. Sun, J.: Impedance-based stability criterion for grid-connected inverters. *IEEE Trans. Power Electron.* **20**(11), 3075–3078 (2011)
7. Yang, S., Lei, Q., Peng, F.Z., Qian, Z.: A robust control scheme for grid-connected voltage-source inverters. *IEEE Trans. Ind. Electron.* **58**(1), 202–212 (2011)
8. Podlubny, I.: Fractional-order systems and PI λ D μ controllers. *IEEE Trans. Autom. Control* **41**(1), 208–213 (1999)
9. Valerio, D.: Fractional robust system control. Technical Univ. Lisbon, Ph.D. thesis (2005)
10. Agrawal, O.P.: A general formulation and solution scheme for fractional optimal control problems. *Nonlinear Dynamics* **38**(1–4), 323–337 (2006)

11. Jelicic, Z.D., Petrovacki, N.: Optimality conditions and a solution scheme for fractional optimal control problems. *Struct. Multidiscip. Opti.* **38**(6), 571–581 (2009)
12. Bartolini, G., Fridman, L., Pisano, A., Usai, E., (Eds.): *Modern sliding mode control theory: new perspectives and applications*. Springer, Berlin (2008)
13. Edwards, C., Fossas, Colet. E., Fridman, L., (Eds.): *Advances in variable structure and sliding mode control*. Springer, Berlin (2006)
14. Hosseinnia, S.H., Tejado, I., Vinagre, B.M., Sierociuk, D.: Boolean-based fractional order SMC for switching systems: application to a DC-DC buck converter. *Signal Image and Video Processing* **6**(3), 445–451 (2012)
15. Pisano, A., Rapaic, M.R., Jelicic, Z.D., Usai, E.: Sliding mode control approaches to the robust regulation of linear multivariable fractional-order systems. *Int. J. Robust Nonlinear Control* **20**(18), 2045–2056 (2010)
16. Efe, M.O.: Fractional order sliding mode control with reaching law approach. *Turk J Electr Eng. Comput Sci.* **18**(5), 731–747 (2010)
17. IEEE standard for interconnecting distributed resources with electric power systems, IEEE standard 1547-2003 (July 2003)

Erratum to: Selection of Large-Scale 3D Point Cloud Data Using Gesture Recognition

Robin Burgess^(✉), António J. Falcão, Tiago Fernandes, Rita A. Ribeiro, Miguel Gomes, Alberto Krone-Martins, and André Moitinho de Almeida

UNINOVA / CTS, Campus FCT/UNL, Monte da Caparica,
2829-516 Caparica, Portugal
{rb,tmf}@ca3-uninova.org, {rar,ajf,mdg}@uninova.pt,
{algol,andre}sim.ul.pt

Erratum to: Chapter 20 in: L.M. Camarinha-Matos et al. (Eds.) Technological Innovation for Cloud-Based Engineering Systems, DOI: 10.1007/978-3-319-16766-4_20

In the original publication the legends of Figs. 1 and 2 did not include the statement that they were used with permission from IEEE. The correct statement is:

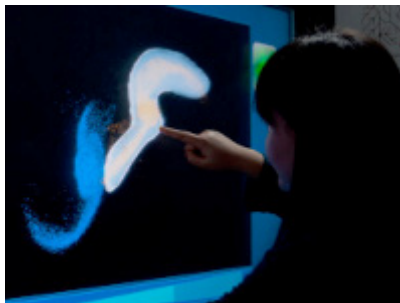


Fig. 1. 3D selection using a touch-based interface [5]. © 2015 IEEE. Reprinted, with permission, from Yu, L., Efstathiou, K., Isenberg, P., Isenberg, T.: Efficient Structure-Aware Selection Techniques for 3D Point Cloud Visualizations with 2DOF Input. IEEE Transactions on Visualization and Computer Graphics **18**(12), 2245–2254 (2012)

The online version of the original chapter can be found under DOI: 10.1007/978-3-319-16766-4_20

© IFIP International Federation for Information Processing 2015
L.M. Camarinha-Matos et al. (Eds.): DoCEIS 2015, IFIP AICT 450, pp. E1–E2, 2015.
DOI: 10.1007/978-3-319-16766-4_55

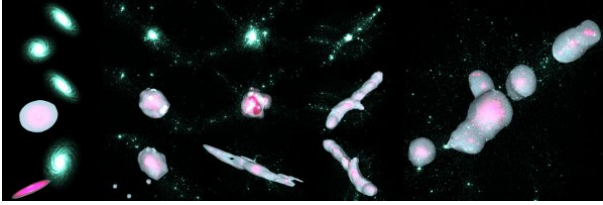


Fig. 2. 3D selection of galaxies using TeddySelection and CloudLasso techniques [5]. © 2015 IEEE. Reprinted, with permission, from Yu, L., Efstathiou, K., Isenberg, P., Isenberg, T.: Efficient Structure-Aware Selection Techniques for 3D Point Cloud Visualizations with 2DOF Input. *IEEE Transactions on Visualization and Computer Graphics* **18**(12), 2245–2254 (2012)

Author Index

- Abdenebaoui, Larbi 137
Adabi, Jafar 502
Adamski, Marian 157
Altsach, Ádám 239
Álvarez, Alfredo 415, 451, 467
Alves, M. 486
Amaro, Nuno 374
Andres, Beatriz 13
Andrzejewski, Grzegorz 157
Arnaudov, Rumen 459
Arsénio, Pedro 415
- Bánáti, Anna 129
Bándi, István Imre 239
Barata, Diogo 82, 101
Barata, José 82, 101, 196
Barata, M. 265
Barrero-González, Fermín 357
Beko, Marko 204
Blos, Maurício F 93
Burgess, Robin 188
- Camarinha-Matos, Luis M. 3, 22, 31, 42
Campos-Rebello, Rogério 147
Caramelo, T. 327
Casimiro, Luís 374
Catalão, João P.S. 296, 309, 317, 327
395, 431, 502
Ceballos, José M. 374, 467
Collares-Pereira, M. 285, 385, 423, 440
Cordeiro, Hugo 217
Costa, Anikó 147
Cseri, Orsolya Eszter 239
- da Silva, Robson Marinho 93
Damavandi, M.Y. 431
de Almeida, André Moitinho 188
de Sousa, Jorge 365
Di Orio, Giovanni 82, 101
Dias Pereira, J.M. 486
Dimic, Goran 204
Dineva, Adrienn 179
Dinis, Rui 204
- dos Santos, M.P. 440
Drozdov, Dmitrii 73
Dubinin, Victor 73
- Esteves, J. 285
Eusébio, Eduardo 365
- Falcão, António J. 188
Fernandes, Tiago 188
Ferrada, Filipa 42
Ferreira, Tiago 196
Fialho, L. 423
Filho, Diolino J Santos 65
Filip, Florin Gheorghe 405
Fonseca, J.M. 486
Fonseca, José 217
Freire, P. 285
- Galvão, João 337
Ghimire, Sudeep 273
Godina, R. 327
Godina, Radu 296
Goes, João 3
Golshan, M.E.H. 309
Gomes, Luis 3, 147, 165, 345
Gomes, Miguel 188
Görner, Manja 259
Göschel, Thomas 259
Graça, Paula 22
- Haghifam, M.-R. 431
Herscheid, Lena 121
Heydarian-Forushani, E. 309
- Inácio, David 451, 467
- Jardim-Goncalves, Ricardo 273
Jonas, Viktor Zoltan 231
Junqueira, Fabrício 65, 93
- Kacsuk, Péter 129
Kail, Eszter 129
Kassel, Stephan 259
Kazem Hoseini, S. 502

- Kiss, Gábor 239
 Klein, Thomas 259
 Könnnyú, Zsolt 225
 Kovács, Levente 239
 Kozlovsky, Miklos 129, 225, 231, 239
 Kreowski, Hans-Jörg 137
 Krone-Martins, Alberto 188
 Krzywicki, Kazimierz 157
 Kuske, Sabine 137

 Laia, R. 385
 Leitão, Sérgio 337
 Louro, P. 265
 Luis-Ferreira, Fernando 273
 Lujano-Rojas, J.M. 317

 Madeira, Ricardo 477
 Maló, Pedro 345
 Martins, João 3, 374
 Matias, João C.O. 296, 317
 Melício, R. 385, 423, 440
 Mendes, Tiago D.P. 296, 327
 Mendes, V.M.F. 285, 385, 423, 440
 Meneses, Carlos 217
 Mihaylov, Kaloyan 459
 Milanés-Montero, María Isabel 357
 Miranda, Fábio 196
 Miyagi, Paulo E 65, 93
 Moghaddam, M.P. 431
 Molnar, Bela 231
 Moreira, Licínio 337
 Murta-Pina, João 415

 Neves, Mário Ventim 451, 467
 Nunes, Francisco 54

 O'Neill, Henrique 54
 Oliveira, Ana Inês 31
 Oliveira, José Antonio Barata 111
 Onofre, Sérgio 251
 Osório, G.J. 317

 Paterakis, Nikolaos G. 395
 Patil, Sandeep 73
 Paulino, Nuno 477
 Peixoto, João Alvarez 111
 Pereira Cabrita, C. 285
 Pereira, Carlos Eduardo 111
 Pereira, Fernando 165
 Pimentão, João Paulo 251, 196
 Pina, João Murta 374, 451, 467

 Pinto, Sónia F. 494
 Pisching, Marcos A 65
 Poler, Raul 13
 Polze, Andreas 121
 Pouresmaeil, Edris 502
 Pousinho, H.M.I. 285, 385
 Pronto, Anabela Gonçalves 415

 Ribeiro, Rita A. 188
 Richter, Daniel 121
 Rocha, André Dionísio 82, 101, 111
 Rodrigues, Eduardo M.G. 296, 327
 Rodrigues, João 345
 Romero-Cadaval, Enrique 357
 Rudas, Imre 225
 Ruiz-Cortés, Mercedes 357

 Sander, Sabrina 259
 Santos Filho, Diolino J 93
 Santos, Nelson 494
 Santos, Sérgio F. 395
 Santos, Tiago 101
 Seixas, M. 440
 Serra, Hugo 477
 Shafie-khah, M. 309, 431
 Silva, Edgar M. 345
 Silva, J. Fernando 494, 265
 Skala, Tibor 225
 Soares, Vasco 494
 Sousa, Duarte 494
 Sousa, Pedro 196, 251
 Stănescu, Ioana Andreea 405
 Sütő, Balázs 225

 Tar, József K. 179
 tefan, Antoniu 405
 Tölgyesi, Zsolt 225
 Tomic, Slavisa 204
 Tuba, Milan 204

 Vale, Zita 337
 Valtchev, Stanimir 459
 Várkonyi-Kóczy, Annamária R. 179
 Ventim Neves, Mário 365, 451, 467
 Vieira, M. 265
 Vieira, M.A. 265
 Vilhena, Nuno 415
 Vyatkin, Valeriy 73

 Watanabe, Edson H 93